SYNTHESIS AND BIOLOGICAL ACTIVITY OF CYANOBACTERIAL AERUGINOSINS

Inauguraldissertation

zur

Erlangung der Würde eines Doktors der Philosophie

vorgelegt der

Philosophisch-Naturwissenschaftlichen Fakultät

der Universität Basel

von

Manuel Eugen Scherer

aus Basel (BS), Schweiz

Basel, 2016

Genehmigt von der Philosophisch-Naturwissenschaftlichen Fakultät
auf Antrag von

Prof. Dr. Karl Gademann und Prof. Dr. Olivier Baudoin

Basel, den 20.09.2016

Prof. Dr. Jörg Schibler
Dekan

Die edelste Art Erkenntnis zu gewinnen ist die durch Nachdenken und Überlegung. Die einfachste Art ist die durch Nachahmung und die bitterste Art ist die durch Erfahrung.

Buddha

Für Jana und Lilly

TABLE OF CONTENTS

ABSTRACT

In this thesis, the chemical synthesis and biological activity of aeruginosins are described. Aeruginosins are a class of secondary metabolites produced by cyanobacteria. Cyanobacteria belong to the oldest living organisms on Earth, capable of inhabiting the most remote and hostile areas.

Chapter I: Over the past years, an augmentation of harmful algal blooms (HABs) has been observed in waters all over the world. HABs pose a threat for animals and humans alike. In the past, the research focus was mainly laid on the investigation of the toxicity of microcystins and nodularins. Recent results showed that also chlorinated and sulfated aeruginosins such as 828A have to be considered as cyanotoxins. In this chapter, the successful synthesis of four congeners of aeruginosin 828A bearing different permutations of the chlorine and sulfate substituents is reported. Performed toxicity tests against the crustacean *Thamnocephalus platyurus* indicate that especially the sulfate group exerts a notable influence on the toxicity of the aeruginosins.

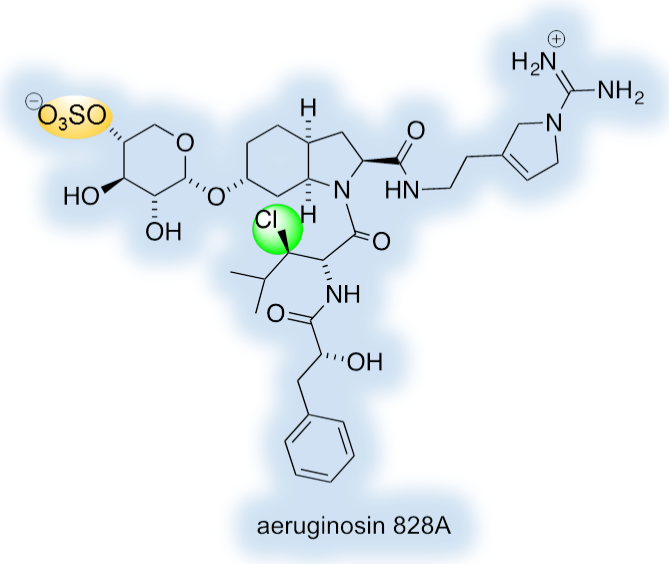

aeruginosin 828A

Chapter II: In this chapter, the results of a purely synthetically driven research project are described. The efforts which were taken in order to elucidate strategies towards the total synthesis of the recently isolated aeruginosin KT608A are summarized. Two novel synthetic approaches were developed for the preparation of the D-*diepi*-Choi core structure present in KT608A. Substantial differences in the NMR spectral data between the synthetic material and the isolated natural product resulted in proposing a revised structure for aeruginosin KT608A.

Parts of this work have been published:

Manuel Scherer, Dominik Bezold and Karl Gademann, *Investigating the Toxicity of the Aeruginosin Chlorosulfopeptides by Chemical Synthesis*, *Angew. Chem. Int. Ed.* **2016**, *55*, 9427–9431.

ACKNOWLEDGMENTS

First of all, I want to thank Prof. Dr. Karl Gademann for giving me the opportunity to conduct research in his group and providing me with an exciting research topic. His support and motivational speeches always pushed me forward during my PhD, especially in times when chemistry was treating me badly.

I am very grateful to Prof. Dr. Olivier Baudoin for agreeing to be the co-examiner of my thesis.

I would like to thank Prof. Dr. Christof Sparr not only for chairing my PhD defense but also for his helpful advice during my PhD.

Big thanks go to Dr. Regina Berg, Dr. Florian Huber, Dr. Christophe Däppen, Dr. Cathrin Ertl, Raphael Liffert and Mathieu Szponarski for proofreading my thesis.

I am very thankful to Dominik Bezold for the work he performed during his Wahlpraktikum and Master thesis project as well as to Agron Ilazi for his work during the Schlussversuch.

I would like to thank all members of Labs 106 and Y32E68 for the always nice working atmosphere, namely Dr. Malika Makhlouf, Dr. Christophe Thommen, Dr. Samuel Bader, Dr. Christophe Däppen, Dominik Bezold, Achim Link, Christian Fischer, Dominik Lotter, Jan Hanusch, Andrea Meier and Joel Rösslein.

Special thanks go to the XXXXx crew including Dr. Patrick Burch, Dr. Samuel Bader, Dr. Elias Kaufmann and Dr. Christophe Däppen for the good vibes after the working hours in the lab.

Very special thanks go to Dr. Christophe Däppen for being the pillar of strength beside me in the lab during the whole period of my PhD. Your musical entertainment really raised the atmosphere in the lab.

I would like to thank Roy Lips not only for the supply with laboratory material but in particular for the fruitful discussions.

I am grateful for the support I received for analytical measurements by PD Dr. Daniel Häussinger and Simon Jurt for NMR measurements, Dr. Heinz Nadig and Laurent Bigler for HRMS measurements and Dr. Markus Neuburger and Prof. Dr. Anthony Linden for X-ray crystallographic analysis.

I thank the whole staff of the universities of Basel and Zurich, Marina Mambelli Johnson, Beatrice Erismann and Miriam Plichta for taking care of administrative affairs and the "Werkstatt-teams" of both universities for technical support.

Big thanks go to the remaining present and former group members of the Gademann research group: Dr. Fabian Schmid, Ellen Piel, Hiromu Hattori, Robin Wehlauch, Raphael Liffert and Mathieu Szponarski.

I would like to thank the ESOC team including Dr. Elias Kaufmann, Dr. Christophe Däppen and Isabel Kerschgens for the lovely time we spent in Lisbon.

I want to thank Dr. Nadine Bohni, Dr. Verena Grundler and Dr. Simon Sieber for their assistance during HPLC purification.

The wisdom of the former and current postdocs of the group, Dr. Hideki Miyatake, Dr. Suman de Sarkar, Dr. Erika Crane, Dr. Nadine Bohni, Dr. Regina Berg, Dr. Chien-Chi Hsiao and Dr. Florian Huber is especially honored.

I really enjoyed the tabletop and real soccer battles with Dr. José Gomes, Dr. Johannes Hoecker and Dr. Simon Sieber.

I am thankful to the Panini Gang around Dr. Florian Huber, Joel Rösslein and Simone Grendelmeier for helping me collecting football stickers and Dr. Cathrin Ertl for her assistance with putting them into our album.

Big thanks go to our friendly neighbors of the Sparr Group in Basel, Achim Link, Dominik Lotter, Christian Fischer, Reto Witzig and Vincent Fäseke.

I would like to thank my friends from high-school, Gian Looser, Matthias Pflugi, Anna Rinne and David Tschirky and the NERDS team around Ina Bodoky, Lukas Felix, Natalie Huber and Philipp Raschle who reminded me that there is a life beside the laboratory.

Nicht genug kann ich meinen Eltern Maya und Hanspeter danken. Ihr seid die Baumeister, die das Fundament für diese Arbeit gelegt haben. Eure vollumfängliche Unterstützung war mir zu jeder Zeit meiner Ausbildung gewiss – dafür bin ich euch enorm dankbar. Auch meine Geschwister Raphael und Seraina haben einen grossen Anteil an dem, was aus mir geworden ist.

To Cathrin, thank you for acting as a peacemaker between me and Office Word and as a pacemaker in my PhD and life. Without your care and your support, especially in the last months, the writing of this thesis would not have been possible for me.

LIST OF ABBREVIATIONS AND ACRONYMS

°	degree
°C	degree Celsius
$[\alpha]_D^T$	optical rotation
Å	Ångström
A	aeruginosin
AAA	asymmetric allylic alkylation
Aap	1-amidino-2-aminopyrrolidine
Ac	acetyl
Adc	1-(*N*-amidino-Δ^3-pyrrolino)ethyl
Aer	aeruginosin gene cluster
Agma	agmantin
Ahap	1-amidino-2-hydroxy-3-aminopiperidine
Amap	1-amidino-2-methoxy-3-aminopiperidine
aq.	aqueous
Argal	argininal
Argol	argininol
Bar	barbamide
BAr_F	tetrakis[3,5-bis(trifluoromethyl)phenyl]borate
BDA	butane diacetal
Bn	benzyl
Boc	*tert*-butyloxycarbonyl
Bp	boiling point
br	broad
Bu	butyl
Bz	benzoyl
Cbz	carboxybenzyl
Ccoi	2-carboxy-6-chlorooctahydroindole
Choi	2-carboxy-6-hydroxyoctahydroindole
CHT	chymotrypsin
CIP	contact ion pair
Cleu	chloroleucine

COSY	correlation spectroscopy
CPO	chloroperoxidases
CSA	camphorsulfonic acid
δ	chemical shift
Δ	difference
d	doublet
d.r.	diastereomeric ratio
DAST	diethylaminosulfur trifluoride
DBU	1,8-diazabicyclo[5.4.0]undec-7-ene
DCE	dichloroethane
DEAD	diethyl azodicarboxylate
DEBPT	3-(diethoxyphosphoryloxy)-1,2,3-benzotriazin-4(3*H*)-one
DFW	diluted standard freshwater
DIBAL	diisobutylaluminium hydride
DIPEA	*N*,*N*-diisopropylethylamine
DMAP	4-dimethylaminopyridine
DMF	*N*,*N*-dimethylformamide
DMSO	dimethyl sulfoxide
DMTMM	4-(4,6-dimethoxy-1,3,5-triazin-2-yl)-4-methylmorpholinium chloride
DTBMP	2,6-di-*tert*-butyl-4-methylpyridine
E^+	electrophile
EDC	1-ethyl-3-(3-dimethylaminopropyl)carbodiimide
ee	enantiomeric excess
epi	epimeric
ESI	electrospray ionization
Et	ethyl
FTIR	Fourier transform infrared spectroscopy
g	gram
Glu	glucose
h	hour(s)
HAB	harmful algal blooms
HATU	1-[bis(dimethylamino)methylene]-1*H*-1,2,3-triazolo[4,5-*b*]pyridinium 3-oxid hexafluorophosphate

HCT	human colon tumor
HMBC	heteronuclear multiple bond correlation
HMDS	bis(trimethylsilyl)amine
HMPA	hexamethylphosphoramide
HOBt	hydroxybenzotriazole
Hpla	4-hydroxyphenyllactic acid
HPLC	high-performance liquid chromatography
HRMS	high-resolution mass spectrometry
HSQC	heteronuclear single quantum coherence spectroscopy
HWE	Horner-Wadsworth-Emmons
Hz	Hertz
i	*iso*
IC_{50}	50% inhibitory concentration
Ile	isoleucine
J	coupling constant
K	Kelvin
KG	ketoglutarate
L	liter
LC_{50}	50% lethal concentration
LDA	lithium diisopropylamide
Leu	leucine
LG	leaving group
LRMS	low-resolution mass spectrometry
μ	micro
m	meter; milli; multiplet (NMR)
M	molarity
m-CPBA	*meta*-chloroperoxybenzoic acid
M.	*Microcystis*
m/*z*	mass to charge ratio
ManA	mannuronic acid
MC	microcystin
mcy	microcystin synthase
Me	methyl

MeCN	acetonitrile
min	minute(s)
MOM	chloromethyl methyl ether
MP	melting point
Ms	mesyl
MS	molecular sieves
n	nano
N.	*Nodularia*
NASA	national aeronautics and space administration
NBS	*N*-bromosuccinimide
NIS	*N*-iodosuccinimide
NMM	*N*-methylmorpholine
NMO	*N*-methylmorpholine *N*-oxide
NMR	nuclear magnetic resonance
NOE	nuclear Overhauser effect
NOESY	nuclear Overhauser effect spectroscopy
NRP	nonribosomal peptide(s)
O.	*Oscillatoria*
P	nonparticipating substituent
P.	*Planktothrix*
PA	picolinamide
PAP	papain
Pen	pentose
PG	protection group
Ph	phenyl
PHOX	phosphinooxazolines
Pla	phenyllactic acid
PLM	plasmin
ppm	parts per million
Pr	propyl
Pren	prenyl
PyBOP	benzotriazol-1-yl-oxytripyrrolidinophosphonium hexafluorophosphate
PyBrOP	bromotri(pyrrolidino)phosphonium hexafluorophosphate

q	quartet
quant.	quantitative
R	residue
r.t.	room temperature
RCM	ring closing metathesis
R_f	retention factor
ROESY	rotating-frame nuclear Overhauser effect correlation spectroscopy
s	singlet
S	solvent
SAM	*S*-adenosylmethionine
SAR	structure–activity relationship
sat.	saturated
sept	septet
SM	starting material
sp.	*species*
SFW	standard freshwater
t	*tert*
t	triplet
T.	*Thamnocephalus*
TBAF	tetra-*N*-butylammonium fluoride
TBDPS	*tert*-butyldiphenylsilane
TBS	*tert*-butyldimethylsilyl
TCE	trichloroethyl
TES	triethylsilyl ether
Tf	triflate
TFA	trifluoroacetic acid
THB	thrombin
THF	tetrahydrofuran
Thr	threonine
TIPS	triisopropylsilyl ether
TLC	thin layer chromatography
TMS	trimethylsilyl
TOCSY	total correlation spectroscopy

TOX	toxic
TRP	trypsin
Tyr	tyrosine
UPLC	ultra performance liquid chromatography
UV	ultraviolet (spectroscopy/light)
v/*v*	volume per volume
w/*w*	weight per weight
X^-	counterion
Xyl	xylose

General Introduction

1. Cyanobacteria – Tiny Organisms with a Toxic Punch

Cyanobacteria are a phylum of prokaryotic organisms belonging to the domain of bacteria. The name cyano (Greek for blue) is derived from the colorful appearance of some cyanobacteria strains (Figure 1). Owing to their distinct color, cyanobacteria are also referred to as "blue-green algae", albeit this name can be deceptive in a sense that algae are eukaryotes in contrast to the prokaryotic cyanobacteria. The name "blue-green algae" originates from earlier days in which the distinction of biological fine structures of algae and cyanobacteria was difficult. Due to fossil findings in Australia it is estimated that the evolution of cyanobacteria occurred 3.5 billion years ago, making them one of the oldest organisms on Earth.[1,2] During these 3.5 billion years, cyanobacteria had a tremendous influence on the life on Earth: for instance led their ability to perform photosynthesis to O_2 enrichment in the atmosphere 2.4 billion years ago. This change from a reductive to an oxidative atmosphere paved the way for aerobic terrestrial life and can therefore be considered as one of the most significant events in the history of life on Earth.[3] Cyanobacteria preferably grow in marine and fresh water. Besides aquatic cyanobacteria, also strains exist which are known to grow in terrestrial habitats and in soil.[4] Thereby, cyanobacteria show a remarkable adaptability to environmental stress. For example, strains were found enduring very low temperatures in the Antarctic but also others which tolerate high temperatures of up to 74 °C in hot springs, such as in the Yellowstone National Park (Figure 1).[5,6] Even extremely dry desert regions and volcanic ash can be inhabited by cyanobacteria.[7,8]

Figure 1 Cyanobacteria in the Grand Prismatic hot spring at Yellowstone National Park.[9]

1.1. Cyanobacterial Secondary Metabolites

Besides ordinary metabolites including fatty acids, polysaccharides and lipopeptides, cyanobacteria produce various carotenoids which are responsible for the distinct cyanobacterial colors. A further characteristic of cyanobacteria is the production of structurally diverse peptide-like secondary metabolites created over nonribosomal biosynthetic pathways. Cyanobacteria incorporate various modified amino acids into these nonribosomal peptides (NRP), thereby allowing for tuning of the NRP biological function. Examples for NRPs include the cyclic polypeptides microcystins (MC) and cyanopeptolins. Because of their diversity and pharmacological functions, cyanobacterial metabolites have attracted attention as potential drug candidates.[10] Among the biologically active metabolites produced by cyanobacteria, there are numerous toxic compounds. The most prevalent cyanotoxins are depicted in Figure 2, including microcystin-LR (**A**), anatoxin-a (**B**), cylindrospermopsin (**C**), saxitoxin (**D**), β-methylamino-L-alanine (**E**) and nodularin-R (**F**). Whereas microcystins, cylindrospermopsin and nodularins, such as compounds **A**, **C** and **F** for example, show a hepatotoxic effect by damaging the liver, anatoxin-a (**B**), saxitoxin (**D**) and β-methylamino-L-alanine (**E**) exhibit neurotoxic effects.[11]

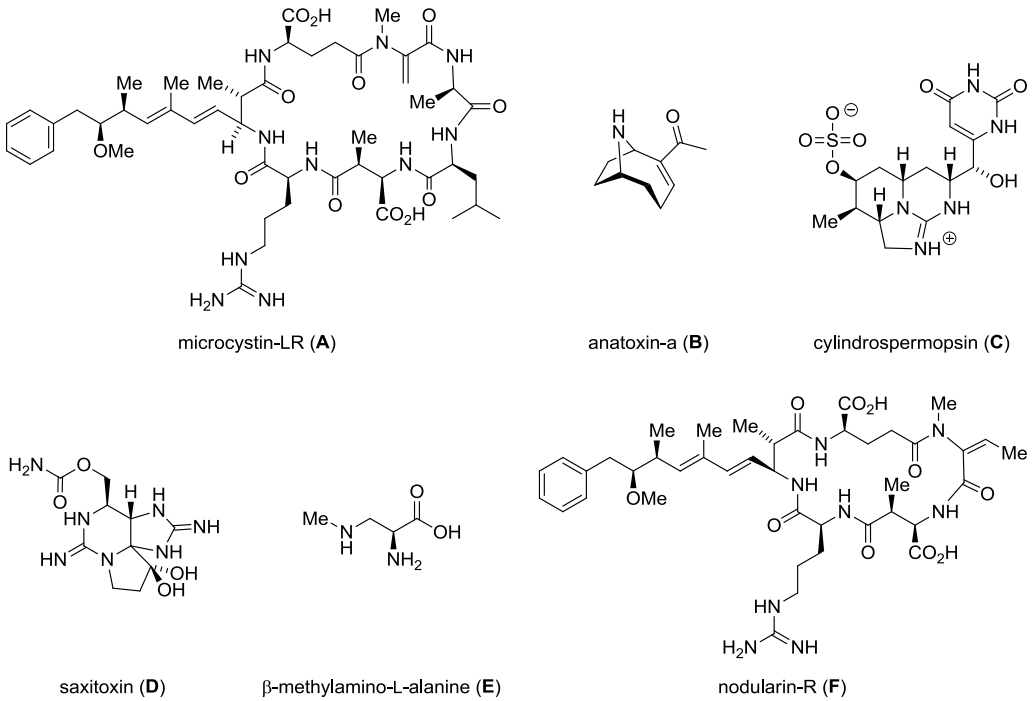

Figure 2 A selection of the most prevalent cyanotoxins: microcystin-LR (**A**), anatoxin-a (**B**), cylindrospermopsin (**C**), saxitoxin (**D**), β-methylamino-L-alanine (**E**) and nodularin-R (**F**).

1.2. Harmful Algal Blooms (HABs)

As described in the previous section, cyanobacteria are capable of producing potent toxins. These venomous metabolites produced by aquatic cyanobacteria can be a threat for animals and humans alike: Eutrophication of waters in combination with rising temperatures caused by the climate change led to an augmentation of harmful algal blooms (HABs) all over the world.[12,13] HABs are described by an uncontrollable growth of cyanobacteria spreading over large areas, thereby intoxicating the waters. In 2014, one of the largest blooms ever was observed in Lake Erie[14,15] (Figure 3) resulting in a cut-off of the local drinking water supply of half a million people. Other examples for the formation of HABs are the Baltic Sea[16] in summer 2015 or the Yellow Sea in China in 2013. Recently, also lakes in Switzerland and Germany have been affected by the occurrence of toxic cyanobacteria blooms.[17]

That water intoxication by cyanobacteria can have dramatic consequences is illustrated by a tragic case in Brazil in 1996. In a clinic in Curuaru, dialysis patients were treated with cyanobacteria contaminated water. Caused by the cyanotoxins, 116 people showed severe intoxications and 52 even lost their lives.[18] All in all, an increase of intoxications triggered by cyanobacteria has been observed over the past years. Uptake of the cyanotoxins usually occurs *via* oral intake but other mechanisms such as skin contact or inhalation are also possible.[19]

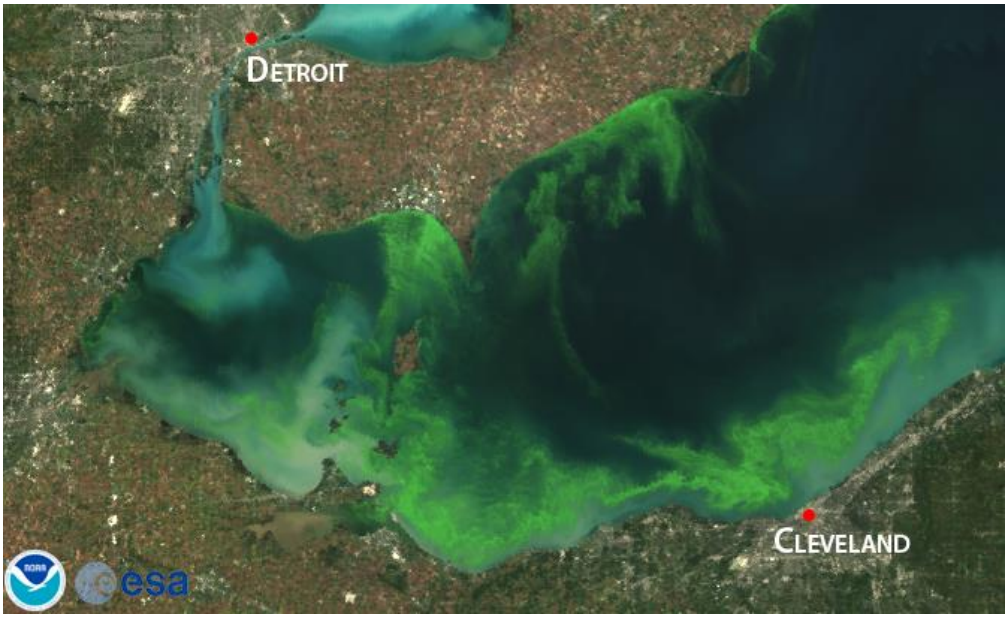

Figure 3 Satellite picture recorded by NASA showing the harmful algal bloom in Lake Erie in 2014.[20]

2. Aeruginosins

Besides the secondary metabolites described in the previous sections, cyanobacteria produce another group of natural products which are linear modified NRPs, called aeruginosins. The first member of this new class of natural products was isolated by Murakami and co-workers in 1994. By screening metabolites of the cyanobacterium *Microcystis aeruginosa*, Murakami *et al*. were able to isolate and characterize aeruginosin 298A (**1**).[21] Unlike the cyclic NRPs microcystin and cyanopeptolin, aeruginosin 298A (**1**) is built up in a linear fashion. Further, compound **1** showed the presence of a thus far unknown, unique 2-carboxy-6-hydroxyoctahydroindole (Choi) moiety. Such a modified amino acid as presented by the Choi unit had not been observed in natural products until the isolation of A298A (**1**). As a result, A298 (**1**) was classified as a new class of secondary metabolites named aeruginosin in allusion to the cyanobacteria strain *M*. *aeruginosa*. Aside from the Choi motif, the group of Murakami described a 4-hydroxyphenyllactic acid (Hpla) and an L-leucine (L-Leu) residue on the N-terminus and an argininol (Argol) side chain on the C-terminus of aeruginosin 298A (**1**) (left, Figure 4). Since Murakami *et al*. were not able to determine all stereochemical information in aeruginosin 298A (**1**), the absolute configuration of natural product **1** remained unclear until Tulinsky and co-workers succeeded in recording an X-ray crystallographic structure of aeruginosin **1**. Tulinsky and his group managed to grow single crystals of a ternary complex of aeruginosin 298 (**1**) bound to hirugen-thrombin.[22] The obtained crystallographic data at 2.1 Å resolution indicated the presence of L-Choi, L-Argol, L-Leu and D-Hpla moieties in compound **1** (center, Figure 4). However, total syntheses reported simultaneously by Bonjoch[23] and Wipf[24] revealed that the absolute configuration of the leucine residue in A298A (**1**) is D and not L as reported by Tulinsky (right, Figure 4).

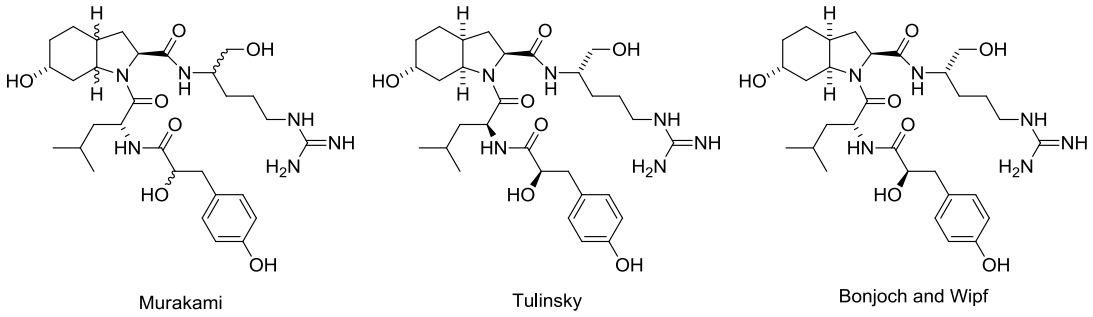

Figure 4 Proposed structures of aeruginosin 298A (**1**) by Murakami (left, 1994), Tulinksy (center, 1998) and Bonjoch and Wipf (right, 2000).

From the structure of aeruginosin 298A (**1**), a general configuration for the class of aeruginosins can be derived (Figure 9, page 13): Aeruginosins consist of four modified or unmodified amino acids which are linked in a linear manner. The core unit comprises the proline-based Choi unit onto which a guanidine-containing residue is joined on the C-terminus. The N-terminus is normally enclosed by a bulky hydrophobic acid at the first position (with respect to the Choi) and a phenyllactic acid (Pla) or Hpla derivative at the second position (with respect to the Choi). To date the structures of around 60 naturally occurring aeruginosins are known (see Table on pages 14 and 15). For a better overview over the structures, the different aeruginosins were divided into four groups. The affiliation to a particular group was executed according to the special characteristics of the respective aeruginosins. Group one comprises ordinary aeruginosins which do not contain any additional distinctive features (Figure 5, page 8). Group two consists of aeruginosins bearing a halogenated Hpla residue on the N-terminus (Figure 6, page 9). Group three contains glycosylated aeruginosins (Figure 7, page 11) and group four involves aeruginosins which exhibit an alteration in the L-Choi motif (Figure 8, page 12). Of course, an alternative classification of the different aeruginosins based on other criteria would also be possible: for example a classification not by structural features but by isolation source.

2.1. Ordinary Aeruginosins

One year after the isolation of aeruginosin 298A (**1**), Murakami and co-workers reported the identification of aeruginosin 98B (**2**) in *M. aeruginosa*. Aeruginosin 98B (**2**) bears an agmantin (Agma) residue on the N-terminus and contains a sulfated hydroxyl group on the L-Choi (Figure 5).[25] In the following years, researchers from the Boehringer Mannheim GmbH reported on the isolation and characterization of oscillarin (**3**) from *Oscillatoria agardhii*.[26] Oscillarin (**3**) featured a novel 1-(*N*-amidino-Δ^3-pyrrolino)ethyl (Adc) unit on the N-terminus. In 1996 and 1998, Murakami *et al*. disclosed three new members of the aeruginosin family, namely aeruginosins 102A (**4**), 102B (**5**) and 103A (**6**) from *M. viridis*.[27,28] These newly isolated aeruginosins were characterized by a C-terminal 1-amidino-2-hydroxy-3-aminopiperidine (Ahap). Due to a tautomeric equilibrium arising from the Ahap subunit, the analysis and characterization of natural products **4**, **5** and **6** turned out to be difficult. Nonetheless, Murakami *et al*. were able to elucidate the structures of aeruginosins **4**, **5** and **6**. Microcin SF608 (**7**) was discovered in 1999 by Carmeli and his group while screening protease inhibitors from *M. aeruginosa*. Natural product **7** featured the known Agma residue on the C-terminus and L-Phe and L-Hpla subunits on the N-terminus.[29] In the same year, Murakami *et al*. published the isolation of aeruginosin 298B (**8**). The special feature of A298B (**8**) is the lack of the arginine-mimicking residue on the C-terminus.[30] Most recently, Sivonen and co-workers reported the isolation of a series of aeruginosins from *Nodularia spumigena*. The aeruginosins disclosed by Sivonen *et al*. were characterized by fatty acid residues on the N-terminus.[31] The C-terminal unit of these aeruginosins was either decorated with an argininal moiety (Argal) (present in aeruginosins NAL1 (**9**), NAL2 (**10**) and NAL3 (**11**)) or an argininol residue (Argol) (present in aeruginosins NOL1 (**12**), NOL2 (**13**), NOL3 (**14**) and NOL4 (**15**), see Figure 5).

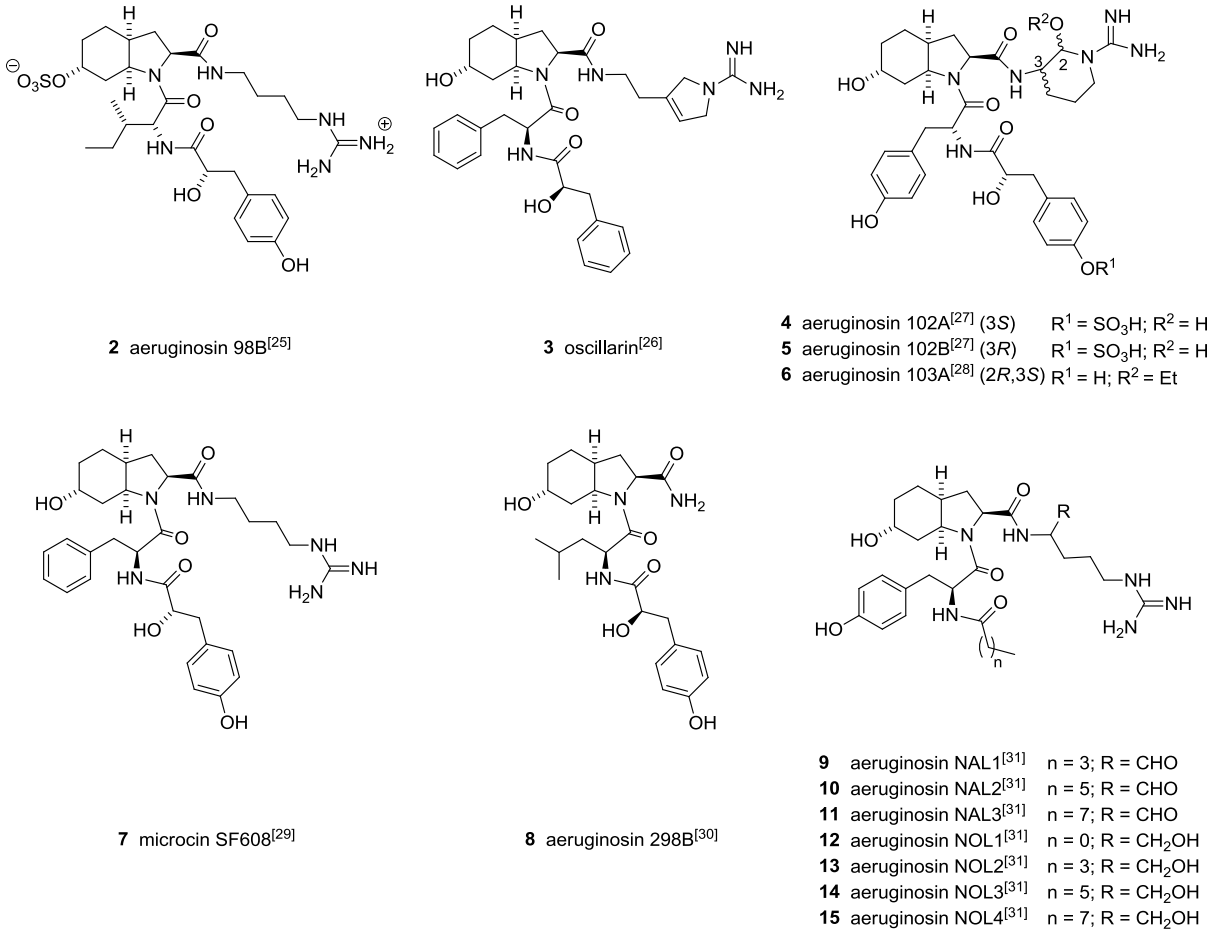

Figure 5 Structures of known ordinary aeruginosins.

2.2. Aeruginosins Bearing Halogenated Hpla Residues

Already in 1995, Murakami and co-workers described the presence of a *meta* chlorinated 4-hydroxyphenyllactic acid residue (*m*-Cl-Hpla) in aeruginosin 98A (**16**).[25] Later, with aeruginosin 98C (**17**), they could isolate a brominated variant of **16** together with congeners featuring an *O*-sulfated-*m*-Cl-Hpla moiety (aeruginosins 89 A (**33**) and 89 B (**34**)). In aeruginosin 101 (**18**), even a dichlorinated Hpla residue (*m*-Cl_2-Hpla) was observed (Figure 6).[30] Further, Carmeli *et al*. demonstrated that halogenation of the Hpla unit in aeruginosins isolated from *M*. *aeruginosa* is highly likely.[32–36] With aeruginosins KY608 (**19**), KY642 (**20**), GE766 (**21**), GE686 (**22**), GE810 (**23**) and GE730 (**24**), they identified congeners of aeruginosin 98A (**16**) containing various permutations regarding the bromine, chlorine and sulfate substituents. In the case of aeruginosin DA495B (**25**), also a chlorinated variant lacking the agmantin residue on the C-terminus could be isolated, together with four

additional chlorinated congeners. All of them possessed the prevalent agmantin pharmacophore on the C-terminus but differed in the amino acid present in the second position. Aeruginosins DA688 (**26**) and DA722 (**27**) featured a Leu residue whereas DA642A (**31**) and DA642B (**32**) contained a Phe moiety.[34] Further, with the isolation of aeruginosins LH650A (**35**), LH650B (**36**) and LH606 (**37**) from *Microcystis spp*.[36] and aeruginosins IN608 (**29**) and IN652 (**30**) from *Microcystis sp*.,[33] Carmeli *et al*. could show that chlorination of the Hpla unit is not restricted to the cyanobacteria strain *M*. *aeruginosa*: Natural products **35** and **36** contained a 1-amidino-2-methoxy-3-aminopiperidine (Amap) moiety on the C-terminus whereas compound **37** featured a novel 1-amidino-2-aminopyrrolidine (Aap) residue. IN608 (**29**) and IN652 (**30**) exhibited a similar structure to aeruginosins DA688 (**26**) and DA722 (**27**) as well as to GE642 (**28**) (Figure 6).

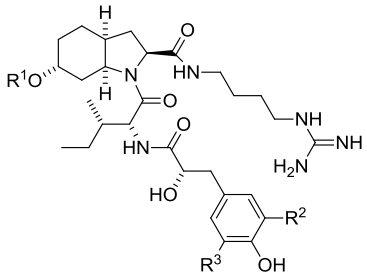

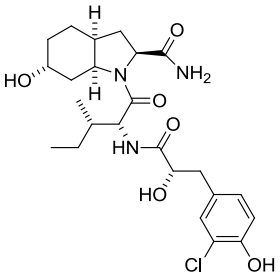

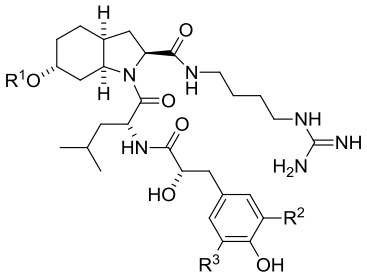

16 aeruginosin 98A[25] $R^1 = SO_3H$; $R^2 = Cl$; $R^3 = H$
17 aeruginosin 98C[30] $R^1 = SO_3H$; $R^2 = Br$; $R^3 = H$
18 aeruginosin 101[30] $R^1 = SO_3H$; $R^2 = Cl$; $R^3 = Cl$
19 aeruginosin KY608[32] $R^1 = H$; $R^2 = Cl$; $R^3 = H$
20 aeruginosin KY642[32] $R^1 = H$; $R^2 = Cl$; $R^3 = Cl$
21 aeruginosin GE766[35] $R^1 = SO_3H$; $R^2 = Cl$; $R^3 = Br$
22 aeruginosin GE686[35] $R^1 = H$; $R^2 = Cl$; $R^3 = Br$
23 aeruginosin GE810[35] $R^1 = SO_3H$; $R^2 = Br$; $R^3 = Br$
24 aeruginosin GE730[35] $R^1 = H$; $R^2 = Br$; $R^3 = Br$

25 aeruginosin DA495B[34]

26 aeruginosin DA688[34] $R^1 = SO_3H$; $R^2 = Cl$; $R^3 = H$
27 aeruginosin DA722[34] $R^1 = SO_3H$; $R^2 = Cl$; $R^3 = Cl$
28 aeruginosin GE642[35] $R^1 = H$; $R^2 = Cl$; $R^3 = Cl$
29 aeruginosin IN608[33] $R^1 = H$; $R^2 = Cl$; $R^3 = H$
30 aeruginosin IN652[33] $R^1 = H$; $R^2 = Br$; $R^3 = H$

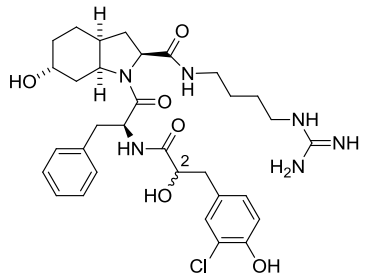

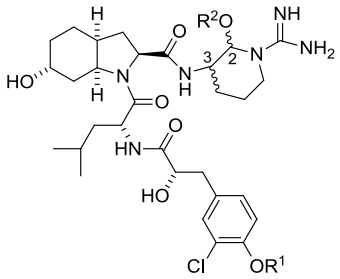

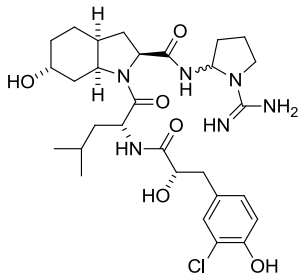

31 aeruginosin DA642A[34] (2*S*)
32 aeruginosin DA642B[34] (2*R*)

33 aeruginosin 89A (3*S*)[30] $R^1 = SO_3H$; $R^2 = H$
34 aeruginosin 89B (2*S*, 3*R*)[30] $R^1 = SO_3H$; $R^2 = H$
35 aeruginosin LH650A[36] (2*R*, 3*S*) $R^1 = H$; $R^2 = Me$
36 aeruginosin LH650B[36] (2*S*, 3*S*) $R^1 = H$; $R^2 = Me$

37 aeruginosin LH606[36]

Figure 6 Structures of aeruginosins bearing a halogenated Hpla residue.

2.3. Glycopeptidic Aeruginosins

A further class of aeruginosins is characterized by an additional carbohydrate substituent (Figure 7). In 1997, Murakami disclosed the first members of this aeruginosin group by isolating aeruginosins 205A (**38**) and 205B (**39**) from *Oscillatoria sp*.[37] Murakami *et al*. proposed a structure featuring a central 6-chloro-Choi unit (Ccoi) and a 3-hydroxyleucine residue onto which a xylopyranose (Xyl) moiety is added (top left, Figure 7). NMR data obtained from the total synthesis of the Ccoi unit by Bonjoch and co-workers revealed distinct deviations compared to those of isolated natural products **38** and **39**. Therefore, doubts concerning the structure of the Ccoi moiety arose.[38] Synthetic studies towards the synthesis of aeruginosin 205A (**38**) and 205B (**39**) performed by Hanessian *et al*. strongly support a structure featuring a chloroleucine (Cleu) residue and a xylosylated L-Choi motif with a sulfate group at the xylose O4 position.[39] In 2004, Quinn and co-workers reported on the isolation of dysinosin B, another aeruginosin containing a glycosyl residue attached to the L-Choi unit.[40] In contrast to the xylose moiety present in aeruginosins 205A (**38**) and 205B (**39**), Dysinosin B (**41**) consists of a glucose (Glu) residue. In 2007, the groups of Hemscheidt and Dittmann discovered further congeners of aeruginosin 205 with the isolation of aeruginoside 126A (**42**) and 126B (**40**) from *Planktothrix agardhii*.[41] Compound **40** had the same structural motifs as aeruginosins 205, but lacked the chlorine and sulfate groups. Aeruginoside 126A (**42**) differed from aeruginoside 126B (**40**) by the substituent on the C-terminus, which is an Adc residue in 126A (**42**) and an Agma moiety in 126B (**40**). In 2014, Blom *et al*. published the isolation of aeruginosin 828A (**43**) from *P*. *rubescens*.[42] Natural product **43** constitutes the chlorinated and sulfated congener of aeruginoside 126A (**42**). Further glycopeptidic aeruginosin species were described by Sivonen and co-workers who found four aeruginosins bearing pentose (Pen) substituents on the L-Choi moiety in the strain *N*. *spumigena* with NAL4 (**44**), NOL4 (**45**), NOL6 (**46**) and NOL7 (**47**).[31] Most recently, Hrouzek and his group reported the isolation of aeruginosin 865 (**48**) from *Nostoc sp*.[43] A865A (**48**) concurs with the group of glycosylated aeruginosins by featuring a mannuronic acid (ManA) moiety on the L-Choi motif. In conclusion, the addition of a carbohydrate unit displays a common structural variation in aeruginosins.

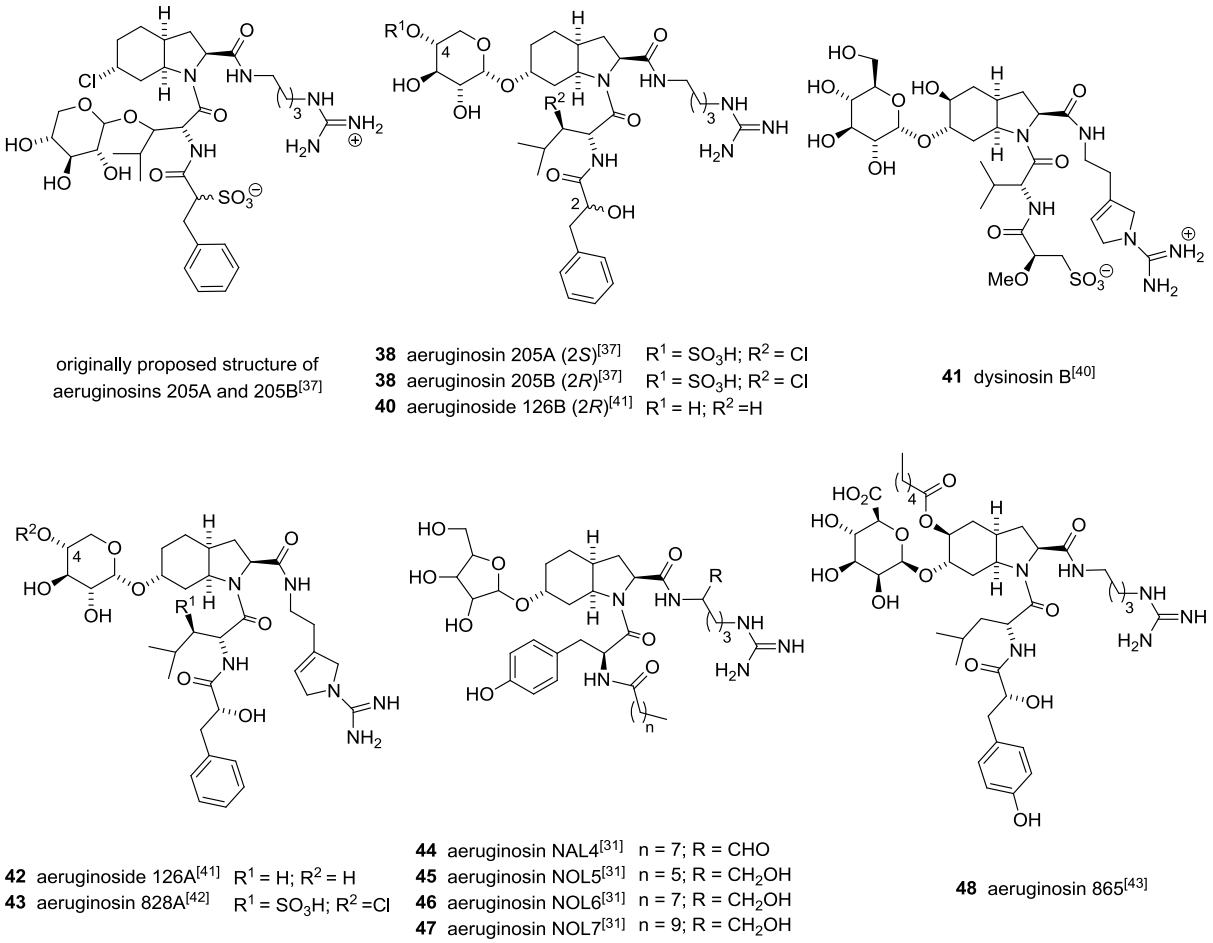

Figure 7 Structures of the known glycopeptidic aeruginosins.

2.4. Aeruginosins with an Altered Choi Unit

The aeruginosins presented in the previous sections were defined by a central 2-L-carboxy-6-hydroxyoctahydroindole (L-Choi) unit. However, variations of the Choi motif were also detected in a couple of isolated aeruginosins. The presence of a core unit divergent from the ordinary L-Choi is the characteristic feature of the aeruginosins described in this section (Figure 8). Dysinosins are one series of natural products matching this criterion. Dysinosins A (**49**), C (**51**) and D (**52**) are special in different respects: First, they were isolated from Australian sponges and not from cyanobacteria strains like other aeruginosins and second, they comprise an extra hydroxyl group at the Choi C5 position (5-OH-L-Choi). Additional to this unique 5-OH-L-Choi subunit, the dysinosins are characterized by a glyceric acid residue on the N-terminus which is sulfated in the case of dysinosins A (**49**) and C (**50**).[40,44] With chlorodysinosin A (**51**), a variant containing a Cleu residue could be isolated.[45] A further aeruginosin not constituting of the L-Choi core is aeruginosin EI461 (**53**). Carmeli *et al*. identified differences in the chemical shifts for the Choi unit of

EI461 (**53**) compared to the typical shifts attributed to the L-Choi. They concluded therefore that compound **53** must feature a different diastereoisomer of the Choi and proposed the presence of a D-*diepi*-Choi core in EI461 (**53**).[46] Later, the originally proposed structure of EI461 (**53**) was revised by Bonjoch and co-workers proving – through total synthesis – that aeruginosin EI461 (**53**) indeed consists of an L-*diepi*-Choi instead of the proposed D-*diepi*-Choi.[47] Nonetheless, the D-*diepi*-Choi motif was later identified in aeruginosins KT608A (**54**), KT608B (**55**) and KT650 (**56**).[48] Aeruginosin GH553 (**57**) possesses the same D-*diepi*-Choi core but with an additional acetyl group on the O atom at C5 position (*O*-Ac-D-*diepi*-Choi).[48] The last L-Choi variation is exhibited by aeruginosins DA495A (**58**), DA511 (**59**) and KB676 (**60**). These aeruginosins all contain an L-6-*epi*-Choi instead of the L-Choi unit in their structure.[34,49] Furthermore, KB676 (**60**) features a novel prenylated agmantin (pren-Agma) residue on the C-terminus.

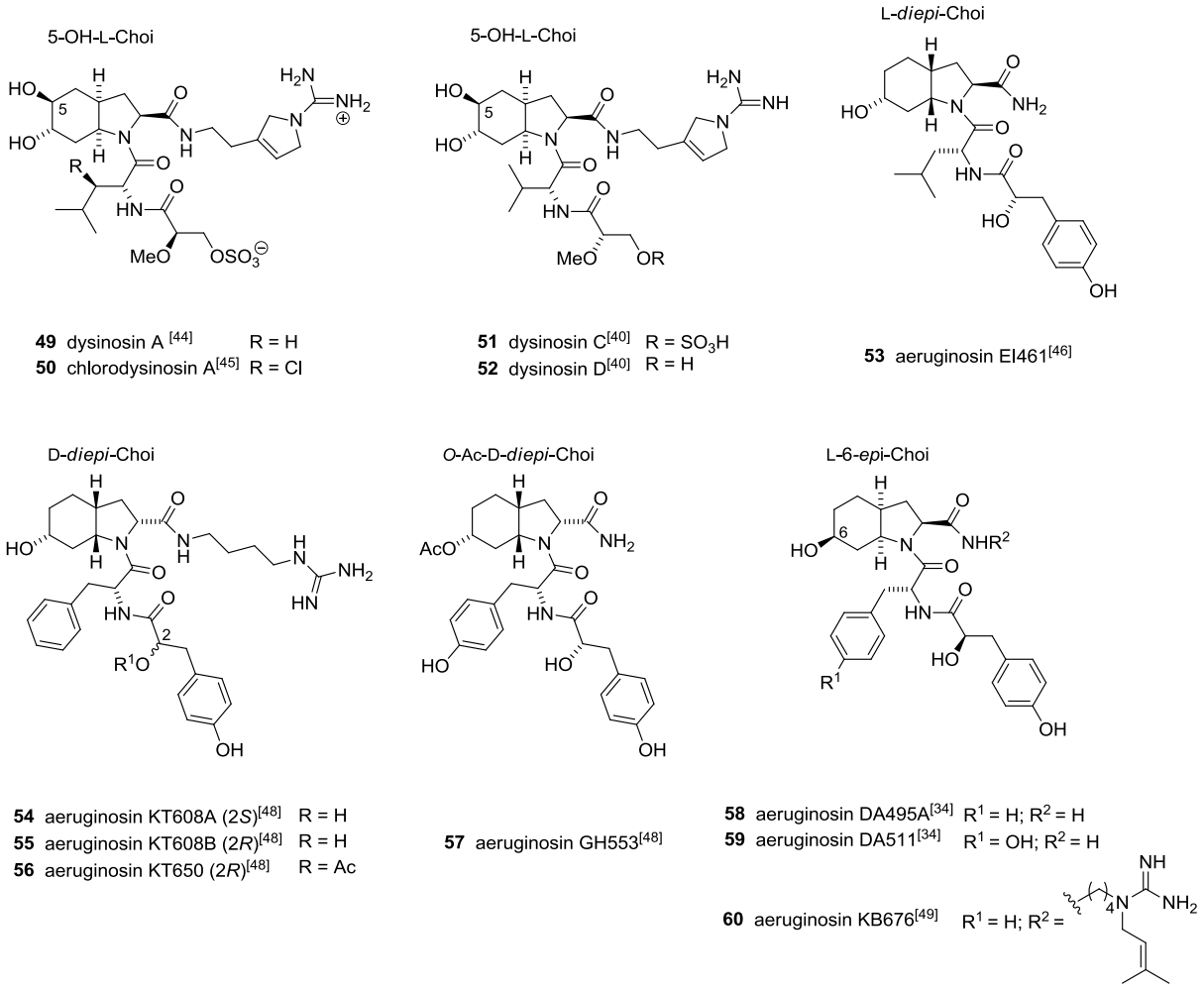

Figure 8 Known aeruginosins with a modified L-Choi unit.

2.5. General Structure and Biological Activity

In the past two decades, aeruginosins gained attention because of their potential as inhibitors of serine proteases like thrombin and trypsin.[50] Serine proteases are important enzymes that control a number of physiological processes, including blood coagulation, digestion and immune response processes.[51] Potential applications for serine protease inhibitors, such as aeruginosins, therefore lie in the treatment of thrombosis or the use as potential dietary supplements. Serine proteases like trypsin are optimized for the cleavage of peptide bonds which are in proximity to positively charged amino acids like lysine and arginine.[52] The inhibition of such proteases is therefore related to the arginine mimicking residues on the C-terminus (R3) of aeruginosins. These basic residues can be recognized by the enzymes, hence inducing their inhibition. The most potent inhibition for thrombin and trypsin has so far been reported for chlorodysinosin A (**50**) with IC_{50} values of 0.0038 μg mL^{-1} and 0.025 μg mL^{-1}, respectively.[53] Other aeruginosin members like oscillarin (**3**)[54] or aeruginosin 828A (**43**) have also revealed potent enzyme inhibition of thrombin and trypsin. Recent results by Blom *et al*. suggest that especially chlorinated and sulfated aeruginosins have to be considered not only as protease inhibitors but also as potent biotoxins.[42] The investigation of venomous aeruginosins forms the topic of the first chapter of this thesis and will be discussed in more detail below. For an overview on enzyme inhibition and biological activity of all known aeruginosins, see the Table on pages 14–15. IC_{50} values are not indicated in the table but can be obtained from the corresponding references. Further, the source of isolation as well as the structural features of each aeruginosin is reported. Concerning structural characterization, R^1 represents the residue on the N-terminus, R^2 the amino acid in the second position and R^3 the arginine mimicking moiety on the C-terminus (Figure 9).

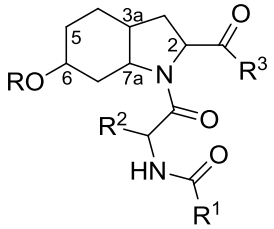

Figure 9 General structure of aeruginosins.

Aeruginosin	Isolation Source	R^1	R^2	Choi	R^3	Biological Activity
298A (**1**)[21]	*M. aeruginosa*	Hpla	Leu	L-Choi	Argol	TRP, THB, PLM, PAP, CHT
98B (**2**)[25]	*M. aeruginosa*	Hpla	*allo*-Ile	*O*-SO_3-L-Choi	Agma	TRP, THB, PLM, PAP, CHT
Oscillarin (**3**)[26]	*O. agardhii*	Pla	Phe	L-Choi	Adc	TRP, THB
102A (**4**)[27]	*M. viridis*	*O*-SO_3-Hpla	Tyr	L-Choi	Ahap (3*S*)	TRP, THB, PLM
102B (**5**) [27]	*M. viridis*	*O*-SO_3-Hpla	Tyr	L-Choi	Ahap (3*R*)	TRP, THB, PLM
103A (**6**) [28]	*M. viridis*	Hpla	Tyr	L-Choi	*O*-Et-Ahap	TRP, THB, PLM
Microcin SF608 (**7**)[29]	*M. aeruginosa*	Hpla	Phe	L-Choi	Agma	TRP, CHT
298B (**8**)[30]	*M. aeruginosa*	Hpla	Leu	L-Choi	NH_2	TRP, THB, PLM, PAP, CHT
NAL1 (**9**)[31]	*N. spumigena*	C_4H_9	Tyr	L-Choi	Argal	n.d.
NAL2 (**10**)[31]	*N. spumigena*	C_6H_{13}	Tyr	L-Choi	Argal	n.d.
NAL3 (**11**)[31]	*N. spumigena*	C_8H_{17}	Tyr	L-Choi	Argal	n.d.
NOL1 (**12**)[31]	*N. spumigena*	CH_3	Tyr	L-Choi	Argol	n.d.
NOL2 (**13**)[31]	*N. spumigena*	C_4H_9	Tyr	L-Choi	Argol	n.d.
NOL3 (**14**)[31]	*N. spumigena*	C_6H_{13}	Tyr	L-Choi	Argol	n.d.
NOL4 (**15**)[31]	*N. spumigena*	C_8H_{17}	Tyr	L-Choi	Argol	n.d.
98A (**16**)[25]	*M. aeruginosa*	*m*-Cl-Hpla	*allo*-Ile	*O*-SO_3-L-Choi	Agma	TRP, THB, PLM, PAP, CHT
98C (**17**)[30]	*M. aeruginosa*	*m*-Br-Hpla	*allo*-Ile	*O*-SO_3-L-Choi	Agma	TRP, THB, PLM, CHT
101 (**18**)[30]	*M. aeruginosa*	*m*-Cl_2-Hpla	*allo*-Ile	*O*-SO_3-L-Choi	Agma	TRP, THB, PLM, CHT
KY608 (**19**)[32]	*M. sp.*	*m*-Cl-Hpla	*allo*-Ile	L-Choi	Agma	TRP
KY642 (**20**)[32]	*M. sp.*	*m*-Cl_2-Hpla	*allo*-Ile	L-Choi	Agma	TRP
GE766 (**21**)[35]	*M. aeruginosa*	*m*-Cl/Br-Hpla	*allo*-Ile	*O*-SO_3-L-Choi	Agma	TRP, THB
GE686 (**22**)[35]	*M. aeruginosa*	*m*-Cl/Br-Hpla	*allo*-Ile	L-Choi	Agma	TRP, THB
GE810 (**23**)[35]	*M. aeruginosa*	*m*-Br_2-Hpla	*allo*-Ile	*O*-SO_3-L-Choi	Agma	TRP, THB
GE730 (**24**)[35]	*M. aeruginosa*	*m*-Br_2-Hpla	*allo*-Ile	L-Choi	Agma	TRP, THB
DA495B (**25**)[34]	*M. aeruginosa*	*m*-Cl-Hpla	*allo*-Ile	L-Choi	NH_2	TRP, THB
DA688 (**26**)[34]	*M. aeruginosa*	*m*-Cl-Hpla	Leu	*O*-SO_3-L-Choi	Agma	TRP, THB
DA722 (**27**)[34]	*M. aeruginosa*	*m*-Cl-Hpla	Leu	L-Choi	Agma	TRP, THB
GE642 (**28**)[35]	*M. aeruginosa*	*m*-Cl_2-Hpla	Leu	*O*-SO_3-L-Choi	Agma	TRP, THB
IN608 (**29**)[33]	*M. sp.*	*m*-Cl_2-Hpla	Leu	L-Choi	Agma	TRP
IN652 (**30**)[33]	*M. sp.*	*m*-Br-Hpla	Leu	L-Choi	Agma	TRP
DA642A (**31**)[34]	*M. aeruginosa*	*m*-Cl-Hpla (2*S*)	Phe	L-Choi	Agma	TRP, THB
DA642B (**32**)[34]	*M. aeruginosa*	*m*-Cl-Hpla (2*R*)	Phe	L-Choi	Agma	TRP, THB

89A (**33**)[30]	*M. aeruginosa*	*O*-SO_3-*m*-Cl-Hpla	Leu	L-Choi	Ahap (3S)	TRP, THB, PLM, PAP, CHT
89B (**34**)[30]	*M. aeruginosa*	*O*-SO_3-*m*-Cl-Hpla	Leu	L-Choi	Ahap (3*R*)	TRP, THB, PLM, PAP, CHT
LH650A (**35**)[36]	*M. spp.*	*m*-Cl-Hpla	Leu	L-Choi	Amap (2*R*)	TRP, THB
LH650B (**36**)[36]	*M. spp.*	*m*-Cl-Hpla	Leu	L-Choi	Amap (2*S*)	TRP, THB
LH606 (**37**)[36]	*M. spp.*	*m*-Cl-Hpla	Leu	L-Choi	Aap (2*S*)	TRP, THB
205A (**38**)[37]	*O. agardhii*	Pla	Cleu	*O*-Xyl-L-Choi	Agma	TRP, THB
205B (**39**)[37]	*O. agardhii*	Pla	Cleu	*O*-Xyl-L-Choi	Agma	TRP, THB
126B (**40**)[41]	*P. agardhii*	Pla	Leu	*O*-Xyl-L-Choi	Agma	n.d.
Dysinosin B (**41**)[40]	*L. chlorea*	*O*-SO_3-glyceric acid	Val	*O*-Glu-L-Choi	Adc	THB
126A (**42**)[41]	*P. agardhii*	Pla	Leu	*O*-Xyl-L-Choi	Adc	TRP, THB
828A (**43**)[42]	*P. rubescens*	Pla	Cleu	*O*-Xyl-L-Choi	Adc	TRP, THB, TOX
NAL4 (**44**)[31]	*N. spumigena*	C_8H_{17}	Tyr	*O*-Pen-L-Choi	Argal	n.d.
NOL5 (**45**)[31]	*N. spumigena*	C_6H_{13}	Tyr	*O*-Pen-L-Choi	Argol	n.d.
NOL6 (**46**)[31]	*N. spumigena*	C_8H_{17}	Tyr	*O*-Pen-L-Choi	Argol	n.d.
NOL7 (**47**)[31]	*N. spumigena*	$C_{10}H_{21}$	Tyr	*O*-Pen-L-Choi	Argol	n.d.
865 (**48**)[43]	*Nostoc sp.*	Hpla	Leu	*O*-ManA-L-Choi	Agma	anti-inflammatory
Dysinosin A (**49**)[44]	*Dysideidae**	*O*-SO_3-glyceric acid	Leu	5-OH-L-Choi	Adc	THB
Chlorodysin. A (**50**)[45]	*Dysideidae**	*O*-SO_3-glyceric acid	Cleu	5-OH-L-Choi	Adc	THB
Dysinosin C (**51**)[40]	*L chlorea**	*O*-SO_3-glyceric acid	Val	5-OH-L-Choi	Adc	THB
Dysinosin D (**52**)[40]	*L. chlorea**	glyceric acid	Val	5-OH-L-Choi	Adc	THB
EI461 (**53**)[46]	*M. aeruginosa*	Hpla	Leu	L-*diepi*-Choi	NH_2	TRP
KT608A (**54**)[48]	*M. aeruginosa*	Hpla (2*S*)	Phe	D-*diepi*-Choi	Agma	TRP
KT608B (**55**)[48]	*M. aeruginosa*	Hpla (2*R*)	Phe	D-*diepi*-Choi	Agma	TRP
KT650 (**56**)[48]	*M. aeruginosa*	2-OAc-Hpla (2*R*)	Phe	D-*diepi*-Choi	Agma	TRP
GH553 (**57**)[48]	*M. aeruginosa*	Hpla	Tyr	*O*-Ac-D-*diepi*-Choi	NH_2	TRP
DA495A (**58**)[34]	*M. aeruginosa*	Hpla	Phe	L-6-*epi*-Choi	NH_2	TRP, THB
DA511 (**59**)[34]	*M. aeruginosa*	Hpla	Tyr	L-6-*epi*-Choi	NH_2	TRP, THB
KB676 (**60**)[49]	*M. spp.*	Hpla	Phe	L-6-*epi*-Choi	pren-Agma	TRP

CHT = Chymotrypsin; PAP = Papain; PLM = Plasmin; TOX = toxic against *T. Platyurus*; TRP = Trypsin; THB = Thrombin. Aeruginosins not isolated from cyanobacteria are indicated by an asterisk (*).

2.6. Biosynthesis of the L-Choi Moiety

Scheme 1 shows the proposed biosynthesis of the L-Choi core occurring in cyanobacteria. Arogenate (**65**) is assumed to be the key intermediate in the L-Choi (**69**) biosynthesis.[41] The biosyntheses of amino acids phenylalanine and tyrosine are also supposed to involve arogenate intermediate **65**.[55] Arogenate (**65**) is synthesized *via* the known shikimate pathway starting from phosphoenolpyruvate (**61**) and erythrose 4-phosphate (**62**). Coupling of compound **61** with **62** followed by several enzymatic steps gives rise to chorismate (**63**). A Claisen rearrangement of chorismate (**63**) forms prephenate (**64**), followed by amination of **64** by an aminotransferase to afford arogenate (**65**).[56] The further biosynthesis of the L-Choi (**69**) is carried out by the aeruginosin specific enzymes AerC-AerF:[41] Oxidation of arogenate (**65**) by the enzyme AerC leads to ketone **66**. Subsequent intramolecular aza-Michael addition of the amine on the α,β-unsaturated ketone is induced by AerE to achieve ring closure yielding bicyclic compound **67**. Decarboxylation of **67** by enzyme AerD leads to the formation of intermediate **68** which is reduced by AerF to the L-Choi core structure **69** in the last step (Scheme 1).[41]

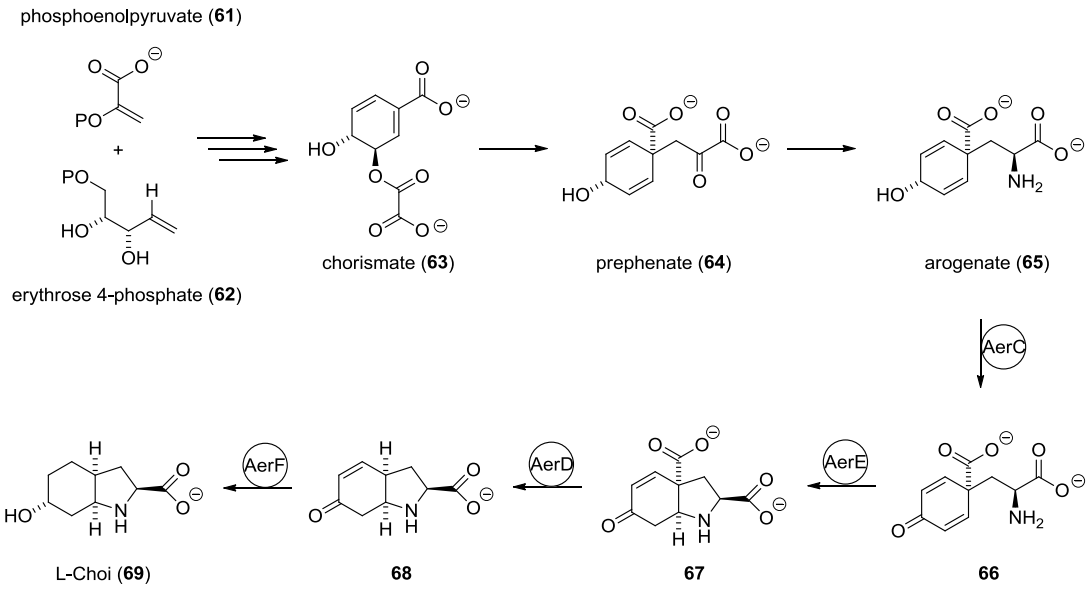

Scheme 1 Biosynthetic pathway of the L-Choi core structure **69** present in aeruginosins.

3. References

[1] W. Altermann, J. Kazmierczak, *Res*. *Microbiol*. **2003**, *154*, 611–617.

[2] J. J. Brocks, G. A. Logan, R. Buick, R. E. Summons, *Science* **1999**, *285d*, 1033–1036.

[3] D. E. Canfield, *Annu*. *Rev*. *Earth Planet*. *Sci*. **2005**, *33*, 1–36.

[4] S. N. Tripathi, I. K. Chung, J. A. Lee, *J*. *Plant Biol*. **2007**, *50*, 50–59.

[5] A. D. Jungblut, C. Lovejoy, W. F. Vincent, *ISME J*. **2010**, *4*, 191–202.

[6] D. M. Ward, M. J. Ferris, S. C. Nold, M. M. Bateson, *Microbiol*. *Mol*. *Biol*. *Rev*. **1998**, *62*, 1353–1370.

[7] I. Dor, A. Danin, *J*. *Arid Environ*. **1998**, *38*, 161–174.

[8] L. M. Gerasimenko, V. K. Orleanskii, G. A. Karpov, G. T. Ushatinskaya, *Microbiology* **2013**, *82*, 111–118.

[9] Picture recorded in July 2011 at Yellowstone National Park. Used with permission of Natalie Huber and Ina Bodoky.

[10] R. B. Dixit, M. R. Suseela, *Antonie van Leeuwenhoek, Int*. *J*. *Gen*. *Mol*. *Microbiol*. **2013**, *103*, 947–961.

[11] I. Chorus, J. Bartram, *Toxic Cyanobacteria in Water: A Guide to Their Public Health Consequences, Monitoring and Management*, London, **1999**.

[12] H. W. Paerl, J. Huisman, *Science* **2008**, *320*, 57–58.

[13] P. M. Visser, J. M. H. Verspagen, G. Sandrini, L. J. Stal, H. C. P. Matthijs, T. W. Davis, H. W. Paerl, J. Huisman, *Harmful Algae* **2016**, *54*, 145–159.

[14] T. T. Wynne, R. P. Stumpf, *Toxins* **2015**, *7*, 1649–1663.

[15] A. M. Michalak, E. J. Anderson, D. Beletsky, S. Boland, N. S. Bosch, T. B. Bridgeman, J. D. Chaffin, K. Cho, R. Confesor, I. Daloglu, J. V. DePinto, M. A. Evans, G. L. Fahnenstiel, L. He, J. C. Ho, L. Jenkins, T. H. Johengen, K. C. Kuo, E. LaPorte, X. Liu, M. R. McWilliams, M. R. Moore, D. J. Posselt, R. P. Richards, D. Scavia, A. L. Steiner, E. Verhamme, D. M. Wright, M. A. Zagorski, *Proc*. *Natl*. *Acad*. *Sci*. *U*. *S*. *A*. **2013**, *110*, 6448–6452.

[16] M. Kahru, R. Elmgren, *Biogeosciences* **2014**, *11*, 3619–3633.

[17] T. Posch, O. Köster, M. M. Salcher, J. Pernthaler, *Nat*. *Clim*. *Chang*. **2012**, *2*, 809–813.

[18] S. M. F. O. Azevedo, W. W. Carmichael, E. M. Jochimsen, K. L. Rinehart, S. Lau, G. R. Shaw, G. K. Eaglesham, *Toxicology* **2002**, *181-182*, 441–446.

[19] I. Stewart, P. M. Webb, P. J. Schlutter, G. R. Shaw, *Environ*. *Heal*. **2006**, *5*, 1–13.

[20] Picture in the public domain: http://www.noaanews.noaa.gov/stories2014/images/MERIS_2011Oct08_truecolor_cropped.jpg, 30.08.2016.

[21] M. Murakami, Y. Okita, H. Matsuda, T. Okino, K. Yamaguchi, *Tetrahedron Lett*. **1994**, *35*, 3129–3132.

[22] J. L. Rios Steiner, M. Murakami, A. Tulinsky, *J*. *Am*. *Chem*. *Soc*. **1998**, *120*, 597–598.

[23] N. Valls, M. Lopez-Canet, M. Vallribera, J. Bonjoch, *J*. *Am*. *Chem*. *Soc*. **2000**, *122*, 11248–11249.

[24] P. Wipf, J. L. Methot, *Org*. *Lett*. **2000**, *2*, 4213–4216.

[25] M. Murakami, K. Ishida, T. Okino, Y. Okita, H. Matsuda, K. Yamaguchi, *Tetrahedron Lett*. **1995**, *36*, 2785–2788.

[26] S. Konetschny-Rapp, H.-W. Krell, U. Martin, PCT WO96/11941, 1996 [Chem. Abst. 1996, 124, 315175].

[27] H. Matsuda, T. Okino, M. Murakami, K. Yamaguchi, *Tetrahedron* **1996**, *52*, 14501–14506.

[28] S. Kodani, K. Ishida, M. Murakami, *J*. *Nat*. *Prod*. **1998**, *61*, 1046–1048.

[29] R. Banker, S. Carmeli, *Tetrahedron* **1999**, *55*, 10835–10844.

[30] K. Ishida, Y. Okita, H. Matsuda, T. Okino, M. Murakami, *Tetrahedron* **1999**, *55*, 10971–10988.

[31] D. P. Fewer, J. Jokela, E. Paukku, J. Österholm, M. Wahlsten, P. Permi, O. Aitio, L. Rouhiainen, G. V. Gomez-Saez, K. Sivonen, *PLoS One* **2013**, *8*, 1–10.

[32] A. Raveh, S. Carmeli, *Phytochem*. *Lett*. **2009**, *2*, 10–14.

[33] S. Elkobi-Peer, R. K. Singh, T. M. Mohapatra, S. P. Tiwari, S. Carmeli, *J*. *Nat*. *Prod*. **2013**, *76*, 1187–1190.

[34] S. Adiv, S. Carmeli, *J*. *Nat*. *Prod*. **2013**, *76*, 2307–2315.

[35] S. Elkobi-Peer, R. Faigenbaum, S. Carmeli, *J*. *Nat*. *Prod*. **2012**, *75*, 2144–2151.

[36] M. Vegman, S. Carmeli, *Tetrahedron* **2014**, *70*, 6817–6824.

[37] H. J. Shin, H. Matsuda, M. Murakami, K. Yamaguchi, *J. Org. Chem.* **1997**, *62*, 1810–1813.

[38] N. Valls, M. Vallribera, M. Font-Bardía, X. Solans, J. Bonjoch, *Tetrahedron Asymmetry* **2003**, *14*, 1241–1244.

[39] S. Hanessian, X. Wang, K. Ersmark, J. R. Del Valle, E. Klegraf, *Org. Lett.* **2009**, *11*, 4232–4235.

[40] A. R. Carroll, M. S. Buchanan, A. Edser, E. Hyde, M. Simpson, R. J. Quinn, *J. Nat. Prod.* **2004**, *67*, 1291–1294.

[41] K. Ishida, G. Christiansen, W. Y. Yoshida, R. Kurmayer, M. Welker, N. Valls, J. Bonjoch, C. Hertweck, T. Börner, T. Hemscheidt, E. Dittmann, *Chem. Biol.* **2007**, *14*, 565–576.

[42] E. Kohler, V. Grundler, D. Häussinger, R. Kurmayer, K. Gademann, J. Pernthaler, J. F. Blom, *Harmful Algae* **2014**, *39*, 154–160.

[43] A. Kapuścik, P. Hrouzek, M. Kuzma, S. Bártová, P. Novák, J. Jokela, M. Pflüger, A. Eger, H. Hundsberger, J. Kopecký, *ChemBioChem* **2013**, *14*, 2329–2337.

[44] A. R. Carroll, G. K. Pierens, G. Fechner, P. de Almeida Leone, A. Ngo, M. Simpson, E. Hyde, J. N. A. Hooper, S. L. Boström, D. Musil, R. J. Quinn, *J. Am. Chem. Soc.* **2002**, *124*, 13340–13341.

[45] G. H. Goetz, G. G. Harrigan, J. J. Likos, T. P. Kasten, PCTWO03/051831, 2003 [Chem. Abst. 2003, 139, 47155].

[46] A. Ploutno, M. Shoshan, S. Carmeli, *J. Nat. Prod.* **2002**, *65*, 973–978.

[47] N. Valls, M. Vallribera, S. Carmeli, J. Bonjoch, *Org. Lett.* **2003**, *5*, 447–450.

[48] M. Lifshits, S. Carmeli, *J. Nat. Prod.* **2012**, *75*, 209–219.

[49] S. Elkobi-Peer, S. Carmeli, *Mar. Drugs* **2015**, *13*, 2347–2375.

[50] K. Ersmark, J. R. Del Valle, S. Hanessian, *Angew. Chem. Int. Ed.* **2008**, *47*, 1202–1223.

[51] L. Hedstrom, *Chem. Rev.* **2002**, *102*, 4501–4524.

[52] L. B. Evnin, J. R. Vasquez, C. S. Craik, *Proc. Natl. Acad. Sci.* **1990**, *87*, 6659–6663.

[53] S. Hanessian, J. R. Del Valle, Y. F. Xue, N. Blomberg, *J. Am. Chem. Soc.* **2006**, *128*, 10491–10495.

[54] S. Hanessian, M. Tremblay, J. F. W. Petersen, *J*. *Am*. *Chem*. *Soc*. **2004**, *126*, 6064–6071.

[55] G. C. Hall, M. B. Flick, R. L. Gherna, R. A. Jensen, *J*. *Bacteriol*. **1982**, *149*, 65–78.

[56] A. R. Knaggs, *Nat*. *Prod*. *Rep*. **1999**, *16*, 525–560.

CHAPTER I: TOXICITY AND SYNTHESIS OF AERUGINOSIN CHLOROSULFOPEPTIDES

1. Introduction

In this chapter, the results of a research project founded on the observation that particular cyanobacteria strains had stopped the production of toxic microcystins at a certain evolutionary point are reported. Driven by curiosity we addressed this biological singularity by using chemical total synthesis combined with biological testing.

1.1. Isolation and Bioactivity of Aeruginosin 828A

Aeruginosin 828A (A828A) (**2.1**) was isolated in collaboration with the group of PD Dr. Judith Blom from the limnological station of the University of Zurich. The toxicity of six cyanobacterial *Planktothrix* strains collected from lakes in Switzerland was evaluated by Dr. Esther Kohler using HPLC-guided fractionation. All fractions were subjected to acute toxicity screenings against the crustacean *Thamnocephalus platyurus*, in order to detect fractions containing toxic compounds. Besides the detection of already known cyanotoxins like microcystins (MC), the presence of ten chlorosulfopeptides was observed. Interestingly, the chlorosulfopeptides were found only in four microcystin deficient cyanobacteria strains such as *Planktothrix rubescens* (Figure 10). Therefore, the venomousness of these cyanobacteria strains could not be derived from microcystins.

Figure 10 Epifluorescence micrograph of *Planktothrix rubescens* (left); *Planktothrix rubescens* bloom in Lake Hallwil, Switzerland (right).[1]

More detailed investigations on these microcystin deficient strains showed that the toxicity assigned to these strains is attributed to aeruginosin 828A (**2.1**), a thus far unknown member of the aeruginosin family. For structural elucidation a purified sample of isolated A828A (**2.1**) was sent to Dr. Verena Grundler from the research group of Prof. Karl Gademann, who could assign the structure of aeruginosin 828A (**2.1**) to be as shown in Figure 11.[2]

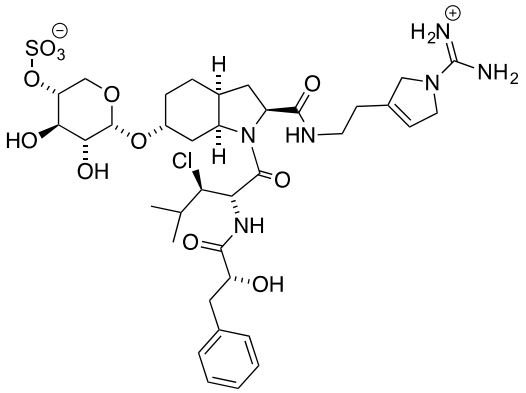

aeruginosin 828A (**2.1**)

Figure 11 Structure of the cyanotoxin aeruginosin 828A (**2.1**) isolated form *P. rubescens*

1.1.1. Bioactivity of aeruginosin A828A

With the pure, isolated A828A (**2.1**) several biological assays were performed. The toxicity towards the freshwater crustacean *Thamnocephalus platyurus* revealed an LC_{50} value of 22.8 μM, which is comparable to already known toxic microcystins.[3] This points out the high venomousness potential of A828A (**2.1**). Furthermore, the enzyme inhibition property of **2.1** on the serine proteases trypsin and thrombin was found to be in the nanomolar range for both trypsin (IC_{50} = 112 nm) and thrombin (IC_{50} = 21.8 nm).[2] Recently, Fent and co-workers also reported anti-inflammatory activity of A828A (**2.1**) in human hepatoma cell lines.[4]

1.1.2. Microcystin deficient cyanobacteria

As mentioned before, A828A (**2.1**) was isolated form a *Planktothrix* strain lacking microcystin (MC) production. Analysis of the genome of microcystin deficient *Planktothrix* strains revealed that mutations in the microcystin synthase (mcy) gene cluster might be responsible for the loss of microcystin production during evolution. Strains lacking MC production showed either insertions in the mcyA or mcyD genes or a deletion in the mcyHA gene (Figure 12).[5,6] These mutations are responsible for the inactivation of the mcy gene cluster, thus, the MC production is shut down. It is estimated that the loss of MC production of certain *Planktothrix* strains occurred millions of years ago.[7] However, the exact site of these mutations in the phylogenetic lineage could not be determined. Interestingly, a loss of the capability to produce MCs does not seem to have a disadvantageous effect on the total population of cyanobacteria. This has been shown by Ostermaier and Kurmayer *via* comparison of the total population of MC producing and MC deficient *Planktothrix* strains over a period of two years.[5] Consequently, a valid hypothesis is that the evolutionary disadvantage caused by the loss of MC production is counterbalanced by the production of other secondary metabolites, such as A828A (**2.1**), which are able to restore the toxic phenotype of the cyanobacterium.

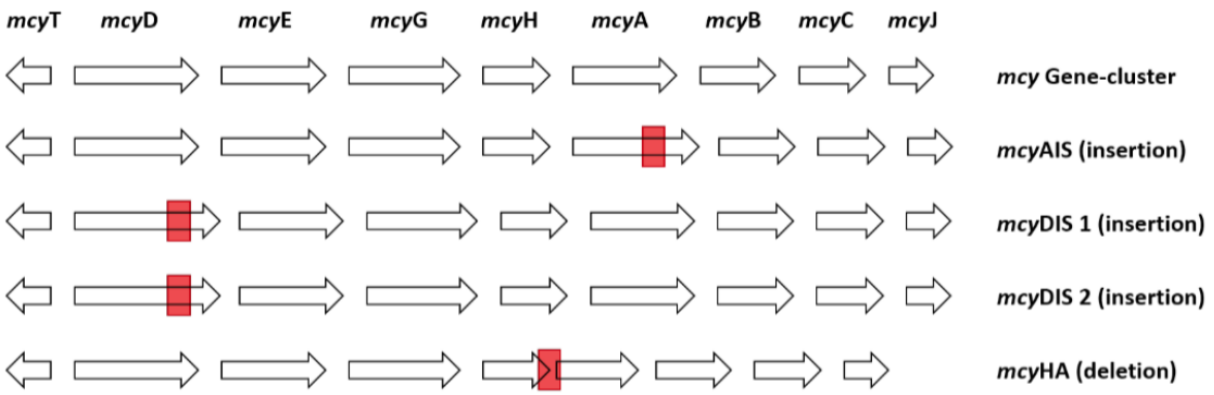

Figure 12 Microcystin synthase (mcy) gene cluster of *Planktothrix* (topmost). Mutations responsible for the inactivation of the mcy gene cluster: insertion in the mcyA gene (2nd from top), insertion in the mcyD gene (3rd and 4th from top) and deletion in the mcyHA gene (bottom).[8]

1.2. Chlorinated Natural Products – Bioactivity and Biosynthesis

Halogenated secondary metabolites are widely spread in nature and have been found in over 4000 natural products. Among these, compounds containing a carbon-chlorine bond are most abundant with over 2300 isolated examples.[9] The reason why nature incorporates halogen and especially chlorine atoms into secondary metabolites is due to the versatile role these substituents can have on the function of a molecule. With the simple exchange of a hydrogen to a chloride atom, the whole bioactivity of a compound can be altered.[10] The remarkable influence of chlorinations on the bioactivity of natural products is illustrated by the following examples vancomycin, salinosporamide A, neomangicol A and rebeccamycin (Figure 13). Vancomycin was isolated from the bacterium *Amycolatopsis orientalis* in 1953 and is used as antibiotic for the treatment of multi-drug resistant bacterial infections. Harris and co-workers have shown that the two chlorine substituents in vancomycin are essential for its clinically active conformation, due to the controlling effect on the atropisomeric distribution expressed by the chlorine atoms.[11] Salinasporamide A was isolated from the bacteria *Salinaspora tropica* and is currently in clinical trials for multiple myeloma treatment. The mechanism of action of salinasporamide A rests on the potent inhibition of the proteasome 20S. The densely functionalized β-lactone of salinasporamide A serves as electrophile, which is attacked by the hydroxyl group of the Thr21 unit of proteasome 20S. The obtained hydroxyl group from the former lactone can then attack the chlorinated carbon atom in an intramolecular fashion to form a tetrahydrofuran ring. With this, the reforming of the β-lactone accompanied by the release of the inhibitor from the enzyme is prevented, thus leading to an irreversible, covalent inhibition of proteasome 20S.[12] A further example is the sesterterpene neomangicol A: Renner and co-workers demonstrated that only neomangicol A shows cytotoxic effects *in vitro* against HCT-116 human colon tumor cell lines whereas the dechloro congener is inactive.[13] A similar behavior was observed for rebeccamycin. While rebeccamycin showed antimicrobial activity, its derivative lacking the chlorine substituent displayed no such activity.[14] All these examples demonstrate the tremendous influence chlorine atoms can have on the bioactivity of a specific compound.

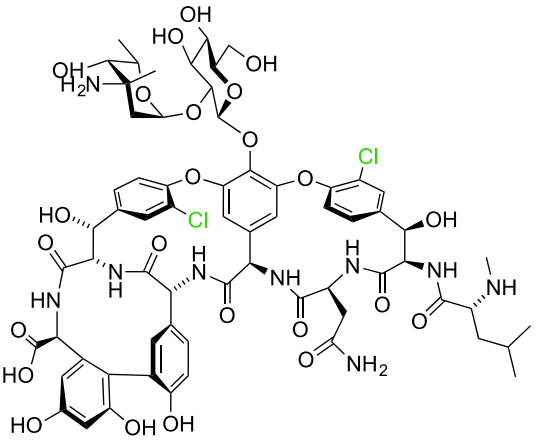

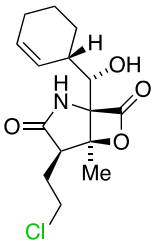

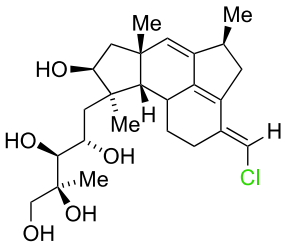

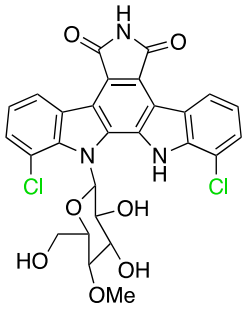

Figure 13 Selected chlorinated natural products with biological activities: vancomycin, salinosporamide A, neomangicol A and rebeccamycin.

1.2.1. Chlorine effect in aeruginosins

Studies on a chlorine dependent bioactivity for natural products of the aeruginosin family was described by Hanessian and co-workers. They observed a remarkably enhanced *in vitro* enzyme inhibitory activity against thrombin Factor IIA and Factor VIIA of one order of magnitude going from non-chlorinated dysinosin A (IC_{50} = 46.0 nM and 0.326 μM) to chlorodysinosin A (IC_{50} = 5.70 nM and 0.039 μM) (Figure 14).[15] The results of this observable 'chlorine effect' were further supported by the synthesis of unnatural chlorinated and non-chlorinated aeruginosin hybrids, which showed the same effect for enzyme inhibition as described for dysinosin A and chlorodysinosin A.[15]

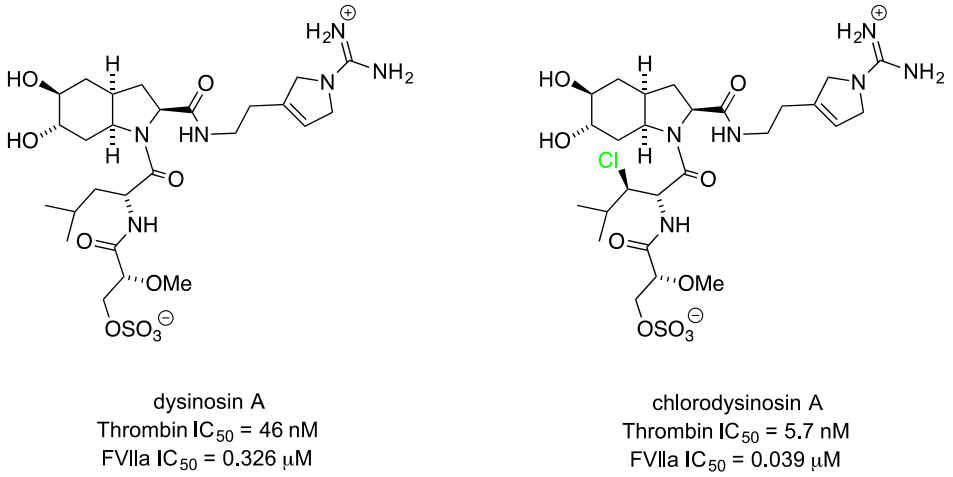

Figure 14 Enzyme inhibitory activity against thrombin Factor IIA and Factor VIIA of dysinosin A and chlorodysinosin A.

1.2.2. Chlorination of unreactive carbon centers in natural products biosynthesis

Nature provides a variety of different chlorination pathways.[10] Most common is the incorporation of the chlorine atom as a hypochlorite (Cl^+) using heme-iron (Fe-CPO)[16,17] or vanadium (V-CPO)[18,19] dependent chloroperoxidases or flavin dependent chlorogenases.[20] The discovery of CPOs goes back to the work of Hager and co-workers in the 1960s and they have since been intensively studied.[16] While heme-iron CPOs find a broad application in nature's biosynthesis, V-CPOs are especially common in the biosynthesis of halogenated marine natural products.[19] Furthermore, the enzymatic incorporation of chlorine atoms as a chloride (Cl^-) using S-adenosylmethionine (SAM) has been reported recently.[21] However, for unreactive carbon centers like the C3 position of chloroleucine (Cleu), these chlorination methods are unlikely to occur, due to the poor reactivity of this center against electrophilic Cl^+ from the CPOs and nucleophilic Cl^- from the enzymatic pathway.

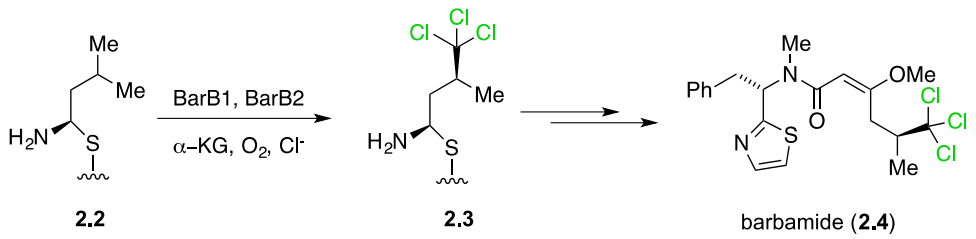

Figure 15 Chlorination of the leucine residue in the barbamide biosynthesis, investigated by Hartung and co-workers.[22]

Therefore, it was presumed that yet another chlorination pathway might exist which indeed was discovered in the late 1990s by the groups of Hartung[22] and Sitachitta[23] during the investigation of the biosynthesis of the natural product barbamide (**2.4**) (Figure 15). In 2006, Walsh *et al*. were then able to fully characterize the catalytic, radical mechanism for the chlorination of the methyl group of the leucine residue in barbamide (**2.4**).[24] The chlorination pathway comprises the enzymes BarB1 and BarB2 which contain a ferrous ion chelated by the co-factor α-ketoglutarate (α-KG) in the active pocket. Oxidation accompanied by decarboxylation of the ketoglutarate **2.6** leads to the Fe^{IV} species **2.8**. Ligand exchange of the obtained succinic acid by chloride yields chlorine-iron complex **2.9**. Single electron transfer from the substrate to complex **2.9** leads to the reduction of the Fe^{IV} center to Fe^{III} and to the formation of an alkyl radical. Homolytic cleavage of the Cl-Fe bond reduces the Fe^{III} core to Fe^{II} and allows formation of the C-Cl bond by radical recombination. Chelation of the co-factor α-KG closes the catalytic cycle (Scheme 2).[24]

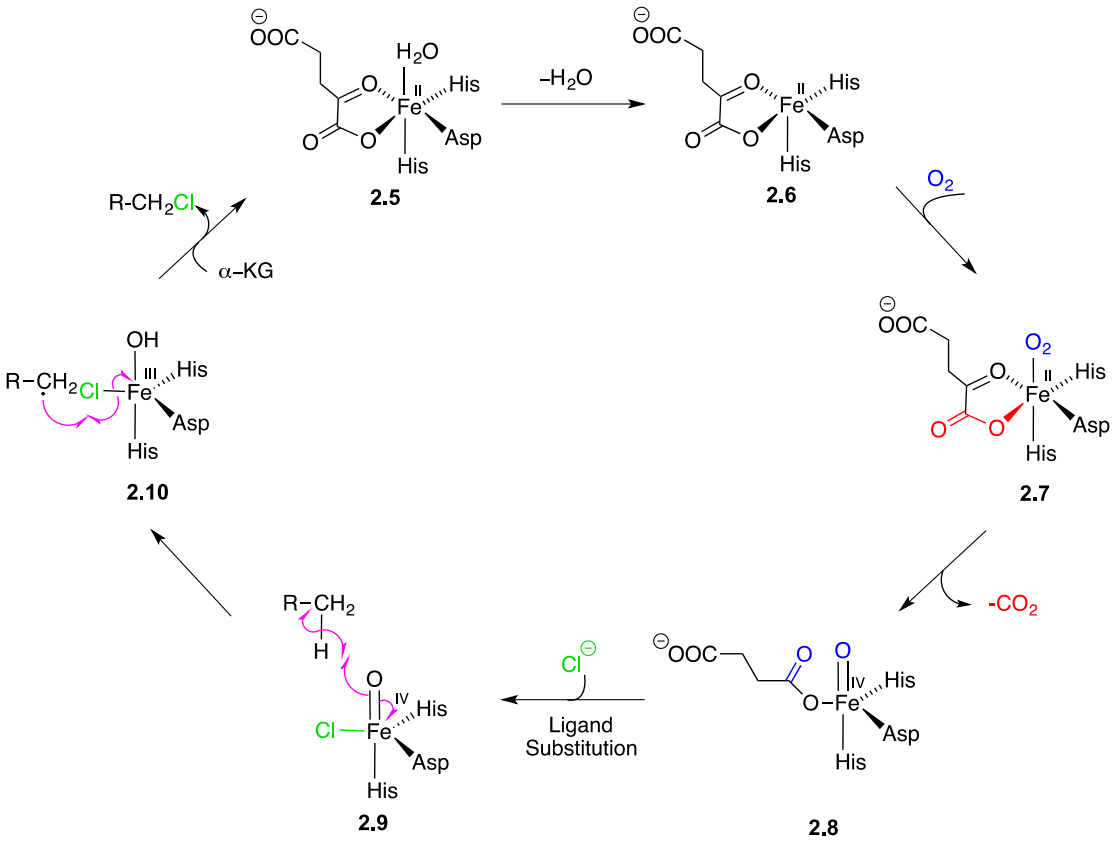

Scheme 2 Radical chlorination mechanism for the chlorination of unreactive carbon centers, proposed by Walsh and co-workers.[24]

2. Aim of the Project

This project builds on the results obtained by Dr. Esther Kohler, who reported on the toxicity of aeruginosin 828A (**2.1**).[2] Our goal was to investigate an efficient fully synthetic route to A828A (**2.1**), which allows for the confirmation of the elucidated structure by Dr. Verena Grundler on the one hand and the toxicity against the freshwater crustacean *Thamnocephalus platyurus* on the other hand. With pure synthetic A828A (**2.1**) in hand, contamination derived toxicity, which is possible in isolated compounds, can be excluded. After the elaboration of a synthetic strategy towards A828A (**2.1**) it was envisioned to synthesize and characterize other chlorosulfopeptides with all possible permutations with regard to the sulfate and chloride groups present, namely A126A (**2.11**), A748A (**2.12**) and A794A (**2.13**) (Figure 16). Biological testing of these congeners shall clarify the effect of sulfate and chlorine groups on the toxicity. Interestingly, congener A126A (**2.11**) is also a naturally occurring aeruginosin, isolated from a cyanobacterium capable of producing MCs,[25,26] making it especially interesting for the comparison with A828A (**2.1**).

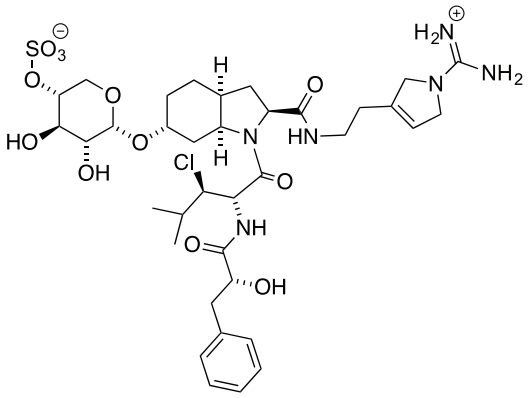

aeruginosin 828A (**2.1**)

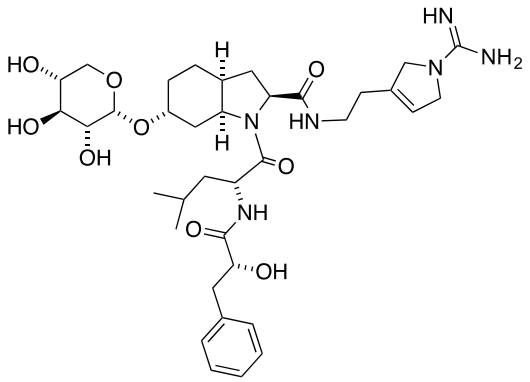

aeruginoside 126A (**2.11**)

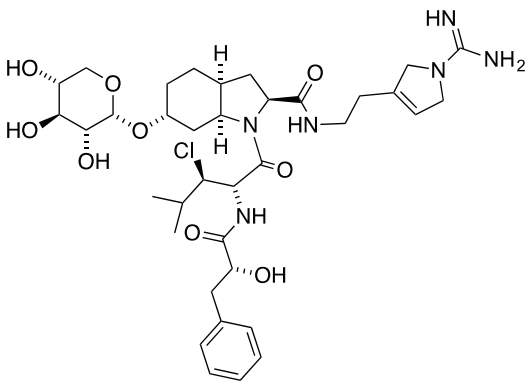

aeruginosin 748A (**2.12**)

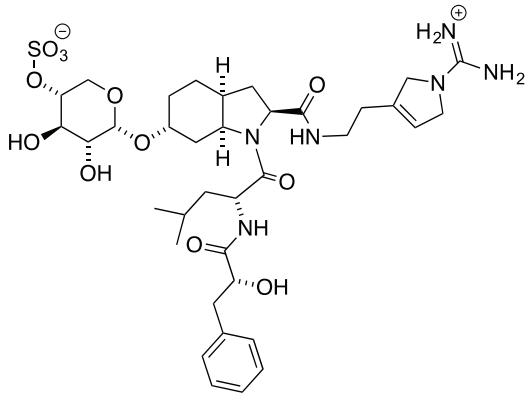

aeruginosin 794A (**2.13**)

Figure 16 Naturally occurring aeruginosin 828A (**2.1**) and aeruginoside 126A (**2.11**) as well as derivatives aeruginosin 748A (**2.12**) and aeruginosin 794A (**2.13**)

3. Retrosynthetic Considerations and Synthetic Strategies

3.1. Retrosynthetic Analysis of A828A

Aeruginosin 828A (**2.1**) is built up of five different subunits, linked together through three peptide bonds and one glycosyl linkage (Figure 17). The core unit consists of an L-2-carboxy-6-octahydroindole (L-Choi) residue which is attached to an 1-(N-amidino-Δ^3-pyrrolino)ethyl (Adc) side chain on the C-terminus and to a chloroleucine (Cleu) amino acid on the N-terminus. Further, the oxygen at C6 position of the L-Choi is linked to a sulfated xylose (Xyl) residue. Finally, the structure of A828A is accomplished by a phenyllactic acid (Pla) unit at the N-terminus of the Cleu unit. For the synthesis of congeners A748A (**2.12**), A794A (**2.13**) and A126A (**2.11**) the same disconnections as for A828A (**2.1**) can be considered, leading to five similar fragments as described above: For A748A (**2.12**), the Xyl residue would be exchanged by a Xyl unit bearing no sulfate group at the oxygen at C4 position; for A794A (**2.13**), the Cleu residue is replaced by a leucine (Leu) unit and for A126A (**2.11**), a Leu moiety and a non-sulfated Xyl residue would be required. Retrosynthetic considerations for the different building blocks will be discussed in the subsequent section.

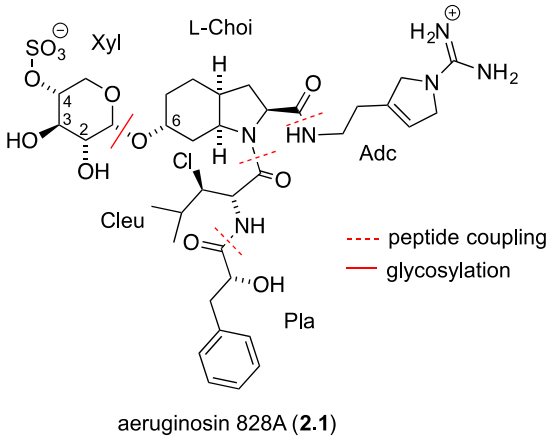

aeruginosin 828A (**2.1**)

Figure 17 A828A (**2.1**) consists of five different subunits (Xyl, L-Choi, Adc, Cleu and Pla), linked together *via* three peptide bonds and one glycosyl linkage.

3.2. Retrosynthetic Analysis of the Building Blocks

The synthetic strategies for the Adc side chain (**2.14**) and the Cleu moiety (**2.15**) have already been reported in the syntheses of dysinosin A and chlorodysinosin A,[27,28] respectively, and could be adopted for the synthesis of A828A (**2.1**). The Adc side chain is prepared starting from α-methylene-γ-butyrolactone (**2.16**) and the Cleu residue starting from isobutyraldehyde (**2.17**). D-phenyllactic building block **2.18** can be derived from D-phenyllactic acid which is accessible from D-phenylalanine (**2.19**) according to known literature procedures.[29,30] Protection of the hydroxyl group of D-phenyllactic acid provides a suitable Pla building block. For the L-Choi center structure **2.20** various syntheses have been reported by different research groups. Hanessian and co-workers reported a straightforward synthesis for L-Choi starting from L-glutamic acid (**2.21**).[31] Finally, the Xyl residue **2.22** can be obtained from D-xylose (**2.23**) using orthogonal protection strategies for the hydroxyl group at C4 position (PG) with regard to the hydroxyl groups at positions C2 and C3 (PG^1) to allow for a late stage introduction of the sulfate group at O4 position. Further, installation of an appropriate leaving group (LG) at the anomeric center of the Xyl residue is envisioned (Scheme 3). The preparation of the different building blocks will be described in Section 4.

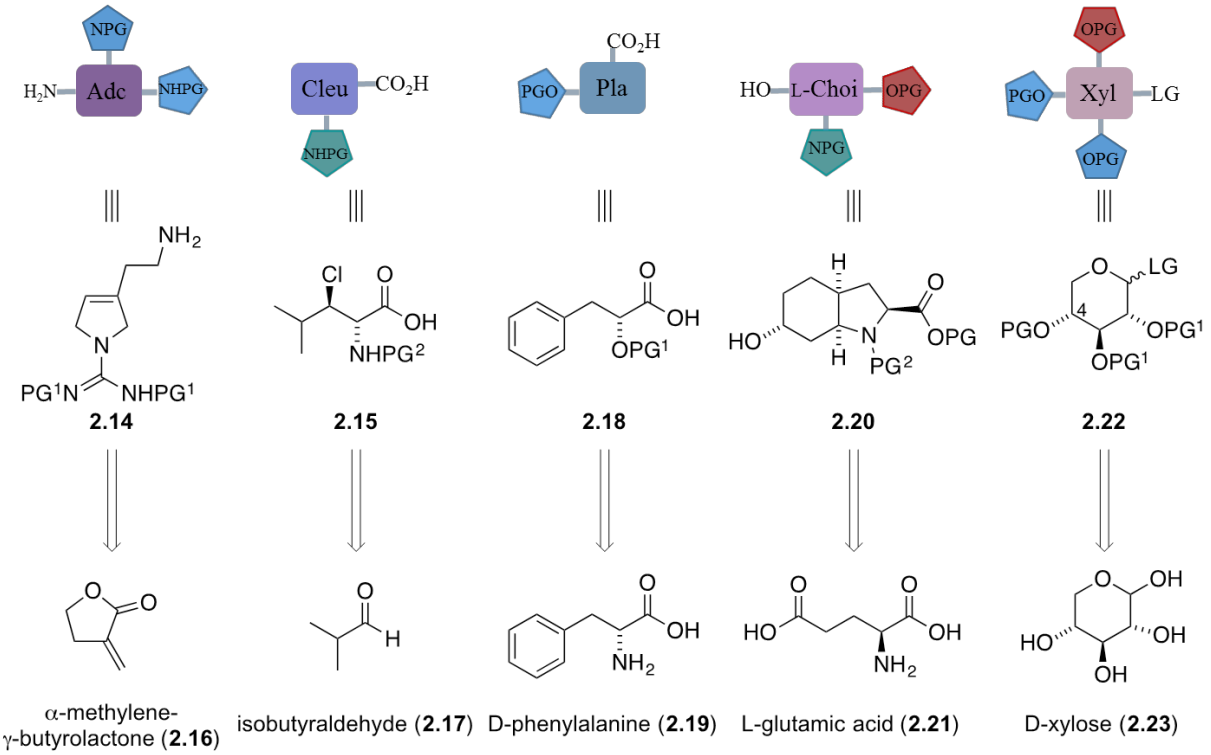

Scheme 3 Cartoons of the simplified building blocks (top). Retrosynthetic analysis of the different building blocks (bottom).

3.3. Different Assembly Strategies

For the assembly of the building blocks, several different strategies can be considered and three selected strategies will be discussed in more detail.

Strategy A (left, Scheme 4) includes glycosylation of the L-Choi with the Xyl residue. Deprotection of the amine of the L-Choi allows for peptide coupling with the Pla-Cleu-OH dipeptide. Liberation of the acid of the L-Choi and the hydroxyl group at C4 position of the Xyl residue is performed in a single step. Further, the Xyl-Pla-Cleu-L-Choi-OH tripeptide is coupled to the Adc building block. Sulfonation of the oxygen at C4 position of the Xyl residue followed by global deprotection gives access to A828A (**2.1**). The advantage of this strategy is that the challenging α-xylosylation takes place at the very beginning of the assembly. Furthermore, the introduction of the Pla-Cleu-OH as a dipeptide saves two synthetic steps. The disadvantage is the global deprotection at the end in the presence of the labile sulfate group. The pursuit of this strategy will be discussed in Section 5.

Strategy B (middle, Scheme 4) comprises a more classical peptide synthesis approach *via* an assembly from the C to the N terminus.[32] Peptide coupling of the L-Choi with the Adc unit is followed by glycosylation with the Xyl residue. Further, deprotection of the L-Choi amine is followed by coupling to the Cleu residue. Deprotection of the Cleu amine followed by peptide coupling with the Pla-OH unit provides the glycosylated tetrapeptide. Sulfonation and subsequent deprotection yield A828A (**2.1**). The poor step economy as well as the low orthogonality of the protecting groups makes this route unfavorable.

Strategy C (right, Scheme 4) starts with an early peptide coupling of the L-Choi unit with the Pla-Cleu-OH dipeptide, followed by glycosylation with the Xyl moiety. In this strategy a xylosyl donor which already bears a masked sulfate group is used for the glycosylation step. After saponification of the methyl ester of the L-Choi, the glycosylated Pla-Cleu-L-Choi-OH is coupled to the Adc side chain. Global deprotection followed by final unmasking of the sulfate provides A828A (**2.1**). The advantages of this strategy are the early introduction of the sulfate and the increased stability and convenience of its masked analogue. A drawback is that glycosylations with masked sulfates are relatively unexplored. The results following this strategy will be discussed in Section 8.

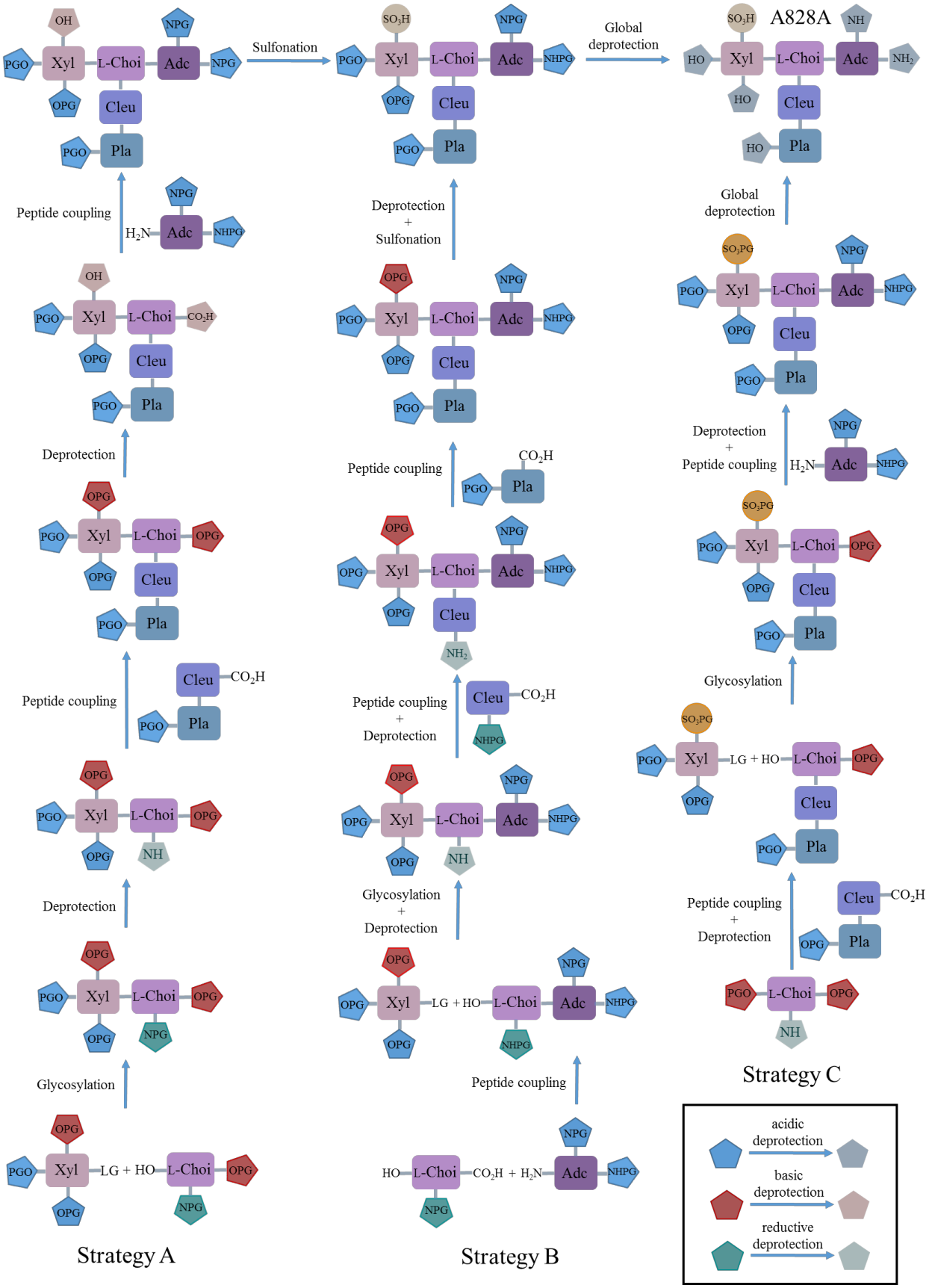

Scheme 4 Strategies A, B and C for the assembly of the building blocks of A828A (**2.1**).

4. Synthesis of the Different Building Blocks

4.1. L-Choi-Synthesis

The L-Choi building block was synthesized following a procedure of Hanessian and co-workers[31] (Scheme 5): The free amine group of L-glutamic methyl ester (**2.24**) was protected with a *tert*-butyloxycarbonyl (Boc) group to give **2.25**. Further, α-functionalization was carried out with LiHMDS as base and but-3-en-1-yl trifluoromethanesulfonate as the electrophile to give alkylated glutamic methyl ester **2.26** in a moderate yield. Removal of the Boc protecting group in formic acid was followed by ring closure in refluxing toluene to give lactame **2.27** in an excellent yield. The obtained lactame **2.27** was either protected with a Boc or with a carboxybenzyl (Cbz) protecting group to give the corresponding protected lactames **2.28** and **2.29**, respectively. Reduction of both lactames was performed with $LiHBEt_3$ to yield a diastereomeric mixture of cyclic hemiaminals which were subsequently acetylated using Ac_2O to give acetyl esters **2.30** and **2.31**. Intermediates **2.30** and **2.31** were the precursors for the aza-Prins carbocyclization and gave access to octahydroindoles **2.32** and **2.33**. The chair-like transition state of the aza-Prins carbocyclization, followed by the favored equatorial attack of the bromide on the carbocation provides the formation of a single desired diastereomer of 6-bromo-octahydroindole compounds **2.32** and **2.33**. Replacement of the bromide atom by an acetate group was achieved by treating the 6-bromo-octahydroindoles with an excess of *tert*-butylammonium acetate under inversion of the stereochemistry at C6 position giving octahydroindoles **2.34** and **2.35**. Finally, saponification of acetyl esters **2.34** and **2.35** to the corresponding alcohols gave rise to the protected (2*S*,3*aS*,6*R*-hydroxy,7*aS*)octahydroindole 2-carboxylic acid (L-Choi) core units **2.36** and **2.37** in excellent yields.

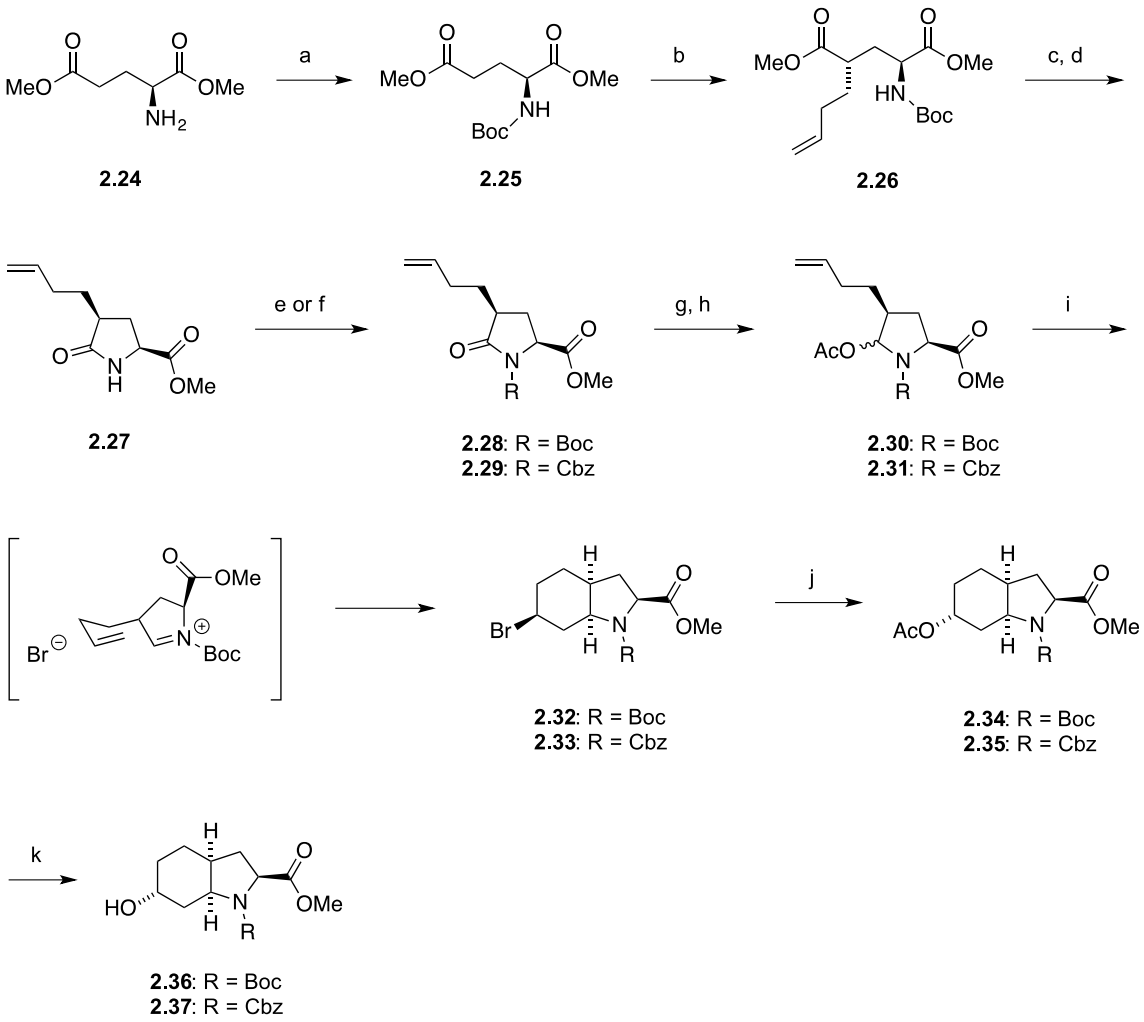

Scheme 5 Synthesis of L-Choi derivatives **2.36** and **2.37**. Reagents and conditions: a) Boc_2O, NEt_3, CH_2Cl_2, 0 °C to r.t., 20 h, 99%; b) LiHMDS, THF, –78 °C, 45 min, then but-3-en-1-yl trifluoromethanesulfonate, –78 °C, 20 min, 63%; c) formic acid, r.t., 5 h, quant.; d) toluene, reflux, 1.5 h, quant.; e) Boc_2O, Et_3N, DMAP, CH_2Cl_2, 0 °C to r.t., 16 h, 68% for **2.28**; f) LiHMDS, THF, –78 °C, 20 min, then benzyl chloroformate, –78 °C, 1 h, 71% for **2.29**; g) $LiHBEt_3$, THF, –78 °C, 1 h; h) Ac_2O, Et_3N, DMAP, CH_2Cl_2, r.t., 20 h (**2.30**: 44% over two steps from **2.28**, **2.31**: 72% over two steps from **2.29**); i) $SnBr_4$, CH_2Cl_2, –78 °C, 30 min (**2.32**: 87% from **2.30**, **2.33**: 84% from **2.31**); j) Bu_4NOAc, toluene, 45–47 °C, 3 h (**2.34**: 62% from **2.32**, **2.35**: 53% from **2.33**); k) NaOMe, MeOH, r.t., 6 h (**2.36**: 86% from **2.34**, **2.37**: 86% from **2.35**).

4.2. Synthesis of Pla-Cleu-OH Dipeptide 2.47

Chloroleucine derivative **2.47** was synthesized according to a procedure developed towards the total synthesis of chlorodysinosin A[28] and aeruginosin 205A[33] (Scheme 6): Isobutyraldehyde (**2.21**) was converted into ester **2.38** in a good yield in a Horner-Wadsworth-Emmons (HWE) reaction. Subsequently, ester **2.38** was reduced to the corresponding allyl alcohol **2.39** using DIBAL, followed by an enantioselective epoxidation of the olefin using Sharpless conditions to access epoxide **2.40**.[34] Protection of the free primary alcohol of **2.40** with a *tert*-butyldimethylsilyl (TBS) group followed by epoxide opening by treatment with NaN_3 yielded a regioisomeric mixture of azides **2.41** and **2.42**.

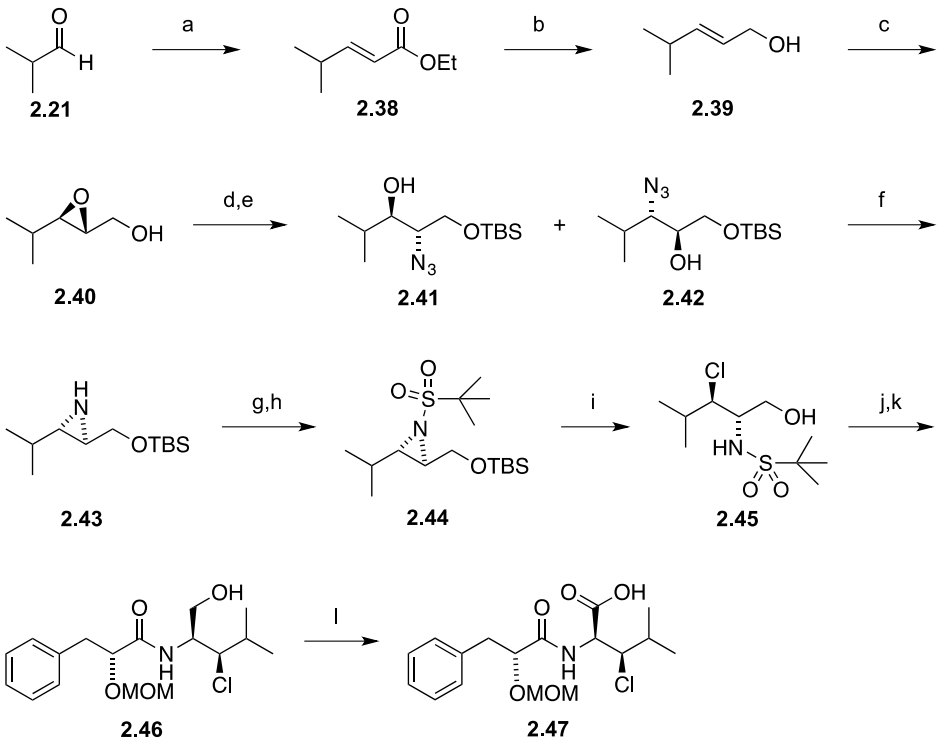

Scheme 6 Synthesis of Pla-Cleu-OH dipeptide **2.47**. Reagents and conditions: a) triethyl phosphonoacetate, NaH, benzene, 70 °C, 1.5 h, 65%; b) DIBAL, CH_2Cl_2, –78 °C, 1.5 h, 75%; c) D(–)-diethyl tartrate, *t*-BuOOH, Ti(*i*-OPr)$_4$, 4 Å MS, CH_2Cl_2, –20 °C, 14 h, 46%; d) NaN_3, MeOEtOH/H_2O (20:1), 120 °C, 24 h; e) TBSCl, Et_3N, DMAP, CH_2Cl_2, 0 °C, 2 h, 89% over two steps; f) PPh_3, MeCN, 50 °C, 18 h, 79%; g) *tert*-butylsulfinyl chloride, Et_3N, CH_2Cl_2, 0 °C, 2 h; h) *m*-CPBA, CH_2Cl_2, 0 °C, 1.5 h, 84% over two steps; i) $CeCl_3 \cdot H_2O$, MeCN, 85 °C, 84 h, 54%; j) TfOH, anisole, CH_2Cl_2, r.t., 20 h; k) Pla-OH **2.51**, PyBOP, 2,6-lutidine, CH_2Cl_2, 0 °C to r.t., 16 h, 68% over two steps; l) CrO_3, H_5IO_6, MeCN/H_2O (99.3:0.7), 0 °C, 1 h, 90%.

Reduction of the azides to the corresponding amines was achieved using Staudinger conditions and was accompanied by the elimination of H_2O and the formation of aziridine **2.43**. Protection of the aziridine with a *tert*-butylsulfinyl group using *tert*-butylsulfinyl chloride was followed by subsequent oxidation of the sulfoxide to the sulfone using *m*-CPBA to give access to **2.44**. The key step of this building block synthesis was the regiocontrolled opening of aziridine **2.44** using an excess of $CeCl_3 \cdot H_2O$ as the chloride donor yielding α-chloro-amine **2.45** as a single regioisomer.[28] The conditions for the chlorination of aziridine **2.44** also resulted in the cleavage of the TBS protecting group. The desired confirmation of α-chloro-amino alcohol **2.45** was confirmed by X-ray crystallographic analysis (Figure 18).

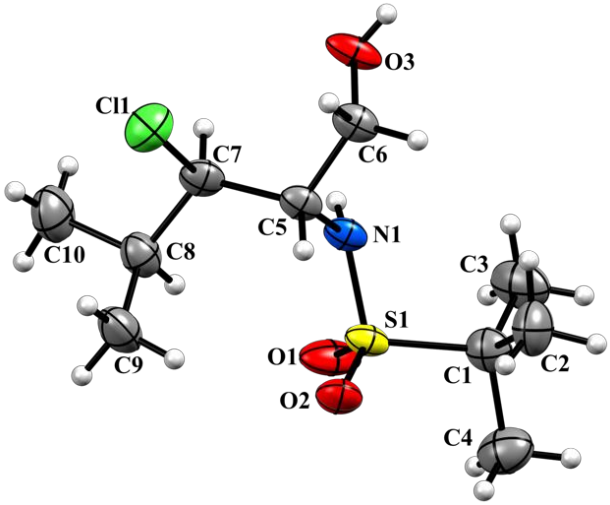

Figure 18 X-ray crystallographic structure of α-chloro-amino alcohol **2.45**, ellipsoids plotted at 40% probability level. Selected bond parameters: Cl1–C7 = 1.824(3), N1–S1 = 1.619(2), S1–O1 = 1.427(2), S1–O2 = 1.4224(19) Å; S1–N1–C5 = 124.81(16), O1–S1–O2 = 118.92(13) °.

Continiung with the literature procedure[33], cleavage of the *tert*-butylsulfonyl group followed by peptide coupling of the free amine with the Pla-OH side chain **2.51** was investigated (for the synthesis of **2.51** see Section 4.3). The conditions described in the literature for this two-step sequence are as follows: Treatment of α-chloro-amino alcohol **2.45** with an excess of TfOH (5.0 eq.) and anisole (20.0 eq.) in CH_2Cl_2 gives the free amine as a triflate salt and coupling to the Pla-OH acid **2.51** is conducted using PyBOP as coupling reagent and 2,6-lutidine as base. However, these synthetic conditions resulted in a poor yield (< 20%). Changing the coupling reagent from PyBOP to DEBPT or DMTMM and the base from 2,6-lutidine to NMM did not lead to an improvement. In the literature procedure, lyophilization techniques were performed to

remove the excess TfOH from the crude product. However, with this method we were not able to fully remove the TfOH from the crude residue, which might be the reason for the low yield of the subsequent peptide coupling. Therefore, focus was set on a more efficient removal of the TfOH by using a basic resin or neutralization with NH_3 (g). Unfortunately, the TfOH could not be removed using these methods but we were finally pleased to find a rather simple solution for this problem by leaving the excess of TfOH in the crude product but instead and consequently adding two more equivalents of the base 2,6-lutidine during the peptide coupling step. With this alteration of the literature procedure the yield of dipeptide **2.46** could be increased from less than 20% to 68%, an even higher value than the reported 60%. In order to finish the synthesis of the Pla-Cleu-OH side chain, the alcohol of dipeptide **2.46** was oxidized to the corresponding acid in an excellent yield using CrO_3 and H_5IO_6. To summarize, Pla-Cleu-OH dipeptide **2.47** was successfully synthesized over twelve steps with an overall yield of 4.3% starting from commercially available isobutyraldehyde **2.21**.

4.3. Synthesis of Pla-Leu-OH Dipeptide 2.53

For the syntheses of aeruginoside 126A (**2.11**) and the analogue aeruginosin 794A (**2.13**), a building block containing a leucine (Leu) instead of a chloroleucine residue was required. The synthesis of Pla-Leu-OH dipeptide **2.53** started with commercially available D-phenylalanine (**2.23**) which upon treatment with $NaNO_2$ in aqueous 2 M sulphuric acid was converted into D-phenyllactic acid (Pla) (**2.48**) with retention of the stereochemistry and in a good yield of 77%.[29,30] Phenyllactic acid (**2.48**) was esterified to the corresponding methyl ester **2.49** in an almost quantitative yield followed by protection of the free secondary hydroxyl group with an acid labile MOM group to access **2.50**. Saponification of the methyl ester of **2.50** yielded acid **2.51** which was coupled with H-D-Leu-OMe using PyBOP as peptide coupling reagent and 2,6-lutidine as base. Subsequent saponification of the leucine methyl ester **2.52** finally gave access to Pla-Leu-OH dipeptide **2.53** in an excellent yield (Scheme 7).

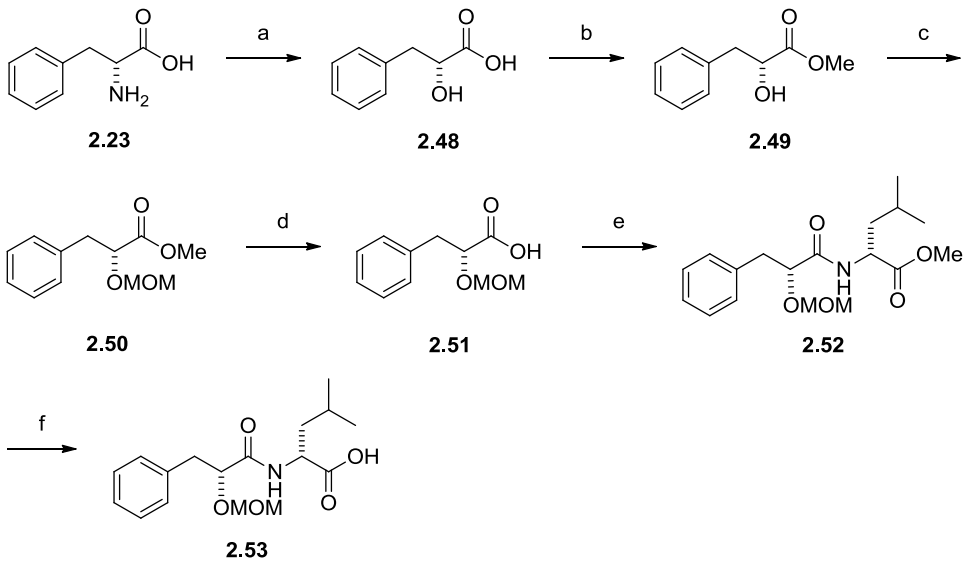

Scheme 7 Synthesis of Pla-Leu-OH dipeptide **2.53**. Reagents and conditions: a) $NaNO_2$, aq. 2 M H_2SO_4, r.t., 20 h, 77%; b) HCl, MeOH, toluene, 75 °C, 4 h, 94%; c) MOMBr, DIPEA, CH_2Cl_2, r.t., 15 h, 73%; d) LiOH, THF/H_2O (5:3), r.t., 1 h, 97%; e) H-D-Leu-OMe, PyBOP, 2,6-lutidine, CH_2Cl_2, r.t., 20 h, 81%; g) LiOH, THF/H_2O 5:3, r.t., 2 h, 98%.

4.4. Synthesis of the Adc Building Block

4.4.1. Synthesis of Adc precursor 2.62

The Adc subunit **2.62** was synthesized following a procedure from Hanessian and co-workers[27] (Scheme 8): Commercially available α-methylene-γ-butyrolactone (**2.17**) was transformed to the corresponding methyl ester **2.54** by treatment with fuming sulfuric acid in methanol.[35] Since reclosing to the lactone was observed during flash column chromatography (SiO_2), the primary alcohol of ester **2.54** was directly protected with a *tert*-butyldiphenylsilane (TBDPS) group without further purification, to prevent lactone formation. Unfortunately, this sequence provided **2.55** in a poor yield of only 30% over two steps. Nevertheless, ester **2.55** was reduced with a 1 M DIBAL solution in toluene to give alcohol **2.56** in an excellent yield of 90%.

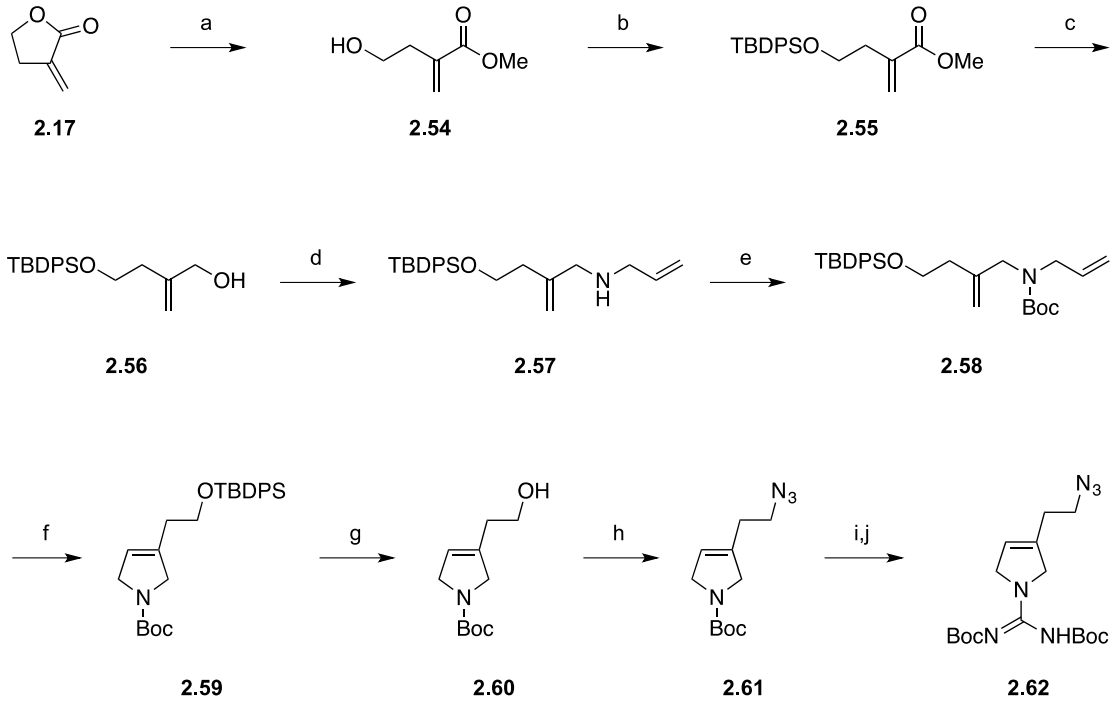

Scheme 8 Synthesis of the Adc subunit precursor **2.62**. Reagents and conditions: a) MeOH, H_2SO_4, r.t., 16 h; b) TBDPSCl, imidazole, DMF, r.t., 15 h, 30% over two steps; c) 1 M DIBAL, DCM, −78 °C, 1 h, 90%; d) MsCl, TEA, allylamine, DCM, r.t., 16 h, 76%; e) Boc_2O, TEA, CH_2Cl_2, r.t., 1 h, 96%; f) Grubbs' II, CH_2Cl_2, r.t., 16 h, 96%; g) TBAF, THF, r.t., 1 h, 77%; h) PPh_3, DEAD, diphenylphosphoryl azide, r.t., 1 h, 72%; i) TFA, CH_2Cl_2, r.t., 4 h; j) Goodman's reagent, Et_3N, $CHCl_3$, r.t., 17 h, 78% over two steps.

In situ mesylation of the primary alcohol of **2.56** allowed S_N2 attack of allylamine to yield amine **2.57** which was subsequently reacted with Boc_2O to obtain the protected amine **2.58** in a yield of 73% over two steps. Ring closing metathesis (RCM) using Grubbs' 2nd generation catalyst converted amine **2.58** into pyrroline **2.59** in an almost quantitative yield of 96%. Deprotection of the primary alcohol of pyrroline **2.59** was achieved by treatment with a TBAF solution in THF and resulted in the formation of free alcohol **2.60** in a good yield of 77%. Using Mitsunobu's reaction conditions, alcohol **2.60** was converted into the corresponding azide **2.61** with diphenylphosphoryl azide as azide source. Further, the Boc protecting group was cleaved under acidic conditions and the obtained free amine reacted with Goodman's reagent giving access to Adc precursor **2.62**.

4.4.2. Reduction of azide 2.62 to Adc subunit 2.63

With the Adc precursor **2.62** in hand, we focused on the reduction of the azide functionality to the corresponding primary amine present in the Adc subunit **2.63**. Using Staudinger's conditions for this transformation as described by Hanessian and co-workers successfully reduced the azide to the amine (Scheme 9). However, separation of the side product triphenylphosphine oxide from the desired product turned out to be problematic, because flash column chromatography (SiO_2 or Al_2O_3) led to decomposition and purification by recrystallization was not successful. We opted then for an alternative to the Staudinger reduction. Since pyrroline **2.62** possesses two sensitive functions (the Boc-protected guanidine and the double bond of the pyrroline) prone to undergo overreduction, well-known methods such as reduction with lithium aluminium hydride or hydrogenation with Pd/C under a H_2 atmosphere are unsuitable.[36] We were delighted to find a catalytic hydrogenation reaction using Lindlar's catalyst which remained the dihydropyrrole untouched (Scheme 9).[37,38]

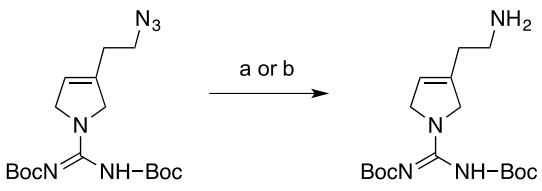

2.62 **2.63**

Scheme 9 Reduction of azide **2.62** to Adc subunit **2.63**. Reagents and conditions: a) PPh_3, H_2O, THF, r.t., 16 h, then AcOH, 72%; b) Lindlar's catalyst, H_2 (1 bar), MeOH, r.t., 90 min, 96%.

Using these conditions, not only could the yield be increased from 72% (lit.) to 96%, but also the purity of Adc subunit **2.63** was enhanced as illustrated in Figure 19. The ^{1}H NMR spectrum from the Adc subunit **2.63** gained *via* the Staudinger reduction (red) shows impurities of triphenylphosphine oxide (~7.75 to 8.00 ppm) and an acetate peak (singlet at 1.91 ppm) derived from the work up with acetic acid, whereas the compound obtained by the catalytic hydrogenation only shows negligible impurities (blue).

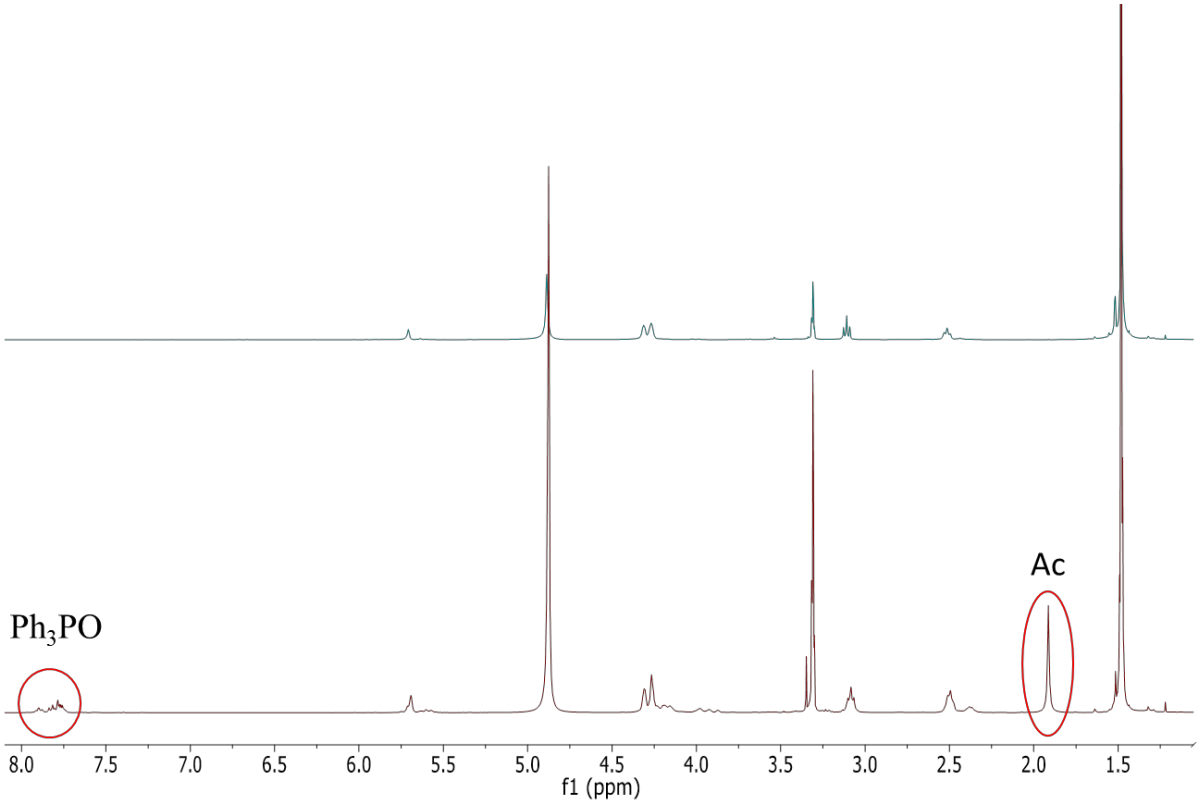

Figure 19 Comparison of the ^{1}H NMR spectra obtained from the reduction of azide **2.62** to Adc subunit **2.63**. In red: the reduction using Staudinger conditions; in blue: the reduction by catalytic hydrogenation using Lindlar's catalyst.

4.4.3. Unexpected oxidation of 2,5-dihydropyrrole 2.61 to pyrrole 2.64

A main challenge towards the synthesis of aeruginosin 828A (**2.1**) and its congeners was the coordinated synthesis of the different building blocks in a sense that each building block had to be available at the exact stage of the synthesis when they were incorporated into the total synthesis. 2,5-dihydropyrrole **2.61**, a late stage precursor of the Adc subunit **2.63**, illustrates an example that this proved to be problematic at some points of the synthesis: 2,5-dihydropyrrole **2.61** was synthesized as described in Section 4.4.1. and obtained in a scale of 440 mg over eight steps. For the completion of Adc subunit **2.63** two additional steps were

required (for details see Section 4.4.1.). These final steps were performed on a 100 mg scale leading to 66 mg of the desired Adc subunit **2.63**. Since these 66 mg of **2.63** contained minor impurities (for details see Section 4.4.2), additional purification of **2.63** had to be performed just before merging **2.63** into the building block assembly. As described in Section 4.4.2, purification by flash column chromatography of Adc subunit **2.63** led to decomposition thereof. Unfortunately, by that time the remaining 340 mg of late stage precursor **2.61** had almost entirely been oxidized to the corresponding pyrrole **2.64** during storage in the refrigerator (Scheme 10). As the reverse of the oxidation reaction – the reduction of the pyrrole to the 2,5-dihydropyrrole – is precarious in the presence of the azide and Boc functionalities, the whole synthesis of the Adc building block had to be repeated. Surprisingly, this type of oxidation was only observed for 2,5-dihydropyrrole **2.61** and neither natural product aeruginosin 828A (**2.1**) nor Adc subunit **2.63** showed observable traces of the pyrrole compound during isolation or storage.

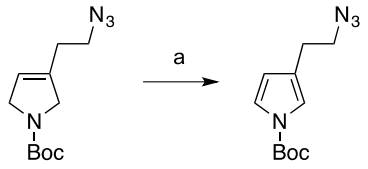

2.61 **2.64**

Scheme 10 Spontaneous oxidation of 2,5-dihydropyrrole **2.61** to pyrrole **2.64**. Reagents and conditions: a) O_2, 4 °C, 90 d, 80%.

4.5. Synthesis of Xyl Donor 2.69

The synthesis of xylose donor **2.69** was achieved starting form commercially available D-xylose (**2.15**) (Scheme 11). Global acetylation of all the hydroxyl groups provided fully acetylated xylose moiety **2.65** as a mixture of α and β anomers. Further, the acetate group at the anomeric position was replaced by a thiophenol group, catalyzed by $BF_3 \cdot Et_2O$, to give xyloside **2.66** as the single β-anomer.[39] The exclusive formation of the β-anomer can be explained by a neighboring group participation of the acetyl group at C2 position which interacts with the oxonium ion, obtained as intermediate during the glycosylation, thereby blocking the α-position for a possible attack by the thiophenol.[40] Removal of all acetyl groups was achieved by treating **2.66** with a methanolic NaOMe solution to yield **2.67**. Subsequently, regioselective protection of the OH-group at C4 position of **2.67** with a benzoyl (Bz) protecting group was achieved in 81% yield using benzoyl chloride and Me_2SnCl_2 as

catalyst.[41] The 2-OH and 3-OH groups were protected with a butane diacetal (BDA) group using 2,3-butanedione, trimethyl orthoformate and camphorsulfonic acid.[42] Initial attempts of BDA protection always led to an inseparable mixture of two isomers caused by a non-steroselective formation of the acetals within the BDA group (see bottom ^{1}H NMR spectrum in Figure 21). Since the BDA group only serves as protecting group during the synthesis, it would in fact be possible to use a mixture of isomers for future synthetic steps. However, in order to avoid the challenging interpretation of analytical data due to the presence of diastereomeric mixtures in the successive total synthesis, we opted for an optimization of the reaction conditions and found the reaction time to be crucial for product formation. Increasing the reaction time from 20 h to 64 h led to the formation of a single diastereoisomer of xylosyl donor **2.69** (Scheme 11). The configuration of xylose donor **2.69** was confirmed by X-ray crystallographic analysis (Figure 20).

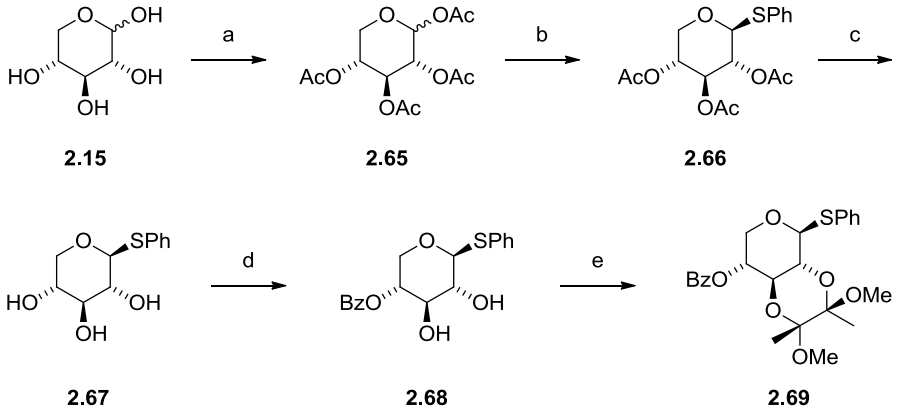

Scheme 11 Synthesis of Xyl donor **2.69**. Reagents and conditions: a) AcCl, pyridine, 0 °C, 24 h; b) $BF_3 \cdot Et_2O$, thiophenol, CH_2Cl_2, 0 °C to r.t., 98% over two steps; c) NaOMe, MeOH, r.t., 2 h, 61%; d) Me_2SnCl_2, DIPEA, BzCl, THF/H_2O (9:1), r.t., 4 h, 76%; e) 2,3-butanedione, trimethyl orthoformate, CSA, MeOH, 66 °C, 64 h, 69%.

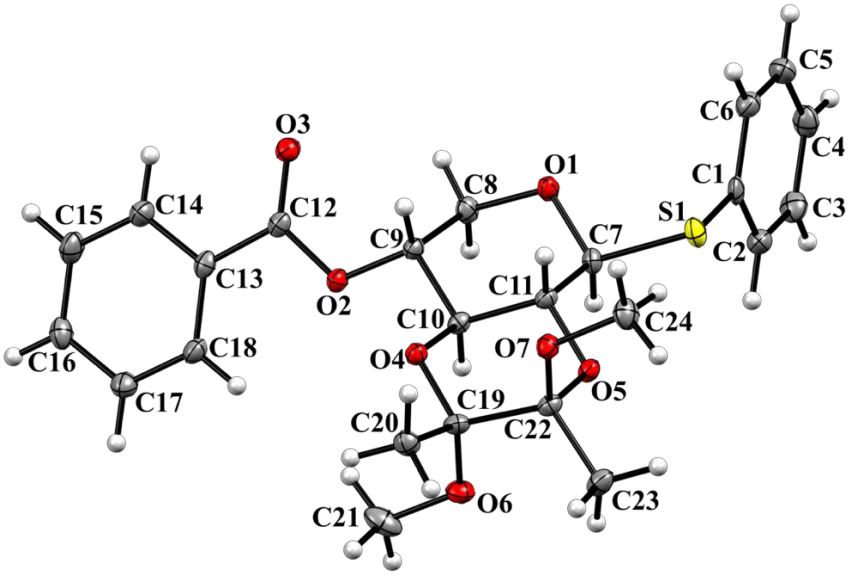

Figure 20 X-ray crystallographic structure of xyloside **2.69**, showing the relative orientation of the methyl and methoxy groups at C19 and C22. Ellipsoids plotted at 40% probability level.

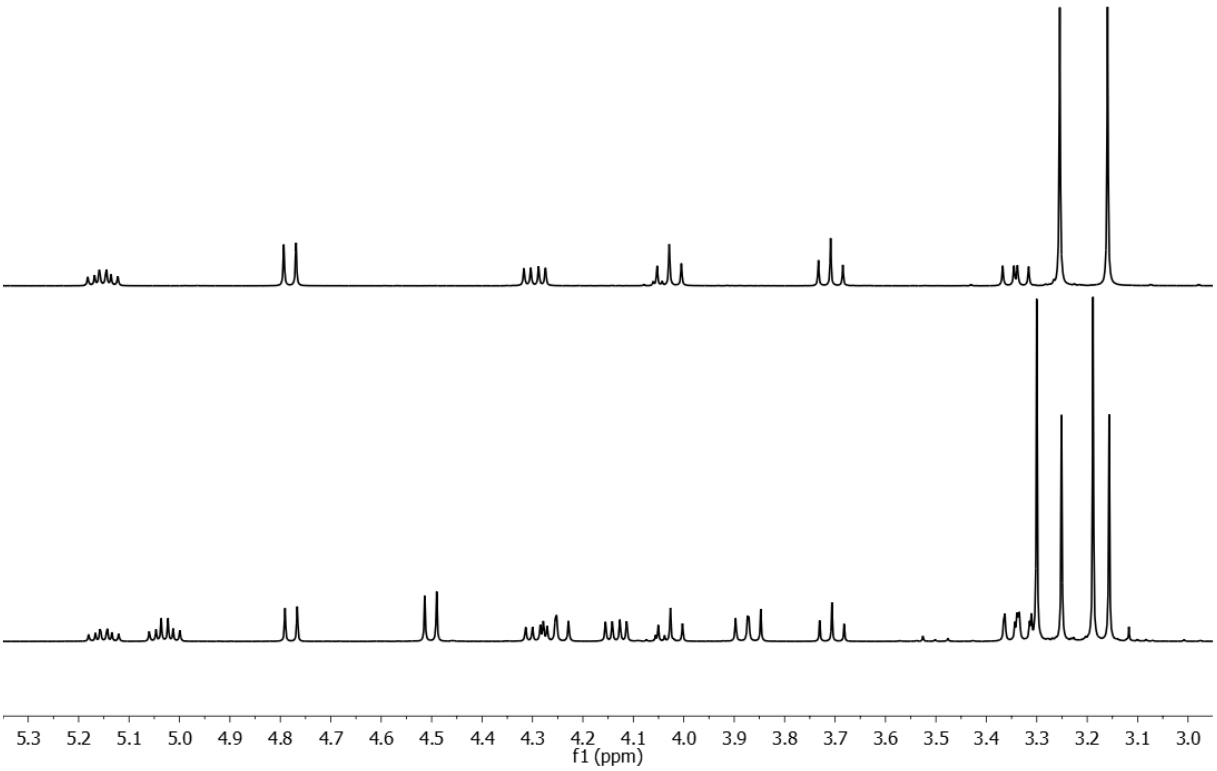

Figure 21 Selected part of the ^{1}H NMR spectra of xyloside **2.69** (top) and the diastereomeric mixture of xyloside **2.69** (bottom).

5. Synthesis of Aeruginosin 828A and Aeruginosin 748A – Assembly of the Different Building Blocks

5.1. Xylosylation

With all the different building blocks in hand, we started to focus on the assembly thereof. Since the α-xylosylation appeared to be synthetically most challenging, we sought for an incorporation of the xylosyl moiety at an early stage of the assembly. For this, xylosyl donor **2.69**, with a thiophenol group at the anomeric carbon atom, was treated with NIS as activator and AgOTf as promoter to form an iodo-sulfonium species *in situ*,[43] allowing for an attack of the hydroxyl group of the respective L-choi derivative. The glycosylation with L-choi derivative **2.36** proceeded with a moderate yield of 42%. Fortunately, the formation of the desired α-anomer was favored in contrast to the β-anomer by a ratio of 2:1 (according to ^{1}H NMR spectra analysis) (Scheme 12).

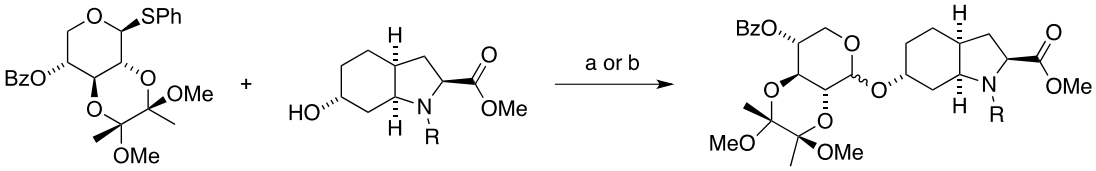

2.69

2.36: R = Boc
2.37: R = Cbz

2.70: R = Boc
2.71: R = Cbz

Scheme 12 Glycosylation of L-choi derivatives **2.36** and **2.37** with xylosyl donor **2.69**. Reagents and conditions: a) NIS, AgOTf, 4 Å MS, CH_2Cl_2, 0 °C to r.t., 2 h, (**2.70**: 42% from **2.36**, α/β (2:1)); b) NIS, AgOTf, Et_2O, 0 °C to r.t., 2 h, (**2.71**: 79% from **2.37**, α/β (5:3)).

Because the separation of the two anomers of **2.70** turned out to be arduous, the anomeric mixture was used for the next step, cleaving the Boc group from the secondary amine of the L-Choi unit. Various acidic conditions for this deprotection always harmed not only the Boc group but also the BDA protecting group of the xylosyl residue. To overcome the problem of the poor orthogonality of the BDA and Boc groups, there were two options: either exchange the BDA group of xylosyl moiety **2.69** by a more stable group or exchange the Boc group of L-choi derivative **2.36** by a more orthogonal group with respect to the BDA group. The latter strategy was chosen by preparing L-choi derivative **2.37** containing a Cbz group on the secondary amine. Since the glycosylation system with NIS as activator and AgOTf as promoter provided a favored selectivity for the desired α-anomer, these conditions were also applied for the glycosylation of xylosyl donor **2.69** with L-choi derivative **2.37**, to achieve a

comparable anomeric selectivity and yield for **2.71** as obtained before for **2.70**. Fortunately, the two anomers of **2.71** could be separated from each other. Minor optimizations, mainly by changing the solvent from CH_2Cl_2 to Et_2O, finally allowed the xylosylation to proceed with a good yield of 79% and an anomeric ratio of 5:3 favoring the α-anomer (Scheme 12).

5.2. Amine Deprotection

To progress with the total synthesis of aeruginosin 828A and the assembly of the different building blocks, the Cbz protecting group had to be cleaved from the xylosylated L-choi derivative **2.71**. As similar transformations for this deprotection had already been investigated for aglycon derivatives of L-Choi by other research groups,[27] we were optimistic to rapidly find suitable conditions for this deprotection. Unfortunately, the catalytic hydrogenation reaction with Pd/C described in the literature only resulted in the recovery of the starting material (Table 1, Entry 1). Furthermore, neither increasing the catalyst loading from 0.3 to 3.0 equivalents (Entry 2), nor raising the H_2 pressure from 1 to 10 bar (Entry 3) led to any conversion of the starting material. In pursue of enhancing the reactivity of the catalyst, an excess of acetic acid was added to the reaction mixture, which was rewarded with no success (Entry 4). Changing the catalytic species from Pd/C to the more active $Pd(OH)_2$ did not lead to any progress either, since no conversion was observed applying low pressure (Entry 5) or decomposition of the starting material was witnessed at a high pressure of 15 bar (Entry 6). Neither did the use of additives such as acetic acid or triethylamine result in an enhancement of the reactivity (Entries 7 and 8). Pleasingly, **2.71** was treated with $PdCl_2$ and Et_3N dissolved in triethylsilane, according to a protocol of Birkofer and co-workers,[44] which led to 88% yield of the desired free amine (Entry 9).

Table 1 Conditions for the Cbz deprotection of Xyl-L-Choi-Cbz derivative **2.71**.

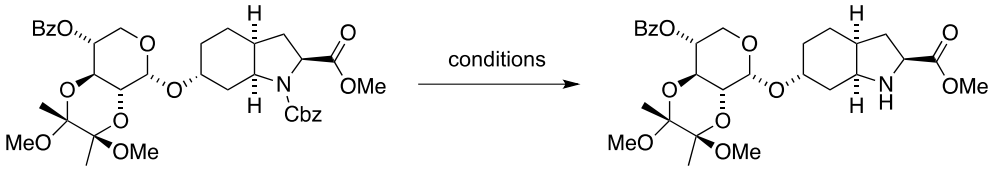

2.71 **2.72**

Entry	Catalyst	Additive	H_2 pressure	Observation
1	Pd/C (0.3 eq.)	-	1 bar	SM
2	Pd/C (3.0 eq.)	-	1 bar	SM
3	Pd/C (0.3 eq.)	-	10 bar[a]	SM
4	Pd/C (0.3 eq.)	AcOH	1 bar	SM
5	$Pd(OH)_2$ (3.0 eq.)	-	1 bar	SM
6	$Pd(OH)_2$ (3.0 eq.)	-	15 bar[a]	decomposition
7	$Pd(OH)_2$ (3.0 eq.)	AcOH	1 bar	SM
8	$Pd(OH)_2$ (3.0 eq.)	Et_3N	1 bar	SM
9[b]	$PdCl_2$ (1.0 eq.)	Et_3SiH	-	88% of **2.72**

All reactions were performed in MeOH at room temperature unless otherwise stated. Reaction vessel were repeatedly evacuated and flushed with H_2. [a]Reactions were performed in a low-pressure autoclave. [b]Reaction was perfomed under neat conditions.

5.2.1. Cleavage of the undesired amino silylether 2.73 by treatment with SiO_2

The reaction conditions described in Table 1, Entry 9 proved to be sensitive in a sense that the yields varied over a wide range. We propose that *N*-triethylsilyl intermediate **2.73** (Scheme 13) was formed as by-product during the reaction. Similar by-products had been observed by Ohfune and co-workers[45] which had used comparable conditions for their deprotection. Therefore, we assume that amino silylether **2.73** interacted with the silica gel during purification and that the free amine was not been formed until in contact with the silica gel. The amount of liberated free amine is therefore dependent on the time used for purification, leading to the poor reproducibility of this reaction. This problem was circumvented by simply stirring the obtained crude residue containing amino silylether **2.73** in a suspension of SiO_2 in MeOH for 30 min prior to purification.

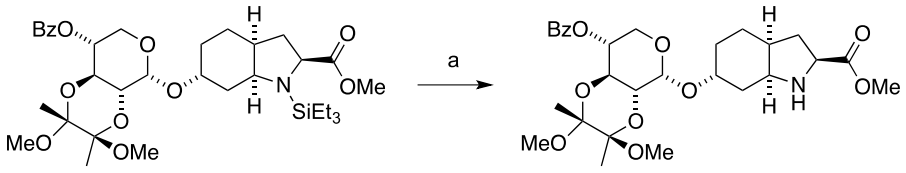

2.73 **2.72**

Scheme 13 Cleavage of the undesired amino silylether **2.73**. Reagents and Conditions: a) SiO_2, MeOH, r.t., 30 min.

5.3. Peptide Coupling of Xyl-L-Choi Unit 2.72 with Pla-Cleu-OH Dipeptide 2.47

With Xyl-L-Choi amine **2.72** in hand, the investigation of the peptide coupling of this amine residue to the Pla-Cleu-OH dipeptide **2.47** was started (for the synthesis of dipeptide **2.47** see Section 4.2.). First attempts with benzotriazol-1-yl-oxytripyrrolidinophosphonium hexafluorophosphate (PyBOP) (Figure 22) as coupling reagent and NMM as base (Entry 1, Table 2) led to the formation of a single product. Unfortunately, the mass of the isolated product did not correspond to the desired tripeptide **2.74**, but to product **2.75** containing a double bond in the Cleu residue, obtained *via* elimination of HCl. Similar HCl elimination and racemization had already been described in the literature for the synthesis of other aeruginosins.[28,46] The mechanism of racemization followed by elimination of HCl during peptide coupling will be discussed in the following Section 5.3.1. We then started to screen different conditions and coupling reagents for the peptide coupling: First, the base NMM was replaced by the slightly less basic and sterically more demanding 2,6-lutidine, to again obtain exclusively eliminated product **2.75** (Entry 2, Table 2). Further, the coupling reagent was changed from PyBOP to bromotri(pyrrolidino)phosphonium hexafluorophosphate (PyBrOP) (Figure 22), since PyBrOP is described in the literature as an efficient peptide coupling reagent for *N*-methylated amino esters,[47,48] which should be suitable for the L-Choi-derivative **2.72** also containing a secondary amine. This exchange of the coupling reagent did not give the desired product **2.74** either, but again the eliminated product **2.75** (Entry 3, Table 2). Next, more classical peptide coupling conditions were attempted with the well-known coupling reagent (1-[bis(dimethylamino)methylene]-1*H*-1,2,3-triazolo[4,5-*b*]pyridinium 3-oxid hexafluorophosphate) (HATU) (Figure 22) and DIPEA as base. This time, traces of the desired product were observed accompanied by eliminated product and starting material, which were the major products according to UPLC mass analysis (Entry 4, Table 2).

Table 2 Conditions for the peptide coupling of Xyl-L-Choi amine **2.72** with Pla-Cleu-OH dipeptide **2.47**.

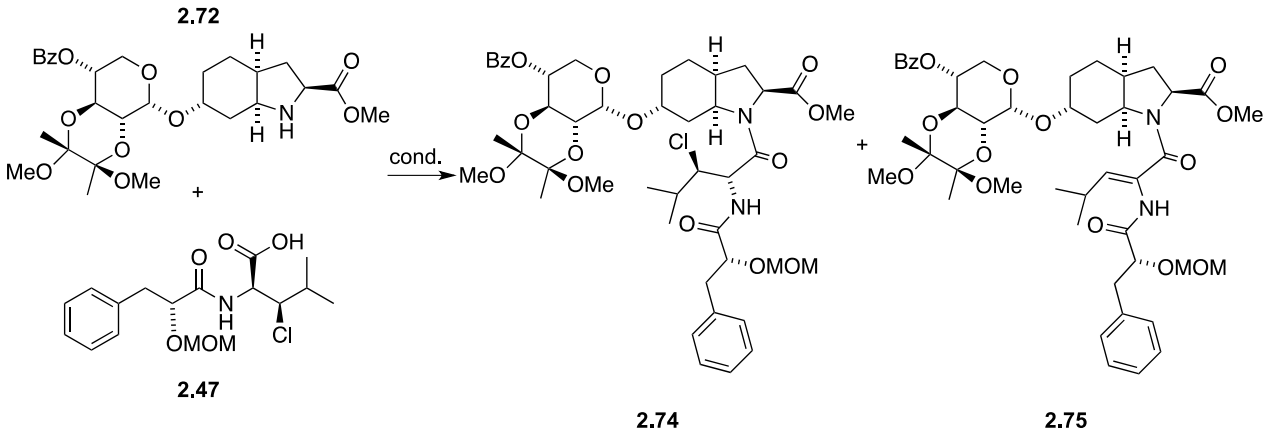

Entry	Coupling Reagent	Base	Solvent	Temp.	Observation[a]
1	PyBOP (1.5 eq.)	NMM (3.0 eq.)	CH_2Cl_2	r.t.	80% of 2.75
2	PyBOP (1.5 eq.)	2,6-lutidine (3.0 eq.)	CH_2Cl_2	r.t.	2.75
3	PyBrOP (1.5 eq.)	DIPEA (3.0 eq.)	CH_2Cl_2	r.t.	2.75
4	HATU (1.2 eq.)	DIPEA (1.2 eq.)	CH_2Cl_2	r.t.	Mainly 2.75 + SM
5	DEPBT (1.5 eq.)[b]	2,6-lutidine (3.0 eq.)	CH_2Cl_2	r.t.	Mainly 2.75 + SM
6	DEPBT (1.5 eq.)[b]	2,6-lutidine (1.5 eq.)	CH_2Cl_2	r.t.	Mainly 2.75 + SM
7	DEPBT (1.5 eq.)[b]	2,6-lutidine (3.0 eq.)	CH_2Cl_2	0 °C	Mainly 2.75 + SM
8	DEPBT (1.5 eq.)[b]	DIPEA (3.0 eq.)	CH_2Cl_2	r.t.	Mainly 2.75 + SM
9	DEPBT (1.5 eq.)[b]	NMM (3.0 eq.)	CH_2Cl_2	r.t.	Mainly 2.75 + SM
10	DEPBT (1.5 eq.)[b]	2,6-lutidine (3.0 eq.)	THF	r.t.	Mainly 2.75 + SM
11	DEPBT (1.5 eq.)[b]	2,6-lutidine (3.0 eq.)	THF/CH_2Cl_2	r.t.	Mainly 2.75 + SM
12	DEPBT (1.5 eq.)[b]	2,6-lutidine (3.0 eq.)	$CHCl_3$	r.t.	Mainly 2.75 + SM
13	DEPBT (1.5 eq.)[b]	2,6-lutidine (3.0 eq.)	DMF	r.t.	Mainly 2.75 + SM
14	DEPBT (1.5 eq.)[b]	$NaHCO_3$ (10.0 eq.)	THF	0 °C	SM
15	DEPBT (1.5 eq.)[b]	-	THF	0 °C	SM
16	DMTMM (1.5 eq.)	NMM (2.0 eq.)	CH_2Cl_2	r.t.	87% of 2.74

The reactions were carried out under careful exclusion of water under argon. [a]The screening was performed with small amounts, thus the yield was not always determined, but the conversion was monitored by UPLC. [b]The DEPBT was recrystallized before usage.

Thereafter, the conditions described in the total synthesis of aeruginosin 205 A and B, containing similar Cleu and L-Choi residues, were tested.[33] The peptide coupling in the synthesis of aeruginosin 205 A and B was performed with (3-(diethoxyphosphoryloxy)-1,2,3-benzotriazin-4(3*H*)-one (DEPBT) (Figure 22) and an excess of three equivalents of 2,6-lutidine as base. Applying these reaction conditions to the coupling of **2.72** and **2.47** provided a mixture of the desired compound **2.74** as minor product and eliminated compound **2.75** as the major product (Entry 5, Table 2). Further, the reaction was accompanied by a long reaction time of over 24 h with still no full consumption of the starting materials. Since DEPBT as coupling reagent provided the best results so far, optimizations were carried out. First by reducing the excess of the base 2,6-lutidine from three equivalents to 1.5 equivalents, leading to no improvement (Entry 6, Table 2). Further, the reaction temperature was decreased from room temperature to 0 °C in order to prevent the elimination reaction, which was not successful either (Entry 7, Table 2). The influence of the base was investigated by exchanging 2-6-lutidine with DIPEA and NMM, without observing any critical effect on the outcome of the reaction (Entries 8 and 9, Table 2). Additionally, a screening of the solvent influence on the result of the reaction was carried out by using THF, THF/CH_2Cl_2, $CHCl_3$ and DMF as solvents instead of CH_2Cl_2. Unfortunately also this screening was not rewarded with success and provided a similar outcome as before (Entries 10–13, Table 2). Next, an excess of the inorganic base $NaHCO_3$ was incorporated into the reaction system instead of the organic base 2,6-lutidine, leading to poor reaction conversion and mainly to recovery of the starting material (Entry 14, Table 2). The same holds for the peptide coupling without addition of a base (Entry 15, Table 2). Unable to optimize the reaction conditions with DEPBT as coupling reagent, yet another alternative coupling reagent was sought after, identifying 4-(4,6-dimethoxy-1,3,5-triazin-2-yl)-4-methylmorpholinium chloride (DMTMM) (Figure 22) to be the ideal promoter for the peptide coupling reaction of amine **2.72** and acid **2.47**. With DMTMM as coupling reagent and NMM as base,[49] the coupling was completed after only two hours resulting in an excellent yield of 87% with no observable elimination of HCl.

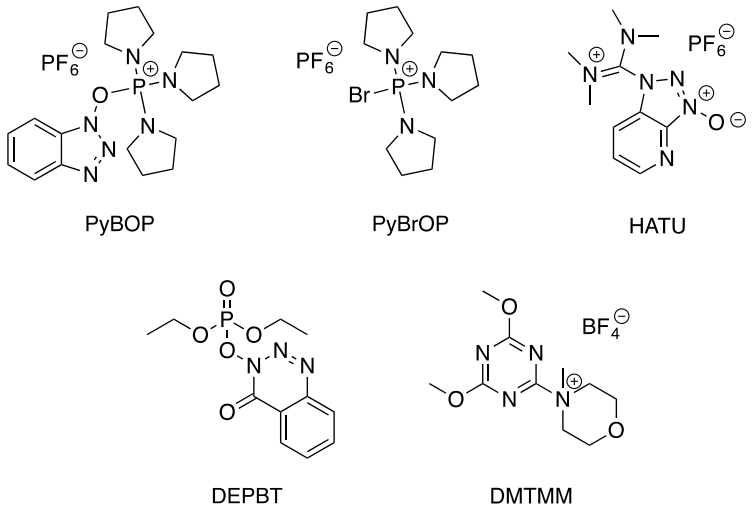

Figure 22 Peptide coupling reagents: PyBOP, PyBrOP, HATU, DEPBT and DMTMM.

5.3.1. Racemization and elimination mechanism for the peptide coupling

The elimination of HCl during the peptide coupling might proceed *via* the two following E1cB mechanism pathways:[50–52] In pathway A (Scheme 14, right), activation of the acid of dipeptide **2.47** leads to the active ester **2.76**. Abstraction of the α-proton by the base gives enolate **2.77**, leading to racemization of the amino acid. With the chlorine atom in β-position, there is a good leaving group present. Consequently, not only racemization – as in other peptide couplings – but also elimination of HCl in an E1 fashion becomes possible. Thus, α,β-unsaturated active ester **2.78** is obtained, which is subsequently attacked by the secondary amine of Xyl-L-Choi derivative **2.72** yielding tripeptide **2.75**. Active ester **2.76** is again the first intermediate formed in pathway B (Scheme 14, left), as described before for pathway A. In this pathway, carboximidate **2.79** is produced which allows for an intramolecular attach on the active ester to form oxazolone intermediate **2.80**. Oxazolone **2.80** can now be readily deprotonated to anionic intermediate **2.81** due to a stabilization of the anion caused by a mesomeric effect. Further, elimination of HCl gives intermediate **2.82** which is opened by the amine of Xyl-L-Choi derivative **2.72**, again providing α,β-unsaturated tripeptide **2.75**. Pathway B is more probable to occur, as the deprotonation of oxazolone **2.80** is more likely to happen compared to the α-deprotonation of active ester **2.77**. Consequently, it is recommendable to synthesize a polypeptide starting from the C-terminus rather than from the N-terminus, since in this case oxazolone formation is prevented due to the missing carbonyl function at the γ-position. Our established route for the synthesis of aeruginosin 828A was started from the N-terminus due to the more straightforward synthesis of Pla-Cleu-OH

dipeptide **2.47** with respect to the synthesis of the Cleu amino acid. In addition, the incorporation of Pla-Cleu-OH as a dipeptide allows for a more convergent synthesis, shortening the total synthesis by two steps. An assembly of the different building blocks starting from the C-terminus might have had spared the problem of racemization but would have also extended the total synthesis (for more details see Section 3.3).

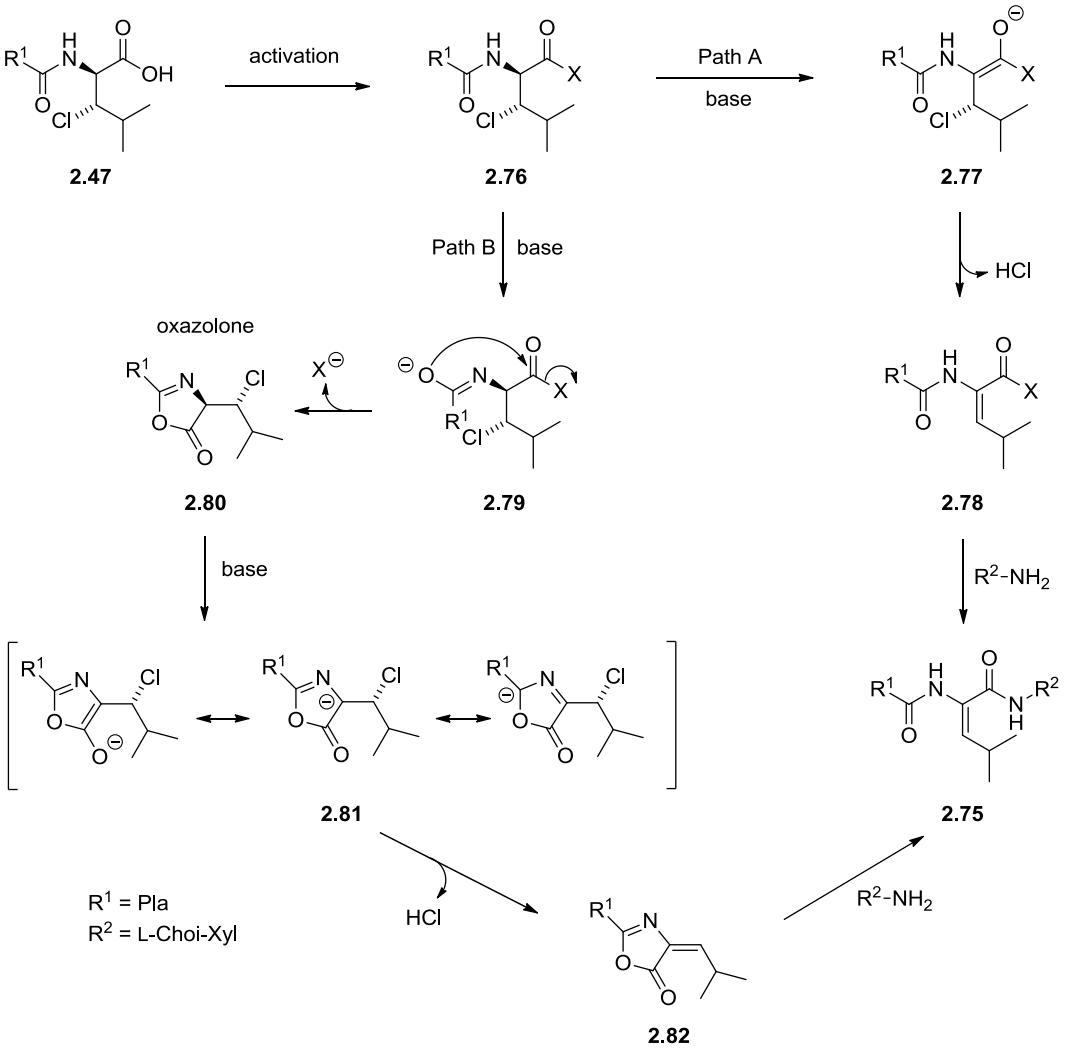

Scheme 14 Possible mechanistic pathways for the elimination of HCl.[50–52]

5.4. Saponification and Attachment of the Adc Subunit

The next synthetic step towards the preparation of aeruginosin 828A (**2.1**) comprised the saponification of the methyl ester of the L-Choi residue in **2.74** and the cleavage of the benzoyl protecting group from the O4 position of the xylose moiety, preparing the molecule for coupling with Adc subunit **2.63** (Scheme 15). The saponification was carried out by the treatment of **2.74** with LiOH to access acid **2.83** in a good yield of 77%. Close monitoring of the reaction progression by UPLC was crucial, to allow for timely quenching of the reaction (~12 h), since longer reaction times again led to elimination of HCl. The subsequent peptide coupling of tripeptide **2.83** with the amine of Adc subunit **2.63** was performed with PyBOP as coupling reagent and 2,6-lutidine as base, yielding tetrapeptide **2.84** in a moderate yield of 60%. Among other factors, the arduous purification of tetrapeptide **2.84** was responsible for the relatively poor yield of the peptide coupling: Repeated flash column chromatography was required to separate the desired product **2.84** from tri(pyrrolidin-1-yl)phosphine oxide obtained as side product during the peptide coupling.

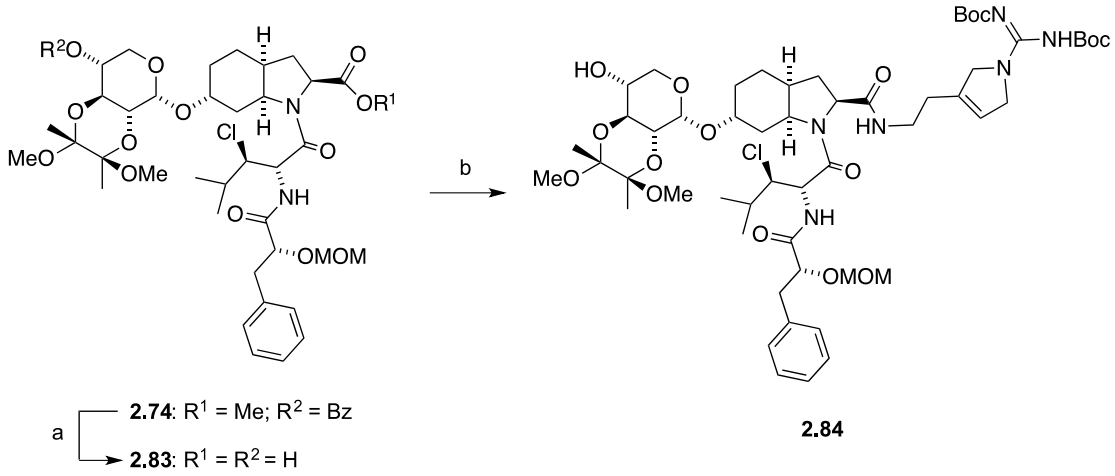

Scheme 15 Saponification of methyl ester **2.74** and further peptide coupling to Adc subunit **2.63**. Reagents and conditions: a) 0.1 M LiOH, THF/H_2O (5:3), r.t., 12 h, 77%; b) Adc subunit **2.63**, PyBOP, 2,6-lutidine, CH_2Cl_2, 0 °C to r.t., 5 h, 60%.

5.5. Sulfonation and Global Deprotection

Tetrapeptide **2.84** with the free hydroxyl group on C4 position of the xylose moiety was treated with an excess of SO_3·pyridine (50.0 eq.) to obtain the required sulfate group on the xylose residue (Scheme 16).[33] After completion of the reaction, sulfated tetrapeptide **2.85** was directly used for the next step without purification. Cleavage of the two Boc, the MOM and the BDA protecting groups was performed in a single acidic global deprotection by treating a solution of tetrapeptide **2.85** in CH_2Cl_2 with TFA. The deprotection proceeded smoothly at room temperature as monitored by UPLC, which showed first the cleavage of the Boc groups, followed by the BDA group. Finally, after 5 h also the MOM group was entirely cleaved from the phenyllactic acid residue. Timely quenching of the deprotection reaction was important in order to prevent cleavage of the sulfate group, since this functionality is known to be labile under acidic conditions.[33][53] The obtained crude residue containing aeruginosin 828A (**2.1**) was then subjected to HPLC purification, discussed in more detail in the following Section 5.6.

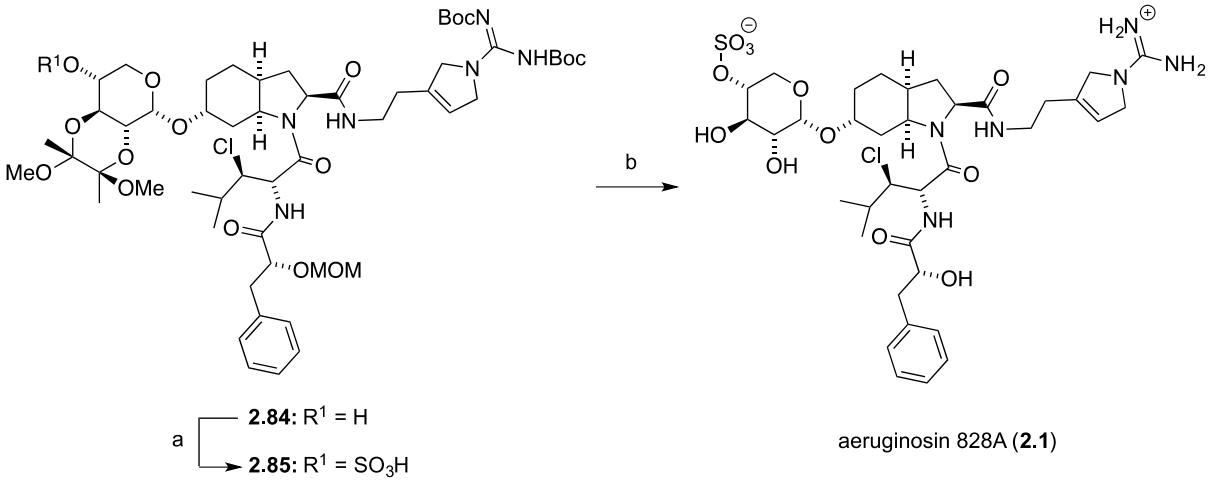

Scheme 16 Sulfonation of intermediate **2.84** and global deprotection – synthesis of aeruginosin 828A (**2.1**). Reagents and conditions: a) SO_3·pyridine (50.0 eq.), pyridine, 50 °C, 15 h; b) CH_2Cl_2/TFA (10:1), r.t., 5 h, 72% over two steps.

5.6. Isolation of Aeruginosin 828A

The crude residue obtained after deprotection was purified by reversed phase HPLC ($MeCN/H_2O$ + 0.1% formic acid). The HPLC chromatogram at 210 nm showed two main peaks: a minor one at 6.58 min and a major one at 8.32 min (Figure 23). The minor and major peaks corresponded to masses of $m/z = 749^+$ and 829^+ (ESI-MS), respectively. The mass of 829^+ could rapidly be assigned to the natural product aeruginosin 828A. Due to the mass difference of $m/z = 80$, an absence of the SO_3 group was suggested in the case of the minor peak which was therefore assigned to the synthetic analogue aeruginosin 748A or a diastereoisomer thereof. The lack of the SO_3 group might either be derived from an incomplete introduction of this functionality before the global deprotection step or from a partial cleavage of the group during acidic deprotection. Fractionated HPLC finally provided 996 µg of aeruginosin 828A (**2.1**) as a white amorphous solid.

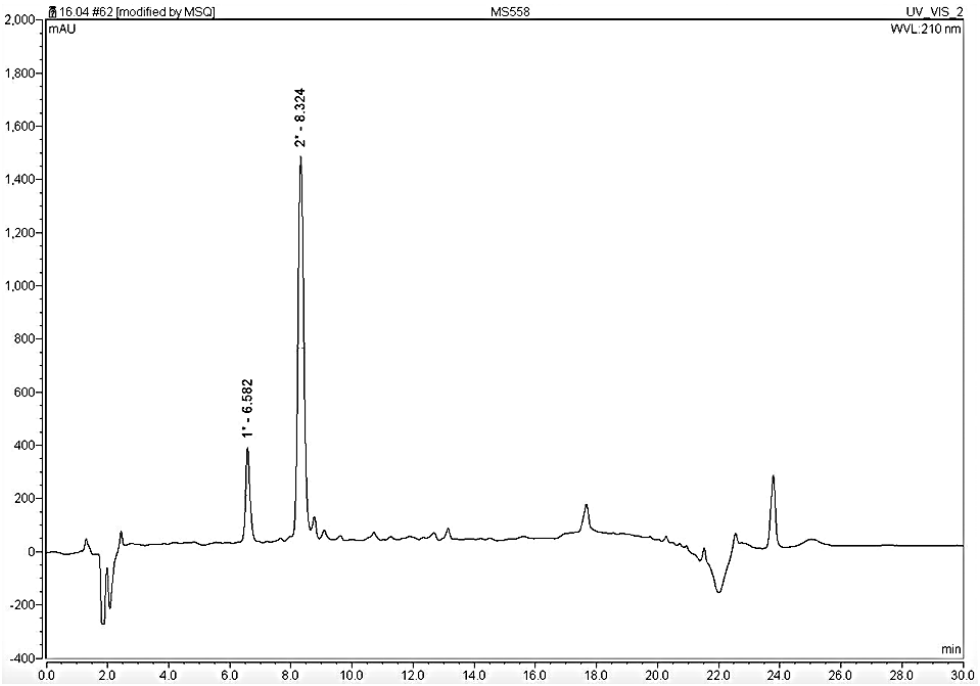

Figure 23 HPLC chromatogram at 210 nm of the isolation of aeruginosin 828A (**2.1**): peak 2^* at 8.32 min corresponds to a mass of 829^+ assigned to the natural product A828A; peak 1^* at 6.58 min to a mass of 749^+ assigned to a compound lacking the SO_3 group.

5.7. Comparison of the ^{1}H and ^{13}C NMR Spectra of Natural and Synthetic A828A

In general, the NMR spectra of aeruginosin 828A (**2.1**) proved to be very sensitive in a sense that the water and salt content of the sample as well as the counterion present had an influence on the chemical shifts. In the ^{1}H NMR spectrum, the shifts of the O-H and N-H protons were affected the most. Also the C-H protons in close proximity to one of the ionic species of **2.1** – such as Adc-H5 and H6 – showed slight differences of 0.03 to 0.04 ppm in the chemical shift in a first measured sample (for numbering see Figure 24). Adjustment of the salt content in the NMR sample finally provided NMR spectra which were in an excellent accordance with the spectra of the isolated compound described in the literature (Table 3).[2] Most of the ^{1}H NMR shifts were either exactly the same or shifted by only +/–0.01 ppm, only the chemical shift of Adc N-H proton showed a difference of –0.02 ppm. For the ^{13}C NMR spectra, the situation was similar: most of the carbon signals exhibited precisely the same chemical shift or were shifted by only +/–0.1 ppm. An exception was the ^{13}C signal of Adc-C3 displaying a difference of –0.2 ppm. The recorded 2D NMR experiments such as HMBC, HSQC, COSY, NOESY and TOCSY were also in superb agreement with the spectra reported in the literature.[2] Thus, it was possible to conclude without any doubt that aeruginosin 828A (**2.1**) had been successfully synthesized *via* the developed synthetic strategy.

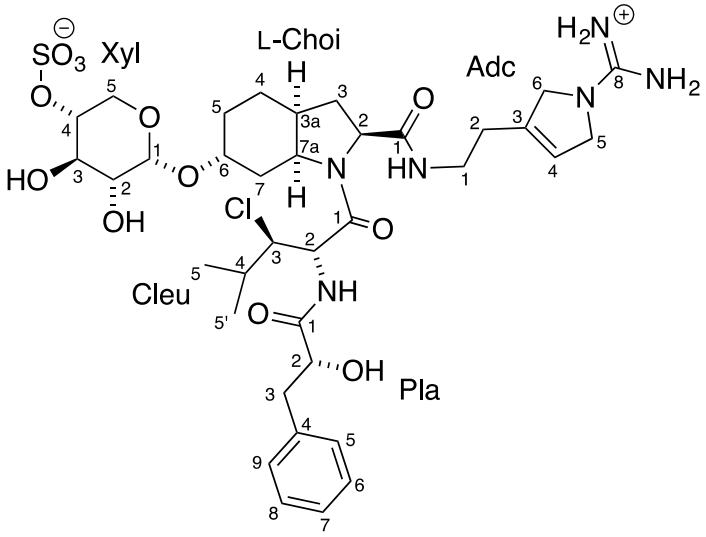

Figure 24 Atom numbering in aeruginosin 828A (**2.1**).

Table 3 Comparison of the ^{1}H and ^{13}C NMR shifts of natural[2] and synthetic A828A

		^{1}H shifts (ppm)			^{13}C shifts (ppm)		
Subunit	Position	A828A natural	A828A synthetic	$\Delta\delta$	A828A natural	A828A synthetic	$\Delta\delta$
Xyl	1eq	4.94	4.94	0.00	95.0	95.0	0.0
	2ax	3.28	3.28	0.00	71.8	71.8	0.0
	3ax	3.57	3.57	0.00	71.4	71.4	0.0
	4ax	3.93	3.93	0.00	74.7	74.7	0.0
	5ax	3.36	3.36	0.00	59.3	59.3	0.0
	5eq	3.67	3.66	–0.01	-	-	-
	2-OH	4.41	4.40	–0.01	-	-	-
	3-OH	4.96	4.95	–0.01	-	-	-
Choi	1	-	-	-	171.1	171.1	0.0
	2	4.18	4.17	–0.01	59.5	59.5	0.0
	3	2.01	2.00	–0.01	30.5	30.6	+0.1
	3'	1.81	1.80	–0.01	-	-	-
	3a	2.25	2.24	–0.01	35.6	35.6	0.0
	4	2.14	2.15	+0.01	19.1	19.1	0.0
	4'	1.48	1.47	–0.01	-	-	-
	5	1.49	1.49	0.00	24.4	24.5	+0.1
	5'	1.54	1.54	0.00	-	-	-
	6	3.83	3.83	0.00	68.4	68.4	0.0
	7	1.58	1.57	–0.01	28.4	28.4	0.0
	7'	2.25	2.25	0.00	-	-	-
	7a	4.32	4.32	0.00	54.1	54.1	0.0
Pla	1	-	-	-	172.5	172.3	–0.2
	2	4.18	4.18	0.00	71.5	71.4	–0.1
	3	2.79	2.79	0.00	39.7	39.8	+0.1
	3'	2.96	2.96	0.00	-	-	-
	4	-	-	-	137.9	137.8	–0.1
	5,9	7.23	7.24	+0.01	129.5	129.5	0.0
	6,8	7.26	7.26	0.00	127.7	127.7	0.0
	7	7.18	7.18	0.00	125.8	125.8	0.0
Cleu	1	-	-	-	167.4	167.3	–0.1
	2	4.93	4.92	–0.01	50.9	51.0	+0.1
	3	4.00	3.99	–0.01	68.6	68.6	0.0
	4	1.71	1.71	0.00	27.3	27.4	+0.1
	5	0.87	0.87	0.00	15.3	15.3	0.0
	5'	0.86	0.86	0.00	20.6	20.6	0.0
	NH	7.68	7.67	–0.01	-	-	-
Adc	1	3.16	3.16	0.00	36.3	36.3	0.0
	1'	3.23	3.24	+0.01	-	-	-
	2,2’	2.25	2.25	0.00	28.1	28.2	+0.1
	3	-	-	-	136.1	135.9	–0.2
	4	5.61	5.61	0.00	119.0	119.0	0.0
	5	4.07	4.07	0.00	53.6	53.6	0.0
	6	4.07	4.07	0.00	54.9	54.9	0.0
	NH	8.00	7.98	–0.02	-	-	-
	8	-	-		154.9	154.9	0.0

5.8. Synthesis and Isolation of Synthetic Analogue Aeruginosin 748A

Late stage intermediate **2.84** served as precursor for the synthetic analogue aeruginosin 748A (**2.12**). Global deprotection of tetrapeptide **2.84** by treatment with a diluted TFA solution in CH_2Cl_2 provided analogue A748A (**2.12**) as crude residue (Scheme 17). After fractionated HPLC purification, 1.0 mg of pure A748A (**2.12**) was obtained as a white amorphous solid in a good yield of 70%.

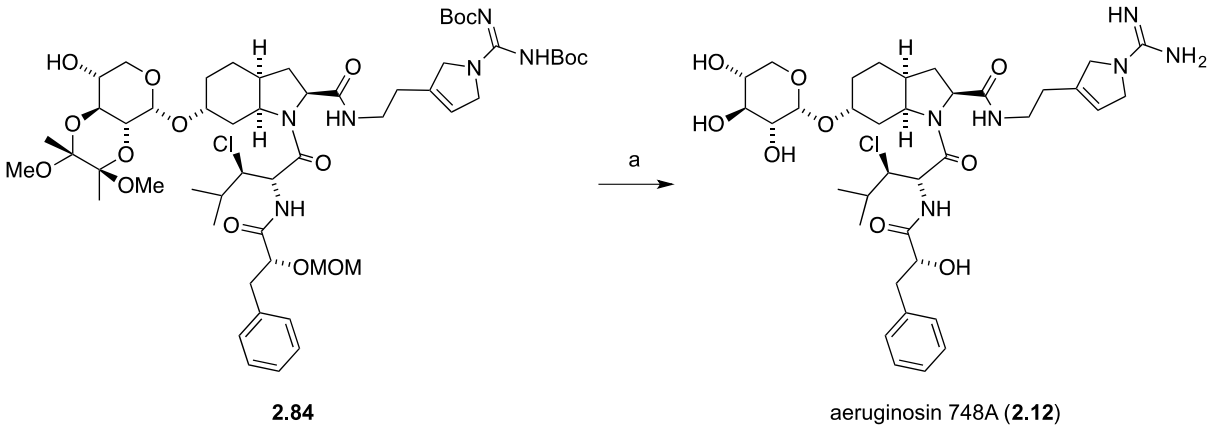

2.84 aeruginosin 748A (**2.12**)

Scheme 17 Preparation of synthetic analogue aeruginosin 748A (**2.12**). Reagents and conditions: a) CH_2Cl_2/TFA (10:1), r.t., 7 h, 70%.

5.9. Comparison of the ^{1}H and ^{13}C NMR Spectra of A748A and A828A

Confirmation of the obtained desired structure of A748A (**2.12**) was achieved by analysis of 1D (^{1}H and ^{13}C) and 2D NMR spectra (HMBC, HSQC, COSY and NOESY) as well as by comparison of the spectra with those of A828A (**2.1**). Table 4 shows the compared values of the ^{1}H and ^{13}C chemical shifts of the Xyl moiety of A748A (**2.12**) and A828A (**2.1**), which is affected the most. Expected upfield shifts are observed for the Xyl-H4 and Xyl-C4 signals of –0.64 ppm and –4.9 ppm, respectively, caused by the electron-withdrawing nature of the SO_3 group at O4 position (see highlighted entries in Table 4). Minor shifts to higher field were also detected for all other proton signals within the Xyl residue. Further, expected deshielding effects for the carbon atoms in β position to O4 were observed for C3 (+1.9 ppm) and C5 (+2.4 ppm), going from sulfated (A828A) to hydroxyl containing Xyl (A748A).[54] The ^{1}H and ^{13}C NMR signals of the L-Choi, Adc, Cleu and Adc residues of **2.12** showed very similar shifts and coupling constants to those of A828A (**2.1**), constituting that the desired compound A748A (**2.12**) had effectively been synthesized.

Table 4 Comparison of the ^{1}H and ^{13}C NMR shifts of the Xyl moieties of natural A828A (**2.1**) and synthetic analogue A748A (**2.12**).

		^{1}H shifts (ppm)			^{13}C shifts (ppm)		
Subunit	Position	A828A	A748A	$\Delta\delta$	A828A	A748A	$\Delta\delta$
Xyl	1eq	4.94	4.96	–0.02	95.0	95.2	+0.2
	2ax	3.28	3.24	–0.04	71.8	71.8	0.0
	3ax	3.57	3.43	–0.14	71.4	73.3	+1.9
	4ax	3.93	3.29	–0.64	74.7	69.8	–4.9
	5ax	3.36	3.30	–0.16	59.3	61.7	+2.4
	5eq	3.67	3.40	–0.27	-	-	-

5.10. Synthesis of Aeruginoside 126A

Following the strategy developed for the synthesis of aeruginosin 828A (**2.1**) and synthetic analogue aeruginosin 748A (**2.12**), the preparation and isolation of aeruginoside 126A (**2.11**) was investigated (Scheme 18). For the synthesis of **2.11**, the Cleu-Pla-OH dipeptide **2.47**, used for the synthesis of A828A (**2.1**), was replaced by Leu-Pla-OH dipeptide **2.53** in the first peptide coupling step to access tripeptide **2.86** in a moderate yield of 58%. For the peptide coupling the same conditions with DMTMM as coupling reagent were used as in the synthesis of A828A (**2.1**). Further, under basic conditions, the methyl ester of the xylosylated Pla-Cleu-L-Choi tripeptide **2.86** was converted into the corresponding acid and the hydroxyl group at O4 position of the xylosyl moiety was liberated giving acid **2.87** in an excellent yield. The improved yield of 95% for the saponification and deprotection, compared to the 77% obtained in the synthesis of A828A (**2.1**), can be explained by the fact that an elimination reaction is not possible in tripeptide **2.86**. Second peptide coupling of tripeptide **2.87** with Adc subunit **2.63** promoted by PyBOP and 2-6-lutidine afforded tetrapeptide **2.88** in a yield of 64%. The only step missing to complete the total synthesis of aeruginoside 126A (**2.11**) was the global removal of the protecting groups, which was carried out in a diluted TFA/CH_2Cl_2 solution. The reaction progression was followed by UPLC showing a fast cleavage of the Boc and the BDA groups, whereas the MOM group proved to be more stable. After seven hours the reaction was stopped in order to prevent side reactions regardless of the incomplete deprotection of the MOM group. The obtained crude residue was subjected to fractionated HPLC purification leading to a separation of A126A (**2.11**) from the product which still contained the MOM protecting group on the Pla residue. Doing so, 1.3 mg of A126A (**2.11**) could be isolated as a white amorphous solid.

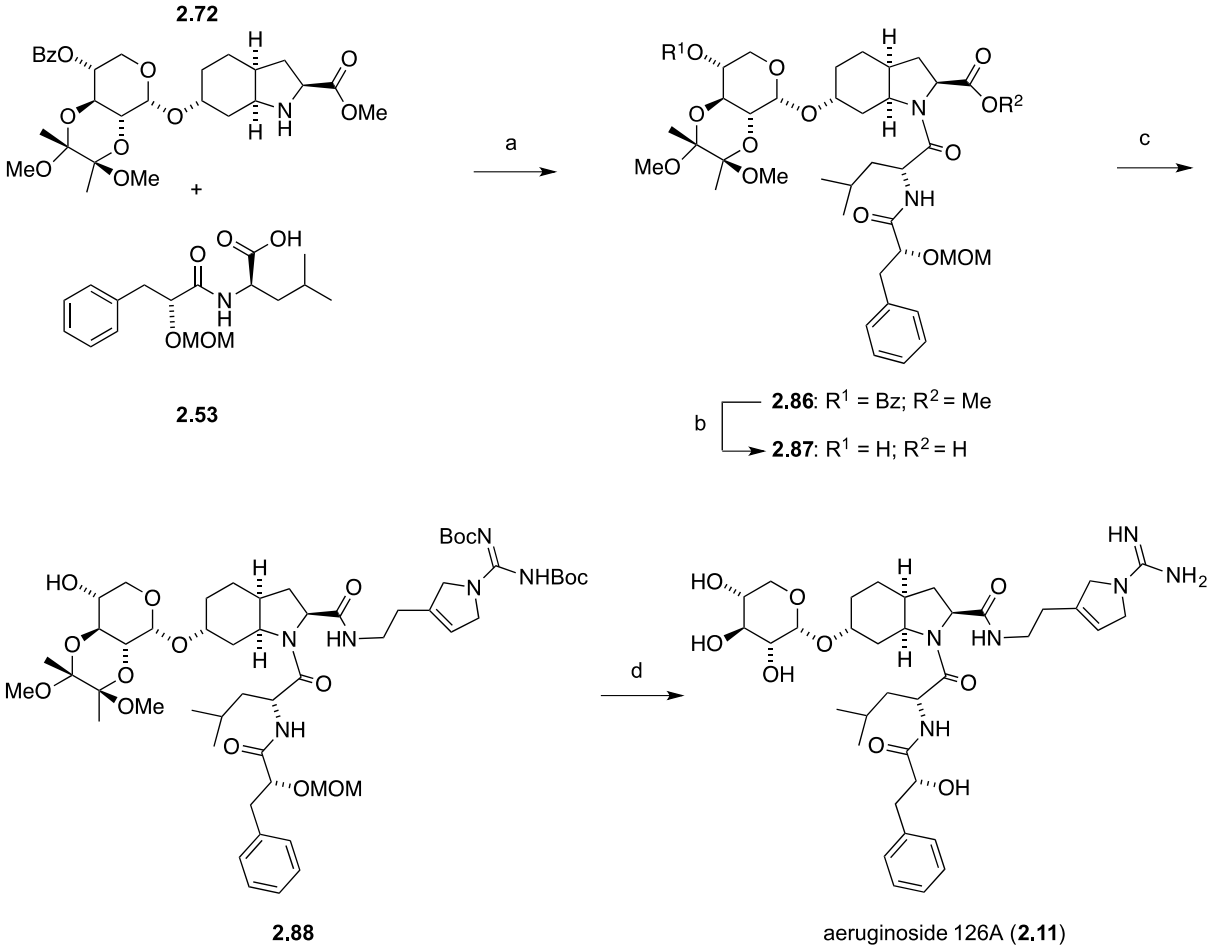

Scheme 18 Synthesis of aeruginoside 126A (**2.11**). Reagents and conditions: a) DMTMM, NMM, CH_2Cl_2, 0 °C to r.t., 3 h, 58%; b) 0.1 M LiOH, THF/H_2O (5:3), r.t., 12 h, 95%; c) Adc subunit **2.63**, PyBOP, 2,6-lutidine, CH_2Cl_2, 0 °C to r.t., 4.5 h, 64%; d) CH_2Cl_2/TFA (10:1), r.t., 7 h, 73%.

5.11. Comparison of ^{1}H and ^{13}C NMR Spectra of Natural and Synthetic A126A

The NMR spectra obtained from our synthesized A126A (**2.11**) and the spectra from the isolation work were compared.[25] Both spectra showed the presence of two conformers, further referred to as rotamers, in a ratio of 3.5:1 and 3:1, respectively. The conformational behavior of the synthesized aeruginosins will be discussed in more detail in Section 5.14. Furthermore, the ^{1}H NMR spectra of synthetic and natural A126A (**2.11**) revealed a good but not an excellent accordance (Table 5). All required proton signals from the ^{1}H NMR spectrum of natural A126A (**2.11**)[25] could be assigned to signals in our recorded ^{1}H NMR spectrum of synthetic A126A (**2.11**). Small differences in the chemical shifts were, however, observed (for the largest divergences see entries highlighted in red in Table 5). These chemical shift deviations are in a range of –0.08 ppm for Leu H3' to +0.08 ppm for Pla H3, except for the shift of Leu N-H which shows a difference of –0.23 ppm (for labeling and numbering see Figure 25). All necessary carbon signals of the literature[25] ^{13}C NMR spectrum could also be assigned to signals in our recorded spectrum. The chemical shift differences in the ^{13}C NMR spectrum lie in a range of –1.0 ppm for Pla C1 to +0.2 ppm for Leu C2 (for labeling and numbering see Figure 25). In general, the ^{13}C signals of synthetic A126A (**2.11**) are shifted to lower frequency than the signals of natural A126A (**2.11**).[25] Examining the differences of the spectra in more detail, it was revealed that the Pla and Leu units showed the largest deviations. However, a wrong configuration of these units can be excluded: the absolute stereochemistry of the Pla and Leu units was determined after acidic hydrolysis by chromatography on a chiral stationary phase. By comparison of the retention times to those of authentic standards during isolation work, a D configuration of the Pla and Leu moieties was identified. In our synthetic work, the absolute stereochemistry of the Pla and Leu units was determined by comparison of the optical rotation values to those described in the literature: a positive value for the rotation of the Pla moiety and a negative value for the Leu unit were obtained, both corresponding to a D configuration. Another reason for the differences in the NMR spectra could be that natural A126A (**2.11**) incorporates a xylose moiety with L configuration instead of the D-xylose in synthetic A126A (**2.11**), since the absolute configuration of the xylose residue could not be determined during isolation work. Nevertheless, the scarcity of L-xylose in nature and the almost identical shifts of the ^{1}H and ^{13}C signals in the xylose moiety of natural and synthetic A126A (**2.11**) suggest a D configuration of the xylose in natural A126A (**2.11**). Also the chemical shifts of the L-Choi and Adc units in the natural and synthetic A126A (**2.11**) were in a very good agreement with each other confirming the right confirmation of these units. So where do the observed

differences in the shifts of the NMR spectra arise from? As already described in Section 5.9, the recorded NMR spectra are sensitive with respect to water and salt concentration within the sample. Further, the counterion present in the compound can affect the chemical shifts of the signals. In the isolation work, HPLC purification was performed with aqueous acetonitrile containing 0.05% *v/v* TFA instead of the 0.1% *v/v* formic acid we used as eluent. Therefore, the counterions of natural and synthetic A126A (**2.11**) were not the same, which might be one explanation for differences in the shifts of the ^{1}H and ^{13}C spectra. Additionally, the spectra of the isolation work were recorded on a 500 MHz spectrometer[25] whereas our samples were measured on a 600 MHz spectrometer. Moreover, the temperature at which the NMR experiments were carried out is not apparent from the supporting information of the literature. A difference of the temperature could also be a reason for small deviations in the chemical shifts in the spectra (the influence of the temperature on the shifts of the rotamers will be discussed in more detail in Section 5.14.1). To conclude, the desired natural product A126A (**2.11**) was successfully synthesized with very high probability, regardless of the circumstance that the recorded NMR spectra were not in full agreement with those reported in literature.[25] However, definite confirmation could only be gained by either mixing equimolar amounts of synthetic and isolated samples for NMR experiments or by HPLC co-injection of both samples.

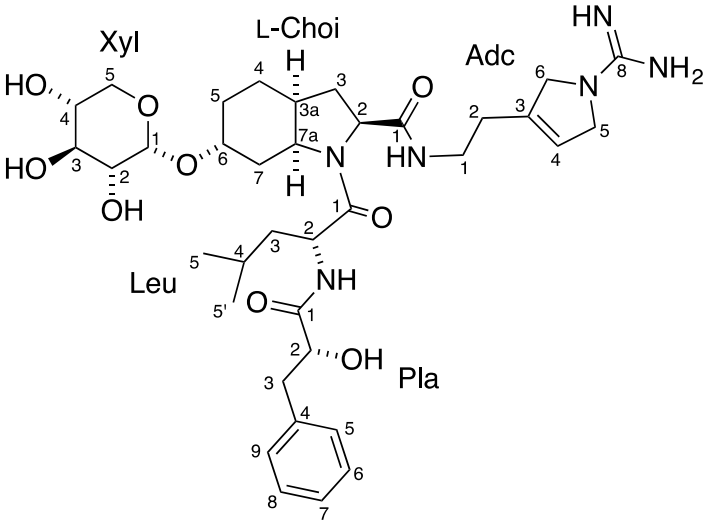

Figure 25 Atom labeling and numbering in aeruginosin 126A (**2.11**).

Table 5 Comparison of the ^{1}H and ^{13}C NMR shifts of natural[25] and synthetic A126A (**2.11**)

		^{1}H shifts (ppm)			^{13}C shifts (ppm)		
Subunit	Position	A126A natural	A126A synthetic	$\Delta\delta$	A126A natural	A126A synthetic	$\Delta\delta$
Xyl	1eq	4.81	4.81	0.00	96.5	96.4	–0.1
	2ax	3.21	3.22	+0.01	71.9	71.7	–0.2
	3ax	3.40	3.40	0.00	73.4	73.2	–0.2
	4ax	3.28	3.28	0.00	70.0	69.8	–0.2
	5ax	3.34	3.34	0.00	62.1	62.0	–0.1
	5eq	3.39	3.40	+0.01	-	-	-
Choi	1	-	-	-	171.4	170.8	–0.6
	2	4.18	4.14	–0.04	59.8	59.7	–0.1
	3	2.04	2.01	–0.03	30.5	30.4	–0.1
	3'	1.78	1.77	–0.01	-	-	-
	3a	2.28	2.31	+0.01	36.1	35.8	–0.3
	4	2.08	2.09	+0.01	19.5	19.3	–0.2
	4'	1.47	1.47	0.00	-	-	-
	5	1.49	1.49	0.00	24.5	24.2	–0.3
	5'	1.56	1.56	0.00	-	-	-
	6	3.84	3.84	0.00	70.1	69.8	–0.3
	7	1.57	1.61	+0.04	29.2	29.1	–0.1
	7'	2.27	2.26	–0.01	-	-	-
	7a	4.15	4.12	–0.03	54.1	53.7	–0.4
Pla	1	-	-	-	173.2	172.2	–1.0
	2	4.11	4.12	+0.01	72.0	71.5	–0.5
	3	2.65	2.73	+0.08	40.4	39.9	–0.5
	3'	2.95	2.99	+0.04	-	-	-
	4	-	-	-	138.4	137.7	–0.7
	5,9	7.21	7.22	+0.01	129.3	129.3	0.0
	6,8	7.24	7.25	+0.01	127.9	127.6	–0.3
	7	7.16	7.18	+0.02	125.9	125.7	–0.2
Leu	1	-	-	-	169.9	-	-
	2	4.50	4.56	+0.06	48.6	47.8	–0.8
	3	1.34	1.28	–0.06	41.0	41.2	+0.2
	3’	1.46	1.38	–0.08	-	-	-
	4	1.48	1.48	0.00	24.1	24.2	+0.1
	5	0.86	0.86	0.00	21.8	21.6	–0.2
	5'	0.84	0.82	–0.02	23.3	23.3	0.0
	NH	7.76	7.53	–0.23	-	-	-
Adc	1	3.17	3.19	+0.02	36.6	36.3	–0.3
	1'	3.21	3.19	–0.02	-	-	-
	2	2.28	2.26	–0.02	28.2	28.1	–0.1
	2’	2.26	-	-	-	-	-
	3	-	-	-	136.2	-	-
	4	5.61	5.62	+0.01	119.1	119.0	–0.1
	5	4.10	4.07	–0.03	54.1	53.7	–0.4
	6	4.09	4.07	–0.02	55.3	54.9	–0.4
	NH	7.74	7.81	+0.07	-	-	-
	8	-	-	-	154.2	-	-

5.12. Synthesis and Isolation of Synthetic Analogue Aeruginosin 794A

Late stage intermediate **2.88** figured also as precursor for the synthesis of aeruginosin 794A (**2.13**). Introduction of the SO_3-group with a large excess of SO_3·pyridine complex gave tetrapeptide **2.89**. Further, global deprotection was carried out in a diluted TFA/CH_2Cl_2 solution, closely monitored by UPLC. Subsequent fractionated HPLC purification afforded 1.5 mg of the desired A794A (**2.13)** as a white amorphous solid in a yield of 75% over two steps (Scheme 19).

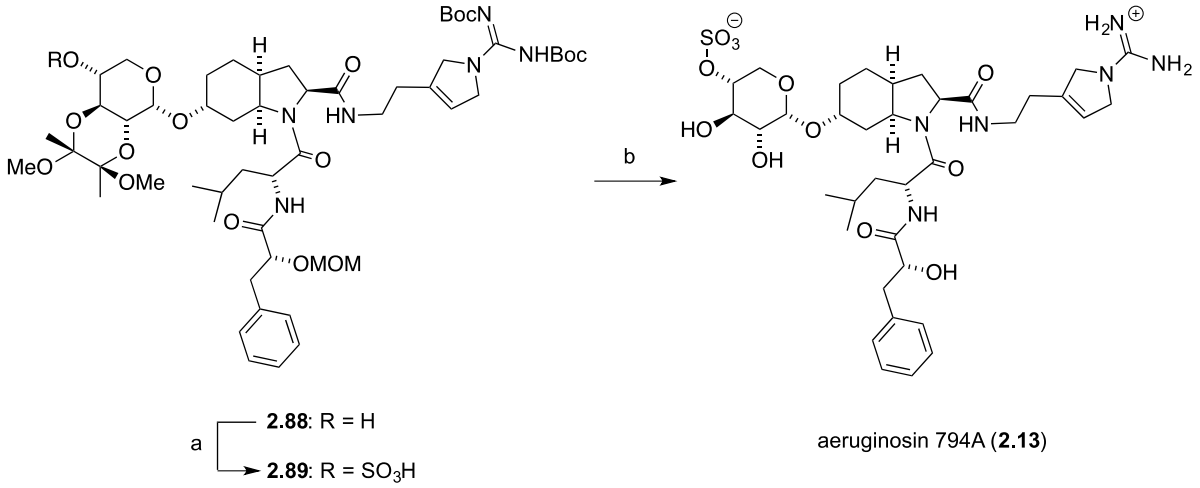

Scheme 19 Sulfonation of intermediate **2.88** and global deprotection – synthesis of aeruginosin 794A (**2.13**). Reagents and conditions: a) SO_3·pyridine (50.0 eq.), pyridine, 50 °C, 15 h; b) CH_2Cl_2/TFA (10:1), r.t., 5 h, 75% over two steps.

5.13. Comparison of the ^{1}H and ^{13}C NMR Spectra of A126A and A794A

The structure of A794A (**2.13**) was confirmed by 1D (^{1}H and ^{13}C) and 2D (HMBC, HSQC, COSY and NOESY) NMR spectroscopies as well as by comparison of the spectra with those of A126A (**2.11**). Like A126A (**2.11**), A794A (**2.13**) showed the presence of two different rotamers in a ratio of 4:1 in the NMR spectra. Table 6 shows the comparison of the ^{1}H NMR and ^{13}C chemical shifts of the Xyl moieties of A126A (**2.11**) and A794A (**2.13**) which are affected the most. Expected downfield shifts are observed for the Xyl-H4 and Xyl-C4 signals of +0.64 ppm and +4.9 ppm, respectively, caused by the electron-withdrawing nature of the SO_3 group at O4 position (see entries highlighted in red in Table 6). Minor shifts to higher field were detected for the other proton signals within the Xyl residue. Further, an expected shielding effect for the carbon atoms in β position to O4 was observed for C3 (–1.8 ppm) and C5 (–2.5 ppm), going from hydroxyl (A126A (**2.11**)) to sulfated Xyl (A794A (**2.13**)).[54] The

^{1}H and ^{13}C NMR signals of the L-Choi, Adc, Leu and Adc residues showed very similar shifts to those of A126A (**2.13**), corroborating that the desired compound A794A (**2.13**) had effectively been synthesized.

Table 6 Comparison of the 1H and 13C NMR shifts of the Xyl moieties of synthetic A126A and synthetic analogue A794A.

		^{1}H shifts (ppm)			^{13}C shifts (ppm)		
Subunit	Position	A126A	A794A	$\Delta\delta$	A126A	A794A	$\Delta\delta$
Xyl	1eq	4.81	4.81	0.00	96.4	96.2	–0.2
	2ax	3.22	3.27	+0.04	71.7	71.8	+0.1
	3ax	3.40	3.56	+0.16	73.2	71.4	–1.8
	4ax	3.28	3.92	+0.64	69.8	74.7	+4.9
	5ax	3.34	3.40	+0.06	62.0	59.5	–2.5
	5eq	3.40	3.67	+0.27	-	-	-

5.14. Conformational Analysis – The Presence of Rotamers

An interesting feature observed during the synthesis of A828A (**2.1**) and its analogues was the modulating impact of the chlorine atom on the conformation of the entire molecule: All the late stage intermediates containing the Cleu moiety, including A828A (**2.1**) and A748A (**2.12**), appeared as a single or as a high excess of one rotamer (>50:1). The congeners lacking the chlorine atom, including A126A (**2.11**) and A794A (**2.13**), were on the other hand present as a rotameric mixture of around 3.5:1, as visible in the ^{1}H and the ^{13}C NMR spectra. The ^{1}H NMR spectra of A828A (**2.1**) and A794A (**2.13**) are illustrated in Figure 28; for the ^{1}H NMR spectra of A748A (**2.12**) and A126A (**2.11**), see Figure 29. The presence of two conformers is caused by a rotational equilibrium of the L-Choi-Leu peptide bond which can possess either *cis* or *trans* conformation (Figure 26). Analysis of the ROESY spectra of A828A (**2.1**) and A748A (**2.12**) revealed the existence of the *trans* rotamer in **2.1** and **2.12**, as concluded due to observed NOEs between Cleu H2 and Choi (H7, H7' and H7a), respectively. As mentioned before, intermediates devoid of the chlorine atom appeared as a rotameric mixture. The presence of two rotamers in A126A (**2.11**) has already been reported in the isolation work of **2.11** by Dittmann and co-workers.[25] Additionally, it could be confirmed for A126A (**2.11**) and A794A (**2.13**) by exchange crosspeaks visible in the ROESY spectra between the methyl groups of both rotameric leucine units (Figure 27). Further, the *trans* rotamer was assigned as the major conformer, verified by similar NOEs as described before for **2.1** and **2.12**. The minor *cis* rotamer was identified by an observed NOE between

Leu H2 and L-Choi H2. To conclude, the halogen atom appears to have a critical effect on the conformation of the different aeruginosins by restricting the torsion angle of the L-Choi-Leu amide bond. A related phenomenon has already been described earlier by Hanessian and co-workers for unnatural aeruginosin hybrids.[15]

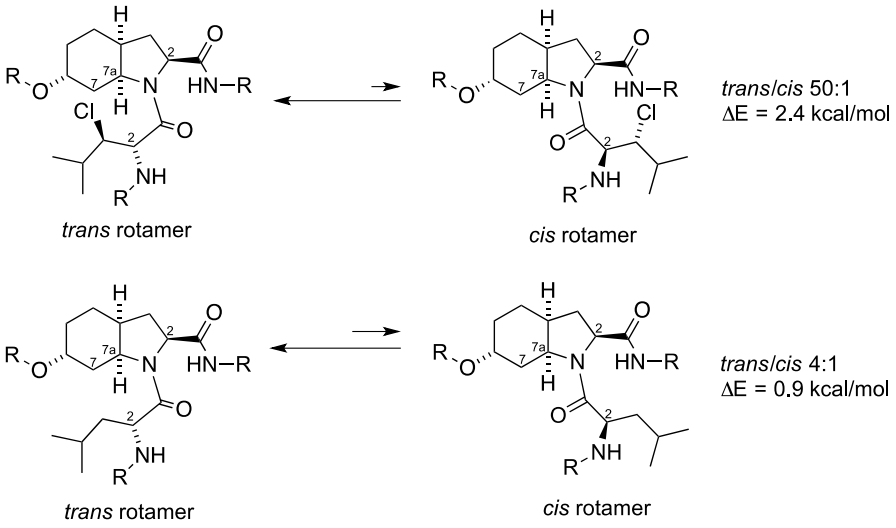

Figure 26 Amide isomer equilibria of the L-Choi-Cleu (top) and the L-Choi-Leu (bottom) peptide bonds.

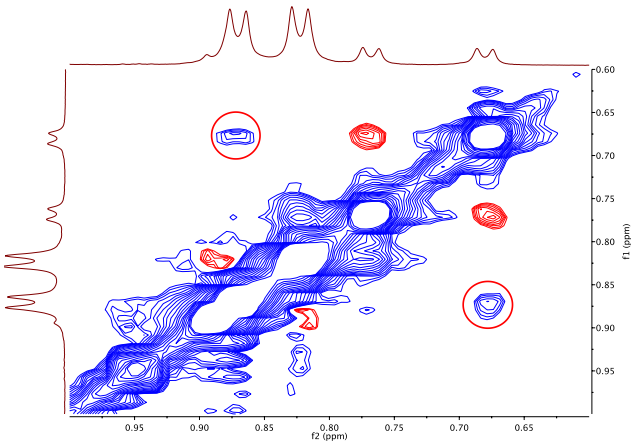

Figure 27 Selected part of the 2D ROESY NMR spectrum of A126A (**2.11**); exchange cross-peaks between the methyl groups of both rotameric leucine units are highlighted in red.

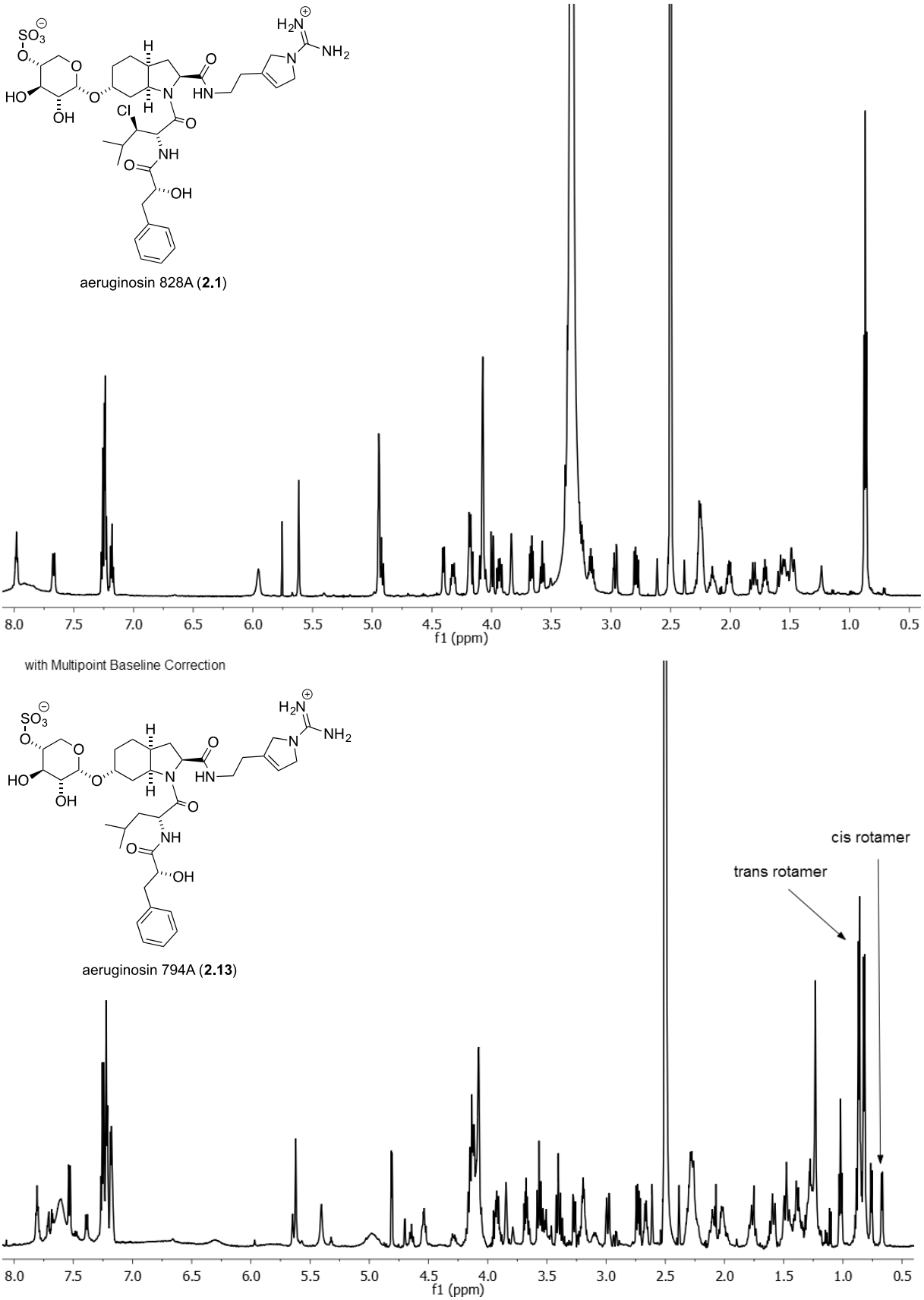

Figure 28 ^{1}H NMR spectra of A828A (**2.1**) (top) and A794A (**2.13**) (bottom), showing the presence of two rotamers in A794A (**2.13**).

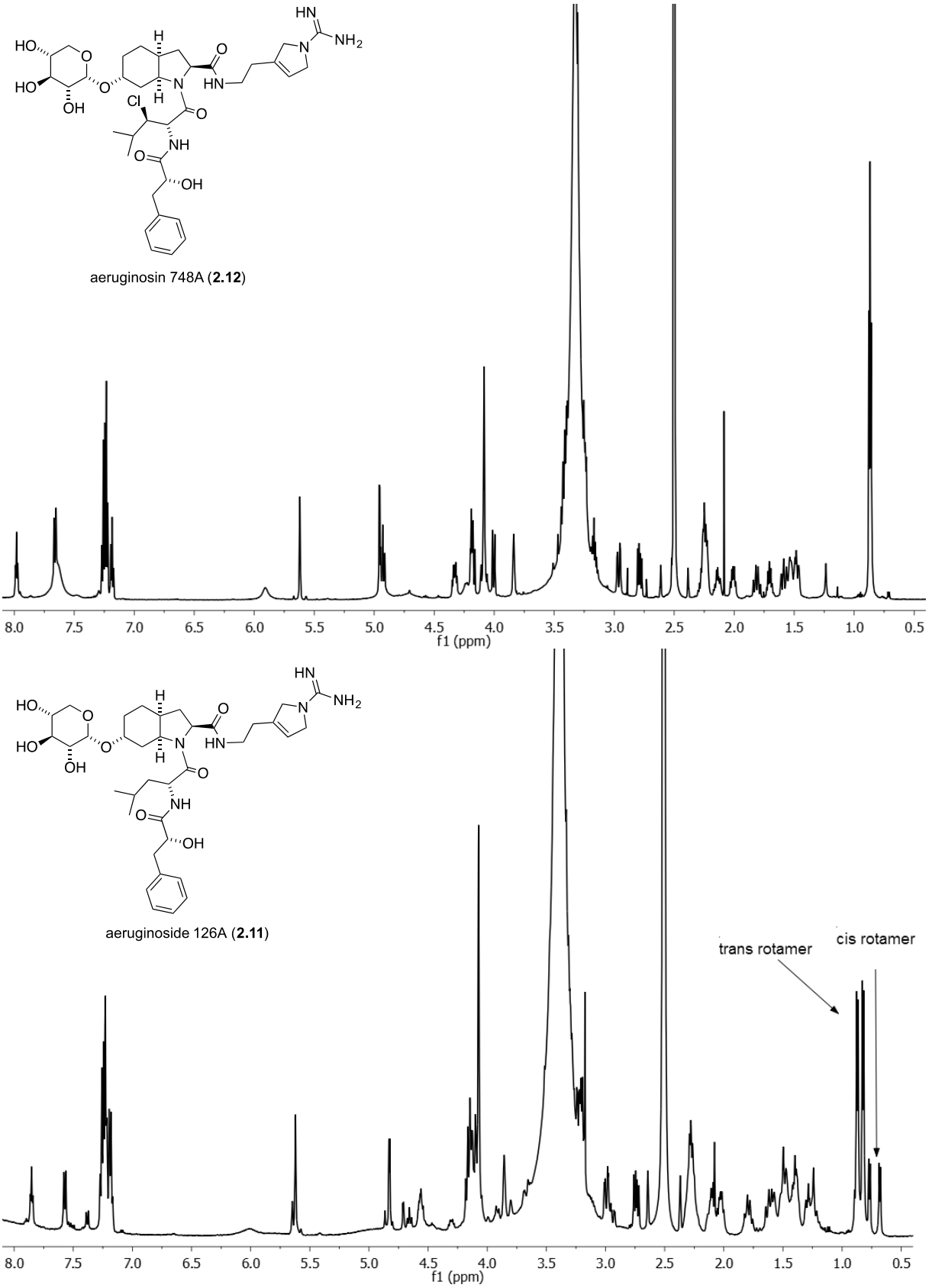

Figure 29 ^{1}H NMR spectra of A748A (**2.12**) (top) and A126A (**2.11**) (bottom), showing the presence of two rotamers in A126A (**2.11**).

5.14.1. Variable temperature NMR spectroscopy of L-Choi-Leu-Pla 2.90

For further investigations on the behavior of the two rotameric conformers, ^{1}H NMR experiments were conducted at elevated temperatures (300–400 K). NMR experiments were performed with the model substrate L-Choi-Leu-Pla (**2.90**) (Figure 30) which lacks the Xyl and Adc units (for the synthesis of **2.90** see Section 8.2.1). The Adc and Xyl residues showed to exert a negligible influence on the conformation of the rotamers, observed during the synthesis of A126A (**2.11**) and A794A (**2.13**). Therefore, **2.90** was chosen as model substrate. First, the NMR spectra are more easily interpreted when lacking two units and second, **2.90** should be more stable during the heating process since the Xyl and Adc units bear rather labile BDA and Boc protecting groups, respectively.[55] The proton signals of **2.90** showed sharp signals at room temperature and a rotameric mixture of 5:1. The most distinct effects upon increasing the temperature are illustrated with the following examples: The singlets of the L-Choi methyl esters of the *cis* and *trans* rotamers underwent a broadening of the peaks while increasing the temperature. At 400 K, just one broad merged signal for the methyl group was finally observed (highlighted in red, Figure 31). The signals for the Pla-H3' proton first showed a pair of doublets of doublets caused by the two rotamers. Elevating the temperature first led to broadening and merging of the two signals (360 K). Higher temperatures (>360K) induced a sharpening of the two merged signals to one defined doublet of doublet (highlighted in blue, Figure 31). The two singlets corresponding to the acetate group only showed merging of the two signals to one sharp singlet at 360 K (highlighted in yellow, Figure 31). No broadening of the peaks was observed for this signal while heating. The most distinctive effect was observed for the doublets of the *cis* and *trans* Leu H5 and H5', respectively: Heating the sample did not only lead to merging of the signals of the *cis* and *trans* rotamers, but also of the two H5 and H5' doublets to just one signal, when going from 360 K to 380 K (highlighted in green, Figure 31). This effect is caused by a slow, restricted rotation of the Leu C3-C4 bond at room temperature, resulting in two doublets for H5 and H5'. Increasing the temperature causes a faster rotation of the Leu C3-C4 bond and the formation of just one signal for H5 and H5'. Heating the sample to 400 K did not prove enough in order to access a sharp, fully merged signal for H5 and H5', since a small shoulder could still be detected. Nevertheless, the tendency of a merging process of the signals is clearly evident. Higher temperatures than 400 K were avoided to prevent the sample from decomposition.

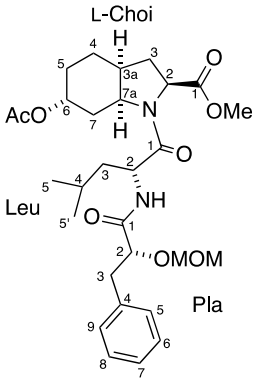

Figure 30 Atom labeling and numbering in L-Choi-Leu-Pla derivative **2.90**.

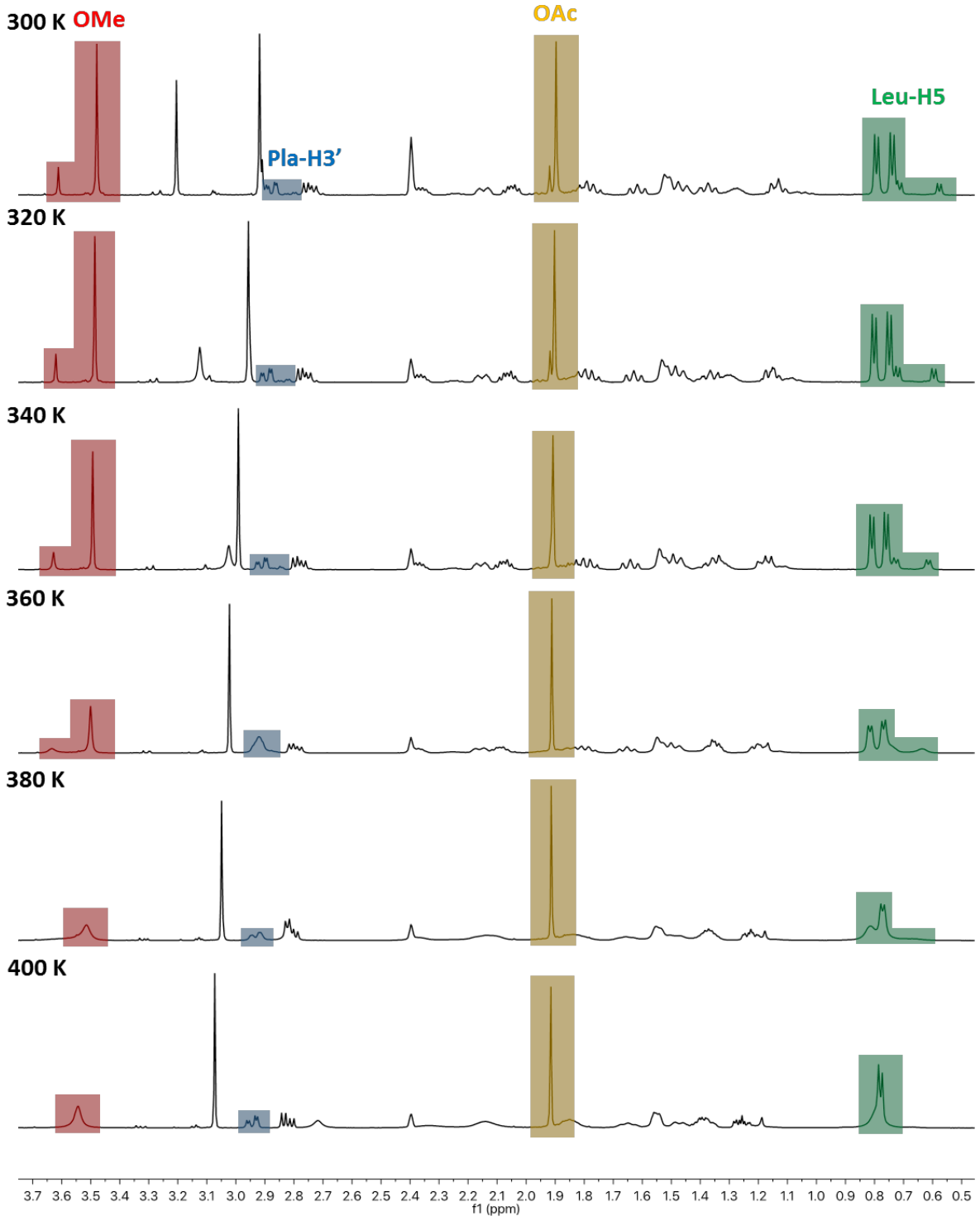

Figure 31 Selected region of the ^{1}H NMR spectra of **2.90** at different temperatures, from 300 to 400 K, with intervals of 20 K (top to bottom). Proton signals showing distinctive effects upon increasing temperature are shown in color. The ^{1}H NMR spectra were recorded in DMSO-*d6* on a 500 MHz spectrometer.

6. Evaluating the Toxicity of A828A, A126A, A748A and A794A

For the evaluation of the environmental toxicity of natural products A828A (**2.1**) and A126A (**2.11**) as well as for synthetic analogues A748A (**2.12**) and A794A (**2.13**), a standard assay with the sensitive freshwater crustacean *Thamnocephalus platyurus* was conducted. Following the standard procedure, six concentrations ranging from 0.41 µM to 100 µM for **2.1** and 1.2 µM to 150 µM for **2.11**, **2.12**, and **2.13** were prepared and tested in an acute toxicity assay (24 h). For every concentration, three to four experiments with 10 to 16 animals per experiment were performed. The mortality rates of the test organisms were determined by visual inspection of the animals after exposing them to a certain concentration for 24 h in the dark (Figure 32). A first topic of interest was the confirmation of the toxicity reported for **2.1** by Blom *et al*., who indicated an LC_{50} value of 22.4 µM for **2.1** against *T*. *platyurus*.[2] In fact, our assay with synthetic aeruginosin 828A (**2.1**) showed a reproducible toxicity with an LC_{50} value of 34.5 µM. Therefore, it could be proven that **2.1** is indeed responsible for the toxicity and that the toxicity assigned to **2.1** by Blom *et al*. had not been derived from a contamination with other toxins during isolation. The next focus lay on the evaluation of the effect of the chlorine atom and the sulfate group on the bioactivity. Conducting the assay with synthetic analogue A748A (**2.12**), which lacks the sulfate group, showed a toxicity of 24.2 µM, which is in the same range as that of A828A (**2.1**). Further, tests with dechloro derivative A794A (**2.13**) revealed an increased toxicity with an LC_{50} value of 12.8 µM, compared to 34.5 µM of A828A (**2.1**). As already discussed in Section 5.14, the chlorine substituent has a strong impact on the conformation of the aeruginosin. Reported SAR studies with unnatural aeruginosin hybrids bearing either a Cleu or a Leu residue revealed that the chlorine substituent in the leucine moiety is important for the inhibition of enzymes such as thrombin (for more details see Section 1.2.1).[15] In terms of toxicity, however, this "chlorine effect" appears to be detrimental, which is likely due to restricted rotation around the L-Choi-Leu peptide bond, which could result in an entropic penalty. Most interestingly, the natural occurring A126A (**2.11**), which contains neither the sulfate group nor a chlorine substituent, showed a significantly lower toxicity with an LC_{50} of 57.7 µM. From the conducted toxicity assays, the following conclusions can be drawn: 1) the introduction of either chloride or sulfate functionalities leads to an increased toxicity, and 2) the chloride group in combination with the sulfate moiety results in a slight attenuation of the toxicity. These hypotheses go along with the ecological observations that chlorosulfopeptides such as A828A (**2.1**) are produced in microcystin deficient, but still toxic cyanobacteria, in contrast to non-chlorinated

and non-sulfated aeruginosins, like A126A (**2.11**), which are present in cyanobacteria strains able to produce microcystins.[1,23,24] Further, one can assume that the toxicity of aeruginosins is caused by a mode of action other than the inhibition of proteases like thrombin and trypsin, since chlorinated aeruginosins **2.1** and **2.12** showed no enhanced toxicity compared to dechloro congener **2.13**. An enhanced protease inhibition can however be expected for chlorinated aeruginosins **2.1** and **2.12**, since such a "chlorine effect" has also been observed for similar aeruginosins[15] and strong protease inhibition has indeed been detected for A828A (**2.1**).[2] This hypothesis is supported by Blom and co-workers who reported on the absence of correlation between toxicity and protease inhibitory action of MCs.[3] However, this theory can only be proven by comparison of the enzyme inhibition of chlorinated aeruginosins **2.1** and **2.12** with those of non-chlorinated **2.11** and **2.13**. This dual use of A828A (**2.1**) – not only as strong protease inhibitor but also as toxin – might be the reason for the loss of MC production of certain bacteria strains, since MC production became obsolete in the presence of A828A (**2.1**). Therefore, the production of MCs provided no further advantage for the bacteria but only required a lot of energy to create. This might be an explanation for the evolutionary inactivation of the mcy gene cluster of some strains. All in all, the obtained results support the hypothesis that chlorosulfopeptides restore the toxic phenotype of cyanobacteria.

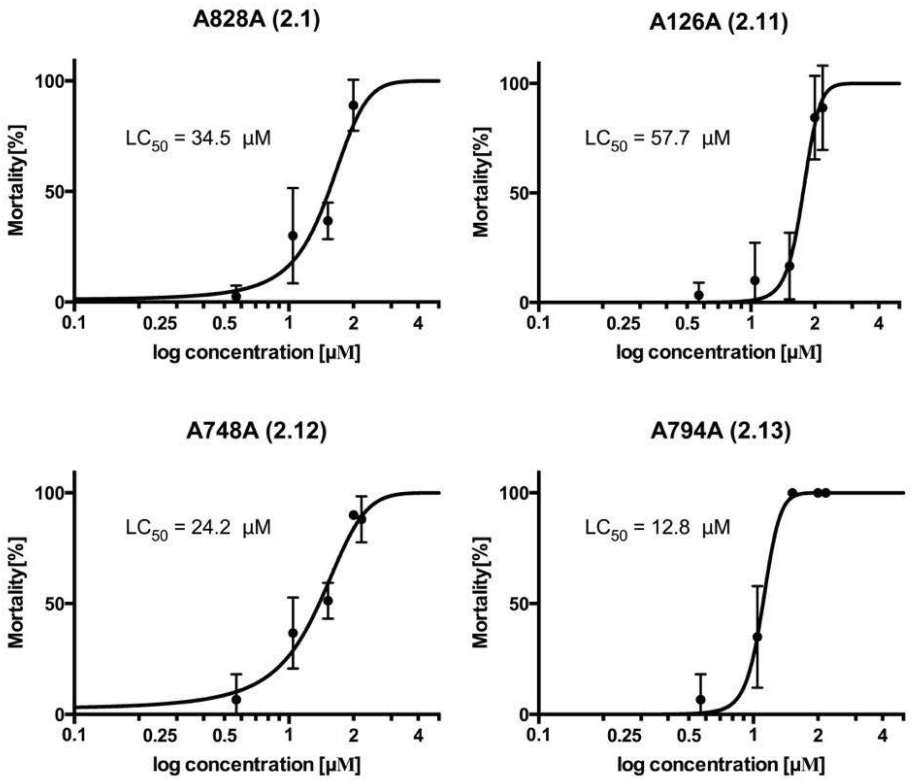

Figure 32 Mortality of *T. platyurus* as a function of the concentration of A828A (**2.1**), A126A (**2.11**), A748A (**2.12**) and A794A (**2.13**). Values are given as the mean of three independent experiments with 10 to 16 animals; error bars denote the standard error of the mean value.

7. Synthesis and Biological Activity of Aglycone A616A

7.1. Synthesis of Aglycone A616A

For further investigations on the toxicity and for studies on the influence of the xylose moiety, the aglycone A616A (**2.91**) of natural product A828A (**2.1**) was synthesized (Scheme 20): Cbz protected L-Choi derivative **2.35** was transferred to the corresponding free amine using a catalytic hydrogenation reaction with Pd/C to give amine **2.92** in a good yield.[27] The poor reactivity of the catalytic hydrogenation seen for the deprotection of Xyl-L-Choi-Cbz **2.71** (for details see Section 5.2.) was not observed for substrate **2.35**. Therefore, the prevented reactivity of **2.71** against catalytic hydrogenation seems to be derived from the Xyl moiety attached to the L-Choi, caused *e.g.* by an increase of the sterical hindrance of the substrate.

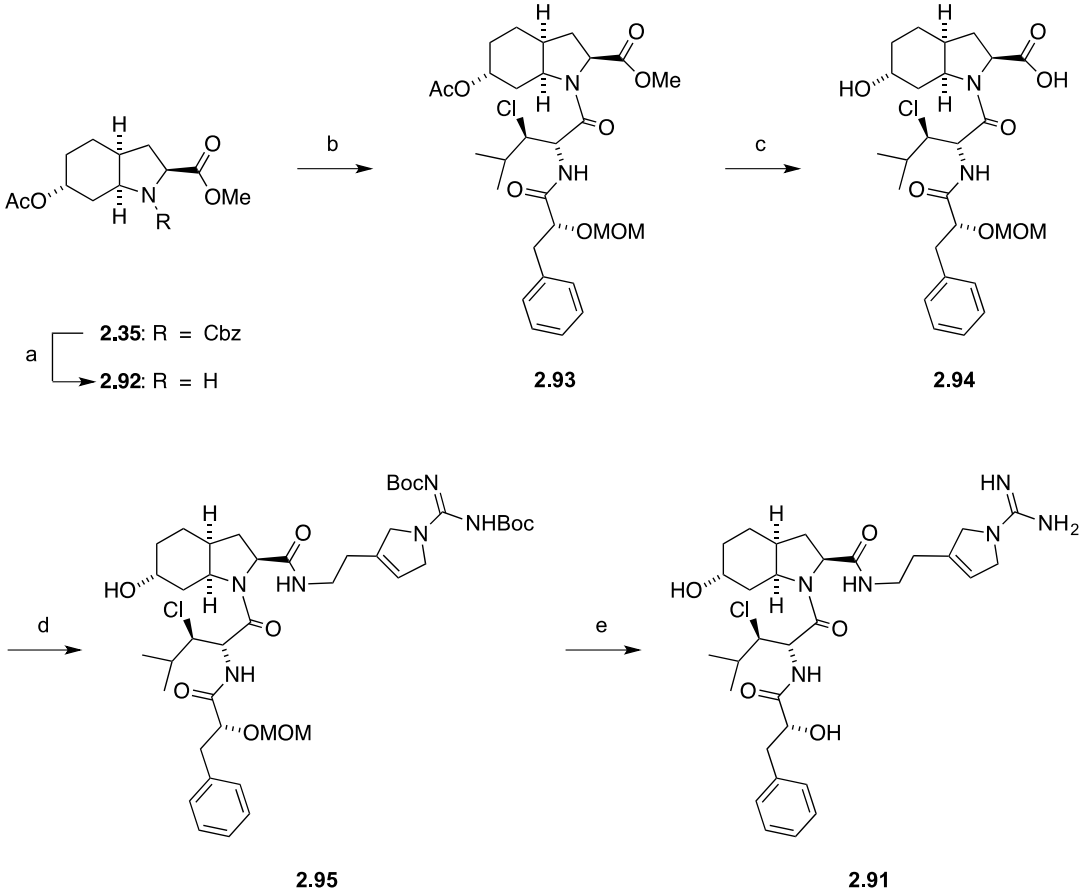

Scheme 20 Synthesis of aglycone A616A (**2.91**). Reagents and conditions: a) Pd/C, H_2 (1 bar), MeOH, r.t., 3.5 h, 76%; b) Pla-Cleu-OH **2.47**, DMTMM, NMM, CH_2Cl_2, 0 °C to r.t., 2 h, 83%; c) 0.1 M LiOH, THF/H_2O (5:3), r.t., 12 h, 76%; d) Adc subunit **2.63**, PyBOP, 2,6-lutidine, CH_2Cl_2, 0 °C to r.t., 5 h, 51%; e) CH_2Cl_2/TFA (10:1), r.t., 8 h, then K_2CO_3, H_2O, r.t., 30 min, 45%.

Peptide coupling of the obtained amine **2.92** with Pla-Cleu-OH subunit **2.47** provided tripeptide **2.93** in an excellent yield. Subsequent saponification of the methyl and acetyl ester in **2.93** to the corresponding acid and alcohol functionalities was carried out under basic conditions to afford Pla-Cleu-L-Choi-OH tripeptide **2.94**. Attachment of the Adc subunit **2.63** to the tripeptide **2.94** yielded tetrapeptide **2.95** in a moderate yield. Removal of the Boc and the MOM groups with a diluted TFA/CH_2Cl_2 solution was accompanied by the formation of trifluoroacetylated intermediate **2.96** (Scheme 21).[56] However, treatment of **2.96** with an aqueous K_2CO_3 solution for 30 min at room temperature finally provided aglycone A616A (**2.91**).

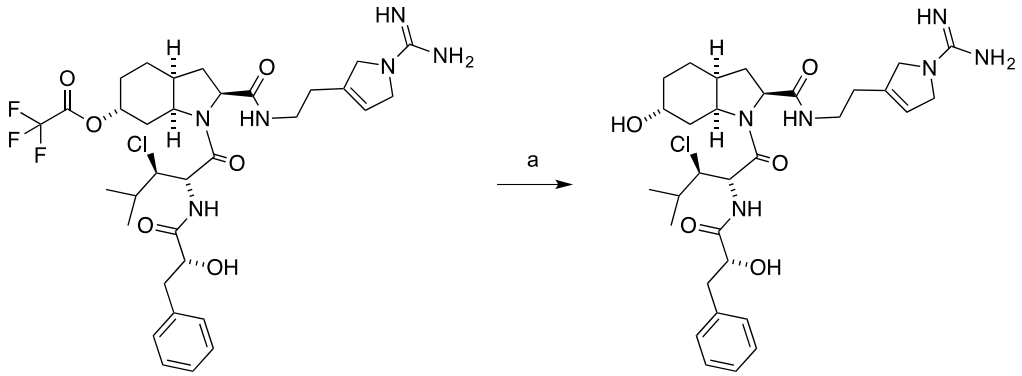

2.96 **2.91**

Scheme 21 Conversion of the trifluoroacetate intermediate **2.96** into aglycone A616A (**2.91**). Reagents and conditions: a) K_2CO_3, H_2O, r.t., 30 min.

7.2. Comparison of the NMR Spectra of A828A and A616A

The comparison of the ^{1}H and ^{13}C NMR signals of A828A (**2.1**) and A616A (**2.91**) is shown in Table 7; for atom numbering see Figure 33. The chemical shifts of the Adc and Pla groups of A828A (**2.1**) and A616A (**2.91**) were almost identical with deviations of only –0.02 to +0.03 ppm in the proton and –0.2 to +0.2 ppm in the carbon NMR spectra. The small chemical shift differences are due to the long distance of at least seven bonds of the Pla and Adc units from the site of xylosylation. Consequently, the signals of the L-Choi unit should be affected the most, which was confirmed by the recorded spectra, showing a deviation for the L-Choi ranging from –0.20 to +0.06 ppm in the proton and from –4.8 to +4.6 ppm in the carbon NMR spectra. The most distinct differences in the carbon NMR of the L-Choi unit are assigned to the signals of C5, C6 and C7. This agrees well with the theory which predicts a shielding of the carbon atom in α position, C6 (–4.8 ppm), and a deshielding of the carbon atoms in β position, C5 (+1.4 ppm) and C7 (+4.6 ppm), going from an acetal (A828A (**2.1**)) to a hydroxyl (A616A (**2.91**)) group.[54] Concerning the chemical shifts of the proton signals, shielding of the α position and deshielding of the β positions are expected for the aglycone.[54] Indeed, the recorded ^{1}H NMR spectrum showed a downfield shift for H6 (+0.06 ppm) and upfield shifts for H5 (–0.07 ppm), H5' (–0.11 ppm) and H7' (–0.20 ppm). Only for the signal of H7 (+0.05 ppm), a reversed shift was observed. The Cleu unit exhibited minor differences in the chemical shifts which can be explained by the *cis* configuration of the molecule, bringing the Cleu and the Xyl moiety in close proximity to each other, as is confirmed by NOEs arising between Cleu-H5 and Xyl (H2, H3 and 2-OH). In conclusion, the NMR spectra were in perfect agreement with the predictions, proving that aglycone A616A (**2.91**) had successfully been synthesized.

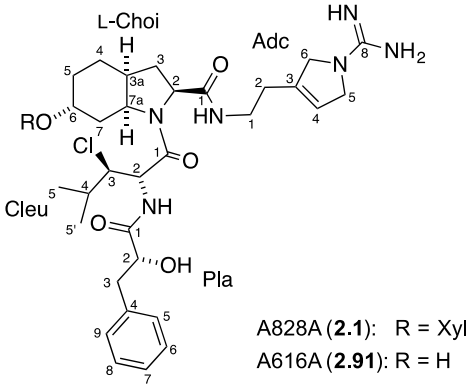

Figure 33 Atom numbering and labeling of A828A (**2.1**) and A616A (**2.91**).

Table 7 Comparison of the ^{1}H and ^{13}C NMR spectra of aglycone A616A (**2.91**) and natural product A828A (**2.1**). Most distinct deviations are highlighted in red.

		^{1}H shifts (ppm)			^{13}C shifts (ppm)		
Subunit	Position	A828A	A616A	$\Delta\delta$	A828A	A616A	$\Delta\delta$
Choi	1	-	-	-	171.1	171.0	–0.1
	2	4.17	4.17	+0.03	59.5	59.5	0.0
	3	2.00	1.98	–0.02	30.6	30.5	–0.1
	3'	1.80	1.79	–0.01	-	-	-
	3a	2.24	2.19	–0.05	35.6	35.6	0.0
	4	2.15	2.02	–0.13	19.1	18.7	–0.4
	4'	1.47	1.41	–0.06	-	-	-
	5	1.49	1.42	–0.07	24.5	25.9	+1.4
	5'	1.54	1.43	–0.11	-	-	-
	6	3.83	3.89	+0.06	68.4	63.6	–4.8
	7	1.57	1.62	+0.05	28.4	33.0	+4.6
	7'	2.25	2.05	–0.20	-	-	-
	7a	4.32	4.27	–0.05	54.1	54.4	+0.3
Pla	1	-	-	-	172.3	172.1	–0.2
	2	4.18	4.20	+0.02	71.4	71.4	0.0
	3	2.79	2.82	+0.03	39.8	39.7	–0.1
	3'	2.96	2.96	0.00	-	-	-
	4	-	-	-	137.8	137.8	0.0
	5,9	7.24	7.22	–0.02	129.5	129.5	0.0
	6,8	7.26	7.25	–0.01	127.7	127.6	–0.1
	7	7.18	7.19	+0.01	125.8	125.8	0.0
Cleu	1	-	-	-	167.3	167.6	+0.3
	2	4.92	4.89	–0.03	51.0	50.8	–0.2
	3	3.99	3.94	–0.05	68.6	68.8	+0.2
	4	1.71	1.65	–0.06	27.4	27.3	–0.1
	5	0.87	0.85	–0.02	15.3	14.9	–0.4
	5'	0.86	0.84	–0.02	20.6	20.4	–0.2
	NH	7.67	7.55	–0.12	-	-	-
Adc	1	3.16	3.17	+0.01	36.3	36.3	0.0
	1'	3.24	3.24	0.00	-	-	-
	2,2’	2.25	2.24	–0.01	28.2	28.1	–0.1
	3	-	-	-	135.9	136.1	+0.2
	4	5.61	5.61	0.00	119.0	119.0	0.0
	5	4.07	4.07	0.00	53.6	53.7	+0.1
	6	4.07	4.07	0.00	54.9	54.9	0.0
	NH	7.98	7.96	–0.02	-	-	-
	8	-	-		154.9	-	-

7.3. Toxicity of Aglycone 616A

For the evaluation of the environmental toxicity of A616A (**2.91**), a standard assay with the sensitive freshwater crustacean *Thamnocephalus platyurus* was conducted. Six concentrations of A616A (**2.91**) ranging from 1.2 µM to 150 µM were prepared and tested in an acute toxicity assay (24 h); the results are shown in Figure 34. For each concentration, three experiments with ten animals were performed. The mortality rate of the test organisms was determined by visual inspection of the animals after exposing them to a defined concentration for 24 h in the dark. The thus obtained LC_{50} value of 21.0 µM for A616A (**2.91**) was in the same range as the toxicity of A828A (**2.1**) and A748A (**2.12**). Therefore, the bioassay supports the hypothesis that the Xyl residue has a negligible effect on the toxicity of the aeruginosin. However, incorporation of the Xyl residue leads to a better solubility in water of the corresponding aeruginosin. Since the tested concentrations of 1.2 µM to 150 µM corresponded to high dilution, solubility was not an issue in this case. A possible advantageous effect of the Xyl moiety on the toxicity might hence be only observed at higher concentrations. Another reason for the incorporation of the Xyl residue in A828A (**2.1**) could be a facilitated cell uptake of the glycosylated aeruginosin compared to the aglycone. However, these hypotheses need to be investigated in more detail.

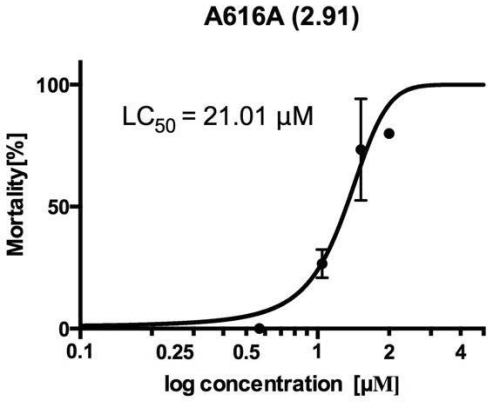

Figure 34 Mortality of *T. platyurus* as a function of the concentration of A616A (**2.91**). Values are given as the mean of three independent experiments with 10 animals; error bars denote the standard error of the mean value.

8. Alternative Approaches – Synthesis of Aeruginosin 828B

In the following sections alternative synthetic approaches, which were performed in the pursuit of the successful total synthesis of aeruginosin 828A (**2.1**), will be discussed. The focus was laid especially on an alternative introduction of the sulfate group and a different assembly of the building blocks, including a late stage glycosylation.

8.1. Introduction of the Sulfate Group as a Protected Trichloroethyl (TCE) Ester

One anticipated drawback in the synthetic strategy for the assembly of A828A (**2.1**), as described in Section 5, was the introduction of the sulfate group with subsequent global acidic deprotection, regarding that sulfate groups are known to be sensitive to acidic conditions.[57] This assumption was supported by first experiments which indeed indicated a loss of the sulfate group according to UPLC mass analysis. Moreover, using a large excess of 50 equivalents of SO_3·pyridine complex for the introduction of the sulfate group is inconvenient in terms of reaction conditions. A much more elegant way for the incorporation of the sulfate group would therefore constitute of its introduction in a masked form at an early stage of the synthetic pathway. Thus, the stability of the sulfate towards acidic conditions would be increased.[58] Following this strategy, the sulfate group would not be unmasked until the very end of the synthesis. The advantage of this approach is that intermediates containing the protected sulfate can be easily purified whereas purification of unmasked sulfate containing compounds can prove difficult. In the literature, a large scope of protecting groups is provided, *e.g*. for hydroxyls, amines and acids. However, protection/deprotection strategies for sulfates are rarely known and are largely unexplored, despite the important role sulfates play in a large variety of biologically active compounds.[59,60] In 1981, Penney and Perlin reported the introduction of a sulfate group as a protected phenyl sulfate, using phenyl chlorosulfate (left, Figure 35).[61] Unmasking of the sulfate by cleavage of the phenyl group was performed through catalytic hydrogenation. Due to the poor stability of the dihydropyrrole of the Adc unit with regard to hydrogenation conditions, the strategy of Penney and Perlin is not suitable for our substrate. Next, Flitsch and co-workers approached the problem of sulfate protection in 1997. Flitsch *et al*. described the formation of a 2,2,2-trifluoroethyl sulfate ester by treating sulfate monoesters with 2,2,2-trifluorodiazoethane (center, Figure 35).[62] The fact that 2,2,2-trifluorodiazoethane is highly toxic and potentially explosive and that the unmasking conditions by treatment with potassium *tert*-butoxide at high temperatures are vigorous, resulted in a discharge of this protection strategy in our case.

In 2006 finally, Taylor *et al*. elaborated a convenient method for the masking and unmasking of sulfates by the introduction of a trichloroethyl (TCE) group (right, Figure 35).[63] TCE protected sulfate esters showed remarkable stabilities against various different reaction conditions: strongly acidic conditions among others, thereby allowing unmasking under highly selective and mild conditions using a methanolic zinc and ammonium formate solution.[63] Furthermore, TCE sulfate esters can be readily obtained by the reaction of an adequate alcohol with TCE imidazolium salt **2.97** under mild conditions. The reported advantages of the TCE group encouraged us to further investigate this protection strategy in our synthesis.

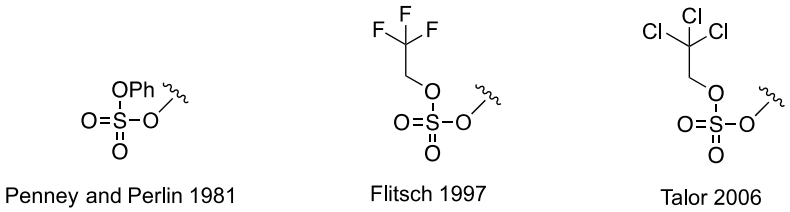

Figure 35 Masking of the sulfate group with a phenyl group (left), trifluoroethyl ester (center) and trichloroethyl ester (right).

8.1.1. Preparation of the trichloroethyl protected sulfuryl imidazolium salt 2.97

To incorporate the TCE group in our synthesis, the TCE protected sulfuryl imidazolium salt **2.97** had to be prepared first. According to the literature procedure,[63] sulfuryl chloride was reacted with 2,2,2-trichloroethanol (**2.98**) to give sulfurochloridate **2.99** in a high yield. Subsequent replacement of the chlorine atom of **2.99** by an imidazole substituent was achieved by treating **2.99** with imidazole to access imidazole sulfonate **2.100** in a good yield. Finally, **2.100** was transferred to the corresponding imidazolium salt **2.96** in an excellent yield using methyl triflate (Scheme 22).

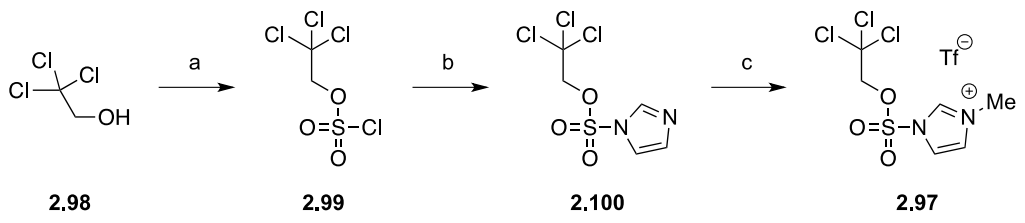

Scheme 22 Synthesis of trichloroethyl protected sulfuryl imidazolium salt **2.97**. Reagents and conditions: a) sulfuryl chloride, pyridine, Et_2O, −78 °C, 1 h, 85%; b) imidazole, THF, 0 °C to r.t., 1 h, 67%; c) methyl triflate, Et_2O, 0 °C, 3 h, 89%.

8.1.2. Preparation of the TCE ester and stability testing under acidic conditions

For the investigation of the stability of the TCE group under acidic conditions, as used in the global deprotection step, model substrate **2.102** was synthesized (Scheme 23). For this, thioglycoside **2.69** was treated with a methanolic NaOMe solution to access the free hydroxyl group at C4 position of the glycoside **2.101**, thus allowing the introduction of the TCE sulfate ester. The preparation of TCE sulfate ester **2.102** was achieved in a high yield by the reaction of **2.101** with the prepared imidazolium salt **2.97**. Further, TCE sulfate ester **2.102** was suspended in a diluted CH_2Cl_2/TFA solution for 20 h, in order to examine whether the TCE sulfate ester is stable under such acidic conditions. Pleasingly, exclusively deprotection of the BDA group was observed to give diol **2.103**, whereas the TCE sulfate ester was not harmed (Scheme 23). Hence, the TCE sulfate ester proved to be an ideal candidate for our synthetic strategy.

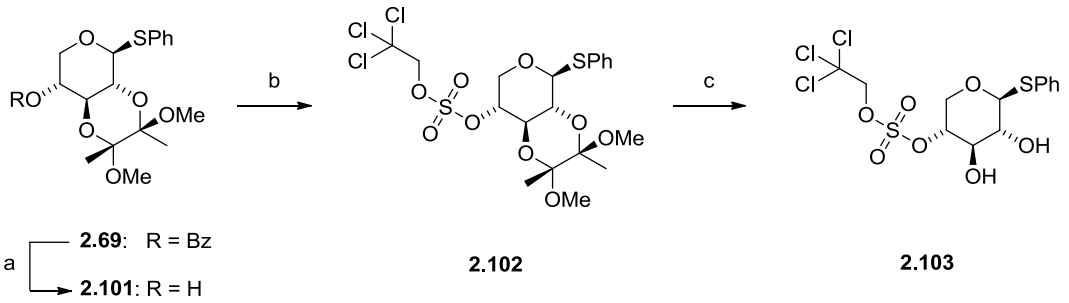

Scheme 23 Introduction and cleavage of the TCE protecting group. Reagents and conditions: a) NaOMe, MeOH, CH_2Cl_2, r.t., 2 h, 83%; b) **2.97**, 1-methylimidazole, THF, r.t., 66 h, 88%; c) CH_2Cl_2/TFA (10:1), r.t., 20 h, quant.

8.1.3. Incorporation of the TCE sulfate ester into late stage intermediates

Encouraged by the results described in the previous section, several attempts were performed to introduce the TCE sulfate ester at a late stage of the synthesis (Scheme 24). First, introduction at the stage of tetrapeptide **2.84** was investigated, unfortunately resulting in no formation of TCE protected sulfate **2.105**. Next, tripeptide intermediates **2.83** and **2.87** were subjected to the same protection conditions, yet again leading to no observable conversion to sulfate esters **2.106** and **2107**, respectively. Tripeptides **2.83** and **2.87** contain the free acid function at the L-Choi moiety, which could interfere with the outcome of the reaction. Thus, tripeptide **2.104**, containing a methyl ester instead of the free acid, was prepared. However, reaction of tripeptide **2.104** with reagent **2.97** showed no formation of the desired TCE sulfate ester **2.108** either. The reasons for the poor reactivity of the tested substrates regarding the protection with a TCE sulfate ester remain unclear and have to be further investigated. One explanation could be the complexity of the intermediates causing more steric interference, since the protection worked well and reliably with the much less complex model substrate **2.101**. In conclusion, introduction of the TCE sulfate ester did not prove successful at a late stage of the synthesis.

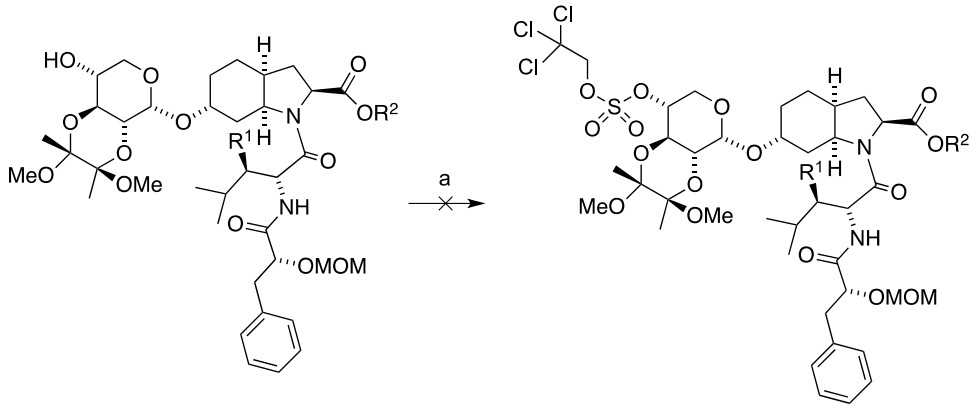

2.84: R^1 = Cl; R^2 = Adc
2.83: R^1 = Cl; R^2 = H
2.87: R^1 = R^2 = H
2.104: R^1 = H; R^2 = Me

2.105: R^1 = Cl; R^2 = Adc
2.106: R^1 = Cl; R^2 = H
2.107: R^1 = R^2 = H
2.108: R^1 = H; R^2 = Me

Scheme 24 Introduction of the TCE sulfate ester at a late stage of the synthesis. Reagents and conditions: a) **2.97**, 1-methylimidazole, THF, r.t., 42–86 h.

8.2. One Step Back – Incorporating the TCE Sulfate Ester before Glycosylation

Since late stage introduction of the TCE sulfate ester was not successful, a new synthetic strategy had to be investigated. This new route incorporated the use of a xylosyl donor already bearing the TCE sulfate ester on C4 position of the glycoside for the glycosylation reaction. The straightforward synthesis of such a xylosyl donor had already been investigated in Section 8.1.2. Because subjecting TCE sulfate xylosyl donor **2.102** to the conditions used for removing the Cbz group from the L-Choi led to cleavage of the TCE group in a test experiment, another strategy for the assembly of the different subunits had to be considered (for cleavage of the Cbz group from the L-Choi see Section 5.2). The new assembly comprises a first peptide coupling of the L-Choi core unit **2.92** with Cleu-Pla-OH **2.47** and Leu-Pla-OH **2.53**, respectively. Subsequently, L-Choi-Cleu-Pla unit **2.109** and L-Choi-Leu-Pla unit **2.110** serve as acceptors in the xylosylation step, building up the Xyl-L-Choi-Cleu-Pla and Xyl-L-Choi-Leu-Pla fragments, respectively. With this assembling strategy, a possible cleavage of the TCE group during Cbz deprotection can be avoided.

8.2.1. Preparation of different acceptors

The two acceptors **2.109** and **2.110** were synthesized in a straightforward manner starting from L-Choi derivative **2.92**. Peptide coupling of amine **2.92** with Pla-Cleu-OH unit **2.47** and Pla-Leu-OH unit **2.53** using DMTMM and NMM gave the corresponding tripeptides L-Choi-Cleu-Pla **2.93** and L-Choi-Leu-Pla **2.90** in a high yield. Selective saponification of the acetyl ester at L-Choi-C6 position was achieved by treatment with a methanolic K_2CO_3 suspension, which did not harm the L-Choi methyl ester (Scheme 25). Using these reaction conditions, acceptors **2.109** and **2.110** were obtained, ready to be used in the xylosylation step.

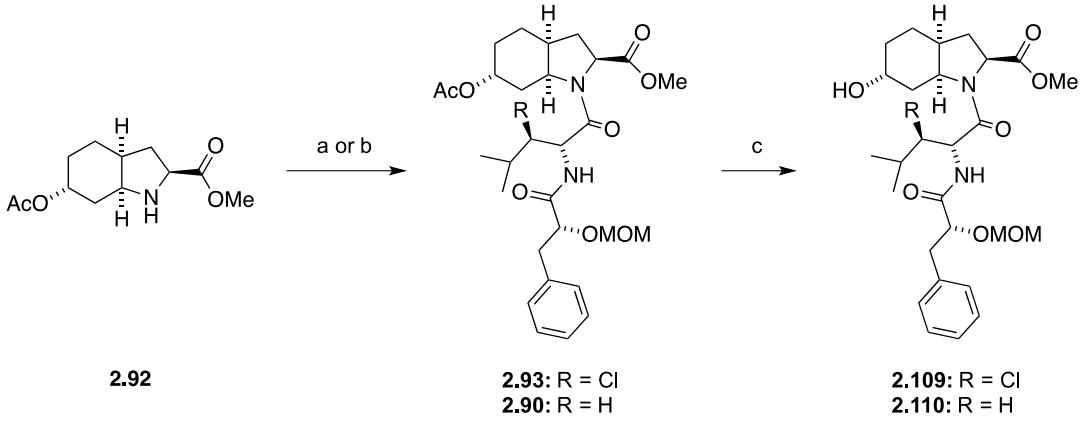

2.92

2.93: R = Cl
2.90: R = H

2.109: R = Cl
2.110: R = H

Scheme 25 Preparation of L-Choi acceptors **2.109** and **2.110**. Reagents and conditions: a) Pla-Cleu-OH **2.47**, DMTMM, NMM, CH_2Cl_2, 0 °C to r.t., 2 h, 83%; b) Pla-Leu-OH **2.53**, DMTMM, NMM, CH_2Cl_2, 0 °C to r.t., 3.5 h, 80%; c) K_2CO_3, MeOH, r.t., 2–3.5 h, (**2.109**: 85% from **2.93**; **2.110**: 61% from **2.90**).

8.2.2. Preparation of different donors

To increase the scope of the glycosylation reactions, several different xylosyl donors containing the TCE sulfate ester were synthesized starting from thioglycoside **2.102** (Scheme 26): Xylosyl donor **2.111**, bearing a bromine atom at the anomeric position, was obtained as an anomeric mixture α/β of 6:1 by treating **2.102** with bromine.[64] Introduction of the trichloroacetimidate was carried out by reaction of **2.102** with Cl_3CCN under basic conditions to access trichloroacetimidate **2.112** in a mixture α/β of 2:1.[65] Oxidation of the thiophenol group of **2.102** with *m*-CPBA gave the corresponding sulfoxide xylosyl donor **2.113** as a 1:1 diastereomeric mixture.[66] Hydrolysis of the thiophenol group of **2.102** to the alcohol yielded xylosyl donor **2.114** as a mixture α/β of 2:1.[67] Fluorination of the anomeric position of **2.102** using diethylaminosulfur trifluoride (DAST) provided fluorinated xylosyl donor **2.115**.[68] All prepared xylosyl donors were then tested in the glycosylation step together with acceptors **2.109** and **2.110** (Section 8.3.3.).

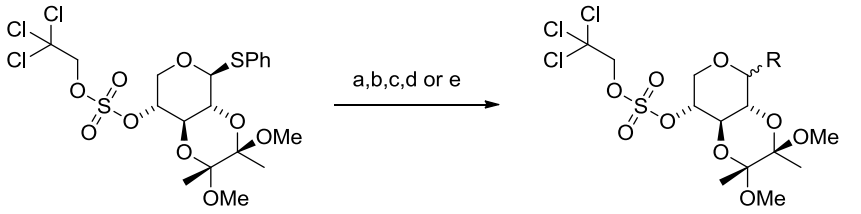

2.102

a) **2.111:** R = Br (α/β 6:1)
b) **2.112:** R = $OCNHCCl_3$ (α/β 2:1)
c) **2.113:** R = S(O)Ph (d.r. 1:1)
d) **2.114:** R = OH (α/β 2:1)
e) **2.115:** R = F (α/β 3:1)

Scheme 26 Synthesis of the different xylosyl donors. Reagents and conditions: a) Br_2, CH_2Cl_2, r.t., 1 h, 86%; b) Cl_3CCN, DBU, CH_2Cl_2, r.t., 2 h, 55%; c) *m*-CPBA, KF, MeCN/H_2O (5:1), 0 °C, 5 min, 71%; d) NBS, acetone/H_2O (9:1), −10 °C, 2 h, 53%; e) DAST, NBS, CH_2Cl_2, −15 °C, 2 h, 76%.

8.3. Late Stage Glycosylation

8.3.1. A closer look on the mechanism of glycosylations

The elaboration of effective glycosylation methods with a manageable control over the diasteromeric outcome of the formed *O*-glycosidic linkage has been challenging organic chemists ever since the first reported glycosylation by Michael in 1879.[69] The term glycosylation generally describes the condensation of an alcohol, sometimes referred to as the acceptor, with a glycoside group bearing a leaving group (LG) at the anomeric position, referred to as the donor. Usually the glycosyl donor is activated with a promotor (E^+X^-), which transfers the substituent at the anomeric position into a better leaving group (LG-E^+), thus enabling a facilitated cleavage thereof. Through cleavage of the activated leaving group an oxocarbenium ion is formed as active intermediate (highlighted in red, Figure 36). The creation of this oxocarbenium ion is the reason why the stereochemical control of a glycosylation is so difficult to manage and predict, since many parameters are involved in the stabilization of the oxocarbenium ion leading to different possible pathways. Pathway A: The former leaving group of the donor stays in close proximity to the oxocarbenium ion, thus, forming a contact ion pair (CIP). Depending on the nature of the leaving group, different orientations of the leaving group can be accessed in the CIP, favoring either an α or β attack of the alcohol. A solvent-separated ion pair of the LG^- with the oxocarbenium ion is also possible.[70] Pathway B: The solvent (S) participates by forming weak covalent bonds to the oxocarbenium ion, this behavior has been observed with acetonitrile and diethyl ether, for example.[71] Depending on the preferred position of the solvent donor, an α or β attack of the alcohol is favored. The used solvent exerts a tremendous impact on the outcome of the glycosylation in any case, since polar solvents can lead to a stabilization of the oxocarbenium ion.[70] Path C: The counter ion (X^-) of the promoter affects the stereochemical outcome of the glycosylation by forming either a CIP or a covalent bond with the oxocarbenium ion.[70] Concluding, the diasteromeric outcome of a glycosylation reaction depends on the leaving group, promoter, solvent and temperature. Determined by the reaction conditions, one intermediate will be dominant and hence responsible for the stereochemical outcome.

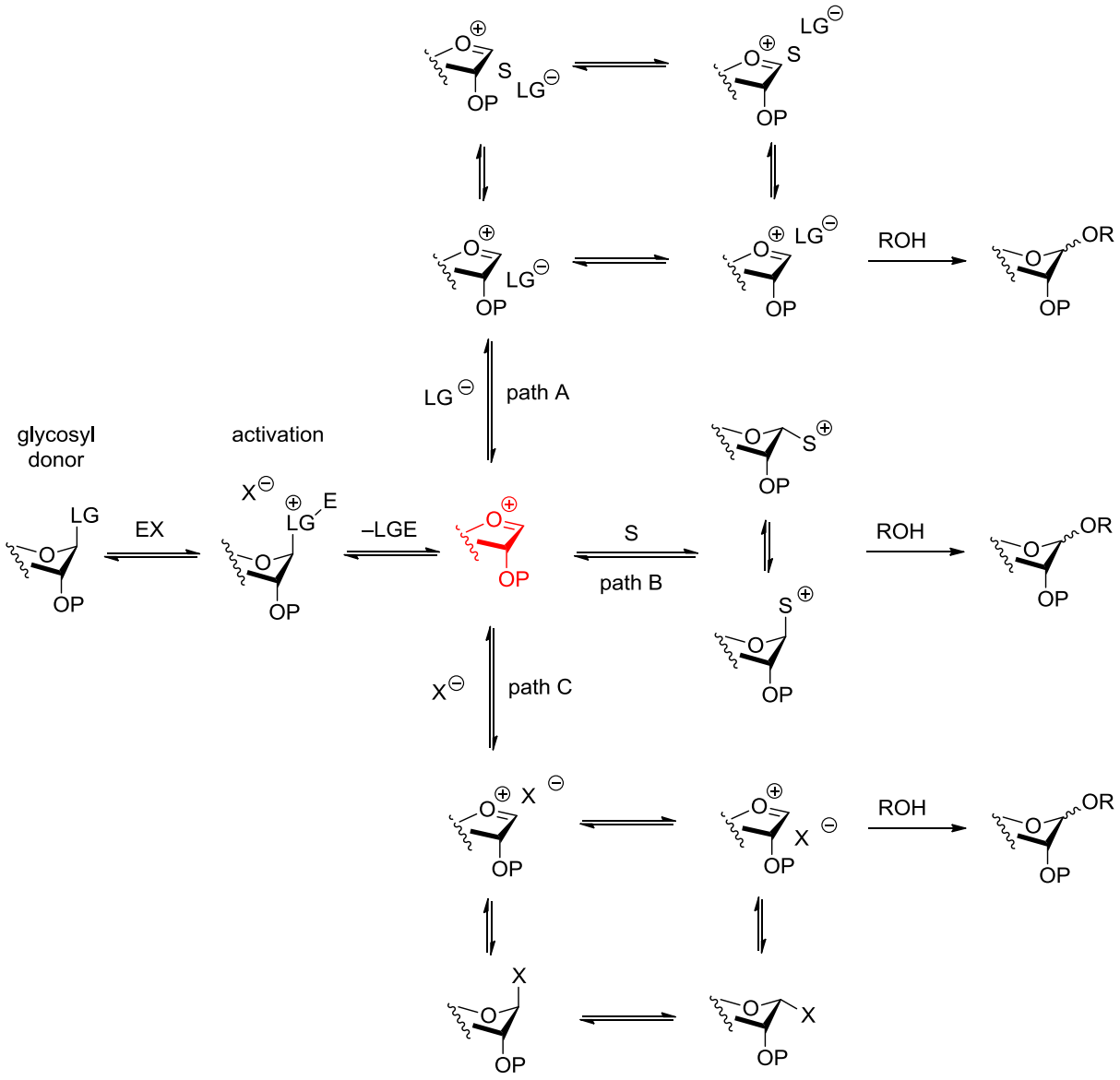

Figure 36 Possible intermediates occurring during a glycosylation reaction. LG = leaving group; P = nonparticipating substituent; EX = promoter (electrophile and leaving group), S = solvent.

8.3.2. The principle of armed and disarmed glycosyl donors

The reactivity and selectivity of a glycosylation is also affected by the substituents the glycosyl donor is decorated with. Freiser-Reid and co-workers first described an enhanced reactivity rate of benzyl-protected donors compared to acetyl-protected donors during glycosylations reactions (Figure 37).[72,73] They introduced the terms "armed" and "disarmed" for donors with enhanced and reduced reactivity. The increased reactivity of an armed donor can be explained by the electron-pushing nature of *e.g.* benzyl groups, which stimulates the dissociation of the bond between the leaving group and the anomeric carbon atom by a stabilization of the positive charge of the obtained oxocarbenium ion intermediate. On the contrary, electron-withdrawing moieties such as acetyl protecting groups lead to a destabilization of the oxocarbenium ion intermediate. The principle of armed and disarmed donors especially meets applications in the oligosaccharide one-pot-synthesis, since it allows for directing the reactivity of two co-existing donors.

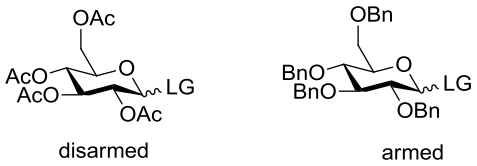

Figure 37 Armed and disarmed glycosyl donors.

8.3.3. Glycosylations with TCE-protected sulfate

With the L-Choi-Cleu-Pla (**2.109**) and L-Choi-Leu-Pla (**2.110**) acceptors in hand, coupling to the Xyl donors was investigated. First attempts using thioglycoside donor **2.102** and the conditions developed for the glycosylation step during the synthesis of A828A (**2.1**) (Section 5.1.) led to no conversion (Entry 1, Table 8). Changing the activator/promoter system from NIS/AgOTf to $Tf_2O/Ph_2SO/SnCl_4$[74] showed no improvement, leading to no conversion, but only decomposition (Entry 2, Table 8). As described in Section 8.3.2, the introduction of electron-withdrawing substituents leads to disarming of the corresponding donor. The poor reactivity of the glycosylations can therefore be explained by the electron-withdrawing nature of the TCE sulfate ester, leading to disarming of the Xyl donors. Next, donor **2.114**, with a hydroxyl leaving group, was treated with acceptors **2.109** and **2.110** under Appel-like conditions.[75] Again, no conversion was observable for both reactions (Entries 3 and 4, Table 8). Further, the reactivity of fluorinated donor **2.115** was investigated.

Table 8 Conditions for the glycosylation of different Xyl donors with acceptors **2.109** and **2.110**

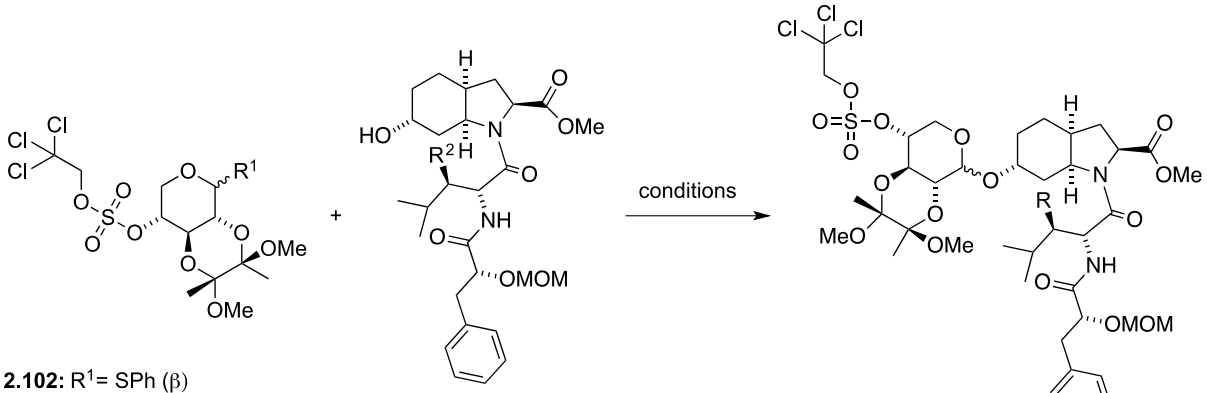

2.102: R^1= SPh (β)
2.111: R^1 = Br (α/β 6:1)
2.112: R^1= $OCNHCCl_3$ (α/β 2:1)
2.113: R^1= S(O)Ph (d.r. 1:1)
2.114: R^1 = OH (α/β 2:1)
2.115: R^1= F (α/β 3:1)

2.109: R^2 = Cl
2.110: R^2 = H

2.116: R = Cl
2.117: R = H

Entry	Donor	Acceptor	Conditions[a]	Observation[b]	α/β[c]
1	SPh	2.109	NIS, AgOTf, Et_2O, r.t.	no reaction	-
2	SPh	2.110	Tf_2O, Ph_2SO, $SnCl_4$, CH_2Cl_2, −78 °C	decomposition	-
3	OH	2.110	CBr_4, PPh_3, DMF, r.t.	no reaction	-
4	OH	2.109	CBr_4, PPh_3, DMF, r.t.	no reaction	-
5	F	2.110	$SnCl_2$, $AgClO_4$, Et_2O, r.t.[d]	no reaction	-
6	F	2.110	$SnCl_2$, $AgClO_4$, Et_2O, r.t.[e]	no reaction	-
7	F	2.109	NIS, AgOTf, CH_2Cl_2, r.t.	decomposition	-
8[f]	$OCNHCCl_3$	2.109	TMSOTf, DTBMP, CH_2Cl_2, −20 °C	conversion	1:5
9[g]	$OCNHCCl_3$	2.109	TMSOTf, DTBMP, CH_2Cl_2, −20 °C	conversion	1:5
10	S(O)Ph	2.109	Tf_2O, DTBMP, PhMe, −78 °C	conversion	1:2
11	S(O)Ph	2.109	Tf_2O, DTBMP, CH_2Cl_2, −78 °C	conversion	1:4
12	Br	2.110	AgOTf, DTBMP, Et_2O, r.t.	hydrolysis	-
13	Br	2.110	AgOTf, DTBMP, MeCN, r.t.	hydrolysis	-
14	Br	2.109	AgOTf, DTBMP, Et_2O, r.t.	full conversion	1:5
15	Br	2.109	AgOTf, DTBMP, CH_2Cl_2, r.t.	full conversion	1:5
16	Br	2.109	AgOTf, DTBMP, MeCN, r.t.	decomposition	-
17	Br	2.109	AgOTf, DTBMP, PhMe, r.t.	full conversion	1:20
18	Br	2.109	Ag_2O, CH_2Cl_2, r.t	no reaction	-
19	Br	2.109	Ag_2O, PhMe, r.t	no reaction	-
20	Br	2.109	$AgClO_4$, CH_2Cl_2, r.t	full conversion	3:5

[a]The reactions were carried out under careful exclusion of water and in the presence of 4 Å molecular sieves. [b]The screening was performed with small amounts, thus the yield was not always determined, but the conversion was monitored by TLC and/or UPLC. [c]The anomeric ratio was determined either by the isolated yields or by integration of the characteristic shifts of the anomeric proton signals in the crude ^{1}H NMR spectra. [d]2.50 equivalents of $SnCl_2$ and $AgClO_4$ were used. [e]6.0 equivalents of $SnCl_2$ and $AgClO_4$ were used. [f]An anomeric mixture of α/β (2:1) of donor 2.112 was used. [g]β anomer of donor 2.112 was used.

Nicolaou and co-workers reported the use of fluorinated donors in the synthesis of the natural product avermectin B_{1a}. They used $SnCl_2$ and $AgClO_4$ as promoter system for linking a sterically demanding secondary alcohol with a fluorinated glycosyl donor.[68] The fact that these reaction conditions did not result in any conversion supports the assumption that the problem lies in the poor reactivity of the different donors, since Nicolaou successfully used a much less reactive acceptor in his glycosylation (Entries 5 and 6, Table 8).[68] Furthermore, by changing to a stronger activator/promoter system with NIS/AgOTf, only decomposition could be observed (Entry 7, Table 8). As a next step, the use of trichloroacetimidate donor **2.112** was explored. Trichloroacetimidates were first introduced by Schmidt and co-workers in the 1980s and have since become a useful tool in glycosyl chemistry.[65] Indeed, by using the Schmidt conditions the formation of the *O*-glycosidic linkage between acceptor **2.109** and donor **2.112** was achieved, although the undesired β anomer was favored in a ratio of 5:1 (Entry 8, Table 8).[67] Since an anomeric mixture of α/β 2:1 of donor **2.112** had been used in the previous experiment, the pure β anomer of **2.112** was tested next. With this experiment, it was investigated whether the configuration of the donor has an influence on the stereochemical outcome. Unfortunately, the observed ratio of α/β did not change and stayed 1:5 in favor of the β anomer, indicating that the glycosylation reaction undergoes a pure S_N1 reaction pathway (Entry 9, Table 8). Seeing that the Schmidt conditions favored the formation of the β anomer, other donors and conditions were investigated in order to access the formation of the favored α anomer. Kahne and co-workers reported a rapid method for the glycosylation of unreactive substrates by the use of sulfoxides as donors, promoted by Tf_2O and 2,6-di-*tert*-butyl-4-methylpyridine (DTBMP). Further, they could control the stereochemical outcome of the glycosylation by changing the solvent from toluene (α/β 20:1), to CH_2Cl_2 (α/β 1:3) and to propionitrile (α/β 1:8).[76] Kahne's conditions led to good conversion of donor **2.113** and acceptor **2.109** in toluene in combination with an anomeric ratio α/β of 1:2, which were the best results obtained so far (Entry 10, Table 8). Since Kahne *et al*. reported the strong influence of the solvent on the stereochemical outcome of this reaction, the solvent was switched from toluene to CH_2Cl_2, to find the same tendency such as that more polar solvents favor the formation of the β anomer (Entry 11, Table 8). Last, the traditional Koenigs-Knorr conditions were investigated by the use of brominated donor **2.111**. Brominated donors are known to be very reactive, therefore donor **2.111** was formed *in situ* during the glycosylation, since purification of donor **2.111** already led to its hydrolysis.[64] First attempts with acceptor **2.110** and AgOTf/DTBMP as activator/promoter system were accompanied by hydrolysis of the xylosyl donor (Entries 12 and 13, Table 8). Careful

exclusion of water finally led to a clean reaction in Et_2O under full conversion of donor **2.113** and acceptor **2.109** with a preference for the β anomer of 5:1 (Entry 14, Table 8). Knowing about the influence of the solvent on the stereochemical outcome, a screening of different solvents was performed (Entries 15, 16 and 17, Table 8). While the use of CH_2Cl_2 led to a comparable ratio as before (Entry 15), the use of MeCN showed only decomposition products (Entry 16). Surprisingly, toluene induced an even more pronounced favoritism for the β anomer of 20:1 (Entry 17), which is in contradiction to the results obtained with Kahne's method (Entries 10 and 11, Table 8).[76] This exemplifies the difficulty assigned to glycosylations, which is that general predictions of the stereochemical outcome are difficult to predict. Albeit in the literature[77] some tendencies for the stereochemical outcome are described by changing a specific parameter, these tendencies can heavily vary for each condition and as shown before, even the opposite can occur. This demonstrates the great importance of experimental synthetic work. Since the brominated donor proved to be very active, a weak activator/promoter system with Ag_2O instead of AgOTf/DTBMP was investigated. However, neither in CH_2Cl_2 nor in toluene any conversion was observed (Entries 18 and 19, Table 8). Finally, the best results were obtained using the moderate activator $AgClO_4$ with full conversion and an anomeric ratio α/β of 3:5. Because in the meantime the approach described in Section 5 gave rise to the successful synthesis of A828A, this approach with the late stage glycosylation using TCE sulfate ester donors was not further optimized.

8.4. Synthesis of Aeruginosin 828B

Disregarding the success of the glycosylation step described in the previous section, we were interested in the endgame of the synthesis A828A (**2.1**). Since only very little amounts of the α anomer of Xyl-L-Choi-Cleu-Pla **2.116** were obtained, the last steps of the synthesis were performed with the β anomer of **2.116** (Scheme 27). Due to the poor stability of the TCE group under basic conditions, the general conditions for the saponification of the L-Choi methyl ester could not be used. Instead, milder conditions were used by treatment of **2.116** with an excess of Me_3SnOH,[78,79] resulting in a slow reaction rate.

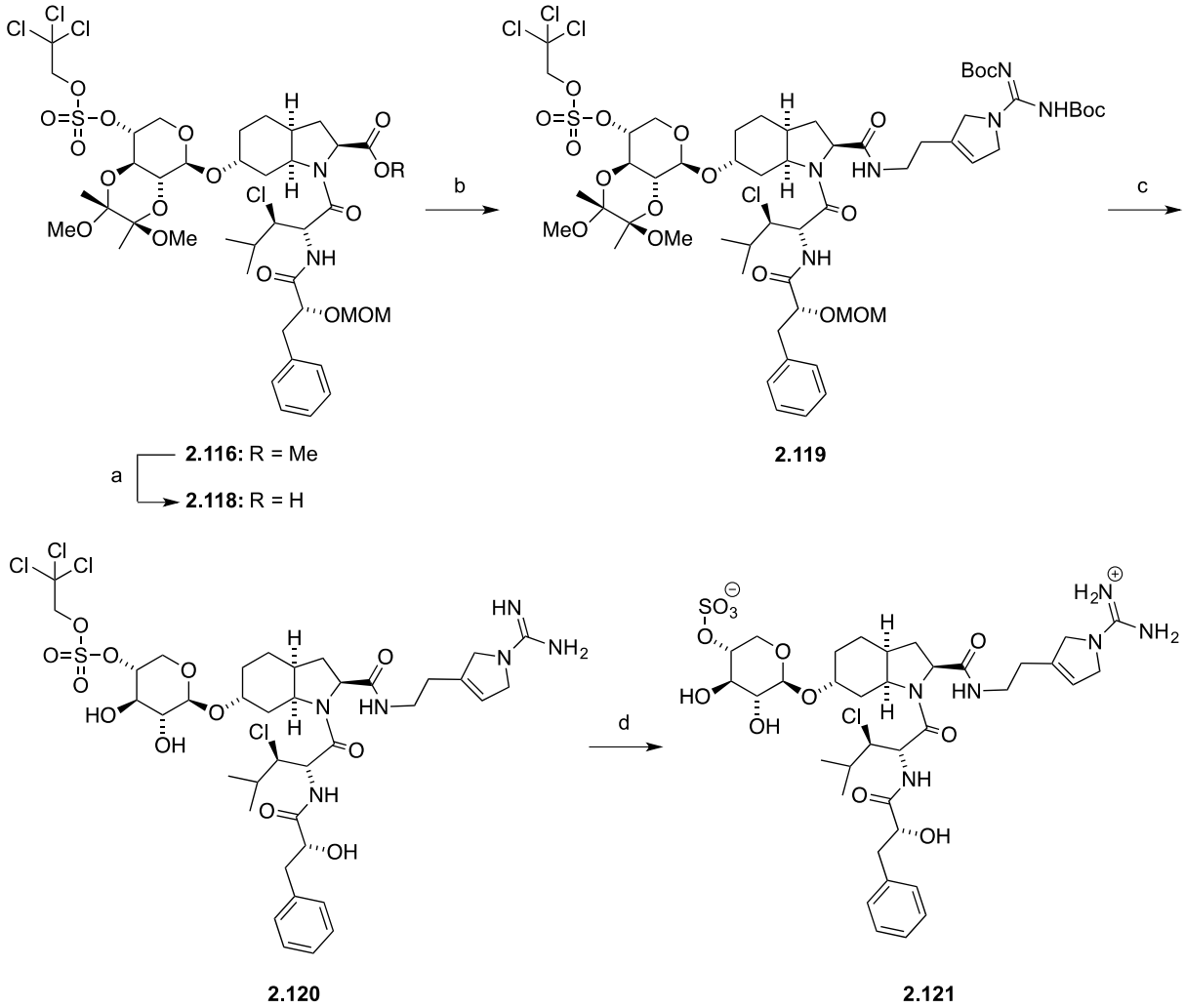

Scheme 27 Synthesis of aeruginosin 828B. Reagents and conditions: a) Me_3SnOH, DCE, 85 °C, 90 h, 34% (97% brsm); b) Adc subunit **2.63**, PyBOP, 2,6-lutidine, CH_2Cl_2, 0 °C to r.t., 4 h, 95%; c) CH_2Cl_2/TFA (10:1), r.t., 10 h; d) Zn powder, ammonium formate, MeOH, r.t., 2 h, 44% over two steps.

Even after several days a yield of only 34% of acid **2.118** was observed, accompanied by the recovery of 63% of starting material **2.116**. Acid **2.118** was further coupled with Adc subunit **2.63** to give tetrapeptide **2.119** in an excellent yield. Cleavage of the Boc, BDA and MOM protecting groups was performed in a diluted TFA/CH_2Cl_2 solution, giving access to tetrapeptide **2.120**. Final unmasking of the sulfate group in **2.120** was performed in a methanolic zinc powder/ammonium formate solution. Thus, 350 µg of aeruginosin 828B (**2.121**) could be obtained in 44% yield over the last two deprotection steps and after HPLC purification. It has to be mentioned that the five last steps were performed only once and on a very small scale, which leaves room for optimizations. Nevertheless, the feasibility of this synthetic strategy could be undoubtedly demonstrated.

8.4.1. Comparison of the ^{1}H NMR spectra of A828A and A828B

Due to the small quantities obtained for A828B (**2.121**), no 2D NMR spectra were recorded. Therefore, the full assignment of the signals of A828B (**2.121**) could not be conducted. In general, the proton signals of the L-Choi, Adc, Cleu and Pla units of A828A (**2.1**) and A828B (**2.121**) are very similar. Differences were observed of course for the proton signals of the Xyl residue going from A828A (**2.1**) to A828B (**2.121**).

9. Conclusion

In this chapter, the first total synthesis of the cyanobacterial toxin aeruginosin 828A (**2.1**) was reported. In the beginning, the synthesis of all required building blocks for the synthesis of A828A (**2.1**) was accomplished. The subsequent assembly of the building blocks featured a stereoselective α-xylosylation of L-Choi building block **2.37** with xylosyl donor **2.69**. By screening different coupling reagents and conditions, the problem of HCl elimination during the peptide coupling of Xyl-L-Choi-H **2.72** with Pla-Cleu-OH dipeptide **2.47** was solved using DMTMM as coupling reagent. Completion of the total synthesis was achieved by another peptide coupling of xylosylated Pla-Cleu-L-Choi-OH **2.83** with Adc unit **2.63**, followed by sulfonation and global deprotection. In summary, A828A (**2.1**) was successfully synthesized over a longest linear sequence of 18 steps incorporating 50 synthetic steps in total.

Further, the developed synthetic strategy for A828A (**2.1**) was successfully adopted in the synthesis of the natural congener aeruginoside 126A (**2.11**) and the synthetic analogues A748A (**2.12**) and A794A (**2.13**). Comparison of the NMR spectra of chlorinated congeners A828A (**2.1**) and A748A (**2.12**) with non-chlorinated A126A (**2.11**) and A794A (**2.13**) revealed an interesting modulating effect of the chlorine atom on the conformation of the particular aeruginosins. While A828A (**2.1**) and A748A (**2.12**) appeared as a single rotamer, A126A (**2.11**) and A794A (**2.13**) were present as a rotameric mixtures of around 4:1, which was proven by 2D ROESY and variable temperature ^{1}H NMR experiments. The synthesized compounds A828A (**2.1**), A794A (**2.13**), A748A (**2.12**) and A126A (**2.11**) were tested with regard to their toxicity against the freshwater crustacean *T. platyurus*, demonstrating that the sulfate group has a critical effect on the toxicity, whereas a "chlorine effect" like in the inhibition of proteases was not observed. This finding led to the assumption that the toxicity of the chlorosulfopeptides has to be explained by another mode of action than the inhibition of protease enzymes. Further, the findings support the hypothesis that chlorosulfopeptides have to be considered not only as potent protease inhibitors but also as cyanobacterial biotoxins. This dual function of chlorosulfopeptides such as A828A (**2.1**) might be the reason for the inactivation of the mcy gene cluster in some cyanobacteria strains, which resulted in the loss of microcystin production in these strains. Therefore, MC formation became obsolete in cyanobacteria strains which produced chlorosulfopeptidic toxins like A828A (**2.1**). Further, aglycone A616A (**2.91**) of A828A (**2.1**) was synthesized. The determined potent toxicity of aglycone A616A (**2.91**) revealed that the aglycone of each particular aeruginosin has to be considered as cyanobacterial toxin, too.

In the course of the total synthesis of A828A (**2.1**) alternative approaches were also investigated. These incorporated a late stage glycosylation with a xylosyl donor bearing a masked sulfate group. This alternative approach resulted in the synthesis of aeruginosin 828B (**2.121**) which contains a β linkage to the xylosyl residue. In general, the work described in this chapter contributes to a better understanding of the toxicity related to chlorosulfopeptides produced by particular cyanobacterium strains.

10. References

[1] Pictures are used with permission of PD Dr. Thomas Posch (Picture of Epifluorescence micrograph) and PD Dr. Judith Blom (Picture of Lake Hallwil) from the University of Zurich.

[2] E. Kohler, V. Grundler, D. Häussinger, R. Kurmayer, K. Gademann, J. Pernthaler, J. F. Blom, *Harmful Algae* **2014**, *39*, 154–160.

[3] J. F. Blom, F. Jüttner, *Toxicon* **2005**, *46*, 465–470.

[4] S. Faltermann, S. Hutter, V. Christen, T. Hettich, K. Fent, *Toxins* **2016**, *8*, 219–233.

[5] V. Ostermaier, R. Kurmayer, *Microb. Ecol.* **2009**, *58*, 323–333.

[6] G. Christiansen, R. Kurmayer, Q. Liu, T. Börner, *Appl. Environ. Microbiol.* **2006**, *72*, 117–123.

[7] R. Kurmayer, J. F. Blom, L. Deng, J. Pernthaler, *ISME J.* **2015**, *9*, 909–921.

[8] E. Kohler, *Structural Characterization, Bioactivity and Biodegradation of Cyanobacterial Toxins*, PhD Thesis, University of Zurich, **2015**.

[9] G. W. Gribble, *J. Chem. Educ.* **2004**, *81*, 1441–1449.

[10] C. S. Neumann, D. G. Fujimori, C. T. Walsh, *Chem. Biol.* **2008**, *15*, 99–109.

[11] C. M. Harris, R. Kannan, H. Kopecka, T. M. Harris, *J. Am. Chem. Soc.* **1985**, *107*, 6652–6658.

[12] M. Groll, R. Huber, B. C. M. Potts, *J. Am. Chem. Soc.* **2006**, *128*, 5136–5141.

[13] M. K. Renner, P. R. Jensen, W. Fenical, *J. Org. Chem.* **1998**, *63*, 8346–8354.

[14] E. R. Pereira, L. Belin, M. Sancelme, M. Prudhomme, M. Ollier, M. Rapp, D. Sevère, J. F. Riou, D. Fabbro, T. Meyer, *J. Med. Chem.* **1996**, *39*, 4471–4477.

[15] S. Hanessian, K. Ersmark, X. Wang, J. R. Del Valle, N. Blomberg, Y. Xue, O. Fjellström, *Bioorganic Med. Chem. Lett.* **2007**, *17*, 3480–3485.

[16] L. P. Hager, D. R. Morris, F. S. Brown, H. Eberwein, *J. Biol. Chem.* **1965**, *241*, 1769–1777.

[17] J. H. Dawson, M. Sono, *Chem. Rev.* **1987**, *87*, 1255–1276.

[18] A. Messerschmidt, R. Wever, *Proc. Natl. Acad. Sci. U. S. A.* **1996**, *93*, 392–396.

[19] A. Butler, J. N. Carter-Franklin, *Nat. Prod. Rep.* **2004**, *21*, 180–188.

[20] S. Keller, T. Wage, K. Hohaus, M. Hölzer, E. Eichhorn, K. H. van Pée, *Angew. Chem. Int. Ed.* **2000**, *39*, 2300–2302.

[21] A. S. Eustáquio, F. Pojer, J. P. Noel, B. S. Moore, *Nat. Chem. Biol.* **2008**, *4*, 69–74.

[22] J. Hartung, *Angew. Chem. Int. Ed.* **1999**, *38*, 1209–1211.

[23] N. Sitachitta, J. Rossi, M. A. Roberts, W. H. Gerwick, M. D. Fletcher, C. L. Willis, *J.*

Am. *Chem*. *Soc*. **1998**, *120*, 7131–7132.

[24] F. H. Vaillancourt, J. Yin, C. T. Walsh, *Proc*. *Natl*. *Acad*. *Sci*. *U*. *S*. *A*. **2005**, *102*, 10111–10116.

[25] K. Ishida, G. Christiansen, W. Y. Yoshida, R. Kurmayer, M. Welker, N. Valls, J. Bonjoch, C. Hertweck, T. Börner, T. Hemscheidt, E. Dittmann, *Chem*. *Biol*. **2007**, *14*, 565–576.

[26] L. Tonk, P. M. Visser, G. Christiansen, E. Dittmann, E. O. F. M. Snelder, C. Wiedner, L. R. Mur, J. Huisman, *Appl*. *Environ*. *Microbiol*. **2005**, *71*, 5177–5181.

[27] S. Hanessian, R. Margarita, A. Hall, S. Johnstone, M. Tremblay, L. Parlanti, *J*. *Am*. *Chem*. *Soc*. **2002**, *124*, 13342–13343.

[28] S. Hanessian, J. R. Del Valle, Y. F. Xue, N. Blomberg, *J*. *Am*. *Chem*. *Soc*. **2006**, *128*, 10491–10495.

[29] N. Stuhr-Hansen, S. Padrah, K. Strømgaard, *Tetrahedron Lett*. **2014**, *55*, 4149–4151.

[30] P. Brewster, E. D. Hughes, C. K. Ingold, P. A. D. S. Rao, *Nature* **1950**, *166*, 179–180.

[31] S. Hanessian, M. Tremblay, J. F. W. Petersen, *J*. *Am*. *Chem*. *Soc*. **2004**, *126*, 6064–6071.

[32] R. B. Merrifield, *J*. *Am*. *Chem*. *Soc*. **1963**, *85*, 2149–2154.

[33] S. Hanessian, X. Wang, K. Ersmark, J. R. Del Valle, E. Klegraf, *Org*. *Lett*. **2009**, *11*, 4232–4235.

[34] M. T. Crimmins, R. S. Al-awar, I. M. Vallin, W. G. Hollis, R. O'Mahony, J. G. Lever, D. M. Bankaitis-Davis, *J*. *Am*. *Chem*. *Soc* **1996**, *118*, 7513–7528.

[35] R. Grigg, J. Markand, T. Perriorb, S. Surendrakuma, W. J. Warnocka, *Tetrahedron* **1992**, *48*, 6929–6952.

[36] T. W. Greene, P. G. M. Wuts, *Protective Groups In Organic Synthesis*, John Wiley & Sons, INC., New York, **1999**.

[37] S. Mukherjee, R. Sivappa, M. Yousufuddin, C. J. Lovely, *Org*. *Lett*. **2010**, *12*, 4940–4943.

[38] P. G. Reddy, T. V. Pratap, G. D. K. Kumar, S. K. Mohanty, S. Baskaran, *Eur*. *J*. *Org*. *Chem*. **2002**, 3740–3743.

[39] S. Tamura, H. Abe, A. Matsuda, S. Shuto, *Angew*. *Chem*. *Int*. *Ed*. **2003**, *42*, 1021–1023.

[40] J. Guo, X. S. Ye, *Molecules* **2010**, *15*, 7235–7265.

[41] Y. Demizu, Y. Kubo, H. Miyoshi, T. Maki, Y. Matsumura, N. Moriyama, O. Onomura, *Org*. *Lett*. **2008**, *10*, 5075–5077.

[42] L. S. Khasanova, F. A. Gimalova, S. A. Torosyan, A. A. Fatykhov, M. S. Miftakhov, *Russ. J. Org. Chem.* **2011**, *47*, 1125–1129.

[43] O. Kanie, Y. Ito, T. Ogawa, *J. Am. Chem. Soc.* **1994**, *116*, 12073–12074.

[44] L. Birkofer, E. Bierwirth, A. Ritter, *Chem. Ber.* **1961**, *94*, 821–824.

[45] M. Sakaitani, N. Kurokawa, Y. Ohfune, *Tetrahedron Lett.* **1986**, *27*, 3753–3754.

[46] S. Diethelm, C. S. Schindler, E. M. Carreira, *Chem. Eur. J.* **2014**, *20*, 6071–6080.

[47] J. Coste, E. Frérot, P. Jouin, B. Castro, *Tetrahedron Lett.* **1991**, *32*, 1967–1970.

[48] C. A. G. N. Montalbetti, V. Falque, *Tetrahedron* **2005**, *61*, 10827–10852.

[49] A. Falchi, G. Giacomelli, A. Porcheddu, M. Taddei, *Synlett* **2000**, *2*, 275–277.

[50] M. Goodman, L. Levine, *J. Am. Chem. Soc* **1964**, *86*, 2918–2922.

[51] D. S. Kemp, J. J. Rebek, *J. Am. Chem. Soc* **1970**, *92*, 5792–5793.

[52] M. Goodman, W. J. McGahren, *Tetrahedron* **1967**, *23*, 2031–2050.

[53] J. Guiard, A. Collmann, M. Gilleron, L. Mori, G. De Libero, J. Prandi, G. Puzo, *Angew. Chem. Int. Ed.* **2008**, *47*, 9734–9738.

[54] M. Hesse, H. Meier, B. Zeeh, *Spektroskopische Methoden in Der Organischen Chemie*, Georg Thieme Verlag, Stuttgart, **2005**.

[55] V. H. Rawal, M. P. Cava, *Tetrahedron Lett.* **1985**, *26*, 6141–6142.

[56] N. Valls, M. Vallribera, M. López-Canet, J. Bonjoch, *J. Org. Chem.* **2002**, *67*, 4945–4950.

[57] A. Liang, J. N. Thakkar, U. R. Desai, *J. Pharm. Sci.* **2010**, *99*, 1207–1216.

[58] R. A. Al-Horani, U. R. Desai, *Tetrahedron* **2010**, *66*, 2907–2918.

[59] T. C. McKee, J. H. Cardellina, R. Riccio, M. V. D'Auria, M. Iorizzi, L. Minale, R. A. Moran, R. J. Gulakowski, J. B. McMahon, R. W. Buckheit, K. M. Snader, M. R. Boyd, *J. Med. Chem.* **1994**, *37*, 793–797.

[60] D. J. Faulkner, *Nat. Prod. Rep.* **2000**, *17*, 7–55.

[61] C. L. Penney, A. S. Perlin, *Carbohydr. Res.* **1981**, *93*, 241–246.

[62] A. D. Proud, J. C. Prodger, S. L. Flitsch, *Tetrahedron Lett.* **1997**, *38*, 7243–7246.

[63] L. J. Ingram, S. D. Taylor, *Angew. Chem. Int. Ed.* **2006**, *45*, 3503–3506.

[64] S. Kaeothip, J. P. Yasomanee, A. V. Demchenko, *J. Org. Chem.* **2012**, *77*, 291–299.

[65] R. R. Schmidt, J. Michel, *Angew. Chem. Int. Ed.* **1980**, *19*, 731–732.

[66] G. Agnihotri, A. K. Misra, *Tetrahedron Lett.* **2005**, *46*, 8113–8116.

[67] Q. Liu, Y. Yu, P. Wang, Y. Li, *New J. Chem.* **2013**, *37*, 3647–3661.

[68] K. C. Nicolaou, R. E. Dolle, D. P. Papahatjis, J. L. Randall, *J. Am. Chem. Soc.* **1984**, *106*, 4189–4192.

[69] A. Michael, *Am*. *Chem*. *J*. **1879**, *1*, 305–312.

[70] Y. Yang, X. Zhang, B. Yu, *Nat*. *Prod*. *Rep*. **2015**, *32*, 1331–1355.

[71] A. J. Ratcliffe, B. Fraser-Reid, *J*. *Chem*. *Soc*. *Perkin Trans*. *1* **1990**, 747–750.

[72] D. R. Mootoo, P. Konradsson, U. Udodong, B. Fraser-Reid, *J*. *Am*. *Chem*. *Soc*. **1988**, *110*, 5583–5584.

[73] B. Fraser-Reid, Z. Wu, C. W. Andrews, E. Skowronski, *J*. *Am*. *Chem*. *Soc*. **1991**, *113*, 1434–1435.

[74] Y. Geng, Q. Qin, X. S. Ye, *J*. *Org*. *Chem*. **2012**, *77*, 5255–5270.

[75] Y. Nishida, Y. Shingu, H. Dohi, K. Kobayashi, *Org*. *Lett*. **2003**, *5*, 2377–2380.

[76] D. Kahne, S. Walker, Y. Cheng, D. Van Engen, *J*. *Am*. *Chem*. *Soc*. **1989**, *111*, 6881–6882.

[77] K. Toshima, K. Tatsuta, *Chem*. *Rev*. **1993**, *93*, 1503–1531.

[78] K. C. Nicolaou, W. E. Brenzovich, G. Bulger, T. M. Francis, *Org*. *Biomol*. *Chem*. **2006**, *4*, 2119–2157.

[79] R. L. E. Furlán, E. G. Mata, O. A. Mascaretti, *Tetrahedron Lett*. **1996**, *37*, 5229–5232.

CHAPTER II: SYNTHETIC STUDIES ON AERUGINOSIN KT608A

1. Introduction

In this chapter, the results of a purely synthesis driven research project are described. The efforts which were made in order to elucidate strategies for the synthesis of the recently isolated aeruginosin KT608A (**3.1**) are summarized. A special focus was laid on the efficient synthesis of the D-*diepi*-Choi unit present in KT608A (**3.1**).

1.1. Isolation and Bioactivity of Aeruginosins KT608A, KT608B and KT650

In 2012, Carmeli and co-workers reported the isolation of aeruginosin KT608A (**3.1**), KT608B (**3.2**) and KT650 (**3.3**) from *Microcystis aeruginosa* bloom material obtained from Lake Kinneret in Israel.[1] The especialness of these three isolated aeruginosins is the presence of a novel D-*diepi*-Choi motif instead of the L-Choi moiety usually observed in aeruginosins.[2] Further, Carmeli *et al*. investigated the inhibitory activities against serine proteases trypsin and thrombin of **3.1**, **3.2** and **3.3**. While aeruginosin KT608A (**3.1**) and KT608B (**3.2**) revealed a potent inhibition of trypsin with IC_{50} values of 1.9 and 1.3 µM, KT650 (**3.3**) showed an activity an order of magnitude lower with an IC_{50} value of 19.9 µM.[1] Interestingly, KT608A (**3.1**) induced an enhanced thrombin activity of 30% at a concentration of 45.5 µM, whereas KT608B (**3.2**) and KT650 (**3.3**) inhibited the activity of thrombin by 50% at this concentration.[1]

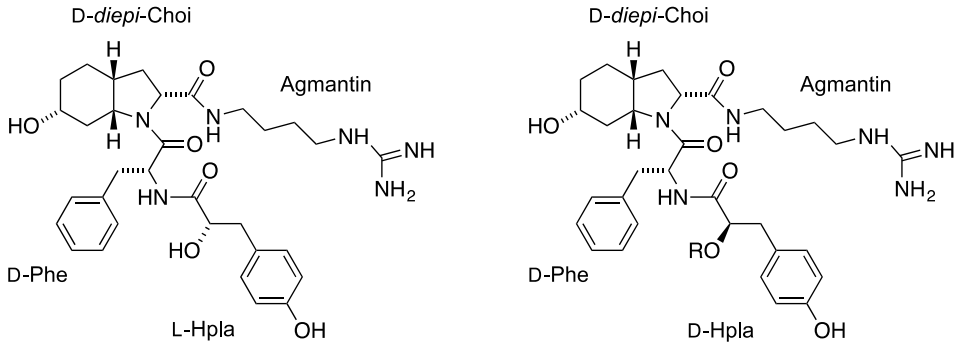

aeruginosin KT608A (**3.1**)

aeruginosin KT608B (**3.2**): R = H
aeruginosin KT650 (**3.3**): R = Ac

Figure 38 Elucidated structures of aeruginosin KT608A (**3.1**), KT608B (**3.2**) and KT650 (**3.3**) by Carmeli and co-workers.[1]

1.2. Previous Syntheses

In this section, previously described syntheses of aeruginosins performed by other research groups will be discussed. Thereby, the focus is laid on the reported strategies for the preparation of the different Choi units.

1.2.1. Bonjoch's contributions to the syntheses of aeruginosins

Bonjoch and co-workers effectively synthesized a variety of different aeruginosins.[3–7] The total syntheses of Bonjoch *et al*. build on a straightforward synthesis of the L-Choi core, which they had already developed in 1996.[8] This synthesis was later successfully implemented in the first total synthesis of aeruginosin 298A (**1**).[3] Bonjoch's preparation of the L-Choi unit commenced with the Birch reduction of L-tyrosine derivative **3.4** to give compound **3.5**. Further, the methoxy ether of **3.5** was cleaved under acidic conditions and the *in situ* formed α,β-unsaturated ketone was attacked intramolecularly by the amine in an aza Michael type addition providing a diasteromeric mixture of ketone **3.6** (Scheme 28).

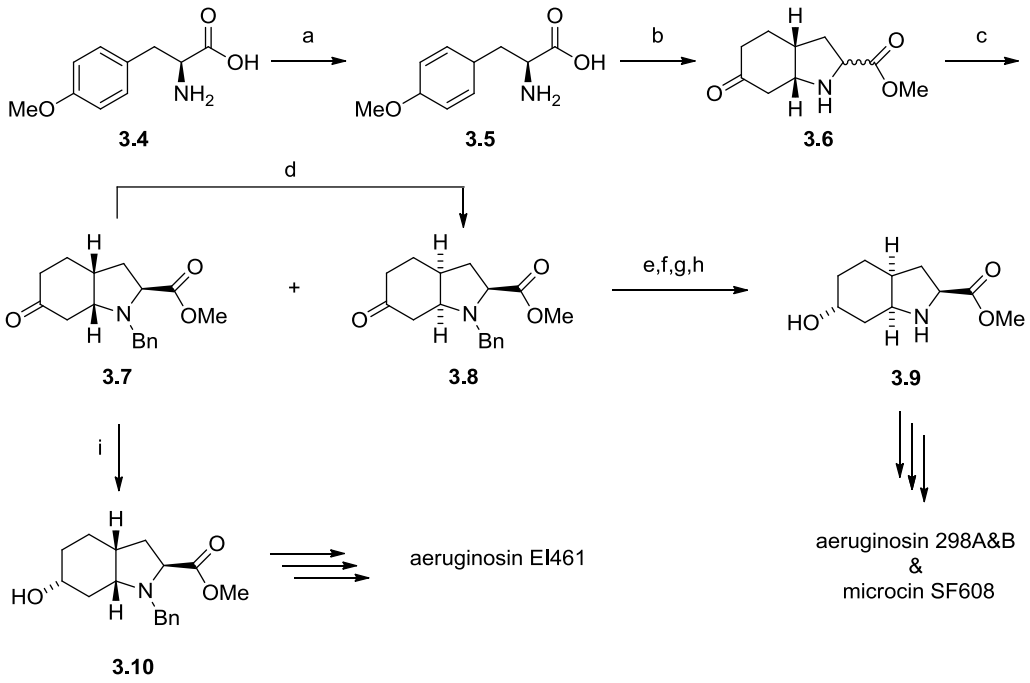

Scheme 28 Bonjoch's synthesis of L-Choi derivative **3.9** and L-*diepi*-Choi building block **3.10**. Reagents and conditions: a) Li, NH_3, THF/^{t}BuOH, –78 °C; b) MeOH, 7.5 N HCl, 35 °C; c) BnBr, $NaHCO_3$, EtOH, 70 °C; d) MeOH, 8 N HCl, 65 °C, 44% over four steps; e) H_2, $Pd(OH)_2$; f) Boc_2O, EtOAc; g) LS-Selectride, THF, –78 °C, 42% over three steps; h) TFA, CH_2Cl_2, 0 °C, quant.; i) $NaBH_4$, MeOH, –78 °C, 72%.

Subsequent benzyl protection yielded ketones **3.7** and **3.8**. Under acidic conditions, ketone **3.7** could be isomerized to **3.8**. For the completion of the L-Choi synthesis, the Bn group was replaced by a Boc group, followed by diastereoselective reduction of the ketone to the octahydroindole. Removal of the Boc group finally gave access to L-Choi derivative **3.9** (Scheme 28). Usage of L-Choi building block **3.9** subsequently led to the total synthesis of aeruginosins 298A (**1**)[3] and 298B (**8**)[5] and microcin SF608 (**7**)[4]. (For the structures of the different aeruginosins see pages 5 and 8 in the general introduction). Branching off at intermediate **3.7** provided L-*diepi*-Choi building block **3.10**, which was implemented in the synthesis of aeruginosin EI461 (Scheme 28).[6] Bonjoch *et al*. also reported the so far only synthesis of a D-*diepi*-Choi building block. For this, they used the same synthetic strategy as for the L-Choi synthesis, yet starting from D-tyrosine derivative **3.11** instead of L-tyrosine. Consequently, ketone **3.12**, the enantiomer of intermediate **3.8** from the L-Choi synthesis, could be prepared. Further, reduction of ketone **3.12** followed by protection of the hydroxyl group and deprotection of the amine gave D-*diepi*-Choi building block **3.13** (Scheme 29).

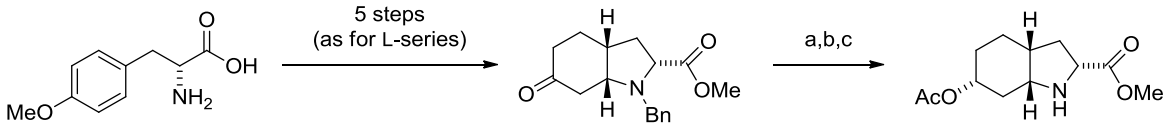

3.11 **3.12** **3.13**

Scheme 29 Bonjoch's synthesis of D-*diepi*-Choi building block **3.13**. Reagents and conditions: a) $NaBH_4$, MeOH, 80%; b) Ac_2O, DMAP, PyBOP, 95%; c) TFA, CH_2Cl_2, 0 °C, quant.

1.2.2. Wipf's contribution to the syntheses of aeruginosins

Instead of the reductive route described by Bonjoch,[3] Wipf and co-workers reported an oxidative route starting from Cbz-L-Tyr (**3.14**) (Scheme 30). Oxidative amination of **3.14** induced by a hypervalent iodine species provided bicyclic intermediate **3.15**. Protection of the tertiary alcohol of **3.15** yielded compound **3.16**, which could be isomerized under basic conditions to the thermodynamically more stable isomer **3.17**. Further, reductive cleavage of the benzoyl ester gave access to intermediate **3.18**. Hydrogenation of the alkene function in **3.18** provided *cis* fused bicyclic system **3.19**. The ketone of **3.19** could be diastereoselectively reduced to the alcohol in a similar fashion as described by Bonjoch.[3] Subsequent protection of the hydroxyl group with a TBS group finally provided the fully protected L-Choi building block **3.20** (Scheme 30). First, Wipf *et al*. incorporated building block **3.20** in the synthesis of aeruginosin 298A (**1**).[9] Later, they could also adopt the same strategy for the total synthesis of the natural product tuberostemonin.[10]

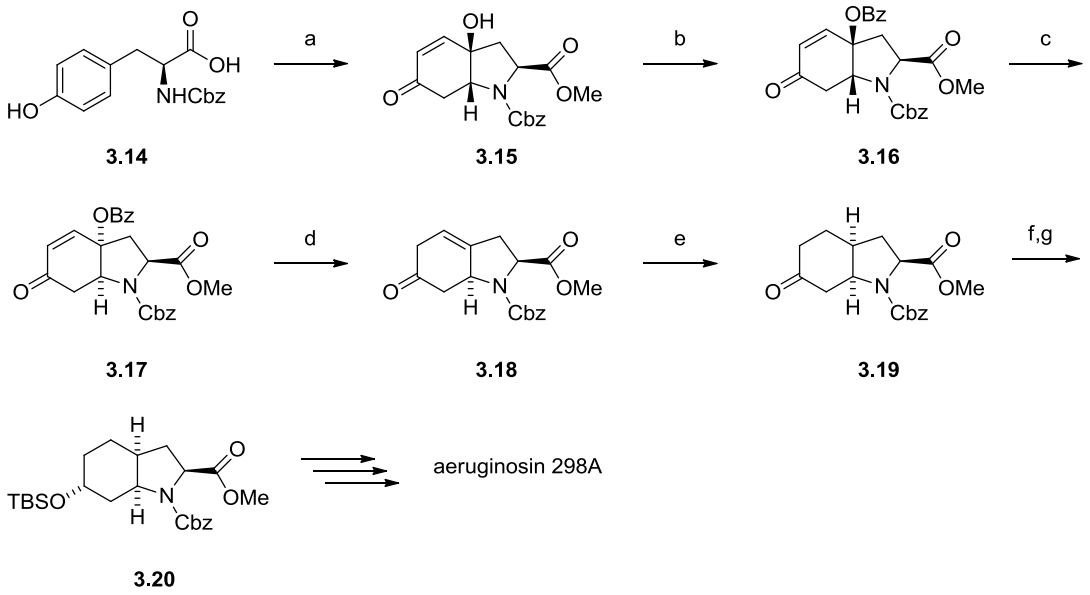

Scheme 30 Wipf's synthesis of the fully protected L-Choi building block **3.20**. Reagents and conditions: a) $PhI(OAc)_2$, $NaHCO_3$, MeOH, 55%; b) Bz_2O, DMAP, pyridine, CH_2Cl_2, 90%; c) $NaHCO_3$, DMSO, 90 °C, 78%; d) Zn dust, AcOH/THF, 65 °C, 75%; e) H_2, PtO_2, AcOH/EtOH, 0 °C, 95%; f) L-Selectride, THF, –78 °C; g) TBSOTf, imidazole, CH_2Cl_2, 87% over two steps.

1.2.3. Hanessian's contributions to the syntheses of aeruginosins

Besides the work of Bonjoch, the group of Hanessian probably contributed the most to the synthesis and structural confirmation of aeruginosins. Hanessian's efforts led to the preparation of numerous aeruginosins, *e.g.* oscillarin (**3**)[11], dysinosin A (**49**)[12], chlorodysinosin A (**50**)[13] and aeruginosin 205A (**38**) and B (**39**)[14] (for the structures of the different aeruginosins see pages 7, 10 and 11 in the general introduction). The successful syntheses of the above mentioned aeruginosins build on a facile synthesis of the L-Choi moiety (Scheme 31). To start with, *N*-Protected glutamate **3.21** was transformed to the terminal olefin **3.22**. Deprotection of the amine of **3.22** followed by an intramolecular lactame formation in refluxing toluene with subsequent Boc protection provided lactame **3.23**. Reduction of lactame **3.23** with superhydride and successive acetyl protection of the alcohol provided intermediate **3.24**. The key step consisted of a *N*-acyloxyiminium ion aza-Prins halocarbocyclization of **3.24** leading to the second ring closure and thus to octahydroindole structure **3.25**. Replacement of the bromine substituent at C6 position with an OAc group under inversion of the stereochemical configuration provided acetyl ester **3.26**. Removal of the Boc group of **3.26** finally gave access to L-Choi building block **3.27**.

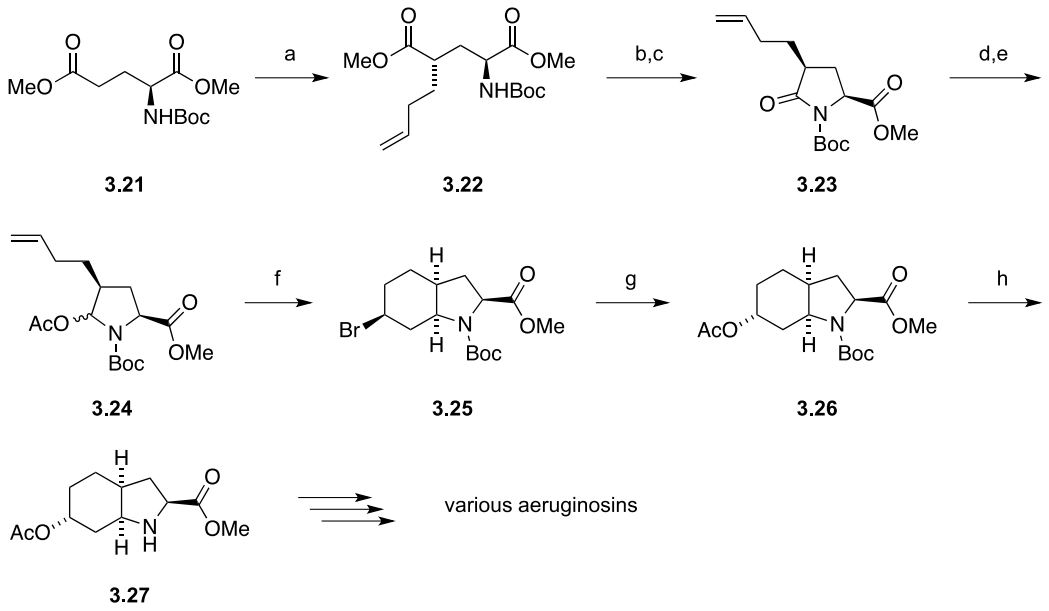

3.21 **3.22** **3.23**

3.24 **3.25** **3.26**

3.27

Scheme 31 Hanessian's synthesis of L-Choi building block **3.27**. Reagents and conditions: a) LiHMDS, THF, –78 °C, then 3-butenol triflate, 85%; b) TFA, CH_2Cl_2, then toluene, reflux, 92% over two steps; c) Boc_2O, Et_3N, DMAP, CH_2Cl_2, 90%; d) $LiHBEt_3$, THF, –78 °C; e) Ac_2O, Et_3N, DMAP, CH_2Cl_2, 91% over two steps; f) $SnBr_4$, DCM, –78 °C, 5 min, 78%; g) Bu_4NOAc, toluene, 50 °C, 78%; h) TFA, CH_2Cl_2.

1.2.4. Carreira's synthesis of microcin SF608

Carreira and his group also provided a synthetic route for the synthesis of the L-Choi core, developed during the synthesis of microcin SF608 (**7**) (Scheme 32).[15,16] Carreira's synthesis features *E*-α,β-unsaturated ester (**3.28**)[17] which upon diasteroselective epoxidation and lactone formation was transformed into intermediate **3.29**. Azidation of lactone **3.29** provided azidolactone **3.30**, which was subsequently opened with *O*-TBDPS-protected 4-aminobutanol. Reduction of the azide followed by Cbz protection of the obtained amine afforded intermediate **3.31**. Further, regioselective reduction of the epoxide of **3.31** yielded compound **3.32**. Acetylation of the secondary alcohol in **3.32** was followed by deoxygenation of the tertiary alcohol to give intermediate **3.33**. By removal of the Cbz protecting group followed by intramolecular nucleophilic opening of the oxabicyclo[2.2.1]heptane by the obtained amine, octahydroindole **3.34** was gained with the desired L-Choi configuration. Intermediate **3.34** was further converted into microcin SF608 (**7**) over ten additional synthetic steps.

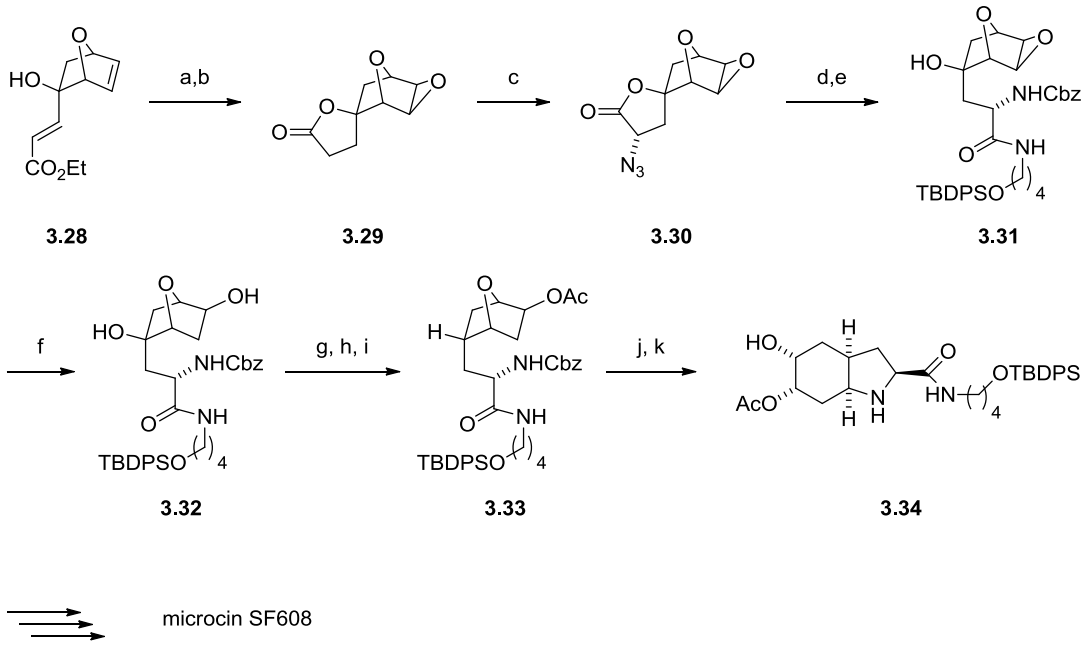

Scheme 32 Carreira's synthesis of microcin SF608 (**7**). Reagents and conditions: a) *m*-CPBA, CH_2Cl_2, 93%; b) H_2, Pd/C, then K_2CO_3, MeOH, 78%; c) LiHMDS, –78 °C, then $TrisN_3$, –45 °C, then AcOH/KOAc, CH_2Cl_2, 58%; d) *O*-TBDPS-4-amino-1-butanol, CH_2Cl_2, 94%; e) H_2, Pd/C, MeOH, then CbzCl, $NaHCO_3$, EtOAc/H_2O 1:1, 88%; f) Cp_2TiCl_2, Zn, 1,4-cyclohexadiene, THF, 0 °C, 75% brsm; g) Ac_2O, Et_3N, DMAP, CH_2Cl_2, 99%; h) *m*-CF_3-C_6H_4COCl, Et_3N, DMAP, CH_2Cl_2, 91%; i) h*v* (UV), *N*-methylcarbazole, 1,4-cyclohexadiene, THF/H_2O 1:1, 68%; j) H_2, Pd/C, MeOH, 93%; k) TMSOTf, Et_3N, CH_2Cl_2, 81%.

1.2.5. Trost's synthesis of aeruginosin 95B

In the total synthesis of aeruginosin 98B (**2**), Trost and co-workers used a Pd-catalyzed asymmetric allylic alkylation (AAA) of late stage intermediates **3.39a** and **3.39b** to form the bicyclic backbone of the L-Choi unit (Scheme 33).[18] Intermediates **3.39a** and **3.39b** were synthesized starting from 4-methoxyphenol (**3.35**), which was reduced in a first step under Birch conditions, followed by TIPS protection of the alcohol and diastereoselective α-hydroxylation to give racemic **3.36**. TES protection of **3.36** followed by treatment with Comin's reagent afforded triflate **3.37**. Heck coupling of the obtained triflate **3.37** with *N*-Boc-3-iodalanine methyl ester provided intermediates **3.38a** and **3.38b**, which could be further converted over three synthetic steps into the AAA reaction precursors **3.39a** and **3.39b**. The obtained bicyclic AAA reaction product **3.40** was finally transferred over two steps into L-Choi derivative **3.41** (Scheme 33).

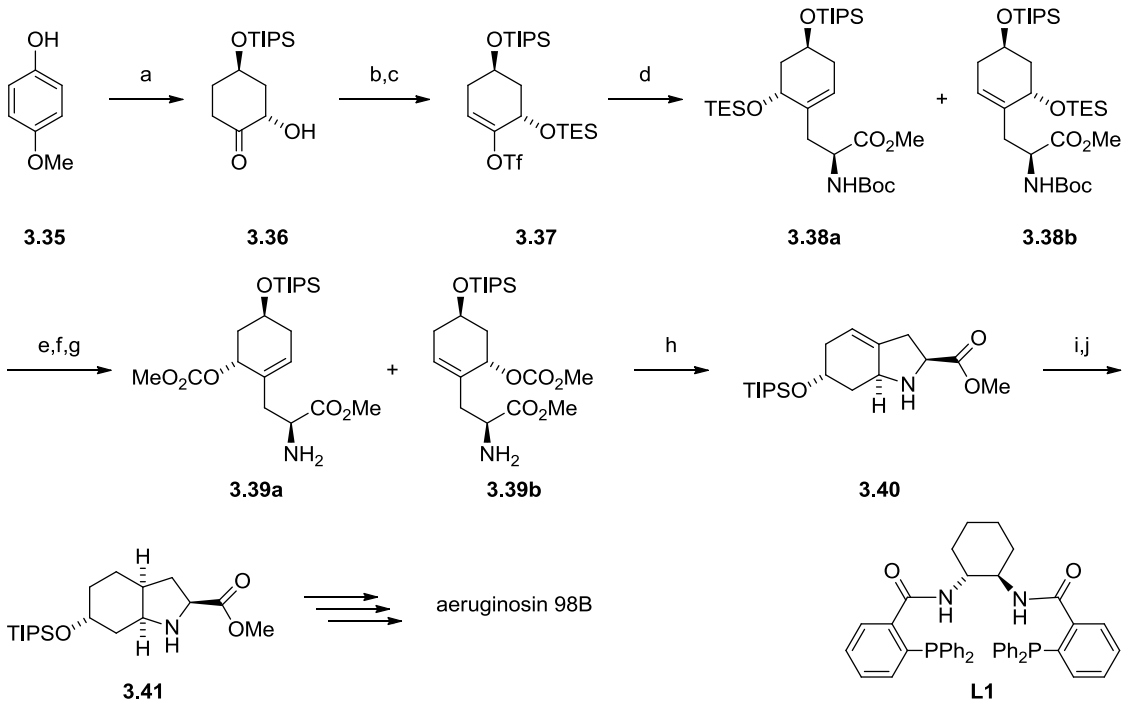

Scheme 33 Trost's synthesis of aeruginosin 98B (**2**). Reagents and conditions: a) Li, NH_3, EtOH, −78 °C, then TIPSOTf, 2,6-lutidine, CH_2Cl_2, 0 °C, then OsO_4, NMO, THF/H_2O 3:1, 0 °C, 96%; b) TESCl, imidazole, DMAP, CH_2Cl_2, 97%; c) LiHMDS, Comin's reagent, –78 °C to –40 °C, 88%; d) *N*-Boc-3-iodalanine methyl ester, Zn, TMSCl, $Pd(PPh_3)_4$, LiCl, DMA, 60 °C, 87%; e) HF-pyridine, CH_2Cl_2, 0 °C, 93%; f) methyl chloroformate, pyridine, DMAP, CH_2Cl_2, 0 °C, 98%; g) TFA, CH_2Cl_2, −10 °C; h) $[(\eta^3\text{-}C_3H_5)PdCl]_2$, racemic **L1**, TFA, THF, 60 °C, 96%; i) BnBr, Et_3N, MeCN, then TBAF, 89%; j) H_2, Pd/C, MeOH, 92%.

1.2.6. Baudoin's contributions to the syntheses of aeruginosins

The most recent contribution to the total synthesis field of aeruginosins arose from Baudoin and his group. Already in 2012, Baudoin *et al*. showed that the octahydroindole core of the Choi can be readily accessed *via* an intramolecular C_{sp3}-H alkenylation.[19] Based on this work, Baudoin and co-workers established an efficient, scalable synthesis for the L-Choi motif (Scheme 34). The synthesis was commenced with commercially available dihomoallylalcohol **3.42**, which after TBDPS protection of the alcohol and ring-closing metathesis afforded cyclopentenol **3.43**. Subsequent dibromocyclopropanation[20] provided cyclopropane **3.44** which upon thermal electrocyclic ring expansion furnished dibromocyclohexene **3.45**. Nucleophilic substitution with a TBS-protected L-alaninol derivative followed by trifluoroacetylation of the amine yielded **3.46**. Intramolecular C_{sp3}-H alkenylation of **3.46** catalyzed by $[Pd(PCy_3)_2]$ rendered hexahydroindole **3.47**. Hydrogenation of the alkene in **3.47** provided octahydroindole **3.48**, which was oxidized to the corresponding methyl ester **3.49** after deprotection of the alcohol. Cleavage of the trifluoroacetate finally furnished L-Choi derivative **3.50** (Scheme 34). Following this readily scalable synthetic strategy, Baudoin and co-workers were able to synthesize up to 700 mg of aeruginosin 298A (**1**).[21] Furthermore, the development of an intermolecular C_{sp3}-H arylation allowed the synthesis of halogenated Hpla fragments, which could be successfully incorporated in the synthesis of aeruginosin 98A(**16**) and C (**17**) (for the structures of the different aeruginosins see pages 5 and 8 in the general introduction).[22]

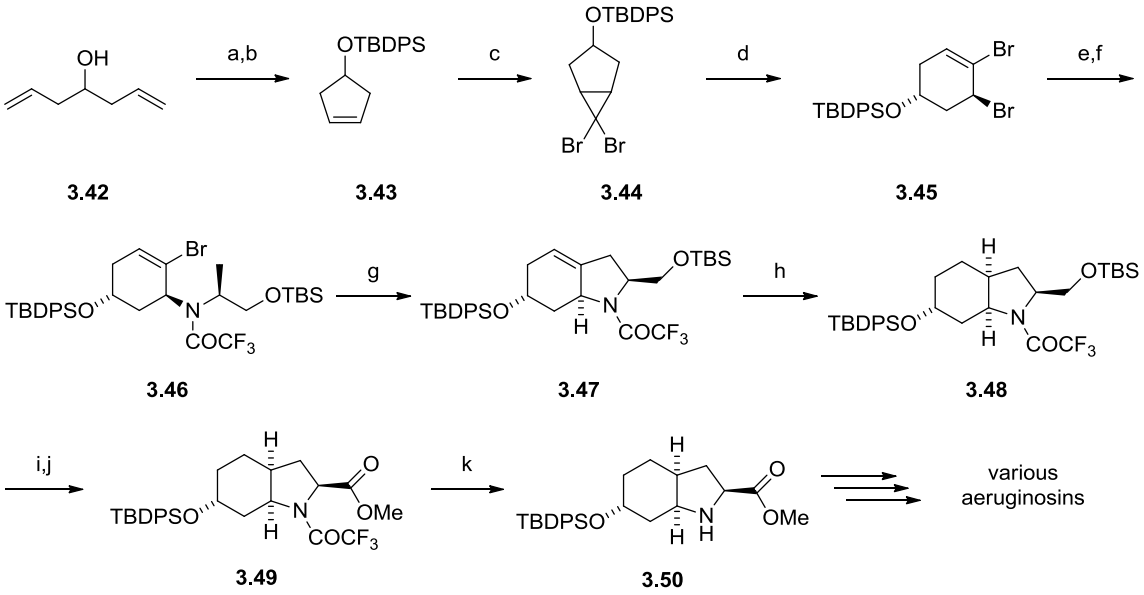

Scheme 34 Baudoin's synthesis of L-Choi building block **3.50**. Reagents and conditions: a) TBDPSCl, imidazole, CH_2Cl_2, 0 °C, quant.; b) Grubbs' first generation catalyst, CH_2Cl_2, quant.; c) $CHBr_3$, NaOH, Et_3BnNCl, CH_2Cl_2, ultrasound; d) 130 °C (neat), 88% over four steps; e) (*S*)-1-((*tert*-butyl dimethylsilyl)oxy)propan-2-amine, K_2CO_3, DMF, 20 °C to 90 °C; f) $(CF_3CO)_2O$, pyridine, CH_2Cl_2, 38% over two steps; g) $Pd(PCy_3)_2$, K_2CO_3, $^tBuCO_2K$, toluene, 120 °C, 71%; h) H_2, Rh/C, EtOAc, then HCl, MeOH, 95%; i) Jones' reagent, acetone, 86%; j) Me_3SiCHN_2, MeOH, 0 °C, 97%; k) $NaBH_4$, MeOH, –10 °C to 20 °C, 83%.

1.2.7. Comparison of the different synthetic strategies

As seen in the last sections, the groups of Bonjoch, Wipf, Carreira and Trost used a final formation of the C7a-N bond for the construction of the octahydroindole skeleton of the L-Choi (Figure 39). On the other hand, Hanessian described the formation of the C7-C7a bond *via* an aza-Prins halocarbocyclization to access the L-Choi. Most recently, Baudoin developed a C_{sp3}-H alkenylation, building up the L-Choi through formation of the C3-C3a bond (Figure 39).

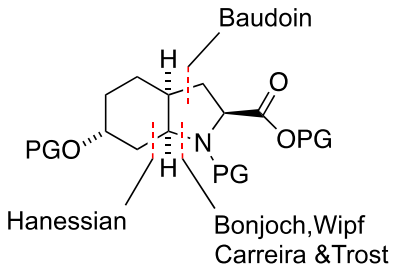

Figure 39 Comparison of the different reported syntheses of the L-Choi moiety with the main disconnections of the respective synthetic strategies marked in red.

2. Aim and Retrosynthetic Considerations

The aim of this project was the investigation of efficient synthetic strategies for the preparation of the D-*diepi*-Choi motif present in aeruginosins KT608A (**3.1**) and B (**3.2**) and KT650 (**3.1**). Further, the prepared D-*diepi*-Choi building block should be incorporated in the total syntheses of the natural products mentioned above. For the preparation of the octahydroindole core of the D-*diepi*-Choi we envisioned a straightforward synthesis from an enantiopure D-indoline precursor. Heterogeneous hydrogenation of this D-indoline precursor should allow for diastereoselective installation of the hydrogen atoms at C3a, C6 and C7a position, induced by substrate control from the carboxyl group of the indoline (Scheme 35). For the synthesis of suitable enantiopure indolines we considered two possible strategies. The first pathway comprises the condensation of an α-azido ester with anisaldehyde leading to an indole after intramolecular amination. Further, enantioselective hydrogenation of the indole should allow for the formation of enantioenriched indoline. The second strategy consists of using a starting material from the chiral pool, namely D-tyrosine, which is decorated with suitable protection and directing groups. Subsequent C-H activation should enable intramolecular amination and thus formation of the desired indoline (Scheme 35).

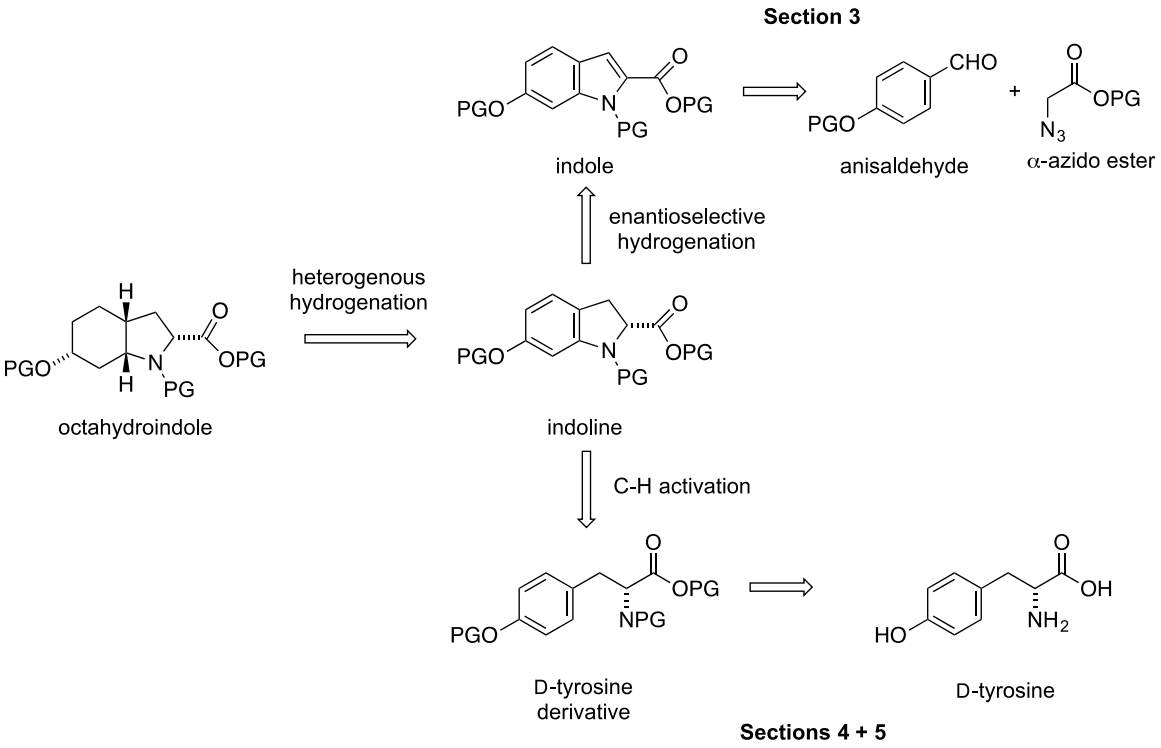

Scheme 35 Retrosynthetic analysis of D-*diepi*-Choi.

3. Synthesis of Aeruginosin KT608A – 1st Generation

3.1. D-*diepi*-Choi Synthesis

3.1.1. Preparation of the indole

The synthesis of aeruginosin KT608A commenced with the preparation of indole **3.55** which was needed for the later enantioselective reduction to access the required indoline. For the synthesis of indole **3.55**, commercially available *p*-anisaldehyde (**3.51**) was reacted with ethyl-2-azidoacetate (**3.52**), which had been prepared from ethyl bromoacetate (**3.53**),[23] in an aldol condensation.[24] First attempts using commercially available NaOEt led to low conversion and a poor yield of condensated product **3.54**. The poor reactivity of the aldol condensation could be enhanced by using freshly prepared NaOEt from solid Na and EtOH. With this modification, a yield of up to 70% on a small scale (~1 g) and 57% on a larger scale (~5.5 g) was achieved for the aldol condensation of **3.51** and **3.52**. The next step was the Hemetsberger-Knittel cyclization[25] of azide **3.54** to the corresponding indole. Initial attempts by catalyzing the intramolecular C-H amination with $Rh_2(OAc)_4$ at room temperature resulted only in moderate conversion and yield.[26,27] Besides the poor reactivity, the use of expensive Rh catalysts is not convenient for reactions on a larger scale. However, azidoacrylate **3.54** could be converted into the indole in an excellent yield of 93% without the addition of any catalyst by simply stirring **3.54** in refluxing *o*-xylene for 1.5 h.[28] The obtained indole was subsequently protected with an acetyl group to give indole derivative **3.55** in a good yield (Scheme 36).

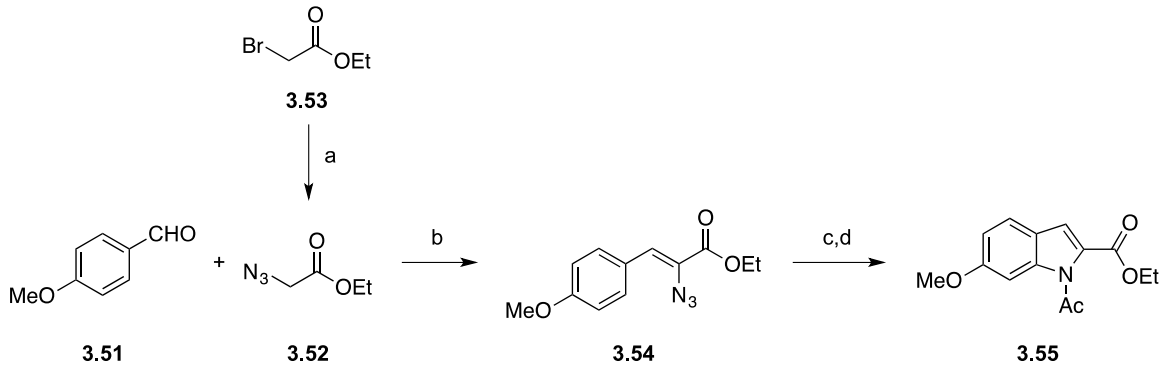

Scheme 36 Synthesis of indole **3.55**. Reagents and conditions: a) NaN_3, H_2O/acetone (1:3), r.t., 1 h, quant.; b) Na, EtOH, −15 °C, 7 h, 57%; c) *o*–xylene, 144 °C, 1.5 h, 93%; d) Ac_2O, DMAP, Et_3N, CH_2Cl_2, 50 °C, 16 h, 75%.

3.1.2. Enantioselective hydrogenation of the indole to the indoline

With indole **3.55** in hand, the focus was laid on the enantioselective hydrogenation to access the D-indoline derivative. Since the investigation of catalytic asymmetric hydrogenation reactions was a dynamic field in chemistry in the last two decades, a big diversity of different catalysts and ligands for a variety of specific substrates has been explored. In the early 2000s Kuwano and Ito were the first to achieve the asymmetric reduction of indoles in a highly enantioselective fashion, providing indolines with up to 95% *ee*.[29] Kuwano and Ito used a rhodium catalyst with a chiral di-ferrocenyl ligand for their asymmetric reduction (left, Figure 40). They successfully applied their catalytic system to a broad scope of 2-substituted indoles including 2-carboxylated indoles and thereby could optimize the reaction conditions to yield indolines with an *ee* of up to 99%.[30,31] Agbossou-Niedercorn and co-workers pursued a similar strategy to the one of Kuwano and Ito for their asymmetric reduction of indoles by using rhodium catalysts with chiral Walphos ligands (second from left, Figure 40). Agbossou-Niedercorn *et al*. achieved yields up to 85% and *ee*s up to 80% using these Walphos ligands.[32] Rueping and co-workers developed the first metal-free asymmetric hydrogenation of 3*H*-indoles by applying a reaction system with chiral Brønsted acids in combination with Hantzsch's ester as hydrogen source (second from right, Figure 40). With their catalytic system, Rueping *et al*. were able to access indolines with up to 99% *ee* and 99% yield from the corresponding 3*H*-indoles.[33] In 2010, Pfaltz and Baeza reported the use of Ir-PHOX catalysts for the asymmetric hydrogenation of 2-, 3- and 5-substituted indoles (right, Figure 40). With their Ir-PHOX catalysts, Pfaltz and Baeza could transfer 2-carboxylated indoles with 97% conversion and 99% *ee* into the corresponding indolines.[34]

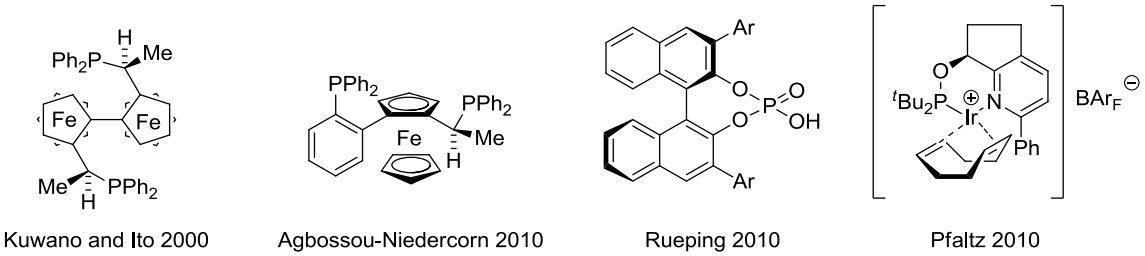

Figure 40 Different ligands and catalysts developed for the enantioselective reduction of indoles and 3*H*-indoles.

Of all the described enantioselective reduction methods, the one of Agbossou-Niedercorn, using chiral Walphos ligands, gave the lowest *ee* values and yields. Therefore, the use of this catalytic system was not investigated. Further, the asymmetric hydrogenation of the Rueping group only works with 3*H*-indoles and was therefore not suitable for our substrate, an indole. Most promising were the methods from Kuwano and Pfaltz, both using similar substrates to our indole for their asymmetric reductions. Both groups reported high *ee* values and yields. Since the Pfaltz group was located in the same department at the University of Basel, they generously provided us with their Ir-PHOX catalysts, whereas the di-ferrocenyl ligands used by Kuwano were not available and are cumbersome to prepare.[35] Therefore, the reduction developed by Pfaltz was investigated further for the asymmetric hydrogenation of indole **3.55** (Table 9). First, a racemic reduction of indole **3.55** was performed using Pd on carbon as catalyst at 75 bar H_2 pressure to access racemic indoline **3.56** (Entry 1). Racemic indoline **3.56** was needed as a reference for the later determination of the *ee* of the asymmetric hydrogenations *via* chiral HPLC. The first asymmetric reduction was carried out with 2 mol% Ir-PHOX catalyst **A** under a H_2 pressure of 100 bar at 60 °C. With these conditions an *ee* of 99% and a yield of 27% were achieved (Entry 2). Since already the first tried conditions gave almost enantiopure indoline **3.56**, the focus was laid on improving the yield. For this, the temperature was increased from 60 to 80 °C which indeed furnished a higher yield of 50% (Entry 3). Beside the isolation of the desired indoline, also starting material **3.55** and deprotected indole could be recovered. To further enhance the yield of the reaction, the catalyst loading was raised from 2 mol% to 3 and 4 mol%. By doing so, the yield was increased from 50% to 80% (Entries 4 and 5). Because no distinct effect was observed going from 3 to 4 mol%, a further increase of the catalyst loading was not tested. Next, the feasibility of the reduction on a larger scale was explored, going from a 0.04 mmol to a 0.4 mmol scale. Unfortunately, scaling up the reaction led to a significant drop of the yield, providing only 10% of the desired indoline **3.56**, with 2 mol% catalyst loading (Entry 6). As mentioned before, the Ir-PHOX catalyst was kindly provided by the research group of Pfaltz. However, the large molecular weight of the Ir-PHOX catalysts (>1600 g/mol) in combination with the relatively high required catalyst loading of up to 4 mol%, results in a catalyst loading of 25% *w*/*w*. For smaller scales these 25% *w*/*w* of catalyst were accessible, but not for larger scales. Therefore, the performance of Ir-PHOX catalyst **B** was investigated, since this catalyst was commercially available in a larger amount from Sigma-Aldrich. First, a catalyst loading of 2 mol% of catalyst **B** was applied, resulting only in traces of the desired product **3.56** (Entry 7). Raising the catalyst loading from 2 to 4 mol% allowed the isolation of 35% of

indoline **3.56**. However, chiral HPLC revealed a moderate *ee* of only 60% for catalyst **B** (Entry 8). Further increasing the catalyst loading to 6 mol% provided 50% of indoline **3.56** (Entry 9). Due to the moderate *ee* in combination with the required high catalyst loadings, the use of catalyst **B** was not further investigated. To conclude, the asymmetric hydrogenation was achieved with a high *ee* and yield using Ir-PHOX catalyst **A**, albeit only on a very small scale.

Table 9 Conditions tested for the asymmetric hydrogenation of indole **3.55** to access indoline **3.56**

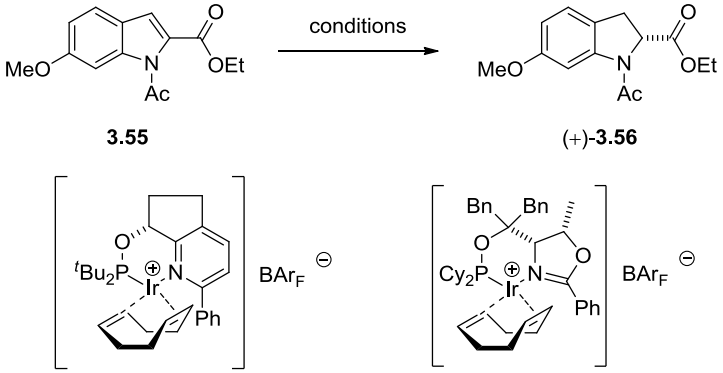

Entry	Catalyst	mol%	Conditions[a]	Observation[b]	*ee*[c]
1	Pd/C	10	CH_2Cl_2, H_2 (75 bar), r.t.	quant.	-
2[d]	A	2	CH_2Cl_2, H_2 (100 bar), 60 °C	27%	99
3[d]	A	2	DCE, H_2 (100 bar), 80 °C	50%[e]	n.d.
4[d]	A	3	DCE, H_2 (100 bar), 80 °C	80%[e]	n.d.
5[d]	A	4	DCE, H_2 (100 bar), 80 °C	80%[e]	n.d.
6[f]	A	2	DCE, H_2 (100 bar), 80 °C	10%[e]	n.d.
7	B	2	DCE, H_2 (100 bar), 80 °C	traces	n.d.
8	B	4	DCE, H_2 (100 bar), 80 °C	35%	60
9	B	6	DCE, H_2 (100 bar), 80 °C	50%	n.d.

[a]All reactions were carried out in a high pressure autoclave, solvents were filtered over aluminium oxide prior to use. [b]The yield was determined by isolation of the product and the conversion by integration of the ^{1}H NMR signals in the crude product. [c]The *ee* was determined by chiral HPLC. [d]The reaction was carried out on a 0.04 mmol scale. [e]Cleavage of the acetyl group was observed. [f]The reaction was carried out on a 0.4 mmol scale.

3.2. D-*diepi*-Choi Formation, 1st Approach

3.2.1. Reduction of the indoline to the octahydroindole

The next sequence of the total synthesis involved the formation of the octahydroindole core of D-*diepi*-Choi. For the reduction of indoline **3.56** to octahydroindole **3.57**, a heterogeneous catalysis was envisioned. The use of a heterogeneous catalyst poses the advantage that all hydrogen atoms are introduced from the side facing the surface of the catalyst, thus, allowing for stereochemical control of the three obtained chiral centers at C3a, C6 and C7a position. Alongside the induced *syn* addition of the hydrogen atoms by the heterogeneous catalyst, substrate control triggered by the carboxylate substituent at C2 position of the indoline takes place. The stereochemical configuration of the carboxylate substituent directs the binding of the indoline to the metal surface. These effects are responsible for the formation of a single diastereoisomer out of eight possible isomers. The groups of Vincent[36], Kim[37] and Cativiela[38–40] have reported on the highly diastereoselective outcome of prepared octahydroindoles from 2-substituted indolines. While the group of Vincent used Pd on carbon as catalyst, the groups of Kim and Cativiela applied PtO_2 as the heterogeneous catalyst. However, all the conditions described in the literature led to no conversion with our substrate. Pleasingly, indoline **3.56** could be converted into octahydroindole **3.57** using Rh on carbon as catalyst at 50 bar hydrogen pressure, according to a patented procedure (Scheme 37).[41] Beside quantitative conversion, the reaction also displayed a high stereoselectivity featuring almost exclusively the formation of the desired compound **3.57**. The correct relative configuration of octahydroindole **3.57** was confirmed by X-ray crystallographic analysis which revealed the *syn* configuration of the hydrogen atoms at positions C2, C3a, C6 and C7a (crystal structure numbering: C1, C3, C6 and C8, respectively), as shown in Figure 41.

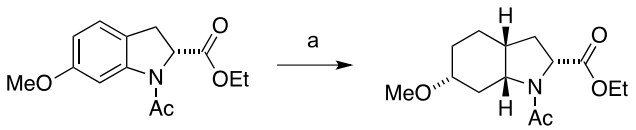

3.56 **3.57**

Scheme 37 Reduction of indoline **3.56** to octahydroindole **3.57**. Reagents and conditions: a) H_2 (50 bar), Rh/C, MeOH, r.t., 9 h, 99%.

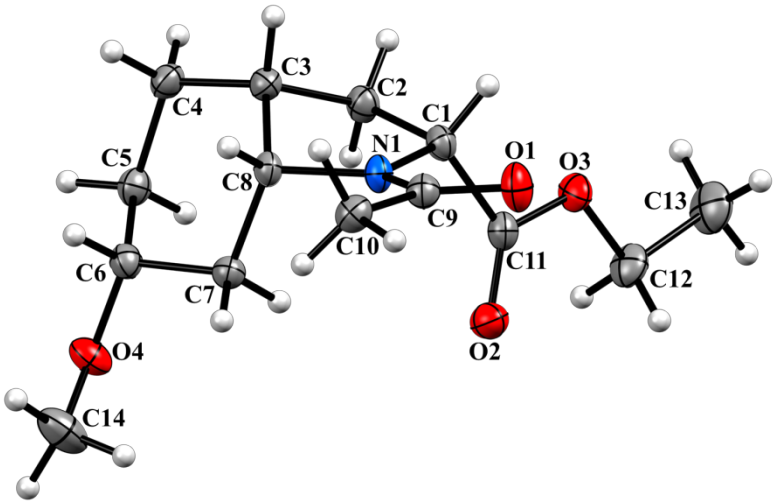

Figure 41 Structure of the D-enantiomer present in the asymmetric unit of racemic **3.57**, ellipsoids plotted at 40% probability level. Selected bond parameters: N1–C9 = 1.3488(15), O1–C9 = 1.2333(15) Å; C1–N1–C8 = 111.65(9), C1–N1–C9 = 119.75(10), N1–C9–O1 = 121.10(11)°.

3.2.2. Deprotection of the octahydroindole

Octahydroindole **3.57** already contained the whole carbon backbone of the D-*diepi*-Choi core structure. Therefore, only global deprotection was required to access D-*diepi*-Choi building block **3.59**. First, cleavage of the methoxy ether was investigated. Initial attempts based on the classical method for this transformation using the strong Lewis acid BBr_3 resulted in no conversion.[42,43] The addition of 18-crown-6-ether and NaI to BBr_3 could not enhance the reactivity either.[44,45] Similar results were obtained when employing $SiCl_4$ and NaI for the deprotection.[46] Finally, a deprotection method utilizing TMSCl and NaI, which has been described by Zutter and co-workers, led to the formation of the desired alcohol **3.58** in a very good yield.[47] Further, removal of the acetyl group and saponification of the ethyl ester were achieved by treating **3.58** with an aqueous 6 M HCl solution giving the hydrochloride salt of D-*diepi*-Choi **3.59** (Scheme 38).

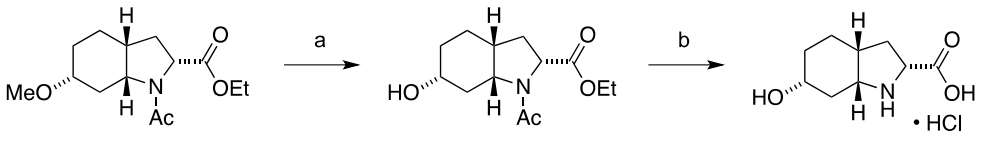

3.57 **3.58** **3.59**

Scheme 38 Synthesis of D-*diepi*-Choi hydrochloride salt **3.59**. Reagents and conditions: a) TMSCl, NaI, MeCN, 40 °C, 16 h, 77%; b) 6 M HCl, H_2O, reflux, 5 h, quant.

3.3. Octahydroindole Formation, 2nd Approach

In the course of the D-*diepi*-Choi synthesis, alternative approaches were also investigated. Since methoxy ethers connected to an sp^3 carbon center are more stable than their analogues linked to an sp^2 carbon center, cleavage of the ether at an earlier stage of the synthesis was examined. Indeed, indoline **3.56** showed an enhanced reactivity compared to that of octahydroindole **3.57** towards the cleavage of the methoxy ether. Treating indoline **3.56** with BBr_3 afforded the desired free alcohol **3.60** in a good yield. However, the following reduction of indoline **3.60** with the conditions developed in Section 3.2.1 led to no conversion. Neither increasing the temperature or the H_2 pressure nor the use of other heterogeneous catalysts such as PtO_2 could convert indoline **3.60** into octahydroindole **3.58** (Scheme 39). Since the free hydroxyl group of indoline **3.60** seemed to be responsible for decreasing the reactivity towards hydrogenations, the alcohol of **3.60** was protected with a MOM group to counterbalance this effect. Doing so, the reduction of indoline **3.61** proceeded smoothly using the conditions described in Section 3.2.1. Further, global acidic deprotection provided *diepi*-Choi core **3.59** in quantitative yield (Scheme 39). Due to the ready availability of racemic indoline **3.60**, all the reactions described in this section were performed with racemic substrates. However, the feasibility of this approach could be proven.

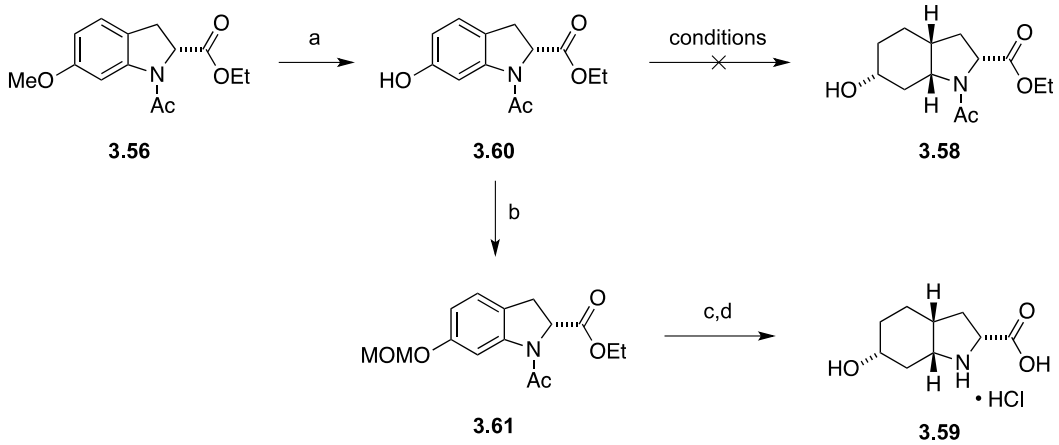

Scheme 39 Synthesis of racemic *diepi*-Choi hydrochloride salt **3.59**. Reagents and conditions: a) BBr_3, CH_2Cl_2, −78 °C, 3 h, 85%; b) MOMCl, DIPEA, CH_2Cl_2, 0 °C to r.t., 20 h, 87%; c) H_2 (50 bar), Rh/C, MeOH, r.t., 14 h, 99%; d) 6 M HCl, H_2O, reflux, 5 h, quant.

3.4. Synthesis of the Different Building Blocks

3.4.1. Agmantin side chain

The agmantin side chain was synthesized from commercially available 2-methyl-2-thiopseudourea hemisulfate (**3.62**) according to literature known procedures. Protection of the imine and the amine of **3.62** with Boc_2O afforded pseudothiourea derivative **3.63**.[48] Replacement of the methyl thioether in **3.63** by 1,4-butanediamine gave access to agmantin side chain **3.64** in an excellent yield (Scheme 40).[49]

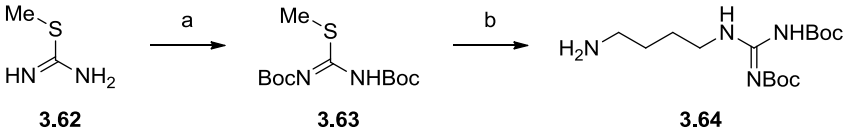

3.62 **3.63** **3.64**

Scheme 40 Synthesis of the agmantin side chain **3.64**. Reagents and conditions: a) Boc_2O, $NaHCO_3$, CH_2Cl_2, r.t., 18 h, 92%; b) 1,4-butanediamine, THF, 50 °C, 1 h, 97%.

3.4.2. L-Hpla building block

The L-Hpla-OH building block **3.67** was prepared *via* a literature known two-step sequence starting from L-Tyr-OH (**3.65**). Protection of the hydroxyl group of **3.65** with a benzyl group furnished amino acid **3.66**.[50] Further transformation of **3.66** into phenyllactic acid derivative **3.67** was achieved by treating **3.66** with isoamyl nitrite and NaOAc (Scheme 41).[51]

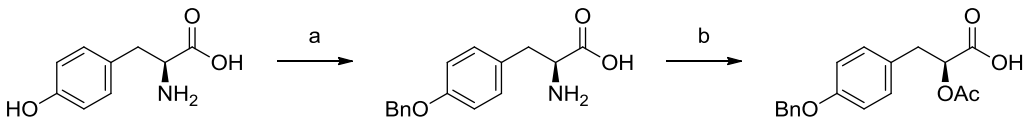

3.65 **3.66** **3.67**

Scheme 41 Synthesis of L-Hpla-OH unit **3.67**. Reagents and conditions: a) BnBr, NaOH, $CuSO_4$, MeOH/H_2O (5:1), r.t., 16 h, 62%; b) isoamyl nitrite, AcOH, NaOAc, r.t., 24 h, 69%.

3.4.3. Boc-D-Phe-OH building block

Boc-D-Phe-OH (**3.69**) was accessed through protection of the amine of commercially available D-Phe-OH (**3.68**) (Scheme 42).

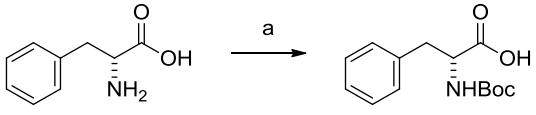

3.68 **3.69**

Scheme 42 Synthesis of Boc-D-Phe-OH (**3.69**). Reagents and conditions: a) Boc_2O, NaOH, dioxane/H_2O (2:1), 0 °C to r.t., 16 h, quant.

3.5. Assembly of the Different Building Blocks

The assembly of the different building blocks is shown in Scheme 43. The preparation of aeruginosin KT608A (**3.1**) commenced with the esterification of D-*diepi*-Choi building block **3.59** to give the hydrochloride salt of methyl ester **3.70**. Peptide coupling of the obtained methyl ester **3.70** with Boc-D-Phe-OH fragment **3.69** delivered dipeptide **3.71**. In the ^{1}H and ^{13}C NMR spectra, three sets of signals in a ratio of 3:1:1 were observed for dipeptide **3.71**. Two of those sets could be assigned to the occurrence of two rotameric conformers of **3.71**, in a ratio of 3:1. Nonetheless, the third set of signals in the NMR spectra indicated the presence of another diastereoisomer of dipeptide **3.71** in the sample probe. The reason for the formation of this second diastereoisomer remains under further investigation, but has to be derived either from a racemization process during peptide coupling or from the use of a non-enantiopure D-*diepi*-Choi building block. Separation of the two diastereoisomers through flash column chromatography was not possible; therefore, the 4:1 diastereomeric mixture was used for the subsequent steps of the assembly. Acidic removal of the Boc protecting group of dipeptide **3.71** provided amine **3.72** which was coupled to L-Hpla building block **3.67** giving tripeptide **3.73** in a yield of 60% over two steps. Simultaneous saponification of the D-*diepi*-Choi methyl ester and the L-Hpla acetyl ester of tripeptide **3.73** gave access to acid **3.74**. Subsequent coupling of acid **3.74** to agmantin side chain **3.64** using PyBOP and NMM furnished tetrapeptide **3.75** in a yield of 61% over two steps. For completion of the total synthesis of KT608A (**3.1**), only global deprotection was required. First, the two Boc groups of the agmantin side chain were removed under acidic conditions, followed by cleavage of the benzyl group of the L-Hpla residue using catalytic hydrogenation (Scheme 43). The crude residue obtained from the deprotection steps was subjected to fractionated HPLC purification leading to the isolation of 1.0 mg of KT608A (**3.1**).

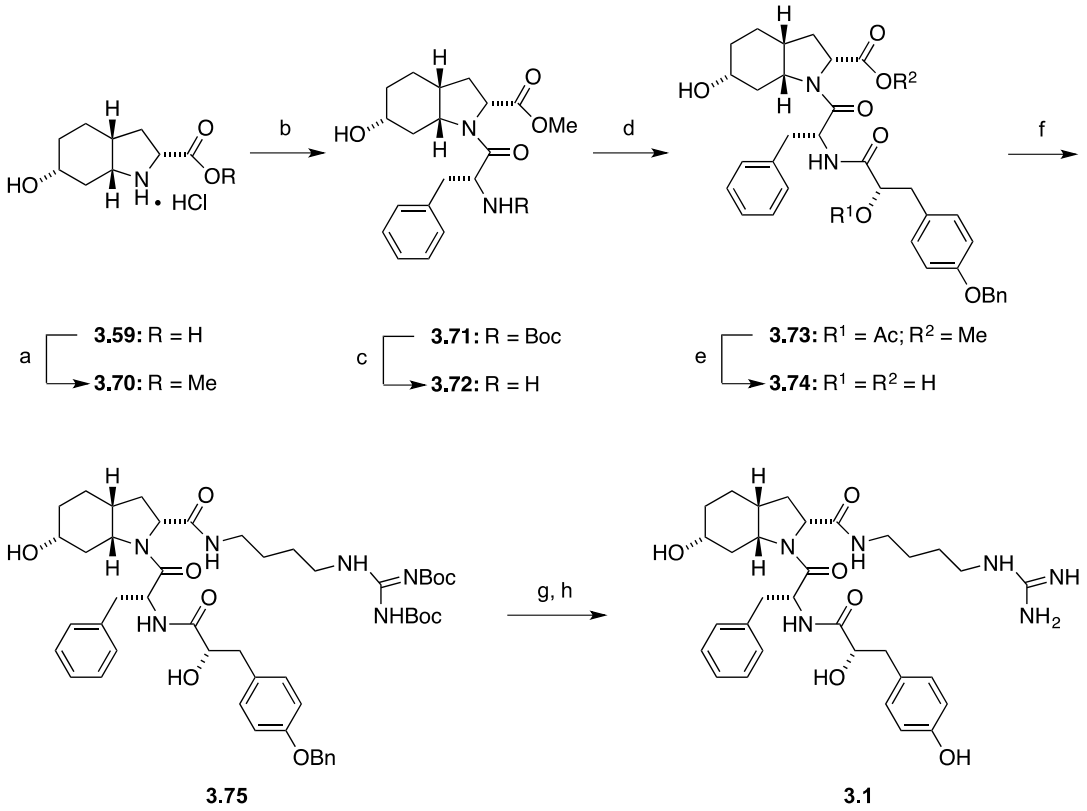

Scheme 43 Synthesis of aeruginosin KT608A (**3.1**). Reagents and conditions: a) $SOCl_2$, MeOH, 60 °C, 4 h, quant.; b) Boc-D-Phe-OH **3.69**, PyBOP, NMM, CH_2Cl_2, r.t., 72 h, 64%; c) TFA, CH_2Cl_2, 0 °C, 1 h; d) L-Hpla-OH **3.67**, PyBOP, NMM, CH_2Cl_2, r.t., 36 h, 60% over two steps; e) 0.1 N LiOH, THF, r.t., 20 h; f) agmantin side chain **3.64**, PyBOP, NMM, DMF, r.t., 48 h, 61% over two steps; g) 1 N HCl, MeCN, r.t., 24 h; h) H_2, Pd/C, EtOAc/MeOH (1:1), r.t., 36 h, 37% over two steps.

3.6. Comparison of the NMR Spectra of Isolated and Synthesized AKT608A

The synthesized aeruginosin KT608A (**3.1**) was characterized by ^1H and ^{13}C NMR as well as COSY, HMBC, HSQC and NOESY 2D NMR experiments. Comparison of our recorded NMR spectra with the spectra of the isolated product reported in the literature[1] revealed significant deviations (Figure 43, Table 10). The most apparent difference is displayed by the ratio of the two rotamers present in the different samples. While the NMR spectra of the isolation work showed a ratio of almost 1:1 of *cis* and *trans* rotamers, our measured spectra indicated the presence of a 3:1 ratio favoring the *trans* rotamer. As already described in Chapter I, the NMR spectra of aeruginosins are strongly influenced by the water and salt concentration of the recorded sample, as well as by the counterion present. However, the influence of these parameters only affected the chemical shifts of the signals, whereas the equilibrium of the *cis* and *trans* rotamers stayed constant under different conditions. Changing the temperature also exerts a negligible effect on the ratio of the two rotamers, as shown in

Section 5.14.1 of Chapter I. The ratio of the two rotameric conformations therefore displays a characteristic feature of a particular aeruginosin. For this reason, the distinct deviation of the recorded rotameric ratios of **3.1** foreboded the existence of two different structures of the isolated and synthesized aeruginosin KT608A (**3.1**). Beside the nonconformity of the rotameric ratios, the chemical shifts in the ^{1}H and ^{13}C NMR spectra also showed tremendous differences (Table 10, page 126). The most pronounced discrepancies in the ^{1}H NMR shifts were found for the signals of the D-*diepi*-Choi unit, namely H7 ($\Delta\delta$ = –0.77 ppm), H7' ($\Delta\delta$ = +1.07 ppm), H3 ($\Delta\delta$ = –0.57 ppm) and H2 ($\Delta\delta$ = –0.58 ppm) (for atom labeling and numbering of **3.1** see Figure 42). Further distinct differences were found for Phe-H2 ($\Delta\delta$ = +0.43 ppm), Agm-NH-1 ($\Delta\delta$ = +0.32 ppm) and Agm-NH-4 ($\Delta\delta$ = +0.40 ppm). Comparison of the ^{13}C NMR spectra resembles the situation described for the ^{1}H NMR spectra: The largest chemical shift deviations were observed for the signals of the D-*diepi*-Choi unit (C7: $\Delta\delta$ = +1.8 ppm; C3a: $\Delta\delta$ = +3.0 ppm; C3: $\Delta\delta$ = –3.3 ppm) and for Phe-C3 ($\Delta\delta$ = +1.3 ppm). The ^{1}H and ^{13}C signals for the Hpla, Phe (except for H2 and C2) and Agm (except for N-H) units were in accordance with each other and showed only minor differences. To conclude, comparison of the NMR spectra indicated that the structures of the isolated and synthesized aeruginosin KT608A (**3.1**) were not identical. This provoked the assumption that either the structure of **3.1** was wrongly assigned during the isolation work or that a mistake had slipped in during the total synthesis. Possible missteps in the synthesis or assignment will be discussed in the following section.

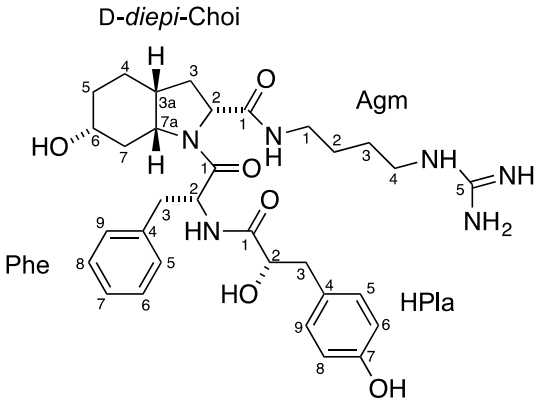

Figure 42 Atom labeling and numbering in aeruginosin KT608A (**3.1**).

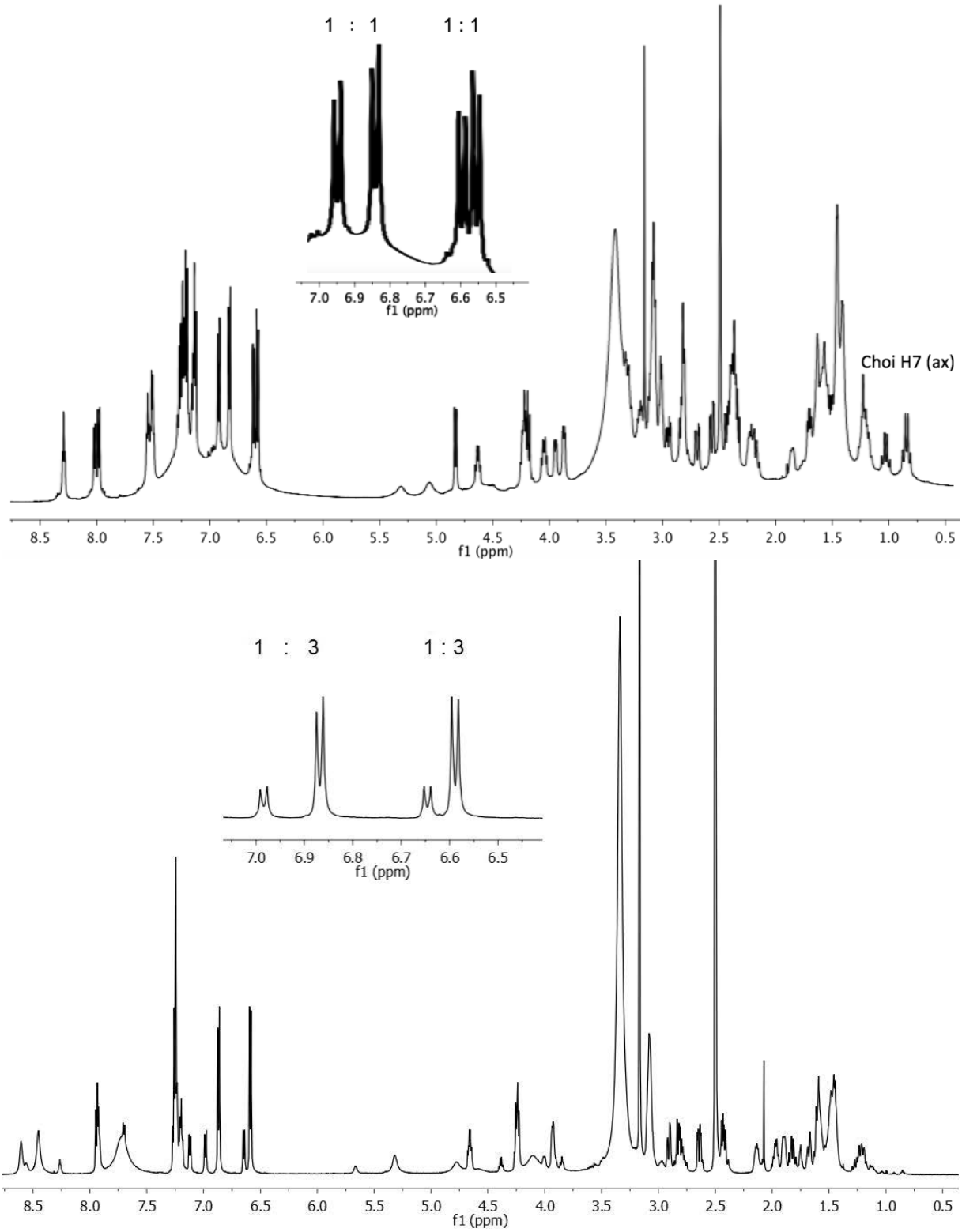

Figure 43 ^{1}H NMR spectra of synthetic aeruginosin KT608A (**3.1**) (top) and isolated aeruginosin KT608A (**3.1**) (bottom).

Table 10 Comparison of the ^{1}H and ^{13}C NMR spectra of natural and synthetic KT608A (**3.1**)

		^{1}H shifts (ppm)			^{13}C shifts (ppm)		
Subunit	Position	KT608A natural	KT608A synthetic	$\Delta\delta$	KT608A natural	KT608A synthetic	$\Delta\delta$
Choi	1	-	-	-	172.3	171.1	–1.2
	2	4.82	4.24	–0.58	59.6	59.8	+0.2
	3	2.38	1.81	–0.57	33.6	30.3	–3.3
	3'	1.70	1.96	+0.26	-	-	-
	3a	2.23	2.13	–0.10	32.7	35.7	+3.0
	4	1.63	1.57	–0.06	22.7	22.4	–0.3
	4'	1.56	1.67	+0.09	-	-	-
	5	1.56	1.60	+0.04	29.9	29.0	–0.9
	5'	1.19	1.20	+0.01	-	-	-
	6	3.30	3.36	+0.06	67.0	66.9	–0.1
	7	2.37	1.60	–0.77	36.1	37.9	+1.8
	7'	0.83	1.90	+1.07	-	-	-
	7a	4.04	4.24	+0.20	56.8	57.3	+0.5
Hpla	1	-	-	-	173.5	173.0	–0.5
	2	3.85	3.93	+0.08	72.0	72.0	0.0
	3	2.33	2.43	+0.10	39.5	39.5	0.0
	3'	2.55	2.64	+0.09	-	-	-
	4	-	-	-	128.5	128.2	–0.3
	5,9	6.82	6.87	+0.05	130.4	130.2	–0.2
	6,8	6.57	6.59	+0.02	114.9	114.6	–0.3
	7	-	-	-	155.7	155.6	–0.1
	2-OH	5.05	5.32	+0.27	-	-	-
	7-OH	9.06	9.28	+0.22	125.8	125.8	0.0
Phe	1	-	-	-	170.0	169.3	–0.7
	2	4.20	4.66	+0.46	51.8	50.9	–0.9
	3	2.84	2.91	+0.07	36.5	37.8	+1.3
	3’	2.81	2.82	+0.01	-	-	-
	4			-	138.4	137.4	–1.0
	5,9	7.12	7.20	+0.08	129.2	129.2	0.0
	6,8	7.19	7.25	+0.06	128.2	128.2	0.0
	7	7.14	7.20	+0.06	126.4	126.4	0.0
	NH	7.97	7.94	–0.03	-	-	-
Agm	1	3.18	3.09	–0.09	38.6	37.8	–0.8
	1'	3.06	3.09	+0.03	-	-	-
	2	1.45	1.46	+0.01	26.2	25.8	–0.4
	3	1.41	1.47	+0.06	26.4	26.3	–0.1
	4	3.08	3.07	–0.01	40.6	40.3	–0.3
	5	-	-	-	156.9	157.3	+0.4
	1-NH	8.29	8.61	+0.32	-	-	-
	4-NH	7.52	7.92	+0.40	154.9	-	-

3.6.1. Elucidation of possible mistakes

Possible mistakes during the total synthesis of KT608A

Since the total synthesis of a natural product is a complex construct, possible mistakes can be manifold. As the analytical data for the building blocks Agm **3.64**,[48,49] L-Hpla-OH **3.67**[50,51] and Boc-D-Phe-OH (**3.69**) were in accordance with the literature, a fault in the synthesis of these units can be excluded. This assumption is supported by the NMR data, which show minor differences for the signals of these building blocks (Table 10). Therefore, possible mistakes have to have occurred in the synthesis of D-*diepi*-Choi unit **3.59** or during assembly of the building blocks. The relative configuration of the D-*diepi*-Choi was confirmed by X-ray crystallographic analysis of compound **3.57**, displaying the *syn* configuration of the hydrogen atoms at C2, C3a, C6 and C7a (Figure 41, page 119). However, crystallization of octahydroindole **3.57** was carried out starting from a racemic sample, thus not allowing for definition of the absolute configuration of **3.57**. Hence, determination of the absolute configuration of indoline **3.57** builds on the work of Baeza and Pfaltz, who reported on the exclusive formation of the R indoline **3.77** from indole **3.76** using Ir-PHOX catalyst **A** (Scheme 44).[34] As in our synthesis the other enantiomer of catalyst **A** was used, the indoline with D configuration should be obtained (R corresponds to an L configuration, S to a D configuration). Since our substrate for the enantioselective hydrogenation was not exactly the same as the one of Baeza and Pfaltz,[34] there remains a possibility that the absolute configuration of the obtained indoline is reversed to that of the literature,[34] though such an inversion would be unusual. However, definite confirmation of the absolute configuration of indoline **3.57** could only be done by comparison of the optical rotation value of **3.57** with that of an authentic substrate with known absolute configuration. The synthesis of such a reference substrate will be discussed in more detail in Section 4.

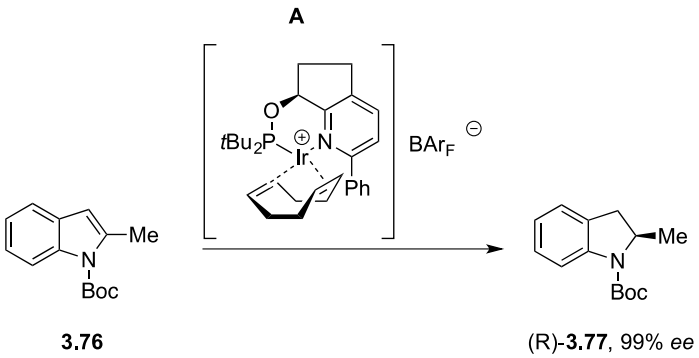

3.76 (R)-**3.77**, 99% *ee*

Scheme 44 Asymmetric hydrogenation reported by Baeza and Pfaltz, including the confirmation of the absolute configuration of the obtained indoline **3.77**.[34]

A more probable misstep in the total synthesis would be that the asymmetric hydrogenation of indole **3.55** did not provide enantiopure indoline **3.56**, since the *ee* was not determined by chiral HPLC for each reaction condition (Section 3.1.2). According to this theory, a mixture of the D-*diepi*-Choi and L-6-*epi*-Choi could have been present in building block **3.59** (for the nomenclature of the different Choi isomers see Figure 45). This hypothesis is supported by the fact that indeed a 4:1 diastereomeric mixture of Phe-D-*diepi*-Choi dipeptide **3.71** was obtained (Section 3.5). The isolation of KT608A diastereoisomer **3.78**, containing an L-6-*epi*-Choi core instead of the D-*diepi*-Choi, can thus not be excluded (Figure 44). To prevent the formation of diastereoisomers, the incorporation of an enantiopure D-*diepi*-Choi building block is required. Doing so, the possibility of a wrong diastereoisomer isolated during final HPLC purification can be excluded. Studies on such a synthesis will be discussed in Section 5.

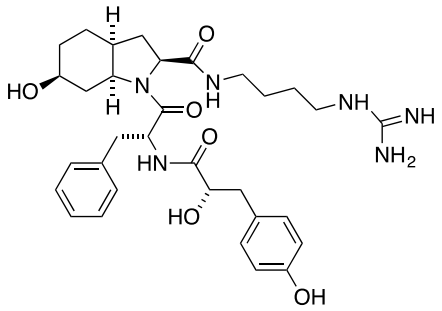

3.78

Figure 44 Compound **3.78** displays a possible diastereoisomer of KT608A (**3.1**) which might have been isolated instead of **3.1** during the final HPLC purification of the total synthesis.

Possible mistakes in the assignment of the structure of KT608A

As already described in the general introduction of this thesis, there have been various misassignments in the structural elucidation of compounds from the aeruginosin family. Among others, Carmeli and co-workers have also contributed to the number of misassigned aeruginosins with the wrong determination of the structure of aeruginosin EI461.[6,52]

The absolute configuration of the Phe and Hpla units of KT608A (**3.1**) were confirmed *via* acidic hydrolysis of the peptide bonds of **3.1** followed by the application of Marfey's method and chiral-phase HPLC on the obtained fragments. Thus, the L configuration of the Hpla moiety and the D configuration of the Phe could be confirmed.[1] A potential wrong assignment of the Carmeli group can therefore be restricted to the conformation of the Choi core, which is supported by the NMR data, revealing large deviations only in the Choi unit signals (Table 10). Four relative configurations of the Choi motif are possible, assuming that the hydrogen atoms at C3a and C7a positions have to be in a *syn* relationship, caused by the biosynthetic pathway of the Choi fragment and the large ring strain of *trans*-fused Choi derivatives.[53,54] These four relative configurations can adopt either an L or D absolute configuration (Figure 45). Beside the D-*diepi*-Choi, only the L-Choi (present in the majority of isolated aeruginosins[2]), the L-*diepi*-Choi (present in aeruginosin EI461[6]) and the L-6-*epi*-Choi (present in aeruginosin DA594A, DA511 and KB676) have been detected in natural aeruginosins.

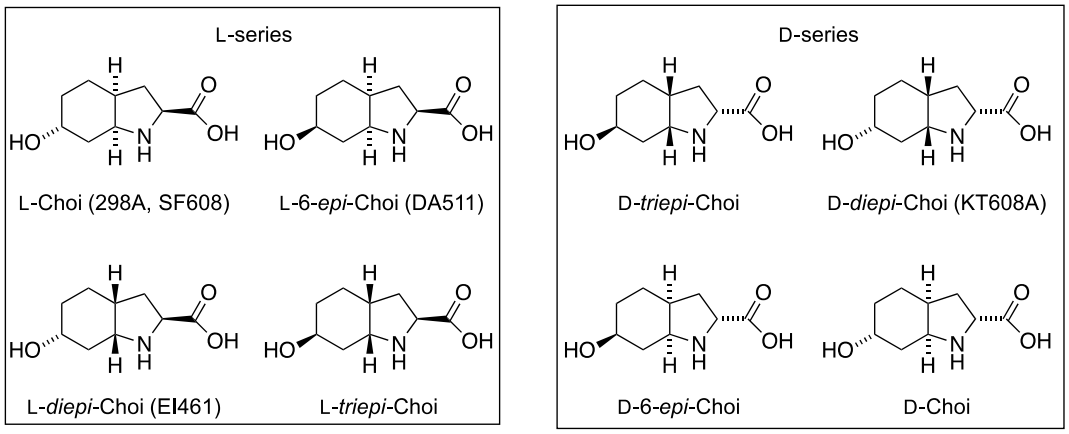

Figure 45 Configurations of the Choi unit: four relative configurations with L and four relative configurations with D absolute configuration are possible. The nomenclature results on the one hand from the configuration at the C2 center (L or D) and on the other hand from the epimerization of centers C3a, C6 and C7a with respect to the L-Choi. Therefore, the enantiomer of *e.g.* L-Choi is named D-*triepi*-Choi. Aeruginosins consisting of the specific Choi structure are shown in brackets.

Now, which one is which member in the Choi family?

The best way to distinguish between the different relative configurations of the Choi family is to analyze the respective ^{1}H NMR spectra. First, we make the assumption that the relative configuration of the Choi motif has a more distinct influence on the chemical shifts than the absolute configuration. Thus, both enantiomers of a relative Choi configuration, *e.g.* L-Choi and D-*triepi*-Choi, will have similar shifts, although the decoration of the Choi with chiral substituents provides different diastereoisomers with slightly different NMR spectra. One example for how the different isomers can be identified is by considering the Choi-H6 signal. The Choi-H6 chemical shift is heavily influenced by the relative configuration of the Choi (Figure 46): In D-*diepi*-Choi and L-*diepi*-Choi, the hydroxyl group at Choi-C6 occupies an equatorial position, leading to chemical shifts of the Choi-H6 of around 3.30 ppm. In D-*triepi*-Choi and L-*triepi*-Choi, however, the hydroxyl group is found in an axial position, so that the ^{1}H NMR signal of Choi-H6 is shifted downfield to around 3.90 to 4.00 ppm. Since the Choi-H6 chemical shift of the isolated aeruginosin KT608A (**3.1**) was reported to be 3.30 ppm, a D-*triepi*-Choi and L-*triepi*-Choi configuration, as well as their respective enantiomers (L-Choi and D-Choi), can be excluded. Aeruginosin KT608A (**3.1**) therefore has to contain either a D-*diepi*-Choi, L-*diepi*-Choi, L-6-*epi*-Choi or D-6-*epi*-Choi core unit. The differences in the ^{1}H NMR spectra of D-*diepi*-Choi and L-*diepi*-Choi and L-6-*epi*-Choi and D-6-*epi*-Choi, respectively, will be discussed in the next section.

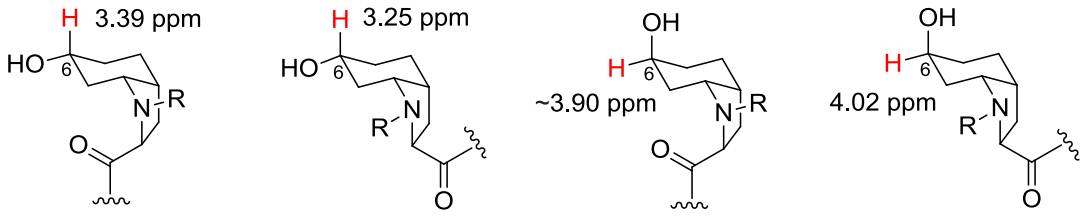

D-*diepi*-Choi L-*diepi*-Choi D-*triepi*-Choi L-*triepi*-Choi

Figure 46 The four possible relative configurations of the Choi family. For a better overview, only one enantiomer of each relative configuration is shown. The chemical shifts were obtained from the following examples reported in the literature: D-*diepi*-Choi from the synthesis of originally proposed aeruginosin EI461 by Bonjoch,[6] L-*diepi*-Choi from the revised structure of aeruginosin EI461 (**53**),[6] D-*triepi*-Choi from aeruginosin 298A (**1**)[55] and microcin SF608 (**7**)[4] and L-*triepi*-Choi from a side product obtained in Wipf's and Methot's synthesis of aeruginosin 298A (**1**).[9] The Choi-H6 atom is highlighted in red.

D-*diepi*-Choi *vs.* L-*diepi*-Choi

Comparing the ^{1}H NMR spectra of aeruginosin EI461[6] containing an L-*diepi*-Choi core with those of KT608A (**3.1**) reveals good accordance of the chemical shifts (Table 11, page 133). Nonetheless, Carmeli and co-workers excluded the presence of an L-*diepi*-Choi unit in aeruginosin KT608A due to observed NOE cross-peaks between Choi H2 and H3a. Carmeli attributed these cross-peaks to a *syn* configuration of H2 and H3a (as in D-*diepi*-Choi). Therefore, Carmeli proposed the presence of a D-*diepi*-Choi instead of an L-*diepi*-Choi unit in aeruginosin KT608A (**3.1**). Figure 47 shows the ROESY spectrum of KT608A (**3.1**) recorded by Carmeli with the highlighted Choi H2-H3a cross-peaks (Figure 47). The conclusion that these cross-peaks are proof for the *syn* configuration of H2 and H3a is problematic in several respects: First, the intensity of the discussed cross-peaks is very low, therefore they might arise from a $^{4}J_{\text{H-H}}$ COSY coupling, since long-range couplings are possible for rigid bicyclic systems with a W shape orientation.[56] Second, from our X-ray crystal structure of the D-*diepi*-Choi core derivative **3.57** (Figure 41, page 119), the distance between protons H2 and H3a can be measured, revealing a value of 2.9 Å. This relatively short distance should result in more intense cross-peaks of H2 and H3a than those observed by Carmeli.[57] Further, the distance for an *anti* configuration of H2 and H3a can also be estimated from the crystal structure and should be less than 4.2 Å. This distance still allows the occurrence of NOE cross-peaks between H2 and H3a.[57] To conclude, the observed NOE cross-peaks between H2 and H3a do not necessarily result from a relative *syn* configuration of these substituents, thus an L-*diepi*-Choi moiety in aeruginosin KT608A cannot be excluded.

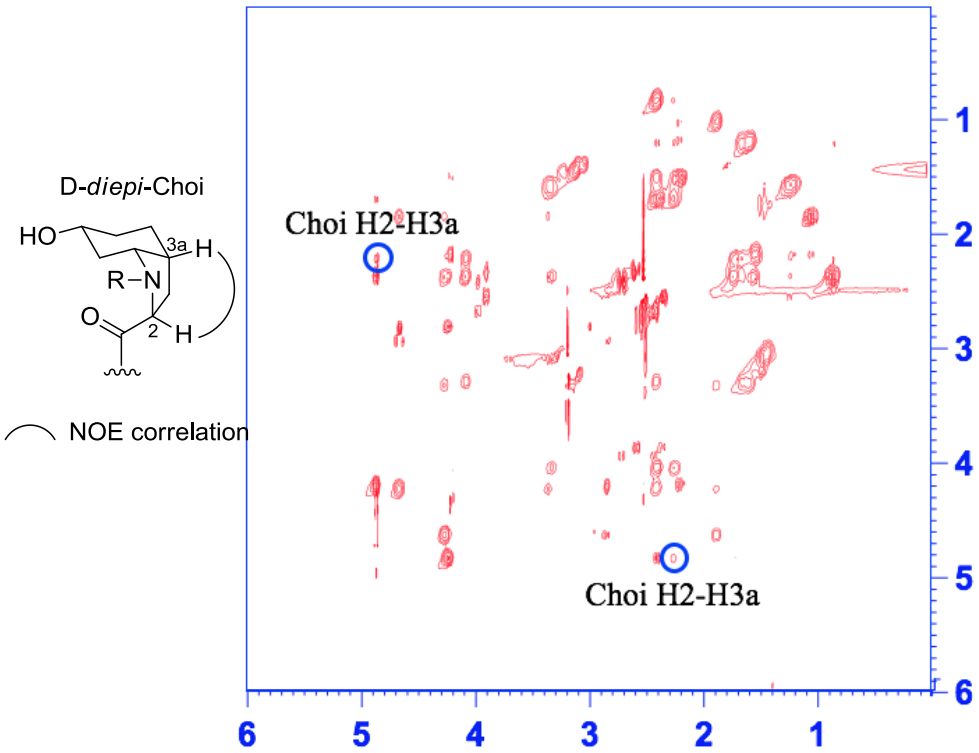

Figure 47 Excerpt of the ROESY spectrum of aeruginosin KT608A, showing cross-peaks between Choi H2 and Choi H3a.[1]

In the course of the structural elucidation of aeruginosin EI461, Carmeli had already proposed the presence of a D-*diepi*-Choi core.[52] However, the structure originally proposed by Carmeli was later revised by Bonjoch and co-workers,[6] who did indeed synthesize the proposed aeruginosin EI461 containing a D-*diepi*-Choi moiety. Bonjoch realized that the NMR spectra of the synthetic material and isolated EI461 were not in accordance with each other. To elucidate the correct structure of aeruginosin EI461, Bonjoch and co-workers synthesized a congener consisting of an L-*diepi*-Choi core. Comparison of the NMR spectra of the synthesized analogue containing the L-*diepi*-Choi core with those of naturally occurring EI461 proved that the L-*diepi*-Choi was the correct structural element present in aeruginosin EI461 (Figure 48).[6]

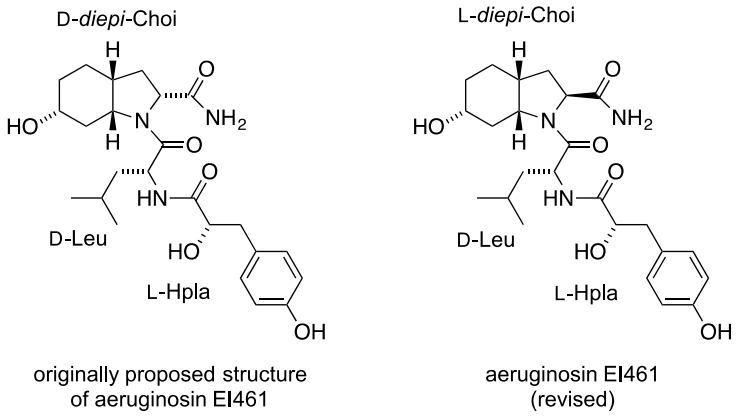

Figure 48 Structure originally proposed for aeruginosin EI461 by Carmeli and co-workers (left),[52] revised structure of aeruginosin EI461 by Bonjoch and co-workers (right).[6]

Table 11 shows the ^{1}H NMR data of revised aeruginosin EI461 containing an L-*diepi*-Choi moiety and the derivative with a D-*diepi*-Choi unit as well as those of isolated aeruginosin KT608A and our synthetic aeruginosin KT608A. There is a distinct similarity between EI461 with its L-*diepi*-Choi unit and isolated KT608A, as well as between the originally proposed EI461 congener with a D-*diepi*-Choi motif and our synthetic KT608A. This supports the hypothesis that aeruginosin KT608A in fact does not contain the proposed D-*diepi*-Choi, but an L-*diepi*-Choi core instead.

Table 11 Comparison of the ^{1}H NMR spectra of the Choi moiety of natural and synthetic aeruginosin KT608A and aeruginosin EI461 and EI461 derivative synthesized by Bonjoch.

	Chemical shifts in ppm, multiplicity (coupling constant in Hz)			
	KT608A natural	EI461 L-*diepi*-Choi	KT608A synthetic	EI461 derivative D-*diepi*-Choi
2	4.82, d (9.5)	4.71, d (9)	4.23, t (8.8)	4.23, t (8.5)
3	2.38, m (ax)	2.28, td (12.5, 9)	1.96, dt (12.3, 7.2)	2.02, m
3'	1.70, dd (12, 6)	1.69, dd (12.0, 6.0)	1.83, dt (12.9, 10.1)	1.84, ddd (12, 10, 0.5)
3a	2.23, m	2.18, m	2.15, m	2.16, ddddd
4	1.63, m	1.63, m	1.57, m	1.70, m
4'	1.63, m	1.63, m	1.67, m	1.70, m
5	1.56, m (eq.)	1.54, m	1.60, m	1.62, m
5'	1.19, m (ax)	1.21 dq (4.2, 12.8)	1.24, m	1.23, ddddd
6	3.30, m	3.25, br t (11)	3.36, m	3.39, m
7	2.37, m (eq.)	2.31, dd (12, 6)	1.90, m	1.96, m
7'	0.83, q (12)	0.78, q (12)	1.60, m	1.57, m
7a	4.04, ddd (12, 8, 6.5)	3.94 ddd, (12, 6.5, 5.5)	4.24, m	4.24, ddd (12, 6, 6)

One characteristic feature of the L-*diepi*-Choi is the presence of a high-field shifted pseudo-quartet (~0.8 ppm for the *cis* and ~1.2 ppm for the *trans* rotamer) arising from H7 (ax). Bonjoch reported a shift of 1.57 ppm for H7 (ax) in the D-*diepi*-Choi of the originally synthesized EI461.[6] This is in accordance with the 1.60 ppm for H7 (ax) that we observed in our ^{1}H NMR spectrum of KT608A (**3.1**). The dramatic downfield shift of the H7 signal (ax) when changing the L-*diepi* to a D-*diepi* configuration of the Choi unit can be explained by an influence of the peptide bond on the C-terminus. In D-*diepi*-Choi, the carboxyl oxygen of the amide bond lies in close proximity to H7 (ax), thus leading to a deshielding effect on H7 (ax) and an upfield shift of its ^{1}H NMR signal. The X-ray structure of D-*diepi*-Choi derivative **3.57** reveals a distance of 2.7 Å between these two atoms. In contrast, such a through-space deshielding effect of the carboxyl oxygen on the H7 (ax) proton is not possible in L-*diepi*-Choi due to the large distance between these two atoms (Figure 49).

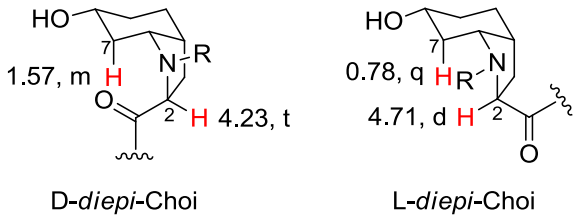

Figure 49 Configuration of D-*diepi*-Choi and L-*diepi*-Choi, showing the respective distances of the carboxyl oxygen to H7 (ax). The chemical shifts were obtained from the following NMR examples described in the literature: D-*diepi*-Choi from aeruginosin EI461, L-*diepi*-Choi from the revised structure of aeruginosin EI461. The Choi-H2 and H7 (ax) atoms are highlighted in red.

Furthermore, epimerization of D-*diepi*- to L-*diepi*-Choi does of course also strongly influence the chemical shift and the coupling pattern of the H2 signal in the ^{1}H NMR spectrum. In D-*diepi*-Choi, the dihedral angles of H2-C2-C3-H3α and H2-C2-C3-H3β correspond to 20 and 140°, respectively (Figure 50). According to the Karplus equation, these two angles induce similar coupling constants,[58,59] resulting in a pseudo-triplet multiplicity of the H2 signal in the ^{1}H NMR spectrum of D-*diepi*-Choi (t, 4.23 ppm). On the other hand, the dihedral angles of H2-C2-C3-H3α and H2-C2-C3-H3β in L-*diepi*-Choi have values of 20 and 100°, respectively. Based on the Karplus equation, this leads to a large and a very small coupling constant for angles of H3α (dihedral angle = 20°) and H3β (dihedral angle = 100°), respectively. As a result, the signal appears as a doublet of doublet or just as a doublet, when the second coupling is too small to be resolved.[58,59] Indeed, the signal of L-*diepi*-Choi-H2 in aeruginosin

EI461 (**53**) is observed as a doublet at 4.71 ppm.[6] These observations are supported by the work of Bonjoch and co-workers, who reported on similar NMR characteristics for the Choi H2 in *exo* and *endo cis*-octahydroindole-2-carboxylic acid derivatives.[5]

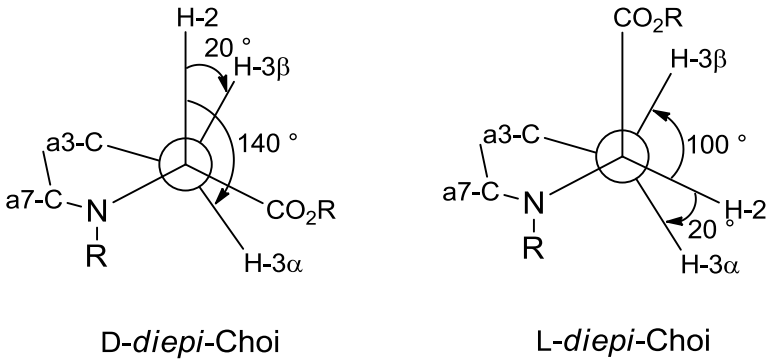

Figure 50 Newman projection of the Choi C2-C3 bond with selected dihedral angles. The dihedral angles for H2-C2-C3-H3α and H2-C2-C3-H3β in D-*diepi*-Choi were obtained from the X-ray structure of **3.57**. The dihedral angles for H2-C2-C3-H3α and H2-C2-C3-H3β in L-*diepi*-Choi were estimated by measuring the C1-C2-C3-H3α and C1-C2-C3-H3β dihedral angles in the X-ray structure of **3.57**.

All these observations strongly support the theory that in fact an L-*diepi*-Choi unit, or the enantiomeric D-6-*epi*-Choi, is present in aeruginosin KT608A (**3.1**). Of course, differentiation between the L-*diepi*-Choi and D-6-*epi*-Choi units cannot be achieved by NMR experiments without the use of chiral shift reagents. However, the fact that the L-*diepi*-Choi motif had already been identified in aeruginosin EI461 and that amino acids with L configuration are favorably formed in nature, hints at the presence of the L-*diepi*-Choi in aeruginosin KT608A (**3.1**).

Isomerization of D-*diepi*-Choi

For the investigation of the drastic shifting effect of the H7 (ax) NMR signal upon changing from a D-*diepi*-Choi to an L-*diepi*-Choi configuration, D-*diepi*-Choi derivative **3.57** was epimerized at its C2 position. First attempts using LDA as base did not bring about the desired epimerization and only led to decomposition of **3.57**. However, treating **3.57** with NaH gave rise to epimerization at the C2 position and yielded an inseparable mixture of the D-*diepi* and L-*diepi*-Choi products (Scheme 45). Figure 51 shows a selected part of the ^{1}H NMR spectrum of D-*diepi*-Choi derivative **3.57** (top) and the ^{1}H NMR spectrum of the mixed D-*diepi*-Choi and L-*diepi*-Choi, obtained after epimerization (bottom). After epimerization,

the characteristic upfield-shifted pseudo-quartets at 1.20 ppm (*trans* rotamer) and 0.91 (*cis* rotamer) for H7 (ax) of the L-*diepi*-Choi were observed. This experiment further supports the hypothesis that an L-*diepi*-Choi instead of a D-*diepi*-Choi configuration is present in aeruginosin KT608A (**3.1**). However, final proof of this hypothesis can only be accomplished by the total synthesis of aeruginosin KT608A (**3.1**) containing an L-*diepi*-Choi moiety and by comparison of the NMR spectra to those of the isolated natural product KT608A (**3.1**).

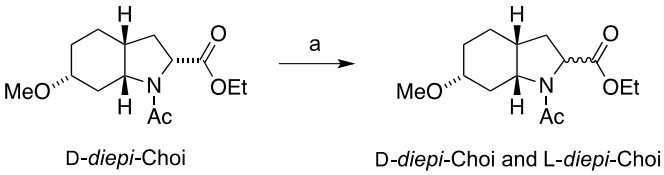

Scheme 45 Epimerization of D-*diepi*-Choi derivative **3.57**. Reagents and conditions: a) NaH, THF, −78 °C to r.t., 20% as a diastereomeric mixture.

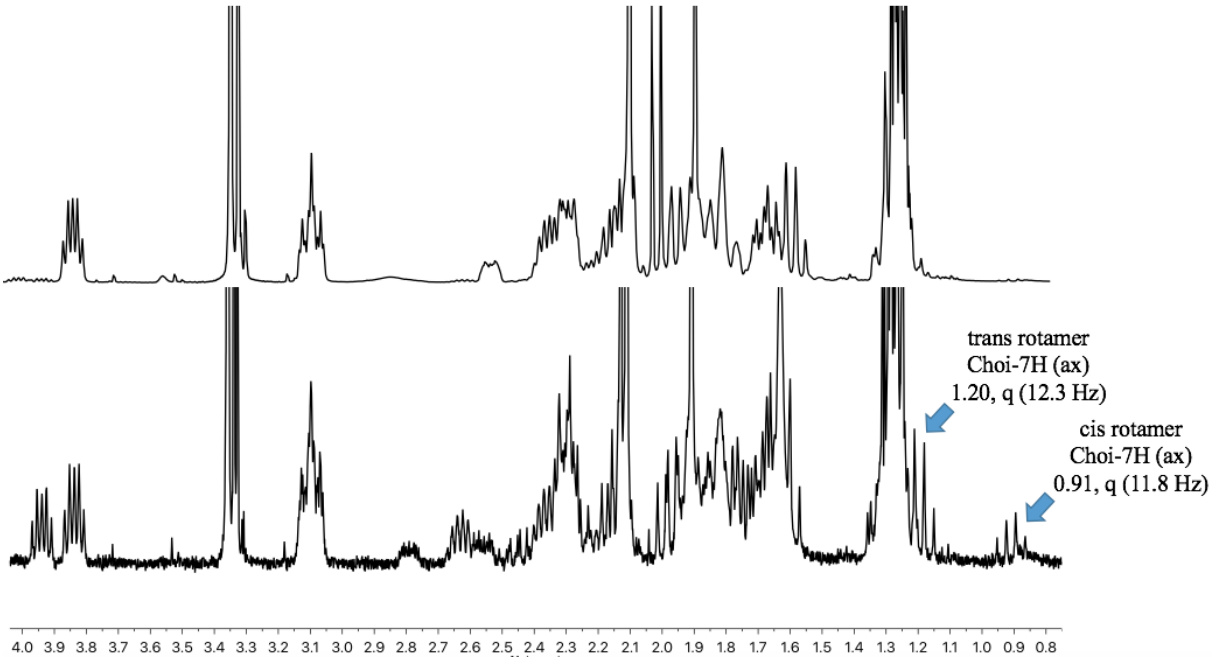

Figure 51 Excerpt of the ^{1}H NMR spectrum of D-*diepi*-Choi derivative **3.57** (top) and a mixture of D-*diepi*-Choi and L-*diepi*-Choi (bottom). The observed upfield-shifted signal for Choi-H7 (ax) for the *trans* and *cis* rotamers in L-*diepi*-Choi are highlighted.

4. Indoline Synthesis *via* C-H Activation – Confirmation of the Absolute Configuration of the Indoline

For the determination of the absolute configuration of indoline **3.56**, an alternative synthetic approach was investigated. The new strategy featured an indoline formation by use of an intramolecular amination, starting from enantiopure L-tyrosine. Beginning with a compound with known absolute configuration is advantageous as the same absolute configuration will be found in indoline **3.56**.

4.1. Intramolecular Amination using Picolinamide as Directing Group

In 2011, Chen and co-workers reported on the highly efficient synthesis of indolines *via* palladium-catalyzed intramolecular amination.[60] They introduced picolinamide as a directing group for the challenging amination of the δ-C(sp^2)-H bond. Catalyzed by $Pd(OAc)_2$ as the Pd^{II} source and $PhI(OAc)_2$ as stoichiometric oxidant, they were able to form indolines **3.81** and **3.82** in excellent yields from 2-phenylethan-1-picolinamide (**3.79**) and phenylalanine methyl ester picolinamide (**3.80**), respectively (Scheme 46). Chen proposed a cyclic nine-membered intermediate containing a Pd^{IV} center for the C-H activation mechanism. Reductive elimination of this cyclic intermediate provides the corresponding indolines.[61] Exchange of the phenylalanine moiety in **3.80** by an O-protected tyrosine picolinamide should therefore provide an indoline suitable for our total synthesis. The preparation of different picolinamide tyrosine derivatives and subsequent amination will be discussed in the following sections.

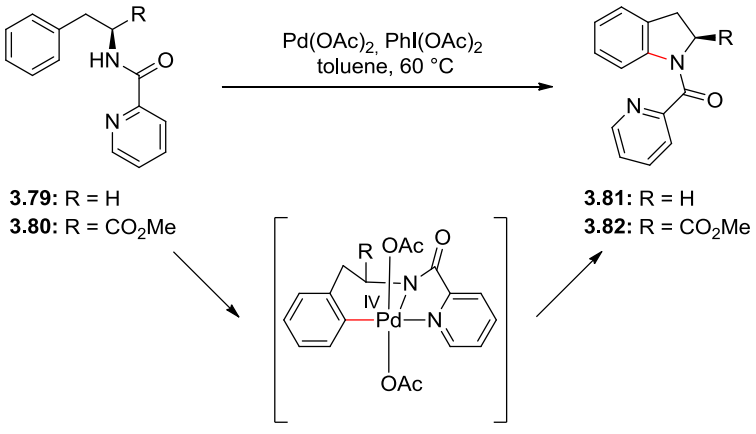

Scheme 46 Chen's preparation of indolines using an intramolecular amination reaction. The C-H activation proceeds *via* a Pd^{IV} species, with a picolinamide substituent as directing group.[60]

4.2. Preparation of Different Picolinamide Tyrosine Derivatives

For the preparation of different picolinamide derivatives of tyrosine, the free amino group of L-tyrosine methyl ester (**3.83**) was coupled with 2-picolinic acid using HOBt and EDC as coupling reagents to give picolinamide **3.84** (Scheme 47). The low yield of 56% for this reaction can be explained by the formation of a side product in which both amino and hydroxyl groups of tyrosine were bound to picolinic acid. Alteration of the procedure by using Schotten-Baumann conditions,[62,63] including the usage of 2-picolinic acid chloride, did not lead to any improvement. Thus, the picolinamide tyrosine methyl ester (**3.84**) was protected on the phenol moiety. First, a TBS group was incorporated by the reaction of **3.84** with TBSCl to give silyl ether **3.85** in excellent yield. Further, **3.84** was protected with a MOM group by treatment with MOMCl providing MOM ether **3.86**. Reaction of **3.84** with MeI afforded methyl ether **3.87** in very good yield (Scheme 47). Derivatives **3.85**, **3.86** and **3.87** were then subjected to the amination conditions described by Chen and co-workers, which will be discussed in the subsequent section in more detail.

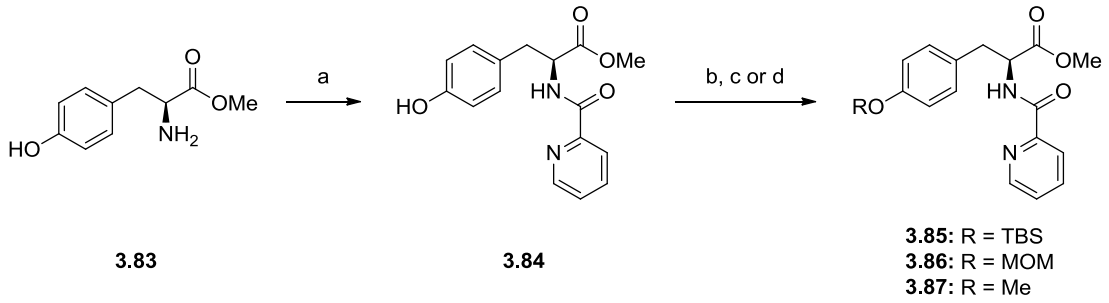

Scheme 47 Synthesis of picolinamide tyrosine derivatives **3.85**, **3.86** and **3.87**. Reagents and conditions: a) 2-picolinic acid, HOBt, EDC, DIPEA, CH_2Cl_2, 16 h, 56%; b) TBSCl, Et_3N, DMAP, CH_2Cl_2/DMF (5:1), r.t., 16 h, 98%; c) MOMCl, DIPEA, CH_2Cl_2, 0 °C to r.t., 24 h, 75%; d) MeI, K_2CO_3, DMF, r.t., 17 h, 95%.

4.3. Investigation of the C-H Activation

With the different picolinamide tyrosine derivatives in hand, their suitability for the intramolecular amination reaction was investigated (Table 12). First, silyl ether **3.85** and MOM ether **3.86** were subjected to the conditions described by Chen and co-workers. However, these conditions led to no conversion, but only the starting materials were recovered (Entries 1 and 2). In order to enforce the intramolecular amination to occur, the catalyst loading of $Pd(OAc)_2$ was increased from 2 to 5 mol%. Indeed, with this change, 60% consumption of silyl ether **3.85** and 100% consumption of MOM ether **3.86** was observed (Entries 3 and 4). Indoline **3.89** containing the MOM ether was isolated in 60% yield, together with 20% of oxidized side product **3.89b**. Since 100% consumption of the starting material had already been observed for derivative **3.86**, further optimizations were carried out only for the cyclization of silyl ether **3.85**. The catalyst loading was increased from 5 to 10 mol%, leading to an enhancement of the consumption from 60 to 80% (Entry 5). Because 10 mol% of catalyst already correspond to the upper limit of a convenient catalytic reaction, the catalyst loading was not further increased. Instead, the influence of the temperature on the outcome of the C-H activation was explored. Increasing the temperature from 60 to 110 °C furnished a 90% consumption of silyl ether **3.85** to the corresponding indoline **3.88** already at 2 mol% catalyst loading (Entry 6). This observation suggests that our substrates required higher temperatures for the amination than the one investigated by Chen and his group. An increase of the catalyst loading to 5 and 10 mol%, respectively, finally led to full consumption of silyl ether **3.85** (Entires 7 and 8). However, the high temperature of 110 °C seemed to be too harsh conditions, provoking decomposition processes, since despite 100% consumption of the starting material only 60% of the desired indoline **3.88** was isolated. Therefore, the cyclization of methyl ether **3.87** was performed at a lower temperature of 60 °C, but with a high catalyst loading. Although the starting material was fully consumed, only 46% of methoxy indoline **3.90** were isolated (Entry 9). One reason for the low yields obtained despite full consumption of the starting material might be the formation of a pyridine *N*-oxide by reaction with the oxidant $PhI(OAc)_2$, resulting in a very polar compound, which is difficult to elute during column chromatography. Therefore, the performance of an F^+ oxidant[64] was investigated, to prevent the possible oxidation of the picolinamide nitrogen, but all attempts incorporating this oxidant led to no observable formation of the desired indoline (results not shown in Table 12).

Table 12 Different reaction conditions for the intramolecular amination of **3.85**, **3.86** and **3.87**.

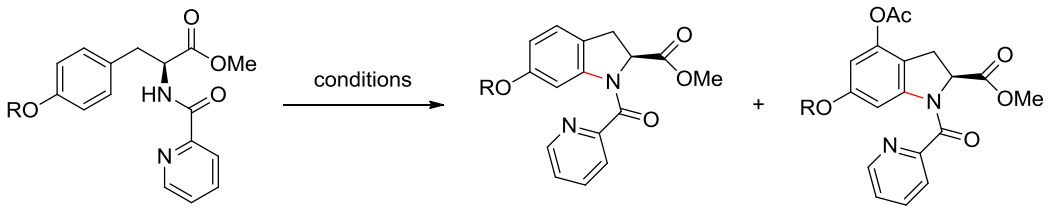

3.85: R = TBS
3.86: R = MOM
3.87: R = Me

3.88: R = TBS
3.89: R = MOM
3.90: R = Me

3.89b: R = MOM

Entry	Substrate	$Pd(OAc)_2$	Temperature	Consumption of starting material[a]	Yield
1	TBS	2 mol%	60 °C	none	-
2	MOM	2 mol%	60 °C	none	-
3	TBS	5 mol%	60 °C	60%	n.d.
4	MOM	5 mol%	60 °C	100%	60% + 20%[b]
5	TBS	10 mol%	60 °C	80%	n.d.
6	TBS	2 mol%	110 °C	90%	n.d.
7	TBS	5 mol%	110 °C	100%	60%
8	TBS	10 mol%	110 °C	100%	60%
9[c]	Me	10 mol%	60 °C	100%	46%

All reactions were carried out by stirring in toluene for 16–20 h with 2.5 eq. of $PhI(OAc)_2$ as oxidant. [a]Consumption of the starting material was determined using UPLC analysis. [b]20% of the oxidized product **3.89b** were isolated. [c]Only 2.0 eq. of $PhI(OAc)_2$ were used.

4.4. Synthesis of Indoline 3.56 and Confirmation of its Absolute Configuration

Focusing on the determination of the absolute configuration of indoline **3.56**, obtained after the enantioselective hydrogenation step described in Section 3.1.2, the transformation of methoxy indoline **3.90** to **3.56** was investigated. For this, the picolinamide group of **3.90** had to be replaced by an acetyl group and a transesterification from methyl to ethyl ester was required. First, the removal of the picolinamide substituent was explored. Chen and co-workers described a facile elimination of the picolinamide auxiliary by subjecting the corresponding picolinamide product either to basic[60,61] or mildly acidic conditions.[65] However, applying Chen's conditions to our substrate **3.90** led to no observable conversion under basic conditions. Treating **3.90** under acidic conditions, led to the cleavage of the picolinamide auxiliary, though in a very poor yield (Scheme 48). Although the picolinamide group has frequently been used in synthesis, for example as directing group for transition-metal catalyzed C-H activation reactions[60,61,66,67] or as chelating ligand coordinated to different metal centers[68,69], only few methods have been established for the cleavage of this

group. Since picolinamides are known to strongly bind to Cu^{II} ions[70], $Cu(OAc)_2$ was added to the reaction mixture under acidic conditions, in order to facilitate cleavage of the picolinamide group. Indeed, the picolinamide functionality was readily removed under these conditions, according to reaction control by TLC. However, purification and separation of the desired product from the Cu^{II} salts turned out to be challenging, due to good water solubility and large binding affinity to Cu^{II} of the obtained desired amino acid product. Therefore, no reasonable yields were obtained. In May 2016, O'Donovan and co-workers reported on the reductive cleavage of picolinamides by the reaction with zinc in aqueous HCl solution.[71] However, this deprotection method was published after we had stopped investigating cleavage of the picolinamide group in **3.90**. Further, the yields of O'Donovan for the removal of the picolinamide auxiliary range from 20 to 95%, revealing that this method cannot be universally used for the picolinamide deprotection either. Despite the problematic cleavage of the picolinamide group, synthesis of the desired indoline **3.56** was achieved: Esterification of the picolinamide deprotected amino acid with ethanol provided intermediate **3.91**, followed by acetyl protection of the free amino group. The optical rotation of the obtained indoline **3.56** was measured, revealing a negative value of –79.4°. Therefore, the negative optical rotation of indoline **3.56** can be attributed to an L-configuration, because the synthesis of **3.56** had started from enantiopure L-tyrosine. Since the indoline obtained *via* enantioselective hydrogenation displayed an optical rotation value of +78.8°, the D-configuration of this indoline could thus be confirmed (for details see Section 3.1.2). Consequently, the D-*diepi*-Choi and not the L-6-*epi*-Choi had effectively been prepared in our previous synthesis of aeruginosin KT608A (**3.1**) (Section 3). Therefore, one possible mistake in our total synthesis of **3.1** could be excluded. Since picolinamide turned out to be problematic as directing group for the C-H activation to furnish reasonable amounts of indoline **3.56**, the use of a different directing group for the intramolecular amination was investigated (Section 5).

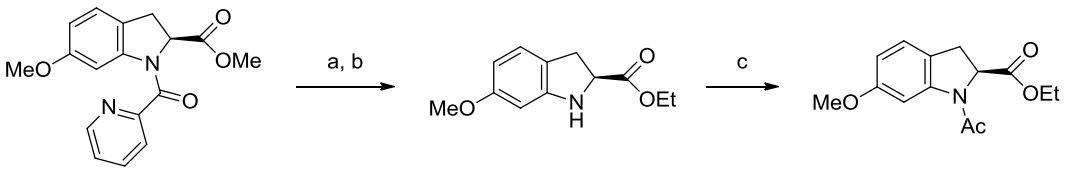

3.90 **3.91** **(–)-3.56**

Scheme 48 Synthesis of indoline **3.56**. Reagents and conditions: a) 6 N aq. HCl, 100 °C, 2 h; b) $SOCl_2$, EtOH, 0 °C to 79 °C, 3 h, 14% over two steps; c) Ac_2O, Et_3N, DMAP, CH_2Cl_2, r.t., 16 h, 71%.

5. Synthesis of Aeruginosin KT608A – 2nd Generation

5.1. Intramolecular Amination using 2-Pyridinesulfonamide as Directing Group

Already in 2008, Yu and co-workers had described the Pd^{II}-catalyzed formation of indolines and tetrahydroisoquinolines form arylethylamines.[72] Yu explored a tandem reaction incorporating a Pd^{II}-catalyzed iodination followed by a Cu^{I}-mediated amination, leading to the cyclization of a broad scope of arylethyltriflamides. Further investigations on this reaction showed that the iodination step is not necessarily required for C-H activation and that arylethyltriflamides can directly be transformed to the corresponding indolines.[73] A drawback of the C-H activation developed by Yu and co-workers was that the amines required a triflate protecting group to successfully undergo the amination. Due to the stability of triflamides and the harsh conditions which are required for their cleavage, *e.g.* using $LiAlH_4$,[74] the liberation of the free amine can cause problems. Fortunately, Yu *et al*. later found a solution to circumvent this problem. Instead of using triflates for the protection of the amine, they incorporated pyridine-2-sulfonamide as the directing group.[75] The use of the pyridine-2-sulfonamide group combines the advantage of the high reactivity of triflamides regarding the C-H activation with the directing capability of the picolinamide group, as described by Chen. Further, Yu and co-workers explored a mild and selective deprotection method for the cleavage of the sulfonamide by simple treatment with a methanolic Mg^0 powder suspension (Scheme 49). An advantage of this mild deprotection method is that no racemization has been observed during the cleavage of sulfonamide **3.93** to give access to indoline **3.94** (Scheme 49). All these benefits encouraged us to further investigate Yu's C-H activation strategy for our synthesis of the D-*diepi*-Choi.

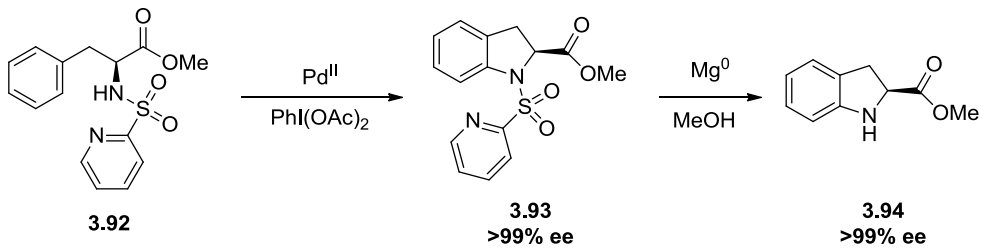

3.92 | **3.93** >99% ee | **3.94** >99% ee

Scheme 49 Yu's amination using pyridine-2-sulfonamide as directing group and cleavage of the sulfonamide auxiliary by treatment with Mg^0.

5.2. Preparation of Sulfonamides 3.98 and 3.100

The synthesis of adequate sulfonamide precursors was started from commercially available D-tyrosine (**3.95**), which was transformed into methyl ester **3.96** (Scheme 50).[76] Further, the hydroxyl group of **3.96** was protected with a TBS group to give silyl ether **3.97**.[76] For the formation of the pyridine-2-sulfonamide, we followed Yu's method by treating amine **3.97** with sulfonyl chloride prepared from 2-mercaptopyridine and sodium hypochlorite *in situ*. However, this procedure did not furnish the desired product **3.98**. Therefore, the sulfonamide was introduced by reaction with freshly prepared pyridine-2-sulfonyl chloride under basic conditions, giving pyridine-2-sulfonamide **3.98** in good yield[77] as starting material for the projected C-H activation. Furthermore, a pyridine-2-sulfonamide derivative was synthesized bearing an electron-withdrawing acetyl group instead of the electron-donating silyl group in order to investigate the influence of electronic properties on the C-H activation. Thus, silyl ether **3.98** was treated with a TBAF solution yielding the free phenol **3.99**. Subsequent acetylation of **3.99** then provided pyridine-2-sulfonamide **3.100** (Scheme 50).

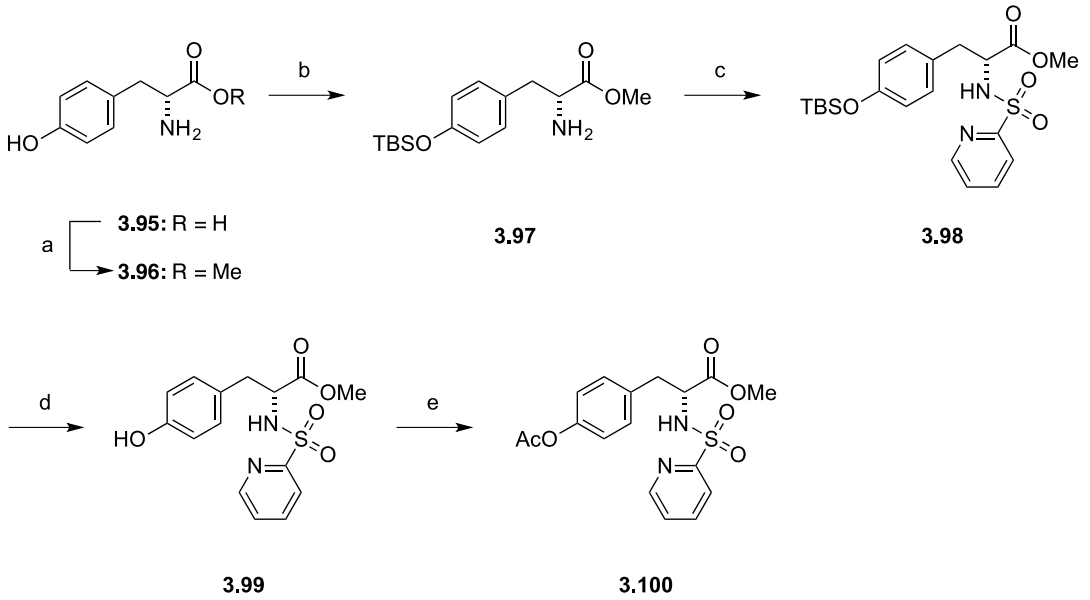

Scheme 50 Preparation of sulfonamides **3.98** and **3.100**. Reagents and conditions: a) $SOCl_2$, MeOH, 0 °C to 66 °C, 12 h, quant.; b) TBSCl, imidazole, CH_2Cl_2, r.t., 16 h, 87%; c) pyridine-2-sulfonyl chloride, Et_3N, CH_2Cl_2, r.t., 2 h, 72%; d) TBAF, THF, 0 °C to r.t., 2 h, 79%; e) AcCl, DMAP, Et_3N, CH_2Cl_2, r.t., 1 h, 86%.

5.3. Different Conditions for the C-H Activation of 3.98 and 3.100

Both tyrosine sulfonamide derivatives **3.98** and **3.100** were tested for their suitability to react in the Pd^{II}-catalyzed intramolecular amination. The results of these experiments are summarized in Table 13. A first test reaction starting from silyl ether **3.98** with 2 mol% catalyst loading and a reaction temperature of 90 °C gave only traces of the desired indoline product **3.101** (Entry 1). Increasing the catalyst loading up to 15 mol% did not lead to a significant improvement of the conversion to indoline **3.101** (Entries 2-4). Since the C-H activation seemed to require higher temperatures than 90 °C, the temperature was raised to 130 °C. However, with 5 mol% of catalyst, this did not change the results (Entry 5). Further, the catalyst loading was increased from 5 to 10 mol% and the dilution of the reaction mixture decreased from 0.01 M to 0.09 M. These changes provided 100% consumption of the starting material sulfonamide **3.98**, although only 40% of the desired indoline **3.101** were isolated (Entry 6). The discrepancy between starting material consumption and isolated yield suggests the occurrence of side reactions leading to decomposition pathways. In order to diminish possible decomposition, the reaction time was reduced from 14 h to 10 h. Indeed, with this modification the isolated yield of **3.101** was raised from 40% to 54% (Entry 7). Next, acetylated tyrosine sulfonamide **3.100** was investigated as substrate. Knowing that 90 °C did not suffice to bring about intramolecular amination, we started our screening directly at a temperature of 130 °C. A first reaction with 10 mol% catalyst loading and 0.01 M substrate concentration provided 30% consumption of the starting material (Entry 8). As observed in the C-H activation of the silyl ether derivative, the dilution of the reaction mixture has a crucial impact on the outcome of the reaction. Therefore, the concentration was increased from 0.01 M to 0.1 M. This alteration of the reaction conditions resulted in an increased consumption of the starting material from 30 to 60% and furnished the isolation of 30% of indoline **3.102** (Entry 9). Since the reaction was not complete after 8 h (Entry 9), the reaction time was extended to 12 h (Entry 10). To reduce possible decomposition pathways, the dilution of the reaction was slightly increased from 0.1 M to 0.08 M. These adjustments of the reaction conditions led to 100% consumption of the starting material **3.100** accompanied by the isolation of 67% of the desired product **3.102** (Entry 10). A reduction of the reaction time from 12 to 11 h finally provided a yield of 80% of the desired indoline **3.102** (Entry 11).

Table 13 Different conditions for the amination of sulfonamides **3.98** and **3.100**.

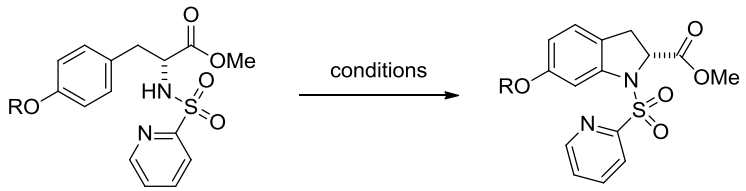

3.98: R = TBS
3.100: R = Ac

3.101: R = TBS
3.102: R = Ac

Entry	Substrate	$Pd(OAc)_2$	Temp.	Time	Consumption of starting material[a]	Yield
1	TBS	2 mol%	90 °C	14 h	<10%	n.d.
2	TBS	5 mol%	90 °C	14 h	<10%	n.d.
3	TBS	10 mol%	90 °C	14 h	<10%	n.d.
4	TBS	15 mol%	90 °C	14 h	<10%	n.d.
5	TBS[c]	5 mol%	130 °C[b]	6 h	<10%	n.d.
6	TBS[d]	10 mol%	130 °C[b]	14 h	100%	40%
7	TBS[d]	10 mol%	130 °C[b]	10 h	100%	54%
8	Ac[c]	10 mol%	130 °C[b]	8 h	30%	n.d.
9	Ac[d]	10 mol%	130 °C[b]	8 h	60%	30%
10	Ac[d]	10 mol%	130 °C[b]	12 h	100%	67%
11	Ac[d]	10 mol%	130 °C[b]	11 h	100%	80%

All reactions were carried out under exclusion of water in toluene with 2.0 eq. $PhI(OAc)_2$ as the oxidant. [a]Consumption of the starting material was determined using UPLC analysis. [b]The reaction was performed in a microwave reactor. [c]The reaction was performed at a 0.01 M substrate concentration. [d]The reactions were performed with a starting material concentration ranging from 0.08 to 0.1 M.

5.4. Synthesis of the D-*diepi*-Choi, 1st Approach

With silyl ether indoline **3.101** in hand, the next focus lay on the cleavage of the sulfonamide auxiliary and reduction of the indoline to the octahydroindole unit (Scheme 51). For this, sulfonamide **3.101** was treated with a methanolic Mg^0 powder suspension, as described by Yu and co-workers.[75] Indeed under these mild conditions, the sulfonamide moiety in **3.101** was smoothly cleaved to give indoline **3.103** in excellent yield. For the preparation of indoline **3.103** as starting material for the subsequent reduction to the octahydroindole, the amine of indoline **3.103** was protected with a trifluoroacetate group yielding indoline **3.104**. Baudoin and co-workers showed that amine trifluoroacetates can be readily and selectively cleaved in

the presence of a silyl ether and methyl ester by treatment with $NaBH_4$,[21] whereas non-fluorinated amides can only be cleaved under harsh acidic conditions (for more details see Section 3.2.2). Further, indoline **3.104** was subjected to the reduction conditions developed in our previous synthesis of the D-*diepi*-Choi (Section 3.2.1). Unfortunately, the applied conditions provoked degradation of the silyl ether, thus leading to a complex mixture of different products. Investigation of the synthetic strategy incorporating the TBS protecting group was therefore stopped and the focus was laid on the derivative bearing the acetyl group. The results obtained with this route will be the topic of the next section.

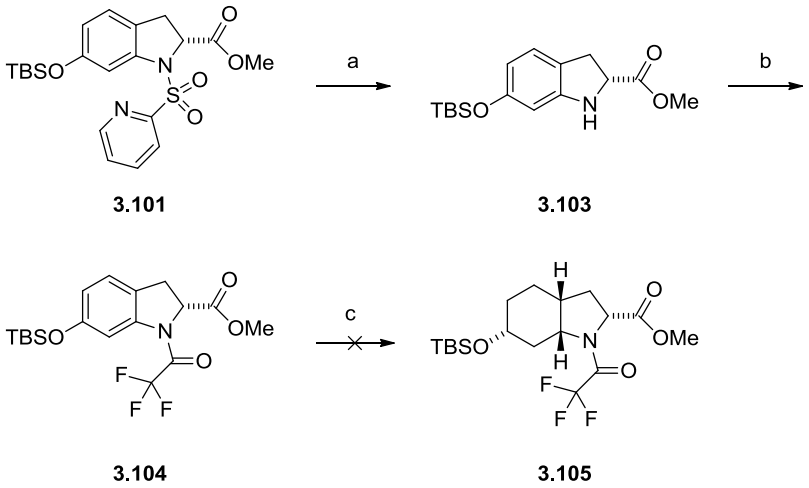

Scheme 51 Studies towards the synthesis of octahydroindole **3.105**. Reagents and conditions: a) Mg powder, MeOH, 0 °C, 3 h, then sat. aq. NH_4Cl, Et_2O, r.t., 1 h, 95%; b) trifluoroacetic anhydride, pyridine, CH_2Cl_2, 0 °C to r.t., 16 h, 89%; c) H_2 (35 bar), Rh/C, MeOH, r.t..

5.5. Synthesis of the D-*diepi*-Choi, 2nd Approach

Due to decomposition of the derivative bearing a TBS group (Section 5.4) under reducing conditions, the synthesis of the D-*diepi*-Choi was continued with acetylated indoline **3.102** (Scheme 52). Not only did subjecting **3.102** to a methanolic Mg^0 powder suspension induce the cleavage of the sulfonamide, but also of the acetyl ester to give indoline **3.106**. Reduction of this unprotected indoline **3.106** to the corresponding octahydroindole using heterogeneous catalysis was not successful. Therefore, the amino group of indoline **3.106** was protected with a trifluoroacetyl group to provide indoline **3.107** (similar to Section 5.4). Since indoline **3.107** could still not be converted into the corresponding octahydroindole *via* catalytic heterogenous hydrogenation, the hydroxyl group of **3.107** was protected with a MOM group. The poor reactivity of unprotected indolines towards hydrogenation has already been observed in our

previous synthesis of the D-*diepi*-Choi (for more details see Section 3.3). Fortunately, the trifluoroacetyl-protected indoline **3.108** could be converted into octahydroindole **3.109**, although the yield of 56% (65% brsm) was moderate. The lower yield compared to the one achieved in our previous synthesis (Section 3.2.1) can be explained by the moderate stability of the trifluoroacetate under the applied conditions. However, optimization of the reaction conditions, *e.g*. by adjusting the H_2 pressure, should prevent degradation of the trifluoroacetate and thus lead to an increased yield of **3.109**. Removal of the trifluoroacetate functionality of **3.109** using the conditions described by Baudoin and co-workers finally gave access to D-*diepi*-Choi derivative **3.110** in a very good yield (Scheme 52). Compound **3.110** was further used as a building block in the assembly of aeruginosin KT608A (**3.1**), which will be discussed in Section 5.7.

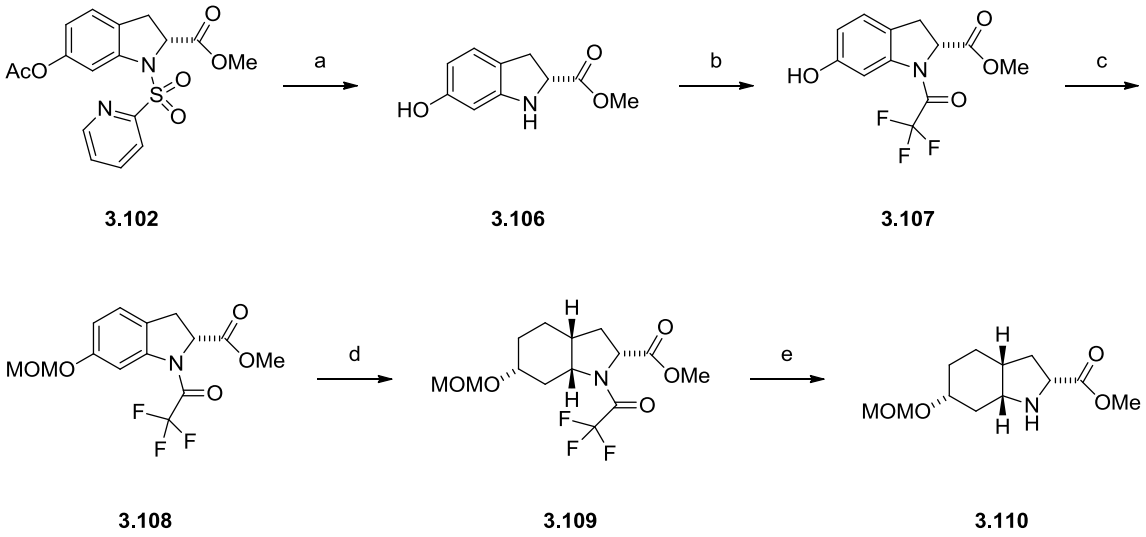

Scheme 52 Synthesis of D-*diepi*-Choi derivative **3.110**. Reagents and conditions: a) Mg powder, MeOH, 0 °C, 3 h, then sat. aq. NH_4Cl, Et_2O, r.t., 1 h; b) trifluoroacetic anhydride, pyridine, CH_2Cl_2, 0 °C to r.t., 16 h; c) MOMBr, DIPEA, CH_2Cl_2, 0 °C to r.t., 24 h, 62% over three steps; d) H_2 (15 bar), Rh/C, MeOH, r.t., 4.5 h, 56% (65% brsm); e) $NaBH_4$, MeOH, 0 °C, 1 h, 81%.

5.6. Synthesis of the Hpla-Phe-OH Dipeptide

For the assembly of aeruginosin KT608A (**3.1**), we envisioned the incorporation of the D-Phe and L-Hpla-OH building blocks as a dipeptide, similar to the strategy described in the synthesis of aeruginosin 828A. Doing so, the step economy of the total synthesis is reduced by two synthetic steps. For the synthesis of Hpla-Phe-OH dipeptide **3.115**, D-Phe-OMe (**3.111**) was coupled to the L-Hpla-OH unit (**3.67**) using PyBOP as coupling reagent, to access dipeptide **3.112** (Scheme 53). Since the acetyl ester of the L-Hpla unit was not orthogonal to the conditions used for the cleavage of the D-Phe methyl ester, the protecting group of this hydroxyl group had to be altered. That way, the problem of a free hydroxyl group which could possibly interfere by an intramolecular attack on the active ester in another peptide coupling was excluded. Thus, acetyl ester **3.112** was treated with K_2CO_3 to give the free hydroxyl group and dipeptide **3.113**. Subsequent protection of the obtained hydroxyl group with TBSCl provided silyl ether **3.114**. Finally, the synthesis of Hpla-Phe-OH dipeptide **3.115** was accomplished by saponification of the D-Phe methyl ester in **3.114** (Scheme 53). The application of dipeptidic building block **3.115** in the assembly of aeruginosin KT608A (**3.1**) will be the content of the next section.

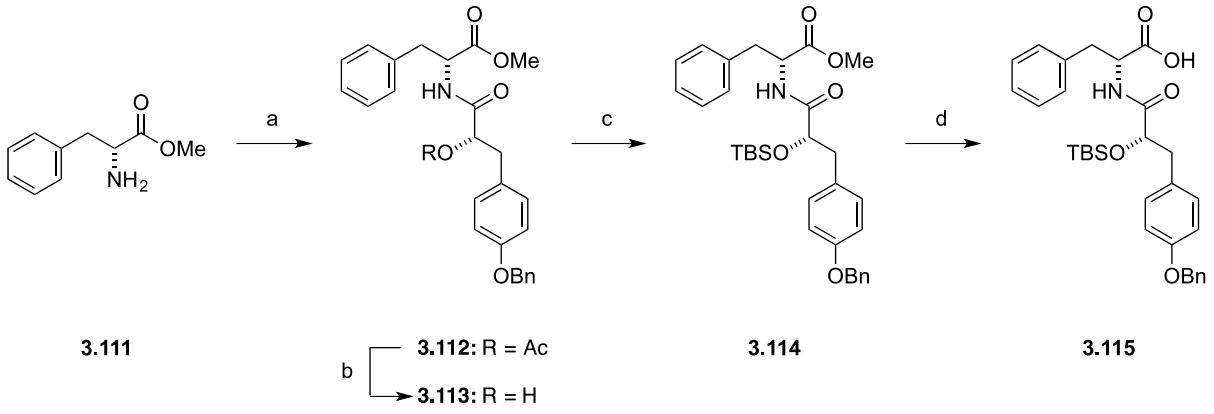

Scheme 53 Synthesis of Hpla-Phe-OH dipeptide **3.115**. Reagents and conditions: a) L-Hpla-OH **3.67**, PyBOP, 2,6-lutidine, CH_2Cl_2, 0 °C to r.t., 20 h, 77%; b) K_2CO_3, MeOH, r.t., 2 h, 84%; c) TBSCl, imidazole, DMAP, DMF, r.t., 18 h, 38% (94% brsm); d) LiOH, THF/H_2O (5:3), r.t., 1 h, 96%.

5.7. Assembly of the Different Building Blocks

The assembly of the building blocks of aeruginosin KT608A commenced with the peptide coupling of D-*diepi*-Choi unit **3.110** to Hpla-Phe-OH dipeptide **3.115** (Scheme 54). For this coupling, the same conditions were applied as in the synthesis of aeruginosin 828A (Section 5.3; Chapter I). Fortunately, these conditions provided tripeptide **3.116** in a high yield as a rotameric mixture of 4:1, without the occurrence of racemization. As tripeptide **3.116** was obtained as a single diastereoisomer (in contrast to the previously described synthesis of aeruginosin KT608A (**3.1**)), we can exclude the formation of an undesired stereoisomer in the course of this synthesis. Saponification of the methyl ester of the L-Choi moiety in tripeptide **3.116** provided acid **3.117**. Further, coupling of this acid **3.117** with the agmantin building block **3.64** gave access to tetrapeptide **3.118** (Scheme 54). At this stage, the desired natural product was fully assembled and global deprotection was required for completion of the total synthesis of KT608A (**3.1**). First, the Bn group of **3.118** was removed using catalytic hydrogenation to provide tetrapeptide **3.119** in excellent yield. Further, tetrapeptide **3.119** was treated with TFA in CH_2Cl_2 to cleave the acid-labile Boc, MOM and TBS groups. Surprisingly, the TBS group was not removed under these conditions. Therefore, the crude residue obtained after acidic treatment was additionally stirred for 1 h in a solution of HF in MeCN to ensure cleavage of the TBS group. During the treatment with diluted TFA solution, a trifluoroacetylated side product was formed as well. Thus, the obtained crude residue was stirred for 30 min in an aqueous Na_2CO_3 solution to cleave the trifluoroacetyl ester (analogously to the synthesis of aeruginosin 616A (Section 7.1, Chapter I)). After deprotection, 2.4 mg of the desired aeruginosin KT608A (**3.1**) were successfully isolated (Scheme 54). With the synthetic aeruginosin KT608A (**3.1**) in hand, ^{1}H and ^{13}C 1D NMR experiments as well as COSY, HMBC, HSQC and NOESY 2D NMR experiments were recorded. The obtained NMR spectra were then compared with those recorded by Carmeli[1] and with the NMR spectra from our previous total synthesis of KT608A (Section 3.6), revealing that the spectra of our previously synthesized KT608A and the synthesized KT608A of the 2nd generation were identical. This strongly supports the hypothesis that the desired aeruginosin does indeed contain a D-*diepi*-Choi core and that the assigned structure for aeruginosin KT608A by Carmeli and co-workers was incorrect. Of course, final prove of this hypothesis can only be accomplished by the total synthesis of aeruginosin KT608A containing the correct core structure.

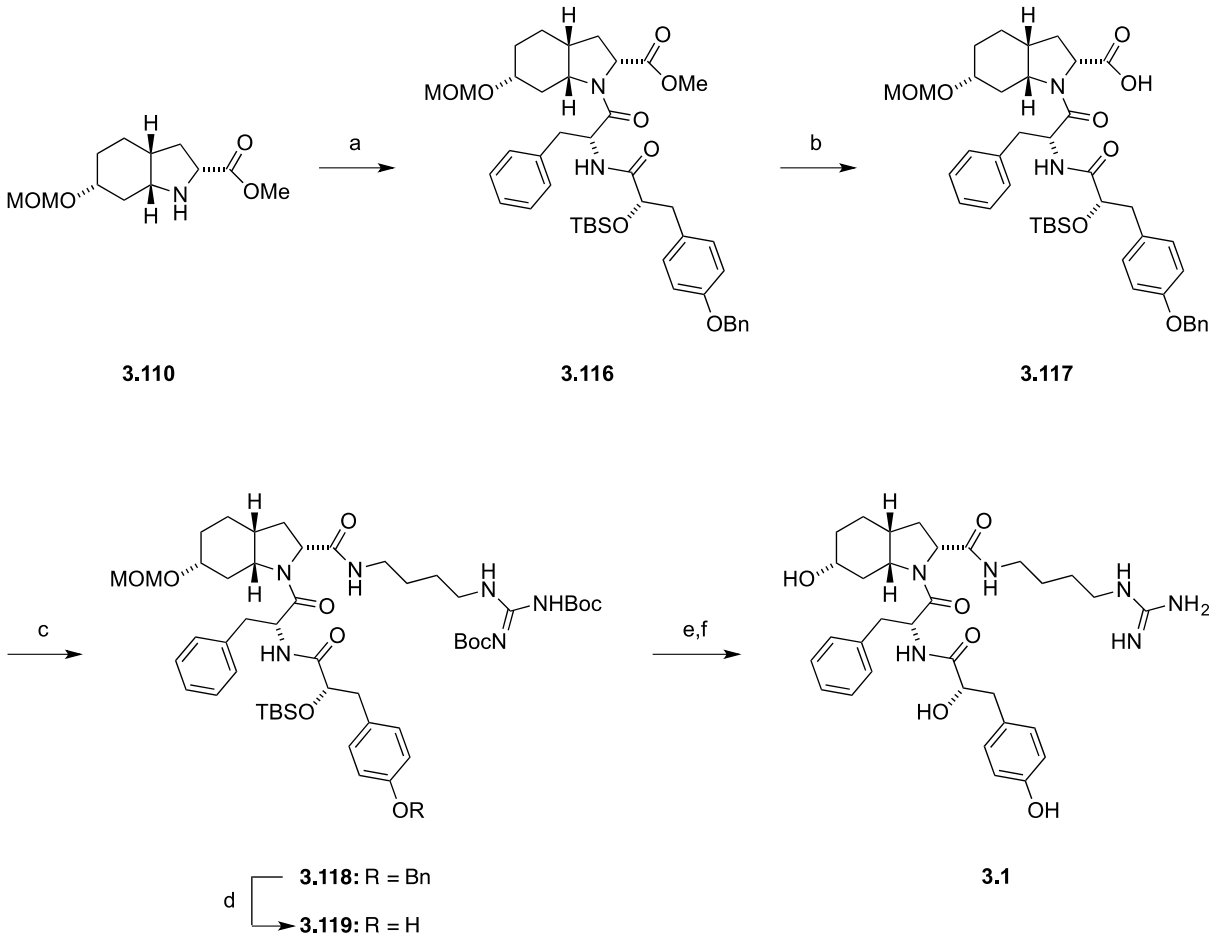

Scheme 54 Assembly of the different building blocks – synthesis of aeruginosin KT608A (**3.1**). Reagents and conditions: a) Hpla-Phe-OH **3.115**, DMTMM, NMM, CH_2Cl_2, 0 °C to r.t., 2 h, 71%; b) 0.1 N LiOH, THF/H_2O (5:3), r.t., 7 h, 77%; c) Agm **3.64**, PyBOP, 2,6-lutidine, CH_2Cl_2, 0 °C to r.t., 5 h, 55%; d) H_2, Pd/C, MeOH/EtOAc (1:1), r.t., 24 h, 97%; e) CH_2Cl_2/TFA (10:1), r.t., 7 h; f) HF (aq.)/MeCN (1:9), r.t., 1 h, then Na_2CO_3, r.t., 30 min, 99% over two steps.

5.8. Isomerization of the D-*diepi*-Choi Unit

As already exemplified in Section 3.6.1, the most probable candidate to be structurally identical with the natural product aeruginosin KT608A (**3.1**) is an aeruginosin consisting of the same L-Hpla, D-Phe and agmantin moieties, but with an L-*diepi*-Choi instead of the D-*diepi*-Choi core. Therefore, investigations towards the isomerization of the D-*diepi*-Choi to the L-*diepi*-Choi were carried out (Scheme 55). First attempts by treating D-*diepi*-Choi derivative **3.110** with LDA or NaH resulted either in no isomerization or in decomposition of **3.110**. Fortunately, a procedure by Wipf and co-workers,[9] developed for the epimerization of L-*triepi*-Choi to D-*triepi*-Choi, also led to the epimerization of our substrate. In general, the formation of the D-*diepi*-Choi is kinetically favored due the sterically less hindered protonation from the convex side compared to protonation from the concave side. Wipf took advantage of this effect by using sterically demanding *tert*-butyl alcohol for quenching and protonation, which gave the desired D-*triepi*-Choi in a 12:1 ratio. In order to minimize steric interaction of L-*diepi*-Choi with the proton source, we used methanol instead of *tert*-butyl alcohol to quench our epimerization reaction. With methanol as proton source, we observed a ratio of 3:1 of D-*diepi*-Choi to L-*diepi*-Choi. However, further inquiry of this epimerization and investigation of the separation of the two epimers have to be explored.

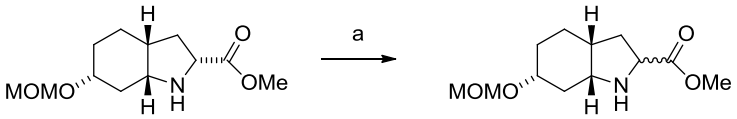

3.110 **3.110 + 3.120**

Scheme 55 Isomerization of D-*diepi*-Choi derivative **3.110**. Reagents and conditions: a) $LiNEt_2$, 10% HMPA/THF, −78 °C, 30 min, then MeOH, no product isolation.

6. Conclusion

In this chapter, the development of two novel synthetic routes for the synthesis of the presumed D-*diepi*-Choi moiety in aeruginosins has been described. The first strategy comprises the homogeneous catalytic enantioselective hydrogenation, followed by heterogeneous catalytic hydrogenation to give the octahydroindole backbone of D-*diepi*-Choi. The second route includes C-H activation of a D-tyrosine derivative providing the corresponding indoline. As in the first strategy, heterogeneous catalytic hydrogenation provides the octahydroindole skeleton of the D-*diepi*-Choi. Both synthetic routes finally led to the total synthesis of the presumed structure of aeruginosin KT608A (**3.1**). However, analysis of the NMR spectra showed substantial differences between the data of our synthetic material and the isolated aeruginosin KT608A (**3.1**). Our synthetic work therefore resulted in a reconsideration of the proposed structure of KT608A, as described by Carmeli and co-workers in the isolation work. Furthermore, by carefully comparing the NMR spectra of natural aeruginosin KT608A (**3.1**) with those of literature known aeruginosins, we have developed a closer understanding of the isomeric Choi core units' spectroscopic properties and propose that aeruginosin KT608A (**3.1**) actually comprises an L-*diepi*-Choi moiety instead of the presumed D-*diepi*-Choi. This hypothesis was supported by epimerization experiments with D-*diepi*-Choi furnishing L-*diepi*-Choi. Further, it is to be expected that the structures of the other aeruginosins reported to contain such a D-*diepi*-Choi core – aeruginosins KT608B (**3.2**) and KT650 (**3.3**) – have also been wrongly assigned, since these natural products show the same characteristics in the NMR spectra as **3.1**. These characteristics indicate the presence of an L-*diepi*-Choi motif in the natural products **3.2** and **3.3** as well. All in all, the presence of a D-*diepi*-Choi unit in natural aeruginosins seems to be a myth from literature. Hence, the natural occurrence of the D-*diepi*-Choi unit has to be strongly questioned as no confirmed structure of a natural product containing this feature has been reported so far.

7. Outlook – Synthesis of Aeruginosin KT608A containing an L-*diepi*-Choi Moiety

For future work, we envision the synthesis of our proposed revised structure of aeruginosin KT608A (**3.121**) containing an L-*diepi*-Choi core (Scheme 56). Careful investigation of the NMR spectra of our synthetic material with the isolated natural product indicates the presence of this stereoisomer of the Choi motif. Epimerization of the D-*diepi*-Choi derivative **3.110** should give access to L-*diepi*-Choi building block **3.120**. Further, assembly of the different building blocks can be performed by the same route as reported in section 5.7, with the only difference being the incorporation of L-*diepi*-Choi **3.120** instead of D-*diepi*-Choi derivative **3.110**. Once the synthesis of aeruginosin KT608A (**3.121**) will be successfully accomplished, the analysis of the NMR spectra of **3.121** and natural **3.1** should lead to the confirmation of our proposed structure of natural aeruginosin KT608A.

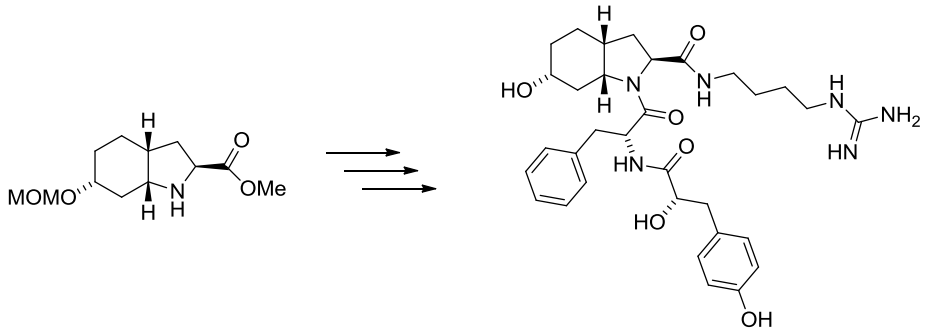

3.120 **3.121**

Scheme 56 Planned synthesis of the proposed revised structure of aeruginosin KT608A (**3.121**), starting from L-*diepi*-Choi building block **3.120**.

8. References

[1] M. Lifshits, S. Carmeli, *J. Nat. Prod.* **2012**, *75*, 209–219.

[2] K. Ersmark, J. R. Del Valle, S. Hanessian, *Angew. Chem. Int. Ed.* **2008**, *47*, 1202–1223.

[3] N. Valls, M. Lopez-Canet, M. Vallribera, J. Bonjoch, *J. Am. Chem. Soc.* **2000**, *122*, 11248–11249.

[4] N. Valls, M. Vallribera, M. López-Canet, J. Bonjoch, *J. Org. Chem.* **2002**, *67*, 4945–4950.

[5] N. Valls, M. López-Canet, M. Vallribera, J. Bonjoch, *Chem. Eur. J.* **2001**, *7*, 3446–3460.

[6] N. Valls, M. Vallribera, S. Carmeli, J. Bonjoch, *Org. Lett.* **2003**, *5*, 447–450.

[7] N. Valls, M. Vallribera, M. Font-Bardía, X. Solans, J. Bonjoch, *Tetrahedron Asymmetry* **2003**, *14*, 1241–1244.

[8] J. Bonjoch, J. Catena, E. Isábal, M. López-Canet, N. Valls, *Tetrahedron Asymmetry* **1996**, *7*, 1899–1902.

[9] P. Wipf, J. L. Methot, *Org. Lett.* **2000**, *2*, 4213–4216.

[10] P. Wipf, S. R. Rector, H. Takahashi, *J. Am. Chem. Soc.* **2002**, *124*, 14848–14849.

[11] S. Hanessian, M. Tremblay, J. F. W. Petersen, *J. Am. Chem. Soc.* **2004**, *126*, 6064–6071.

[12] S. Hanessian, R. Margarita, A. Hall, S. Johnstone, M. Tremblay, L. Parlanti, *J. Am. Chem. Soc.* **2002**, *124*, 13342–13343.

[13] S. Hanessian, J. R. Del Valle, Y. F. Xue, N. Blomberg, *J. Am. Chem. Soc.* **2006**, *128*, 10491–10495.

[14] S. Hanessian, X. Wang, K. Ersmark, J. R. Del Valle, E. Klegraf, *Org. Lett.* **2009**, *11*, 4232–4235.

[15] S. Diethelm, C. S. Schindler, E. M. Carreira, *Org. Lett.* **2010**, *12*, 3950–3953.

[16] S. Diethelm, C. S. Schindler, E. M. Carreira, *Chem. Eur. J.* **2014**, *20*, 6071–6080.

[17] C. S. Schindler, C. R. J. Stephenson, E. M. Carreira, *Angew. Chem. Int. Ed.* **2008**, *47*, 8852–8855.

[18] B. M. Trost, T. Kaneko, N. G. Andersen, C. Tappertzhofen, B. Fahr, *J. Am. Chem. Soc.* **2012**, *134*, 18944–18947.

[19] J. Sofack-Kreutzer, N. Martin, A. Renaudat, R. Jazzar, O. Baudoin, *Angew. Chem. Int. Ed.* **2012**, *51*, 10399–10402.

[20] L. Petit, M. G. Banwell, A. C. Willis, *Org. Lett.* **2011**, *13*, 5800–5803.

[21] D. Dailler, G. Danoun, O. Baudoin, *Angew. Chem. Int. Ed.* **2015**, *54*, 4919–4922.

[22] D. Dailler, G. Danoun, B. Ourri, O. Baudoin, *Chem. Eur. J.* **2015**, *21*, 9370–9378.

[23] F. Shi, J. P. Waldo, Y. Chen, R. C. Larock, *Org. Lett.* **2008**, *10*, 2409–2412.

[24] A. Arques, P. Molina, D. Aunon, M. J. Vilaplana, M. D. Velasco, F. Martinez, D. Bautista, F. J. Lahoz, *J. Organomet. Chem.* **2000**, *598*, 329–338.

[25] H. Hemetsberger, D. Knittel, *Synthesis* **1971**, *103*, 194–204.

[26] R. Wang, H. F. Shi, J. F. Zhao, Y. P. He, H. Bin Zhang, J. P. Liu, *Bioorganic Med. Chem. Lett.* **2013**, *23*, 1760–1762.

[27] B. J. Stokes, H. Dong, B. E. Leslie, A. L. Pumphrey, T. G. Driver, *J. Am. Chem. Soc.* **2007**, *129*, 7500–7501.

[28] J. S. Sawyer, D. W. Beight, E. C. R. Smith, D. W. Snyder, M. K. Chastain, R. L. Tielking, L. W. Hartley, D. G. Carlson, *J. Med. Chem.* **2005**, *46*, 893–896.

[29] R. Kuwano, K. Sato, T. Kurokawa, D. Karube, Y. Ito, *J. Am. Chem. Soc.* **2000**, *122*, 7614–7615.

[30] R. Kuwano, M. Kashiwabara, K. Sato, T. Ito, K. Kaneda, Y. Ito, *Tetrahedron Asymmetry* **2006**, *17*, 521–535.

[31] R. Kuwano, M. Kashiwabara, *Org. Lett.* **2006**, *8*, 2653–2655.

[32] A. M. Maj, I. Suisse, C. Méliet, F. Agbossou-Niedercorn, *Tetrahedron Asymmetry* **2010**, *21*, 2010–2014.

[33] M. Rueping, C. Brinkmann, A. P. Antonchick, I. Atodiresei, *Org. Lett.* **2010**, *12*, 4604–4607.

[34] A. Baeza, A. Pfaltz, *Chem. Eur. J.* **2010**, *16*, 2036–2039.

[35] M. Sawamura, H. Hamashima, M. Sugaeara, R. Kuwano, Y. Ito, *Organometallics* **1995**, *14*, 4549–4558.

[36] M. Vincent, G. Remond, B. Portevin, B. Serkiz, M. Laubie, *Tetrahedron Lett.* **1982**, *23*, 1677–1680.

[37] Y. H. Kim, S. H. Kim, D. H. Park, *Tetrahedron Lett.* **1993**, *34*, 6063–6066.

[38] F. J. Sayago, M. Isabel Calaza, A. I. Jiménez, C. Cativiela, *Tetrahedron* **2008**, *64*, 84–91.

[39] F. J. Sayago, M. Pueyo, M. I. Calaza, A. I. Jiménez, C. Cativiela, *Chirality* **2011**, *23*, 507–513.

[40] F. J. Sayago, A. I. Jiménez, C. Cativiela, *Tetrahedron Asymmetry* **2007**, *18*, 2358–2364.

[41] T. Mezei, M. Porcs-Makkay, G. Simig, *US Patent* **2004**, 198988 A1.

[42] M. V. Bhatt, S. S. El-Morey, *Synthesis* **1982**, *1*, 1048–1050.

[43] M. Demuynck, P. De Clerq, M. Vandewalle, *J. Org. Chem.* **1979**, *44*, 4863–4866.

[44] M. E. Kuehne, J. B. Pitner, *J. Org. Chem.* **1989**, *54*, 4553–4569.

[45] H. Niwa, T. Hida, K. Yamada, *Tetrahedron Lett.* **1981**, *22*, 4239–4240.

[46] P. A. Grieco, M. Nishizawa, T. Oguri, S. D. Burke, N. Marinovic, *J. Am. Chem. Soc.* **1977**, *99*, 5773–5780.

[47] U. Zutter, H. Iding, P. Spurr, B. Wirz, *J. Org. Chem.* **2008**, *73*, 4895–4902.

[48] S. Han, R. A. Moore, R. E. Viola, *Bioorg. Chem.* **2002**, *30*, 81–94.

[49] F. Sarabia, A. Sánchez-Ruiz, S. Chammaa, *Bioorganic Med. Chem.* **2005**, *13*, 1691–1705.

[50] J. B. L. Kristensen, A. L. Nielsen, L. Jørgensen, L. H. Kristensen, C. Helgstrand, L. Juknaite, J. L. Kristensen, J. S. Kastrup, R. P. Clausen, L. Olsen, *FEBS Lett.* **2011**, *585*, 1951–1956.

[51] G. Wang, N. Goyal, B. Hopkinson, *Bioorganic Med. Chem. Lett.* **2009**, *19*, 3798–3803.

[52] A. Ploutno, M. Shoshan, S. Carmeli, *J. Nat. Prod.* **2002**, *65*, 973–978.

[53] K. Ishida, G. Christiansen, W. Y. Yoshida, R. Kurmayer, M. Welker, N. Valls, J. Bonjoch, C. Hertweck, T. Börner, T. Hemscheidt, E. Dittmann, *Chem. Biol.* **2007**, *14*, 565–576.

[54] A. R. Knaggs, *Nat. Prod. Rep.* **1999**, *16*, 525–560.

[55] M. Murakami, Y. Okita, H. Matsuda, T. Okino, K. Yamaguchi, *Tetrahedron Lett.* **1994**, *35*, 3129–3132.

[56] M. Hesse, H. Meier, B. Zeeh, *Spektroskopische Methoden in Der Organischen Chemie*, Georg Thieme Verlag, Stuttgart, **2005**.

[57] J. Keeler, *Understanding NMR Spectroscopy*, John Wiley & Sons, INC., Chichester, **2010**.

[58] M. Karplus, *J. Chem. Phys.* **1959**, *30*, 11–15.

[59] M. Karplus, *J. Am. Chem. Soc.* **1963**, *85*, 2870–2871.

[60] G. He, Y. Zhao, S. Zhang, C. Lu, G. Chen, *J. Am. Chem. Soc.* **2012**, *134*, 3–6.

[61] G. He, C. Lu, Y. Zhao, W. A. Nack, G. Chen, *Org. Lett.* **2012**, *14*, 2944–2947.

[62] E. Baumann, *Berichte der Dtsch. Chem. Gesellschaft* **1886**, *19*, 3218–3222.

[63] C. Schotten, *Berichte der Dtsch. Chem. Gesellschaft* **1884**, *17*, 2544–2547.

[64] K. L. Hull, W. Q. Anani, M. S. Sanford, *J. Am. Chem. Soc.* **2006**, *128*, 7134–7135.

[65] S. Zhang, G. He, Y. Zhao, K. Wright, W. A. Nack, G. Chen, *J. Am. Chem. Soc.* **2012**, *134*, 7312–7316.

[66] V. G. Zaitsev, D. Shabashov, O. Daugulis, *J. Am. Chem. Soc.* **2005**, *127*, 13154–13155.

[67] W. A. Nack, G. He, S. Y. Zhang, C. Lu, G. Chen, *Org. Lett.* **2013**, *15*, 3440–3443.

[68] A. Casnati, N. Della Ca, M. Fontanella, F. Sansone, F. Ugozzoli, R. Ungaro, K. Liger, J. F. Dozol, *European J. Org. Chem.* **2005**, 2338–2348.

[69] J. M. Rowland, M. M. Olmstead, P. K. Mascharak, *Inorg. Chem.* **2002**, *41*, 2754–2760.

[70] L. Wu, Y. Li, *Anal. Chim. Acta* **2003**, *482*, 175–181.

[71] D. H. O' Donovan, C. De Fusco, D. R. Spring, *Tetrahedron Lett.* **2016**, *57*, 2962–2964.

[72] J. J. Li, T. S. Mei, J. Q. Yu, *Angew. Chem. Int. Ed.* **2008**, *120*, 6452–6455.

[73] T. Mei, X. Wang, J. Yu, *J. Am. Chem. Soc.* **2009**, *131*, 10806–10807.

[74] T. W. Greene, P. G. M. Wuts, *Protective Groups In Organic Synthesis*, John Wiley & Sons, INC., New York, **1999**.

[75] T. S. Mei, D. Leow, H. Xiao, B. N. Laforteza, J. Q. Yu, *Org. Lett.* **2013**, *15*, 3058–3061.

[76] B. Cao, D. Xiao, M. M. Joullie, *Org. Lett.* **1999**, *1*, 1799–1801.

[77] D. Yang, S. Mao, Y.-R. Gao, D.-D. Guo, S.-H. Guo, B. Li, Y.-Q. Wang, *RSC Adv.* **2015**, *5*, 23727–23736.

CONCLUSION

In this thesis, our synthetic and biological studies on cyanobacterial aeruginosins were described.

Intoxication of waters caused by cyanobacteria has emerged as an ever growing problem all over the world. Recently, chlorosulfopeptides such as aeruginosin 828A have been shown to exert toxic effects on aquatic organisms. In Chapter I, the first total synthesis of venomous A828A is described, incorporating 18 linear synthetic steps. Solutions for the challenging α-xylosylation and peptide coupling to the Pla-Cleu-OH dipeptide of the L-Choi moiety were reported. In order to get insights into the mode of action of A828A, three congeners with different permutations of the chloride and sulfate groups have successfully been prepared. The synthesized analogues include aeruginosin 748A and 794A, lacking the sulfate and the chloride substituent, respectively, and aeruginoside 126A, missing both sulfate and chloride residues. Performed toxicity tests against the crustacean *Thamnocephalus platyurus* revealed a distinct effect of the sulfate group on increasing the toxicity. Further, no 'chlorine effect' was observed, suggesting that the mode of action of the aeruginosins' toxicity differs from that of protease inhibition. The results described in Chapter I therefore contribute to a more thorough understanding of the chlorosulfopeptides' role as cyanotoxins.

In Chapter II, two different strategies for the synthesis of the D-*diepi*-Choi unit present in aeruginosins such as KT608A are described. The first approach involves a two-step sequence for the ready preparation of octahydroindoles from indoles. This sequence includes a homogeneous enantioselective hydrogenation reaction giving access to enantioenriched indolines followed by a stereocontrolled heterogeneous reduction. The second pathway comprises a C-H activation step providing the indoline intermediates which is again succeeded by a catalytic heterogeneous hydrogenation reaction. The synthesized D-*diepi*-Choi units were successfully incorporated in two independently performed total syntheses of presumed aeruginosin KT608A. Both synthetic materials revealed distinct deviations of the NMR data with respect to the isolated natural product, resulting in the structural revision of aeruginosin KT608A.

EXPERIMENTAL PART

1. General Methods and Materials

Reagents and Solvents were purchased from commercial suppliers (Acros, Fluorochem, Simga Aldrich or TCI) and were used in the reactions without any purification unless otherwise stated. Dry solvents were either purchased from Sigma Aldrich and Acros or were obtained from the Innovative Technology solvent drying system. Technical grade solvents were distilled prior to usage.

Thin Layer Chromatography (TLC) was performed using Merck silica gel 60 F254 plates, visualized with UV light or developed either with aqueous $KMnO_4/Na_2CO_3$ or cerium ammonium molybdate (CAM) stain solution followed by heating.

Flash Chromatography (FC) was carried out on silica gel 60 with a particle size of 0.04–0.063 mm (230–400 mesh) from Silicycle or Merck using a slight overpressure.

Nuclear Magnetic Resonance spectroscopy (NMR) **^{1}H NMR** spectra were recorded on Bruker 400 MHz spectrometers, 500 MHz spectrometers or 600 MHz spectrometers (equipped with a cryo platform) at 298K or 300K in the indicated deuterated solvent. Data are reported as follow: chemical shift (δ, ppm), multiplicity (s, singulet; d, doublet; t, triplet; q, quartet; m, multiplet or not resolved signal; br, broad signal), coupling constant(s) (J, Hz), integration. All signals were referenced to the internal solvent signal as standard ($CHCl_3$ = δ 7.26; DMSO-d_6 = δ 2.50; MeOD-d_4 = δ 3.31). **^{13}C NMR** spectra were recorded with ^{1}H-decoupling on Bruker 101 MHz, Bruker 126 MHz or Bruker 150 MHz spectrometers (equipped with a cryo platform) at 298 K or 300K in the indicated deuterated solvent. All signals were referenced to the internal solvent signal as standard ($CHCl_3$ = δ 77.16; DMSO-d_6 = δ 39.52; MeOD-d_4 = 49.00). **^{19}F NMR** spectra were recorded with ^{1}H-decoupling on Bruker 376 MHz spectrometers.

Melting points (Mp) were determined using a Büchi B-545 apparatus in open capillaries and are uncorrected.

Infrared Spectroscopy (IR) was recorded on a Varian 800 FT-IR ATR spectrometer or on a Spectrum Two (UATR) FT-IR (Perkin Elmer). Data are reported in terms of frequency of absorption ($\tilde{\nu}$, cm^{-1}).

Optical rotations $[\alpha]_D^T$ were recorded at the indicated tempereatre (T) on a Jasco P-2000 digital polarimeter with a path length of 1 dm, using the 589.3 nm D-line of sodium. Concentrations (c) are quoted in g/100 mL.

High Resolution Mass Spectroscopy (HRMS) was recorded by Dr. Heinz Nadig at the University of Basel on a Bruker maXis 4G QTOF ESI mass spectrometer or by the mass spectroscopy service at University of Zurich on a Finnigan MAT95 MS.

Ultra High Performance Liquid Chromatography with Mass Spectrometry (UHPLC-MS) was performed on an Agilent 1290 Infinity instrument equipped with an Eclipse Plus C18 column and an Agilent 6130 ESI-MS detector using a formic acid buffered MeCN/H_2O gradient.

Chiral High Performance Liquid Chromatography (Chiral HPLC) was performed on a Dionex HPLC equipped with a UV-detecor and a chiralpak AS_H column, using isocratic *n*-heptane/^{i}PrOH or *n*-hexane/^{i}PrOH eluents.

Reversed-phase high-performance liquid chromatography (RP-HPLC) was performed on a Dionex HPLC equipped with a P680 HPLC Pump, an ASI-100 automated sample injector, a PDA-100 photodiode array detector, a MSQ- ESI mass spectrometric detector and a Gemini C18 5 µm 150x4.6 mm column using formic acid buffered H_2O/MeCN gradients.

X-ray single crystal structure determination was performed by Dr. Markus Neuburger on a Bruker APEX-II (University of Basel) and by Prof. Dr. Anthony Linden (University of Zurich) on a Nonius KappaCCD diffractometer. Data reduction, solution and refinement used the programs APEX[1] and SHELXL97.[2] Structure analysis was carried out using Mercury v. 3.6.[3]

2. Experimental Procedures

2.1. Toxicity and Synthesis of Aeruginosin Chlorosulfopeptides

2.1.1. L-Choi synthesis

Dimethyl (*tert*-butoxycarbonyl)-L-glutamate (2.25)

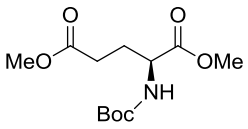

L-Glutamic acid dimethyl ester hydrochloride (**2.24**) (5.80 g, 27.1 mmol, 1.0 eq.) was dissolved in CH_2Cl_2 (45 mL). To this solution, NEt_3 (7.63 mL, 54.2 mmol, 2.0 eq.) and Boc_2O (6.04 g, 27.1 mmol, 1.0 eq.) were added in small portions at 0 °C. The mixture was stirred for 30 min at 0 °C and further 20 h at room temperature. The reaction mixture was quenched by the addition of sat. aq. Na_2CO_3 solution (25 mL). The layers were separated and the aqueous layer was extracted with CH_2Cl_2 (3 x 20 mL). The combined organic layers were dried over Na_2SO_4 and the solvent removed under reduced pressure. The crude product was purified by flash column chromatography (SiO_2, pentane/EtOAc 2:1) to give *N*-Boc-glutamic acid dimethylester (**2.25**) (7.40 g, 26.9 mmol, 99%) a colorless solid.

^{1}H NMR (400 MHz, $CDCl_3$) δ/ppm 5.11 (d, J = 8.4 Hz, 1H), 4.41–4.24 (m, 1H), 3.73 (s, 3H), 3.66 (s, 3H), 2.54–2.32 (m, 2H), 2.17 (dq, J = 13.0, 7.5 Hz, 1H), 1.94 (td, J = 14.6, 8.2 Hz, 1H), 1.42 (s, 9H); **^{13}C NMR** (101 MHz, $CDCl_3$) δ/ppm 173.3, 172.8, 155.5, 53.0, 52.5, 51.9, 30.2, 28.4, 27.9.

Analytical data are in accordance with those reported in the literature.[4]

But-3-en-1-yl trifluoromethanesulfonate

To a solution of pyridine (5.60 mL, 69.1 mmol, 1.2 eq.) in CH_2Cl_2 (70 mL) was added dropwise Tf_2O (9.90 mL, 57.6 mmol, 1.0 eq.) at –78 °C. The mixture was stirred for 15 min at –78 °C before 3-butenol (5.00 mL, 57.6 mmol, 1.0 eq.) was added dropwise, followed by CH_2Cl_2 (20 mL). After stirring at –78 °C for 20 min, the mixture was diluted with CH_2Cl_2 (70 mL). The solution was washed with ice cold HCl solution (1 M, 40 mL), H_2O (40 mL) and the organic layer was dried over Na_2SO_4. The solvent was removed under reduced pressure (300 mbar) at 24 °C. The crude residue was purified by flash column chromatography (SiO_2, pentane/EtOAc 5:1) to give but-3-en-1-yl trifluoromethane-sulfonate (9.80 g, 48.0 mmol, 83%) as a colorless oil.

^{1}H NMR (400 MHz, $CDCl_3$) δ/ppm 5.85–5.67 (m, 1H), 5.23 (dq, J = 5.6, 1.4 Hz, 1H), 5.20 (t, J = 1.4 Hz, 1H), 4.56 (t, J = 6.6 Hz, 2H), 2.58 (qt, J = 6.6, 1.3 Hz, 2H); **^{13}C NMR** (101 MHz, $CDCl_3$) δ/ppm 131.1, 119.7, 76.2, 33.6.

Analytical data are in accordance with those reported in the literature.[4]

Dimethyl (2*S*,4*S*)-2-(but-3-en-1-yl)-4-((*tert*-butoxycarbonyl)amino)pentanedioate (2.26)

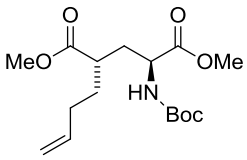

To a solution of *N*-boc-glutamic acid dimethylester (**2.25**) (6.60 g, 24.0 mmol, 1.0 eq.) in THF (130 mL) was added slowly LiHMDS (48.0 mL, 1 M solution in THF, 48.0 mmol, 2.0 eq.) at –78 °C. The mixture was stirred for 45 min at –78 °C before but-3-en-1-yl trifluoromethanesulfonate (9.80 g, 48.0 mmol, 2.0 eq.) was added dropwise. After stirring for 20 min at –78 °C the reaction was quenched by the addition of aq. NH_4Cl solution (2 M, 40 mL) and the mixture was allowed to warm to room temperature. The solvent was removed and the aqueous layer was extracted with CH_2Cl_2 (3 x 60 mL). The combined organic layers were dried over Na_2SO_4 and the solvent was removed under reduced pressure to obtain an orange oil. The crude residue was purified by flash column chromatography (SiO_2, pentane/EtOAc 9:1) to give pentanedioate **2.26** (5.00 g, 15.2 mmol, 63%) as a colorless oil.

^{1}H NMR (400 MHz, $CDCl_3$) δ/ppm 5.75 (ddt, J = 16.9, 10.2, 6.6 Hz, 1H), 5.05–4.90 (m, 3H), 4.40–4.28 (m, 1H), 3.72 (s, 3H), 3.67 (s, 3H), 2.50 (tt, J = 8.1, 5.8 Hz, 1H), 2.07–1.94 (m, 4H), 1.72 (dtd, J = 13.6, 8.3, 6.9 Hz, 1H), 1.66–1.56 (m, 2H), 1.43 (s, 10H); **^{13}C NMR** (101 MHz, $CDCl_3$) δ/ppm 176.2, 173.0, 155.4, 137.5, 115.6, 80.1, 52.5, 52.3, 51.9, 41.6, 34.6, 31.7, 31.2, 28.4.

Analytical data are in accordance with those reported in the literature.[4]

Methyl (2*S*,4*S*)-4-(but-3-en-1-yl)-5-oxopyrrolidine-2-carboxylate (2.27)

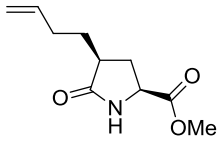

Pentanedioate **2.26** (5.00 g, 15.2 mmol, 1.0 eq.) was dissolved in formic acid (38 mL) and stirred at room temperature for 5 h. The formic acid was removed under reduced pressure and the resulting oil was dissolved in toluene (180 mL) and refluxed for 1.5 h. The solvent was removed under reduced pressure to give pyrrolidinone **2.27** (3.00 g, 15.2 mmol, quant.) as a brown oil which was used in the next step without further purification.

^{1}H NMR (400 MHz, $CDCl_3$) δ/ppm 6.41–6.11 (m, 1H), 5.89–5.67 (m, 1H), 5.07–4.95 (m, 2H), 4.21 (t, J = 8.1 Hz, 1H), 3.78 (s, 2H), 2.66 (ddd, J = 12.8, 8.7, 7.9 Hz, 1H), 2.54–2.39 (m, 1H), 2.24–2.13 (m, 1H), 2.13–1.96 (m, 2H), 1.82 (ddd, J = 12.9, 9.5, 8.2 Hz, 1H), 1.44 (dddd, J = 13.8, 9.7, 8.2, 5.4 Hz, 1H); **^{13}C NMR** (101 MHz, $CDCl_3$) δ/ppm 176.0, 172.2, 137.7, 115.6, 53.8, 52.7, 40.5, 31.6, 31.4, 30.1.
Analytical data are in accordance with those reported in the literature.[4]

1-Benzyl 2-methyl (2*S*,4*S*)-4-(but-3-en-1-yl)-5-oxopyrrolidine-1,2-dicarboxylate (2.29)

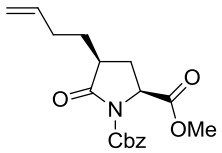

To a solution of pyrrolidinone **2.27** (2.80 g, 14.2 mmol, 1.0 eq.) in THF (35 mL) at –78 °C was added dropwise a solution of LiHMDS (15.8 mL, 1.0 M in THF, 15.8 mmol, 1.1 eq.). After stirring for 30 min at –78 °C, benzyl chloroformate (2.66 mL, 15.8 mmol, 1.1 eq.) was added and the resulting mixture stirred for 1 h at –78 °C. The excess of LiHMDS was quenched by the addition of aq. NH_4Cl solution (2 N, 10 mL) and the resulting mixture was allowed to reach room temperature. THF and H_2O were removed under reduced pressure and the obtained residue was dissolved in H_2O (50 mL) and CH_2Cl_2 (50 mL). The layers were separated and the aqueous layer was extracted with CH_2Cl_2 (2 x 50 mL). The combined organic layers were washed with brine (10 mL), dried over Na_2SO_4 and the solvent was removed under reduced pressure. The crude residue was purified by flash column chromatography (SiO_2, pentane/EtOAc 3:1) to give lactam **2.29** (3.35 g, 10.1 mmol, 71%) as a colorless oil.

^{1}H NMR (400 MHz, $CDCl_3$) δ/ppm 7.43–7.29 (m, 5H), 5.75 (ddt, J = 17.1, 10.2, 6.6 Hz, 1H), 5.33 (d, J = 12.3 Hz, 1H), 5.19 (d, J = 12.3 Hz, 1H), 5.08–4.97 (m, 2H), 4.59–4.50 (m, 1H), 3.64 (s, 2H), 2.64–2.50 (m, 2H), 2.26–2.14 (m, 1H), 2.13–2.06 (m, 1H), 2.05–1.96 (m, 1H), 1.74–1.65 (m, 1H), 1.57–1.47 (m, 1H); **^{13}C NMR** (101 MHz, $CDCl_3$) δ/ppm 174.7, 171.7, 151.2, 137.2, 135.1, 128.7, 128.6, 128.3, 116.0, 68.5, 57.3, 52.7, 41.9, 31.2, 30.3, 28.1.
Analytical data are in accordance with those reported in the literature.[5]

1-Benzyl 2-methyl (2*S*,4*S*)-4-(but-3-en-1-yl)-5-hydroxypyrrolidine-1,2-dicarboxylate (2.29b)

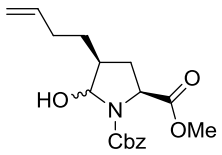

To a solution of lactam **2.29** (3.30 g, 10.0 mmol, 1.0 eq.) in THF (70 mL) at –78 °C was slowly added lithium triethylborohydride (11.1 mL, 1 M solution in THF, 11.1 mmol, 1.1 eq.). The reaction mixture was stirred for 1 h at –78 °C and the excess of lithium triethylborohydride was quenched by the addition of aq. sat. $NaHCO_3$ solution (5 mL). Three drops of H_2O_2 (30% *w*/*w* in H_2O) were added and the solution concentrated under vacuum. The obtained residue was portioned between CH_2Cl_2 (50 mL) and H_2O (50 mL) and the aqueous layer extracted with CH_2Cl_2 (2 x 50 mL). The combined organic layers were washed with brine (20 mL), dried over Na_2SO_4 and the solvent removed under reduced pressure to obtain lactol **2.29b** (3.33 g, 10.0 mmol, quant.) as a colorless oil (dr = 3:1). The crude residue was used in the next step without further purification.

1-Benzyl 2-methyl (2*S*,4*S*)-5-acetoxy-4-(but-3-en-1-yl)pyrrolidine-1,2-dicarboxylate (2.31a and 2.31b)

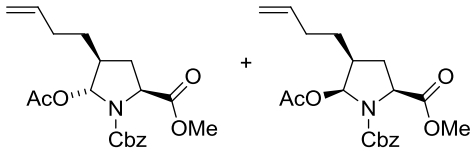

Lactol **2.29b** (3.33 g, 10.0 mmol, 1.0 eq.) was dissolved in CH_2Cl_2 (25 mL) and Et_3N (2.81 mL, 20.0 mmol, 2.0 eq.), Ac_2O (2.82 mL, 30.0 mmol, 3.0 eq.) and DMAP (122 mg, 1.0 mmol, 0.10 eq.) were added. The mixture was stirred at room temperature for 16 h before additional Et_3N (0.70 mL, 5.00 mmol, 0.50 eq.), Ac_2O (0.70 mL, 7.50 mmol, 0.75 eq.) and DMAP (30 mg, 0.25 mmol, 0.030 eq.) were added. The mixture was stirred for further 3 h at room temperature. The reaction was quenched with sat. aq. $NaHCO_3$ solution (20 mL), the resulting layers separated and the aqueous layer extracted with CH_2Cl_2 (2 x 70 mL). The combined organic layers were washed with brine (20 mL), dried over Na_2SO_4 and the solvent removed under reduced pressure. The crude residue was

purified by flash column chromatography (SiO_2, pentane/EtOAc 5:1) to give in a first fraction a rotameric mixture of acetylated lactol **2.31a** (0.600 g, 1.60 mmol, 16%) and in a second fraction a rotameric mixture of acetylated lactol **2.31b** (2.10 g, 5.60 mmol, 56%) as colorless oils. Both diastereoisomers were combined (2.70 g, 7.20 mmol, 72%) and were used as a mixture in the next step.

2.31a: **^{1}H NMR** (400 MHz, $CDCl_3$, major rotamer) δ/ppm 7.43–7.27 (m, 5H), 6.77–6.63 (m, 1H), 5.85–5.62 (m, 1H), 5.29–4.93 (m, 4H), 4.42–4.24 (m, 1H), 3.91–3.46 (m, 3H), 2.43 (dt, J = 12.1, 7.2 Hz, 1H), 2.35–1.96 (m, 6H), 1.94–1.68 (m, 1H), 1.68–1.50 (m, 1H), 1.36 (dq, J = 14.8, 7.7 Hz, 1H); **^{13}C NMR** (101 MHz, $CDCl_3$, major rotamer) δ/ppm 170.0, 153.7, 137.7, 128.6, 128.2, 127.9, 115.5, 82.6, 67.7, 59.2, 52.5, 43.2, 32.9, 31.8, 27.4, 21.1.

2.31b: **^{1}H NMR** (400 MHz, $CDCl_3$, major rotamer) δ/ppm 7.49–7.26 (m, 5H), 6.43–6.32 (m, 1H), 5.85–5.67 (m, 1H), 5.41–5.11 (m, 2H), 5.10–4.94 (m, 3H), 4.55–4.38 (m, 1H), 3.84–3.73 (m, 2H), 3.63–3.50 (m, 2H), 2.65–2.49 (m, 1H), 2.22–2.07 (m, 5H), 1.82–1.64 (m, 1H), 1.47–1.32 (m, 1H); **^{13}C NMR** (101 MHz, $CDCl_3$, major rotamer) δ/ppm 172.5, 154.1, 137.8, 128.6, 128.1, 128.0, 115.3, 87.7, 67.6, 58.9, 52.6, 44.9, 31.6, 30.5, 21.0, 20.7.

1-Benzyl 2-methyl (2*S*,3a*S*,6*S*,7a*S*)-6-bromooctahydro-1*H*-indole-1,2-dicarboxylate (2.33)

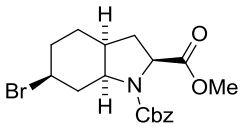

To a solution of protected lactols **2.31a** and **2.31b** (2.25 g, 6.00 mmol, 1.0 eq.) in CH_2Cl_2 (100 mL) at –78 °C was added dropwise a solution of $SnBr_4$ (5.26 g, 12.0 mmol, 2.0 eq.) in CH_2Cl_2 (60 mL). After stirring for 30 min at –78 °C, the solution was quenched with aq. $NaHCO_3$ solution (10% *w*/*w*, 200 mL). The reaction mixture was allowed to warm to room temperature, the layers were separated and the aqueous layer extracted with CH_2Cl_2 (3 x 200 mL). The combined organic layers were dried over Na_2SO_4 and the solvent removed under reduced pressure. The crude residue was purified by flash column chromatography (SiO_2, pentane/EtOAc 5:1) to give a 1:1 rotameric mixture of 6-bromooctahydroindole derivative **2.33** (2.00 g, 5.04 mmol, 84%) as a colorless oil.

^{1}H NMR (400 MHz, $CDCl_3$, mixture of rotamers) δ/ppm 7.37–7.20 (m, 10H), 5.11 (dd, J = 16.2, 12.3 Hz, 2H), 4.96 (dd, J = 25.8, 12.4 Hz, 2H), 4.26 (ddd, J = 16.8, 9.7, 7.3 Hz, 2H), 3.96 (dt, J = 10.9, 6.3 Hz, 1H), 3.86 (dt, J = 11.4, 6.5 Hz, 1H), 3.82–3.74 (m, 1H), 3.71 (s, 3H), 3.50 (s, 3H), 2.74 (ddd, J = 12.5, 6.3, 3.0 Hz, 1H), 2.60 (ddd, J = 13.2, 6.1, 2.8 Hz, 1H), 2.28 (dt, J = 13.6, 6.8 Hz, 2H), 2.12 (dt, J = 12.4, 7.2 Hz, 2H), 2.07–1.88 (m, 6H), 1.83–1.53 (m, 7H); **^{13}C NMR** (101 MHz, $CDCl_3$, mixture of rotamers) δ/ppm 173.3, 173.1, 154.3, 153.7, 136.6, 136.4, 128.7, 128.5, 128.3, 128.2, 128.1, 128.0, 67.4, 67.3, 59.4, 59.3, 58.2, 57.7, 52.5, 52.3, 47.1, 39.2, 38.6, 35.7, 35.0, 32.5, 32.2, 32.1, 31.4, 25.7, 25.6.

Analytical data are in accordance with those reported in the literature.[5]

1-Benzyl 2-methyl (2*S*,3a*S*,6*R*,7a*S*)-6-acetoxyoctahydro-1*H*-indole-1,2-dicarboxylate (2.35)

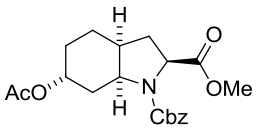

To a solution of 6-bromooctahydroindole derivative **2.33** (1.59 g, 4.00 mmol, 1.0 eq.) in toluene (47 mL) was added Bu_4NOAc (18.1 g, 60.0 mmol, 15 eq.). The mixture was stirred at 44 °C for 3 h. The reaction mixture was allowed to reach room temperature and was diluted with cyclohexane (200 mL). The solution was washed with H_2O (150 mL) and brine (150 mL), dried over Na_2SO_4 and the solvent was removed under reduced pressure. The crude residue was purified by flash column chromatography (SiO_2, pentane/EtOAc 5:1) to give a 1:1 rotameric mixture of octahydroindole **2.35** (0.800 g, 2.13 mmol, 53%) as a colorless oil.

^{1}H NMR (400 MHz, $CDCl_3$, mixture of rotamers) δ/ppm 7.34–7.20 (m, 10H), 5.17–4.92 (m, 4H), 4.27 (dt, J = 16.4, 9.1 Hz, 2H), 4.22–4.12 (m, 1H), 4.10–4.03 (m, 1H), 3.69 (s, 3H), 3.50 (s, 3H), 2.42–2.24 (m, 3H), 2.14 (dt, J = 13.9, 7.2 Hz, 2H), 2.01–1.98 (m, 3H), 1.96–1.83 (m, 5H), 1.77–1.57 (m, 4H), 1.57–1.42 (m, 4H); **^{13}C NMR** (101 MHz, $CDCl_3$, mixture of rotamers) δ/ppm 171.2, 170.5, 153.9, 136.9, 136.6, 128.5, 128.04, 127.96, 127.6, 69.4, 69.2, 67.1, 67.0, 59.4, 59.3, 54.5, 54.1, 52.5, 52.2, 36.5, 35.8, 32.7, 31.7, 31.2, 30.7, 23.8, 21.4, 20.1.

Analytical data are in accordance with those reported in the literature.[5]

1-Benzyl 2-methyl (2*S*,3a*S*,6*R*,7a*S*)-6-hydroxyoctahydro-1*H*-indole-1,2-dicarboxylate (2.37)

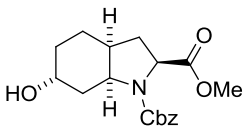

Acetylated ester **2.35** (220 mg, 0.586 mmol, 1.0 eq.) was dissolved in MeOH (12 mL). NaOMe (222 mg, 4.10 mmol, 7.0 eq.) was added and the mixture was stirred for 3 h at room temperature. The excess of NaOMe was quenched with sat. aq. NH_4Cl solution (5 mL), the solvent was removed and the remaining mixture was extracted with EtOAc (3 x 20 mL). The combined organic layers were dried over Na_2SO_4 and the solvent was removed under reduced pressure. The crude mixture was purified by flash column chromatography (SiO_2, pentane/EtOAc 1:1) to obtain a 1:1 rotameric mixture of L-Choi derivative **2.37** (168 mg, 0.504 mmol, 86%) as colorless sticky oil.

R_f = 0.34 (SiO_2, pentane/EtOAc); **Optical rotation** $[\alpha]_D^{25}$ **=** −22.2 (*c* = 0.95, $CHCl_3$); **FTIR** $\tilde{\nu}$/cm^{-1} 3461, 2946, 2890, 1748, 1700, 1417, 1355, 1289, 1199, 1176, 1113, 1012, 907, 746, 699; **^{1}H NMR** (400 MHz, $CDCl_3$) δ/ppm 7.40–7.27 (m, 5H), 5.21–4.97 (m, 2H), 4.40–4.18 (m, 2H), 4.12 (br, 1H), 3.75 (s, 3H), 2.41–2.25 (m, 2H), 2.23–2.10 (m, 3H), 2.01–1.90 (m, 1H), 1.76–1.64 (m, 1H), 1.60–1.45 (m, 3H); **^{13}C NMR** (101 MHz, $CDCl_3$) δ/ppm 173.8, 154.7, 136.9, 128.5, 128.0, 127.9, 67.0, 66.2, 59.4, 53.9, 52.4, 36.7, 33.9, 31.7, 26.6, 19.7; **HRMS ESI** *m*/*z* calc. for $C_{18}H_{23}NO_5Na$ $[M+Na]^+$: 356.1468, found: 356.1474.

1-(*tert*-Butyl) 2-methyl (2*S*,4*S*)-4-(but-3-en-1-yl)-5-oxopyrrolidine-1,2-dicarboxylate (2.28)

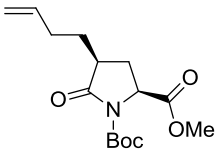

To a solution of pyrrolidinone **2.27** (1.46 g, 7.40 mmol, 1.0 eq.) in CH_2Cl_2 (20 mL) were added Et_3N (3.12 mL, 22.2 mmol, 3.0 eq.), Boc_2O (2.31 g, 10.4 mmol, 1.4 eq.) and DMAP (90.4 mg, 0.740 mmol, 0.10 eq.) at 0 °C. The mixture was stirred for 20 min at 0 °C and further for 16 h at room temperature. Sat. aq. NH_4Cl solution (10 mL) and H_2O (10 mL) were added. The layers were separated and the aqueous layer was extracted with CH_2Cl_2 (2 x 20 mL). The combined organic layers were washed with brine (10 mL), dried over Na_2SO_4 and the solvent removed under reduced pressure. The crude residue was purified by flash column chromatography (SiO_2, pentane/EtOAc 9:1 changing to 5:1) to give lactam **2.28** (1.50 g, 5.04 mmol, 68%) as a colorless oil.

^{1}H NMR (400 MHz, $CDCl_3$) δ/ppm 5.84–5.68 (m, 1H), 5.09–4.94 (m, 2H), 4.54–4.43 (m, 1H), 3.77 (s, 3H), 2.60–2.46 (m, 2H), 2.27–1.95 (m, 3H), 1.72–1.60 (m, 1H), 1.56–1.44 (m, 10H); **^{13}C NMR** (101 MHz, $CDCl_3$) δ/ppm 175.1, 172.1, 149.5, 137.4, 115.9, 83.8, 57.5, 52.6, 42.0, 31.2, 30.3, 28.00, 27.96.

Analytical data are in accordance with those reported in the literature.[4]

1-(*tert*-Butyl) 2-methyl (2*S*,4*S*)-5-acetoxy-4-(but-3-en-1-yl)pyrrolidine-1,2-dicarboxylate (2.30)

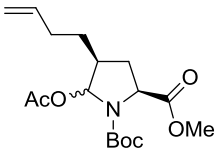

To a solution of lactam **2.28** (1.49 g, 5.00 mmol, 1.0 eq.) in THF (35 mL) at –78 °C was slowly added lithium triethylborohydride (5.55 mL, 1 M solution in THF, 5.55 mmol, 1.1 eq.). The reaction mixture was stirred for 1 h at –78 °C before the excess of lithium triethylborohydride was quenched by the addition of aq. sat. $NaHCO_3$ solution (2 mL). One drop of H_2O_2 (30% *w*/*w* in H_2O) was added and the solution was concentrated under vacuum. The obtained residue was portioned between CH_2Cl_2 (50 mL) and H_2O (50 mL), the layers separated and the aqueous layer extracted with CH_2Cl_2 (2 x 50 mL). The combined organic layers were washed with brine (20 mL), dried over Na_2SO_4 and the solvent removed under reduced pressure to obtain a diastereomeric mixture of the corresponding lactol as a colorless solid. The obtained crude product was dissolved in CH_2Cl_2 (20 mL). To this solution Et_3N (1.40 mL, 10.0 mmol, 2.0 eq.), Ac_2O (1.40 mL, 15.0 mmol, 3.0 eq.) and DMAP (61.0 mg, 0.500 mmol, 0.10 eq.) were added and the mixture was stirred at room temperature for 16 h. Additional Et_3N (0.70 mL, 5.00 mmol, 1.0 eq.) and Ac_2O (0.70 mL, 7.50 mmol, 1.50 eq.) were added and the mixture stirred for further 5 h at room temperature. The reaction was quenched with sat. aq. $NaHCO_3$ solution (10 mL), the layers separated and the aqueous layers extracted with CH_2Cl_2 (2 x 20 mL). The combined organic layers were washed with brine (10 mL), dried over Na_2SO_4 and the solvent removed under reduced pressure. The crude residue was purified by flash column chromatography (SiO_2, pentane/EtOAc 7:1) to give acetylated lactol **2.30** as a mixture of diastereoisomers (0.750 g, 2.20 mmol, 44%) as a colorless oil. Further, the unprotected lactol (0.250 g, 0.850 mmol, 17%) could be isolated as a colorless oil.

1-(*tert*-Butyl) 2-methyl (2*S*,3a*S*,6*S*,7a*S*)-6-bromooctahydro-1*H*-indole-1,2-dicarboxylate (2.32)

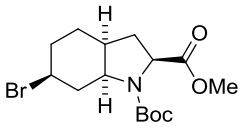

To a solution of protected lactol **2.30** (574 mg, 1.68 mmol, 1.0 eq.) in CH_2Cl_2 (11.5 mL) at –78 °C was added dropwise a solution of $SnBr_4$ (957 mg, 2.18 mmol, 1.3 eq.) in CH_2Cl_2 (2 mL). After stirring for 10 min at –78 °C, the solution was diluted with CH_2Cl_2 (5 mL) and quenched with sat. aq. $NaHCO_3$ solution (0.5 mL). The reaction mixture was allowed to warm to room temperature, filtered over Celite® which was subsequently washed with CH_2Cl_2 (2 x 5 mL). The filtrate was washed with brine (15 mL), dried over Na_2SO_4 and the solvent removed under reduced pressure. A 4:3 rotameric mixture of 6-bromooctahydroindole derivative **2.32** (0.530 g, 1.46 mmol, 87%) was obtained as a colorless oil which was used for the next step without further purification.

^{1}H NMR (400 MHz, $CDCl_3$, mixture of rotamers) δ/ppm 4.21 (dd, J = 10.0, 7.7 Hz, 0.75H), 4.15 (dd, J = 10.1, 7.5 Hz, 1H), 3.91–3.73 (m, 3.5H), 3.69 (s, 2.25H), 3.68 (s, 3H), 3.68–3.64 (m, 1.75H), 2.73 (dddd, J = 13.1, 6.0, 3.7, 2.4 Hz, 1H), 2.60–2.53 (m, 0.75H), 2.35–2.20 (m, 1.75H), 2.15–2.00 (m, 4.5H), 1.99–1.86 (m, 4.5H), 1.83–1.64 (m, 5.25H), 1.39 (s, 6.75H), 1.32 (s, 9H); **^{13}C NMR** (101 MHz, $CDCl_3$, mixture of rotamers) δ/ppm 173.6, 173.4, 153.6, 153.0, 80.29, 80.26, 59.5, 59.0, 57.7, 57.4, 52.3, 52.2, 47.5, 47.4, 39.2, 38.8, 35.6, 34.9, 32.3, 32.2, 32.1, 31.4, 28.5, 28.3, 25.7, 25.6.

Analytical data are in accordance with those reported in the literature.[4]

1-(*tert*-Butyl) 2-methyl (2*S*,3a*S*,6*R*,7a*S*)-6-acetoxyoctahydro-1*H*-indole-1,2-dicarboxylate (2.34)

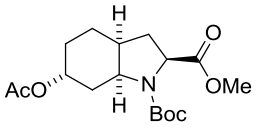

To a solution of 6-bromooctahydroindole derivative **2.32** (0.500 g, 1.38 mmol, 1.0 eq.) in toluene (12 mL) was added Bu_4NOAc (6.20 g, 20.7 mmol, 15.0 eq.). The mixture was stirred at 47 °C for 2 h. The reaction mixture was allowed to reach room temperature and was diluted with cyclohexane (75 mL). The organic layer was washed with H_2O (30 mL), brine (30 mL), dried over Na_2SO_4 and the solvent was removed under reduced pressure. The crude residue was purified by flash column chromatography (SiO_2, pentane/EtOAc 6:1) to give octahydroindole **2.34** (0.260 g, 0.850 mmol, 62%) in a rotameric mixture of 3:1 as a colorless oil.

^{1}H NMR (400 MHz, $CDCl_3$, major rotamer) δ/ppm 5.03 (s, 1H), 4.27–4.13 (m, 1H), 4.13–4.01 (m, 1H), 3.67 (s, 3H), 2.38–2.18 (m, 2H), 2.10 (dt, J = 12.4, 7.3 Hz, 1H), 1.95–1.83 (m, 3H), 1.75–1.58 (m, 2H), 1.56–1.44 (m, 2H), 1.42–1.29 (m, 9H); **^{13}C NMR** (101 MHz, $CDCl_3$, major rotamer) δ/ppm 174.1, 171.2, 153.2, 80.0, 69.2, 59.5, 53.6, 52.1, 35.7, 32.5, 30.8, 28.3, 23.8, 21.1, 20.0.

Analytical data are in accordance with those reported in the literature.[4]

1-(*tert*-Butyl) 2-methyl (2*S*,3a*S*,6*R*,7a*S*)-6-hydroxyoctahydro-1*H*-indole-1,2-dicarboxylate (2.36)

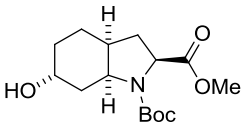

A solution of octahydroindole **2.34** (0.270 g, 0.780 mmol, 1.0 eq.) in MeOH (9.5 mL) was treated with a solution of NaOMe (0.300 g, 5.46 mmol, 7.0 eq.) in MeOH (11 mL). After stirring at room temperature for 6 h, the reaction mixture was diluted with sat. aq. NH_4Cl solution (5 mL). The MeOH was removed under reduced pressure and the obtained aqueous residue extracted with EtOAc (3 x 30 mL). The combined organic layers were dried over Na_2SO_4 and the solvent removed under reduced pressure. The crude residue was purified by flash column chromatography (SiO_2, pentane/EtOAc 3:2) to give octahydroindole **2.36** (0.200 g, 0.670 mmol, 86%) as a colorless solid.

Mp = 160.2−162.1 °C; **Optical rotation** $[\alpha]_D^{25}$ **=** −29.2 (c = 0.23, $CHCl_3$); **FTIR** $\tilde{\nu}$/cm^{-1} 3453, 2973, 2934, 2892, 1751, 1689, 1479, 1402, 1366, 1255, 1197, 1167, 1143, 1116, 1015, 912, 882, 860, 777, 606, 555; **^{1}H NMR** (400 MHz, $CDCl_3$, major rotamer) δ/ppm 4.28–4.06 (m, 3H), 3.71 (s, 3H), 2.39–2.23 (m, 2H), 2.19–2.06 (m, 2H), 1.99–1.85 (m, 1H), 1.72–1.44 (m, 4H), 1.41–1.33 (m, 9H); **^{13}C NMR** (101 MHz, $CDCl_3$, major rotamer) δ/ppm 174.2, 80.0, 66.0, 59.5, 53.6, 52.1, 45.2, 36.0, 33.8, 32.6, 28.4, 26.5, 19.6; **HRMS ESI** m/z calc. for $C_{15}H_{25}NO_5Na$ $[M+Na]^+$: 322.1625, found: 322.1624.

2.1.2. Synthesis of Pla-Cleu-OH dipeptide 2.47

Ethyl (*E*)-4-methylpent-2-enoate (2.38)

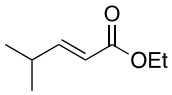

To a solution of NaH (3.68 g, 92.1 mmol, 1.2 eq.) in benzene (110 mL) was slowly added isobutyraldehyde (**2.21**) (5.53 g, 76.7 mmol, 1.0 eq.) at room temperature. The mixture was stirred for 30 min before triethyl phosphonoacetate (1.94 g, 86.7, 1.1 eq.) was added, leading to the formation of a white slurry. The reaction mixture was heated at 70 °C for 1.5 h and was quenched by the addition of H_2O (40 mL). The layers were separated and the organic layer was washed with brine (40 mL), dried over Na_2SO_4 and the solvent was removed under reduced pressure. The obtained crude product was purified by distillation (85 °C, 50 mbar) to give ethyl (*E*)-4-methylpent-2-enoate (**2.38**) (7.12 g, 49.9 mmol, 65%) as a colorless liquid.

Bp: 85 °C (50 mbar); **^{1}H NMR** (400 MHz, $CDCl_3$) δ/ppm 6.94 (dd, J = 15.7, 6.6 Hz, 1H), 5.76 (dd, J = 15.7, 1.5 Hz, 1H), 4.18 (q, J = 7.1 Hz, 2H), 2.59–2.22 (m, 1H), 1.28 (t, J = 7.1 Hz, 3H), 1.05 (d, J = 6.8 Hz, 6H).
Analytical data are in accordance with those reported in the literature.[6]

(*E*)-4-Methylpent-2-en-1-ol (2.39)

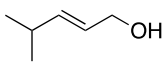

Ethyl (*E*)-4-methylpent-2-enoate (**2.38**) (7.00 g, 49.1 mmol, 1.0 eq.) was dissolved in CH_2Cl_2 (210 mL) and cooled to –78 °C. Then DIBAL (149 mL, 1 M solution in CH_2Cl_2, 143 mmol, 2.9 eq.) was added over a period of 20 min and the mixture stirred for 1.5 h before sat. aq. NH_4Cl solution (100 mL) and aq. HCl solution (1 M, 200 mL) were added at 0 °C. The mixture was diluted with CH_2Cl_2 (250 mL), the layers were separated and the aqueous layer was extracted with CH_2Cl_2 (3 x 250 mL). The combined organic layers were washed with brine (100 mL) and dried over Na_2SO_4. The solvent was removed and the obtained crude product purified by distillation (60 °C, 20 mbar) to give (*E*)-4-methylpent-2-en-1-ol (**2.39**) (3.70 g, 36.8 mmol, 75 %) as a colorless oil.

Bp: 60 °C (20 mbar); **^{1}H NMR** (400 MHz, $CDCl_3$) δ/ppm 5.60 (dd, J = 15.5, 6.1 Hz, 1H), 5.52 (dt, J = 16.4, 5.6 Hz, 1H), 4.02 (d, J = 5.6 Hz, 2H), 2.31–2.15 (m, 1H), 1.39 (s, J = 2.9 Hz, 1H), 0.93 (d, J = 6.8 Hz, 6H); **^{13}C NMR** (101 MHz, $CDCl_3$) δ/ppm 140.3, 125.9, 63.9, 30.79, 22.2.

Analytical data are in accordance with those reported in the literature.[6]

((2*R*,3*R*)-3-Isopropyloxiran-2-yl)methanol (2.40)

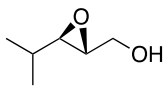

To a suspension of powdered 4 Å molecular sieves in CH_2Cl_2 (60 mL) were added a solution of D(−)-diethyl tartrate (6.20 mL, 36.0 mmol, 0.60 eq.) in CH_2Cl_2 (10 mL) and $Ti(O^iPr)_4$ (8.99 mL, 30.0 mmol, 0.50 eq.) at 0 °C. The solution was stirred for 20 min at the same temperature before cooling to −20 °C. ^{t}BuOOH (16.4 mL, 5.5 M solution in decane, 90.0 mmol, 1.5 eq.) was slowly added over a period of 10 min. The resulting solution was stirred for 30 min at −20 °C before allylalcohol **2.39** (6.01 g, 60.0 mmol, 1.0 eq.) dissolved in CH_2Cl_2 (10 mL) was added dropwise over 20 min. The mixture was stirred at −20 °C for further 14 h and was quenched by the addition of aq. NaOH solution (35% *w*/*w*, 5 mL, sat. with NaCl). The reaction mixture was filtered over Celite® and the filtrate was concentrated under reduced pressure at room temperature. The obtained residue was purified by flash column chromatography (SiO_2, pentane/Et_2O 1:1) to give ((2*R*,3*R*)-3-isopropyloxiran-2-yl)methanol (**2.40**) (3.20 g, 27.6 mmol, 46%) as a colorless oil.

^{1}H NMR (400 MHz, $CDCl_3$) δ/ppm 3.85 (dd, J = 12.6, 2.5 Hz, 1H), 3.55 (dd, J = 12.6, 4.4 Hz, 1H), 2.91 (dt, J = 4.7, 2.5 Hz, 1H), 2.69 (dd, J = 6.9, 2.3 Hz, 1H), 1.60–1.43 (m, 1H), 0.96 (d, J = 6.7 Hz, 3H), 0.90 (d, J = 6.9 Hz, 3H).

Analytical data are in accordance with those reported in the literature.[6]

(2*S*,3*R*)-2-Azido-4-methylpentane-1,3-diol (2.40a) and (2*S*,3*S*)-3-azido-4-methylpentane-1,2-diol (2.40b)

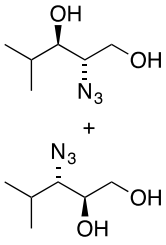

Epoxide **2.40** (1.63 g, 14.0 mmol, 1.0 eq.), NaN_3 (9.10 g, 140 mmol, 10 eq.) and NH_4Cl (1.50 g, 28.0 mmol, 2.0 eq.) were suspended in MeOEtOH (20 mL). H_2O (1 mL) was added and the suspension heated at 120 °C for 24 h. The mixture was let to cool to room temperature and the solvent was removed under reduced pressure. The obtained brown oil was suspended in H_2O (40 mL) and EtOAc (100 mL). The layers were separated, the aqueous layer was extracted with EtOAc (2 x 100 mL) and the combined organic layers were dried over Na_2SO_4. The solvent was removed under reduced pressure to obtain a regioisomeric mixture of azides **2.40a** and **2.40b** as an amber oil (2.25 g, 14.0 mmol, quant.). The crude residue containing azides **2.40a** and **2.40b** was directly used for the next step without further purification.

(2*S*,3*R*)-2-Azido-1-((*tert*-butyldimethylsilyl)oxy)-4-methylpentan-3-ol (2.41) and (2*S*,3*S*)-3-azido-1-((*tert*-butyldimethylsilyl)oxy)-4-methylpentan-2-ol (2.42)

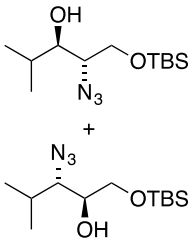

Crude azides **2.40a** and **2.40b** (2.25 g, 14.0 mmol, 1.0 eq.) were dissolved in CH_2Cl_2 (21 mL). To this solution Et_3N (2.83 mL, 20.3 mmol, 1.5 eq.), DMAP (40.0 mg, 0.328 mmol, 0.023 eq.) and TBSCl (2.27 g, 15.4 mmol, 1.1 eq.) were added at 0 °C and the mixture was stirred for 2 h at 0 °C. The reaction mixture was diluted with CH_2Cl_2 (100 mL) and washed with aq. HCl solution (1 M, 20 mL). The organic layer was dried over Na_2SO_4 and the solvent was removed under reduced pressure. The obtained crude product was purified by flash column chromatography (SiO_2, pentane/EtOAc 15:1 to 1:1) to give a 1:1 regioisomeric mixture of azides **2.41** and **2.42** (3.40 g, 12.4 mmol, 89% over two steps) as a colorless oil.

2.41: ^{1}H NMR (400 MHz, $CDCl_3$) δ/ppm 3.97 (dd, J = 10.6, 4.0 Hz, 1H), 3.92 (dd, J = 10.6, 5.9 Hz, 1H), 3.50–3.43 (m, 1H), 3.39 (td, J = 6.2, 3.9 Hz, 1H), 2.30 (d, J = 4.6 Hz, 1H), 1.93–1.80 (m, 1H), 0.98 (d, J = 1.0 Hz, 3H), 0.96 (d, J = 1.2 Hz, 3H), 0.92 (s, 9H), 0.11 (s, 6H); **^{13}C NMR** (101 MHz, $CDCl_3$) δ/ppm 63.99, 63.91, 30.4, 26.0, 25.9, 19.6, 18.3, 16.9, −5.4, −5.5.

2.42: **^{1}H NMR** (400 MHz, $CDCl_3$) δ/ppm 3.78 (dd, J = 10.0, 3.3 Hz, 1H), 3.70 (dd, J = 10.1, 5.6 Hz, 1H), 3.60 (s, 1H), 3.28 (dd, J = 8.0, 4.4 Hz, 1H), 2.51 (s, 1H), 2.09 (septd, J = 6.8, 4.5 Hz, 1H), 1.05 (d, J = 6.9 Hz, 3H), 0.95 (d, J = 6.7 Hz, 3H), 0.92 (s, 9H), 0.11 (s, 3H), 0.11 (s, 3H); **^{13}C NMR** (101 MHz, $CDCl_3$) δ/ppm 71.4, 69.9, 64.0, 29.4, 26.0, 20.6, 18.4, 16.9, −5.2, −5.3.

(2*R*,3*S*)-2-(((*tert*-Butyldimethylsilyl)oxy)methyl)-3-isopropylaziridine (2.43)

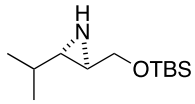

Azides **2.41** and **2.42** (3.40 g, 12.4 mmol, 1.0 eq.) and PPh_3 (3.60 g, 13.6 mmol, 1.1 eq.) were dissolved in MeCN (25 mL) and the mixture was stirred for 2 h at room temperature and further for 18 h at 50 °C. The solvent removed under reduced pressure and the obtained residue was diluted with Et_2O (50 mL) and filtered over a short pad of Celite® to remove precipitated triphenylphosphine oxide. The pad of Celite® was washed with Et_2O (2 x 30 mL) and the filtrate was concentrated under reduced pressure. The obtained crude residue was purified by flash column chromatography (SiO_2, pentane/EtOAc 4:1) to give aziridine **2.43** (2.20 g, 9.80 mmol, 79%) as a colorless oil.

Optical rotation $[\alpha]_D^{25}$ = −19.0 (c = 0.30, $CHCl_3$); **^{1}H NMR** (400 MHz, $CDCl_3$) δ/ppm 3.85–3.63 (m, 1H), 1.88 (q, J = 3.7 Hz, 1H), 1.63 (dd, J = 7.9, 3.2 Hz, 1H), 1.31–1.18 (m, 1H), 1.17–1.07 (m, 1H), 1.02 (d, J = 6.6 Hz, 1H), 0.96 (d, J = 6.8 Hz, 1H), 0.88 (s, J = 2.9 Hz, 4H), 0.05 (d, J = 0.7 Hz, 3H); **^{13}C NMR** (101 MHz, $CDCl_3$) δ/ppm 63.0, 40.9, 37.4, 31.9, 25.9, 20.4, 20.0, 18.3, −5.33, −5.36.

Analytical data are in accordance with those reported in the literature.[7]

(2*R*,3*S*)-2-(((*tert*-Butyldimethylsilyl)oxy)methyl)-1-(*tert*-butylsulfinyl)-3-isopropyl-aziridine (2.43a)

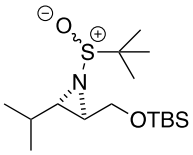

Aziridine **2.43** (2.18 g, 9.50 mmol, 1.0 eq.) was dissolved in CH_2Cl_2 (35 mL) and cooled to 0 °C. Freshly distilled Et_3N (9.61 mL, 95.0 mmol, 10.0 eq.) was slowly added and the solution was stirred for 5 min before *tert*-butylsulfinyl chloride (2.81 g, 20.0 mmol, 2.1 eq.) was added dropwise. The reaction was further stirred at 0 °C for 2 h and then quenched by the addition of aq. Na_2CO_3 soln. (10% *w*/*w*, 35 mL). The layers were separated and the aqueous layer was extracted with CH_2Cl_2 (50 mL). The combined organic layers were washed with H_2O (25 mL), dried over Na_2SO_4 and the solvent was removed under reduced pressure. The obtained crude residue was purified by flash column chromatography (SiO_2, pentane/EtOAc 9:1) to give a 1:1 diastereomeric mixture of protected aziridine **2.43a** (3.20 g, 9.50 mmol, quant.) as a colorless oil.

^{1}H NMR (400 MHz, $CDCl_3$, diastereomeric mixture) δ/ppm 4.01 (dd, J = 11.0, 4.3 Hz, 1H), 3.86 (dd, J = 11.1, 7.4 Hz, 1H), 3.79 (s, 1H), 3.55 (s, 1H), 2.71–2.59 (m, 2H), 2.49 (dt, J = 7.5, 4.2 Hz, 1H), 2.20 (dd, J = 7.5, 3.9 Hz, 1H), 1.92–1.79 (m, 2H), 1.61 (s, 3H), 1.46 (s, 3H), 1.26 (s, 6H), 1.21 (s, 12H), 1.08 (d, J = 6.6 Hz, 3H), 0.98 (d, J = 6.8 Hz, 3H), 0.88 (d, J = 1.1 Hz, 18H), 0.05 (d, J = 1.5 Hz, 12H); **^{13}C NMR** (101 MHz, $CDCl_3$, diastereomeric mixture) δ/ppm 62.5, 57.0, 56.8, 48.8, 46.9, 31.7, 29.6, 27.8, 26.0, 23.9, 22.9, 22.7, 20.3, 19.8, 18.4, 18.3, −5.16, −5.20, −5.21, −5.22.

(2*R*,3*S*)-2-(((*tert*-Butyldimethylsilyl)oxy)methyl)-1-(*tert*-butylsulfonyl)-3-isopropyl-aziridine (2.44)

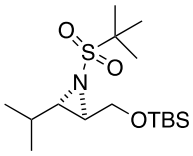

The diastereomeric mixture of sulfoxides **2.43a** (3.20 g, 9.58 mmol, 1.0 eq.) was dissolved in CH_2Cl_2 (22 mL) and cooled to 0 °C. *m*-CPBA (2.58 g, 11.5 mmol, 1.2 eq.) was added and the reaction mixture was stirred for 1.5 h at 0 °C. The mixture was filtered over a short pad of Celite® and the Celite® pad was washed with CH_2Cl_2 (100 mL). The filtrate was washed with sat. aq. $NaHCO_3$ solution (50 mL). The layers were separated and the aqueous layer was extracted with CH_2Cl_2 (50 mL). The combined organic layers were dried over Na_2SO_4 and the solvent was removed under reduced pressure. The crude residue was purified by flash column chromatography (SiO_2, pentane/EtOAc 10:1) to give sulfone **2.44** (2.80 g, 8.05 mmol, 84%) as a colorless oil.

Optical rotation $[\alpha]_D^{25}$ = +34.0 (*c* = 0.26, $CHCl_3$); **^{1}H NMR** (400 MHz, $CDCl_3$) δ/ppm 4.04 (dd, *J* = 10.7, 3.9 Hz, 1H), 3.72 (dd, *J* = 10.9, 7.1 Hz, 1H), 2.73 (dt, *J* = 7.1, 4.6 Hz, 1H), 2.52 (dd, *J* = 7.0, 4.5 Hz, 1H), 1.93 (dsept, *J* = 13.5, 6.6 Hz, 1H), 1.47 (s, 9H), 1.13 (d, *J* = 6.6 Hz, 3H), 0.95 (d, *J* = 6.8 Hz, 3H), 0.89 (s, *J* = 3.0 Hz, 9H), 0.06 (s, *J* = 2.9 Hz, 6H); **^{13}C NMR** (101 MHz, $CDCl_3$) δ/ppm 62.1, 60.0, 52.3, 46.8, 28.5, 25.8, 24.3, 20.6, 18.2, −5.4.
Analytical data are in accordance with those reported in the literature.[7]

***N*-((2*R*,3*S*)-1-((*tert*-Butyldimethylsilyl)oxy)-3-chloro-4-methylpentan-2-yl)-2-methylpropane-2-sulfonamide (2.45)**

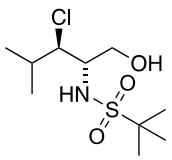

Sulfone **2.44** (2.62 g, 7.50 mmol, 1.0 eq.) was dissolved in MeCN (20 mL). To this solution, $CeCl_3 \cdot H_2O$ (8.38 g, 22.5 mmol, 3.0 eq.) was added in portions over 36 h (1.0 eq. every 12 h) under reflux. The reaction mixture was heated at reflux for additional 48 h. The mixture was let to cool to room temperature and filtered over a pad of Celite®. The filtrate was concentrated under reduced pressure and the obtained crude residue recrystallized from CH_2Cl_2/cyclohexane to give chlorinated sulfone **2.45** (1.10 g, 4.05 mmol, 54%) as a white crystalline solid.

Optical rotation $[\alpha]_D^{25} = -4.5$ (c = 0.29, $CHCl_3$); **^{1}H NMR** (400 MHz, $CDCl_3$) δ/ppm 4.51 (s, J = 8.9 Hz, 1H), 4.06–3.68 (m, 4H), 2.12 (tq, J = 13.2, 6.5 Hz, 2H), 2.09 (br s, 1H), 1.43 (s, 9H), 1.08 (*pseudo*-t, J = 7.0 Hz, 6H); **^{13}C NMR** (101 MHz, $CDCl_3$) δ/ppm 72.3, 62.2, 60.3, 57.7, 31.8, 24.6, 24.4, 20.5, 19.6; **Crystallography** $C_{10}H_{22}ClNO_3S$, M = 271.81, colorless needle, orthorhombic, space group $C222_1$, a = 7.5819(6), b = 20.4433(18), c = 18.8420(16) Å, U = 2920.5(2) Å^3, Z = 8, D_c = 1.236 Mg m^{-3}, μ(Cu-Kα) = 3.618 mm^{-1}, T = 123 K. Total 12499 reflections, 2661 unique, R_{int} = 0.051. Refinement of 2548 reflections (152 parameters) with $I > 2\sigma(I)$ converged at final $R1$ = 0.0430 ($R1$ all data = 0.0438), $wR2$ = 0.0468 ($wR2$ all data = 0.0490), gof = 1.0492.

Analytical data are in accordance with those reported in the literature.[7]

(*R*)-*N*-((2*S*,3*R*)-3-Chloro-1-hydroxy-4-methylpentan-2-yl)-2-(methoxymethoxy)-3-phenylpropanamide (2.46)

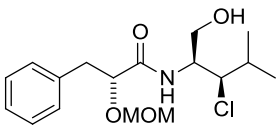

Sulfone **2.45** (70.0 mg, 0.26 mmol, 1.0 eq.) was dissolved in CH_2Cl_2 (13 mL). To this solution were added trifluoromethanesulfonic acid (0.11 mL, 1.29 mmol, 5.0 eq.) and anisole (0.56 mL, 5.16 mmol, 20 eq.) at 0 °C. The mixture was stirred for 20 min at 0 °C and further for 16 h at room temperature. All volatiles were removed under reduced pressure and the obtained crude residue was suspended in H_2O (10 mL). The aqueous layer was washed with Et_2O (3 x 5 mL), frozen and lyophilized to give the triflate salt of the deprotected amine, which was directly used for the next step without further purification. The crude amine salt was suspended in CH_2Cl_2 (2 mL). To this suspension, PyBOP (143 mg, 0.280 mmol, 1.1 eq.), Pla-OH derivative **2.51** (52.6 mg, 0.260 mmol, 1.0 eq.) and 2,6-lutidine (0.20 mL, 1.75 mmol, 7.0 eq.) were

added at 0 °C. The reaction mixture was allowed to warm to room temperature and was further stirred for 16 h. CH_2Cl_2 (15 mL) was added and the mixture was washed with aq. HCl solution (1 M, 5 mL), sat. aq. Na_2CO_3 solution (5 mL) and brine (5 mL). The organic layers were dried over Na_2SO_4 and the solvent was removed under reduced pressure. The obtained crude residue was purified by flash column chromatography (SiO_2, pentane/EtOAc 1:1) to give the desired dipeptide **2.46** (59.0 mg, 0.170 mmol, 68%) as a colorless oil.

Optical rotation $[\alpha]_D^{25}$ = +69.4 (*c* = 0.73, $CHCl_3$); **^{1}H NMR** (400 MHz, $CDCl_3$) *δ*/ppm 7.45–7.17 (m, 1H), 6.92 (d, *J* = 9.3 Hz, 1H), 4.66 (d, *J* = 6.5 Hz, 1H), 4.56 (d, *J* = 6.5 Hz, 1H), 4.34 (dd, *J* = 7.0, 3.8 Hz, 1H), 4.20 (dddd, *J* = 9.4, 7.9, 4.6, 3.2 Hz, 1H), 3.97 (dd, *J* = 11.4, 4.6 Hz, 1H), 3.73 (dd, *J* = 7.9, 4.9 Hz, 1H), 3.71 (dd, *J* = 11.4, 3.2 Hz, 1H) 3.25 (s, 1H), 3.18 (dd, *J* = 14.1, 3.8 Hz, 1H), 3.00 (dd, *J* = 14.1, 7.0 Hz, 1H), 2.49 (s, 1H), 1.71 (dsept, *J* = 6.7, 4.8 Hz 1H), 0.97 (dd, *J* = 7.5, 6.7 Hz, 6H); **^{13}C NMR** (101 MHz, $CDCl_3$) *δ*/ppm 171.6, 136.8, 129.8, 128.3, 126.8, 96.5, 78.7, 68.6, 62.4, 56.1, 52.5, 38.7, 30.4, 20.8, 17.3.
Analytical data are in accordance with those reported in the literature.[5]

(2*S*,3*R*)-3-Chloro-2-((*R*)-2-(methoxymethoxy)-3-phenylpropanamido)-4-methyl-pentanoic acid (2.47)

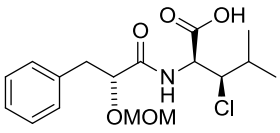

To an ice-cooled solution of dipeptide **2.46** (49.9 mg, 0.150 mmol, 1.0 eq.) dissolved in MeCN (0.83 mL) was added a solution of CrO_3 (1.00 mg, 10.0 µmol, 0.66 eq.) in 0.9 mL of 0.4 M H_5IO_6 in wet MeCN (MeCN/H_2O, 99.3:0.7). The mixture was stirred for 1 h at 0 °C before sat. aq. $NaHCO_3$ solution (1 mL) was added. The solvent was removed under reduced pressure and the aqueous mixture was treated with aq. NaOH solution (0.5 M, 0.3 mL). The aqueous layer was washed with Et_2O (2 x 5 mL) and acidified with aq. HCl solution (1 M, 10 mL). The aqueous layer was extracted with CH_2Cl_2 (2 x 20 mL). The combined organic layers were dried over Na_2SO_4 and the solvent was removed under reduced pressure to obtain Pla-Cleu-OH dipeptide **2.47** (47.0 mg, 0.130 mmol, 90%) as a colorless sticky oil, which was used in the next step without further purification.

Optical rotation $[\alpha]_D^{25}$ = +34.8 (*c* = 0.37, $CHCl_3$); **^{1}H NMR** (400 MHz, $CDCl_3$) *δ*/ppm 9.84 (s, 1H), 7.36 (d, *J* = 8.9 Hz, 1H), 7.30–7.20 (m, 5H), 5.03 (dd, *J* = 8.9, 4.3 Hz, 1H), 4.62 (d, *J* = 6.8 Hz, 1H), 4.55 (d, *J* = 6.8 Hz, 1H), 4.41 (dd, *J* = 7.4, 3.6 Hz, 1H), 3.47 (dd, *J* = 8.5, 4.3 Hz, 1H), 3.20–3.15 (m, 4H), 2.97 (dd, *J* = 14.1, 7.4 Hz, 1H), 2.13–2.00 (m, 1H), 1.09 (d, *J* = 6.7 Hz, 3H), 1.03 (d, *J* = 6.5 Hz, 3H); **^{13}C NMR** (101 MHz, $CDCl_3$) *δ*/ppm 172.2, 171.9, 136.7, 129.9, 128.4, 127.0, 96.2, 77.7, 69.7, 56.2, 54.2, 38.9, 31.9, 20.3, 20.0; **HRMS ESI** *m*/*z* calc. for $C_{17}H_{24}ClNO_5Na$ $[M+Na]^+$: 380.1235, found: 380.1240.

Analytical data are in accordance with those reported in the literature.[5]

2.1.3. Synthesis of Pla-Leu-OH dipeptide 2.53

(*R*)-2-Hydroxy-3-phenylpropanoic acid (2.48)

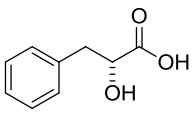

D-Phenylalanine (**2.23**) (3.30 g, 20.0 mmol, 1.0 eq.) was dissolved in aq. H_2SO_4 solution (2 M, 23 mL) and cooled to 0 °C. An aq. $NaNO_2$ solution (40% *w*/*w*, 9 mL) was added over a period of 1 h at 0 °C. The mixture was stirred for 6 h at 0 °C and further 12 h at room temperature. Additional aq. H_2SO_4 solution (2 M, 5 mL) and aq. $NaNO_2$ solution (40% *w*/*w*, 3 mL) were added as above and the mixture was stirred for another 4 h at room temperature. The reaction mixture was saturated with NaCl and extracted with EtOAc (3 x 50 mL). The combined organic layers were washed with brine (100 mL), dried over Na_2SO_4 and the solvent was removed under reduced pressure. The crude product was recrystallized from Et_2O to obtain α-hydroxy acid **2.48** (0.733 g, 4.41 mmol, 22%) as white crystals. The solvent of the mother liquor was removed under reduced pressure to obtain further α-hydroxy acid **2.48** with minor impurities (1.84 g, 11.1 mmol, 55%) as white to light yellow crystals which were used for the next step without further purification.

Mp = 121.0–123.0 °C; $\mathbf{R_f}$ = 0.11 (SiO_2, pentane/EtOAc 4:1 + 0.1% AcOH); **Optical rotation** $[\alpha]_D^{25}$ = +37.5 (*c* = 0.61, $CHCl_3$); **FTIR** $\tilde{\nu}$/cm^{-1} 3442, 2928, 1726, 1494, 1433, 1240, 1189, 1089, 880, 794, 739, 699, 618; **^{1}H NMR** (400 MHz, $CDCl_3$) δ/ppm 7.35–7.25 (m, 5H), 4.53 (dd, *J* = 7.2, 4.3 Hz, 1H), 3.22 (dd, *J* = 14.0, 4.3 Hz, 1H), 3.01 (dd, *J* = 14.0, 7.2 Hz, 1H); **^{13}C NMR** (101 MHz, $CDCl_3$) δ/ppm 177.5, 135.9, 129.7, 128.8, 127.3, 71.1, 40.3.
Analytical data are in accordance with those reported in the literature.[8]

Methyl (*R*)-2-hydroxy-3-phenylpropanoate (2.49)

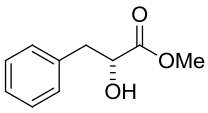

α-Hydroxy acid **2.48** (2.40 g, 14.4 mmol, 1.0 eq.) was dissolved in MeOH/toluene (2:1, 36 mL). Conc. aq. HCl solution (32% *w*/*w*, 0.17 mL, 1.73 mmol, 0.42 eq.) was added dropwise to this solution. The solution was stirred at 75 °C for 4 h. After cooling to room temperature, the mixture was neutralized with aq. $NaHCO_3$ solution (5% *w*/*w*, 70 mL) and extracted with CH_2Cl_2 (3 x 50 mL). The combined organic layers were washed with H_2O (100 mL), dried over Na_2SO_4 and the solvent was removed under reduced pressure to obtain α-hydroxy ester **2.49** (2.49 g, 13.8 mmol, 96%) as a yellow sticky oil, which was used for the next step without further purification.

R_f = 0.26 (SiO_2, pentane/EtOAc 4:1); **Optical rotation** $[\alpha]_D^{25}$ = +7.4 (c = 0.50, $CHCl_3$); **FTIR** $\tilde{\nu}$/cm^{-1} 3029, 2951, 1744, 1433, 1341, 1272, 1210, 1104, 1015, 857, 744, 679; **^{1}H NMR** (400 MHz, $CDCl_3$) δ/ppm 7.34–7.18 (m, 5H), 4.47 (td, J = 6.5, 4.5 Hz, 1H), 3.78 (s, 3H), 3.13 (dd, J = 13.9, 4.4 Hz, 1H), 2.97 (dd, J = 13.9, 6.8 Hz, 1H), 2.70 (d, J = 6.2 Hz, 1H); **^{13}C NMR** (101 MHz, $CDCl_3$) δ/ppm 174.7, 136.4, 129.6, 128.6, 127.1, 71.4, 52.6, 40.7.
Analytical data are in accordance with those reported in the literature.[4]

Methyl (*R*)-2-(methoxymethoxy)-3-phenylpropanoate (2.50)

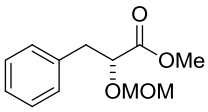

α-Hydroxy ester **2.49** (1.30 g, 7.21 mmol, 1.0 eq.) and DIPEA (3.58 mL, 21.6 mmoL, 3.0 eq.) were dissolved in CH_2Cl_2 (15 mL) and the solution was cooled to 0 °C. MOMBr (1.77 mL, 21.6 mmol, 3.0 eq.) was added dropwise. The solution was stirred for 30 min at 0 °C and for 16 h at room temperature. The mixture was quenched with sat. aq. NH_4Cl solution (20 mL), the layers were separated and the aqueous layer was extracted with CH_2Cl_2 (3 x 20 mL). The combined organic layers were washed with brine (80 mL), dried over Na_2SO_4 and the solvent was removed under reduced pressure. The crude product was purified by flash column chromatography (SiO_2, pentane/EtOAc 4:1) to obtain phenyllactic ester **2.50** (1.18 g, 5.28 mmol, 73%) as a colorless oil.

R_f = 0.41 (SiO_2, pentane/EtOAc 4:1); **Optical rotation** $[\alpha]_D^{25}$ = +64.3 (c = 0.41, $CHCl_3$); **FTIR** $\tilde{\nu}$/cm^{-1} 2953, 2895, 1748, 1605, 1453, 1355, 1279, 1206, 1150, 1111, 1020, 919, 748, 702, 630; **^{1}H NMR** (400 MHz, $CDCl_3$) δ/ppm 7.34–7.20 (m, 5H), 4.64 (d, J = 7.0 Hz, 1H), 4.51 (d, J = 7.0 Hz, 1H), 4.34 (dd, J = 9.0, 4.4 Hz, 1H), 3.73 (s, 3H), 3.11 (dd, J = 13.9, 4.5 Hz, 1H), 3.07 (s, 3H), 2.99 (dd, J = 13.8, 9.0 Hz, 1H); **^{13}C NMR** (101 MHz, $CDCl_3$) δ/ppm 172.7, 137.1, 129.6, 128.5, 126.9, 96.2, 76.5, 55.8, 52.2, 39.3.
Analytical data are in accordance with those reported in the literature.[4]

(*R*)-2-(Methoxymethoxy)-3-phenylpropanoic acid (2.51)

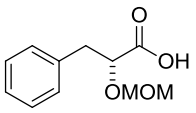

Ester **2.50** (1.30 g, 5.80 mmol, 1.0 eq.) was dissolved in THF/H_2O (5:3, 32 mL). LiOH (0.417 g, 17.4 mmol, 3.0 eq.) was added and the solution stirred for 1 h at room temperature. The mixture was cooled to 0 °C and was neutralized with aq. HCl solution (2 M, 5 mL). The aqueous layer was extracted with EtOAc (3 x 20 mL), the combined organic layers were washed with brine (50 mL) and dried over Na_2SO_4. The solvent was removed under reduced pressure to obtain the phenyllactic acid derivative **2.51** (1.19 g, 5.64 mmol, 97%) as a colorless to light yellow oil, which was used for the next step without further purification .

R_f = 0.19 (SiO_2, pentane/EtOAc 2:1 + 0.2% TFA); **Optical rotation** $[\alpha]_D^{25}$ = +62.8 (*c* = 0.57, $CHCl_3$); **FTIR** $\tilde{\nu}$/cm^{-1} 3063, 2954, 2899, 1722, 1497, 1444, 1212, 1150, 1112, 1023, 918, 701, 633; **^{1}H NMR** (400 MHz, $CDCl_3$) δ/ppm 10.17 (br s, 1H), 7.35–7.20 (m, 5H), 4.67 (d, *J* = 7.0 Hz, 1H), 4.51 (d, *J* = 6.9 Hz, 1H), 4.39 (dd, *J* = 9.1, 3.9 Hz, 1H), 3.19 (dd, *J* = 14.0, 4.0 Hz, 1H), 3.10 (s, 3H), 3.02 (dd, *J* = 14.0, 9.1 Hz, 1H); **^{13}C NMR** (101 MHz, $CDCl_3$) δ/ppm 176.1, 136.7, 129.7, 128.6, 127.1, 96.5, 76.4, 56.1, 39.0.

Analytical data are in accordance with those reported in the literature.[4]

Methyl D-leucinate

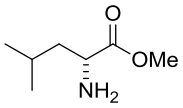

D-Leucine (1.50 g, 11.4 mmol, 1.0 eq.) was dissolved in MeOH (25 mL). $SOCl_2$ (2.50 mL, 34.2 mmol, 3.0 eq.) was added dropwise at 0 °C. The reaction mixture was heated for 3 h under reflux. Then all volatiles were removed under reduced pressure. Semi-saturated aq. Na_2CO_3 soln. (20 mL) was added and the mixture extracted with CH_2Cl_2 (3 x 20 mL). The organic layers were combined and dried over Na_2SO_4. The solvent was removed under reduced pressure to obtain the H-D-Leu-OMe (1.30 g, 8.97 mmol, 79%) as light yellow oil which was used without any further purification.

R_f = 0.26 (SiO_2, CH_2Cl_2/MeOH 20:1); **Optical rotation** $[\alpha]_D^{25}$ = –12.4 (*c* = 0.51, $CHCl_3$); **FTIR** $\tilde{\nu}$/cm^{-1} 3381, 2956, 2871, 1737, 1605, 1438, 1385, 1197, 1172, 1007, 835, 635; **^{1}H NMR** (400 MHz, $CDCl_3$) δ/ppm 3.72 (s, 3H), 3.49 (dd, *J* = 8.7, 5.6 Hz, 1H), 1.83–1.72 (m, 3H), 1.61–1.53 (m, 1H), 1.48–1.39 (m, 1H), 0.93 (t, *J* = 6.6 Hz, 6H); **^{13}C NMR** (101 MHz, $CDCl_3$) δ/ppm 177.3, 53.0, 52.0, 44.3, 24.9, 23.1, 21.9.

Methyl ((*R*)-2-(methoxymethoxy)-3-phenylpropanoyl)-D-leucinate (2.52)

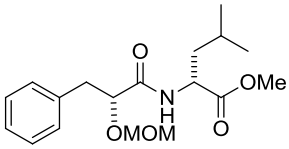

H-D-Leu-OMe (250 mg, 1.72 mmol, 1.0 eq.) and phenyllactic aicd derivative **2.51** (470 mg, 2.24 mmol, 1.3 eq.) were dissolved in CH_2Cl_2 (12 mL). The solution was cooled to 0 °C and 2,6-lutidine (1.00 mL, 8.60 mmol, 5.0 eq.) and PyBOP (1.16 g, 2.24 mmol, 1.3 eq.) were added. The mixture was stirred for 20 min at 0 °C and further 20 h at room temperature. Then the reaction was diluted with CH_2Cl_2 (5.0 mL), washed with aq. HCl solution (1 M, 10 mL), sat. aq. Na_2CO_3 solution (10 mL) and brine (30 mL). The combined organic layers were dried over Na_2SO_4 and the solvent was removed under reduced pressure. The crude residue was purified by flash column chromatography (SiO_2, pentane/EtOAc 3:1 changing to 1:1) to obtain Pla-Leu-OMe dipeptide **2.52** (0.471 g, 1.40 mmol, 81%) as a colorless oil.

R_f = 0.63 (SiO_2, pentane/EtOAc 1:1); **Optical rotation** $[\alpha]_D^{25}$ = +64.0 (*c* = 0.30, $CHCl_3$); **FTIR** $\tilde{\nu}$/cm^{-1} 3317, 2955, 1744, 1667, 1520, 1453, 1339, 1273, 1208, 1151, 1103, 1036, 920, 846, 702, 631; **^{1}H NMR** (400 MHz, $CDCl_3$) δ/ppm 7.29–7.18 (m, 5H), 6.81 (d, *J* = 8.9 Hz, 1H), 4.66–4.56 (m, 3H), 4.37 (dd, *J* = 7.3, 3.7 Hz, 1H), 3.70 (s, 3H), 3.21 (s, 3H), 3.18 (dd, *J* = 14.1, 3.7 Hz, 1H), 2.97 (dd, *J* = 14.1, 7.3 Hz, 1H), 1.59–1.51 (m, 1H), 1.45–1.37 (m, 1H), 1.36–1.24 (m, 1H), 0.87 (d, *J* = 6.5 Hz, 3H), 0.85 (d, *J* = 6.6 Hz, 3H); **^{13}C NMR** (101 MHz, $CDCl_3$) δ/ppm 173.5, 171.3, 137.1, 129.9, 128.3, 126.8, 96.0, 77.7, 56.2, 52.4, 50.1, 41.7, 38.9, 24.6, 23.0, 21.9; **HRMS ESI** *m/z* calc. for $C_{18}H_{27}NO_5Na$ $[M+Na]^+$: 360.1781, found: 360.1785.

((*R*)-2-(Methoxymethoxy)-3-phenylpropanoyl)-D-leucine (2.53)

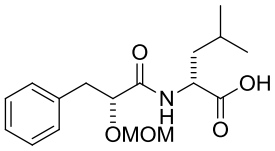

Pla-Leu-OMe dipeptide **2.52** (340 mg, 1.01 mmol, 1.0 eq.) was dissolved in THF/H_2O (5:3, 16 mL). LiOH (71.9 mg, 3.00 mmol, 3.0 eq.) was added and the mixture was stirred for 2 h at room temperature. The reaction was cooled to 0 °C, neutralized with aq. HCl solution (2 M, 5 mL) and the THF was removed under reduced pressure. The residue was extracted with EtOAc (3 x 10 mL), the combined organic layers were washed with brine (50 mL) and dried over Na_2SO_4. The solvent was removed under reduced pressure to obtain Pla-Leu-OH dipeptide **2.53** (318 mg, 0.983 mmol, 98%) as colorless sticky oil.

R_f = 0.12 (SiO_2, pentane/EtOAc 1:1 + 0.5% AcOH); **Optical rotation** $[\alpha]_D^{25}$ = +62.1 (*c* = 0.54, $CHCl_3$); **FTIR** $\tilde{\nu}$/cm^{-1} 3408, 2955, 1728, 1637, 1529, 1453, 1351, 1268, 1201, 1150, 1104, 1037, 920, 746, 700, 652, 621; **^{1}H NMR** (400 MHz, $CDCl_3$) δ/ppm 7.30–7.18 (m, 5H), 6.82 (d, *J* = 8.8 Hz, 1H), 4.65–4.55 (m, 3H), 4.39 (dd, *J* = 7.2, 3.7 Hz, 1H), 3.20–3.15 (m, 4H), 2.97 (dd, *J* = 14.1, 7.2 Hz, 1H), 1.62 (ddd, *J* = 13.9, 9.7, 4.9 Hz, 1H), 1.45 (ddd, *J* = 13.7, 9.7, 5.3 Hz 1H), 1.38–1.29 (m, 1H), 0.86 (d, *J* = 6.6 Hz, 6H); **^{13}C NMR** (101 MHz, $CDCl_3$) δ/ppm 176.6, 172.1, 136.9, 129.9, 128.4, 126.8, 96.0, 77.7, 56.2, 50.2, 41.1, 38.8, 24.7, 23.0, 21.8; **HRMS ESI** *m*/*z* calc. for $C_{17}H_{25}NO_5Na$ $[M+Na]^+$: 346.1625, found: 346.1629.

2.1.4. Synthesis of Adc building block 2.63

Methyl 4-hydroxy-2-methylenebutanoate (2.54)

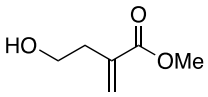

3-Methylenedihydrofuran-2-(3*H*)-one (**2.17**) (4.2 mL, 48.0 mmol, 1.0 eq.) was dissolved in MeOH (180 mL) and cooled to 0 °C. Fuming sulfuric acid (9.5 mL) was added dropwise and the solution was stirred for 16 h at room temperature. The mixture was neutralized with aq. NaOH solution (10 M, 50 mL) and the solvent was removed under reduced pressure at room temperature. The residue was extracted with EtOAc (3 x 150 mL). The combined organic layers were washed with H_2O (200 mL), dried over Na_2SO_4 and the solvent was removed under reduced pressure at room temperature to obtain γ-hydroxy ester **2.54** (4.58 g, 35.2 mmol, 72%) as a colorless oil. The crude product was used for the next step without further purification.

R_f = 0.43 (SiO_2, pentane/EtOAc 10:1); **^{1}H NMR** (400 MHz, $CDCl_3$) δ/ppm 6.27–6.23 (m, 1H), 5.69–5.65 (m, 1H), 3.81–3.74 (m, 2H), 3.76 (s, 3H) 2.58 (t, J = 6.1 Hz, 2H); **^{13}C NMR** (101 MHz, $CDCl_3$) δ/ppm 168.0, 137.5, 127.6, 61.8, 52.2, 35.7.

Methyl 4-((*tert*-butyldiphenylsilyl)oxy)-2-methylenebutanoate (2.55)

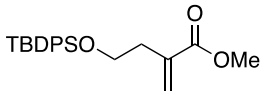

γ-Hydroxy ester **2.54** (4.58 g, 35.2 mmol, 1.0 eq.) was dissolved in DMF (150 mL) and cooled to 0 °C. TBDPSCl (9.20 mL, 35.5 mmol, 1.0 eq.) and imidazole (4.85 g, 73.4 mmol, 2.1 eq.) were added. The solution was stirred for 16 h at room temperature. The solvent was removed under reduced pressure and the obtained residue dissolved in EtOAc (150 mL). The solution was washed with H_2O (4 x 150 mL) and brine (100 mL) and dried over Na_2SO_4. The solvent was removed under reduced pressure and the crude residue purified by flash column chromatography (SiO_2, pentane/EtOAc 15:1 changing to 1:1) to obtain TBDPS protected alcohol **2.55** (3.94 g, 10.7 mmol, 30%) as a colorless oil.

R_f = 0.45 (SiO_2, pentane/EtOAc 15:1); **FTIR** $\tilde{\nu}$/cm^{-1} 3071, 3050, 2954, 2932, 2858, 1722, 1632, 1429, 1305, 1218, 1154, 1108, 998, 931, 821, 705, 631; **^{1}H NMR** (400 MHz, $CDCl_3$) δ/ppm 7.67–7.63 (m, 4H), 7.45–7.35 (m, 6H), 6.22 (d, J = 1.3 Hz, 1H), 5.6–5.61 (m, 1H), 3.79 (t, J = 6.4 Hz, 2H), 3.70 (s, 3H), 2.58 (t, J = 6.5 Hz, 2H), 1.03 (s, 9H); **^{13}C NMR** (101 MHz, $CDCl_3$) δ/ppm 167.6, 137.4, 135.7, 133.9, 129.7, 127.7, 127.2, 62.7, 51.9, 35.3, 27.0, 19.3.

Analytical data are in accordance with those reported in the literature.[9]

4-((*tert*-Butyldiphenylsilyl)oxy)-2-methylenebutan-1-ol (2.56)

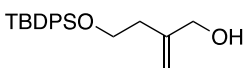

Ester **2.55** (3.85 g, 10.4 mmol, 1.0 eq.) was dissolved in CH_2Cl_2 (60 mL) and cooled to –78 °C. DIBAL (1 M, 26 mL, 26.5 mmol, 2.5 eq.) was added dropwise and the solution was stirred for 1 h at –78 °C. The reaction was quenched with sat. aq. NH_4Cl solution (10 mL). The solvent was removed under reduced pressure and the residue was dissolved in EtOAc (150 mL). The solution was washed with sat. aq. Rochelle salt solution (2 x 50 mL), H_2O (100 mL), brine (100 mL) and dried over Na_2SO_4. The solvent was removed under reduced pressure and the crude product was purified by flash column chromatography (SiO_2, pentane/EtOAc 4:1) to obtain alcohol **2.56** (3.19 g, 9.36 mmol, 90%) as a colorless oil.

R_f = 0.45 (SiO_2, pentane/EtOAc 4:1); **FTIR** $\tilde{\nu}$/cm^{-1} 3363, 3071, 2931, 2858, 1428, 1191, 1109, 901, 822, 705, 632; **^{1}H NMR** (400 MHz, $CDCl_3$) δ/ppm 7.69–7.65 (m, 4H), 7.46–7.36 (m, 6H), 5.06 (d, J = 1.5 Hz, 1H), 4.90–4.88 (m, 1H), 4.08 (d, J = 6.1 Hz, 2H), 3.77 (t, J = 6.2 Hz, 2H), 2.35 (t, J = 6.2 Hz, 2H), 2.23 (t, J = 6.2 Hz, 1H), 1.05 (s, 9H); **^{13}C NMR** (101 MHz, $CDCl_3$) δ/ppm 146.8, 135.7, 133.5, 129.9, 127.8, 112.4, 66.5, 63.9, 36.7, 26.9, 19.3.

Analytical data are in accordance with those reported in the literature.[9]

_N_-Allyl-4-((_tert_-butyldiphenylsilyl)oxy)-2-methylenebutan-1-amine (2.57)

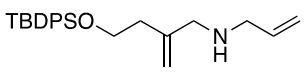

Alcohol **2.56** (3.12 g, 9.16 mmol, 1.0 eq.) was dissolved in CH_2Cl_2 (90 mL) and cooled to 0 °C. Et_3N (1.4 mL, 9.96 mmol, 1.1 eq.) and methanesulfonyl chloride (0.80 mL, 10.3 mmol, 1.1 eq.) were added. After stirring for 2 h at 0 °C, the mixture was allowed to warm to room temperature and prop-2-en-1-amine (3.43 mL, 45.8 mmol, 5.0 eq.) was added and the mixture stirred for 16 h at room temperature. The solvent was removed under reduced pressure and the crude product was purified by flash column chromatography (SiO_2, CH_2Cl_2/MeOH 15:1 changing to 10:1) to obtain allyl amine **2.57** (2.64 g, 6.95 mmol, 76%) as a colorless oil.

R_f = 0.40 (SiO_2, CH_2Cl_2/MeOH 10:1); **FTIR** $\tilde{\nu}$/cm^{-1} 3071, 2931, 2858, 1647, 1463, 1428, 1107, 997, 915, 823, 703, 613; **^{1}H NMR** (400 MHz, $CDCl_3$) δ/ppm 7.69–7.65 (m, 4H), 7.45–7.35 (m, 6H), 5.93–5.83 (m, 1H), 5.18–5.05 (m, 2H), 4.95 (q, J = 1.6 Hz, 1H), 4.86–4.84 (m, 1H), 3.77 (t, J = 6.8 Hz, 2H), 3.19 (dt, J = 6.0, 1.4 Hz, 2H), 3.15 (s, 2H), 2.31 (t, J = 6.6 Hz, 2H), 1.04 (s, 9H); **^{13}C NMR** (101 MHz, $CDCl_3$) δ/ppm 145.1, 137.1, 135.7, 134.0, 129.7, 127.8, 116.0, 111.9, 63.2, 54.1, 51.8, 37.7, 27.0, 19.3.
Analytical data are in accordance with those reported in the literature.[9]

***tert*-Butyl allyl(4-((*tert*-butyldiphenylsilyl)oxy)-2-methylenebutyl)carbamate (2.58)**

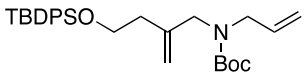

Allyl amine **2.57** (2.60 g, 6.85 mmol, 1.0 eq.) was dissolved in CH_2Cl_2 (38 mL). Et_3N (1.25 mL, 8.91 mmol, 1.3 eq.) and Boc_2O (1.65 g, 7.56 mmol, 1.1 eq.) were added and the solution was stirred for 1 h at room temperature. The solvent was removed under reduced pressure and the crude residue was purified by flash column chromatography (SiO_2, pentane/EtOAc 10:1) to obtain Boc protected allyl amine **2.58** (3.14 g, 6.54 mmol, 96%) as a colorless oil.

R_f = 0.55 (SiO_2, pentane/EtOAc 10:1); **FTIR** $\tilde{\nu}$/cm^{-1} 3072, 2931, 2858, 2360, 1695, 1405, 1246, 1169, 1106, 997, 913, 823, 701, 612; **^{1}H NMR** (400 MHz, $CDCl_3$) δ/ppm 7.68–7.64 (m, 4H), 7.45–7.35 (m, 6H), 5.80–5.67 (m, 1H), 5.14–5.01 (m, 2H), 4.90–4.79 (m, 2H), 3.85–3.66 (m, 6H), 2.24 (t, J = 6.1 Hz, 2H), 1.47–1.38 (m, 9H), 1.04 (s, 9H); **^{13}C NMR** (101 MHz, $CDCl_3$) δ/ppm 155.7, 146.9, 142.2, 135.7, 133.9, 129.7, 127.8, 116.7, 112.4, 79.7, 62.7, 50.8, 48.4, 36.8, 28.5, 27.0, 19.3.

Analytical data are in accordance with those reported in the literature.[9]

tert-Butyl 3-(2-((_tert_-butyldiphenylsilyl)oxy)ethyl)-2,5-dihydro-1-pyrrole-1-carboxylate (2.59)

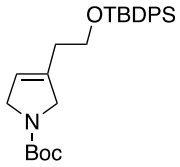

Allyl amine **2.58** (2.81 g, 5.86 mmol, 1.0 eq.) was dissolved in CH_2Cl_2 (200 mL, degassed). Grubbs' catalyst 2nd generation (100 mg, 0.120 mmol, 0.020 eq.) was added and the black solution was stirred for 16 h at room temperature. The solvent was removed under reduced pressure and the crude residue was purified by flash column chromatography (SiO_2, pentane/EtOAc 9:1) to obtain pyrroline **2.59** (2.42 g, 5.41 mmol, 92%) as a light brown oil.

R_f = 0.49 (SiO_2, pentane/EtOAc 9:1); **FTIR** $\tilde{\nu}$/cm^{-1} 3071, 2932, 2858, 1702, 1475, 1401, 1365, 1253, 1164, 1110, 998, 824, 705, 632, 614; **^{1}H NMR** (400 MHz, $CDCl_3$) δ/ppm 7.67–7.63 (m, 4H), 7.46–7.34 (m, 6H), 5.44–5.37 (m, 1H), 4.12–3.95 (m, 4H), 3.75 (td, J = 6.4, 2.3 Hz, 2H), 2.37–2.30 (m, 2H), 1.47 (s, 9H), 1.05 (d, J = 2.2 Hz, 9H); **^{13}C NMR** (101 MHz, $CDCl_3$) δ/ppm 154.4, 137.3, 135.7, 133.7, 129.8, 127.8, 120.4, 79.3, 62.6, 55.5, 53.1, 32.5, 28.7, 27.0, 19.3.

Analytical data are in accordance with those reported in the literature.[9]

***tert*-Butyl 3-(2-hydroxyethyl)-2,5-dihydro-1*H*-pyrrole-1-carboxylate (2.60)**

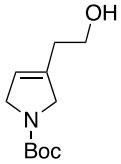

Pyrroline **2.59** (2.30 g, 5.09 mmol, 1.0 eq.) was dissolved in THF (50 mL) and cooled to 0 °C. TBAF (7.70 mL, 1 M in THF, 7.70 mmol, 1.5 eq.) was added dropwise. The reaction mixture was stirred for 10 min at 0 °C and further for 1 h at room temperature. The mixture was quenched with sat. aq. NH_4Cl solution (30 mL). The solvent was evaporated and the residue was diluted with H_2O (10 mL) and extracted with CH_2Cl_2 (3 x 50 mL). The combined organic layers were washed with brine (2 x 50 mL) and dried over Na_2SO_4. The solvent was removed under reduced pressure and the crude product was purified by flash column chromatography (SiO_2, pentane/EtOAc 1:1) to obtain alcohol **2.60** (833 mg, 3.91 mmol, 77%) as a colorless oil.

R_f = 0.29 (SiO_2, pentane/EtOAc 1:1); **FTIR** $\tilde{\nu}$/cm^{-1} 3430, 2972, 2866, 1681, 1653, 1405, 1367, 1250, 1169, 1118, 1050, 984, 873, 621; **^{1}H NMR** (400 MHz, $CDCl_3$) δ/ppm 5.56–5.48 (m, 1H), 4.16–4.02 (m, 4H), 3.80–3.74 (m, 2H), 2.42–2.34 (m, 2H), 1.47 (d, J = 1.5 Hz, 9H); **^{13}C NMR** (101 MHz, $CDCl_3$) δ/ppm 154.4, 136.5, 120.9, 79.5, 60.6, 55.2, 53.2, 32.4, 28.7.
Analytical data are in accordance with those reported in the literature.[9]

***tert*-Butyl 3-(2-azidoethyl)-2,5-dihydro-1*H*-pyrrole-1-carboxylate (2.61)**

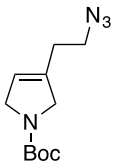

Alcohol **2.60** (790 mg, 3.70 mmol, 1.0 eq.) and PPh_3 (1.95 g, 7.40 mmol, 2.0 eq.) were dissolved in THF (27 mL) and cooled to 0 °C. DEAD (3.40 mL, 40% *w*/*w* solution in toluene, 7.40 mmol, 2.0 eq.) and diphenyl phosphorazidate (1.60 mL, 7.40 mmol, 2.0 eq.) were added. The mixture was stirred for 15 min at 0 °C and further for 1 h at room temperature. The solvent was removed under reduced pressure and the crude product was purified by flash column chromatography (SiO_2, pentane/EtOAc 6:1) to obtain azide **2.61** (633 mg, 2.66 mmol, 72%) as a colorless oil.

R_f = 0.33 (SiO_2, pentane/EtOAc 6:1); **FTIR** $\tilde{\nu}$/cm^{-1} 2976, 2858, 2095, 1697, 1399, 1255, 1173, 1113, 988, 878, 652, 624; **^{1}H NMR** (400 MHz, $CDCl_3$) δ/ppm 5.56–5.48 (m, 1H), 4.15–3.99 (m, 4H), 3.42 (td, J = 6.9, 3.6 Hz, 2H), 2.43–2.35 (m, 2H), 1.47 (d, J = 2.3 Hz, 9H); **^{13}C NMR** (101 MHz, $CDCl_3$) δ/ppm 154.3, 135.9, 121.3, 79.5, 55.0, 53.2, 49.3, 28.7, 28.6; **HRMS ESI** m/z calc. for $C_{11}H_{18}N_4O_2Na$ $[M+Na]^+$: 261.1322, found: 261.1319.
Analytical data are in accordance with those reported in the literature.[9]

tert-Butyl (_E_)-((3-(2-azidoethyl)-2,5-dihydro-1_H_-pyrrol-1-yl)((_tert_-butoxycarbonyl) imino)methyl)carbamate (2.62)

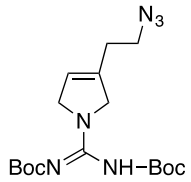

Azide **2.61** (219 mg, 0.919 mmol, 1.0 eq.) was dissolved in CH_2Cl_2 (16 mL). TFA (0.65 mL) was added dropwise to the solution, which turned black after a few minutes. After stirring for 4 h at room temperature, the solution was cooled to 0 °C and Et_3N (1.30 mL, 9.40 mmol, 10 eq.) was added slowly. The solvent was removed under reduced pressure and the resulting dark oil was dissolved in chloroform (10 mL). To this solution Et_3N (0.26 mL, 1.88 mmol, 2.1 eq.) and Goodman's reagent (360 mg, 0.919 mmol, 1.0 eq.) were added and the mixture stirred for 16 h at room temperature. The reaction mixture was diluted with chloroform (20 mL), washed with H_2O (20 mL) and brine (20 mL) and dried over Na_2SO_4. The solvent was removed under reduced pressure and the crude product was purified by flash column chromatography (SiO_2, pentane/EtOAc 4:1) to obtain the azide **2.62** (273 mg, 0.718 mmol, 78%) as a colorless oil.

R_f = 0.26 (SiO_2, pentane/EtOAc 4:1); **FTIR** $\tilde{\nu}$/cm^{-1} 2978, 2932, 2098, 1743, 1598, 1125; **^{1}H NMR** (400 MHz, $CDCl_3$) δ/ppm 10.27 (br s, 1H), 5.58–5.53 (m, 1H), 4.44–4.32 (m, 4H), 3.43 (t, J = 6.9 Hz, 2H), 2.40 (t, J = 6.4 Hz, 2H), 1.50 (s, 18H); **^{13}C NMR** (101 MHz, $CDCl_3$) δ/ppm 154.0, 134.9, 120.1, 80.6, 56.9, 55.4, 49.0, 31.2, 28.3; **HRMS ESI** m/z calc. for $C_{17}H_{29}N_6O_4$ $[M+H]^+$: 381.2245, found: 381.2245.
Analytical data are in accordance with those reported in the literature.[9]

***tert*-Butyl (*E*)-((3-(2-aminoethyl)-2,5-dihydro-1*H*-pyrrol-1-yl)((*tert*-butoxycarbonyl) imino)methyl)carbamate (2.63)**

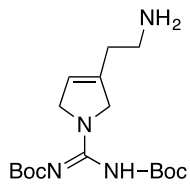

Azide **2.62** (68.0 mg, 0.179 mmol, 1.0 eq.) was dissolved in MeOH (1.5 mL) and Lindlar catalyst (34.0 mg, 50% *w*/*w*) was added. The mixture was stirred at room temperature for 1.5 h under an atmosphere of H_2. The mixture was filtered over a pad of Celite®, the filter cake was washed with MeOH (2.0 mL) and the filtrate concentrated under reduced pressure. After lyophilization, Adc subunit **2.63** (60.7 mg, 0.171 mmol, 96%) was obtained as a colorless solid.

Mp = 109.7–110.4 °C; $\mathbf{R}_f$ = 0.11 (SiO_2, CH_2Cl_2/MeOH 10:1 + 0.2% Et_3N); **FTIR** $\tilde{\nu}$/cm^{-1} 2977, 2934, 1746, 1603, 1479, 1367, 1289, 1241, 1137, 804; **^{1}H NMR** (400 MHz, MeOD) δ/ppm 5.72–5.69 (m, 1H), 4.35–4.24 (m, 4H), 3.11 (t, J = 7.3 Hz, 2H), 2.51 (t, J = 6.8 Hz, 2H), 1.48 (s, 18H); **^{13}C NMR** (101 MHz, MeOD) δ/ppm 153.0, 137.7, 120.5, 81.3, 57.0, 53.7, 40.2, 32.5, 28.6; **HRMS ESI** *m*/*z* calc. for $C_{17}H_{31}N_4O_4$ $[M+H]^+$: 355.2340, found: 355.2340. Analytical data are in accordance with those reported in the literature.[9]

2.1.5. Synthesis of Xyl donor 2.69

(2*S*,3*R*,4*S*,5*R*)-2-(Phenylthio)tetrahydro-2*H*-pyran-3,4,5-triyl triacetate (2.66)

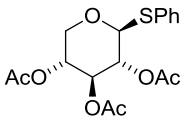

D-(+)-Xylose (5.00 g, 33.3 mmol, 1.0 eq.) was dissolved in pyridine (26.9 mL, 333 mmol, 10 eq.) and cooled to 0 °C. Acetyl chloride (23.8 mL, 333 mmol, 10 eq.) was added slowly and the reaction mixture stirred for 24 h at 0 °C. The reaction mixture was poured into H_2O (150 mL) and extracted with Et_2O (2 x 150 mL). The combined organic layers were washed with sat. aq. NH_4Cl solution (3 x 100 mL) and dried over Na_2SO_4. The solvent was removed under reduced pressure to give an anomeric mixture of (3*R*,4*S*,5*R*)-tetrahydro-2*H*-pyran-2,3,4,5-tetrayl tetraacetate (**2.65**) (10.0 g, 31.4 mmol, 94%) as a brown syrup, which was used for the next step without further purification. The crude residue of acetylated xylose moiety **2.65** (2.20 g, 6.91 mmol, 1.0 eq.) was dissolved in CH_2Cl_2 (9 mL). Thiophenol (0.86 mL, 8.29 mmol, 1.2 eq.) and boron trifluoro etherate (2.60 mL, 20.7 mmol, 3.0 eq.) were slowly added at 0 °C and the mixture was stirred for 20 min at 0 °C and further for 2 h at room temperature. The reaction mixture was diluted with CH_2Cl_2 (10 mL) and washed with sat. aq. $NaHCO_3$ solution (2 x 25 mL) and H_2O (2 x 15 mL). The organic layer was dried over Na_2SO_4 and the solvent was removed under reduced pressure to obtain thioxyloside **2.66** (2.50 g, 6.79 mmol, 98%) as a colorless, viscous oil.

^{1}H NMR (400 MHz, $CDCl_3$) δ/ppm 7.50–7.46 (m, 2H), 7.34–7.29 (m, 3H), 5.18 (t, J = 8.1 Hz, 1H), 4.97–4.88 (m, 2H), 4.80 (d, J = 8.3 Hz, 1H), 4.28 (dd, J = 11.8, 5.0 Hz, 1H), 3.42 (dd, J =11.8, 8.7 Hz, 1H), 2.09 (s, 3H), 2.04 (s, 3H), 2.04 (s, 3H); **^{13}C NMR** (101 MHz, $CDCl_3$) δ/ppm 170.0, 169.9, 169.4, 132.9, 132.4, 129.2, 128.4, 86.4, 72.1, 70.0, 68.5, 65.3, 20.92, 20.86, 20.84.

Analytical data are in accordance with those reported in the literature.[10]

(2*S*,3*R*,4*S*,5*R*)-2-(Phenylthio)tetrahydro-2*H*-pyran-3,4,5-triol (2.67)

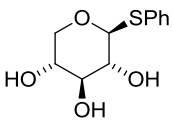

Acetylated thioxyloside **2.66** (2.50 g, 6.79 mmol, 1.0 eq.) was dissolved in MeOH (6 mL). NaOMe (124 mg, 2.30 mmol, 0.34 eq.) was added and the reaction mixture was stirred for 2 h at room temperature. Acidic Amberlite® resin 120 was added to neutralize the reaction solution (the resin was prewashed with H_2O, 1 M HCl and MeOH (2x) prior to use). The resin was filtered off and the solvent was removed under reduced pressure. The crude residue was recrystallized from cyclohexane/acetone (3:1) to afford thioxyloside **2.67** (1.00 g, 4.13 mmol, 61%) as colorless crystals.

Mp = 123.0−124.0 °C; **Optical rotation** $[\alpha]_D^{25}$ **=** +1.7 (*c* = 0.48, MeOH); **FTIR** $\tilde{\nu}$/cm^{-1} 3338, 2932, 2907, 2862, 1568, 1478, 1436, 1345, 1306, 1235, 1092, 1042, 959, 928, 903, 837, 730, 684; **1H NMR** (400 MHz, MeOD) δ/ppm 7.59–7.47 (m, 2H), 7.39–7.23 (m, 3H), 4.55 (d, *J* = 9.3 Hz, 1H), 3.94 (dd, *J* = 11.3, 5.2 Hz, 1H), 3.47 (ddd, *J* = 9.9, 8.7, 5.1 Hz, 1H), 3.37–3.32 (m, 1H), 3.26–3.18 (m, 2H); **^{13}C NMR** (101 MHz, MeOD) δ/ppm 134.9, 133.2, 129.9, 128.5, 90.1, 79.2, 73.7, 70.9, 70.4.
Analytical data are in accordance with those reported in the literature.[10]

(3*R*,4*R*,5*R*,6*S*)-4,5-Dihydroxy-6-(phenylthio)tetrahydro-2*H*-pyran-3-yl benzoate (2.68)

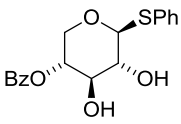

BzCl (0.32 mL, 2.72 mmol, 1.1 eq.) was added dropwise to a stirred solution of thioxyloside **2.67** (598 mg, 2.47 mmol, 1.0 eq.), Me_2SnCl_2 (28.0 mg, 0.120 mmol, 0.050 eq.) and DIPEA (0.82 mL, 4.94 mmol, 2.0 eq.) in THF/H_2O (9:1, 11 mL). The mixture was stirred for 2 h at room temperature before additional Me_2SnCl_2 (28.0 mg, 0.120 mmol, 0.050 eq.) was added. The mixture was stirred for further 2 h after which an aq. HCl solution (3% *w*/*w*, 100 mL) was added. The aqueous layer was extracted with EtOAc (3 x 100 mL), the combined organic layers were dried over Na_2SO_4 and the solvent was removed. The obtained crude product was purified by flash column chromatography (SiO_2, pentane/EtOAc 1:1) to give thioxyloside **2.68** (650 mg, 1.88 mmol, 76%) as a colorless solid.

R$_f$ = 0.51 (SiO_2, pentane/EtOAc 1:1); **Mp** = 89.0−90.0 °C; **Optical rotation** $[\alpha]_D^{25}$ = –40.7 (*c* = 1.09, $CHCl_3$); **FTIR** $\tilde{\nu}$/cm^{-1} 3443, 3064, 2878, 1722, 1602, 1452, 1317, 1261, 1179, 1114, 1086, 1061, 1043, 1026, 968, 906, 847, 804, 744, 708, 688; **^{1}H NMR** (400 MHz, $CDCl_3$) δ/ppm 8.09–7.97 (m, 2H), 7.61–7.53 (m, 3H), 7.44 (dt, *J* = 7.5, 3.0 Hz, 2H), 7.37–7.30 (m,

3H), 5.07 (td, *J* = 9.7, 5.4 Hz, 1H), 4.58 (d, *J* = 9.3 Hz, 1H), 4.30 (dd, *J* = 11.4, 5.4 Hz, 1H), 3.89 (t, *J* = 8.8 Hz, 1H), 3.52–3.41 (m, 2H); **^{13}C NMR** (101 MHz, $CDCl_3$) *δ*/ppm 166.2, 133.5, 133.2, 131.3, 129.8, 129.3, 129.2, 128.5, 128.5, 88.5, 75.5, 72.2, 71.5, 66.6; **HRMS ESI** *m*/*z* calc. for $C_{18}H_{19}O_5S$ $[M+H]^+$: 369.0767; found: 369.0767.

(2*R*,3*R*,4a*R*,5*S*,8*R*,8a*S*)-2,3-Dimethoxy-2,3-dimethyl-5-(phenylthio)hexahydro-5*H*-pyrano[3,4-*b*][1,4]dioxin-8-yl benzoate (2.69)

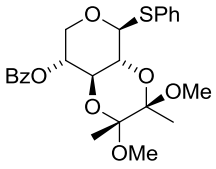

To a solution of thioxyloside **2.68** (600 mg, 1.73 mmol, 1.0 eq.) in MeOH (9.0 mL) were added 2,3-butanedione (0.19 mL, 2.08 mmol, 1.2 eq.), trimethyl orthoformate (0.57 mL, 5.20 mmol, 3.0 eq.) and CSA (4.07 mg, 17.0 µmol, 0.010 eq.). The reaction mixture was heated at 66 °C for 40 h before additional 2,3-butanedione (0.19 mL, 2.08 mmol, 1.2 eq.), trimethyl orthoformate (0.57 mL, 5.20 mmol, 3.0 eq.) and CSA (4.07 mg, 17.0 µmol, 0.010 eq.) were added. The reaction mixture was stirred for additional 24 h at 66 °C. The precipitated product was filtered off and the filter cake was washed with ice cold MeOH (2 x 10 mL) to give the desired thioxyloside **2.69** (550 mg, 1.19 mmol, 69%) as white crystals.

R_f = 0.66 (SiO_2, pentane/EtOAc 10:1); **Mp** = 201.0–203.0 °C; **Optical rotation** $[\alpha]_D^{25}$ = –208.2 (*c* = 0.50, $CHCl_3$); **FTIR** $\tilde{\nu}$/cm^{-1} 2989, 2952, 2937, 2901, 2875, 2825, 1708, 1600, 1450, 1379, 1336, 1316, 1288, 1267, 1203, 1128, 1108, 1044, 979, 924, 884, 850, 749, 708, 691, 654; **^{1}H NMR** (400 MHz, $CDCl_3$) *δ*/ppm 8.09–7.97 (m, 2H), 7.61–7.53 (m, 3H), 7.48–7.41 (m, 2H), 7.33–7.25 (m, 3H), 5.22 (td, *J* = 9.7, 5.4 Hz, 1H), 4.85 (d, *J* = 9.3 Hz, 1H), 4.37 (dd, *J* = 11.6, 5.4 Hz, 1H), 4.10 (t, *J* = 9.3 Hz, 1H), 3.89 (t, *J* = 9.7 Hz, 1H), 3.41 (dd, *J* = 11.6, 8.9 Hz, 1H), 3.32 (s, 3H), 3.23 (s, 3H), 1.35 (s, 3H), 1.28 (s, 3H); **^{13}C NMR** (101 MHz, $CDCl_3$) *δ*/ppm 165.5, 133.3, 133.2, 131.9, 129.6, 128.9, 128.5, 127.6, 100.3, 99.7, 86.0, 71.5, 69.3, 68.2, 67.1, 48.2, 47.9, 17.61, 17.57; **HRMS ESI** *m*/*z* calc. for $C_{24}H_{28}O_7SNa$ $[M+Na]^+$: 483.1448, found: 483.1444; **Crystallography** $C_{24}H_{28}O_7S$, *M* = 460.55, colorless needle, triclinic, space group *P*1, *a* = 5.6090(6), *b* = 8.5370(9), *c* = 12.7740(13) Å, *α* = 71.160(6), *β* = 88.037(7), *γ* = 85.190(7)°, *U* = 576.85(6) Å^3, *Z* = 1, D_c = 1.326 Mg m^{-3}, *μ*(Cu-Kα) = 1.608 mm^{-1}, *T* = 123 K. Total 5847 reflections, 3451 unique, R_{int} = 0.025. Refinement of 3218 reflections (290 parameters) with $I > 2\sigma(I)$ converged at final *R*1 = 0.0294 (*R*1 all data = 0.0308), *wR*2 = 0.0334 (*wR*2 all data = 0.0350), gof = 1.1090.

2.1.6. Assembly of the Different Building Blocks – Synthesis of A828A, A848A, A126A and A794A

1-Benzyl 2-methyl (2*S*,3a*S*,6*R*,7a*S*)-6-(((2*R*,3*R*,4a*R*,5*R*,8*R*,8a*S*)-8-(benzoyloxy)-2,3-dimethoxy-2,3-dimethylhexahydro-5*H*-pyrano[3,4-*b*][1,4]dioxin-5-yl)oxy)octahydro-1*H*-indole-1,2-dicarboxylate (2.71)

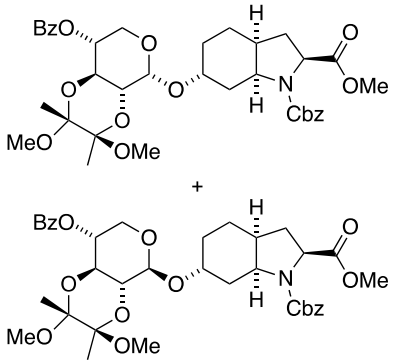

Xylosyl donor **2.69** (203 mg, 0.440 mmol, 1.1 eq.), L-choi derivative **2.37** (133 mg, 0.400 mmol, 1.0 eq.) and NIS (99.0 mg, 0.440 mmol, 1.1 eq.) were dissolved in Et_2O (8.5 mL) containing powdered 4 Å molecular sieves. The mixture was stirred for 20 min at 0 °C before AgOTf (206 mg, 0.800 mmol, 2.0 eq.) was added. The mixture was stirred for another 20 min at 0 °C and further for 2 h at room temperature before four drops of pyridine were added. The mixture was filtered over Celite® and the filtrate was concentrated. The crude product was purified by flash column chromatography (SiO_2, pentane/EtOAc 4:1) to give 1:1 rotameric mixtures of pure α-anomer **2.71** (135 mg, 19.8 mmol, 50%) and pure β-anomer **2.71b** (80.0 mg, 11.7 mmol, 29%). Both anomers were initially obtained as colorless oils, which solidified upon standing.

2.71: Mp = 84.0−86.0 °C; $\mathbf{R}_f$ = 0.53 (SiO_2, pentane/EtOAc 1:1); **Optical rotation** $[\alpha]_D^{25}$ = −107.4 (*c* = 0.13, $CHCl_3$); **FTIR** $\tilde{\nu}$/cm^{-1} 2946, 1704, 1451, 1414, 1353, 1316, 1270, 1197, 1175, 1137, 1111, 1034, 993, 938, 882, 847, 772, 748, 645; **^{1}H NMR** (400 MHz, $CDCl_3$, mixture of rotamers) δ/ppm 8.02 (d, *J* = 7.0 Hz, 2H), 7.56 (t, *J* = 7.4 Hz, 1H), 7.43 (t, *J* = 7.7 Hz, 2H), 7.36–7.75 (m, 5H), 5.28–5.02 (m, 3H), 5.00–4.80 (m, 1H), 4.41–4.24 (m, 3H), 4.00 (br s, 1H), 3.95 (dd, *J* = 10.7, 5.7 Hz, 1H), 3.76 (s, 3H), 3.71–3.60 (m, 2H), 3.28 (s, 3H), 2.96 (s, 3H), 2.51–2.35 (m, 2H), 2.26–2.14 (m, 2H), 2.06–1.93 (m, 1H), 1.75–1.66 (m, 1H), 1.64–1.51 (m, 3H), 1.25 (s, 3H), 1.21 (s, 3H); **^{13}C NMR** (101 MHz, $CDCl_3$, mixture of rotamers) δ/ppm 173.8, 165.7 154.8, 137.0, 136.7, 133.2, 130.0, 129.8, 128.5, 128.0, 127.8, 127.6, 99.9, 99.6, 94.8, 94.3, 71.3, 70.5, 69.8, 68.3, 68.2, 67.0, 66.6, 66.5, 59.8, 59.5, 59.3, 54.5, 53.8, 52.4, 52.1, 48.2, 47.7, 36.6, 36.0, 32.8, 31.9, 29.8, 29.6, 25.7, 20.4, 20.2, 17.8, 17.7, 17.6; **HRMS ESI** *m*/*z* calc. for $C_{36}H_{45}NO_{12}Na$ $[M+Na]^+$: 706.2834, found: 706.2833.

2.71b: $\mathbf{R}_f$ = 0. 46 (SiO_2, pentane/EtOAc 1:1); **Optical rotation** $[\alpha]_D^{25}$ = –124.4 (c = 0.70, $CHCl_3$); **FTIR** $\tilde{\nu}$/cm^{-1} 2950, 1705, 1416, 1354, 1271, 1176, 1138, 1113, 1037, 888, 755, 713; **^{1}H NMR** (400 MHz, $CDCl_3$, mixture of rotamers) δ/ppm 8.05–7.99 (m, 2H), 7.60–7.53 (m, 1H), 7.47–7.40 (m, 2H), 7.35–7.27 (m, 5H), 5.22–4.95 (m, 3H), 4.55 (d, J = 7.4 Hz, 1H), 4.37–4.25 (m, 2H), 4.18 (dt, J = 12.0, 6.5 Hz, 1H), 4.09–4.02 (m, 1H), 4.00–3.91 (m, 1H), 3.75 (s, 3H), 3.71–3.58 (m, 1H), 3.30 (s, 3H), 3.21 (s, 3H), 3.19–3.12 (m, 1H), 2.51–2.30 (m, 2H), 2.23–2.10 (m, 2H), 2.04–1.89 (m, 1H), 1.81–1.74 (m, 1H), 1.68–1.56 (m, 1H), 1.52–1.36 (m, 2H), 1.28 (s, 3H), 1.26 (s, 3H); **^{13}C NMR** (101 MHz, $CDCl_3$, mixture of rotamers) δ/ppm 173.8, 165.6, 154.7, 136.7, 133.3, 133.2, 129.9, 129.7, 128.5, 128.4, 128.1, 127.9, 99.6, 99.0, 98.6, 72.9, 72.0, 70.7, 70.1, 69.8, 69.6, 69.5, 67.1, 66.9, 63.8, 63.5, 59.8, 59.4, 59.2, 54.6, 54.2, 52.4, 52.1, 47.9, 47.7, 36.5, 35.9, 32.8, 32.5, 32.0, 31.8, 23.4, 23.1, 19.6, 17.7, 17.6; **HRMS ESI** m/z calc. for $C_{36}H_{45}NO_{12}Na$ $[M+Na]^+$: 706.2834, found: 706.2833.

Methyl (2*S*,3a*S*,6*R*,7a*S*)-6-(((2*R*,3*R*,4a*R*,5*R*,8*R*,8a*S*)-8-(benzoyloxy)-2,3-dimethoxy-2,3-dimethylhexahydro-5*H*-pyrano[3,4-*b*][1,4]dioxin-5-yl)oxy)octahydro-1*H*-indole-2-carboxylate (2.72)

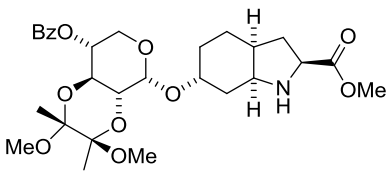

To a solution of Xyl-L-Choi-Cbz derivative **2.71** (90.0 mg, 13.1 mmol, 1.0 eq.) and $PdCl_2$ (23.6 mg, 13.1 mmol, 1.0 eq.) in Et_3SiH (1.5 mL) was added Et_3N (37.1 µL, 26.2 mmol, 2.0 eq.). The reaction was stirred for 2.5 h at room temperature and filtered over a short pad of Celite®. The filtrate was concentrated under reduced pressure and the crude product was purified by flash column chromatography (SiO_2, CH_2Cl_2/MeOH 30:1) to give Xyl-L-Choi-H derivative **2.72** (64.0 mg, 11.6 mmol, 88%) as a colorless oil which solidified upon standing.

Mp = 68.1–68.9 °C; $\mathbf{R}_f$ = 0.45 (SiO_2, CH_2Cl_2/MeOH 20:1); **Optical rotation** $[\alpha]_D^{25}$ = –64.1 (c = 0.58, $CHCl_3$); **FTIR** $\tilde{\nu}$/cm^{-1} 2947, 1727, 1602, 1452, 1375, 1272, 1177, 1140, 1034, 943, 884, 714; **^{1}H NMR** (400 MHz, $CDCl_3$) δ/ppm 8.02 (d, J = 7.5 Hz, 2H), 7.56 (t, J = 7.4 Hz, 1H), 7.43 (t, J = 7.6 Hz, 2H), 5.13 (td, J = 10.1, 5.7 Hz, 1H), 4.91 (d, J = 3.6 Hz, 1H), 4.26 (t, J = 9.9 Hz, 1H), 3.93 (dd, J = 10.8, 5.8 Hz, 1H), 3.87 (dt, J = 10.3, 5.4 Hz, 2H), 3.78 (dd, J = 10.4, 3.5 Hz, 1H), 3.74 (s, 3H), 3.65 (t, J = 10.6 Hz, 1H), 3.45 (q, J = 5.0 Hz, 1H), 3.30 (s, 3H), 3.24 (s, 3H), 3.00 (br s, 1H), 2.30–.20 (m, 1H), 2.10–2.00 (m, 2H), 1.88–1.77 (m, 2H), 1.75–1.65 (m, 2H), 1.55–1.45 (m, 1H), 1.38–1.31 (m, 1H), 1.28 (s, 3H), 1.24 (s, 3H);

^{13}C NMR (101 MHz, $CDCl_3$) δ/ppm 176.0, 165.7, 133.2, 130.0, 129.8, 128.5, 99.9, 99.6, 95.9, 73.2, 70.0, 68.4, 66.7, 59.6, 58.5, 58.4, 48.0, 47.8, 37.4, 35.7, 32.8, 31.2, 25.6, 17.9, 17.7; **HRMS ESI** *m*/*z* calc. for $C_{28}H_{40}NO_{10}$ $[M+H]^+$: 550.2647, found: 550.2655.

Ethyl (2*S*,3a*S*,6*R*,7a*S*)-6-(((2*R*,3*R*,4a*R*,5*R*,8*R*,8a*S*)-8-(benzoyloxy)-2,3-dimethoxy-2,3-dimethylhexahydro-5*H*-pyrano[3,4-*b*][1,4]dioxin-5-yl)oxy)-1-((2*S*,3*R*)-3-chloro-2-((*R*)-2-(methoxymethoxy)-3-phenylpropanamido)-4-methylpentanoyl)-octahydro-1*H*-indole-2-carboxylate (2.74)

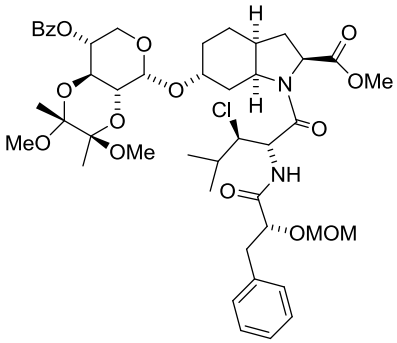

To a solution of amine **2.72** (5.50 mg, 10.0 µmol, 1.0 eq.) and Cleu derivative **2.47** (5.37 mg, 15.0 µmol, 1.5 eq.) in CH_2Cl_2 (0.2 mL) at 0 °C were added DMTMM (4.15 mg, 15.0 µmol, 1.5 eq.) and NMM (2.2 µL, 20.0 mmol, 2.0 eq.). After the addition, the reaction mixture was allowed to reach room temperature and stirred for 2 h. The solvent was removed under reduced pressure and the crude product directly purified by flash column chromatography (SiO_2, pentane/EtOAc 1:1) to give pure tripeptide **2.74** (7.45 mg, 8.70 µmol, 87%) as a white solid.

Mp = 218.0−220.0 °C; **R_f** = 0.41 (SiO_2, pentane/EtOAc 1:1); **Optical rotation** $[\alpha]_D^{25}$ **=** –29.3 (*c* = 0.12, $CHCl_3$); **FTIR** $\tilde{\nu}$/cm^{-1} 2954, 2927, 2855, 1749, 1727, 1682, 1646, 1505, 1451, 1369, 1316, 1271, 1196, 1175, 1143, 1112, 1084, 1036, 939, 881, 803, 754, 713, 613; **^{1}H NMR** (400 MHz, $CDCl_3$) δ/ppm 8.07–7.98 (m, 2H), 7.57 (tt, *J* = 7.4, 1.3 Hz, 1H), 7.44 (t, *J* = 7.7 Hz, 2H), 7.29–7.18 (m, 5H), 6.92 (d, *J* = 10.2 Hz, 1H), 5.22 (d, *J* = 3.4 Hz, 1H), 5.17 (td, *J* = 10.2, 5.8 Hz, 1H), 4.95 (t, *J* = 10.4 Hz, 1H), 4.55 (s, 2H), 4.42–4.31 (m, 4H), 4.04 (br s, 1H), 3.99 (ddd, *J* = 10.6, 3.8, 1.8 Hz, 2H), 3.90 (dd, *J* = 10.1, 3.4 Hz, 1H), 3.67 (s, 3H), 3.53 (t, *J* = 10.6 Hz, 1H), 3.33 (s, 3H), 3.29 (s, 3H), 3.16 (s, 3H), 3.12 (dd, *J* = 14.2, 3.5 Hz, 1H), 2.97 (dd, *J* = 14.2, 6.9 Hz, 1H), 2.53 (td, *J* = 12.5, 6.3 Hz, 1H), 2.47–2.39 (m, 1H), 2.35–2.25 (m, 1H), 2.23–2.13 (m, 1H), 1.95 (dd, *J* = 23.2, 12.8 Hz, 2H), 1.76–1.69 (m, 1H), 1.56 (t, *J* = 12.8 Hz, 3H), 1.50–1.42 (m, 1H), 1.30 (s, *J* = 10.7 Hz, 3H), 1.27 (s, 3H), 0.93 (d, *J* = 6.5 Hz, 3H), 0.87 (d, *J* = 6.7 Hz, 3H); **^{13}C NMR** (101 MHz, $CDCl_3$) δ/ppm 172.7, 170.5, 168.7, 165.8, 136.9, 133.2, 130.11, 130.06, 129.8, 128.5, 128.3, 126.8, 99.8, 99.6, 95.6, 93.5, 77.0, 70.1, 68.5, 68.4, 68.1, 66.6, 59.7, 59.2, 56.2, 54.7, 52.2, 48.2, 47.8, 38.4, 36.9, 30.6, 29.8,

28.9, 27.9, 25.2, 20.9, 19.9, 18.0, 17.6, 16.0; **HRMS ESI** *m/z* calc. for $C_{45}H_{61}ClN_2O_{14}Na$ $[M+Na]^+$: 911.3704, found: 911.3707.

(2*S*,3a*S*,6*R*,7a*S*)-1-((2*S*,3*R*)-3-Chloro-2-((*R*)-2-(methoxymethoxy)-3-phenyl-propanamido)-4-methylpentanoyl)-6-(((2*R*,3*R*,4a*R*,5*R*,8*R*,8a*S*)-8-hydroxy-2,3-dimethoxy-2,3-dimethylhexahydro-5*H*-pyrano[3,4-*b*][1,4]dioxin-5-yl)oxy)-octahydro-1*H*-indole-2-carboxylic acid (2.83)

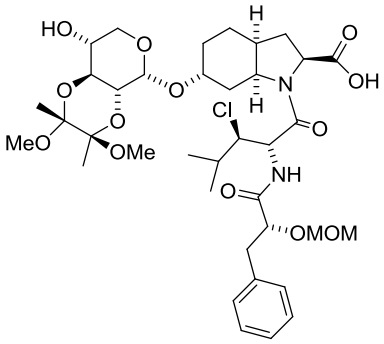

Tripeptide **2.74** (7.20 mg, 8.09 µmol, 1.0 eq.) was dissolved in THF/H_2O (5:3, 1.5 mL) and LiOH monohydrate (6.60 mg, 0.160 mmol, 20 eq.) was added. The reaction was stirred for 12 h at room temperature, H_2O (1 mL) was added and the THF was removed under reduced pressure. Aq. citric acid solution (5% *w*/*w*, 3 mL) was added and the aqueous layer was extracted with CH_2Cl_2 (3 x 5 mL), the combined organic layers were dried over Na_2SO_4 and the solvent was removed under reduced pressure. The crude residue was purified by flash column chromatography (SiO_2, CH_2Cl_2/MeOH 10:1) to obtain tripeptidic acid **2.83** (4.80 mg, 6.22 µmol, 77%) as a colorless solid.

Mp = 183.5–185.0 °C; $\mathbf{R}_f$ = 0.31 (SiO_2, CH_2Cl_2/MeOH 10:1); **Optical rotation** $[\alpha]_D^{25} = -13.9$ (*c* = 0.15, $CHCl_3$); **FTIR** $\tilde{\nu}$/cm^{-1} 3405, 2953, 2927, 2362, 2342, 1741, 1680, 1631, 1510, 1458, 1374, 1334, 1254, 1141, 1117, 1096, 1034, 941, 921, 880, 806, 754, 700, 670, 612; **^{1}H NMR** (400 MHz, $CDCl_3$) δ/ppm 7.27–7.17 (m, 1H), 6.98 (d, *J* = 10.5 Hz, 1H), 5.14 (d, *J* = 3.2 Hz, 1H), 5.03 (t, *J* = 10.5 Hz, 1H), 4.58–4.47 (m, 1H), 4.41–4.31 (m, 1H), 4.07–3.97 (m, 1H), 3.87 (td, *J* = 9.9, 5.7 Hz, 1H), 3.75–3.69 (m, 1H), 3.51 (t, *J* = 10.7 Hz, 1H), 3.29 (s, 1H), 3.27 (s, 1H), 3.17 (s, 1H), 3.12 (dd, *J* = 14.2, 3.5 Hz, 1H), 2.97 (dd, *J* = 14.1, 6.5 Hz, 1H), 2.54–2.42 (m, 1H), 2.39–2.12 (m, 1H), 1.74 (d, *J* = 12.5 Hz, 1H), 1.59 (d, *J* = 9.1 Hz, 1H), 1.46–1.37 (m, 1H), 1.32 (s, 1H), 1.29 (s, 1H), 0.88 (t, *J* = 7.2 Hz, 1H); **^{13}C NMR** (101 MHz, $CDCl_3$) δ/ppm 173.4, 170.7, 170.6, 136.7, 130.07, 128.3, 126.9, 99.8, 99.5, 95.8, 93.9, 69.9, 68.4, 68.3, 68.0, 67.9, 62.3, 59.4, 56.2, 55.9, 52.1, 48.1, 48.0, 38.2, 36.0, 29.9, 29.2, 29.1, 27.9, 24.9, 20.8, 19.8, 18.0, 17.7, 15.9; **HRMS ESI** *m/z* calc. for $C_{37}H_{55}ClN_2O_{13}Na$ $[M+Na]^+$: 793.3285, found: 793.3284.

***tert*-Butyl ((*Z*)-((*tert*-butoxycarbonyl)imino)(3-(2-((2*S*,3a*S*,6*R*,7a*S*)-1-((2*S*,3*R*)-3-chloro-2-((*R*)-2-(methoxymethoxy)-3-phenylpropanamido)-4-methylpentanoyl)-6-(((2*R*,3*R*,4a*R*,5*R*,8*R*,8a*S*)-8-hydroxy-2,3-dimethoxy-2,3-dimethylhexahydro-5*H*-pyrano[3,4-*b*][1,4]dioxin-5-yl)oxy)octahydro-1*H*-indole-2-carboxamido)ethyl)-2,5-dihydro-1*H*-pyrrol-1-yl)methyl)carbamate (2.84)**

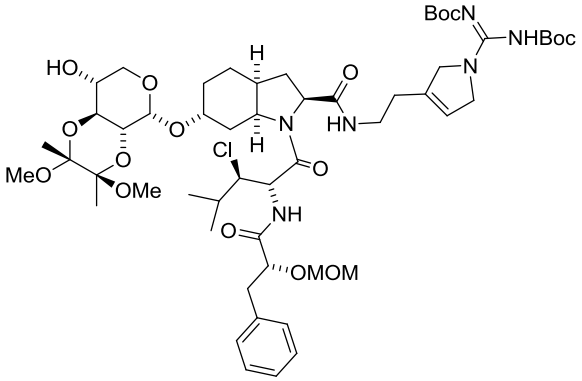

To a solution of tripeptidic acid **2.83** (4.63 mg, 6.00 µmol, 1.0 eq.), Adc side chain **2.63** (4.25 mg, 12.0 µmol, 2.0 eq.) and PyBOP (6.24 mg, 12.0 µmol, 2.0 eq.) in CH_2Cl_2 (0.2 mL) was added 2,6-lutidine (2.1 µL, 18.0 µmol, 3.0 eq.) at 0 °C. The reaction mixture was stirred for 30 min at 0 °C and further for 5 h at room temperature. CH_2Cl_2 (3 mL) was added and the mixture was washed with sat. aq. $NaHCO_3$ solution (1 mL) and brine (1 mL). The organic layer was dried over Na_2SO_4 and the solvent was removed. The crude product was purified by flash column chromatography (SiO_2, CH_2Cl_2/MeOH 30:1) to give tetrapeptide **2.84** (4.00 mg, 3.61 µmol, 60%) as a white amorphous solid.

R_f = 0.40 (SiO_2, CH_2Cl_2/MeOH 10:1); **Optical rotation** $[\alpha]_D^{25}$ = –43.0 (c = 0.10, $CHCl_3$); **FTIR** $\tilde{\nu}$/cm^{-1} 2954, 2926, 2855, 2362, 2336, 1746, 1678, 1631, 1503, 1454, 1369, 1289, 1254, 1141, 1035, 880, 755, 699; **^{1}H NMR** (400 MHz, $CDCl_3$) δ/ppm 10.31 (br s, 1H), 7.25–7.16 (m, 5H), 6.96 (br s, 1H), 6.47 (br s, 1H), 5.51 (s, 1H), 5.12 (d, J = 3.3 Hz, 1H), 4.94 (t, J = 10.2 Hz, 1H), 4.60–4.49 (m, 2H), 4.44–4.27 (m, 5H), 4.09–3.96 (m, 3H), 3.91–3.82 (m, 1H), 3.72 (ddd, J = 10.1, 4.4, 2.4 Hz, 2H), 3.52 (m, J = 10.7 Hz, 1H), 3.37–3.30 (m, 2H), 3.29 (s, 3H), 3.26 (s, 3H), 3.16 (s, 3H), 3.11 (dd, J = 14.1, 3.6 Hz, 1H), 2.95 (dd, J = 14.1, 6.9 Hz, 1H), 2.50–2.38 (m, 1H), 2.36–2.17 (m, 5H), 2.12–2.00 (m, 1H), 1.75–1.57 (m, 5H), 1.50 (s, 18H), 1.32 (s, 3H), 1.29 (s, 3H), 0.91 (d, J = 6.6 Hz, 3H), 0.88 (d, J = 6.6 Hz, 3H); **^{13}C NMR** (101 MHz, $CDCl_3$) δ/ppm 171.2, 170.5, 169.2, 136.7, 135.6 (HMBC), 129.9, 128.1, 126.7, 119.4 (HSQC), 99.6, 99.3, 95.7, 93.9, 82.0 (HMBC), 79.5 (HMBC), 77.2 (HSQC), 69.7, 68.4, 68.3, 68.2, 68.1, 62.2, 60.6, 56.2, 55.3, 52.2, 48.0, 47.8, 38.2, 36.2, 31.2, 29.8, 29.7, 28.9, 28.6, 28.2, 27.9, 24.8, 20.7, 19.8, 17.9, 17.5, 15.8; **HRMS ESI** m/z calc. for $C_{54}H_{84}ClN_6O_{16}$ $[M+H]^+$: 1107.5627, found: 1107.5640.

Synthesis of A828A (2.1)

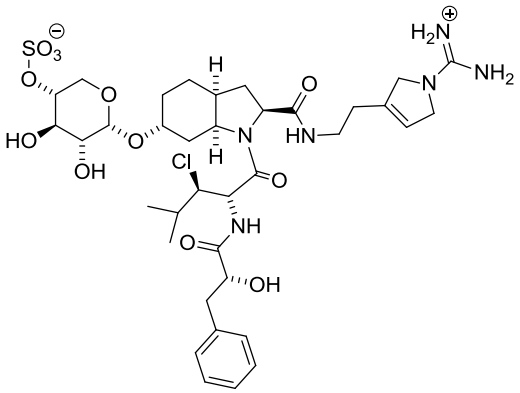

To a solution of tetrapeptide **2.84** (1.80 mg, 1.62 µmol, 1.0 eq.) in pyridine (0.5 mL) was added sulfur trioxide pyridine complex (12.8 mg, 81.0 µmol, 50 eq.). The mixture was heated at 50 °C for 15 h. After cooling to room temperature, the pyridine was removed under reduced pressure. The crude residue was suspended in H_2O (2 mL) and extracted with CH_2Cl_2 (4 x 3 mL). The combined organic layers were dried over Na_2SO_4 and the solvent was removed under reduced pressure to obtain sulfonated tetrapeptide **2.85** as an amorphous white solid, which was used for the next step without further purification. The crude sulfonated tetrapeptide **2.85** was dissolved in CH_2Cl_2 (1.5 mL) and TFA (0.15 mL) was added. After stirring for 5 h at room temperature, toluene (2 mL) was added and all volatiles were removed under reduced pressure. The crude product was purified by reversed phase HPLC (MeCN/H_2O + 0.1% formic acid) to obtain aeruginosin 828A (**2.1**) (996 µg, 1.16 µmol, 72%) as a white amorphous solid.

Optical rotation $[\alpha]_D^{25}$ **=** +23.9 (*c* = 0.023, MeOH); **^{1}H NMR** (600 MHz, DMSO-d_6) δ/ppm 8.51–8.41 (br s, 2H), 7.98 (t, *J* = 5.8 Hz, 1H), 7.67 (d, *J* = 9.6 Hz, 1H), 7.29–7.21 (m, 4H), 7.21–7.15 (m, 1H), 5.99–5.93 (br s, 1H), 5.62 (s, 1H), 4.95 (m, 1H), 4.94 (d, *J* = 3.8 Hz, 2H), 4.92 (*pseudo*-t, *J* = 10.0 Hz, 1H), 4.40 (d, *J* = 7.3 Hz, 1H), 4.32 (dt, *J* = 12.1, 6.3 Hz, 1H), 4.21–4.14 (m, 2H), 4.11–4.04 (m, 4H), 3.99 (dd, *J* = 10.7, 1.8 Hz, 1H), 3.93 (ddd, *J* = 10.8, 8.9, 5.9 Hz, 1H), 3.83 (s, 1H), 3.67 (dd, *J* = 10.8, 5.8 Hz, 1H), 3.58 (*pseudo*-td, *J* = 9.1, 2.4 Hz, 1H), 3.36 (*pseudo*-t, *J* = 11.1 Hz, 1H), 3.28 (m, 1H), 3.29–3.22 (m, 1H), 3.21–3.12 (m, 1H), 2.96 (dd, *J* = 13.9, 3.8 Hz, 1H), 2.82–2.77 (m, 1H), 2.29–2.22 (m, 2H), 2.19–2.10 (m, 1H), 2.01 (dt, *J* = 12.3, 7.3 Hz, 1H), 1.80 (td, *J* = 12.7, 9.8 Hz, 1H), 1.70 (dsept, *J* = 6.3, 1.5 Hz, 1H), 1.62–1.44 (m, 3H), 0.87 (d, *J* = 6.5 Hz, 3H), 0.86 (d, *J* = 6.6 Hz, 2H); **^{13}C NMR** (151 MHz, DMSO-d_6, obtained from 2D NMR spectra) δ/ppm 172.3, 171.1, 167.3, 154.9, 137.8, 135.9, 129.5, 127.7, 125.8, 119.0, 95.0, 74.7, 71.8, 71.4, 68.6, 68.4, 59.5, 59.3, 55.0, 54.1, 53.6, 51.0, 39.8, 36.3, 35.6, 30.6, 28.4, 28.2, 27.4, 24.5, 20.6, 19.1, 15.3; **HRMS ESI** m/z calc. for $C_{36}H_{53}ClN_6O_{12}SNa$ $[M+Na]^+$: 851.3023, found: 851.3017.

Synthesis of A748A (2.12)

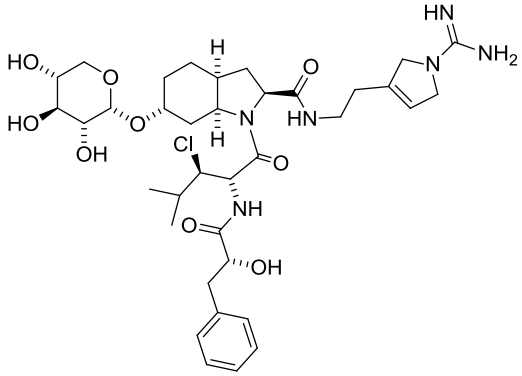

Tetrapeptide **2.84** (2.10 mg, 1.90 μmol, 1.0 eq.) was dissolved in CH_2Cl_2 (2.0 mL) before TFA (0.2 mL) was added. The solution was stirred for 7 h at room temperature. Toluene (2 mL) was added and all volatiles were removed under reduced pressure. The obtained crude product was purified by reversed phase HPLC (MeCN/H_2O + 0.1% formic acid) to obtain aeruginosin 748A (**2.12**) (1.00 mg, 1.33 μmol, 70%) as a white amorphous solid.

Optical rotation $[\alpha]_D^{25}$ **=** +61.0 (*c* = 0.050, MeOH); **^{1}H NMR** (600 MHz, DMSO-d_6) δ/ppm 7.98 (t, *J* = 5.7 Hz, 1H), 7.71–7.57 (br s, 2H), 7.66 (d, *J* = 9.7 Hz, 1H), 7.28–7.21 (m, 4H), 7.20–7.16 (m, 1H), 5.91 (s, 1H), 5.62 (d, *J* = 1.5 Hz, 1H), 4.96 (d, *J* = 3.8 Hz, 1H), 4.93 (*pseudo*-t, *J* = 10.2 Hz, 1H), 4.33 (dt, *J* = 12.1, 6.3 Hz, 1H), 4.20–4.16 (m, 2H), 4.12–4.05 (m, 4H), 4.00 (dd, *J* = 10.7, 1.9 Hz, 1H), 3.84 (s, 1H), 3.43 (*pseudo*-t, *J* = 8.6 Hz, 1H), 3.43–3.37 (m, 1H), 3.35–3.28 (m, 2H), 3.28–3.21 (m, 2H), 3.20–3.13 (m, 1H), 2.96 (dd, *J* = 13.9, 3.8 Hz, 1H), 2.79 (dd, *J* = 13.9, 7.4 Hz, 1H), 2.31–2.20 (m, 4H), 2.13 (ddt, *J* = 13.0, 9.4, 5.2 Hz, 1H), 2.01 (dt, *J* = 12.0, 7.1 Hz, 1H), 1.81 (td, *J* = 12.8, 9.9 Hz, 1H), 1.71 (dsept, *J* = 6.6, 1.9 Hz, 1H), 1.59 (*pseudo*-t, *J* = 12.9 Hz, 1H), 1.55–1.45 (m, 3H), 0.87 (d, *J* = 6.1 Hz, 3H), 0.86 (d, *J* = 6.1 Hz, 3H); **^{13}C NMR** (151 MHz, DMSO-d_6, obtained from 2D NMR spectra) δ/ppm 172.4, 171.1, 167.2, 137.8, 136.1, 129.4, 127.6, 125.8, 118.9, 95.2, 73.3, 71.8, 71.4, 69.8, 68.6, 68.2, 61.7, 59.5, 54.9, 54.0, 53.7, 50.9, 39.7, 36.3, 35.6, 30.5, 28.4, 28.1, 27.3, 24.5, 20.5, 19.1, 15.2; **HRMS ESI** *m*/*z* calc. for $C_{36}H_{54}ClN_6O_9$ $[M+H]^+$: 749.3635, found: 749.3633.

Methyl (2*S*,3a*S*,6*R*,7a*S*)-6-(((2*R*,3*R*,4a*R*,5*R*,8*R*,8a*S*)-8-(benzoyloxy)-2,3-dimethoxy-2,3-dimethylhexahydro-5*H*-pyrano[3,4-*b*][1,4]dioxin-5-yl)oxy)-1-(((*R*)-2-(methoxymethoxy)-3-phenylpropanoyl)-D-leucyl)octahydro-1*H*-indole-2-carboxylate (2.86)

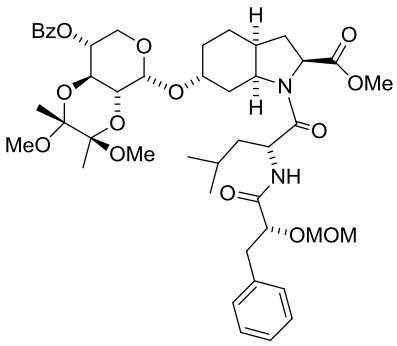

Amine **2.72** (20.0 mg, 36.4 mmol, 1.0 eq.), Pla-Leu-OH dipeptide **2.53** (17.7 mg, 54.6 μmol, 1.5 eq.), NMM (8.0 μL, 72.8 μmol, 2.0 eq.) and DMTMM (15.1 mg, 54.6 μmol, 1.5 eq.) were dissolved in CH_2Cl_2 (0.8 mL) at 0 °C. The mixture was stirred for 30 min at 0 °C and further for 3 h at room temperature. The solvent was removed under reduced pressure and the crude product was purified by flash column chromatography (SiO_2, pentane/EtOAc 1:1) to obtain a 4:1 rotameric mixture of tripeptide **2.86** (18.1 mg, 21.0 μmol, 58%) as a white solid.

Mp = 182.7–183.4 °C; $\mathbf{R}_f$ = 0.24 (SiO_2, pentane/EtOAc 1:1); **Optical rotation** $[\alpha]_D^{25}$ **=** –65.1 (*c* = 0.31, $CHCl_3$); **FTIR** $\tilde{\nu}$/cm^{-1} 3411, 2953, 1726, 1643, 1513, 1450, 1368, 1270, 1140, 1111, 1035, 917, 731; **^{1}H NMR** (400 MHz, $CDCl_3$, major rotamer) δ/ppm 8.05–8.01 (m, 2H), 7.59–7.42 (m, 1H), 7.47–7.40 (m, 2H), 7.25–7.18 (m, 5H), 6.97 (d, *J* = 9.4 Hz, 1H), 5.21–5.09 (m, 2H), 4.82 (dt, *J* = 12.9, 6.5 Hz, 1H), 4.54–4.46 (m, 2H), 4.36–4.27 (m, 3H), 4.18 (dt, *J* = 11.8, 6.1 Hz, 1H), 4.04 (br s, 1H), 3.98 (dd, *J* = 10.7, 5.8 Hz, 1H), 3.90 (dd, *J* = 10.2, 3.5 Hz, 1H), 3.67 (s, 3H), 3.55 (t, *J* = 10.6 Hz, 1H), 3.33 (s, 3H), 3.31 (s, 3H), 3.16 (dd, *J* = 14.0, 3.4 Hz, 1H), 3.11 (s, 3H), 2.92 (dd, *J* = 14.0, 7.9 Hz, 1H), 2.55–2.44 (m, 2H), 2.37–2.13 (m, 3H), 2.05–1.90 (m, 1H), 1.79–1.54 (m, 4H), 1.43–1.38 (m, 2H), 1.30 (s, 3H), 1.27 (s, 3H), 0.92 (d, *J* = 5.9 Hz, 3H), 0.86 (d, *J* = 5.9 Hz, 3H); **^{13}C NMR** (101 MHz, $CDCl_3$, major rotamer) δ/ppm 172.8, 170.6, 170.4, 165.8, 137.4, 133.2, 130.1, 129.9, 129.8, 128.5, 128.3, 126.7, 99.9, 99.6, 95.9, 94.3, 77.7, 70.1, 69.7, 68.5, 66.7, 59.7, 59.4, 56.1, 54.6, 52.3, 48.2, 48.1, 47.9, 42.6, 39.1, 37.3, 30.4, 29.6, 24.9, 24.8, 23.6, 22.9, 20.0, 18.0, 17.8; **HRMS ESI** *m*/*z* calc. for $C_{45}H_{62}N_2O_{14}Na$ $[M+Na]^+$: 877.4093, found: 877.4102.

(2*S*,3a*S*,6*R*,7a*S*)-6-(((2*R*,3*R*,4a*R*,5*R*,8*R*,8a*S*)-8-Hydroxy-2,3-dimethoxy-2,3-dimethyl-hexahydro-5*H*-pyrano[3,4-*b*][1,4]dioxin-5-yl)oxy)-1-(((*R*)-2-(methoxymethoxy)-3-phenylpropanoyl)-D-leucyl)octahydro-1*H*-indole-2-carboxylic acid (2.87)

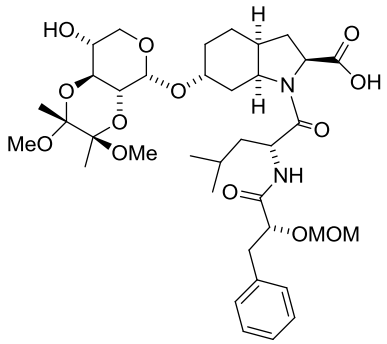

Tripeptide **2.86** (14.0 mg, 16.4 μmol, 1.0 eq.) was dissolved in THF/H_2O (5:3, 4 mL) before LiOH monohydrate (17.6 mg, 0.420 mmol, 26 eq.) was added. The reaction was stirred for 12 h at room temperature, H_2O (2.5 mL) was added and the THF was removed under reduced pressure. Aq. citric acid solution (5% *w*/*w*, 6 mL) was added and extracted with CH_2Cl_2 (3 x 10 mL). The combined organic layers were dried over Na_2SO_4 and the solvent was removed under reduced pressure. The crude residue was purified by flash column chromatography (SiO_2, CH_2Cl_2/MeOH 15:1 changing to 5:1) to obtain a 10:1 rotameric mixture of acid **2.87** (11.5 mg, 15.6 μmol, 95%) as a colorless solid.

Mp = 132.5–135.1 °C; **R_f** = 0.28 (SiO_2, CH_2Cl_2/MeOH 15:1); **Optical rotation** $[\alpha]_D^{25}$ **=** –28.3 (*c* = 0.17, $CHCl_3$); **FTIR** $\tilde{\nu}$/cm^{-1} 3413, 2956, 2929, 1737, 1633, 1520, 1260, 1138, 1094, 1032, 915, 802, 732; **^{1}H NMR** (400 MHz, $CDCl_3$, major rotamer) δ/ppm 7.25–7.18 (m, 5H), 6.97 (d, *J* = 9.0 Hz, 1H), 5.04 (d, *J* = 3.5 Hz, 1H), 4.90–4.82 (m, 1H), 4.55 (d, *J* = 6.7 Hz, 1H), 4.52–4.46 (m, 2H), 4.30 (dd, *J* = 7.3, 3.6 Hz, 1H), 4.24 (dt, *J* = 11.4, 5.6 Hz, 1H), 4.03 (br s, 1H), 4.00–3.93 (m, 1H), 3.86 (td, *J* = 9.8, 9.4, 5.6 Hz, 1H), 3.74–3.69 (m, 2H), 3.53 (t, *J* = 10.7 Hz, 1H), 3.29 (s, 3H), 3.28 (s, 3H), 3.16 (s, 3H), 3.13–3.10 (m, 1H), 2.92 (dd, *J* = 14.0, 7.4 Hz, 1H), 2.56–2.46 (m, 1H), 2.43–2.35 (m, 2H), 2.27–2.08 (m, 3H), 1.80–1.57 (m, 4H), 1.45–1.34 (m, 3H), 1.32 (s, 3H), 1.28 (s, 3H), 0.89 (d, *J* = 6.0 Hz, 3H), 0.86 (d, *J* = 6.2 Hz, 3H); **^{13}C NMR** (101 MHz, $CDCl_3$, major rotamer) δ/ppm 176.1, 173.7, 170.8, 137.1, 129.9, 128.3, 99.9, 99.5, 96.1, 95.0, 77.8, 70.0, 69.9, 68.3, 68.3, 62.4, 59.8, 56.2, 56.0, 48.3, 48.1, 48.0, 42.1, 38.9, 36.0, 29.9, 28.2, 24.8, 24.6, 23.5, 22.8, 19.9, 18.0, 17.8; **HRMS ESI** *m*/*z* calc. for $C_{37}H_{56}N_2O_{13}Na$ $[M+Na]^+$: 759.3675, found: 759.3688.

***tert*-Butyl ((*Z*)-((*tert*-butoxycarbonyl)imino)(3-(2-((2*S*,3a*S*,6*R*,7a*S*)-6-(((2*R*,3*R*,4a*R*,5*R*,8*R*,8a*S*)-8-hydroxy-2,3-dimethoxy-2,3-dimethylhexahydro-5*H*-pyrano[3,4-*b*][1,4]dioxin-5-yl)oxy)-1-(((*R*)-2-(methoxymethoxy)-3-phenyl-propanoyl)-D-leucyl)octahydro-1*H*-indole-2-carboxamido)ethyl)-2,5-dihydro-1*H*-pyrrol-1-yl)methyl)carbamate (2.88)**

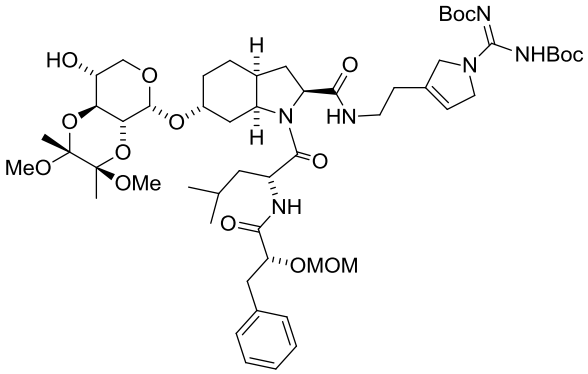

Adc subunit **2.63** (4.00 mg, 5.43 µmol, 1.0 eq.) and acid **2.87** (3.85 mg, 10.9 µmol, 2.0 eq.) were dissolved in CH_2Cl_2 (0.6 mL). At 0 °C, 2,6-lutidine (2.0 µL, 17.2 µmol, 3.2 eq.) and PyBOP (4.24 mg, 8.15 µmol, 1.5 eq.) were added and the mixture was stirred for 20 min at 0 °C and further 4.5 h at room temperature. The mixture was diluted with CH_2Cl_2 (2 mL) and washed with sat. aq. $NaHCO_3$ solution (2 mL) and brine (2 mL). The organic layer was dried over Na_2SO_4 and the solvent was removed under reduced pressure. The crude residue was purified by flash column chromatography (SiO_2, CH_2Cl_2/MeOH 30:1 changing to 20:1) to obtain a 7:1 rotameric mixture of tetrapeptide **2.88** (3.70 mg, 3.45 µmol, 64%) as an amorphous colorless solid.

R_f = 0.15 (SiO_2, CH_2Cl_2/MeOH 20:1); **Optical rotation** $[\alpha]_D^{25}$ **=** –92.7 (*c* = 0.19, $CHCl_3$); **FTIR** $\tilde{\nu}$/cm^{-1} 3348, 2957, 2929, 1747, 1640, 1453, 1369, 1288, 1140, 1034, 938, 846, 801; **^{1}H NMR** (400 MHz, $CDCl_3$, major rotamer) δ/ppm 10.21 (br s, 1H), 7.25–7.19 (m, 5H), 6.95 (t, *J* = 5.7 Hz, 1H), 6.85 (d, *J* = 7.2 Hz, 1H), 5.50 (br s, 1H), 4.94 (d, *J* = 3.5 Hz, 1H), 4.59 (d, *J* = 6.7 Hz, 1H), 4.55–4.50 (m, 2H), 4.42 (t, *J* = 8.7 Hz, 1H), 4.36 (br s, 1H), 4.31 (br s, 1H), 4.25 (dd, *J* = 7.6, 3.7 Hz, 1H), 4.13 (dt, *J* = 11.9, 5.9 Hz, 1H), 4.02 (br s, 1H), 3.96 (t, *J* = 9.6 Hz, 1H), 3.85 (td, *J* = 9.7, 9.2, 5.5 Hz, 1H), 3.75–3.64 (m, 2H), 3.55 (t, *J* = 10.7 Hz, 1H), 3.41 (td, *J* = 6.9, 3.4 Hz, 1H), 3.38–3.31 (m, 2H), 3.28 (s, 3H), 3.26 (s, 3H), 3.15 (s, 3H), 3.15–3.10 (m, 1H), 2.92 (dd, *J* = 14.0, 7.6 Hz, 1H), 2.49–2.40 (m, 1H), 2.38–2.31 (m, 1H), 2.28–2.24 (m, 2H), 2.22–2.10 (m, 3H), 2.02–1.93 (m, 1H), 1.77–1.72 (m, 1H), 1.65–1.55 (m, 4H), 1.49 (s, 18H), 1.45–1.36 (m, 3H), 1.32 (s, 3H), 1.28 (s, 3H), 0.90 (t, *J* = 5.4 Hz, 6H); **^{13}C NMR** (101 MHz, $CDCl_3$, major rotamer) δ/ppm 171.9, 171.7, 171.4, 137.1, 136.0, 129.9, 128.3, 126.8, 119.2, 99.9, 99.5, 96.1, 95.8, 83.2, 80.5, 77.9, 71.5, 70.0, 68.4, 68.3, 62.5, 60.2, 59.5, 57.5, 56.2, 55.8, 55.4, 49.6, 48.1, 48.0, 41.3, 39.1, 37.6, 36.8, 30.2, 29.9, 28.3, 24.9, 24.7, 23.6, 22.7, 20.1, 18.1, 17.8; **HRMS ESI** *m*/*z* calc. for $C_{54}H_{85}N_6O_{16}$ $[M+H]^+$: 1073.6017, found: 1073.6032.

Synthesis of A126A (2.11)

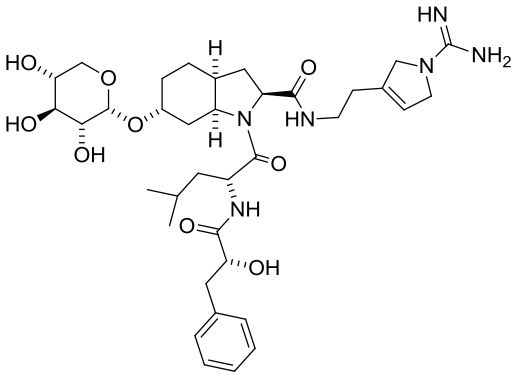

Tetrapeptide **2.88** (2.68 mg, 2.50 μmol, 1.0 eq.) was dissolved in CH_2Cl_2 (2 mL) before TFA (0.2 mL) was added. The solution was stirred for 7 h at room temperature. Toluene (2 mL) was added and all volatiles were removed under reduced pressure. The obtained crude product was purified by reversed phase HPLC (MeCN/H_2O + 0.1% formic acid) to obtain a 3.5:1 rotameric mixture of aeruginoside 126A (**2.11**) (1.30 mg, 1.82 μmol, 73%) as a white amorphous solid.

Optical rotation $[\alpha]_D^{25}$ **=** +39.1 (*c* = 0.070, MeOH); **^{1}H NMR** (600 MHz, DMSO-d_6, major rotamer) δ/ppm 7.85 (t, *J* = 5.7 Hz, 1H), 7.57 (d, *J* = 8.4 Hz, 1H), 7.29–7.14 (m, 5H), 5.62 (s, 1H), 4.83 (d, *J* = 3.7 Hz, 1H), 4.60–4.53 (m, 1H), 4.20–4.02 (m, 4H), 3.43–3.38 (m, 2H), 3.37–3.32 (m, 1H), 3.30–3.25 (m, 1H), 3.23 (dd, *J* = 9.6, 3.4 Hz, 1H), 3.22–3.16 (m, 1H), 2.99 (dd, *J* = 13.8, 3.7 Hz, 1H), 2.74 (dd, *J* = 13.8, 7.7 Hz, 1H), 2.33–2.23 (m, 4H), 2.15–2.07 (m, 1H), 2.03 (dt, *J* = 12.2, 7.6 Hz, 1H), 1.84–1.75 (m, 1H), 1.66–1.54 (m, 2H), 1.54–1.44 (m, 1H), 1.44–1.34 (m, 2H), 1.33–1.19 (m, 1H), 0.87 (d, *J* = 6.3 Hz, 3H), 0.82 (d, *J* = 6.2 Hz, 3H); **^{13}C NMR** (151 MHz, DMSO-d_6, major rotamer, obtained from 2D NMR spectra) δ/ppm 172.2, 170.8, 137.7, 129.3, 127.6, 125.7, 119.0, 96.4, 73.2, 71.7, 71.5, 70.0, 69.8, 62.0, 59.7, 54.9, 53.7, 53.7, 47.8, 41.2, 39.9, 36.3, 35.8, 30.4, 29.1, 28.1, 24.2 (2C), 23.3, 21.6, 19.3; **HRMS ESI** *m/z* calc. for $C_{36}H_{55}N_6O_9$ $[M+H]^+$: 715.4025, found: 715.4026.

Synthesis of A794A (2.13)

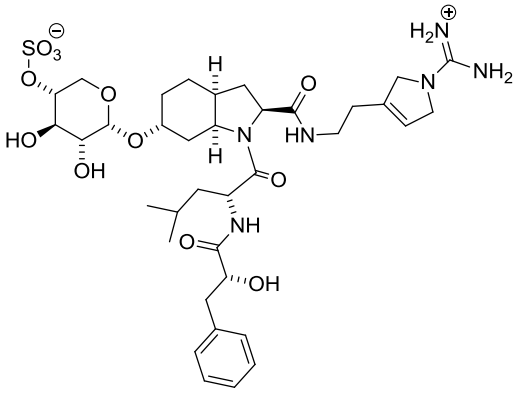

Sulfur trioxide pyridine complex (20.1 mg, 126 µmol, 50 eq.) was added to a solution of tetrapeptide **2.88** (2.70 mg, 2.52 µmol, 1.0 eq) in pyridine (0.6 mL). The mixture was heated at 50 °C for 15 h. After cooling to room temperature, the pyridine was removed under reduced pressure. The crude residue was suspended in H_2O (2 mL) and extracted with CH_2Cl_2 (4 x 3 mL). The combined organic layers were dried over Na_2SO_4 and the solvent was removed under reduced pressure to obtain sulfonated tetrapeptide **2.89** as an amorphous white solid, which was used for the next step without further purification. The crude sulfonated tetrapeptide **2.89** was dissolved in CH_2Cl_2 (2 mL) and TFA (0.2 mL) was added. After stirring for 7 h at room temperature, toluene (2 mL) was added and all volatiles were removed under reduced pressure. The crude product was purified by reversed phase HPLC (MeCN/H_2O + 0.1% formic acid) to obtain a 4:1 rotameric mixture of aeruginosin 794A (**2.13**) (1.50 mg, 1.89 µmol, 75%) as a white amorphous solid.

Optical rotation $[\alpha]_D^{25}$ **=** +17.6 (*c* = 0.042, MeOH); **^{1}H NMR** (600 MHz, DMSO-d_6, major rotamer) δ/ppm 7.81 (t, *J* = 5.8 Hz, 1H), 7.69–7.53 (br s, 2H), 7.53 (d, *J* = 8.2 Hz, 1H), 7.29–7.15 (m, 5H), 5.61 (s, 1H), 5.41, (s, 1H), 4.81 (d, *J* = 3.7 Hz, 1H), 4.54 (td, *J* = 8.8, 4.4 Hz, 1H), 4.19–4.02 (m, 7H), 3.93 (ddd, *J* = 10.6, 8.9, 5.8 Hz, 1H), 3.84 (br s, 1H), 3.68 (dd, *J* = 10.8, 5.8 Hz, 1H), 3.57 (*pseudo*-t, *J* = 9.2 Hz, 1H), 3.40 (*pseudo*-t, *J* = 10.8 Hz, 1H), 3.27 (dd, *J* = 9.5, 3.6 Hz, 1H), 3.21–3.17 (m, 1H), 2.99 (dd, *J* = 13.7, 3.5 Hz, 1H), 2.73 (dd, *J* = 13.7, 7.8 Hz, 1H), 2.34–2.19 (m, 3H), 2.13–2.07 (m, 1H), 2.02 (ddd, *J* = 12.4, 7.4, 7.4 Hz, 1H), 1.82–1.71 (m, 1H), 1.63–1.56 (m, 1H), 1.41–1.35 (m, 1H), 1.31–1.20 (m, 2H), 0.86 (d, *J* = 6.0 Hz, 3H), 0.82 (d, *J* = 6.3 Hz, 3H); **^{13}C NMR** (151 MHz, DMSO-d_6, major rotamer, obtained from 2D NMR spectra) δ/ppm 172.9, 172.6, 171.2, 138.1, 136.1, 129.3, 127.6, 125.8, 119.0, 96.2, 74.7, 71.8, 71.6, 71.4, 70.2, 59.6, 59.5, 54.9, 53.7, 53.0, 47.9, 41.2, 40.0, 36.3, 35.8, 30.4, 29.1, 28.2, 24.2, 23.7, 23.1, 21.6, 19.2; **HRMS ESI** *m/z* calc. for $C_{36}H_{54}N_6O_{12}SNa$ $[M+Na]^+$: 817.3413, found: 817.3408.

2.1.7. Synthesis of Aeruginosin 616A

Methyl (2*S*,3a*S*,6*R*,7a*S*)-6-acetoxyoctahydro-1*H*-indole-2-carboxylate (2.92)

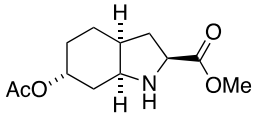

L-Choi-Cbz derivative **2.37** (151 mg, 0.401 mmol, 1.0 eq.) and Pd/C (31.3 mg, 29.4 μmol, 0.070 eq.) were suspended in MeOH (7.5 mL). The mixture was stirred for 3.5 h at room temperature under an atmosphere of H_2. The catalyst was filtered off over Celite® and the crude product was purified by flash column chromatography (SiO_2, CH_2Cl_2/MeOH 20:1) to obtain L-Choi-H derivative **2.92** (73.9 mg, 0.306 mmol, 76%) as a colorless oil.

R_f = 0.29 (SiO_2, CH_2Cl_2/MeOH 20:1); **Optical rotation** $[\alpha]_D^{25}$ = –39.9 (*c* = 0.49, $CHCl_3$); **FTIR** $\tilde{\nu}$/cm^{-1} 3350, 2945, 2864, 1731, 1437, 1365, 1243, 1031, 921, 839, 627; **^{1}H NMR** (400 MHz, $CDCl_3$) δ/ppm 4.99 (tt, *J* = 8.5, 4.0 Hz, 1H), 3.80 (dd, *J* = 10.3, 5.7 Hz, 1H), 3.73 (s, 3H), 3.33 (q, *J* = 5.0 Hz, 1H), 2.25–2.17 (m, 1H), 2.11 (d, *J* = 6.5 Hz, 1H), 2.05–2.03 (m, 1H), 2.02 (s, 3H), 2.01–1.99 (m, 1H), 1.86–1.79 (m, 1H), 1.76–1.68 (m, 2H), 1.66–1.60 (m, 1H), 1.44–1.35 (m, 2H); **^{13}C NMR** (101 MHz, $CDCl_3$) δ/ppm 175.8, 170.6, 69.7, 58.5, 58.1, 52.3, 37.3, 35.3, 32.9, 29.3, 25.0, 21.5; **HRMS ESI** *m*/*z* calc. for $C_{12}H_{20}NO_4$ $[M+H]^+$: 242.1387, found: 242.1389.

Methyl (2*S*,3a*S*,6*R*,7a*S*)-6-acetoxy-1-((2*S*,3*R*)-3-chloro-2-((*R*)-2-(methoxymethoxy)-3-phenylpropanamido)-4-methylpentanoyl)octahydro-1*H*-indole-2-carboxylate (2.93)

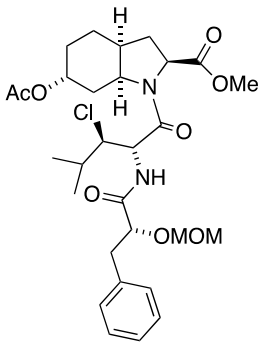

L-Choi derivative **2.92** (13.0 mg, 53.9 μmol, 1.0 eq.) and Pla-Cleu-OH dipeptide **2.47** (25.1 mg, 70.1 μmol, 1.3 eq.) were dissolved in CH_2Cl_2 (1 mL) and cooled to 0 °C. DMTMM (19.4 mg, 70.1 μmol, 1.3 eq.) and NMM (11.9 μL, 0.108 mmol, 2.0 eq.) were added to the solution. The reaction mixture was stirred for 20 min at 0 °C and further for 2 h at room temperature. The solvent was removed under reduced pressure and the crude residue was directly purified by flash column chromatography (SiO_2, pentane/EtOAc 1:1) to give tripeptide **2.93** (26.0 mg, 45.0 μmol, 83%) as a colorless oil.

R_f = 0.30 (SiO_2, pentane/EtOAc 1:1); **Optical rotation** $[\alpha]_D^{25}$ **=** +23.4 (*c* = 0.50, $CHCl_3$); **FTIR** $\tilde{\nu}$/cm^{-1} 3405, 3342, 2956, 2931, 2362, 1740, 1685, 1650, 1579, 1505, 1440, 1365, 1311, 1251, 1198, 1177, 1152, 1100, 1019, 919, 820, 751, 702; **^{1}H NMR** (400 MHz, $CDCl_3$) δ/ppm 7.29–7.19 (m, 5H), 7.04 (d, *J* = 9.9 Hz, 1H), 5.08 (s, 1H), 4.98 (t, *J* = 10.4 Hz, 1H), 4.57–4.53 (m, 1H), 4.46–4.37 (m, 1H), 4.39–4.33 (m, 2H), 3.83 (dd, *J* = 10.8, 1.9 Hz, 1H), 3.66 (s, 3H), 3.19 (s, 3H), 3.14 (dd, *J* = 14.1, 3.7 Hz, 1H), 2.99 (dd, *J* = 14.1, 6.6 Hz, 1H), 2.51–2.41 (m, 1H), 2.36–2.29 (m, 1H), 2.27–2.15 (m, 1H), 2.08 (s, 3H), 2.05–1.90 (m, 2H), 1.84 (d, *J* = 14.9 Hz, 1H), 1.71 (ddd, *J* = 14.5, 11.7, 2.5 Hz, 1H), 1.66–1.56 (m, 2H), 1.56–1.44 (m, 2H), 0.94 (d, *J* = 6.5 Hz, 3H), 0.88 (d, *J* = 6.7 Hz, 3H); **^{13}C NMR** (101 MHz, $CDCl_3$) δ/ppm 172.4, 170.8, 170.2, 168.5, 136.8, 130.1, 128.3, 126.8, 95.7, 77.1, 69.3, 68.6, 58.8, 56.3, 54.9, 52.3, 51.7, 38.3, 36.5, 31.2, 30.7, 28.2, 23.2, 21.3, 20.9, 19.8, 15.0; **HRMS ESI** *m*/*z* calc. for $C_{29}H_{41}ClN_2O_8Na$ $[M+Na]^+$: 603.2444, found: 603.2451.

(2*S*,3a*S*,6*R*,7a*S*)-1-((2*S*,3*R*)-3-Chloro-2-((*R*)-2-(methoxymethoxy)-3-phenylpropanamido)-4-methylpentanoyl)-6-hydroxyoctahydro-1*H*-indole-2-carboxylic acid (2.94)

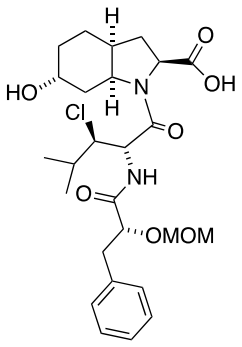

Tripeptide **2.93** (5.81 mg, 10.0 µmol, 1.0 eq.) was dissolved in THF/H_2O (5:3, 2 mL). To this solution was added LiOH monohydrate (8.40 mg, 0.200 mmol, 20 eq.) and the reaction mixture was stirred for 12 h at room temperature. The reaction mixture was acidified with aq. citric acid solution (5% *w*/*w*, 3 mL) to a pH of around 3. The THF was removed under reduced pressure and the residue was extracted with CH_2Cl_2 (3 x 5 mL). The combined organic layers were washed with H_2O (5 mL), dried over $MgSO_4$ and the solvent removed under reduced pressure. The crude residue was purified by flash column chromatography (SiO_2, CH_2Cl_2/MeOH 10:1) to give tripeptide **2.94** (4.00 mg, 8.00 µmol, 76%) as a colorless solid.

FTIR $\tilde{\nu}$/cm^{-1} 3395, 2948, 2924, 2853, 1736, 1634, 1517, 1455, 1368, 1333, 1259, 1187, 1149, 1098, 1079, 1033, 1014, 909, 874, 801, 730, 700, 648, 615, 492; **^{1}H NMR** (400 MHz, $CDCl_3$) δ/ppm 7.30–7.20 (m, 5H), 7.11 (d, *J* = 10.1 Hz, 1H), 5.09 (t, *J* = 10.5 Hz, 1H), 4.59 (q, *J* = 6.8 Hz, 2H), 4.55–4.49 (m, 2H), 4.39 (dd, *J* = 6.1, 3.9 Hz, 1H), 4.15 (s, 1H), 3.92 (dd, *J* = 10.8, 1.9 Hz, 1H), 3.22 (s, 3H), 3.14 (dd, *J* = 14.2, 3.8 Hz, 1H), 3.01 (dd, *J* = 14.2, 6.1 Hz, 1H), 2.47–2.32 (m, 2H), 2.25–2.05 (m, 2H), 1.71–1.53 (m, 3H), 1.50–1.43 (m, 1H), 1.45–1.33 (m, 1H), 0.89 (d, *J* = 3.9 Hz, 3H), 0.87 (d, *J* = 4.0 Hz, 3H); **^{13}C NMR** (101 MHz, $CDCl_3$)

δ/ppm 172.6, 171.0, 170.8, 136.4, 130.1, 128.4, 127.0, 95.9, 67.8, 65.7, 59.4, 56.3, 56.1, 51.9, 38.1, 35.8, 34.1, 29.0, 28.0, 25.7, 20.8, 19.1, 15.3; **HRMS ESI** *m/z* calc. for $C_{26}H_{38}ClN_2O_7$ $[M+H]^+$: 525.2362, found: 525.2365.

***tert*-Butyl ((*E*)-((*tert*-butoxycarbonyl)imino)(3-(2-((2*S*,3a*S*,6*R*,7a*S*)-1-((2*S*,3*R*)-3-chloro-2-((*R*)-2-(methoxymethoxy)-3-phenylpropanamido)-4-methylpentanoyl)-6-hydroxyocta hydro-1*H*-indole-2-carboxamido)ethyl)-2,5-dihydro-1*H*-pyrrol-1-yl)methyl)carbamate (2.95)**

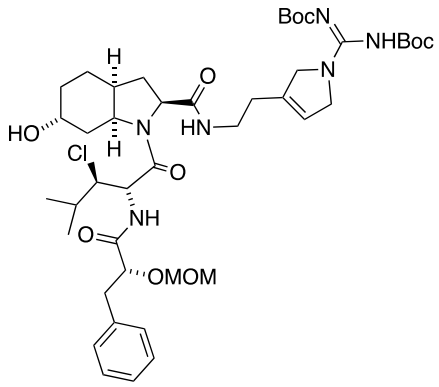

To a solution of tripeptide **2.94** (2.99 mg, 57.0 µmol, 1.0 eq.) and Adc subunit **2.63** (2.63 mg, 74.0 µmol, 1.3 eq.) in CH_2Cl_2 (0.4 mL) were added PyBOP (3.86 mg, 74.0 µmol, 1.3 eq.) and 2,6-lutidine (2.0 µL, 17.1 µmol, 3.0 eq.) at 0 °C. The reaction mixture was stirred for 20 min at 0 °C and further for 5 h at room temperature. CH_2Cl_2 (3 mL) was added and the organic layer was washed with sat. aq. $NaHCO_3$ solution (1 mL) and brine (1 mL). The organic layer was dried over Na_2SO_4 and the solvent was removed under reduced pressure. The crude residue was purified by flash column chromatography (SiO_2, CH_2Cl_2/MeOH 30:1) to give tetrapeptide **2.95** (2.50 mg, 3.00 µmol, 51%) as a white amorphous solid.

FTIR $\tilde{\nu}$/cm^{-1} 3334, 3034, 2971, 2931, 1746, 1673, 1633, 1512, 1454, 1392, 1369, 1285, 1251, 1235, 1149, 1051, 1037, 1016, 920, 841, 732, 701; **^{1}H NMR** (400 MHz, $CDCl_3$) δ/ppm 10.35 (br s, 1H), 7.30–7.20 (m, 5H), 7.09 (br s, 1H), 6.70 (br s, 1H), 5.51 (s, 1H), 4.99 (t, J = 10.2 Hz, 1H), 4.59–4.54 (m, 2H), 4.51–4.38 (m, 5H), 4.37–4.32 (m, 1H), 4.16 (s, 1H), 3.94 (d, J = 10.7 Hz, 1H), 3.33 (dd, J = 12.2, 6.0 Hz, 1H), 3.21 (s, 3H), 3.13 (dd, J = 14.1, 3.7 Hz, 1H), 2.98 (dd, J = 14.1, 6.5 Hz, 1H), 2.33 (d, J = 26.3 Hz, 3H), 2.19–2.04 (m, 3H), 1.77–1.57 (m, 4H), 1.50 (s, 18H), 0.90 (s, 3H), 0.89 (s, 3H); **HRMS ESI** *m/z* calc. for $C_{43}H_{65}ClN_5O_{11}$ $[M+H]^+$: 861.4523, found: 861.4524.

Due to stability problems related to the partial cleavage of the Boc protection groups in the NMR tube, no ^{13}C NMR spectrum could be measured.

Synthesis of A616A (2.91)

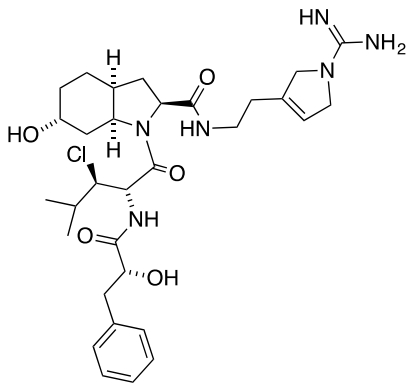

Tetrapeptide **2.95** (2.50 mg, 3.00 µmol, 1.0 eq.) was dissolved in CH_2Cl_2 (2 mL) before TFA (0.2 mL) was added. The solution was stirred for 8 h at room temperature. Toluene (2 mL) was added and all volatiles were removed under reduced pressure. The obtained residue was dissolved in H_2O (2 mL). To this solution K_2CO_3 (0.500 mg, 3.60 mmol, 1.2 eq.) was added and the reaction mixture was stirred for 30 min at room temperature. The H_2O was removed under reduced pressure and the obtained crude product was purified by reversed phase HPLC (MeCN/H_2O + 0.1% formic acid) to obtain aeruginosin 616A (**2.91**) (0.800 mg, 1.30 µmol, 45%) as a white solid.

^{1}H NMR (600 MHz, DMSO-d_6) δ/ppm 8.00 (br s, 1H), 7.95 (t, J = 5.7 Hz, 1H), 7.55 (d, J = 9.4 Hz, 1H), 7.27–.16 (m, 6H), 6.04 (s, 1H), 5.61 (s, 1H), 4.89 (t, J = 10.1 Hz, 1H), 4.53–4.49 (m, 1H), 4.27 (dt, J = 12.3, 6.3 Hz, 1H), 4.19 (s, 1H), 4.17 (dd, J = 10.1, 8.0 Hz, 1H), 4.07 (s, 4H), 3.94 (dd, J = 10.8, 1.8 Hz, 1H), 3.89 (s, 1H), 3.24 (dq, J = 13.0, 6.7 Hz, 1H), 3.17 (td, J = 12.8, 6.4 Hz, 1H), 2.96 (dd, J = 13.9, 3.9 Hz, 1H), 2.82 (dd, J = 13.8, 6.9 Hz, 1H), 2.29–2.16 (m, 3H), 2.07–1.95 (m, 3H), 1.83–1.76 (m, 1H), 1.68–1.59 (m, 2H), 1.48–1.38 (m, 3H), 0.85 (dd, J = 6.7, 2.2 Hz, 7H); **^{13}C NMR** (151 MHz, DMSO-d_6, obtained from 2D NMR spectra) δ/ppm 172.1, 171.0, 167.5, 137.8, 136.1, 129.7, 127.8, 126.1, 119.3, 71.6, 69.0, 63.8, 59.8, 54.7, 55.1, 53.9, 51.0, 40.0, 36.5, 35.9, 33.2, 30.8, 28.4, 27.6, 26.1, 20.6, 18.9, 15.1; **HRMS ESI** m/z calc. for $C_{31}H_{46}ClN_6O_5$ $[M+H]^+$: 617.3213, found: 617.3217.

2.1.8. Alternative Approaches – Synthesis of Aeruginosin 828B

2,2,2-Trichloroethyl sulfurochloridate (2.99)

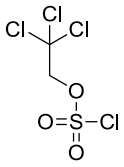

2,2,2-Trichloroethanol (**2.98**) (2.33 mL, 23.9 mmol, 1.0 eq.) and pyridine (1.93 mL, 23.9 mmol, 1.0 eq.) were dissolved in Et_2O (40 mL) and cooled to −78 °C. To this mixture sulfuryl chloride (2.0 mL, 23.9 mmol, 1.0 eq.) was added over a period of 1 h and the mixture stirred for an additional hour at –78 °C. The mixture was allowed to reach room temperature and was stirred for further 3 h. The white precipitate was filtered off and the solvent removed from the filtrate, to give 2,2,2-trichloroethyl sulfurochloridate (**2.99**) (5.06 g, 20.4 mmol, 85%) as a colorless oil.

^{1}H NMR (400 MHz, $CDCl_3$) δ/ppm 4.92 (s, 2H); **^{13}C NMR** (101 MHz, $CDCl_3$) δ/ppm 91.4, 81.3.

Analytical data are in accordance with those reported in the literature.[11]

2,2,2-Trichloroethyl 1*H*-imidazole-1-sulfonate (2.100)

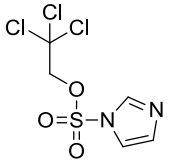

A solution of 2,2,2-trichloroethyl sulfurochloridate (**2.99**) (1.86 g, 7.50 mmol, 1.0 eq.) in THF (1 mL) was added dropwise to a solution of imidazole (1.00 g, 15.0 mmol, 2.0 eq.) in THF (2.5 mL) at 0 °C. The reaction mixture was stirred for 1 h at 0 °C and further for 1 h at room temperature. The obtained precipitate was filtered off and the solvent removed from the filtrate. The obtained crude residue was purified by flash column chromatography (SiO_2, pentane/EtOAc 2:1) to give 2,2,2-trichloroethyl 1*H*-imidazole-1-sulfonate (**2.100**) (1.40 g, 5.01 mmol, 67%) as a colorless solid.

^{1}H NMR (400 MHz, $CDCl_3$) δ/ppm 8.10–7.96 (m, 1H), 7.45–7.37 (m, 1H), 7.24–7.19 (m, 1H), 5.01–4.30 (m, 2H); **^{13}C NMR** (101 MHz, $CDCl_3$) δ/ppm 137.1, 131.8, 118.2, 91.8, 80.3.

Analytical data are in accordance with those reported in the literature.[11]

3-Methyl-1-((2,2,2-trichloroethoxy)sulfonyl)-1*H*-imidazol-3-ium triflate (2.96)

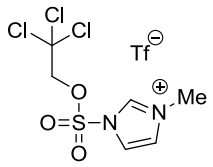

To a solution of 2,2,2-trichloroethyl 1*H*-imidazole-1-sulfonate (**2.100**) (1.06 g, 3.79 mmol, 1.0 eq.) in Et_2O (14 mL) at 0 °C was added dropwise methyl triflate (0.50 mL, 4.29 mmol, 1.1 eq.). The reaction was stirred for 3 h at 0 °C during which time a white precipitate was formed. The precipitate was filtered off and washed with ice cold Et_2O (2 x 10 mL) to give triflate salt **2.96** (1.50 g, 3.38 mmol, 89%) as a colorless solid.

^{1}H NMR (400 MHz, MeOD) δ/ppm 10.12–9.85 (m, 1H), 8.47–8.24 (m, 1H), 8.03–7.74 (m, 1H), 5.43–5.37 (m, 2H), 4.05 (s, 3H); **^{13}C NMR** (101 MHz, MeOD) δ/ppm 141.2, 127.3, 122.3, 93.0, 83.5, 37.8. The triflate ^{13}C signal was not resolved.
Analytical data are in accordance with those reported in the literature.[11]

(4a*R*,5*S*,8*R*,8a*S*)-2,3-Dimethoxy-2,3-dimethyl-5-(phenylthio)hexahydro-5*H*-pyrano[3,4-*b*][1,4]dioxin-8-ol (2.101)

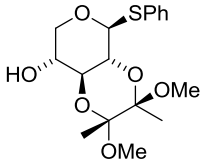

Thioxyloside **2.69** (330 mg, 0.717 mmol, 1.0 eq.) was suspended in MeOH (3 mL) and subsequently dissolved in CH_2Cl_2 (4 mL). NaOMe (79.1 mg, 1.46 mmol, 2.0 eq.) was added and the mixture was stirred for 2 h at room temperature. The solvents were removed under reduced pressure and the obtained residue was dissolved in CH_2Cl_2 (20 mL). The solution was washed with sat. aq. NH_4Cl solution (20 mL), dried over Na_2SO_4 and the solvent was removed under reduced pressure. The crude product was purified by flash column chromatography (SiO_2, pentane/EtOAc 3:1 changing to 2:1) to obtain alcohol **2.101** (212 mg, 0.595 mmol, 83%) as a colorless solid.

Mp = 164.6–165.7 °C; $\mathbf{R}_f$ = 0.26 (SiO_2, pentane/EtOAc 2:1); **Optical rotation** $[\alpha]_D^{25}$ = –161.5 (*c* = 0.79, $CHCl_3$); **FTIR** $\tilde{\nu}$/cm^{-1} 3502, 2924, 2852, 1584, 1454, 1375, 1304, 1219, 1134, 1107, 1068, 1006, 922, 879, 849, 741, 692; **^{1}H NMR** (400 MHz, $CDCl_3$) δ/ppm 7.54–7.49 (m, 2H), 7.33–7.21 (m, 3H), 4.76 (d, *J* = 9.4 Hz, 1H), 4.12 (dd, *J* = 11.3, 5.4 Hz, 1H), 3.96–3.84 (m, 1H), 3.69 (t, *J* = 9.2 Hz, 1H), 3.60 (t, *J* = 9.5 Hz, 1H), 3.31–3.27 (m, 4H), 3.22 (s, 3H), 2.23 (d, *J* = 2.9 Hz, 1H), 1.34 (d, *J* = 1.4 Hz, 6H); **^{13}C NMR** (101 MHz, $CDCl_3$) δ/ppm 133.4, 131.9, 129.0, 127.6, 100.4, 99.8, 86.1, 75.0, 69.8, 68.1, 67.4, 48.3, 48.1, 17.80, 17.76; **HRMS ESI** *m*/*z* calc. for $C_{17}H_{24}O_6SNa$ $[M+Na]^+$: 379.1186, found: 379.1191.

(4a*R*,5*S*,8*R*,8a*R*)-2,3-Dimethoxy-2,3-dimethyl-5-(phenylthio)hexahydro-5*H*-pyrano[3,4-*b*][1,4]dioxin-8-yl (2,2,2-trichloroethyl) sulfate (2.102)

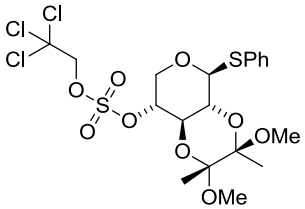

Alcohol **2.101** (200 mg, 0.584 mmol, 1.0 eq.) and triflate salt **2.96** (519 mg, 1.17 mmol, 2.0 eq.) were dissolved in THF (6 mL). 1-Methylimidazole (0.12 mL, 1.51 mmol, 2.6 eq.) was added at 0 °C and the mixture stirred for 66 h at room temperature. The solvent was removed under reduced pressure before H_2O (50 mL) and EtOAc (50 mL) were added. The layers were separated and the organic layer was washed with sat. aq. $NaHCO_3$ solution (30 mL) and brine (30 mL). The organic layer was dried over Na_2SO_4 and the solvent was removed under reduced pressure. The crude product was purified by flash column chromatography (SiO_2, pentane/EtOAc 6:1 changing to 2:1) to obtain sulfate ester **2.102** (293 mg, 0.516 mmol, 88%) as a colorless sticky oil.

$\mathbf{R}_f$ = 0.79 (SiO_2, pentane/EtOAc 4:1); **Optical rotation** $[\alpha]_D^{25}$ = –168.1 (*c* = 0.49, $CHCl_3$); **FTIR** $\tilde{\nu}$/cm^{-1} 2996, 2956, 1585, 1416, 1205, 1140, 1046, 1058, 1012, 964, 884, 774, 729, 692; **^{1}H NMR** (400 MHz, $CDCl_3$) δ/ppm 7.55–7.50 (m, 2H), 7.35–7.26 (m, 3H), 4.95 (d, *J* = 10.5 Hz, 1H), 4.80–4.72 (m, 3H), 4.42 (dd, *J* = 11.8, 5.4 Hz, 1H), 3.97 (t, *J* = 9.6 Hz, 1H), 3.69 (t, *J* = 9.7 Hz, 1H), 3.55 (dd, *J* = 11.9, 9.3 Hz, 1H), 3.30 (s, 3H), 3.23 (s, 3H), 1.35 (s, 3H), 1.33 (s, 3H); **^{13}C NMR** (101 MHz, $CDCl_3$) δ/ppm 132.6, 132.2, 129.1, 127.9, 100.5, 100.2, 92.5, 86.0, 79.6, 78.4, 71.2, 68.1, 66.7, 48.4, 48.2, 17.6, 17.5; **UPLC ESI** *m*/*z* calc. for $C_{19}H_{25}Cl_3O_9S_2Na$ $[M+Na]^+$: 589.0, found: 589.0.

(3*R*,4*R*,5*R*,6*S*)-4,5-Dihydroxy-6-(phenylthio)tetrahydro-2*H*-pyran-3-yl (2,2,2-trichloroethyl) sulfate (2.103)

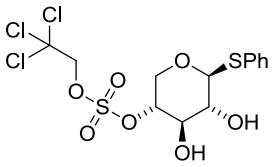

BDA protected thioxyloside **2.102** (20.0 mg, 35.2 µmol, 1.0 eq.) was dissolved in CH_2Cl_2 (0.55 mL), TFA (0.05 mL) was added and the mixture stirred for 20 h at room temperature. Toluene (2 mL) was added and the solvents were removed under reduced pressure to obtain deprotected thioxyloside **2.103** (16.0 mg, 35.2 µmol, quant.) as a colorless solid.

^{1}H NMR (400 MHz, $CDCl_3$) δ/ppm 7.60–7.48 (m, 2H), 7.41–7.31 (m, 3H), 4.94 (d, J = 10.8 Hz, 1H), 4.77 (d, J = 10.7 Hz, 1H), 4.60 (ddd, J = 10.3, 9.1, 5.6 Hz, 1H), 4.46 (d, J = 9.6 Hz, 1H), 4.40 (dd, J = 11.5, 5.5 Hz, 1H), 3.80 (t, J = 8.9 Hz, 1H), 3.50 (dd, J = 11.6, 10.4 Hz, 1H), 3.36 (dd, J = 9.6, 8.7 Hz, 1H), 2.77 (s, 2H); **^{13}C NMR** (101 MHz, $CDCl_3$) δ/ppm 133.6, 130.5, 129.4, 129.2, 92.7, 88.6, 80.2, 80.0, 74.7, 72.3, 66.7.

(4a*R*,8*R*,8a*R*)-5-Hydroxy-2,3-dimethoxy-2,3-dimethylhexahydro-5*H*-pyrano[3,4-*b*][1,4] dioxin-8-yl (2,2,2-trichloroethyl) sulfate (2.114)

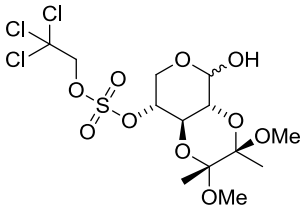

Thioxyloside **2.102** (9.00 mg, 15.8 µmol, 1.0 eq.) was dissolved in acetone/H_2O (0.25 mL, 9:1) and cooled to –10 °C. NBS (8.50 mg, 47.8 µmol, 3.0 eq.) was added and the mixture was stirred for 45 min before additional NBS (2.80 mg, 15.8 µmol 1.0 eq.) was added. After stirring for 1 h at –10 °C, the mixture was quenched with sat. aq. $NaHCO_3$ solution (2 mL). The reaction mixture was concentrated under reduced pressure; the residue was diluted with EtOAc (20 mL) and washed with sat. aq. $NaHCO_3$ solution (2 x 5 mL) and brine (2 x 5 mL). The organic layer was dried over Na_2SO_4 and the solvent was removed under reduced pressure. The crude product was purified by flash column chromatography (SiO_2, pentane/EtOAc 4:1) to obtain an anomeric mixture α/β of 2:1 of hydrolyzed xylosyl donor **2.114** (4.00 mg, 8.00 µmol, 53%) as a white solid.

R_f = 0.16 (SiO_2, pentane/EtOAc 4:1); **FTIR** $\tilde{\nu}$/cm^{-1} 3415, 2954, 2925, 1663, 1414, 1205, 1141, 1037, 967, 883, 779, 729; **^{1}H NMR** (400 MHz, $CDCl_3$, major diastereomer) δ/ppm 5.21 (d, J = 3.1 Hz, 1H), 4.99–4.96 (m, 1H), 4.84–4.66 (m, 2H), 4.25 (t, J = 9.9 Hz, 1H), 4.08–3.97 (m, 2H), 3.77 (ddd, J = 10.0, 3.5, 0.8 Hz, 1H), 3.61–3.51 (m, 1H), 3.29 (s, 3H), 3.25 (s, 3H), 2.94 (br s, 1H), 1.34 (s, 3H), 1.30 (s, 3H).

(4a*R*,8*R*,8a*R*)-5-Bromo-2,3-dimethoxy-2,3-dimethylhexahydro-5*H*-pyrano[3,4-*b*][1,4] dioxin-8-yl (2,2,2-trichloroethyl) sulfate (2.111)

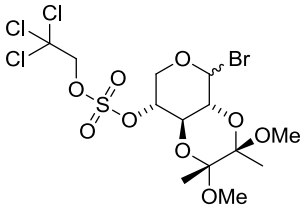

Thioxyloside **2.102** (5.50 mg, 9.93 µmol, 1.0 eq.) was dissolved in CH_2Cl_2 (0.1 mL) and cooled to 0 °C. Bromine (1.53 mL, 29.8 mmol, 3.0 eq.) was added and the mixture was stirred for 30 min at 0 °C and further 1 h at room temperature. The mixture was quenched with aq. $Na_2S_2O_3$ solution (10% *w*/*w*, 2 mL) and the aqueous layer was extracted with $CHCl_3$ (3 x 2 mL). The combined organic layers were washed with brine (5 mL), dried over Na_2SO_4 and the solvent was removed under reduced pressure. Brominated xylosyl donor **2.111** (4.5 mg, 8.58 µmol, 86%) was obtained as an anomeric mixture α/β of 6:1 as a yellow solid which was used without further purification.

R_f = 0.63 (SiO_2, pentane/EtOAc 4:1); **^{1}H NMR** (400 MHz, $CDCl_3$, major diastereomer) δ/ppm 6.26 (d, J = 3.7 Hz, 1H), 4.96 (d, J = 10.5 Hz, 1H), 4.84–4.73 (m, 2H), 4.31–4.21 (m, 2H), 4.05–3.92 (m, 1H), 3.78 (dd, J = 9.8, 3.7 Hz, 1H), 3.31 (s, 3H), 3.25 (s, 3H), 1.34 (s, 3H), 1.31 (s, 3H).

(4a*R*,5*S*,8*R*,8a*R*)-5-Fluoro-2,3-dimethoxy-2,3-dimethylhexahydro-5*H*-pyrano[3,4-*b*][1,4] dioxin-8-yl (2,2,2-trichloroethyl) sulfate (2.115)

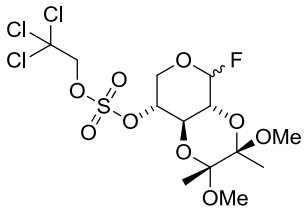

Thioxyloside **2.102** (29.7 mg, 52.3 µmol, 1.0 eq.) was dissolved in CH_2Cl_2 (3.5 mL) and DAST (10.5 µL, 78.4 µmol, 1.5 eq.) and NBS (12.9 mg, 72.5 µmol, 1.4 eq.) were added at –15 °C. The reaction was stirred for 20 min at this temperature before additional NBS (13.0 mg, 73.0 µmol, 1.4 eq.) was added and the mixture was stirred for additional 2 h at –15 °C. Sat. aq. $NaHCO_3$ solution (6 mL) was added and the aqueous layer was extracted with Et_2O (3 x 10 mL). The combined organic layers were washed with brine (15 mL), dried over Na_2SO_4 and the solvent was removed under reduced pressure. The crude product was purified by flash column chromatography (SiO_2, pentane/EtOAc 4:1) to obtain an anomeric mixture α/β of 3:1 of fluorinated xylosyl donor **2.115** (19.0 mg, 39.8 µmol, 76%) was obtained as a sticky colorless oil.

R_f = 0.74 (SiO_2, pentane/EtOAc 4:1); **Optical rotation** $[\alpha]_D^{25}$ = –89.8 (*c* = 0.24, $CHCl_3$); **FTIR** $\tilde{\nu}$/cm^{-1} 2996, 2957, 2838, 1417, 1206, 1142, 1104, 1034, 973, 918, 881, 783, 730; **^{1}H NMR** (400 MHz, $CDCl_3$, major diastereomer) δ/ppm 5.54 (dd, *J* = 53.6, 2.4 Hz, 1H), 4.96 (d, *J* = 10.5 Hz, 1H), 4.80–4.72 (m, 2H), 4.25–4.18 (m, 2H), 3.92 (t, *J* = 11.0 Hz, 1H), 3.78 (ddd, *J* = 24.9, 10.2, 2.5 Hz, 1H), 3.30 (s, 3H), 3.26 (s, 3H), 1.35 (s, 3H), 1.31 (s, 3H); **^{13}C NMR** (101 MHz, $CDCl_3$, major diastereomer) δ/ppm 104.7 (d, *J* = 231.3 Hz), 100.6, 100.4, 92.5, 79.8, 68.2, 68.0, 66.0, 61.3 (d, *J* = 3.6 Hz), 48.4, 48.3, 17.7, 17.6; **^{19}F NMR** (376 MHz, $CDCl_3$) δ/ppm –150.9.

(2*R*,3*R*,4a*R*,8*R*,8a*R*)-2,3-Dimethoxy-2,3-dimethyl-8-(((2,2,2-trichloroethoxy)sulfonyl)-oxy)hexahydro-5*H*-pyrano[3,4-*b*][1,4]dioxin-5-yl 2,2,2-trichloroacetimidate (2.112)

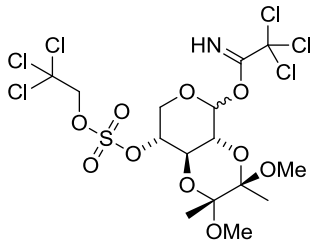

To a solution of an α/β 2:1 anomeric mixture of hydroxyl xyloside **2.114** (33.5 mg, 70.4 µmol, 1.0 eq.) in CH_2Cl_2 (0.5 mL) were added trichloroacetonitrile (44.5 µL, 0.440 mmol, 6.3 eq.) and DBU (10.5 µL, 70.4 µmol, 1.0 eq.) at room temperature. The reaction mixture was stirred for 2 h at room temperature. The solvent was removed and the crude product directly purified by flash column chromatography (SiO_2, pentane/EtOAc 8:1) to obtain an α/β 2:1 anomeric mixture of trichloroacetimidate **2.112** (24.0 mg, 39.0 µmol, 55%) as a colorless oil. A 2nd flash column chromatography (SiO_2, pentane/EtOAc 8:1) led to separation of the α and β anomers.

^{1}H NMR (400 MHz, $CDCl_3$, mixture of diastereomers) δ/ppm 8.71 (s, 0.5H), 8.67 (s, 1H), 6.28 (d, J = 3.2 Hz, 1H), 5.98 (d, J = 7.2 Hz, 0.5H), 4.99 (d, J = 10.5 Hz, 1H), 4.92 (d, J = 10.5 Hz, 0.5H), 4.86–4.74 (m, 3H), 4.38 (dd, J = 7.8, 5.1 Hz, 0.5H), 4.33 (t, J = 10.0 Hz, 1H), 4.21 (dd, J = 11.3, 5.9 Hz, 1H), 4.05 (dd, J = 10.8, 8.4 Hz, 0.5H), 3.97–3.86 (m, 3H), 3.31 (s, 1.5H), 3.28 (s, 1.5H), 3.27 (s, 3H), 3.25 (s, 3H), 1.32 (s, 1.5H), 1.30 (s, 1.5H), 1.30 (s, 3H), 1.25 (s, 3H); **^{13}C NMR** (101 MHz, $CDCl_3$, mixture of diastereomers) δ/ppm 161.04, 160.96, 100.3, 100.2, 100.0, 96.3, 93.5, 92.6, 92.5, 91.1, 90.9, 80.0, 79.8, 79.7, 77.9, 68.7, 68.0, 67.6, 66.2, 64.4, 61.7, 48.4, 48.3, 48.2, 48.1, 17.7, 17.61, 17.59, 17.5.

(2*R*,3*R*,4a*R*,5*S*,8*R*,8a*R*)-2,3-Dimethoxy-2,3-dimethyl-5-((*S*)-phenylsulfinyl)hexahydro-5*H*-pyrano[3,4-*b*][1,4]dioxin-8-yl (2,2,2-trichloroethyl) sulfate (2.113)

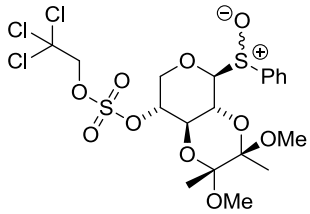

Thioxyloside **2.102** (30.0 mg, 52.8 µmol, 1.0 eq.) and KF (6.14 mg, 106 µmol, 2.0 eq.) were dissolved in MeCN/H_2O (5:1, 0.25 mL) and stirred for 30 min at 0 °C. A solution of *m*-CPBA (26.0 mg, 106 µmol, 2.0 eq.) in MeCN (0.1 mL) was slowly added and the reaction mixture stirred for 5 min at 0 °C before it was quenched with sat. aq. $FeSO_4$ solution (2 mL). The aqueous layer was extracted with CH_2Cl_2 (3 x 2 mL) and the combined organic layers were washed with sat. aq. $NaHCO_3$ solution (1 mL), dried over Na_2SO_4 and the solvent was removed under reduced pressure. The crude residue was purified by flash column chromatography (SiO_2, pentane/EtOAc 4:1) to obtain a 1:1 diastereomeric mixture of sulfoxide **2.113** (22.0 mg, 38.0 µmol, 71%) as a colorless solid.

Mp = 64.0–66.0 °C; $\mathbf{R_f}$ = 0.26 (SiO_2, pentane/EtOAc 4:1); **FTIR** $\tilde{\nu}$/cm^{-1} 2995, 2956, 2922, 2839, 1446, 1415, 1379, 1262, 1204, 1139, 1108, 1093, 1042, 1010, 964, 921, 881, 849, 778, 747, 727, 690, 674, 622; **^{1}H NMR** (400 MHz, $CDCl_3$, mixture of diastereomers) δ/ppm 7.66–7.62 (m, 2H), 7.61–7.57 (m, 2H), 7.55–7.52 (m, 3H), 7.51–7.48 (m, 3H), 4.92 (d, J = 8.2 Hz, 1H), 4.89 (d, J = 8.2 Hz, 1H), 4.79 (dd, J = 9.3, 5.4 Hz, 1H), 4.77–4.68 (m, 3H), 4.46 (dd, J = 12.1, 5.3 Hz, 1H), 4.42–4.36 (m, 2H), 4.33–4.23 (m, 2H), 4.05–3.96 (m, 3H), 3.70 (dd, J = 12.2, 8.0 Hz, 1H), 3.41 (dd, J = 6.6, 2.6 Hz, 1H), 3.41 (s, 3H), 3.37 (s, 3H), 3.31 (s, 3H), 3.23 (s, 3H), 1.40 (s, 3H), 1.36 (s, 3H), 1.26 (s, 3H), 1.04 (s, 3H); **^{13}C NMR** (101 MHz, $CDCl_3$, mixture of diastereomers) δ/ppm 140.0, 138.9, 131.5, 131.3, 129.3, 128.9, 125.08, 125.07, 100.7, 100.6, 100.4, 100.0, 94.3, 92.5, 92.4, 90.9, 79.7, 78.4, 77.9, 70.7, 70.1, 68.2, 67.9, 64.3, 63.9, 49.5, 48.9, 48.4, 48.2, 17.70, 17.67, 17.6, 17.2; **HRMS ESI** m/z calc. for $C_{17}H_{24}O_6SNa$ $[M+Na]^+$: 606.8917, found: 606.8927.

Methyl (2*S*,3a*S*,6*R*,7a*S*)-6-acetoxy-1-(((*R*)-2-(methoxymethoxy)-3-phenylpropanoyl)-D-leucyl)octahydro-1*H*-indole-2-carboxylate (2.90)

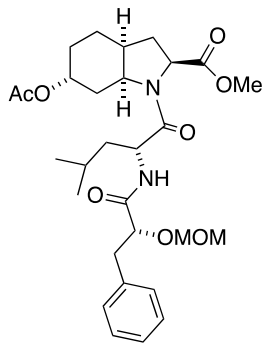

Secondary amine **2.92** (15.1 mg, 62.7 μmol, 1.0 eq.), Pla-Leu-OH dipeptide **2.53** (26.4 mg, 81.7 μmol, 1.3 eq.), DMTMM (22.9 mg, 82.8 μmol, 1.3 eq.) and NMM (14 μL, 125 μmol, 1.6 eq.) were dissolved in CH_2Cl_2 (2 mL) at 0 °C. The mixture was stirred for 30 min at this temperature and further for 4 h at room temperature. The crude product was purified by flash column chromatography (SiO_2, CH_2Cl_2/MeOH 15:1) to obtain a rotameric mixture of 5:1 of tripeptide **2.90** (27.4 mg, 50.1 μmol, 80%) as a colorless sticky oil.

R_f = 0.42 (SiO_2, CH_2Cl_2/MeOH 15:1); **Optical rotation** $[\alpha]_D^{25}$ = +0.3 (*c* = 0.46, $CHCl_3$); **FTIR** $\tilde{\nu}$/cm^{-1} 3414, 2954, 2933, 1739, 1649, 1578, 1516, 1435, 1365, 1236, 1175, 1104, 1020, 919, 817, 747, 702; **^{1}H NMR** (400 MHz, $CDCl_3$, major rotamer) δ/ppm 7.30–7.20 (m, 5H), 7.08 (d, *J* = 9.4 Hz, 1H), 5.15–5.10 (m, 1H), 4.80 (td, *J* = 10.0, 3.4 Hz, 1H), 4.60–4.50 (m, 2H), 4.37–4.32 (m, 1H), 4.11 (dt, *J* = 12.0, 6.1 Hz, 1H), 3.96–3.72 (m, 1H), 3.69 (s, 3H), 3.22–3.19 (m, 1H), 3.17 (s, 3H), 2.97 (dd, *J* = 14.0, 7.6 Hz, 1H), 2.49–2.38 (m, 2H), 2.25–2.17 (m, 1H), 2.07 (s, 3H), 2.02–1.94 (m, 2H), 1.89–1.79 (m, 2H), 1.68–1.61 (m, 1H), 1.59–1.52 (m, 1H), 1.50–1.42 (m, 1H), 1.35–1.29 (m, 1H), 1.25–1.20 (m, 1H), 0.98 (d, *J* = 6.3 Hz, 3H), 0.86 (d, *J* = 6.5 Hz, 3H); **^{13}C NMR** (101 MHz, $CDCl_3$, major rotamer) δ/ppm 172.6, 171.1, 170.4, 170.1, 137.3, 129.9, 128.2, 126.6, 96.0, 77.7, 69.2, 59.1, 56.2, 54.4, 52.3, 48.0, 43.1, 38.9, 37.0, 31.3, 30.5, 29.8, 24.4, 23.5, 21.5, 21.2, 19.8; **HRMS ESI** *m*/*z* calc. for $C_{29}H_{43}N_2O_8$ $[M+H]^+$: 547.3014, found: 547.3018.

Methyl (2*S*,3a*S*,6*R*,7a*S*)-6-hydroxy-1-(((*R*)-2-(methoxymethoxy)-3-phenylpropanoyl)-D-leucyl)octahydro-1*H*-indole-2-carboxylate (2.110)

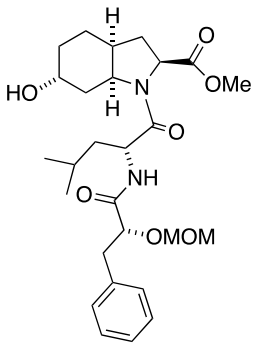

Tripeptide **2.90** (25.0 mg, 45.7 μmol, 1.0 eq.) and K_2CO_3 (20.4 mg, 0.148 mmol, 3.2 eq.) were dissolved in MeOH (0.6 mL) at 0 °C. The reaction mixture was stirred for 5 min at this temperature and further for 3.5 h at room temperature. The reaction was quenched with sat. aq. NH_4Cl solution (4 mL) and the MeOH was removed under reduced pressure. The residue was extracted with CH_2Cl_2 (3 x 5 mL), the combined organic layers were dried over Na_2SO_4 and the solvent was removed under reduced pressure. The crude product was purified by flash column chromatography (SiO_2, CH_2Cl_2/MeOH 30:1) to obtain a rotameric mixture (5:1) of glycosyl acceptor **2.110** (14.1 mg, 27.9 μmol, 61%) as colorless sticky oil.

R_f = 0.46 (SiO_2, CH_2Cl_2/MeOH 20:1); **Optical rotation** $[\alpha]_D^{25}$ = +17.0 (*c* = 0.71, $CHCl_3$); **FTIR** $\tilde{\nu}$/cm^{-1} 3409, 2953, 2932, 1750, 1642, 1579, 1525, 1440, 1364, 1260, 1174, 1104, 1015, 918, 817, 748, 702; **^{1}H NMR** (400 MHz, $CDCl_3$, major rotamer) δ/ppm 7.30–7.19 (m, 5H), 7.07 (d, *J* = 9.6 Hz, 1H), 4.85 (td, *J* = 9.7, 3.9 Hz, 1H), 4.58–4.50 (m, 2H), 4.37–4.30 (m, 2H), 4.25 (dt, *J* = 12.1, 6.3 Hz, 1H), 4.19 (br s, 1H), 3.96–3.74 (m, 1H), 3.68 (s, 3H), 3.16 (s, 3H), 2.96 (dd, *J* = 14.1, 7.5 Hz, 1H), 2.49–2.41 (m, 1H), 2.32–2.25 (m, 2H), 2.23–2.14 (m, 2H), 2.01–1.90 (m, 1H), 1.81–1.73 (m, 1H), 1.70–1.63 (m, 1H), 1.61–1.53 (m, 2H), 1.48–1.41 (m, 1H), 1.35–1.29 (m, 2H), 0.93 (d, *J* = 5.6 Hz, 3H), 0.85 (d, *J* = 5.8 Hz, 3H); **^{13}C NMR** (101 MHz, $CDCl_3$, major rotamer) δ/ppm 172.7, 171.1, 170.2, 137.2, 129.9, 128.3, 126.7, 95.9, 77.6, 65.7, 59.2, 56.2, 54.5, 52.2, 48.1, 42.7, 39.0, 37.3, 34.3, 30.5, 25.8, 24.5, 23.5, 22.0, 19.3; **HRMS ESI** *m/z* calc. for $C_{27}H_{41}N_2O_7$ $[M+H]^+$: 505.2908, found: 505.2915.

Methyl (2*S*,3a*S*,6*R*,7a*S*)-1-((2*S*,3*R*)-3-chloro-2-((*R*)-2-(methoxymethoxy)-3-phenylpropanamido)-4-methylpentanoyl)-6-hydroxyoctahydro-1*H*-indole-2-carboxylate (2.109)

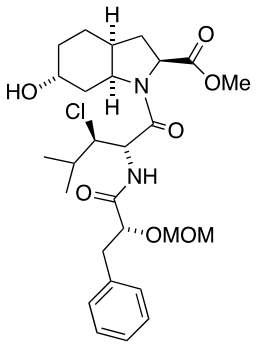

Tripeptide **2.93** (18.8 mg, 32.4 µmol, 1.0 eq.) and K_2CO_3 (13.4 mg, 97.2 µmol, 3.0 eq.) were dissolved in MeOH (0.4 mL) at 0 °C. The reaction mixture was stirred for 5 min at the same temperature and further for 2 h at room temperature. Additional K_2CO_3 (4.30 mg, 32.4 µmol, 1.0 eq.) was added and the reaction mixture was stirred for further 1.5 h. The reaction was quenched with sat. aq. NH_4Cl solution (2 mL) and the MeOH was removed under reduced pressure. The residue was extracted with CH_2Cl_2 (3 x 5 mL), the combined organic layers were dried over Na_2SO_4 and the solvent was removed under reduced pressure. The crude product was purified by flash column chromatography (SiO_2, pentane/EtOAc 1:2) to obtain glycosyl acceptor **2.109** (14.9 mg, 28.0 µmol, 85%) as colorless foam.

R_f = 0.21 (SiO_2, pentane/EtOAc 1:1); **Optical rotation** $[\alpha]_D^{25}$ = +51.8 (*c* = 0.31, $CHCl_3$); **FTIR** $\tilde{\nu}$/cm^{-1} 3399, 2929, 1750, 1640, 1513, 1452, 1361, 1255, 1197, 1176, 1148, 1113, 1035, 919, 887, 804, 752, 701, 695, 667, 605; **^{1}H NMR** (400 MHz, $CDCl_3$) δ/ppm 7.30–7.18 (m, 5H), 7.03 (d, *J* = 10.1 Hz, 1H), 4.99 (t, *J* = 10.4 Hz, 1H), 4.61–4.55 (m, 2H), 4.46 (dt, *J* = 12.2, 6.3 Hz, 1H), 4.42–4.36 (m, 2H), 4.16 (s, 1H), 3.88 (dd, *J* = 10.8, 1.9 Hz, 1H), 3.67 (s, 3H), 3.21 (s, 3H), 3.14 (dd, *J* = 14.2, 3.8 Hz, 1H), 3.00 (dd, *J* = 14.2, 6.4 Hz, 1H), 2.45 (dq, *J* = 12.9, 6.3 Hz, 1H), 2.25–2.11 (m, 3H), 1.93 (td, *J* = 12.9, 10.2 Hz, 1H), 1.85 (s, 1H), 1.74–1.61 (m, 1H), 1.59–1.50 (m, 1H), 1.46–1.37 (m, 1H), 1.29–1.23 (m, 2H), 0.91 (d, *J* = 6.5 Hz, 3H), 0.86 (d, *J* = 6.8 Hz, 3H); **^{13}C NMR** (101 MHz, $CDCl_3$) δ/ppm 172.6, 170.8, 168.4, 136.7, 130.1, 128.3, 126.9, 95.6, 68.4, 65.9, 58.9, 56.4, 54.8, 52.2, 51.9, 38.3, 36.8, 34.3, 30.7, 28.1, 25.8, 20.9, 19.3, 15.4; **HRMS ESI** *m*/*z* calc. for $C_{27}H_{39}ClN_2O_7Na$ $[M+Na]^+$: 561.2338, found: 561.2344.

Methyl (2*S*,3a*S*,6*R*,7a*S*)-1-((2*S*,3*R*)-3-chloro-2-((*R*)-2-(methoxymethoxy)-3-phenylpropanamido)-4-methylpentanoyl)-6-(((4a*R*,5*S*,8*R*,8a*R*)-2,3-dimethoxy-2,3-dimethyl-8-(((2,2,2-trichloroethoxy)sulfonyl)oxy)hexahydro-5*H*-pyrano[3,4-*b*][1,4]dioxin-5-yl)oxy)octahydro-1*H*-indole-2-carboxylate (2.116)

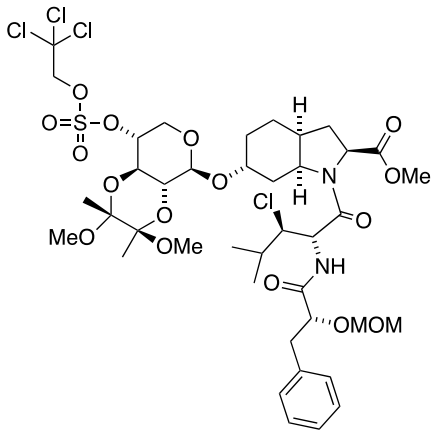

Brominated xylosyl donor **2.111** (3.60 mg, 6.68 µmol, 1.2 eq.), L-Choi-Cleu-Pla derivative **2.109** (3.00 mg, 5.57 µmol, 1.0 eq.) and DTBMP (2.75 mg, 13.4 µmol, 2.4 eq.) were dissolved in CH_2Cl_2 (0.3 mL) containing 4 Å powdered molecular sieves. AgOTf (3.44 mg, 13.4 µmol, 2.4 eq.) was added to this suspension at 0 °C and the mixture was stirred at the same temperature for 30 min and further for 1 h at room temperature. Et_3N (30 µL) was added and the reaction mixture was filtered over Celite®. The Celite® pad was washed with CH_2Cl_2 (2 x 5 mL) and the solvent removed from the filtrate. The crude product was purified by flash column chromatography (SiO_2, pentane/EtOAc 1:2) to give in a first fraction the α-anomer of Xyl-L-Choi-Cleu-Pla derivative **2.116a** (0.800 mg, 0.840 µmol, 15%) and in a second fraction the β-anomer of Xyl-L-Choi-Cleu-Pla derivative **2.116b** (2.40 mg, 2.40 µmol, 43%) as colorless oils.

2.116b: ^{1}H NMR (250 MHz, $CDCl_3$) δ/ppm7.26 (s, 5H), 6.98 (d, J = 10.1 Hz, 1H), 4.97 (t, J = 10.4 Hz, 1H), 4.97 (d, J = 10.5 Hz, 1H), 4.79 (d, J = 10.5 Hz, 1H), 4.74–4.65 (m, 1H), 4.64–4.46 (m, 3H), 4.44–4.33 (m, 2H), 4.01 (s, 1H), 3.95 (dd, J = 10.3, 9.2, 1H), 3.81 (dd, J = 10.8, 1.8 Hz, 1H), 3.74–3.67 (m, 1H), 3.65 (s, 3H), 3.57 (dd, J = 10.3, 7.5 Hz, 1H), 3.31 (s, 3H), 3.27 (s, 3H), 3.20 (s, 3H), 3.13 (dd, J = 14.2, 3.9 Hz, 1H), 3.01 (dd, J = 14.1, 6.3 Hz, 1H), 2.42 (d, J = 16.7 Hz, 2H), 2.16 (d, J = 7.8 Hz, 2H), 2.00–1.81 (m, 1H), 1.68 (d, J = 21.9 Hz, 1H), 1.56 (s, 3H), 1.32 (s, 3H), 1.31 (s, 3H), 0.93 (d, J = 6.4 Hz, 3H), 0.85 (d, J = 6.7 Hz, 3H).

(2*S*,3a*S*,6*R*,7a*S*)-1-((2*S*,3*R*)-3-Chloro-2-((*R*)-2-(methoxymethoxy)-3-phenylpropanamido)-4-methylpentanoyl)-6-(((4a*R*,5*S*,8*R*,8a*R*)-2,3-dimethoxy-2,3-dimethyl-8-(((2,2,2-trichloroethoxy)sulfonyl)oxy)hexahydro-5*H*-pyrano[3,4-*b*][1,4]dioxin-5-yl)oxy)octahydro-1*H*-indole-2-carboxylic acid (2.118)

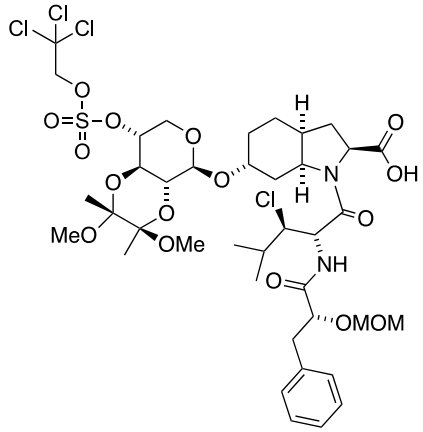

β-Xyl-L-Choi-Cleu-Pla methyl ester **2.116b** (5.90 mg, 5.92 µmol, 1.0 eq.) was dissolved in 1,2-dichloroethane (0.3 mL). Trimethyltin hydroxide (3.60 mg, 19.9 µmol, 3.3 eq.) was added and the reaction mixture stirred for 14 h at 85 °C, before additional trimethyltin hydroxide (3.60 mg, 19.9 µmol, 3.3 eq.) was added. Additional trimethyltin hydroxide (3.60 mg, 19.9 µmol, 3.3 eq.) was again added after further 14 h. The reaction mixture was stirred for additional 68 h at 85 °C before it was partitioned between CH_2Cl_2 (2 mL) and aq. HCl solution (1 M, 1 mL). The layers were separated and the organic layer was washed with aq. HCl solution (1 M, 5 x 1 mL), dried over Na_2SO_4 and the solvent was removed under reduced pressure. The crude product was purified by flash column chromatography (SiO_2, CH_2Cl_2/MeOH 10:1) to obtain Xyl-L-Choi-Cleu-Pla acid **2.118** (2.00 mg, 2.01 µmol, 34%) as a colorless oil. Further, starting material **2.116b** could be recovered (3.70 mg, 3.72 µmol, 63%).

^{1}H NMR (400 MHz, $CDCl_3$) δ/ppm 7.31–7.19 (m, 5H), 7.08–7.00 (m, 1H), 5.06 (t, J = 10.3 Hz, 1H), 4.97 (d, J = 10.5 Hz, 1H), 4.79 (d, J = 10.5 Hz, 1H), 4.71–4.57 (m, 2H), 4.51 (dd, J = 12.4, 5.0 Hz, 1H), 4.39–4.33 (m, 1H), 3.99 (s, 1H), 3.94 (t, J = 9.8 Hz, 1H), 3.82 (d, J = 10.8 Hz, 1H), 3.66 (dd, J = 12.3, 9.0 Hz, 1H), 3.55 (dd, J = 10.2, 7.6 Hz, 1H), 3.30 (s, 3H), 3.26 (s, 3H), 3.24 (s, 3H), 3.11–3.03 (m, 2H), 2.47–2.32 (m, 3H), 2.16–2.04 (m, 3H), 1.80–1.72 (m, 1H), 1.63–1.49 (m, 1H), 1.32 (s, 3H), 1.31 (s, 3H), 1.40–1.21 (m, 4H), 0.89 (d, J = 6.3 Hz, 3H), 0.85 (d, J = 6.6 Hz, 3H).

(4a*R*,5*S*,8*R*,8a*R*)-5-(((2*S*,3a*S*,6*R*,7a*S*)-2-((2-(1-((*Z*)-*N*,*N*'-Bis(*tert*-butoxycarbonyl)-carbamimidoyl)-2,5-dihydro-1*H*-pyrrol-3-yl)ethyl)carbamoyl)-1-((2*S*,3*R*)-3-chloro-2-((*R*)-2-(methoxymethoxy)-3-phenylpropanamido)-4-methylpentanoyl)octahydro-1*H*-indol-6-yl)oxy)-2,3-dimethoxy-2,3-dimethylhexahydro-5*H*-pyrano[3,4-*b*][1,4]dioxin-8-yl (2,2,2-trichloroethyl) sulfate (2.119)

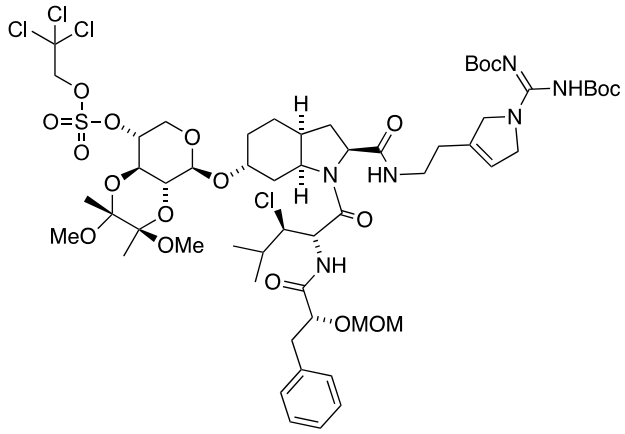

PyBOP (1.82 mg, 3.50 µmol, 2.0 eq.) was added to a solution of Xyl-L-Choi-Cleu-Pla acid **2.118** (1.70 mg, 1.75 µmol, 1.0 eq.) and Adc subunit **2.63** (1.24 mg, 3.50 µmol, 2.0 eq.) in CH_2Cl_2 (50 µL) containing 2,6-lutidine (0.6 µL, 5.15 µmol, 2.9 eq.) at 0 °C. The reaction mixture was stirred for 30 min at 0 °C and further for 4 h at room temperature. CH_2Cl_2 (2 mL) was added and the mixture was washed with sat. aq. $NaHCO_3$ solution (1 mL) and brine (1 mL). The organic layer was dried over Na_2SO_4 and the solvent removed under reduced pressure. The crude product was purified by flash column chromatography (SiO_2, CH_2Cl_2/MeOH 15:1) to obtain tetrapeptide **2.119** (2.20 mg, 1.67 µmol, 95%) as a colorless amorphous solid.

R_f = 0.36 (SiO_2, CH_2Cl_2/MeOH 15:1); **^{1}H NMR** (400 MHz, $CDCl_3$) δ/ppm 10.24 (s, 1H), 7.31–7.19 (m, 5H), 6.92 (d, *J* = 9.6 Hz, 1H), 6.65 (s, 1H), 5.49 (s, 1H), 4.97 (d, *J* = 10.5 Hz, 1H), 4.94 (t, *J* = 9.5 Hz, 1H), 4.79 (d, *J* = 10.5 Hz, 1H), 4.67 (td, *J* = 9.0, 5.2 Hz, 1H), 4.61–4.55 (m, 3H), 4.48 (dd, *J* = 12.3, 5.2 Hz, 1H), 4.42–4.25 (m, 4H), 4.00 (s, 1H), 3.94 (t, *J* = 9.7 Hz, 1H), 3.82 (dd, *J* = 10.8, 1.9 Hz, 1H), 3.71–3.61 (m, 1H), 3.55 (dd, *J* = 10.2, 7.6 Hz, 1H), 3.30 (s, 3H), 3.26 (s, 3H), 3.23 (s, 3H), 3.13 (dd, *J* = 14.1, 3.9 Hz, 1H), 3.02 (dd, *J* = 14.2, 6.2 Hz, 1H), 2.41–2.29 (m, 2H), 2.28–2.20 (m, 2H), 2.11–2.00 (m, 1H), 1.81–1.70 (m, 1H), 1.50–1.45 (m, 25H), 1.33–1.23 (m, 4H), 1.32 (s, 3H), 1.30 (s, 3H), 0.90 (d, *J* = 6.4 Hz, 3H), 0.86 (d, *J* = 6.7 Hz, 3H); **LRMS ESI** *m*/*z* calc. for $C_{56}H_{85}Cl_4N_6O_{19}S$ $[M+H]^+$: 1317.4, found: 1317.6.

Synthesis of A828B (2.121)

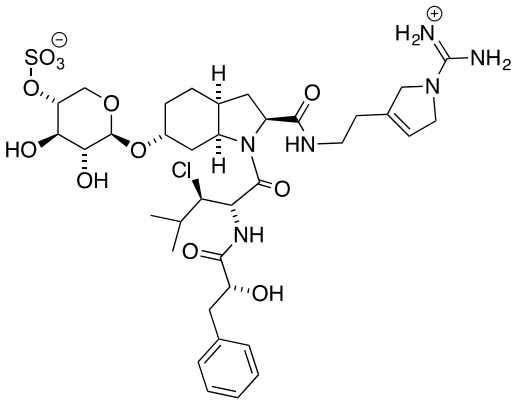

Tetrapeptide **2.119** (1.25 mg, 0.96 µmol, 1.0 eq.) was dissolved in CH_2Cl_2 (1 mL) and cooled to 0 °C. TFA (0.1 mL) was added and the mixture was stirred for 5 min at 0 °C and further for 10 h at room temperature. Solvent and TFA were removed under reduced pressure and the obtained crude residue was directly dissolved in MeOH (50 µL). Ammonium formate (0.59 µL, 11.5 µmol, 12 eq.) and zinc powder (0.980 mg, 14.4 µmol, 15 eq.) were added and the suspension was stirred for 2 h at room temperature. The reaction mixture was diluted with MeOH (2 mL), filtered over Celite® and the filtrate was concentrated under reduced pressure. The crude product was purified by reversed phase HPLC (MeCN/H_2O + 0.1% formic acid) to obtain aeruginosin 828B (**2.121**) (340 µg, 0.420 µmol, 44%) as a white amorphous solid.

^{1}H NMR (600 MHz, DMSO-d_6) δ/ppm 7.85 (t, J = 5.8 Hz, 1H), 7.51 (d, J = 9.0 Hz, 1H), 7.26–7.12 (m, 5H), 5.84 (d, J = 5.8 Hz, 1H), 5.59 (s, 1H), 5.16 (d, J = 2.5 Hz, 1H), 4.96 (d, J = 5.1 Hz, 1H), 4.82 (t, J = 9.7, 1H), 4.25 (dt, J = 12.3, 6.3 Hz, 1H), 4.16–4.12 (m, 3H), 4.10–4.03 (m, 4H), 3.98 (dd, J = 11.5, 5.5 Hz, 1H), 3.93–3.84 (m, 2H), 3.41–3.36 (m, 1H), 3.20–3.12 (m, 2H), 2.93 (dd, J = 13.6, 3.7 Hz, 1H), 2.78 (dd, J = 13.9, 7.1 Hz, 1H), 2.33–2.14 (m, 2H), 2.03–1.94 (m, 2H), 1.79–1.72 (m, 1H), 1.66–1.56 (m, 2H), 1.56–1.37 (m, 2H), 1.34–1.25 (m, 1H), 0.85 (d, J = 6.5 Hz, 3H), 0.82 (d, J = 6.6 Hz, 3H); **LRMS ESI** m/z calc. for $C_{36}H_{54}ClN_6O_{12}S$ $[M+H]^+$: 829.3, found: 829.4.

2.2. Aeruginosin KT608A Synthesis

2.2.1. D-diepi-Choi Synthesis

Ethyl 2-azidoacetate (3.52)

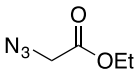

Ethyl bromoacetate (**3.53**) (17.0 g, 102 mmol, 1.0 eq.) and sodium azide (13.3 g, 204 mmol, 2.0 eq.) were dissolved in H_2O/acetone (1:3, 300 mL) and stirred for 1 h at room temperature. The reaction mixture was diluted with CH_2Cl_2 (100 mL), the layers were separated and the aqueous layer was extracted with CH_2Cl_2 (3 x 50 mL). The combined organic layers were dried over Na_2SO_4 and the solvent was removed under reduced pressure to obtain ethyl 2-azidoacetate (**3.52**) (13.0 g, 100 mmol, quant.) as a colorless oil, which was used without further purification.

^{1}H NMR (400 MHz, $CDCl_3$) δ/ppm 4.26 (q, J = 7.2 Hz, 2H), 3.86 (s, 2H), 1.31 (t, J = 7.2 Hz, 3H).
Analytical data are in accordance with those reported in the literature.[12]

Ethyl (*Z*)-2-azido-3-(4-methoxyphenyl)acrylate (3.54)

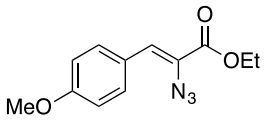

Sodium (1.98 g, 85.2 mmol, 2.2 eq.) was dissolved in EtOH (100 mL) and cooled to −15 °C. Ethyl 2–azidoacetate (**3.52**) (11.0 g, 85.2 mmol, 2.2 eq.) dissolved in EtOH (20 mL) and *p*–anisaldehyde (**3.51**) (4.70 mL, 38.7 mmol 1.0 eq.) dissolved in EtOH (8 mL) were added dropwise at −15 °C. The reaction mixture was stirred for 7 h at −15 °C and quenched by the addition of sat. aq. NH_4Cl solution (30 mL). The aqueous layer was extracted with Et_2O (2 x 50 mL) and the combined organic layers were washed with H_2O (15 mL), dried over Na_2SO_4 and the solvent was removed under reduced pressure. The obtained crude residue was purified by flash column chromatography (SiO_2, pentane/EtOAc 4:1) to give ethyl (*Z*)-2-azido-3-(4-methoxyphenyl)acrylate (**3.54**) (5.50 g, 22.2 mmol, 57%) as a yellow oil.

R_f = 0.63 (SiO_2, pentane/EtOAc 4:1); **^{1}H NMR** (400 MHz, $CDCl_3$) δ/ppm 8.06–7.63 (m, 1H), 7.04–6.43 (m, 1H), 4.36 (q, J = 7.1 Hz, 1H), 3.84 (s, 2H), 1.39 (t, J = 7.1 Hz, 2H); **^{13}C NMR** (101 MHz, $CDCl_3$) δ/ppm 163.9, 160.6, 132.5, 126.2, 125.5, 123.5, 114.0, 62.2, 55.4, 14.4.
Analytical data are in accordance with those reported in the literature.[13]

Ethyl 6-methoxy-1*H*-indole-2-carboxylate (3.54b)

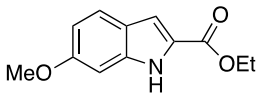

Azide **3.54** (6.00 g, 24.3 mmol, 1.0 eq.) was dissolved in *o*–xylene (180 mL) and added dropwise over a period of 1 h to refluxing *o*-xylene (240 mL). The reaction mixture was heated at reflux for 1.5 h. The solvent was removed under reduced pressure to give pure indole **3.54b** (4.95 g, 22.6 mmol, 93%) as a yellow solid which was used without further purification.

R_f = 0.48 (SiO_2, pentane/EtOAc 3:1); **Mp** = 130.3–131.5 °C; **FTIR** $\tilde{\nu}$/cm^{-1} 2980, 2940, 2906, 1706, 1613, 1347, 1213, 1184, 1110, 1025, 842, 806; **^{1}H NMR** (400 MHz, $CDCl_3$) δ/ppm 8.97 (s, 1H), 7.55 (dt, *J* = 8.5, 0.8 Hz, 1H), 7.17 (dd, *J* = 2.1, 0.8 Hz, 1H), 6.85–6.83 (m, 1H), 6.81 (d, *J* = 2.2 Hz, 1H), 4.40 (q, *J* = 7.1 Hz, 2H), 3.85 (s, 3H), 1.41 (t, *J* = 7.1 Hz, 3H); **^{13}C NMR** (101 MHz, $CDCl_3$) δ/ppm 162.2, 159.0, 138.1, 126.5, 123.5, 122.0, 112.4, 109.1, 93.9, 60.9, 55.6, 14.6.

Analytical data are in accordance with those reported in the literature.[14]

Ethyl 1-acetyl-6-methoxy-1*H*-indole-2-carboxylate (3.55)

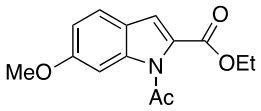

Indole **3.54b** (4.95 g, 24.3 mmol, 1.0 eq.) was dissolved in CH_2Cl_2 (170 mL), then DMAP (30.0 mg, 0.240 mmol, 0.010 eq.), acetic anhydride (3.10 g, 30.3 mmol, 1.3 eq.) and Et_3N (8.50 mL, 60.8 mmol, 2.5 eq.) were added and the mixture was stirred for 70 min at 40 °C. Additional DMAP (30.0 mg, 0.240 mmol, 0.010 eq.) and Et_3N (8.50 mL, 60.8 mmol, 2.5 eq.) were added. After stirring for 16 h at 50 °C, additional DMAP (300 mg, 24.3 mmol, 0.10 eq.), acetic anhydride (7.5 mL, 80.0 mmol, 3.3 eq.) and Et_3N (2.0 mL, 15.2 mmol, 0.63 eq.) were added and the reaction mixture was stirred for 16 h at 50 °C. The mixture was washed with sat. aq. $NaHCO_3$ solution (2 x 200mL) and the combined aqueous layers were extracted with CH_2Cl_2 (50 mL). The combined organic layers were dried over Na_2SO_4 and the solvent was removed under reduced pressure. The obtained crude residue was purified by flash column chromatography (SiO_2, pentane/EtOAc 4:1) to give indole **3.55** (4.77 g, 18.3 mmol, 75%) as a yellow oil.

R_f = 0.57 (SiO_2, pentane/EtOAc 8:1); **FTIR** $\tilde{\nu}$/cm^{-1} 2980, 2940, 2906, 1706, 1613, 1347, 1213, 1184, 1110, 1025, 842, 806; **^{1}H NMR** (400 MHz, $CDCl_3$) δ/ppm 7.62 (d, J = 2.3 Hz, 1H), 7.38 (d, J = 8.7 Hz, 1H), 7.21 (d, J = 0.8 Hz, 1H), 6.81 (dd, J = 8.7, 2.3 Hz, 1H), 4.29 (q, J = 7.1 Hz, 2H), 3.78 (s, 3H), 2.50 (s, 3H), 1.31 (t, J = 7.1 Hz, 3H); **^{13}C NMR** (101 MHz, $CDCl_3$) δ/ppm 212.8, 202.7, 201.9, 181.4, 169.4, 164.2, 161.9, 160.5, 155.4, 139.4, 102.6, 96.8, 68.5, 55.5; **HRMS ESI** m/z calc. for $C_{14}H_{15}NO_4Na$ $[M+Na]^+$: 284.0893, found: 284.0893.

Ethyl (*R*)-1-acetyl-6-methoxyindoline-2-carboxylate (3.56)

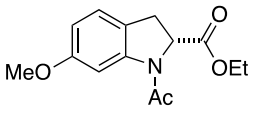

For enantiomerically enriched (+)-**3.56**: Indole derivate **3.55** (20.0 mg, 76.5 µmol, 1.0 eq.) and IrPHOX cat. **A** (1.20 mg, 0.765 µmol, 0.010 eq.) were dissolved in DCE (0.3 ml). The reaction mixture was stirred at 80 °C for 16 h under H_2 pressure (100 bar) in an autoclave, the pressure was released and the system allowed to cool to room temperature. Additional IrPHOX cat. **A** (1.20 mg, 0.765 µmol, 0.010 eq.) was added and the reaction mixture was stirred at 80 °C for further 24 h under H_2 pressure (100 bar). The pressure was released and the system was allowed to cool to room temperature. The residue was diluted with Et_2O/EtOAc (1:1, 2 mL) and filtered over a short pad of silica gel. The solvents were removed under reduced pressure and the obtained crude residue was purified by flash column chromatography (SiO_2, pentane/EtOAc 10:1 changing to 2:1) to give enantiomerically enriched indoline **3.56** (10.1 mg, 38.3 µmol, 50%) as a colorless solid. Further, starting material **3.55** (2.00 mg, 7.65 µmol, 10%) and deprotected indole **3.54b** (1.90 mg, 8.42 µmol, 11%) could be recovered.

Mp = 89.0–90.1 °C; **R_f** = 0.37 (SiO_2, pentane/EtOAc 4:1); **Optical rotation** $[\alpha]_D^{25}$ **=** +78.8 (c = 0.10, MeOH); **FTIR** $\tilde{\nu}$/cm^{-1} 3129, 2985, 2833, 1727, 1655, 1596, 1495, 1445, 1217, 1171, 1020, 848; **^{1}H NMR** (400 MHz, $CDCl_3$, major rotamer) δ/ppm 7.91 (s, 1H), 7.01 (d, J = 8.2 Hz, 1H), 6.58 (d, J = 9.2 Hz, 1H), 4.89 (d, J = 10.1 Hz, 1H), 4.30–4.12 (m, 2H), 3.81 (s, 3H), 3.55 (dd, J = 16.0, 10.9 Hz, 1H), 3.18 (d, J = 16.0 Hz, 1H), 2.17 (s, 3H), 1.27 (t, J = 7.1 Hz, 3H); **^{13}C NMR** (101 MHz, $CDCl_3$, major rotamer) δ/ppm 171.5, 169.1, 159.9, 144.0, 124.5, 120.3, 110.5, 103.4, 62.4, 62.2, 55.7, 33.0, 23.9, 14.2; **HRMS ESI** m/z calc. for $C_{14}H_{17}NO_4Na$ $[M+Na]^+$: 286.1050, found: 286.1050.

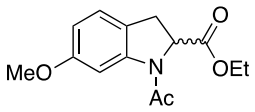

For racemic **3.56**: Indole derivate **3.55** (100 mg, 0.383 mmol, 1.0 eq.) and activated Pd/C (5% *w*/*w*, 81.5 mg, 38.3 µmol, 0.10 eq.) were dissolved in CH_2Cl_2 (5 ml). The reaction mixture was stirred for 8 h at room temperature under H_2 pressure (75 bar) in an autoclave. The pressure was released and the catalyst was filtered off over a short pad of silica gel, the silica gel was washed with Et_2O (2 x 10 mL) and the solvent was removed under reduced pressure. The obtained crude residue was purified by flash column chromatography (SiO_2, pentane/EtOAc 10:1 changing to 5:1) to give racemic indoline **3.56** (80.0 mg, 0.304 mmol, 79%) as a colorless solid.

Ethyl (2*R*,3a*R*,6*R*,7a*R*)-1-acetyl-6-methoxyoctahydro-1*H*-indole-2-carboxylate (3.57)

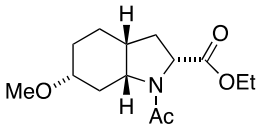

Rh/C (5% *w*/*w*, 73.5 mg, 35.3 µmol, 0.10 eq.) was added to a solution of indoline **3.56** (94.0 mg, 0.353 mmol, 1.0 eq.) in MeOH (3 mL). The reaction mixture was stirred for 9 h at room temperature under H_2 pressure (50 bar). The catalyst was filtered off over Celite®, the Celite® was washed with MeOH (2 x 5 mL) and the solvent was removed under reduced pressure. The obtained crude residue was purified by flash column chromatography (SiO_2, pentane/EtOAc 1:3) to give a 3:1 rotameric mixture of octahydroindole **3.57** (94.0 mg, 0.353 mmol, 99%) as a colorless oil which crystallized upon storing in the refrigerator.

R_f = 0.40 (SiO_2, pentane/MeOH 1:3); **Optical rotation** $[\alpha]_D^{25}$ **=** +42.7 (*c* = 0.12, MeOH); **FTIR** $\tilde{\nu}$/cm^{-1} 2938, 2826, 1731, 1646, 1406, 1182, 1121, 1020; **^{1}H NMR** (400 MHz, $CDCl_3$, major rotamer) δ/ppm 4.36–4.29 (m, 1H), 4.20–4.09 (m, 2H), 3.80 (dt, *J* = 12.0, 6.2 Hz, 1H), 3.30 (s, 3H), 3.05 (tt, *J* = 11.5, 3.8 Hz, 1H), 2.35–2.20 (m, 1H), 2.16–2.07 (m, 1H), 2.06 (s, 3H), 1.94–1.72 (m, 3H), 1.69–1.51 (m, 2H), 1.24–1.19 (m, 5H); **^{13}C NMR** (101 MHz, $CDCl_3$, major rotamer) δ/ppm 172.2, 168.4, 77.1, 61.0, 59.1, 58.5, 55.7, 37.0, 33.7, 30.7, 25.8, 22.9, 21.6, 14.1; **HRMS ESI** *m*/*z* calc. for $C_{14}H_{23}NO_4Na$ $[M+Na]^+$: 292.1519, found: 292.1525; **Crystallography** $C_{14}H_{23}NO_4$, *M* = 269.33, colorless prism, monoclinic, space group $P2_1/n$, *a* = 6.81580(10), *b* = 19.4328(3), *c* = 11.29430(10) Å, β = 106.5055(8)°, *U* = 1434.29(3) Å^3, *Z* = 4, D_c = 1.247 Mg m^{-3}, μ(Mo-Kα) = 0.091 mm^{-1}, *T* = 160 K. Total 31512 reflections, 3396 unique, R_{int} = 0.0477. Refinement of 3392 reflections (176 parameters) with $I > 2\sigma(I)$ converged at final *R*1 = 0.0415 (*R*1 all data = 0.0536), *wR*2 = 0.1008 (*wR*2 all data = 0.1099), gof = 1.026.

Ethyl (2*R*,3a*R*,6*R*,7a*R*)-1-acetyl-6-hydroxyoctahydro-1*H*-indole-2-carboxylate (3.58)

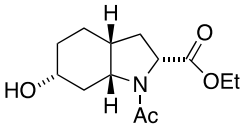

To a suspension of NaI (211 mg, 1.41 mmol, 4.0 eq.) in MeCN (0.6 mL) was added H_2O (2 µL) and the suspension was stirred for 30 min at 40 °C. TMSCl (0.18 mL, 1.41 mmol, 4.0 eq.) was added and the reaction mixture was stirred for further 30 min at 40 °C before a solution of octahydroindole **3.57** (95.0 mg, 0.353 mmol, 1.0 eq.) in MeCN (0.4 mL) was added. The reaction mixture was stirred for further 16 h at 40 °C. EtOAc (15 mL) was added and the organic layer was washed with H_2O (5 mL), sat. aq. $Na_2S_2O_3$ solution (5 mL) and brine (5 mL). The organic layer was dried over Na_2SO_4 and the solvent was removed under reduced pressure. The obtained crude residue was purified by flash column chromatography (SiO_2, EtOAc/MeOH 8:1) to give a 4:1 rotameric mixture of octahydroindole **3.58** (69.0 mg, 0.270 mmol, 77%) as a yellow oil.

R_f = 0.40 (SiO_2, EtOAc/MeOH 15:1); **FTIR** $\tilde{\nu}$/cm^{-1} 3399, 2935, 2865, 1739, 1622, 1415, 1182, 1049, 826; **^{1}H NMR** (400 MHz, $CDCl_3$, major rotamer) δ/ppm 4.35 (dd, J = 10.1, 8.1 Hz, 1H), 4.24–4.06 (m, 2H), 3.84 (dt, J = 12.1, 6.3 Hz, 1H), 3.53 (tt, J = 11.8, 3.7 Hz, 1H), 2.40–2.27 (m, 1H), 2.26–2.18 (m, 1H), 2.17–2.09 (m, 1H), 2.08 (s, 3H), 2.01–1.89 (m, 1H), 1.82–1.72 (m, 2H), 1.72–1.58 (m, 2H), 1.42–1.29 (m, 2H), 1.25 (t, J = 7.2 Hz, 3H); **^{13}C NMR** (101 MHz, $CDCl_3$, major rotamer) δ/ppm 172.6, 168.7, 68.5, 61.2, 59.1, 58.5, 37.2, 36.7, 30.9, 29.6, 23.1, 21.6, 14.2; **HRMS ESI** *m*/*z* calc. for $C_{13}H_{21}NO_4Na$ $[M+Na]^+$: 278.1368, found: 278.1363.

Ethyl 1-acetyl-6-hydroxyindoline-2-carboxylate (3.60)

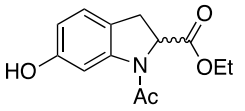

Racemic indoline **3.56** (75.0 mg, 0.285 mmol, 1.0 eq.) was dissolved in CH_2Cl_2 (7.5 mL) and cooled to −78 °C. BBr_3 (1.99 mL, 1 M solution in CH_2Cl_2, 1.99 mmol, 7.0 eq.) was added dropwise to this solution and the reaction mixture was stirred for 3 h at −78 °C. Pentane (10 mL) was added, leading to precipitation of the desired product. Filtration afforded indoline **3.60** (60.0 mg, 0.241 mmol, 85%) as a 3:1 rotameric mixture as a colorless solid, which was used without further purification.

^{1}H NMR (400 MHz, MeOD, major rotamer) δ/ppm 7.71–7.62 (m, 1H), 6.98 (d, J = 8.2 Hz, 1H), 6.48 (dd, J = 8.1, 2.5 Hz, 1H), 5.09 (dd, J = 10.8, 2.5 Hz, 1H), 4.28–4.14 (m, 2H), 3.53 (dd, J = 16.1, 10.9 Hz, 1H), 3.17 (dd, J = 15.9, 2.7 Hz, 1H), 2.16 (s, 3H), 1.27 (t, J = 7.3 Hz, 3H).

Ethyl 1-acetyl-6-(methoxymethoxy)indoline-2-carboxylate (3.61)

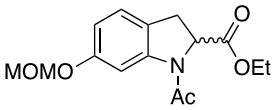

Indoline **3.60** (75.0 mg, 0.301 mmol, 1.0 eq.) and MOMCl (45.7 µL, 0.602 mmol, 2.0 eq.) were dissolved in CH_2Cl_2 (6 mL) and cooled to 0 °C. DIPEA (149 µL, 0.903 mmol, 3.0 eq.) was added at 0 °C and the reaction mixture was stirred for 20 h at room temperature. The solvent was removed under reduced pressure and the crude residue was directly purified by flash column chromatography (SiO_2, CH_2Cl_2/EtOAc 10:1) to give a 3:2 rotameric mixture of racemic indoline **3.61** (77.0 mg, 0.263 mmol, 87%) as a colorless solid.

^{1}H NMR (400 MHz, $CDCl_3$, major rotamer) δ/ppm 7.98 (s, 1H), 7.05 (dd, J = 17.7, 8.0 Hz, 1H), 6.72 (dd, J = 8.2, 2.3 Hz, 1H), 5.16 (s, 2H), 4.94–4.84 (m, 1H), 4.21 (td, J = 11.7, 8.8, 4.8 Hz, 2H), 3.61–3.49 (m, 1H), 3.48 (s, 3H), 3.19 (d, J = 16.1 Hz, 1H), 2.16 (s, 3H), 1.27 (t, J = 7.1 Hz, 3H).

Ethyl 1-acetyl-6-(methoxymethoxy)octahydro-1*H*-indole-2-carboxylate (3.61b)

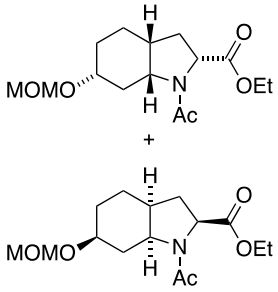

Rh/C (5% *w*/*w*, 52.9 mg, 25.7 µmol, 0.10 eq.) was added to a solution of racemic indoline **3.57** (75.0 mg, 0.257 mmol, 1.0 eq.) in MeOH (1.2 mL). The reaction mixture was stirred for 14 h at room temperature under H_2 pressure (50 bar). The catalyst was filtered off over Celite®, the Celite® was washed with MeOH (2 x 5 mL) and the solvent was removed under reduced pressure to obtain a 2:1 rotameric mixture of racemic octahydroindole **3.61b** (76.5 mg, 0.257 mmol, quant.) as a colorless oil.

^{1}H NMR (400 MHz, MeOD, major rotamer) δ/ppm 4.69 (s, 2H), 4.36 (dd, J = 10.2, 8.1 Hz, 1H), 4.17 (qd, J = 7.1, 3.0 Hz, 2H), 4.05 (dt, J = 12.1, 6.3 Hz, 1H), 3.52 (tt, J = 11.5, 3.7 Hz, 1H), 3.36 (s, 3H), 2.49–2.32 (m, 1H), 2.32–2.23 (m, 1H), 2.19 (ddd, J = 12.6, 8.2, 6.8 Hz, 1H), 2.11 (s, 3H), 2.04–1.93 (m, 1H), 1.88–1.80 (m, 2H), 1.80–1.70 (m, 1H), 1.61 (q, J = 12.1 Hz, 1H), 1.45–1.32 (m, 1H), 1.27 (t, J = 7.1 Hz, 3H).

D-*diepi*-Choi (3.59)

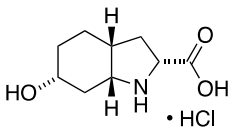

From **3.58**: Octahydroindole **3.58** (37.5 mg, 0.14 mmol, 1.0 eq.) was suspended in aq. HCl solution (6 M, 1.9 mL) and heated at reflux for 5 h. The H_2O was removed under reduced pressure to give D-*diepi*-Choi hydrochloride salt (**3.59**) (26.0 mg, 0.140 mmol, quant.) as a colorless solid, which was used without further purification.

From racemic **3.61b**: Octahydroindole **3.61b** (35.9 mg, 0.120 mmol, 1.0 eq.) was suspended in aq. HCl solution (6 M, 1.6 mL) and heated at reflux for 5 h. The H_2O was removed under reduced pressure to give racemic *diepi*-Choi hydrochloride salt (**3.59**) (26.6 mg, 0.120 mmol, quant.) as a colorless solid.

^{1}H NMR (400 MHz, MeOD) δ/ppm 4.45 (dd, J = 11.8, 4.2 Hz, 1H), 4.12–4.05 (m, 1H), 3.80 (dd, J = 4.5 Hz, 1H), 2.63 (ddd, J = 13.5, 11.7, 6.6 Hz, 1H), 2.45–2.37 (m, 1H), 2.18–2.03 (m, 2H), 1.97 (ddd, J = 15.1, 4.3, 2.8 Hz, 1H), 1.86–1.73 (m, 1H), 1.67–1.56 (m, 3H); **^{13}C NMR** (101 MHz, MeOD) δ/ppm 172.9, 65.9, 61.1, 58.7, 37.3, 35.3, 31.0, 30.6, 21.6.

2.2.2. Synthesis of the Agmantin Side Chain

1,3-Bis(*tert*-butoxycarbonyl)-2-methyl-2-thiopseudourea (3.63)

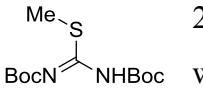

2-Methyl-2-thiopseudourea hemisulfate (**3.62**) (0.630 g, 4.49 mmol, 1.0 eq.) was dissolved in CH_2C1_2 (15 mL). Boc_2O (2.40 g, 10.8 mmol, 2.4 eq.) and sat. aq. $NaHCO_3$ solution (14.4 mL) were added to this solution at room temperature. The reaction mixture was stirred for 18 h at room temperature and was then diluted with CH_2Cl_2 (20 ml). The layers were separated and the aqueous layer was extracted with CH_2Cl_2 (2 x 20 mL) and the combined organic layers were washed with brine (10 mL), dried over Na_2SO_4 and the solvent was removed under reduced pressure. The crude product was purified by flash column chromatography (SiO_2, pentane/EtOAc 15:1) to give thiopseudourea derivative **3.63** (1.20 g, 4.13 mmol, 92%) as a colorless solid.

^{1}H NMR (400 MHz, $CDCl_3$) δ/ppm 2.40 (s, 3H), 1.51 (s, 18H); **^{13}C NMR** (101 MHz, $CDCl_3$) δ/ppm 171.6, 28.2, 14.6. The remaining ^{13}C signals could not be resolved.
Analytical data are in accordance with those reported in the literature.[15]

tert-Butyl (*Z*)-(*N*-(4-aminobutyl)-*N*'-(_tert_-butoxycarbonyl)carbamimidoyl)-λ^2-azane-carboxylate (3.64)

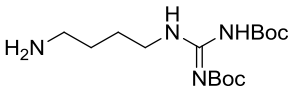

A solution of thiopseudourea derivative **3.63** (0.200 g, 0.689 mmol, 1.0 eq.) in THF (1.7 mL) was added dropwise to a solution of 1,4-butanediamine (0.17 mL, 1.72 mmol, 2.5 eq.) in THF (2.6 mL) and H_2O (0.1 mL) at room temperature. The resulting mixture was stirred for 1 h at 50 °C. $CHCl_3$ (20 mL) and sat. aq. $NaHCO_3$ solution (20 mL) were added, the layers were separated and the aqueous layer was extracted with $CHCl_3$ (2 x 20 mL). The combined organic layers were dried over $MgSO_4$ and the solvent was removed under reduced pressure to give agmantin side chain **3.64** (0.220 g, 0.666 mmol, 97%) as a colorless solid.

Mp = 86.7–87.5 °C; **FTIR** $\tilde{\nu}$/cm^{-1} 3335, 3134, 2979, 2933, 2866, 1715, 1633, 1611, 1568, 1475, 1452, 1413, 1392, 1366, 1324, 1286, 1251, 1227, 1152, 1125, 1051, 1024, 926, 877, 852, 808, 757, 663, 617, 505, 461; **^{1}H NMR** (400 MHz, $CDCl_3$) δ/ppm 11.49 (s, 1H), 8.33 (s, 1H), 3.43 (td, J = 7.1, 5.2 Hz, 2H), 2.72 (t, J = 6.9 Hz, 2H), 1.67–1.57 (m, 2H), 1.55–1.45 (m, 2H) 1.50 (s, 9H), 1.49 (s, 9H); **^{13}C NMR** (101 MHz, $CDCl_3$) δ/ppm 163.8, 156.3, 153.5, 83.2, 79.4, 42.0, 40.9, 31.1, 28.5, 28.2, 26.6; **HRMS ESI** m/z calc. for $C_{15}H_{31}N_4O_4$ $[M+H]^+$: 331.2340, found: 331.2336.

Analytical data are in accordance with those reported in the literature.[16]

2.2.3. Synthesis of the L-Hpla building block

(*S*)-2-Amino-3-(4-(benzyloxy)phenyl)propanoic acid (3.66)

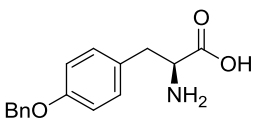

L-Tyrosine (**3.65**) (3.10 g, 17.1 mmol, 1.0 eq.) was dissolved in aq. NaOH solution (2 M, 17 mL). A solution of $CuSO_4 \cdot 5H_2O$ (2.13 g, 8.55 mmol, 0.50 eq.) in H_2O (12.8 mL) was added and the reaction mixture was stirred for 15 min at room temperature. The mixture was diluted with MeOH (64 mL) and additional aq. NaOH solution (2 M, 2.6 ml) was added. After stirring for 30 min at room temperature, benzyl bromide (2.05 mL, 17.1 mmol, 1.0 eq.) was added and the mixture was stirred for 16 h. The blue-violet precipitate was filtered off and the filter cake was washed with H_2O/MeOH (3:1, 40 mL) and MeOH (5 mL). The solid was washed with aq. HCl solution (1 M, 6 x 15 mL), H_2O (2 x 10 mL), aq. NH_4OH solution (2 M, 5 x 10 mL) and H_2O (2 x 10 mL) to give tyrosine derivative **3.66** (3.37 g, 12.4 mmol, 62%) as a colorless solid which was used without further purification.

(*S*)-2-Acetoxy-3-(4-(benzyloxy)phenyl)propanoic acid (3.67)

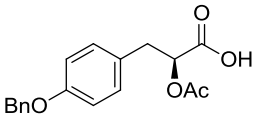

Isoamyl nitrite (1.74 mL, 12.9 mmol, 3.5 eq.) and NaOAc (1.06 g, 12.9 mmol, 3.5 eq.) were slowly added to a solution of tyrosine derivative **3.66** (1.0 g, 3.69 mmol, 1.0 eq.) in glacial acetic acid (15 mL). The reaction mixture was stirred for 24 h at room temperature before the acetic acid was removed under reduced pressure. The obtained residue was partitioned between aq. HCl solution (1 M, 20 mL) and EtOAc (20 mL). The layers were separated and the aqueous layer was extracted with EtOAc (3 x 20 mL). The combined organic layers were washed with H_2O (10 mL) and brine (10 mL), dried over $MgSO_4$ and the solvent was removed under reduced pressure. The crude product was purified by flash column chromatography (SiO_2, pentane/EtOAc/AcOH 1:9:1) to give L-Hpla building block **3.67** (0.800 g, 2.55 mmol, 69%) as a colorless solid.

Optical rotation $[\alpha]_D^{25}$ **=** –4.7 (*c* = 0.44, $CHCl_3$); **FTIR** $\tilde{\nu}$/cm^{-1} 3033, 1742, 1611, 1585, 1513, 1454, 1375, 1235, 1178, 1114, 1075, 1042, 1026, 917, 829, 736, 697, 609, 525; **^{1}H NMR** (400 MHz, $CDCl_3$) δ/ppm 7.46–7.32 (m, 6H), 7.20–7.13 (m, 2H), 6.96–6.84 (m, 2H), 5.21 (dd, *J* = 8.7, 4.1 Hz, 1H), 5.05 (s, 2H), 3.17 (dd, *J* = 14.5, 4.2 Hz, 1H), 3.07 (dd, *J* = 14.4, 8.7 Hz, 1H), 2.09 (s, 3H); **^{13}C NMR** (101 MHz, $CDCl_3$) δ/ppm 170.5, 158.1, 137.1, 130.5, 128.7, 128.1, 127.6, 115.0, 72.8, 70.2, 36.5, 20.7.

Analytical data are in accordance with those reported in the literature.[17]

2.2.4. Assembly of the Different Building Blocks – Synthesis of AKT608A

Methyl (2*R*,3a*R*,6*R*,7a*R*)-1-((*tert*-butoxycarbonyl)-D-phenylalanyl)-6-hydroxyoctahydro-1*H*-indole-2-carboxylate (3.71)

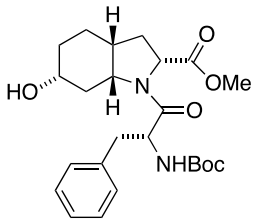

$SOCl_2$ (30.0 µL, 0.150 mmol, 1.1 eq.) was added dropwise to a solution of D-*diepi*-Choi hydrochloride salt (**3.59**) (26.0 mg, 0.140 mmol, 1.0 eq.) in MeOH (0.9 mL) at 0 °C. The reaction mixture was stirred for 4 h at 70 °C. The solvent was removed under reduced pressure to give the corresponding D-*diepi*-Choi methyl ester hydrochloride salt (**3.70**) which was dissolved in CH_2Cl_2 (3.0 mL). Boc-D-Phe-OH (**3.69**) (48.3 mg, 0.180 mmol, 1.3 eq.) was added to this solution. The mixture was cooled to 0 °C before PyBOP (94.7 mg, 0.180 mmol, 1.3 eq.) and NMM (53.9 µL, 0.490 mmol, 3.5 eq.) were added. The reaction mixture was stirred for 30 min at 0 °C and further for 72 h at room temperature The solvent was removed under reduced pressure and the crude residue directly purified by flash column chromatography (SiO_2, pentane/EtOAc 1:1) to give a 3:1 rotameric mixture of dipeptide **3.71** (40.2 mg, 90.0 µmol, 64%) as a colorless, viscous oil.

R_f = 0.43 (SiO_2, pentane/EtOAc 1:1); **Optical rotation** $[\alpha]_D^{25}$ **=** +8.7 (*c* = 0.10, $CHCl_3$); **FTIR** $\tilde{\nu}$/cm^{-1} 2933, 2866, 1741, 1703, 1635, 1498, 1439, 1366, 1249, 1053, 1022, 984, 844, 700, 661; **^{1}H NMR** (400 MHz, $CDCl_3$, major rotamer) δ/ppm 7.28–7.13 (m, 5H), 5.31 (dd, *J* = 12.8, 8.7 Hz, 1H), 5.02 (d, *J* = 9.4 Hz, 1H), 4.51 (q, *J* = 7.1 Hz, 1H), 4.38 (dd, *J* = 10.4, 8.0 Hz, 1H), 4.23–4.09 (m, 1H), 3.70 (s, 3H), 3.41 (tq, *J* = 11.7, 4.0 Hz, 1H), 3.35–3.26 (m, 1H), 3.08 (dd, *J* = 13.0, 6.6 Hz, 1H), 2.96 (dd, *J* = 12.8, 4.6 Hz, 1H), 2.83–2.78 (m, 1H), 2.26 (dt, *J* = 13.0, 6.4 Hz, 1H), 2.06 (dt, *J* = 12.5, 7.4 Hz, 1H), 1.88 (dd, *J* = 12.9, 10.4 Hz, 1H), 1.76–1.40 (m, 3H), 1.30 (s, 9H); **^{13}C NMR** (101 MHz, $CDCl_3$, major rotamer) δ/ppm 172.4, 171.3, 155.4, 136.7, 129.8, 129.5, 128.6, 126.9, 80.0, 68.3, 59.3, 57.8, 53.0, 52.4, 37.7, 36.6, 29.2, 28.5, 28.4, 22.9; **HRMS ESI** *m*/*z* calc. for $C_{24}H_{35}N_2O_6$ $[M+H]^+$: 447.2490, found: 447.2493.

Methyl (2*R*,3a*R*,6*R*,7a*R*)-1-(((*S*)-2-acetoxy-3-(4-(benzyloxy)phenyl)propanoyl)-D-phenylalanyl)-6-hydroxyoctahydro-1*H*-indole-2-carboxylate (3.73)

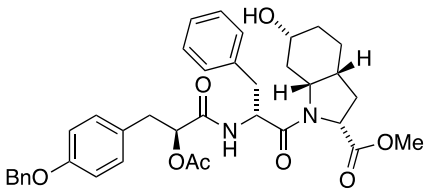

Dipeptide **3.71** (34.6 mg, 80.0 µmol, 1.0 eq.) was dissolved in CH_2Cl_2 (1.0 mL) and cooled to 0 °C. TFA (0.2 mL) was added and the mixture was stirred for 1 h at 0 °C. TFA and CH_2Cl_2 were removed under reduced pressure to obtain crude dipeptide **3.72**. The obtained residue was dissolved in CH_2Cl_2 (0.5 mL) and NMM (14.0 µL, 0.130 mmol, 1.6 eq.) was added. The obtained solution was treated with an ice-cooled solution of L-Hpla-OH derivate **3.67** (30.2 mg, 96.0 µmol, 1.2 eq.) in CH_2Cl_2 (1 mL) which had been stirring for 30 min at 0 °C with PyBOP (50.0 mg, 96.0 µmol, 1.2 eq.) and NMM (17.6 µL, 0.160 mmol, 2.0 eq.). The reaction mixture was stirred for 36 h at room temperature. CH_2Cl_2 (5 mL) was added and the solution was washed with aq. HCl solution (1 M, 3 x 2 mL), sat. aq. $NaHCO_3$ solution (2 mL) and brine (2 mL). The organic layer was dried over Na_2SO_4 and the solvent was removed under reduced pressure. The crude residue was purified by flash column chromatography (SiO_2, pentane/EtOAc 1:1) to give a 3:1 rotameric mixture of tripeptide **3.73** (31.0 mg, 48.2 µmol, 60%) as a colorless, viscous oil.

R_f = 0.31 (SiO_2, pentane/EtOAc 1:2); **Optical rotation** $[\alpha]_D^{25}$ **=** –3.84 (*c* = 0.25, $CHCl_3$); **FTIR** $\tilde{\nu}$/cm^{-1} 3276, 3063, 3036, 2360, 2342, 1743, 1678, 1627, 1512, 1254, 1370, 1299, 1232, 1177, 1059, 1027, 920, 755, 700, 669, 607; **^{1}H NMR** (400 MHz, $CDCl_3$, major rotamer) δ/ppm 7.38–7.28 (m, 4H), 7.27–7.15 (m, 4H), 7.14–7.02 (m, 2H), 6.98–6.93 (m, 2H), 6.79–6.74 (m, 2H), 6.48 (d, *J* = 8.5 Hz, 1H), 5.26 (dt, *J* = 7.9, 4.8 Hz, 1H), 5.18 (dd, *J* = 7.7, 4.4 Hz, 1H), 4.95 (s, 2H), 4.82–4.72 (m, 1H), 4.34 (dd, *J* = 10.4, 8.0 Hz, 1H), 4.14 (dt, *J* = 12.2, 6.1 Hz, 1H), 3.68 (s, 3H), 3.49–3.39 (m, 1H), 3.07 (dd, *J* = 13.8, 7.1 Hz, 1H), 2.97 (dd, *J* = 14.4, 4.5 Hz, 1H), 2.86 (dd, *J* = 14.4, 7.7 Hz, 1H), 2.78 (dd, *J* = 13.8, 6.6 Hz, 1H), 2.29–2.19 (m, 1H), 2.10–1.97 (m, 2H), 1.91 (s, 3H), 1.77–1.52 (m, 3H), 1.40–1.13 (m, 3H); **^{13}C NMR** (101 MHz, $CDCl_3$, major rotamer) δ/ppm 172.3, 169.8, 169.4, 168.9, 157.9, 137.1, 135.9, 130.6, 129.9, 128.70, 128.66, 128.2, 128.1, 127.7, 127.64, 127.61, 127.2, 114.8, 74.3, 70.1, 68.4, 59.3, 57.9, 52.4, 51.2, 39.2, 37.7, 37.1, 36.7, 29.2, 22.9, 20.9; **HRMS ESI** *m*/*z* calc. for $C_{37}H_{43}N_2O_8$ $[M+H]^+$: 643.3014, found: 643.3017.

(2*R*,3a*R*,6*R*,7a*R*)-1-(((*S*)-3-(4-(Benzyloxy)phenyl)-2-hydroxypropanoyl)-D-phenylalanyl)-6-hydroxyoctahydro-1*H*-indole-2-carboxylic acid (3.74)

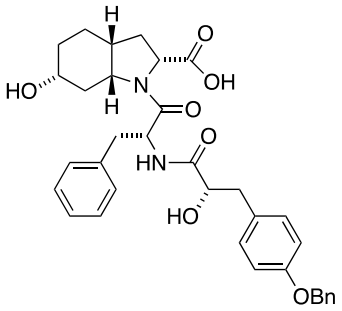

At 0 °C, a solution of LiOH (2.87 mg, 0.120 mmol, 3.0 eq.) in H_2O (1.2 mL) was added dropwise to a solution of tripeptide methyl ester **3.73** (25.7 mg, 40.0 µmol, 1.0 eq.) in THF (1 mL). The obtained suspension was stirred for 20 h at room temperature. The solvents were removed under reduced pressure and the obtained residue was dissolved in H_2O (5 mL) and washed with Et_2O (2 x 5 mL). The aqueous layer was acidified with aq. HCl solution (1 M, 0.2 mL) and extracted with CH_2Cl_2/^{i}PrOH (4:1, 4 x 5 mL). The combined organic layers were dried over Na_2SO_4 and the solvent was removed under reduced pressure to give carboxyl tripeptide **3.74** (23.5 mg, 0.120 mmol, quant.) as a colorless solid, which was used without further purification.

***tert*-Butyl ((*Z*)-*N*-(4-((2*R*,3a*R*,6*R*,7a*R*)-1-(((*S*)-3-(4-(benzyloxy)phenyl)-2-hydroxypropanoyl)-D-phenylalanyl)-6-hydroxyoctahydro-1*H*-indole-2-carboxamido)butyl)-*N*'-(*tert*-butoxycarbonyl)carbamimidoyl)-λ^2-azanecarboxylate (3.75)**

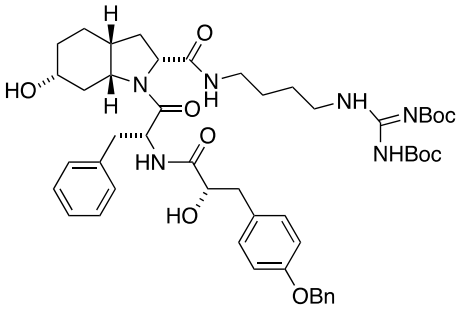

Crude tripeptidic acid **3.74** (23.5 mg, 40.0 µmol, 1.0 eq.) and agmantine side chain **3.64** (17.6 mg, 53.2 µmol, 1.3 eq.) were dissolved in DMF (1 mL) and cooled to 0 °C. PyBOP (20.8 mg, 40.0 mmol, 1.0 eq.) and NMM (11.0 µL, 0.100 mmol, 2.5 eq.) were added and the mixture was stirred for 30 min at 0 °C and further 48 h at room temperature. EtOAc (10 mL) was added and the solution was washed with sat. aq. $NaHCO_3$ solution (5 mL) and H_2O (4 x 5 mL). The combined aqueous layers were extracted with EtOAc (5 mL) and the combined organic layers were dried over Na_2SO_4. The solvent was removed under reduced pressure and the crude residue was purified by flash column chromatography (SiO_2, EtOAc/MeOH 50:1) to give a 3:1 rotameric mixture of tetrapeptide **3.75** (22.0 mg, 24.0 µmol, 61%) as a colorless amorphous solid.

R_f = 0.72 (SiO_2, EtOAc/MeOH 2:1); **FTIR** $\tilde{\nu}$/cm^{-1} 3391, 2928, 2860, 1720, 1627, 1511, 1455, 1416, 1367, 1330, 1230, 1134, 1053, 1027, 801, 752, 698, 668, 649, 611; **^{1}H NMR**

(400 MHz, $CDCl_3$, major rotamer) δ/ppm 11.49 (s, 1H), 8.31 (t, J = 5.4 Hz, 1H), 7.46–7.34 (m, 4H), 7.33–7.19 (m, 4H), 7.18–7.13 (m, 1H), 7.12–7.04 (m, 2H), 6.96–6.83 (m, 2H), 6.65 (t, J = 5.9 Hz, 1H), 5.03 (s, 2H), 4.87 (q, J = 8.0 Hz, 1H), 4.43 (t, J = 8.8 Hz, 1H), 4.31–4.18 (m, 2H), 3.52–3.36 (m, 2H), 3.34–3.02 (m, 3H), 2.99–2.86 (m, 1H), 2.81–2.68 (m, 1H), 2.37 (td, J = 12.9, 9.1 Hz, 1H), 2.24–2.13 (m, 1H), 2.03–1.72 (m, 2H), 1.69–1.53 (m, 1H), 1.49 (s, 9H), 1.47 (s, 9H); **^{13}C NMR** (101 MHz, $CDCl_3$, major rotamer) δ/ppm 172.5, 170.9, 170.7, 163.7, 158.1, 156.3, 153.4, 137.1, 136.1, 130.6, 129.5, 128.9, 128.8, 128.74, 128.70, 128.1, 127.7, 127.5, 115.2, 83.3, 79.4, 72.9, 70.2, 68.6, 59.9, 58.8, 51.9, 40.7, 40.0, 39.5, 39.3, 37.3, 36.3, 29.8, 28.4, 28.2, 27.0, 26.8, 23.0; **HRMS ESI** m/z calc. for $C_{49}H_{67}N_6O_{10}$ $[M+H]^+$: 899.4913, found: 899.4919.

Aeruginosin KT608A (3.1)

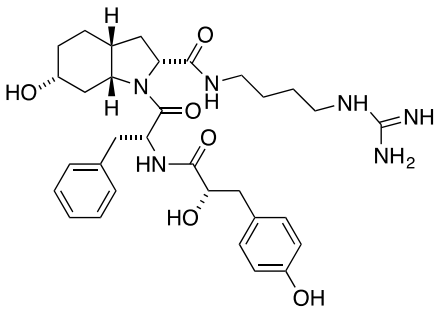

Tetrapeptide **3.75** (4.00 mg, 4.45 µmol, 1.0 eq.) was dissolved in MeCN (0.3 mL). Aq. HCl solution (6 M, 60 µL) was added and the reaction mixture was stirred for 24 h at room temperature. The solvent was removed under reduced pressure and the obtained residue was dissolved in EtOAc/MeOH (1:1, 0.3 mL). Pd/C (10% *w*/*w*, 1.70 mg, 1.60 µmol, 0.36 eq.) was added and the reaction mixture was stirred for 12 h under a H_2 atmosphere. Additional Pd/C (10% *w*/*w*, 1.70 mg, 1.60 µmol, 0.36 eq.) was added and the reaction mixture was stirred for 24 h at room temperature. The catalyst was filtered off over a short pad of Celite® and the Celite® was washed with MeOH (2 x 3 mL). The solvents were removed under reduced pressure and the obtained crude residue was purified by reversed phase HPLC (MeCN/H_2O + 0.1% formic acid) to obtain a 3:1 rotameric mixture of aeruginosin KT608A (**3.1**) (1.00 mg, 1.65 µmol, 37%) as a white amorphous solid.

^{1}H NMR (600 MHz, DMSO-d_6, major rotamer) δ/ppm 9.27 (s, 1H), 8.61 (s, 1H), 7.97–7.90 (m, 2H), 7.32–7.18 (m, 6H), 6.87 (d, J = 8.4 Hz, 2H), 6.61–6.56 (m, 2H), 5.32 (s, 1H), 4.66 (td, J = 8.9, 4.6 Hz, 1H), 4.27–4.21 (m, 2H), 4.02–3.84 (m, 1H), 3.39–3.31 (m, 1H), 3.13–3.01 (m, 3H), 2.91 (dd, J = 14.1, 4.5 Hz, 1H), 2.82 (dd, J = 14.1, 9.3 Hz, 1H), 2.64 (dd, J = 13.9, 3.9 Hz, 1H), 2.43 (dd, J = 13.8, 8.3 Hz, 1H), 2.17–2.08 (m, 1H), 2.01–1.94 (m, 1H), 1.92–1.86 (m, 1H), 1.86–1.78 (m, 1H), 1.77–1.66 (m, 1H), 1.64–1.54 (m, 2H), 1.53–1.42 (m, 2H), 1.31–1.17 (m, 1H).; **^{13}C NMR** (151 MHz, DMSO-d_6, major rotamer) δ/ppm 173.1,

171.1, 169.3, 157.3, 155.6, 137.4, 130.2, 129.2, 128.24, 128.16, 126.4, 114.6, 72.0, 66.9, 59.8, 57.3, 50.9, 40.3, 39.9, 37.9, 37.8, 36.0, 30.6, 29.2, 26.3, 25.8, 22.7. **LRMS ESI** *m/z* calc. for $C_{32}H_{45}N_6O_6$ $[M+H]^+$: 609.3, found: 609.3.

2.2.5. Synthesis of Indoline 3.56 via C-H Activation

Methyl picolinoyl-L-tyrosinate (3.84)

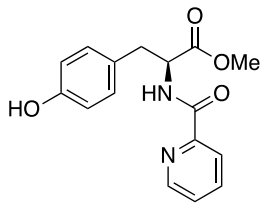

Tyrosine methyl ester (**3.83**) (3.51 g, 18.0 mmol, 1.0 eq.) was dissolved in CH_2Cl_2 (90 mL). 2-picolinic acid (2.44 g, 19.8 mmol, 1.1 eq.), benzotriazol-1-ol (2.68 g, 19.8 mmol, 1.1 eq.), EDC (3.80 g, 19.8 mmol, 1.1 eq.) and DIPEA (8.89 mL, 53.8 mmol, 2.9 eq.) were added and the reaction mixture was stirred for 16 h at room temperature. H_2O (40 mL) was added, the layers were separated and the aqueous layer was extracted with CH_2Cl_2 (2 x 60 mL). The combined organic layers were washed with H_2O (20 mL) and brine (20 mL) and dried over Na_2SO_4. The solvent was removed under reduced pressure and the residue was purified by flash column chromatography (SiO_2, pentane/EtOAc 1:1) to give methyl picolinoyl-L-tyrosinate (**3.84**) (3.00 g, 9.99 mmol, 56%) as a very viscous, colorless oil.

R_f = 0.39 (SiO_2, pentane/EtOAc 1:1); **Optical rotation** $[\alpha]_D^{25}$ **=** +45.9 (*c* = 0.23, $CHCl_3$); **FTIR** $\tilde{\nu}$/cm^{-1} 3366, 3067, 3011, 2950, 1739, 1658, 1615, 1513, 1465, 1434, 1364, 1267, 1215, 1172, 1109, 998, 841, 820, 748, 734, 698, 620, 535, 490; **^{1}H NMR** (400 MHz, $CDCl_3$) δ/ppm 8.55 (ddd, *J* = 4.8, 1.7, 0.9 Hz, 1H), 8.51 (d, *J* = 8.6 Hz, 1H), 8.14 (ddd, *J* = 7.8, 0.9 Hz, 1H), 7.83 (td, *J* = 7.7, 1.7 Hz, 1H), 7.42 (ddd, *J* = 7.6, 4.8, 1.2 Hz, 1H), 7.07–6.99 (m, 2H), 6.78–6.68 (m, 2H), 5.03 (ddd, *J* = 8.5, 6.6, 5.7 Hz, 1H), 3.73 (s, 3H), 3.20 (dd, *J* = 14.0, 5.7 Hz, 1H), 3.11 (dd, *J* = 14.0, 6.7 Hz, 1H); **^{13}C NMR** (101 MHz, $CDCl_3$) δ/ppm 172.1, 164.3, 155.2, 149.3, 148.5, 137.5, 130.5, 127.8, 126.6, 122.5, 115.7, 53.8, 52.5, 37.7; **HRMS ESI** *m/z* calc. for $C_{16}H_{17}N_2O_4$ $[M+H]^+$: 301.1183, found: 301.1180.

Methyl (*S*)-3-(4-methoxyphenyl)-2-(picolinamido)propanoate (3.87)

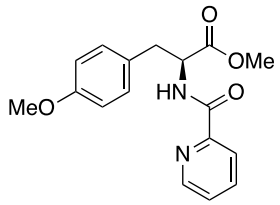

A suspension of methyl picolinoyl-L-tyrosinate (**3.84**) (2.22 g, 7.40 mmol, 1.0 eq.) and K_2CO_3 (1.33 g, 9.62 mmol, 1.3 eq.) in DMF (5 mL) was treated with MeI (0.51 mL, 8.14 mmol, 1.1 eq.) and stirred at room temperature for 17 h. The solvent was removed under reduced pressure and the residue was suspended in H_2O (50 mL). The aqueous layer was extracted with EtOAc (3 x 50 mL) and the combined organic layers were washed with brine (20 mL), dried over Na_2SO_4 and the solvent was removed under reduced pressure. The obtained crude residue was purified by flash column chromatography (SiO_2, pentane/EtOAc 5:1) to give picoline tyrosinate derivative **3.87** (2.20 g, 7.00 mmol, 95%) a colorless oil.

R_f = 0.20 (SiO_2, pentane/EtOAc 5:1); **Optical rotation** $[\alpha]_D^{25}$ **=** +57.5 (*c* = 1.09, $CHCl_3$); **FTIR** $\tilde{\nu}$/cm^{-1} 3385, 3006, 2955, 1739, 1674, 1612, 1509, 1465, 1433, 1362, 1301, 1246, 1213, 1177, 1112, 1032, 998, 839, 820, 750, 699, 620, 539; **^{1}H NMR** (400 MHz, $CDCl_3$) δ/ppm 8.55 (ddd, *J* = 4.8, 1.7, 0.9 Hz, 1H), 8.52–8.48 (m, 1H), 8.16 (dt, *J* = 7.8, 1.1 Hz, 1H), 7.84 (td, *J* = 7.7, 1.7 Hz, 1H), 7.43 (ddd, *J* = 7.6, 4.8, 1.2 Hz, 1H), 7.10 (d, *J* = 8.7 Hz, 2H), 6.81 (d, *J* = 8.7 Hz, 2H), 5.02 (dt, *J* = 8.3, 6.1 Hz, 1H), 3.77 (s, 3H), 3.73 (s, 3H), 3.24–3.13 (m, 2H); **^{13}C NMR** (101 MHz, $CDCl_3$) δ/ppm 172.0, 164.0, 158.8, 149.4, 148.3, 137.5, 130.4, 128.1, 126.5, 122.5, 114.1, 55.3, 53.8, 52.4, 37.6; **HRMS ESI** *m/z* calc. for $C_{17}H_{19}N_2O_4$ $[M+H]^+$: 315.1339, found: 315.1339.

Methyl (*S*)-6-methoxy-1-picolinoylindoline-2-carboxylate (3.90)

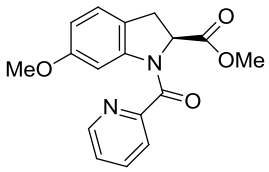

$PhI(OAc)_2$ (653 mg, 1.99 mmol, 2.5 eq.) and $Pd(OAc)_2$ (17.8 mg, 80.0 mmol, 0.10 eq.) were added to a solution of picoline tyrosinate derivative **3.87** (250 mg, 0.795 mmol, 1.0 eq.) in toluene (8 mL). The reaction mixture was stirred for 20 h at 60 °C. The solvent was removed under reduced pressure and the obtained residue purified by flash column chromatography (SiO_2, pentane/EtOAc 3:2) to give indoline **3.90** (113 mg, 0.360 mmol, 46%) as a colorless oil.

R_f = 0.53 (SiO_2, pentane/EtOAc 1:1); **Optical rotation** $[\alpha]_D^{25}$ **=** –46.7 (*c* = 1.03, $CHCl_3$); **FTIR** $\tilde{\nu}$/cm^{-1} 3006, 2959, 2833, 1742, 1648, 1497, 1436, 1387, 1334, 1284, 1232, 1199, 1174, 1160, 1105, 1030, 1010, 997, 911, 852, 811, 728, 691; **^{1}H NMR** (400 MHz, $CDCl_3$) *δ*/ppm 8.52 (d, *J* = 3.4 Hz, 1H), 8.18–8.04 (m, 2H), 7.85 (t, *J* = 7.8 Hz, 1H), 7.38 (t, *J* = 6.3 Hz, 1H), 7.07 (d, *J* = 8.2 Hz, 1H), 6.66 (d, *J* = 8.3 Hz, 1H), 5.83 (d, *J* = 11.0 Hz, 1H), 3.86 (s, 3H), 3.63 (s, 3H), 3.56 (dd, *J* = 15.9, 11.1 Hz, 1H), 3.18 (d, *J* = 15.9 Hz, 1H); **^{13}C NMR** (101 MHz, $CDCl_3$) *δ*/ppm 172.9, 165.5, 159.7, 153.2, 147.2, 144.9, 137.3, 125.5, 125.2, 124.5, 121.1, 111.3, 104.1, 63.6, 55.7, 52.4, 33.2; **HRMS ESI** *m*/*z* calc. for $C_{17}H_{17}N_2O_4$ $[M+H]^+$: 313.1183, found: 313.1185.

Ethyl (*S*)-6-methoxyindoline-2-carboxylate (3.91)

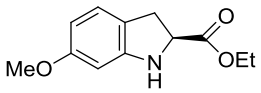

Indoline **3.90** (40.0 mg, 0.128 mmol, 1.0 eq.) was dissolved in aq. HCl solution (6 M, 3 mL) at room temperature and stirred at 100 °C for 2 h. The reaction mixture was let to cool to room temperature and the solvent was removed under reduced pressure to give (*S*)-6-methoxyindoline-2-carboxylic acid as crude product which was subsequently dissolved in EtOH (5 mL) and cooled to 0 °C. $SOCl_2$ (28.0 µL, 0.384 mmol, 3.0 eq.) was added dropwise and the reaction mixture was stirred for 3 h at 79 °C. The solvent was removed under reduced pressure and the obtained crude residue was purified by flash column chromatography (SiO_2, pentane/EtOAc 1:1) to give indoline ethyl ester **3.91** (4.00 mg, 18.0 µmol, 14%) as a colorless oil.

^{1}H NMR (400 MHz, $CDCl_3$) δ/ppm 6.97 (dt, J = 8.4, 1.2 Hz, 1H), 6.40 (d, J = 2.3 Hz, 1H), 6.34 (dd, J = 8.1, 2.3 Hz, 1H), 4.43 (dd, J = 10.3, 5.2 Hz, 1H), 4.21 (qd, J = 7.1, 1.0 Hz, 2H), 3.75 (s, 3H), 3.36 (ddd, J = 15.6, 10.3, 1.1 Hz, 1H), 3.25 (dd, J = 15.5, 5.2 Hz, 1H), 1.29 (t, J = 7.1 Hz, 3H).

Ethyl (*S*)-1-acetyl-6-methoxyindoline-2-carboxylate (3.56)

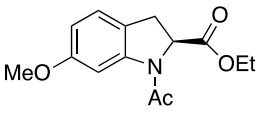

Indoline **3.91** (4.00 mg, 18.0 µmol, 1.0 eq.) was dissolved in CH_2Cl_2 (0.5 mL) and acetic anhydride (4.37 µL, 45.3 µmol, 2.5 eq.), Et_3N (6.36 µL, 45.3 µmol, 2.5 eq.) and DMAP (0.220 mg, 1.81 µmol, 0.10 eq.) were added. The reaction mixture was stirred for 16 h at room temperature before CH_2Cl_2 (5 mL) was added. The organic layer was washed with sat. aq. $NaHCO_3$ solution (2 mL), dried over $MgSO_4$ and the solvent was removed under reduced pressure. The obtained crude residue was purified by flash column chromatography (SiO_2, pentane/EtOAc 4:1) to give a 2:1 rotameric mixture of (–)-indoline **3.56** (3.40 mg, 13.0 µmol, 71%) as a colorless solid.

R_f = 0.37 (SiO_2, pentane/EtOAc 4:1); **Optical rotation** $[\alpha]_D^{25}$ **=** –79.4 (c = 0.17, $CHCl_3$); **^{1}H NMR** (400 MHz, $CDCl_3$, major rotamer) δ/ppm 7.91 (s, 1H), 7.01 (d, J = 8.1 Hz, 1H), 6.57 (d, J = 8.9 Hz, 1H), 4.89 (dd, J = 10.8, 2.6 Hz, 1H), 4.32–4.09 (m, 2H), 3.80 (s, 3H), 3.55 (dd, J = 16.0, 10.8 Hz, 1H), 3.18 (d, J = 16.5 Hz, 1H), 2.16 (s, 3H), 1.27 (t, J = 7.1 Hz, 3H); **^{1}H NMR** (400 MHz, $CDCl_3$, minor rotamer) δ/ppm 7.08 (d, J = 8.3 Hz, 1H), 6.76 (s, 1H), 6.61–6.54 (m, 1H), 5.13 (d, J = 10.7 Hz, 1H), 4.32–4.09 (m, 2H), 3.80 (s, 3H), 3.39 (dd, J = 16.2, 10.9 Hz, 1H), 3.00 (d, J = 16.0 Hz, 1H), 2.47 (s, 3H), 1.27 (t, J = 7.1 Hz, 3H).

2.2.6. Synthesis of D-diepi-Choi 3.110

D-Tyrosine methyl ester hydrochloride (3.96)

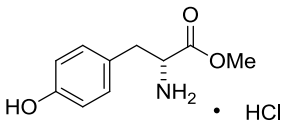

$SOCl_2$ (4.01 mL, 55.2 mmol, 2.0 eq.) was added dropwise to a suspension of D-tyrosine (**3.95**) (5.00 g, 27.6 mmol, 1.0 eq.) in MeOH (37 mL) at 0 °C. The solution was stirred for 20 min at 0 °C and further 12 h at 67 °C. The reaction mixture was allowed to reach room temperature and the solvent was removed under reduced pressure to obtain D-tyrosine methyl ester hydrochloride (**3.96**) (6.40 g, 27.6 mmol, quant.) as a colorless solid which was used without further purification.

^{1}H NMR (400 MHz, MeOD) δ/ppm 7.14–7.02 (m, 2H), 6.82–6.75 (m, 2H), 4.24 (dd, J = 7.3, 6.0 Hz, 1H), 3.81 (s, 3H), 3.17 (dd, J = 14.5, 6.0 Hz, 1H), 3.08 (dd, J = 14.5, 7.4 Hz, 1H); **^{13}C NMR** (101 MHz, MeOD) δ/ppm 170.5, 158.4, 131.5, 125.6, 116.9, 55.4, 53.5, 36.6.
Analytical data are in accordance with those reported in the literature.[18]

Methyl (*R*)-2-amino-3-(4-((*tert*-butyldimethylsilyl)oxy)phenyl)propanoate (3.97)

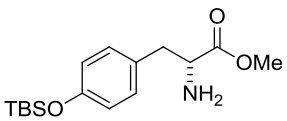

Imidazole (4.14 g, 60.8 mmol, 2.2 eq.) and TBSCl (5.80 mL, 33.2 mmol, 1.2 eq.) were added to a solution of D-tyrosine methyl ester hydrochloride (**3.97**) (6.40 g, 27.6 mmol, 1.0 eq.) in CH_2Cl_2 (90 mL). The reaction mixture was stirred at room temperature for 16 h before quenching with sat. aq. NH_4Cl solution (50 mL). The layers were separated and the aqueous layer was extracted with CH_2Cl_2 (3 x 100 mL). The combined organic layers were dried over $MgSO_4$ and the solvent was removed under reduced pressure to obtain TBS protected tyrosine methyl ester **3.97** (7.40 g, 23.9 mmol, 87%) as a very viscous colorless oil which was used without further purification.

^{1}H NMR (400 MHz, $CDCl_3$) δ/ppm 7.10–6.95 (m, 2H), 6.86–6.70 (m, 2H), 3.70 (s, 3H), 3.00 (dd, J = 13.6, 5.3 Hz, 1H), 2.80 (dd, J = 13.6, 7.7 Hz, 1H), 1.43 (s, 2H), 0.97 (s, 9H), 0.18 (s, 6H).
Analytical data are in accordance with those reported in the literature.[18]

Pyridine-2-sulfonyl chloride

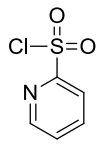

A two necked flask was charged with 2-mercaptopyridine (5.00 g, 45.0 mmol, 1.0 eq.) and sulphuric acid (96-98% *w*/*w*, 73 mL). The reaction mixture was cooled to 0 °C in an ice bath and aq. sodium hypochlorite solution (13% *w*/*w*, 220 mL) was slowly added with a dropping funnel over a period of 1.5 h. Vigorous chlorine gas evolution was observed upon addition. After the addition was complete, the reaction mixture was stirred for 20 min at 0 °C before CH_2Cl_2 (400 mL) was added. The layers were separated and the aqueous layer was extracted with CH_2Cl_2 (400 mL). The combined organic layers were washed with brine (100 mL), dried over $MgSO_4$ and the solvent was removed under reduced pressure to give pyridine-2-sulfonyl chloride (5.40 g, 30.4 mmol, 67%) as a colorless oil which was used without further purification.

^{1}H NMR (400 MHz, $CDCl_3$) δ/ppm 8.88–8.78 (m, 1H), 8.12 (ddt, J = 7.9, 1.5, 0.8 Hz, 1H), 8.06 (ddd, J = 8.0, 7.5, 1.7 Hz, 1H), 7.69 (ddd, J = 7.5, 4.7, 1.3 Hz, 1H); **^{13}C NMR** (101 MHz, $CDCl_3$) δ/ppm 159.4, 150.8, 139.2, 129.2, 122.1.
Analytical data are in accordance with those reported in the literature.[19]

Methyl (*R*)-3-(4-((*tert*-butyldimethylsilyl)oxy)phenyl)-2-(pyridine-2-sulfonamido)-propanoate (3.98)

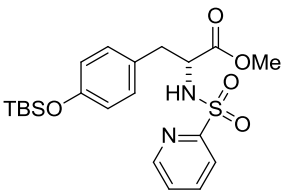

Et_3N (4.76 mL, 33.9 mmol, 1.50 eq.) was added to a solution of TBS protected tyrosine methyl ester **3.97** (6.99 g, 22.6 mmol, 1.0 eq.) and pyridine-2-sulfonyl chloride (4.39 g, 24.9 mmol, 1.1 eq.) in CH_2Cl_2 (70 mL). The reaction mixture was stirred for 16 h at room temperature, then the solvent was removed under reduced pressure. The crude product was purified by flash column chromatography (SiO_2, pentane/EtOAc 1:1) to give sulfonamide **3.98** (7.30 g, 16.2 mmol, 72%) as a very viscous, colorless oil.

R_f = 0.61 (SiO_2, pentane/EtOAc 1:1); **Optical rotation** $[\alpha]_D^{25}$ **=** –5.9 (*c* = 1.0, $CHCl_3$); **FTIR** $\tilde{\nu}$/cm^{-1} 3723, 2955, 2931, 2856, 1739, 1510, 1428, 1345, 1251, 1216, 1175, 1121, 1109, 1086, 992, 910, 838, 778, 738, 688, 620, 594, 537, 468; **^{1}H NMR** (400 MHz, $CDCl_3$) *δ*/ppm 8.62 (ddd, *J* = 4.7, 1.7, 0.9 Hz, 1H), 7.92 (dt, *J* = 7.9, 1.2 Hz, 1H), 7.86 (dt, *J* = 7.5, 1.7 Hz, 1H), 7.45 (ddd, *J* = 7.5, 4.7, 1.3 Hz, 1H), 7.02–6.92 (m, 2H), 6.76–6.65 (m, 2H), 5.29 (d, *J* = 8.8 Hz, 1H), 4.58 (dt, *J* = 8.9, 5.8 Hz, 1H), 3.54 (s, 3H), 3.12–2.99 (m, 2H), 0.97 (s, 9H), 0.17 (s, 6H); **^{13}C NMR** (101 MHz, $CDCl_3$) *δ*/ppm 171.4, 157.9, 155.0, 149.9, 138.1, 130.5, 127.7, 126.8, 121.8, 120.3, 57.8, 52.4, 39.1, 25.8, 18.3, −4.3; **HRMS ESI** *m*/*z* calc. for $C_{21}H_{31}N_2O_5SSi$ $[M+H]^+$: 451.1718, found: 451.1719.

Methyl (pyridin-2-ylsulfonyl)-D-tyrosinate (3.99)

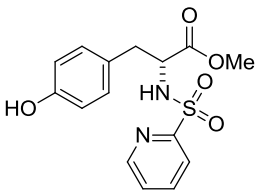

Sulfonamide **3.98** (4.82 g, 10.7 mmol, 1.0 eq.) was dissolved in THF (90 mL) and cooled to 0 °C. TBAF (1 M solution in THF, 16.0 mL, 16.0 mmol, 1.5 eq.) was added dropwise and the reaction mixture was stirred for 10 min at 0 °C and further 2 h at room temperature. The reaction mixture was quenched by the addition of sat. aq. NH_4Cl solution (150 mL). The layers were separated and the aqueous layer was extracted with EtOAc (3 x 100 mL). The combined organic layers were washed with brine (2 x 25 mL), dried over $MgSO_4$ and the solvent was removed under reduced pressure. The crude product was purified by flash column chromatography (SiO_2, pentane/EtOAc 1:2) to give sulfonamide **3.99** (2.84 g, 8.44 mmol, 79%) as a colorless solid.

R_f = 0.43 (SiO_2, pentane/EtOAc 1:2); **Mp** = 137.4–138.4 °C; **Optical rotation** $[\alpha]_D^{25}$ **=** –6.2 (*c* = 0.50, $CHCl_3$); **FTIR** $\tilde{\nu}$/cm^{-1} 3277, 1736, 1514, 1427, 1339, 1331, 1248, 1232, 1172, 1108, 1082, 851, 822, 781, 741, 619, 607, 569, 550, 533, 486; **^{1}H NMR** (400 MHz, MeOD) *δ*/ppm 8.54 (ddd, *J* = 4.8, 1.8, 0.9 Hz, 1H), 7.94 (td, *J* = 7.8, 1.8 Hz, 1H), 7.80 (dt, *J* = 7.9, 1.1 Hz, 1H), 7.54 (ddd, *J* = 7.6, 4.7, 1.2 Hz, 1H), 7.08–6.87 (m, 2H), 6.66–6.54 (m, 2H), 4.30 (dd, *J* = 8.3, 6.1 Hz, 1H), 3.52 (s, 3H), 2.94 (dd, *J* = 13.8, 6.2 Hz, 1H), 2.80 (dd, *J* = 13.8, 8.3 Hz, 1H); **^{13}C NMR** (101 MHz, MeOD) *δ*/ppm 173.3, 159.3, 157.3, 150.7, 139.6, 131.3, 128.2, 127.9, 122.7, 116.2, 59.7, 52.6, 39.2; **HRMS ESI** *m*/*z* calc. for $C_{15}H_{17}N_2O_5S$ $[M+H]^+$: 337.0853, found: 337.0855.

Methyl (*R*)-3-(4-acetoxyphenyl)-2-(pyridine-2-sulfonamido)propanoate (3.100)

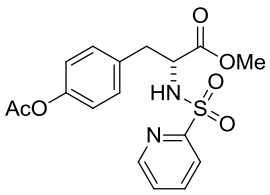

Et_3N (1.63 mL, 11.6 mmol, 1.4 eq.) and DMAP (50.6 mg, 0.410 mmol, 0.050 eq.) were added to a solution of sulfonamide **3.99** (2.80 g, 8.29 mmol, 1.0 eq.) in CH_2Cl_2 (44 mL). The reaction mixture was stirred for 5 min at room temperature before acetyl chloride (0.59 mL, 8.29 mmol, 1.0 eq.) was added. The reaction mixture was stirred for 1 h at room temperature before quenching by the addition of sat. aq. NH_4Cl solution (50 mL). The layers were separated and the aqueous layer was extracted with CH_2Cl_2 (2 x 50 mL). The combined organic layers were dried over $MgSO_4$ and the solvent was removed under reduced pressure. The crude product was purified by flash column chromatography (SiO_2, pentane/EtOAc 1:1) to give sulfonamide **3.100** (2.29 g, 7.16 mmol, 86%) as colorless crystals.

R_f = 0.30 (SiO_2, pentane/EtOAc 1:1); **Mp** = 129.8–130.8 °C; **Optical rotation** $[\alpha]_D^{25}$ **=** –7.0 (*c* = 0.72, $CHCl_3$); **FTIR** $\tilde{\nu}$/cm^{-1} 3178, 1742, 1353, 1217, 1197, 1182, 1170, 1155, 1124, 1111, 1087, 912, 776, 741, 737, 622, 604, 570, 534, 527, 509; **^{1}H NMR** (400 MHz, $CDCl_3$) δ/ppm 8.61 (ddd, *J* = 4.7, 1.7, 1.0 Hz, 1H), 7.91 (dt, *J* = 7.9, 1.1 Hz, 1H), 7.87 (dt, *J* = 7.6, 1.7 Hz, 1H), 7.45 (ddd, *J* = 7.4, 4.7, 1.4 Hz, 1H), 7.18–7.09 (m, 2H), 7.01–6.89 (m, 2H), 5.30 (d, *J* = 8.6 Hz, 1H), 4.63 (dt, *J* = 8.7, 5.9 Hz, 1H), 3.58 (s, 3H), 3.27–2.96 (m, 2H), 2.28 (s, 3H); **^{13}C NMR** (101 MHz, $CDCl_3$) δ/ppm 171.3, 169.5, 157.9, 150.03, 149.98, 138.2, 132.8, 130.6, 126.9, 121.81, 121.77, 57.6, 52.6, 39.3, 21.3; **HRMS ESI** *m*/*z* calc. for $C_{17}H_{19}N_2O_6S$ $[M+H]^+$: 379.0958, found: 379.0970.

Methyl (*R*)-6-((*tert*-butyldimethylsilyl)oxy)-1-(pyridin-2-ylsulfonyl)indoline-2-carboxylate (3.101)

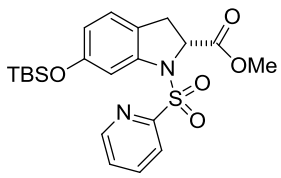

$PhI(OAc)_2$ (1.22 g, 3.78 mmol, 2.0 eq.) and $Pd(OAc)_2$ (42.4 mg, 0.189 mmol, 0.10 eq.) were added to a solution of sulfonamide **3.98** (852 mg, 1.89 mmol, 1.0 eq.) in toluene (20 mL). The reaction mixture was heated for 10 h at 130 °C in a microwave reactor. The solvent was removed under reduced pressure and the crude residue purified by flash column chromatography (SiO_2, pentane/EtOAc 2:1) to give indoline **3.101** (460 mg, 1.03 mmol, 54%) as a colorless, viscous oil.

R_f = 0.33 (SiO_2, pentane/EtOAc 2:1); **Optical rotation** $[\alpha]_D^{25}$ **=** –132.5 (*c* = 0.29, $CHCl_3$); **FTIR** $\tilde{\nu}$/cm^{-1} 2955, 2931, 2887, 2858, 1757, 1612, 1592, 1579, 1566, 1494, 1473, 1452, 1428, 1391, 1360, 1282, 1257, 1197, 1179, 1153, 1122, 1101, 1086, 1027, 991, 937, 859, 840, 801, 780, 737, 667, 622, 602, 567; **^{1}H NMR** (400 MHz, $CDCl_3$) δ/ppm 8.58 (ddd, *J* = 4.7, 1.7, 0.9 Hz, 1H), 7.95 (dt, *J* = 7.9, 1.0 Hz, 1H), 7.81 (td, *J* = 7.8, 1.8 Hz, 1H), 7.41 (ddd, *J* = 7.7, 4.7, 1.2 Hz, 1H), 7.02 (d, *J* = 2.1 Hz, 1H), 6.87 (dt, *J* = 8.2, 1.1 Hz, 1H), 6.42 (dd, *J* = 8.1, 2.3 Hz, 1H), 5.54 (dd, *J* = 10.9, 4.2 Hz, 1H), 3.78 (s, 3H), 3.48 (ddd, *J* = 15.8, 10.9, 1.1 Hz, 1H), 3.11 (dd, *J* = 16.0, 4.2 Hz, 1H), 0.94 (s, 9H), 0.14 (s, 6H); **^{13}C NMR** (101 MHz, $CDCl_3$) δ/ppm 172.0, 156.8, 155.8, 150.3, 142.0, 137.8, 127.1, 125.1, 123.3, 122.4, 116.2, 107.9, 64.5, 52.9, 32.7, 25.8, 18.3, −4.3, −4.4; **HRMS ESI** *m*/*z* calc. for $C_{21}H_{29}N_2O_5SSi$ $[M+H]^+$: 449.1561, found: 449.1558.

Methyl (*R*)-6-((*tert*-butyldimethylsilyl)oxy)indoline-2-carboxylate (3.103)

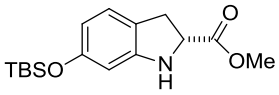

Magnesium powder (250 mg, 10.3 mmol, 10 eq.) was added to a solution of indoline **3.101** (462 mg, 1.03 mmol, 1.0 eq.) in MeOH (30 mL) at 0 °C. The reaction mixture was stirred for 3 h at 0 °C. Sat. aq. NH_4Cl solution (25 mL) and Et_2O (25 mL) were added and the mixture was stirred for 1 h at room temperature until the remaining magnesium powder was quenched. The layers were separated and the aqueous layer was extracted with Et_2O (3 x 25 mL). The combined organic layers were dried over $MgSO_4$ and the solvent was removed under reduced pressure to give indoline **3.103** (302 mg, 0.983 mmol, 95%) as a very viscous, brown syrup which was used without further purification.

R_f = 0.77 (SiO_2, pentane/EtOAc 2:1); **Optical rotation** $[\alpha]_D^{25}$ **=** +3.2 (*c* = 0.42, $CHCl_3$); **FTIR** $\tilde{\nu}$/cm^{-1} 3375, 2955, 2930, 2895, 1740, 1618, 1594, 1498, 1472, 1463, 1390, 1362, 1321, 1298, 1254, 1203, 1160, 1093, 1008, 973, 940, 877, 840, 799, 780, 688, 661, 587; **^{1}H NMR** (400 MHz, $CDCl_3$) δ/ppm 6.92–6.85 (m, 1H), 6.24–6.20 (m, 2H), 4.38 (dd, *J* = 10.2, 5.5 Hz, 1H), 3.75 (s, 3H), 3.31 (ddd, *J* = 15.6, 10.3, 0.9 Hz, 1H), 3.22 (ddd, *J* = 15.6, 5.6, 0.8 Hz, 1H), 0.97 (s, 9H), 0.17 (s, 6H); **^{13}C NMR** (101 MHz, $CDCl_3$) δ/ppm 174.8, 156.0, 151.4, 124.7, 119.5, 111.2, 102.9, 60.6, 52.6, 33.2, 25.9, 18.3, −4.3; **HRMS ESI** *m*/*z* calc. for $C_{16}H_{26}NO_3Si$ $[M+H]^+$: 308.1677, found: 308.1674.

Methyl (*R*)-6-((*tert*-butyldimethylsilyl)oxy)-1-(2,2,2-trifluoroacetyl)indoline-2-carboxylate (3.104)

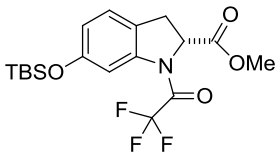

Pyridine (0.30 mL, 3.77 mmol, 4.0 eq.) and trifluoroacetic anhydride (0.53 mL, 3.77 mmol, 4.0 eq.) were added to a solution of indoline **3.103** (290 mg, 0.940 mmol, 1.0 eq.) in CH_2Cl_2 (15 mL) at 0 °C. The reaction mixture was stirred for 20 min at 0 °C and further 16 h at room temperature. The mixture was diluted with CH_2Cl_2 (10 mL) and quenched with sat. aq. $NaHCO_3$ solution (25 mL). The layers were separated and the aqueous layer was extracted with CH_2Cl_2 (3 x 20 mL). The combined organic layers were washed with H_2O (15 mL) and brine (15 mL), dried over $MgSO_4$ and the solvent was removed under reduced pressure. The crude product was purified by flash column chromatography (SiO_2, pentane/EtOAc 6:1) to give indoline **3.104** (337 mg, 0.840 mmol, 89%) as a viscous, colorless oil.

R_f = 0.54 (SiO_2, pentane/EtOAc 6:1); **Optical rotation** $[\alpha]_D^{25}$ **=** +60.7 (*c* = 0.65, $CHCl_3$); **FTIR** $\tilde{\nu}$/cm^{-1} 2957, 2932, 2888, 2860, 1757, 1702, 1610, 1490, 1474, 1440, 1392, 1362, 1349, 1304, 1282, 1265, 1240, 1195, 1155, 1100, 1079, 1010, 964, 940, 876, 862, 841, 819, 801, 783, 750, 729, 698, 667, 633, 585, 527, 458; **^{1}H NMR** (400 MHz, $CDCl_3$) δ/ppm 7.78 (d, *J* = 2.2 Hz, 1H), 7.05 (d, *J* = 8.1 Hz, 1H), 6.65 (dd, *J* = 8.1, 2.3 Hz, 1H), 5.20 (dt, *J* = 10.2, 1.6 Hz, 1H), 3.75 (s, 3H), 3.61 (dd, *J* = 15.8, 10.7 Hz, 1H), 3.22 (d, *J* = 15.9 Hz, 1H), 0.98 (s, 9H), 0.24–0.21 (m, 6H); **^{13}C NMR** (101 MHz, $CDCl_3$) δ/ppm 171.1, 156.0, 154.6 (q, *J* = 37.9 Hz), 142.7, 124.8, 121.3, 117.9, 116.0 (q, *J* = 288.2 Hz), 110.8, 61.40 (q, *J* = 3.2 Hz), 53.2, 33.8, 25.8, 18.4, −4.28, −4.33; **^{19}F NMR** (376 MHz, $CDCl_3$) δ/ppm −71.4; **HRMS ESI** *m*/*z* calc. for $C_{18}H_{25}F_3NO_4$ $[M+H]^+$: 404.1500, found: 404.1494.

Methyl (*R*)-6-acetoxy-1-(pyridin-2-ylsulfonyl)indoline-2-carboxylate (3.102)

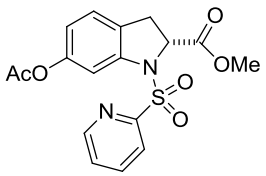

$PhI(OAc)_2$ (1.06 g, 3.30 mmol, 2.0 eq.) and $Pd(OAc)_2$ (37.0 mg, 0.170 mmol, 0.10 eq.) were added to a solution of sulfonamide **3.100** (625 mg, 1.65 mmol, 1.0 eq.) in toluene (20 mL). The reaction mixture was heated for 11 h at 130 °C in a microwave reactor. The solvent was removed under reduced pressure and the obtained residue purified by flash column chromatography (SiO_2, pentane/EtOAc 2:3) to give indoline **3.102** (495 mg, 1.32 mmol, 80%) as a slightly brown solid.

R_f = 0.62 (SiO_2, pentane/EtOAc 1:2); **Mp** = 45.6–46.7 °C; **Optical rotation** $[\alpha]_D^{25}$ **=** –106.8 (*c* = 0.34, $CHCl_3$); **FTIR** $\tilde{\nu}$/cm^{-1} 2959, 1751, 1490, 1428, 1356, 1274, 1202, 1175, 1142, 1119, 1085, 1042, 1013, 990, 926, 894, 775, 736, 621, 601; **^{1}H NMR** (400 MHz, $CDCl_3$) δ/ppm 8.60 (ddd, *J* = 4.7, 1.8, 0.9 Hz, 1H), 7.96 (dt, *J* = 7.9, 1.0 Hz, 1H), 7.84 (td, *J* = 7.8, 1.7 Hz, 1H), 7.43 (ddd, *J* = 7.7, 4.7, 1.2 Hz, 1H), 7.03 (d, *J* = 8.1 Hz, 1H), 6.68 (dd, *J* = 8.1, 2.1 Hz, 1H), 5.54 (dd, *J* = 11.0, 4.1 Hz, 1H), 3.79 (s, 3H), 3.52 (ddd, *J* = 16.2, 11.0, 1.2 Hz, 1H), 3.19 (dd, *J* = 16.2, 4.1 Hz, 1H), 2.26 (s, 3H); **^{13}C NMR** (101 MHz, $CDCl_3$) δ/ppm 171.7, 169.4, 156.4, 150.6, 150.3, 141.9, 138.0, 127.4, 125.2, 123.4, 117.6, 109.6, 64.3, 53.0, 32.8, 21.2; **HRMS ESI** *m/z* calc. for $C_{17}H_{17}N_2O_6S$ $[M+H]^+$: 377.0802, found: 377.0799.

Methyl (*R*)-6-hydroxyindoline-2-carboxylate (3.106)

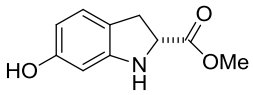

Magnesium powder (352 mg, 14.5 mmol, 10 eq.) was added to a solution of indoline **3.102** (545 mg, 1.45 mmol, 1.0 eq.) in MeOH (34 mL) at 0 °C and the mixture was stirred for 3.5 h at 0 °C. Sat. aq. NH_4Cl solution (50 mL) and Et_2O (50 mL) were added and the mixture was stirred for 1 h at room temperature until the remaining magnesium powder was quenched. The layers were separated and the aqueous layer was extracted with Et_2O (2 x 50 mL). The combined organic layers were dried over $MgSO_4$ and the solvent was removed under reduced pressure. To remove residual H_2O from the product, the residue was diluted with CH_2Cl_2 (10 mL) and H_2O was added (5 mL). The layers were separated and the aqueous layer was extracted with CH_2Cl_2 (10 mL). The combined organic layers were dried over $MgSO_4$ and the solvent was removed to give indoline **3.106** (280 mg, 1.45 mmol, quant.) as a viscous brown syrup. The crude product was of sufficient purity to be used without further purification. For analytical measurements, a small amount of the crude residue was purified by flash column chromatography (SiO_2, pentane/EtOAc 1:2) to give indoline **3.106** as a colorless oil.

R_f = 0.65 (SiO_2, pentane/EtOAc 1:2); **Optical rotation** $[\alpha]_D^{25}$ **=** –28.0 (*c* = 0.30, $CHCl_3$); **FTIR** $\tilde{\nu}$/cm^{-1} 3369, 3029, 2953, 2857, 1729, 1619, 1502, 1469, 1436, 1329, 1294, 1271, 1201, 1178, 1144, 1096, 1079, 1010, 959, 939, 833, 794, 734, 639, 600, 566, 514; **^{1}H NMR** (400 MHz, $CDCl_3$) δ/ppm 6.88 (d, *J* = 8.6 Hz, 1H), 6.23–6.18 (m, 2H), 4.38 (dd, *J* = 10.2, 5.2 Hz, 1H), 3.74 (s, 3H), 3.30 (ddd, *J* = 15.6, 10.2, 1.1 Hz, 1H), 3.19 (ddd, *J* = 15.6, 5.2, 1.0 Hz, 1H); **^{13}C NMR** (101 MHz, $CDCl_3$) δ/ppm 175.0, 156.2, 151.3, 125.0, 118.8, 106.6, 98.5, 60.6, 52.7, 33.1; **HRMS ESI** *m/z* calc. for $C_{10}H_{12}NO_3$ $[M+H]^+$: 194.0812, found: 194.0807.

Methyl (*R*)-6-hydroxy-1-(2,2,2-trifluoroacetyl)indoline-2-carboxylate (3.107)

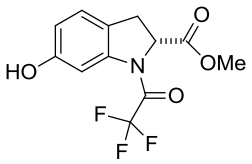

Pyridine (0.42 mL, 5.24 mmol, 4.0 eq.) and trifluoroacetic anhydride (0.73 mL, 5.24 mmol, 4.0 eq.) were added to a solution of indoline **3.106** (253 mg, 1.31 mmol, 1.0 eq.) in CH_2Cl_2 (19 mL) at 0 °C. The reaction mixture was stirred for 20 min at 0 °C and further 16 h at room temperature. The reaction mixture was diluted with CH_2Cl_2 (10 mL) and quenched with sat. aq. $NaHCO_3$ solution (25 mL). The layers were separated and the aqueous layer was extracted with CH_2Cl_2 (3 x 20 mL). The combined organic layers were washed with H_2O (15 mL) and brine (15 mL), dried over $MgSO_4$ and the solvent was removed under reduced pressure. Toluene (3 x 5 mL) was added and removed under reduced pressure to remove residual pyridine, giving indoline **3.107** (380 mg, 1.31 mmol, quant.) as a slightly brown syrup, which was used without further purification. For analytical measurements, a small amount of the crude residue was purified by flash column chromatography (SiO_2, pentane/EtOAc 4:1) to give indoline **3.107** as a colorless solid.

R_f = 0.33 (SiO_2, pentane/EtOAc 4:1); **Mp** = 90.8–91.9 °C; **Optical rotation** $[\alpha]_D^{25}$ = +113.6 (*c* = 0.23, $CHCl_3$); **FTIR** $\tilde{\nu}$/cm^{-1} 3374, 2960, 2928, 1748, 1671, 1619, 1609, 1506, 1461, 1439, 1370, 1352, 1324, 1284, 1197, 1147, 1099, 1079, 1008, 972, 945, 859, 821, 749, 733, 668, 638, 590, 528, 502; **^{1}H NMR** (400 MHz, $CDCl_3$) δ/ppm 7.96 (d, *J* = 2.3 Hz, 1H), 7.09 (d, *J* = 8.3 Hz, 1H), 6.73 (dd, *J* = 8.2, 2.3 Hz, 1H), 6.65 (s, 1H), 5.23 (dt, *J* = 10.1, 1.6 Hz, 1H), 3.76 (s, 3H), 3.62 (ddd, *J* = 15.9, 10.1, 1.3 Hz, 1H), 3.24 (d, *J* = 16.0 Hz, 1H); **^{13}C NMR** (101 MHz, $CDCl_3$) δ/ppm 170.9, 156.7, 155.2 (q, *J* = 37.9 Hz), 142.2, 125.4, 120.3, 116.0 (q, *J* = 287.8 Hz), 113.9, 106.3, 61.7 (q, *J* = 3.4 Hz), 53.4, 33.7; **^{19}F NMR** (376 MHz, $CDCl_3$) δ/ppm –71.2; **HRMS ESI** *m/z* calc. for $C_{12}H_{10}F_3NO_4Na$ $[M+Na]^+$: 312.0454, found: 312.0450.

Methyl (*R*)-6-(methoxymethoxy)-1-(2,2,2-trifluoroacetyl)indoline-2-carboxylate (3.108)

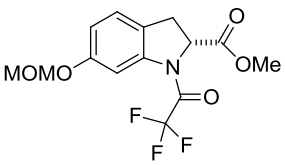

DIPEA (0.43 mL, 2.62 mmol, 2.0 eq.) and MOMBr (0.23 mL, 2.62 mmol, 2.0 eq.) were added to a solution of crude indoline **3.107** (380 mg, 1.31 mmol, 1.0 eq.) in CH_2Cl_2 (20 mL) at 0 °C. The reaction mixture was stirred for 20 min at 0 °C and further 16 h at room temperature. The reaction mixture was quenched with sat. aq. NH_4Cl solution (25 mL), the layers were separated and the aqueous layer was extracted with CH_2Cl_2 (3 x 20 mL). The combined organic layers were washed with brine (15 mL), dried over $MgSO_4$ and the solvent was removed under reduced pressure. The crude product was purified by flash column chromatography (SiO_2, pentane/EtOAc 4:1) to give indoline **3.108** (270 mg, 0.81 mmol, 62% over three steps from indoline **3.102**) as a colorless solid.

R_f = 0.54 (SiO_2, pentane/EtOAc 4:1); **Mp** = 93.6–94.7 °C; **Optical rotation** $[\alpha]_D^{25}$ = +69.4 (c = 0.32, $CHCl_3$); **FTIR** $\tilde{\nu}$/cm^{-1} 2958, 2069, 1753, 1700, 1614, 1600, 1496, 1439, 1352, 1299, 1278, 1262, 1206, 1185, 1151, 1105, 1088, 1069, 1007, 924, 873, 816, 774, 750, 730, 673, 581, 527; **^{1}H NMR** (400 MHz, $CDCl_3$) δ/ppm 7.97 (d, J = 2.3 Hz, 1H), 7.14–7.10 (m, 1H), 6.86 (dd, J = 8.3, 2.3 Hz, 1H), 5.23–5.19 (m, 1H), 5.18 (s, 2H), 3.75 (s, 3H), 3.62 (dd, J = 16.2, 9.4 Hz, 1H), 3.49 (s, 3H), 3.24 (d, J = 16.0 Hz, 1H); **^{13}C NMR** (101 MHz, $CDCl_3$) δ/ppm 171.0, 157.6, 154.6 (q, J = 37.5 Hz), 142.7, 125.0, 122.1, 116.0 (q, J = 287.9 Hz), 114.2, 107.5, 94.9, 61.4 (q, J = 3.6 Hz), 56.3, 53.3, 33.8; **^{19}F NMR** (376 MHz, $CDCl_3$) δ/ppm −71.4; **HRMS ESI** m/z calc. for $C_{14}H_{15}F_3NO_5$ $[M+H]^+$: 334.0897, found: 334.0892.

Methyl (2*R*,3a*R*,6*R*,7a*R*)-6-(methoxymethoxy)-1-(2,2,2-trifluoroacetyl)octahydro-1*H*-indole-2-carboxylate (3.109)

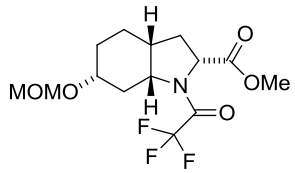

Rh/C (5% *w*/*w*, 54.3 mg, 26.0 µmol, 0.10 eq.) was added to a solution of indoline **3.108** (88.0 mg, 0.260 mmol, 1.0 eq.) in MeOH (2.5 mL). The reaction mixture was stirred for 4.5 h at room temperature in an autoclave under H_2 pressure (15 bar). The catalyst was filtered off over a short pad of Celite®, the Celite® was washed with MeOH (2 x 10 mL) and the solvent was removed under reduced pressure. The crude product was purified by flash column chromatography (SiO_2, pentane/EtOAc 4:1) to give octahydroindole **3.109** (50.0 mg, 0.150 mmol, 56%) as a colorless solid and recovered starting material **3.108** (8.00 mg, 24.0 µmol, 9%).

R_f = 0.36 (SiO_2, pentane/EtOAc 3:1); **Optical rotation** $[\alpha]_D^{25}$ = +72.8 (*c* = 0.13, $CHCl_3$); **FTIR** $\tilde{\nu}$/cm^{-1} 2955, 1751, 1684, 1447, 1360, 1312, 1274, 1256, 1238, 1204, 1166, 1142, 1105, 1058, 1038, 951, 939, 917, 868, 836, 804, 763, 726, 668, 623, 571, 529, 458; **^{1}H NMR** (500 MHz, $CDCl_3$) δ/ppm 4.67 (s, 2H), 4.55 (dd, *J* = 10.0, 8.5 Hz, 1H), 4.16 (dt, *J* = 12.0, 6.0 Hz, 1H), 3.77 (s, 3H), 3.48 (tt, *J* = 11.5, 3.9 Hz, 1H), 3.37 (s, 2H), 2.43–2.34 (m, 1H), 2.33–2.20 (m, 2H), 2.09–2.00 (m, 1H), 1.92–1.83 (m, 2H), 1.77–1.63 (m, 2H), 1.47–1.36 (m, 1H); **^{13}C NMR** (126 MHz, $CDCl_3$) δ/ppm 170.1, 154.5 (q, *J* = 38.0 Hz), 115.1 (q, *J* = 287.0 Hz), 93.6, 71.9, 59.0, 57.5 (q, *J* = 2.5 Hz), 54.3, 51.6, 36.3, 33.2, 28.2, 25.4, 21.5; **^{19}F NMR** (376 MHz, $CDCl_3$) δ/ppm −71.1; **HRMS ESI** *m/z* calc. for $C_{14}H_{20}F_3NO_5Na$ $[M+Na]^+$: 362.1186, found: 362.1187.

Methyl (2*R*,3a*R*,6*R*,7a*R*)-6-(methoxymethoxy)octahydro-1*H*-indole-2-carboxylate (3.110)

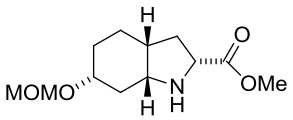

$NaBH_4$ (24.1 mg, 0.640 mmol, 5.8 eq.) was added to a solution of octahydroindole **3.109** (36.0 mg, 0.110 mmol, 1.0 eq.) in MeOH (2.5 mL) at 0 °C. The reaction mixture was stirred for 1 h at 0 °C and subsequently diluted with MeOH (2.5 mL). One spatula of silica gel was added and the solvent was removed under reduced pressure. The impregnated silica gel containing the crude product was purified by flash column chromatography (SiO_2, CH_2Cl_2/MeOH 20:1 changing to 2:1) to give octahydroindole **3.110** (21.0 mg, 86.0 μmol, 81%) as a colorless solid.

R_f = 0.32 (SiO_2, CH_2Cl_2/MeOH 10:1); **Optical rotation** $[\alpha]_D^{25}$ = +2.4 (*c* = 0.22, $CHCl_3$); **FTIR** $\tilde{\nu}$/cm^{-1} 3418, 2930, 1739, 1632, 1442, 1374, 1332, 1305, 1256, 1211, 1148, 1103, 1035, 919, 825, 713, 642, 498; **^{1}H NMR** (400 MHz, $CDCl_3$) δ/ppm 4.71–4.60 (m, 2H), 3.82 (dd, *J* = 10.1, 6.3 Hz, 1H), 3.74 (s, 4H), 3.38 (s, 3H), 3.11 (q, *J* = 5.4 Hz, 1H), 2.99 (br s, 1H), 2.19 (ddd, *J* = 12.9, 10.1, 7.0 Hz, 1H), 2.11–2.00 (m, 1H), 1.94–1.79 (m, 3H), 1.74–1.64 (m, 2H), 1.62–1.49 (m, 2H), 1.47–1.37 (m, 1H); **^{13}C NMR** (101 MHz, $CDCl_3$) δ/ppm 176.0, 94.8, 71.9, 59.0, 58.0, 55.5, 52.3, 38.0, 35.9, 32.9, 28.2, 22.3; **HRMS ESI** *m/z* calc. for $C_{12}H_{22}NO_4$ $[M+H]^+$: 244.1543, found: 244.1543.

2.2.7. Synthesis of Hpla-Phe-OH Dipeptide

D-Phenylalanine methyl ester hydrochloride (3.111)

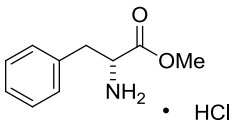

D-Phenylalanine (0.500 g, 3.03 mmol, 1.0 eq.) was dissolved in MeOH (6 mL) and cooled to 0 °C. $SOCl_2$ (0.33 mL, 4.54 mmol, 1.5 eq.) was slowly added at 0 °C and the reaction mixture was heated at reflux for 12 h. The solvent was removed under reduced pressure to give D-phenylalanine methyl ester hydrochloride (**3.111**) (0.540 g, 3.01 mmol, 99%) as a colorless solid, which was used without further purification.

Optical rotation $[\alpha]_D^{25}$**=** −16.6 (*c* = 0.92, MeOH); **^{1}H NMR** (400 MHz, MeOD) *δ*/ppm 7.41–7.29 (m, 3H), 7.29–7.25 (m, 2H), 4.33 (t, *J* = 6.7 Hz, 1H), 3.80 (s, 3H), 3.27 (dd, *J* = 14.4, 6.1 Hz, 1H), 3.19 (dd, *J* = 14.3, 7.2 Hz, 1H); **^{13}C NMR** (101 MHz, MeOD) *δ*/ppm 170.4, 135.3, 130.4, 130.2, 129.0, 55.2, 53.6, 37.4.

Analytical data are in accordance with those reported in the literature.[20]

Methyl ((*S*)-2-acetoxy-3-(4-(benzyloxy)phenyl)propanoyl)-D-phenylalaninate (3.112)

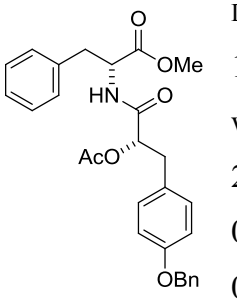

D-Phenylalanine methyl ester hydrochloride (**3.111**) (161 mg, 0.750 mmol, 1.0 eq.) and phenyllactic acid derivative **3.67** (306 mg, 0.970 mmol, 1.3 eq.) were dissolved in CH_2Cl_2 (9 mL). The solution was cooled to 0 °C and 2,6-lutidine (0.44 mL, 3.75 mmol, 5.0 eq.) and PyBOP (507 mg, 0.970 mmol, 1.3 eq.) were added. The mixture was stirred for 20 min at 0 °C and further 20 h at room temperature. The reaction mixture was diluted with CH_2Cl_2 (10 mL), washed with aq. HCl solution (1 M, 10 mL), sat. aq. Na_2CO_3 solution (10 mL) and brine (10 mL). The organic layer was dried over Na_2SO_4 and the solvent was removed under reduced pressure. The crude product was purified by flash column chromatography (SiO_2, pentane/EtOAc 3:2) to give dipeptide **3.112** (265 mg, 0.550 mmol, 77%) as a colorless solid.

R_f = 0.66 (SiO_2, pentane/EtOAc 3:2); **Mp** = 105.4–107.0 °C; **Optical rotation** $[\alpha]_D^{25}$ **=** –57.5 (*c* = 0.40, $CHCl_3$); **FTIR** $\tilde{\nu}$/cm^{-1} 3324, 3063, 3032, 2952, 1742, 1679, 1611, 1584, 1512, 1455, 1436, 1371, 1297, 1220, 1177, 1114, 1026, 921, 818, 741, 699, 639, 608, 530; **^{1}H NMR** (400 MHz, $CDCl_3$) δ/ppm 7.44–7.29 (m, 6H), 7.26–7.22 (m, 2H), 7.13–7.05 (m, 2H), 7.01–6.95 (m, 2H), 6.92–6.84 (m, 2H), 6.32 (d, *J* = 7.9, 1H), 5.33 (dd, *J* = 8.0, 4.6 Hz, 1H), 5.02 (s, 2H), 4.86 (dt, *J* = 7.9, 5.5 Hz, 1H), 3.72 (s, 3H), 3.15 (dd, *J* = 14.4, 4.6 Hz, 1H), 3.09 (dd, *J* = 5.5, 4.1 Hz, 2H), 2.97 (dd, *J* = 14.3, 8.1 Hz, 1H), 1.97 (s, 3H); **^{13}C NMR** (101 MHz, $CDCl_3$) δ/ppm 171.5, 169.5, 168.9, 158.0, 137.1, 135.5, 130.6, 129.4, 128.7, 128.3, 128.1, 127.6, 127.4, 114.9, 74.5, 70.1, 52.7, 52.5, 37.8, 37.1, 20.9; **HRMS ESI** *m*/*z* calc. for $C_{28}H_{30}NO_6$ $[M+H]^+$: 476.2068, found: 476.2070.

Methyl ((*S*)-3-(4-(benzyloxy)phenyl)-2-hydroxypropanoyl)-D-phenylalaninate (3.113)

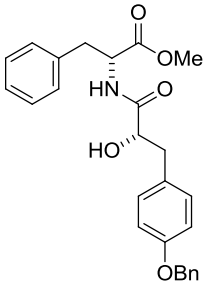

Hpla-Phe-OMe dipeptide **3.112** (130 mg, 0.270 mmol, 1.0 eq.) was dissolved in MeOH (4 mL). K_2CO_3 (113 mg, 0.820 mmol, 3.0 eq.) was added and the mixture stirred for 2 h at room temperature. Sat. aq. NH_4Cl solution (5 mL) was added and the mixture was extracted with CH_2Cl_2 (3 x 10 mL). The combined organic layers were dried over $MgSO_4$ and the solvent was removed under reduced pressure. The crude residue was purified by flash column chromatography (SiO_2, pentane/EtOAc 3:2) to give dipeptide **3.113** (100 mg, 0.226 mmol, 84%) as a colorless solid.

R_f = 0.53 (SiO_2, pentane/EtOAc 1:1); **Mp** = 117.5–118.6 °C; **Optical rotation** $[\alpha]_D^{25}$ **=** –75.0 (*c* = 0.27, $CHCl_3$); **FTIR** $\tilde{\nu}$/cm^{-1} 3394, 3063, 3030, 2952, 2925, 2096, 1743, 1655, 1611, 1584, 1511, 1455, 1437, 1362, 1240, 1177, 1112, 1080, 1025, 917, 819, 740, 698, 609, 572, 527; **^{1}H NMR** (400 MHz, $CDCl_3$) δ/ppm 7.45–7.35 (m, 4H), 7.35–7.23 (m, 4H), 7.16–7.07 (m, 4H), 6.95–6.90 (m, 2H), 6.88 (d, *J* = 8.3 Hz, 1H), 5.04 (s, 2H), 4.88 (dt, *J* = 8.2, 6.1 Hz, 1H), 4.23 (dt, *J* = 8.7, 4.3 Hz, 1H), 3.70 (s, 3H), 3.19–3.05 (m, 3H), 2.79 (dd, *J* = 14.1, 8.7 Hz, 1H), 2.27 (d, *J* = 4.6 Hz, 1H); **^{13}C NMR** (101 MHz, $CDCl_3$) δ/ppm 172.4, 171.8, 158.1, 137.1, 135.9, 130.7, 129.3, 128.8, 128.7, 128.1, 127.6, 127.3, 115.4, 73.0, 70.2, 53.0, 52.5, 40.0, 38.2; **HRMS ESI** *m*/*z* calc. for $C_{26}H_{23}NO_5$ $[M+H]^+$: 434.1962, found: 434.1958.

Methyl ((*S*)-3-(4-(benzyloxy)phenyl)-2-((*tert*-butyldimethylsilyl)oxy)propanoyl)-D-phenylalaninate (3.114)

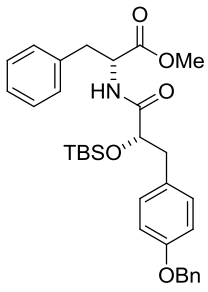

TBSCl (21.1 mg, 0.140 mmol, 1.5 eq.), imidazole (18.9 mg, 0.280 mmol, 3.0 eq.) and DMAP (0.560 mg, 5.00 µmol, 0.050 eq.) were added to a solution of dipeptide **3.113** (40.0 mg, 92.0 µmol, 1.0 eq.) in DMF (1 mL) and stirred for 18 h at room temperature. The reaction mixture was partitioned between H_2O (10 mL) and CH_2Cl_2 (10 mL), the layers were separated and the aqueous layer was extracted with CH_2Cl_2 (2 x 10 mL). The combined organic layers were washed with brine (10 mL), dried over $MgSO_4$ and the solvent was removed under reduced pressure. The crude product was purified by flash column chromatography (SiO_2, pentane/EtOAc 2:1) to give dipeptide **3.114** (18.0 mg, 33.0 µmol, 36%) as a colorless solid. Further, starting material **3.113** could be recovered (23.0 mg, 53.0 µmol, 58%).

R_f = 0.78 (SiO_2, pentane/EtOAc 2:1); **Optical rotation** $[\alpha]_D^{25}$ **=** −72.7 (*c* = 0.055, $CHCl_3$); **FTIR** $\tilde{\nu}$/cm^{-1} 3416, 2927, 2856, 1747, 1679, 1612, 1511, 1456, 1362, 1251, 1176, 1093, 1027, 940, 832, 781, 737, 697, 509; **^{1}H NMR** (400 MHz, $CDCl_3$) *δ*/ppm 7.43–7.34 (m, 4H), 7.33–7.19 (m, 4H), 7.14–7.07 (m, 4H), 6.95 (d, *J* = 7.6 Hz, 1H), 6.88–6.83 (m, 2H), 5.04 (s, 2H), 4.79 (dt, *J* = 7.6, 6.4 Hz, 1H), 4.21 (dd, *J* = 7.7, 3.4 Hz, 1H), 3.67 (s, 3H), 3.18 (dd, *J* = 14.1, 6.1 Hz, 1H), 3.07 (dd, *J* = 14.1, 6.7 Hz, 1H), 3.03 (dd, *J* = 13.9, 3.4 Hz, 1H), 2.79 (dd, *J* = 13.8, 7.7 Hz, 1H), 0.78 (s, 9H), −0.23 (s, 3H), −0.35 (s, 3H); **^{13}C NMR** (101 MHz, $CDCl_3$) *δ*/ppm 173.2, 171.8, 157.7, 137.3, 136.0, 131.2, 129.8, 129.2, 128.71, 128.66, 128.0, 127.5, 127.2, 114.7, 74.9, 70.1, 53.1, 52.4, 41.0, 38.3, 25.8, 18.0, −5.3, −5.4; **HRMS ESI** *m*/*z* calc. for $C_{32}H_{42}NO_5Si$ $[M+H]^+$: 548.2827, found: 548.2830.

((*S*)-3-(4-(Benzyloxy)phenyl)-2-((*tert*-butyldimethylsilyl)oxy)propanoyl)-D-phenylalanine (3.115)

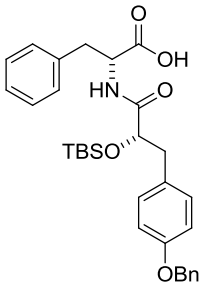

LiOH monohydrate (3.68 mg, 88.0 µmol, 3.0 eq.) was added to a solution of dipeptide **3.114** (16.0 mg, 29.0 µmol, 1.0 eq.) in THF/H_2O (5:3, 0.5 mL) and stirred for 1 h at room temperature. The reaction mixture was acidified with aq. citric acid solution (5% *w*/*w*, 5 mL) to a pH of around 3. The THF was removed under reduced pressure and the residue was extracted with CH_2Cl_2 (3 x 10 mL). The combined organic layers were washed with H_2O (10 mL), dried over $MgSO_4$ and the solvent was removed under reduced pressure to obtain Hpla-Phe-OH dipeptide **3.115** (15.0 mg, 28.0 µmol, 96%) as a colorless solid which was used without further purification.

R_f = 0.16 (SiO_2, pentane/EtOAc 2:1); **Mp** = 157.7–158.3 °C; **Optical rotation** $[\alpha]_D^{25}$ **=** −50.6 (*c* = 0.16, $CHCl_3$); **FTIR** $\tilde{\nu}$/cm^{-1} 3404, 3032, 2952, 2929, 2858, 1733, 1629, 1585, 1512, 1455, 1382, 1348, 1298, 1242, 1177, 1095, 1026, 939, 921, 831, 811, 782, 734, 697, 613, 548, 520, 488; **^{1}H NMR** (400 MHz, $CDCl_3$) δ/ppm 7.43–7.34 (m, 4H), 7.33–7.22 (m, 4H), 7.17–7.14 (m, 2H), 7.10–7.05 (m, 2H), 6.89–6.83 (m, 2H), 5.03 (s, 2H), 4.83–4.73 (m, 2H), 4.23 (dd, *J* = 7.4, 3.6 Hz, 1H), 3.28 (dd, *J* = 14.5, 5.7 Hz, 1H), 3.12–2.97 (m, 2H), 2.80 (dd, *J* = 13.9, 7.5 Hz, 1H), 0.75 (s, 9H), −0.28 (s, 3H), −0.34 (d, *J* = 1.3 Hz, 3H); **^{13}C NMR** (101 MHz, $CDCl_3$) δ/ppm 174.5, 173.4, 157.8, 137.3, 135.7, 131.2, 129.4, 129.2, 128.9, 128.7, 128.0, 127.6, 127.3, 114.8, 74.7, 70.1, 53.2, 41.0, 37.3, 25.9, 18.0, −5.3, −5.5; **HRMS ESI** *m*/*z* calc. for $C_{31}H_{40}NO_5Si$ $[M+H]^+$: 534.2670, found: 534.2674.

2.2.8. Assembly of the Different Building Blocks

Methyl (2*R*,3a*R*,6*R*,7a*R*)-1-(((*S*)-3-(4-(benzyloxy)phenyl)-2-((*tert*-butyldimethylsilyl)-oxy)propanoyl)-D-phenylalanyl)-6-(methoxymethoxy)octahydro-1*H*-indole-2-carboxylate (3.116)

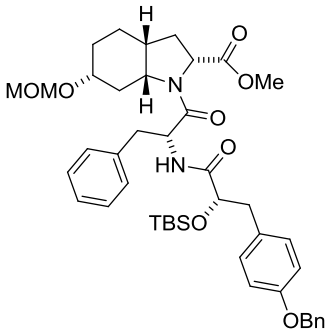

DMTMM (7.77 mg, 28.0 µmol, 1.2 eq.) and NMM (5.15 µL, 47.0 µmol, 2.0 eq.) were added to a solution of D-*diepi*-derivative **3.110** (5.59 mg, 23.0 µmol, 1.0 eq.) and Hpla-Phe-OH dipeptide **3.115** (15.0 mg, 28.0 µmol, 1.2 eq.) in CH_2Cl_2 (0.5 mL) at 0 °C. The reaction mixture was stirred for 20 min at 0 °C and further 2 h at room temperature. The solvent was removed under reduced pressure and the crude product was purified by flash column chromatography (SiO_2, pentane/EtOAc 1:1) to give a 4:1 rotameric mixture of tripeptide **3.116** (12.6 mg, 17.0 µmol, 71%) as a colorless amorphous solid.

R_f = 0.70 (SiO_2, pentane/EtOAc 3:2); **FTIR** $\tilde{\nu}$/cm^{-1} 3415, 2928, 2857, 1751, 1648, 1512, 1436, 1362, 1250, 1196, 1176, 1144, 1103, 1041, 921, 833, 781, 739, 699, 509; **^{1}H NMR** (400 MHz, $CDCl_3$, major rotamer) δ/ppm 7.45–7.40 (m, 2H), 7.39–7.34 (m, 2H), 7.34–7.28 (m, 1H), 7.28–7.24 (m, 2H), 7.23–7.20 (m, 3H), 7.08–7.04 (m, 2H), 6.95 (d, *J* = 8.8 Hz, 1H), 6.86–6.81 (m, 2H), 4.90–4.79 (m, 1H), 4.61–4.48 (m, 2H), 4.38 (dd, *J* = 10.4, 8.0 Hz, 1H), 4.22 (dt, *J* = 12.3, 6.4 Hz, 1H), 4.17 (dd, *J* = 7.7, 3.3 Hz, 1H), 3.73 (s, 3H), 3.40 (tt, *J* = 11.9, 4.0 Hz, 1H), 3.31 (s, 3H), 3.23 (dd, *J* = 13.9, 7.3 Hz, 1H), 2.95 (dd, *J* = 13.8, 3.3 Hz, 1H), 2.83 (dd, *J* = 14.0, 7.2 Hz, 1H), 2.75 (dd, *J* = 13.9, 7.7 Hz, 1H), 2.34–2.25 (m, 1H), 2.08 (dt, *J* = 12.4, 7.3 Hz, 1H), 1.91 (td, *J* = 12.9, 10.4 Hz, 1H), 1.82–1.73 (m, 2H), 1.71–1.52 (m, 3H), 1.37–1.21 (m, 3H), 0.82 (s, 9H), −0.22 (s, 3H), −0.32 (s, 3H); **^{13}C NMR** (101 MHz, $CDCl_3$, major rotamer) δ/ppm 172.9, 172.3, 169.9, 157.7, 137.3, 136.3, 131.12, 131.09, 129.7, 129.6, 129.5, 128.69, 128.66, 128.0, 127.6, 127.1, 114.6, 94.4, 74.8, 72.9, 70.1, 59.3, 57.8, 55.3, 52.3, 51.1, 40.9, 39.4, 36.8, 34.9, 30.5, 26.8, 25.9, 23.0, 18.1, −5.3, −5.5; **HRMS ESI** *m/z* calc. for $C_{43}H_{58}N_2O_8SiNa$ $[M+Na]^+$: 781.3855, found: 781.3853.

(2*R*,3a*R*,6*R*,7a*R*)-1-(((*S*)-3-(4-(Benzyloxy)phenyl)-2-((*tert*-butyldimethylsilyl)oxy)-propanoyl)-D-phenylalanyl)-6-(methoxymethoxy)octahydro-1*H*-indole-2-carboxylic acid (3.117)

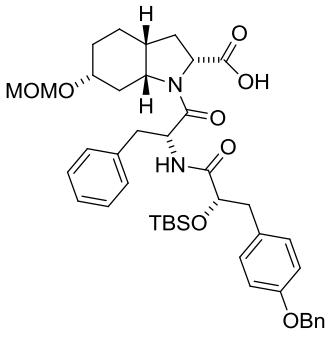

Tripeptide **3.116** (12.5 mg, 16.5 µmol, 1.0 eq.) was dissolved in THF/H_2O (5:3, 0.3 mL) and LiOH monohydrate (2.08 mg, 49.5 µmol, 3.0 eq.) was added. The reaction was stirred for 7 h at room temperature before aq. citric acid solution (5% *w*/*w*, 3 mL) was added. The aqueous layer was extracted with CH_2Cl_2 (3 x 5 mL), the combined organic layers were dried over Na_2SO_4 and the solvent was removed under reduced pressure. The crude residue was purified by flash column chromatography (SiO_2, CH_2Cl_2/MeOH 10:1) to obtain a 4:1 rotameric mixture of tripeptidic acid **3.117** (9.50 mg, 13.0 µmol, 77%) as a colorless solid.

R_f = 0.59 (SiO_2, CH_2Cl_2/MeOH 10:1); **Optical rotation** $[\alpha]_D^{25}$ **=** –14.2 (*c* = 0.20, $CHCl_3$); **FTIR** $\tilde{\nu}$/cm^{-1} 3408, 3059, 3033, 2927, 2856, 1739, 1645, 1612, 1512, 1455, 1362, 1302, 1247, 1177, 1144, 1104, 1042, 939, 918, 833, 781, 738, 698, 542, 509; **^{1}H NMR** (400 MHz, $CDCl_3$, major rotamer) δ/ppm 7.44–7.38 (m, 2H), 7.38–7.34 (m, 1H), 7.34–7.30 (m, 1H), 7.30–7.23 (m, 3H), 7.22–7.17 (m, 2H), 7.09–7.05 (m, 2H), 6.99 (d, *J* = 8.6 Hz, 1H), 6.86–6.82 (m, 3H), 5.04 (d, *J* = 1.8 Hz, 2H), 4.79 (td, *J* = 8.6, 6.3 Hz, 1H), 4.55–4.47 (m, 2H), 4.22 (dd, *J* = 7.4, 3.4 Hz, 1H), 3.43–3.34 (m, 1H), 3.31 (s, 3H), 3.21 (dd, *J* = 13.4, 8.5 Hz, 1H), 2.96 (dd, *J* = 13.9, 3.4 Hz, 1H), 2.86 (dd, *J* = 13.4, 6.1 Hz, 1H), 2.78 (dd, *J* = 13.8, 7.4 Hz, 1H), 2.29–2.21 (m, 2H), 2.07–2.00 (m, 1H), 1.82–1.73 (m, 2H), 1.72–1.57 (m, 1H), 1.38–1.16 (m, 5H), 0.86 (s, 9H), −0.14 (s, 3H), −0.25 (s, 3H); **^{13}C NMR** (101 MHz, $CDCl_3$, major rotamer) δ/ppm 173.0, 172.6, 171.7, 157.7, 137.2, 135.7, 131.1, 129.5, 128.9, 128.71, 128.67, 128.6, 128.1, 127.6, 127.4, 114.6, 94.2, 74.7, 72.5, 70.2, 59.5, 58.7, 55.4, 51.7, 40.8, 39.5, 36.1, 34.1, 29.9, 25.9, 22.8, 18.2, −5.2, −5.4; **HRMS ESI** *m*/*z* calc. for $C_{42}H_{56}N_2O_8SiNa$ $[M+Na]^+$: 767.3698, found: 767.3698.

***tert*-Butyl ((*E*)-*N*-(4-((2*R*,3a*R*,6*R*,7a*R*)-1-(((*S*)-3-(4-(benzyloxy)phenyl)-2-((*tert*-butyldimethylsilyl)oxy)propanoyl)-D-phenylalanyl)-6-(methoxymethoxy)octahydro-1*H*-indole-2-carboxamido)butyl)-*N*'-(*tert*-butoxycarbonyl)carbamimidoyl)-λ^2-azanecarboxylate (3.118)**

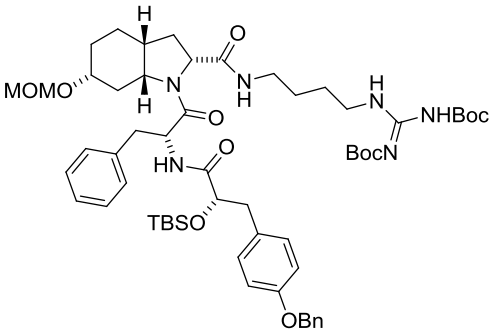

2-6-lutidine (4.2 µL, 36.3 µmol, 3.0 eq.) was added to a solution of tripeptidic acid **3.117** (9.01 mg, 12.1 µmol, 1.0 eq.), agmantin side chain **3.64** (8.00 mg, 24.2 µmol, 2.0 eq.) and PyBOP (12.6 mg, 24.2 µmol, 2.0 eq.) in CH_2Cl_2 (0.4 mL) at 0 °C. The reaction mixture was stirred for 30 min at 0 °C and further 5 h at room temperature. CH_2Cl_2 (3 mL) was added and the solution was washed with sat. aq. $NaHCO_3$ solution (1 mL) and brine (1 mL). The organic layer was dried over Na_2SO_4 and the solvent was removed under reduced pressure. The crude product was purified by flash column chromatography (SiO_2, pentane/EtOAc 2:3) to give a 7:1 rotameric mixture tetrapeptide **3.118** (7.00 mg, 6.70 µmol, 55%) as a white amorphous solid.

R_f = 0.72 (SiO_2, pentane/EtOAc 2:3); **Optical rotation** $[\alpha]_D^{25}$ **=** –3.4 (*c* = 0.17, $CHCl_3$); **FTIR** $\tilde{\nu}$/cm^{-1} 3422, 3336, 2929, 2858, 1720, 1679, 1639, 1584, 1511, 1472, 1446, 1417, 1368, 1332, 1253, 1228, 1158, 1134, 1043, 940, 919, 833, 810, 780, 751, 698, 666, 537, 508, 462; **^{1}H NMR** (400 MHz, $CDCl_3$, major rotamer) δ/ppm 11.49 (s, 1H), 8.32 (t, *J* = 5.3 Hz, 1H), 7.45–7.34 (m, 4H), 7.33–7.28 (m, 1H), 7.25–7.21 (m, 2H), 7.18–7.15 (m, 2H), 7.10–7.05 (m, 2H), 6.98 (d, *J* = 8.3 Hz, 1H), 6.87–6.83 (m, 2H), 6.59 (t, *J* = 5.9 Hz, 1H), 5.04 (s, 2H), 4.83 (td, *J* = 8.6, 6.1 Hz, 1H), 4.60–4.50 (m, 2H), 4.41 (t, *J* = 8.9 Hz, 1H), 4.26–4.18 (m, 2H), 3.46–3.35 (m, 2H), 3.32 (s, 3H), 3.19–3.11 (m, 2H), 2.98 (dd, *J* = 13.8, 3.4 Hz, 1H), 2.87 (dd, *J* = 13.4, 6.0 Hz, 1H), 2.74 (dd, *J* = 13.9, 7.9 Hz, 1H), 2.55 (s, 1H), 2.36 (td, *J* = 12.9, 9.2 Hz, 1H), 2.15 (dt, *J* = 13.2, 6.2 Hz, 1H), 1.91 (dt, *J* = 12.7, 8.0 Hz, 1H), 1.76 (d, *J* = 12.0 Hz, 2H), 1.69–1.54 (m, 4H), 1.50 (s, 9H), 1.48 (s, 9H), 1.44–1.29 (m, 1H), 1.14 (q, *J* = 12.2 Hz, 1H), 0.85 (s, 9H), −0.16 (s, 3H), −0.29 (s, 3H); **^{13}C NMR** (101 MHz, $CDCl_3$, major rotamer) δ/ppm 172.9, 170.8, 170.5, 163.8, 157.7, 156.3, 153.4, 137.2, 136.1, 131.1, 129.7, 129.4, 128.8, 128.7, 128.1, 127.5, 127.4, 114.7, 94.3, 83.2, 79.4, 75.0, 73.0, 70.2, 59.8, 58.8, 55.3, 51.6, 41.0, 40.7, 39.6, 39.4, 36.4, 34.2, 28.5, 28.2, 27.1, 26.8, 25.9, 23.0, 18.2, −5.3, −5.4; **HRMS ESI** *m*/*z* calc. for $C_{57}H_{85}N_6O_{11}Si$ $[M+H]^+$: 1057.6040, found: 1057.6060.

***tert*-Butyl ((*E*)-*N*'-(*tert*-butoxycarbonyl)-*N*-(4-((2*R*,3a*R*,6*R*,7a*R*)-1-(((*S*)-2-((*tert*-butyldimethylsilyl)oxy)-3-(4-hydroxyphenyl)propanoyl)-D-phenylalanyl)-6-(methoxymethoxy)octahydro-1*H*-indole-2-carboxamido)butyl)carbamimidoyl)-λ^2-azanecarboxylate (3.119)**

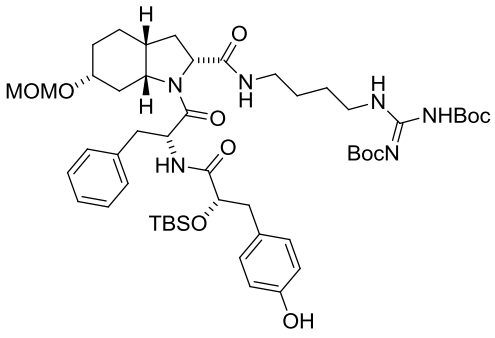

Tetrapeptide **3.118** (4.00 mg, 3.78 µmol, 1.0 eq.) was dissolved in EtOAc/MeOH (1:1, 0.4 mL). Pd/C (10% *w*/*w*, 4.00 mg, 1.0 eq.) was added, the reaction mixture was stirred for 16 h at room temperature under an atmosphere of H_2 and was monitored by UPLC. Additional Pd/C (10% *w*/*w*, 1.30 mg, 12.6 µmol, 0.33 eq.) was added and the mixture was stirred for 4 h at room temperature under an atmosphere of H_2. The catalyst was filtered off over Celite® and the Celite® was washed with EtOAc/MeOH (1:2, 2 x 5 mL). The solvent was removed under reduced pressure to give a 3:1 rotameric mixture of tetrapeptide **3.119** (3.50 mg, 3.67 µmol, 97%) as a colorless amorphous solid which was used without further purification.

R_f = 0.30 (SiO_2, pentane/EtOAc 1:2); **^{1}H NMR** (500 MHz, $CDCl_3$, major rotamer) *δ*/ppm 11.52 (d, *J* = 13.0 Hz, 1H), 8.41 (s, 1H), 7.33–7.17 (m, 5H), 7.15–7.10 (m, 1H), 7.03–6.94 (m, 2H), 6.84 (d, *J* = 9.0 Hz, 1H), 6.72–6.65 (m, 2H), 4.78–4.71 (m, 1H), 4.57–4.48 (m, 2H), 4.33–4.26 (m, 2H), 4.26–4.20 (m, 1H), 3.48–3.42 (m, 1H), 3.39–3.32 (m, 1H), 3.31 (s, 3H), 3.10 (dd, *J* = 13.3, 8.7 Hz, 1H), 2.92–2.83 (m, 1H), 2.79 (dd, *J* = 13.4, 6.3 Hz, 1H), 2.26 (dd, *J* = 12.7, 9.4 Hz, 1H), 2.20–2.11 (m, 1H), 1.95 (dt, *J* = 11.9, 7.3 Hz, 1H), 1.81–1.55 (m, 12H), 1.50 (s, 9H), 1.43 (s, 9H), 1.39–1.24 (m, 2H), 0.90 (s, 9H), −0.04 (s, 3H), −0.07 (s, 3H); **^{13}C NMR** (126 MHz, $CDCl_3$, major rotamer) *δ*/ppm 172.5, 171.0, 170.2, 156.4, 155.3, 153.4, 136.2, 131.1, 130.9, 129.5, 129.4, 129.1, 128.8, 127.3, 115.4, 94.2, 83.5, 74.4, 73.0, 60.3, 58.5, 55.3, 51.2, 41.0, 40.5, 39.3, 36.3, 34.4, 29.2, 28.3, 28.2, 27.1, 26.8, 26.7, 26.0, 23.1, 18.3, −4.9, −5.3; **HRMS ESI** *m*/*z* calc. for $C_{50}H_{79}N_6O_{11}Si$ $[M+H]^+$: 967.5571, found: 967.5581.

Aeruginosin KT608A (3.1)

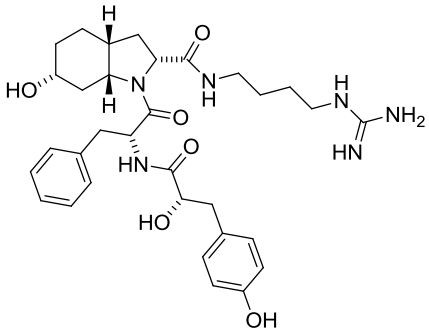

Tetrapeptide **3.119** (3.5 mg, 3.62 µmol, 1.0 eq.) was dissolved in CH_2Cl_2 (2 mL). To this solution TFA (0.2 mL) was added and the reaction mixture stirred for 3 h at room temperature and further for 3.5 h at 40 °C. Toluene (2 mL) was added and the TFA and CH_2Cl_2 removed under reduced pressure. The obtained residue was dissolved in MeCN/aq. HF (48% *w*/*w*) (9:1, 0.5 mL) and the reaction stirred for 1 h at room temperature. The reaction was quenched by the addition of sat. aq. Na_2CO_3 solution (2 mL) and the layers were separated. The aqueous layer was extracted with MeCN (2 mL) and the combined organic layers dried over $MgSO_4$. The solvent was removed under reduced pressure and the obtained crude product dissolved in H_2O. The aqueous solution was subjected to solid phase extraction using a C18 cartridge. The C18 cartridge was eluted with MeOH/H_2O (9:1, 10 mL) to give a 2:1 rotameric mixture of aeruginosin KT608A (**3.1**) (2.20 mg, 3.61 µmol, quant.) as an amorphous white solid.

^{1}H NMR (600 MHz, DMSO-d_6, major rotamer) δ/ppm 9.08 (s, 1H), 7.88 (d, J = 8.4 Hz, 1H), 7.83 (t, J = 5.7 Hz, 1H), 7.42 (t, J = 5.4 Hz, 1H), 7.29–7.19 (m, 6H), 6.88 (d, J = 8.5 Hz, 2H), 6.59 (d, J = 8.4 Hz, 2H), 5.27 (d, J = 6.5 Hz, 1H), 4.73–4.64 (m, 2H), 4.30–4.19 (m, 2H), 3.96–3.92 (m, 1H), 3.42–3.24 (m, 1H), 3.16–3.04 (m, 3H), 2.92 (dd, J = 14.1, 4.6 Hz, 1H), 2.81 (dd, J = 14.2, 9.5 Hz, 1H), 2.65 (dd, J = 13.9, 3.9 Hz, 1H), 2.42 (dd, J = 13.9, 8.3 Hz, 1H), 2.20–2.12 (m, 1H), 2.00–1.94 (m, 1H), 1.93–1.87 (m, 1H), 1.85–1.75 (m, 1H), 1.71–1.64 (m, 1H), 1.62–1.53 (m, 2H), 1.51–1.40 (m, 2H), 1.32–1.17 (m, 1H); **^{13}C NMR** (151 MHz, DMSO-d_6, major rotamer) δ/ppm 173.0, 171.1, 169.3, 156.6, 155.5, 137.4, 130.2, 129.3, 129.2, 128.3, 128.1, 126.4, 114.6, 71.9, 66.8, 59.8, 57.3, 50.9, 40.4, 39.4, 37.9, 37.8, 37.8, 36.0, 30.5, 29.2, 26.3, 25.8, 22.6; **HRMS ESI** *m*/*z* calc. for $C_{32}H_{45}N_6O_6$ $[M+H]^+$: 609.3395, found: 609.3398.

3. Toxicity Assays

The assay "Thamnotokit F^{TM}" was purchased from MicrobioTest Inc., Kleimoer 15, 9030 Mariakerke (Gent), Belgium. The assay was conducted as described in the operating procedure. The standard freshwater (SFW) was prepared as described and oxygenated prior use by bubbling air for 20 minutes through it. Diluted standard freshwater (DFW) was prepared by mixing SFW (2.5 ml) with deionized water (17.5 ml). The *T. platyurus* cysts were hydrated in DFW (1.0 ml) for 30 minutes before they were added to DFW (9 ml) and incubated in a Petri dish for 24 hours at 25 °C under continuous light (Philips TL-D 36W/840 lamp). Aqueous solutions in SFW with concentrations of 150, 100, 33.3, 11.1, 3.7, 1.3 µM of the different test compounds (A828A, A126A, A748A, A794A and A616A) were prepared. For the blank SFW was used. In a 24 well plate, four repetitions of each concentration were prepared. About 40 larvae were added to the first vial of each dilution by a pipette. From there, 10 larvae were transported to each of the remaining three vials of each concentration. Only these three vials were counted for compounds A126A, A748A, A794A and A616A; for A828A all four repetitions were counted. The plate was covered with parafilm and incubated for 24 hours at 25 °C in the dark. The mortality was determined by counting the dead larvae. Dead was defined as no movement within 10 seconds.

Test Substance	0 µM Dead/ Total	1.23 µM Dead/ Total	3.70 µM Dead/ Total	11.1 µM Dead/ Total	33.3 µM Dead/ Total	100 µM Dead/ Total	150 µM Dead/ Total
A828A	0/10	0/10	0/10	0/10	4/10	10/10	
	0/10	0/10	1/10	3/10	3/10	8/11	
	0/10	0/10	0/10	4/10	3/10	8/9	
				8/16	7/15	15/16	
A126A	0/10	1/10	0/10	0/10	3/10	7/11	6/6
	1/10	0/10	0/10	3/10	0/10	9/10	6/6
	0/10	0/10	1/10	0/10	2/10	10/10	4/6
A748A	0/10	0/10	0/10	3/10	5/10	9/10	9/11
	0/10	0/10	0/10	3/12	4/9	9/10	10/10
	0/10	0/10	0/10	5/9	6/10	9/10	9/11
A794A	0/10	0/10	0/10	4/10	10/10	10/10	10/10
	1/10	0/10	0/10	5/10	10/10	10/10	10/10
	0/10	0/10	2/10	1/10	10/10	10/10	10/10
A616A	0/10	0/10	0/10	2/10	5/10	8/10	
	0/10	0/10	0/10	3/10	9/10	8/10	
	0/10	0/10	0/10	3/10	8/10	8/10	

4. References

[1] *APEX2, version 2 user Manual*, M86-E01078, Bruker Analytical X-ray Systems, Inc., Madison, WI, **2006**.

[2] G. M. Sheldrick, *Acta Crystallogr. Sect. A Found. Crystallogr.* **2007**, *64*, 112–122.

[3] P. W. Betteridge, J. P. Carruthers, R. I. Cooper, K. Prout, D. J. Watkin, *J. Appl. Crystallogr.* **2003**, *36*, 1487.

[4] S. Hanessian, M. Tremblay, J. F. W. Petersen, *J. Am. Chem. Soc.* **2004**, *126*, 6064–6071.

[5] S. Hanessian, X. Wang, K. Ersmark, J. R. Del Valle, E. Klegraf, *Org. Lett.* **2009**, *11*, 4232–4235.

[6] M. T. Crimmins, R. S. Al-awar, I. M. Vallin, W. G. Hollis, R. O'Mahony, J. G. Lever, D. M. Bankaitis-Davis, *J. Am. Chem. Soc* **1996**, *118*, 7513–7528.

[7] S. Hanessian, J. R. Del Valle, Y. F. Xue, N. Blomberg, *J. Am. Chem. Soc.* **2006**, *128*, 10491–10495.

[8] N. Stuhr-Hansen, S. Padrah, K. Strømgaard, *Tetrahedron Lett.* **2014**, *55*, 4149–4151.

[9] S. Hanessian, R. Margarita, A. Hall, S. Johnstone, M. Tremblay, L. Parlanti, *J. Am. Chem. Soc.* **2002**, *124*, 13342–13343.

[10] R. López, A. Fernández-Mayoralas, *J. Org. Chem.* **1994**, *59*, 737–745.

[11] L. J. Ingram, S. D. Taylor, *Angew. Chem. Int. Ed.* **2006**, *45*, 3503–3506.

[12] F. Shi, J. P. Waldo, Y. Chen, R. C. Larock, *Org. Lett.* **2008**, *10*, 2409–2412.

[13] A. Arques, P. Molina, D. Aunon, M. J. Vilaplana, M. D. Velasco, F. Martinez, D. Bautista, F. J. Lahoz, *J. Organomet. Chem.* **2000**, *598*, 329–338.

[14] R. Wang, H. F. Shi, J. F. Zhao, Y. P. He, H. Bin Zhang, J. P. Liu, *Bioorganic Med. Chem. Lett.* **2013**, *23*, 1760–1762.

[15] S. Han, R. A. Moore, R. E. Viola, *Bioorg. Chem.* **2002**, *30*, 81–94.

[16] F. Sarabia, A. Sánchez-Ruiz, S. Chammaa, *Bioorganic Med. Chem.* **2005**, *13*, 1691–1705.

[17] G. Wang, N. Goyal, B. Hopkinson, *Bioorganic Med. Chem. Lett.* **2009**, *19*, 3798–3803.

[18] B. Cao, D. Xiao, M. M. Joullie, *Org. Lett.* **1999**, *1*, 1799–1801.

[19] D. Yang, S. Mao, Y.-R. Gao, D.-D. Guo, S.-H. Guo, B. Li, Y.-Q. Wang, *RSC Adv.* **2015**, *5*, 23727–23736.

[20] L. Dong, J. Marakovits, X. Hou, C. Guo, S. Greasley, E. Dagostino, R. Ferre, M. C. Johnson, E. Kraynov, J. Thomson, *Bioorganic Med. Chem. Lett.* **2010**, *20*, 2210–2214.

APPENDIX

1. Chiral HPLC

Racemic Ethyl-1-acetyl-6-methoxyindoline-2-carboxylate (3.56)

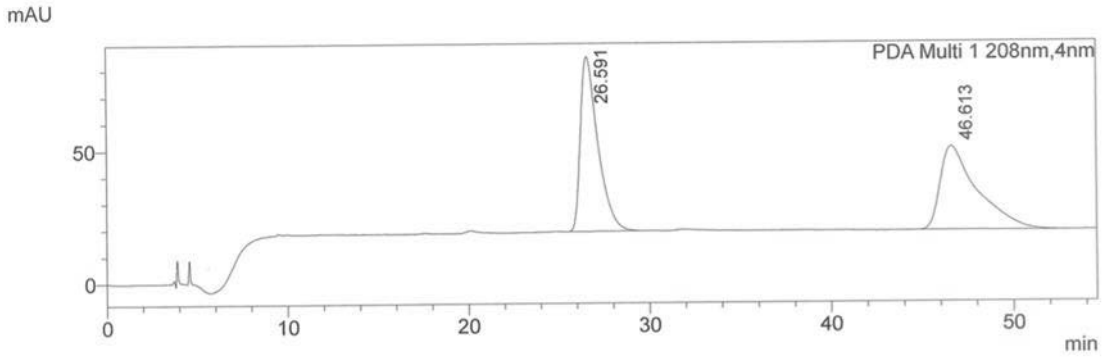

PDA Ch1 208nm

Peak#	Ret. Time	Height	Area	Area%
1	26.591	65908	4447158	50.003
2	46.613	31620	4446586	49.997
Total		97529	8893744	100.000

Chiralpak AS-H column, heptane/iPrOH (90:10), 0.8 mL/min, 30 °C, 208 nm

Ethyl (R)-1-acetyl-6-methoxyindoline-2-carboxylate (3.56)

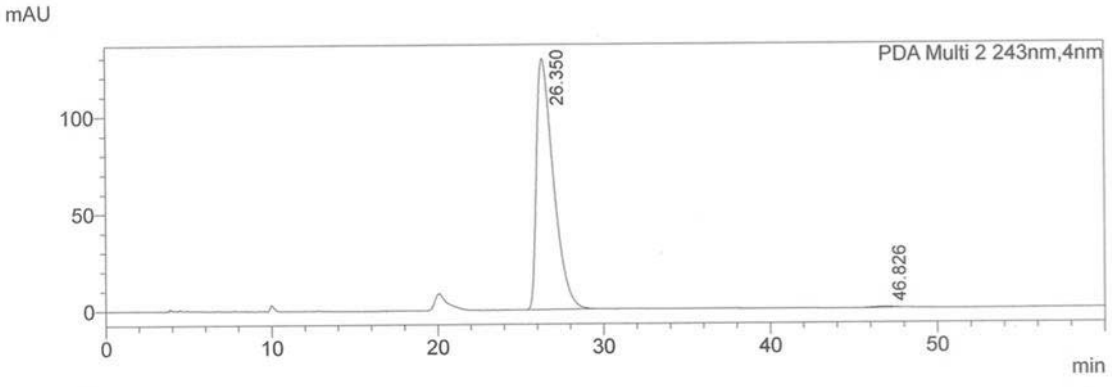

PDA Ch2 243nm

Peak#	Ret. Time	Height	Area	Area%
1	26.350	129235	9185479	99.570
2	46.826	490	39701	0.430
Total		129725	9225181	100.000

Chiralpak AS-H column, heptane/iPrOH (90:10), 0.8 mL/min, 30 °C, 208 nm

2. NMR Spectra

^{1}H, ^{13}C and ^{19}F NMR spectra of previously unreported compounds can be found on the accompanying CD to this PhD thesis.